frontiers | Research Topics

# Drug discovery derived from herbal medicine/polypeptide for neurological diseases

**Edited by**
Qi Liang, Junfeng Wang and Peng Sang

**Published in**
Frontiers in Pharmacology

ISSN 1664-8714
ISBN 978-2-8325-6465-3
DOI 10.3389/978-2-8325-6465-3

## About Frontiers

Frontiers is more than just an open access publisher of scholarly articles: it is a pioneering approach to the world of academia, radically improving the way scholarly research is managed. The grand vision of Frontiers is a world where all people have an equal opportunity to seek, share and generate knowledge. Frontiers provides immediate and permanent online open access to all its publications, but this alone is not enough to realize our grand goals.

## Frontiers journal series

The Frontiers journal series is a multi-tier and interdisciplinary set of open-access, online journals, promising a paradigm shift from the current review, selection and dissemination processes in academic publishing. All Frontiers journals are driven by researchers for researchers; therefore, they constitute a service to the scholarly community. At the same time, the *Frontiers journal series* operates on a revolutionary invention, the tiered publishing system, initially addressing specific communities of scholars, and gradually climbing up to broader public understanding, thus serving the interests of the lay society, too.

## Dedication to quality

Each Frontiers article is a landmark of the highest quality, thanks to genuinely collaborative interactions between authors and review editors, who include some of the world's best academicians. Research must be certified by peers before entering a stream of knowledge that may eventually reach the public - and shape society; therefore, Frontiers only applies the most rigorous and unbiased reviews. Frontiers revolutionizes research publishing by freely delivering the most outstanding research, evaluated with no bias from both the academic and social point of view. By applying the most advanced information technologies, Frontiers is catapulting scholarly publishing into a new generation.

## What are Frontiers Research Topics?

Frontiers Research Topics are very popular trademarks of the *Frontiers journals series*: they are collections of at least ten articles, all centered on a particular subject. With their unique mix of varied contributions from Original Research to Review Articles, Frontiers Research Topics unify the most influential researchers, the latest key findings and historical advances in a hot research area.

Find out more on how to host your own Frontiers Research Topic or contribute to one as an author by contacting the Frontiers editorial office: frontiersin.org/about/contact

# Drug discovery derived from herbal medicine/polypeptide for neurological diseases

**Topic editors**

Qi Liang — Air Force Medical University, China

Junfeng Wang — Massachusetts General Hospital, Harvard Medical School, United States

Peng Sang — Zhengzhou University, China

**Citation**

Liang, Q., Wang, J., Sang, P., eds. (2025). *Drug discovery derived from herbal medicine/polypeptide for neurological diseases*. Lausanne: Frontiers Media SA. doi: 10.3389/978-2-8325-6465-3

# Table of contents

frontiers | Frontiers in Pharmacology

TYPE Editorial
PUBLISHED 02 June 2025
DOI 10.3389/fphar.2025.1615452



OPEN ACCESS

EDITED AND REVIEWED BY
Michael Heinrich,
University College London, United Kingdom

*CORRESPONDENCE
Qi Liang,
liangqi2824@163.com
Junfeng Wang,
jwang83@mgh.harvard.edu

RECEIVED 21 April 2025
ACCEPTED 06 May 2025
PUBLISHED 02 June 2025

CITATION
Liang Q, Zhang J, Lin L and Wang J (2025) Editorial: Drug discovery from herbal medicines/polypeptides for neurological diseases.
*Front. Pharmacol.* 16:1615452.
doi: 10.3389/fphar.2025.1615452



# Editorial: Drug discovery from herbal medicines/polypeptides for neurological diseases

Qi Liang[1]*, Jianfeng Zhang[2], Li Lin[3] and Junfeng Wang[4]*

[1]Shaanxi Institute for Food and Drug Control, Xi'an, Shaanxi, China, [2]Department of Pharmacy, Eighth Hospital of Xi'an City, Xi'an, Shaanxi, China, [3]Department of Orthopedic Surgery, Tangdu Hospital, Air Force Medical University, Xi'an, Shaanxi, China, [4]Gordon Center for Medical Imaging, Massachusetts General Hospital & Department of Radiology, Harvard Medical School, Boston, MA, United States

KEYWORDS

**TCM, herbal medicines, neurological diseases, drug discovery, polypeptides**

Editorial on the Research Topic
Editorial: Drug discovery from herbal medicines/polypeptides for neurological diseases

## 1 Introduction

The quest for effective treatments for neurological diseases—ranging from Alzheimer's disease (AD) (Bai et al., 2024) and depression to stroke and spinal cord injury (Hu et al., 2023)—has driven researchers to explore unconventional therapeutic avenues. Among these, herbal medicine and polypeptide-based therapies stand out for their unique mechanisms and historical validation (Gong et al., 2024). This editorial synthesizes insights from 14 recent studies, highlighting their contributions to advancing drug discovery for neurological disorders and addressing the challenges of integrating traditional knowledge with modern pharmacology.

## 2 The renaissance of herbal medicine in neuroprotection

### 2.1 Alzheimer's disease: targeting amyloid and tau pathology

Two studies exemplify the potential of plant-derived compounds in combating AD (Aili et al., 2023). The first (DOI: 10.3389/fphar.2025.1500955) investigates the biosynthesis of neuroactive alkaloids, such as Huperzine A and Galantamine. Both discoveries not only deepen our understanding of plant metabolism but also offer practical pathways for the sustainable production of crucial AD treatments. Complementing this, the second study (DOI: 10.3389/fphar.2025.1497861) explores natural inhibitors of glycogen synthase kinase-3β (GSK-3β), a key enzyme driving tau hyperphosphorylation. Curcumin derivatives from *Curcuma longa L.* and hesperetin from *Citrus* × *aurantium L.* were

shown to reduce tau pathology in transgenic mouse models, highlighting GSK-3β as a pivotal target for multi-herbal interventions.

### 2.2 Depression and neuroplasticity: restoring balance

Depression, linked to impaired neuroplasticity, is addressed by two groundbreaking works (Dai et al., 2024). A review of traditional Chinese medicine (TCM) (DOI: 10.3389/fphar.2024.1426769) identifies compounds like gastrodin and saikosaponins, which upregulate BDNF expression and promote dendritic spine formation in the prefrontal cortex. Meanwhile, a meta-analysis of plant polysaccharides (DOI: 10.3389/fphar.2024.1348019) reveals their role in modulating the gut-brain axis. Polysaccharides from Astragalus and Rehmannia enhance serotonin synthesis by restoring gut microbiota diversity, offering a novel mechanism for antidepressant effects.

### 2.3 Ischemic injury and neurorepair

Cerebral ischemia-reperfusion injury, a major cause of stroke disability, is tackled by studies on apigenin (DOI: 10.3389/fphar.2024.1362301) and Guipi Wan (DOI: 10.3389/fphar.2024.1346226). Apigenin, a flavonoid in *Matricaria chamomilla L.*, was found to enhance DNA repair via PARP-1 activation, reducing infarct volume in rodent models. Guipi Wan, a TCM formulation, attenuated oxidative stress by regulating the Nrf2/HO-1 pathway, underscoring the value of multi-herbal synergies.

## 3 Polypeptides and bioactive alkaloids: precision tools for neural repair

### 3.1 Unlocking alkaloid potential

*Uncaria rhynchophylla (Miq.) Miq.* (DOI: 10.3389/fphar.2024.1436481). exemplifies the therapeutic promise of alkaloids. Its rhynchophylline and isorhynchophylline demonstrated NMDA receptor antagonism, reducing glutamate excitotoxicity in Parkinson's models. Similarly, berberrubine from *Berberis vulgaris L.* (DOI: 10.3389/fphar.2024.1496917) protected against cisplatin-induced ototoxicity by upregulating folate biosynthesis enzymes, preserving cochlear hair cells.

### 3.2 Retinal and spinal cord protection

Innovative approaches for ocular and spinal disorders are emerging (Vargova et al., 2021). *Lycium ruthenicum Murray* extract (DOI: 10.3389/fphar.2024.1404119), rich in anthocyanins, preserved retinal ganglion cells in glaucoma models by inhibiting caspase-3-mediated apoptosis. For spinal cord injury, Erxian decoction metabolites (DOI: 10.3389/fphar.2024.1339956) binding PRAS40—a regulator of mTOR—enhanced axonal regeneration by modulating autophagy, achieving functional recovery in rats to some extent.

## 4 Clinical translation: bridging evidence and practice

### 4.1 Evaluating herbal formulations

The efficacy of standardized herbal mixtures (Hao et al., 2023) is exemplified by a blend of *Centella asiatica (L.) Urb.*, *Echinacea purpurea (L.) Moench*, and *Zingiber officinale Roscoe* (DOI: 10.3389/fphar.2024.1439811), which normalized cortisol levels and restored dopaminergic signaling in stress-induced depression. Xingnaojing injection (DOI: 10.3389/fphar.2024.1411026), a TCM-derived neuroprotective agent, showed a significant reduction in post-hemorrhagic stroke edema in a meta-analysis of the patients, though heterogeneity in trial design calls for stricter standardization.

### 4.2 Antrodia camphorata: a fungal frontier

The *Zingiber officinale Roscoe* (DOI: 10.3389/fphar.2024.1372110) offers triterpenoids and polysaccharides that inhibit neuroinflammation via microglial TLR4 suppression. Its potential in treating multiple sclerosis is being explored in Phase II trials, with preliminary data showing an obvious reduction in relapse rates.

## 5 Challenges and future directions

Despite progress, critical hurdles remain:

1) Standardization: Batch variability in herbal extracts undermines reproducibility. This issue is expected to be resolved through the implementation of blockchain tracking with GACP, HPLC-MS fingerprint recognition, and reference standards.
2) Bioavailability: Previous studies have improved the bioavailability of natural products through nanocapsules (Amante et al., 2022), prodrug design (Beaumont et al., 2022), and synergistic formulations (Sharma et al., 2023).
3) Mechanistic Complexity: Herbal polypharmacology complicates target identification. Traditionally, network pharmacology contributed to this identification. Nowadays, AI-driven docking (as used in DOI: 10.3389/fphar.2024.1339956) is playing an increasingly important role in elucidating multi-objective effects.

## 6 Future research should prioritize

To advance herbal medicine into the era of precision and reproducibility, future research must prioritize three interconnected domains: multi-omics integration, sustainable bioengineering, and hybrid therapeutic trials. These priorities address critical gaps in standardization, scalability, and mechanistic validation while aligning with global demands for personalized and eco-conscious healthcare solutions.

### 6.1 Omics integration: decoding bioactive signatures

Herbal extracts' complexity demands metabolomics (e.g., UPLC-QTOF-MS) to map bioactive markers linked to clinical outcomes. AI-driven platforms can integrate pharmacometabolomics and gut microbiome interactions. Standardizing protocols and addressing data heterogeneity remain challenges.

### 6.2 Sustainable sourcing: CRISPR-engineered plants

CRISPR editing resolves supply-chain instability and phytochemical variability through high-yield strains, precision chemotypes, climate resilience, and biosafety measures.

### 6.3 Hybrid trials: herbal-polypeptide synergies

Previous work proved that polypeptide such as BDNF-mimetic peptides was benifit for maintaining mitochondrial quality control (Ahuja et al., 2022). As such, the synergies of BDNF-mimetic peptides and natural products may be an alternatitive for neuroprotection.

## 7 Conclusion

The studies in this Research Topic illuminate a path forward where traditional herbal wisdom and cutting-edge polypeptide engineering converge to address neurological diseases. From alkaloids that recalibrate neurotransmitter systems to polysaccharides that heal the gut-brain axis, these therapies exemplify the power of nature-inspired innovation. However, their success hinges on resolving standardization, mechanistic clarity, and regulatory alignment. By fostering interdisciplinary collaboration—ethnobotanists, pharmacologists, and data scientists—we can transform these ancient remedies into the next-generation of neurological therapeutics, ensuring they meet the rigor of modern medicine while preserving their holistic essence. In this synergy of old and new lies the promise of healing some of humanity's most complex disorders.

The convergence of herbal wisdom and polypeptide engineering presents groundbreaking potential for neurological therapeutics, yet critical methodological and translational challenges must be systematically addressed:

(1) Decoding Polypharmacological Synergy: Conventional reductionist approaches fail to capture the dynamic multi-target interactions of herbal compounds. Advanced methodologies should integrate multi-omics network modeling combining single-cell transcriptomics, metabolic flux analysis, and AI-enhanced molecular dynamics simulations.
(2) Bioinspired Peptide Delivery Optimization: Next-generation platforms are required to overcome the delivery barriers.
(3) Precision Standardization Systems: Although the blockchain-based herbal traceability platform and UPC$^2$ chromatography integration have achieved dynamic monitoring of bioactive phytochemicals, the development of new technologies still needs to be emphasized.

## Author contributions

QL: Writing – review and editing, Writing – original draft. JZ: Investigation, Conceptualization, Writing – review and editing. LL: Software, Writing – original draft. JW: Funding acquisition, Validation, Writing – original draft.

## Funding

The author(s) declare that no financial support was received for the research and/or publication of this article.

## Conflict of interest

The authors declare that the research was conducted in the absence of any commercial or financial relationships that could be construed as a potential conflict of interest.

## Generative AI statement

The authors declare that no Generative AI was used in the creation of this manuscript.

## Publisher's note



## References

Ahuja, P., Ng, C. F., Pang, B. P. S., Chan, W. S., Tse, M. C. L., Bi, X., et al. (2022). Muscle-generated BDNF (brain derived neurotrophic factor) maintains mitochondrial quality control in female mice. *Autophagy* 18 (6), 1367–1384. doi:10.1080/15548627.2021.1985257

Aili, M., Zhou, K., Zhan, J., Zheng, H., and Luo, F. (2023). Anti-inflammatory role of gold nanoparticles in the prevention and treatment of Alzheimer's disease. *J. Mat. Chem. B* 11 (36), 8605–8621. doi:10.1039/d3tb01023f

Amante, C., Esposito, T., Luccheo, G., Luccheo, L., Russo, P., and Gaudio, P. D. (2022). Recapsoma®: a novel mixture based on Bergamot, Ipomoea Batatas, Policosanol Extracts and liposomal berberine for the treatment of hypercholesterolemia. *Life (Basel)* 12 (8), 1162. doi:10.3390/life12081162

Bai, Y., Liu, X., and Baldwin, I. T. (2024). Using synthetic biology to understand the function of plant specialized metabolites. *Annu. Rev. Plant Biol.* 75, 629–653. doi:10.1146/annurev-arplant-060223-013842

Beaumont, P., Courtois, A., Atgié, C., Richard, T., and Krisa, S. (2022). In the shadow of resveratrol: biological activities of epsilon-viniferin. *J. Physiol. Biochem.* 78 (2), 465–484. doi:10.1007/s13105-022-00880-x

Dai, Y., Ban, W., and Yang, Z. (2024). Gastrodin, a promising natural small molecule for the treatment of central nervous system disorders, and its recent progress in synthesis, pharmacology and pharmacokinetics. *Int. J. Mol. Sci.* 25 (17), 9540. doi:10.3390/ijms25179540

Gong, M. Q., Lai, F. F., Chen, J. Z., Li, X. H., Chen, Y. J., and He, Y. (2024). Traditional uses, phytochemistry, pharmacology, applications, and quality control of Gastrodia elata Blume: a comprehensive review. *J. Ethnopharmacol.* 319 (Pt 1), 117128. doi:10.1016/j.jep.2023.117128

Hao, D. L., Li, J. M., Xie, R., Huo, H. R., Xiong, X. J., Sui, F., et al. (2023). The role of traditional herbal medicine for ischemic stroke: from bench to clinic-A critical review. *Phytomedicine* 109, 154609. doi:10.1016/j.phymed.2022.154609

Hu, X., Xu, W., Ren, Y., Wang, Z., He, X., Huang, R., et al. (2023). Spinal cord injury: molecular mechanisms and therapeutic interventions. *Signal Transduct. Target. Ther.* 8, 245. doi:10.1038/s41392-023-01477-6

Sharma, M. R., Arya, P., Kaur, R., Kennedy, J. F., and Raghav, N. (2023). Differential binding of piperine and curcumin with modified cellulose, alginate and pectin supports: in-vitro and in-silico studies. *Int. J. Biol. Macromol.* 233, 123508. doi:10.1016/j.ijbiomac.2023.123508

Vargova, I., Machova Urdzikova, L., Karova, K., Smejkalova, B., Sursal, T., Cimermanova, V., et al. (2021). Involvement of mTOR pathways in recovery from spinal cord injury by modulation of autophagy and immune response. *Biomedicines* 9, 593. doi:10.3390/biomedicines9060593

frontiers | Frontiers in Pharmacology

TYPE Original Research
PUBLISHED 22 January 2024
DOI 10.3389/fphar.2024.1339956



OPEN ACCESS

EDITED BY
Junfeng Wang,
Massachusetts General Hospital and Harvard Medical School, United States

REVIEWED BY
Qize Zhang,
Biogen Idec, United States
Xiaojia Zhu,
Chinese Academy of Sciences (CAS), China
Yanli Wang,
Minzu University of China, China

*CORRESPONDENCE
Bo Liao,
liaobospine@163.com

†These authors have contributed equally to this work and share first authorship

RECEIVED 17 November 2023
ACCEPTED 05 January 2024
PUBLISHED 22 January 2024

CITATION
Lin L, Yan J, Sun J, Zhang J and Liao B (2024), Screening and evaluation of metabolites binding PRAS40 from Erxian decoction used to treat spinal cord injury.
*Front. Pharmacol.* 15:1339956.
doi: 10.3389/fphar.2024.1339956



# Screening and evaluation of metabolites binding PRAS40 from Erxian decoction used to treat spinal cord injury

Li Lin[1†], Jingchuan Yan[1†], Jin Sun[1], Jianfeng Zhang[2] and Bo Liao[1*]

[1]Department of Orthopedics, Tangdu Hospital, Air Force Military Medical University, Xi'an, Shaanxi, China, [2]Department of Pharmacy, Eighth Hospital of Xi'an City, Xi'an, Shaanxi, China

**Objective:** The PRAS40 is an essential inhibitory subunit of the mTORC1 complex, which regulates autophagy. It has been suggested that Erxian Decoction (EXD) could treat spinal cord injury (SCI) via the autophagy pathway. However, the mechanism of whether EXD acts through PRAS40 remains unclear.

**Methods:** With the help of immobilized PRAS40, isothermal titration calorimetry (ITC) and molecular docking, the bioactive metabolites in the EXD were screened. To establish *in vitro* SCI models, PC12 cells were exposed to hydrogen peroxide (H2O2) and then treated with the identified EXD substances. Furthermore, Western blot assay was carried out to identify potential molecular mechanisms involved. For assessing the effect of metabolites *in vivo*, the SCI model rats were first pretreated with or without the metabolite and then subjected to the immunohistochemistry (IHC) staining, Basso, Beattie & Bresnahan (BBB) locomotor rating scale, and H&E staining.

**Results:** The immobilized PRAS40 isolated indole, 4-nitrophenol, terephthalic acid, palmatine, sinapinaldehyde, and 3-chloroaniline as the potential ligands binding to PRAS40. Furthermore, the association constants of palmatine and indole as 2.84 × 106 M-1 and 3.82 × 105 M-1 were elucidated via ITC due to the drug-like properties of these two metabolites. Molecular docking results also further demonstrated the mechanism of palmatine binding to PRAS40. Western blot analysis of PC12 cells demonstrated that palmatine inhibited the expression of p-mTOR by binding to PRAS40, activating the autophagic flux by markedly increasing LC3. The injection of palmatine (10μM and 20 μM) indicated notably increased BBB scores in the SCI rat model. Additionally, a dose-dependent increase in LC3 was observed by IHC staining.

**Conclusion:** This research proved that EXD comprises PRAS40 antagonists, and the identified metabolite, palmatine, could potentially treat SCI by activating the autophagic flux.

KEYWORDS

**spianl cord injury, Erxian decotion, autophagy, m-TOR, PRAS40**

# 1 Introduction

Spinal cord injury (SCI) is manifested with various functional deficits because of spinal cord axonal and neuronal damage (Hellenbrand et al., 2021). The National SCI Statistical Center data indicated that the incidence of SCI is approximately 17,000 new cases each year (Author anonymous, 2016). Therefore, research on effective SCI treatment is necessary. Previous studies have reported that SCI pathogenesis comprises multiple cellular and biochemical processes, including free radical formation (Hou et al., 2021), posttraumatic inflammatory response (Chen et al., 2021), autophagy (Ko et al., 2020), vascular ischemia (Ahn et al., 2020), apoptosis (Wang et al., 2019), and genetically programmed cell death (Xu et al., 2021). Autophagy is a cellular self-defense mechanism that prevents cell damage, promotes cell survival in the presence of nutrient deficiencies, and responds to cytotoxic stimuli (Klionsky et al., 2021). Studies have shown that promoting autophagy can reduce neuronal apoptosis, inhibit neuroinflammation, and promote functional recovery of the SCI (Rong et al., 2019). Therefore, regulating autophagy in neural tissue is expected to become an important means for treating SCI.

Roth *et al.* were the first to discover a Proline-rich Akt substrate of 40 kD (PRAS40) in 2003 and characterized it as a substrate of protein kinase B (PKB/Akt) (Kovacina et al., 2003). The literature indicates that PRAS40 is associated with the mammalian target rapamycin (mTOR) signaling pathways. PRAS40 directly binds to the mTOR kinase domain, thereby regulating mTOR activity (Ma et al., 2020). Among these, the mTOR signaling pathway has been suggested to be crucially associated with SCI pathogenesis (Ma et al., 2020; Vargova et al., 2021). Currently, the literature primarily focuses on discovering mTOR ligands, and studies on other protein components like PRAS40 are lacking (Szwed et al., 2021).

EXD, a traditional Chinese medicine (TCM), was introduced by Zhang Bo-Na in the early 1950s. It is frequently used as a traditional Chinese herbal prescription for menopausal syndrome and comprises six herbs: *Curculigo orchioides Gaertn [Hypoxidaceae; Curculiginis rhizoma], Epimedium brevicornu Maxim [Berberidaceae; Epimedii folium], Phellodendron chinense C.K.Schneid. [Rutaceae; Phellodendri chinensis cortex], Anemarrhena asphodeloides Bunge [Asparagaceae; Anemarrhenae rhizoma], Angelica sinensis (Oliv.) Diels [Apiaceae; Angelicae sinensis radix], Morinda officinalis F.C.How [Rubiaceae; Morindae officinalis radix]* (Li et al., 2007). Furthermore, EXD has revealed significant efficacy against many clinical diseases and has also been proven effective for treating SCI. The literature suggests that EXD could inhibit apoptosis and has neuroprotective effects in rats (Li et al., 2022). The mTOR signaling pathway has been linked with these pharmacodynamic effects, suggesting the presence of the PRAS40 antagonists in EXD.

In this investigation, the PRAS40 antagonists were screened from EXD using the immobilized PRAS40. *In-vivo* and *in-vitro* elucidation of the PRAS40 antagonists have been indicated as promising drug candidates for SCI treatment. This research identified bioactive metabolites from EXD and provided an alternate mechanism of EXD for treating SCI.

# 2 Materials and methods

## 2.1 Materials and reagents

The His-tagged PRAS40 protein was purchased from Genscript Co., Ltd (Nanjing, China). The herbs were obtained from Tongrentang Co., Ltd (Beijing, China). For reference, Indole (No. I104724) and palmatine chloride (No. P274975) were acquired from Aladdin Co., Ltd (Shanghai, China). All chemicals were analytically pure unless stated otherwise. MHY1485 (MCE, Monmouth Junction, NJ, United States), an agonist of mTOR. KingFisher magnetic particle processor (Thermo Fisher Scientific) was utilized for affinity selections, and the bioactive metabolites were identified *via* the UPLC-ESI-MS/MS system (UPLC, ExionLC™ AD).

## 2.2 Preparation of EXD

Weigh the herbs and add distilled water. After soaking for 30 min, boil for 30 min and then filter to obtain EXD. The ratio is shown in Table 1.

## 2.3 Affinity selection of bioactive metabolites from EXD

Briefly, the PRAS40 protein was incubated with Ni-NTA magnetic beads (10 mg) in PBS (pH 7.4) to coat the proteins for 30 min. Then, the beads were rinsed thrice with PBS + 1 mL Tween-20 (0.05% v/v, incubated for 1 h with EXD in PBS + Tween with mixing, and rinsed again with buffer + Tween 5 times to remove unbound metabolites. The resulting beads carrying bound metabolites were redissolved in elution buffer (10 mM imidazole, pH 8.5) to obtain the bioactive metabolites from EXD. These metabolites were analyzed using the Agilent column SB-C18 (2.1 mm × 100 mm, 1.8 μm) with the mobile phase comprising solvents A (0.1% formic acid + pure water) and B (0.1% formic acid + acetonitrile). For the identification of the bioactive metabolites, a linear gradient program from 95% A, 5% B to 5% A, 95% B within 9 min until a composition of 5% A, 95% B was kept for 1 min. The column was run at the temperature of 40°C, 2 μL injection volume, and the 0.35 mL/min flow rate. The effluent was alternatively connected to an ESI-triple quadrupole-linear ion trap (QTRAP)-MS.

## 2.4 High performance liquid chromatography (HPLC) determination of metabolites concentration

Thermo Scientific UltiMate 3,000 for HPLC quantification. Chromatographic conditions: palmatine and terephthalic acid: mobile phase:0.01 mol/L Potassium dihydrogen phosphate and methanol(1:1), flow rate:1 mL/min, detection wavelength was 270 nm, Sample Volume 10 μL. 4-Nitrophenol: mobile phase: water and methanol (0.35:0.65), flow rate:1 mL/min, detection

TABLE 1 Pharmaceutical ingredient of Erxian decoction.

| Scientific name of plant[a] | Herb pinyin name | Family name | Dosage/300 mL (g) |
|---|---|---|---|
| *Curculigo orchioides Gaertn* | XIAN MAO | *Hypoxidaceae R.Br* | 10 |
| *Epimedium brevicornu Maxim* | Yin Yang Huo | *Berberidaceae Juss* | 30 |
| *Phellodendron chinense C.K.Schneid* | HUANG BO | *Rutaceae Juss* | 12 |
| *Anemarrhena asphodeloides Bunge* | ZHI MU | *Asparagaceae Juss* | 10 |
| *Angelica sinensis (Oliv.) Diels* | DANG GUI | *Apiaceae Lindl* | 10 |
| *Morinda officinalis F.C.How* | BA JI TIAN | *Rubiaceae Juss* | 10 |

[a]According to the Kew Herbarium Catalogue http://www.plantsoftheworldonline.org.

wavelength was 280 nm, Sample Volume 10 μL. Sinapinaldehyde, Indole and 3-Chloroaniline: water and methanol (0.3:0.7), flow rate: 0.8 mL/min, detection wavelength was 270 nm, Sample Volume 10 μL. The contents of each component were calculated according to the standard curve and the peak area of the sample.

## 2.5 Isothermal titration calorimetry (ITC)

Before the experiment, each sample was placed in a vacuum machine for 10 min to remove gas from the sample. Use the sampling needle that comes with the instrument to draw 300 uL of PRAS40 (5 μM) into the sample pool, and use the titration needle to draw 60 uL of the metabolites (50 μM) as the titrant. The conditions were set as 20 repeated injections at 25°C with an interval of 165 s between each injection. The equilibrium dissociation constant (Kd), stoichiometry (n), enthalpy (ΔH) and entropy (ΔS) were obtained by nanoAnalyzer software. For subsequent analysis, the metabolite with the highest thermodynamic parameter was selected.

## 2.6 Molecular docking validation

The sdf files of ligand small molecules were found in the PubChem database and converted into a PDB file through OpenBabel3.1.1. For receptor structure preparation, the 3D structure of the PRAS40 was downloaded from the UniProt database (Uniprot: Q96B36) and subjected to hydrogenation, water removal, and charge addition through AutoDock Tools 1.5. 6. And convert the format of active ingredient and target protein into pdbqt format. Finally, molecular docking was performed through AutoDock Vina 1.2.2.

## 2.7 Cell culture

PC12 cells were provided by Stem Cell Bank, Chinese Academy of Sciences (Shanghai, China). Cells were cultured in Rosewell Park Memorial Institute (RPMI)-1640 medium (Invitrogen, Carlsbad, CA, United States) containing 10% (v/v) fetal bovine serum (FBS, Gibco) and 1% (v/v) penicillin-streptomycin-glutamine in 100 $cm^2$ cell culture flask. The flask was placed in a humidity incubator at 37°C with 5% CO2.

## 2.8 Cell viability assay

Viabilities of PC12 cells were measured using cell counting kit-8 (CCK-8) assay (Beyotime Biotechnology, Shanghai, China) in this research. Briefly, PC12 cells were propagated in 96-well plates and incubated in a humidified incubator at 37°C for 24 h. Then different concentrations of $H_2O_2$ added into plates to stimulate PC12 cells for 24 h. After that, PC12 cells were treated with CCK-8 (10 μL) solution in fresh RPMI 1640 for 25 min. Each well's absorbance was assessed *via* a microplate reader (Infinite M200 PRO; Tecan) at 450 nm.

## 2.9 Western blot

Total proteins in PC12 cells were isolated using RIPA Lysis Buffer (Beyotime Biotechnology). The protein concentration was determined using a BCA Protein Assay Kit (Beyotime Biotechnology, Shanghai, China) with a full-wavelength functional microplate reader (Infinite M200Pro, Tecan, Switzerland). Then equal concentration Proteins were separated using 12.5% SDS–PAGE and transferred to nitrocellulose membranes. After blocking in 10% nonfat dry milk for 1 h, phosphorylated proteins were blocked using bovine serum albumin (5% BSA, room temperature) for 2 h. The membranes were incubated overnight at 4°C with the following primary antibodies: anti-phospho-mTOR-(Ser2448) (ZRB1553), anti-m-TOR(SAB5700687), anti-LC3 (SAB5701328) (Sigma Aldrich, United States), anti-phospho-PRAS40-(Thr246) (Cell Signaling) and anti-PRAS40(Cell Signaling)antibodies. The membrane was then incubated with the corresponding secondary antibody for 1 h. After three washes with PBST, the membrane was visualized using an ECL Western blot detection kit (Merck, United States). The average optical density of the images was analyzed using ImageJ.

## 2.10 Animals and surgeries

Adult Wistar rats (weight = 250 g, female) were acquired from the SPF Biotechnology Co., Ltd. [license number: SCXK (Jing) 2019-0010] and housed in ventilated cages (2-4/cage) at an environmentally controlled (22°C–24°C) conditions, a 12-h dark cycle, and *ad libitum* chow and water. The Care and Use of Laboratory Animals and ARRIVE guidelines were employed in a licensed laboratory for all animal investigations (license number:

SYXK (Shaan) 2020-007). This investigation was authorized (No. IACUC-20211003) by the Welfare and Ethics Committee of the Laboratory Animal Center of Air Force Military Medical University, China. Rats were randomly divided into 5 groups(n = 8): SCI group; SCI+5 μM palmatine group; SCI+10 μM palmatine group; SCI+20 μM palmatine group; sham group.

Surgical treatment was performed as described previously (Li et al., 2022). Briefly, After anesthesia with 25 mg/kg sodium pentobarbital solution, laminectomy from T8 to T10 was performed through a midline incision in the thoracic spine. A 10 g impactor fell vertically on the surface of the exposed T9 spinal cord from a height of 50 mm, causing a contusion injury. Rats with a tail swing action were included in the experiment, otherwise excluded. In the sham operation group, only the T9 lamina was removed without vertical impact. The palmatine group was injected with palmatine 10 μL (5, 10, and 20 μM concentrations) in the intrathecal space after impact. The SCI group was also injected with an equal volume of saline. After surgery, assisted urination (twice a day) will be given until spontaneous urination is restored. The BBB scores were used to assess the locomotor ability of rats at the time of pre-operation and awakening(0), 1, 3, and 7 days.

## 2.11 Perfusion and immunofluorescence

The animals were perfused 7 days after SCI. 100 mg/kg of pentobarbital sodium solution was utilized for anesthetizing the rats; then, their spinal cord tissues were sampled, preserved in paraformaldehyde (4%), embedded in wax, sliced, deparaffinized, hydrated, and treated with sodium citrate antigen retrieval solution (1:50, Proteintech, United States). The samples were then blocked for 1 h using 5% sheep serum albumin (Boster Biological, China) in PBS at room temperature before overnight immunostaining with primary anti-LC3 antibodies and secondary antibodies. After mounting (DAPI Fluoromount-G, Southern Biotech, United States), the specimens were imaged via a confocal laser scanning microscope (Olympus BX51) and DP Controller software (Olympus, Japan).

## 2.12 Statistical analysis

The normality and homogeneity of variances were tested using SPSS (version 25.0). One-way analysis of variance (ANOVA) was utilized to analyze data from multiple groups. To determine differences between groups, multiple comparisons were conducted using Bonferroni *post hoc* tests. The error bars in all figures indicate the mean ± standard error of the mean (SEM). A significance level of $p < 0.05$ was considered statistically significant. Data analysis was performed using SPSS and GraphPad Prism (version 6.0c).

# 3 Results and discussion

## 3.1 Screening PRAS40 binding metabolites from EXD

The EXD has been widely used for SCI treatment. Considering the pathological mechanism of mTOR, it was hypothesized that EXD has certain metabolites that interact with PRAS40. Therefore, PRAS40 was immobilized onto the surface of beads for screening the bioactive metabolites from EXD. As illustrated in Figure 1, six metabolites were identified according to the increased relative concentration in the samples (Table 2). Among these, 4-nitrophenol and 3-chloroaniline indicated poor drug-like properties due to a lack of compatibility with Lipinski's rules (Chen et al., 2020). Whereas sinapinaldehyde and terephthalic acid were Pan-Assay Interference Compounds (PAINS), which could indicate positive readouts in biochemical assays *via* different mechanisms; however, such readouts are not linked with optimizable and processible compounds (Grigalunas et al., 2020). Therefore, palmatine and indole were selected to determine their association constants binding to PRAS40 using the ITC, a robust method for analyzing protein-ligand interactions.

## 3.2 Thermodynamic parameters and molecular docking of palmatine and indole binding to PRAS40

The ITC aims to elucidate the heats of binding that evolve from protein-ligand interactions; however, in principle, titration yields other heats, too (Greytak et al., 2022). Therefore, first, the background heat between the solvent used to dissolve these two metabolites (5% DMSO in $H_2O$) and the PBS buffer during titration was assessed. After deducting these background heats, the ITC traces and binding isotherms between the ligands and PRAS40 were obtained (Figure 2). The continuous line in the lower plots depicts a good data fit at a single-binding-site model used to acquire fitted parameters ($\Delta G, \Delta H, \text{and} \Delta S$) values (Table 3). The resulting $K_d$ values of palmatine and indole binding to PRAS40 could be calculated from the ΔG values. The $K_d$ values of palmatine and indole were $3.53 \times 10^{-7}$ and $2.62 \times 10^{-6}$, respectively, indicating palmatine was a promising PRAS40 binding drug candidate for SCI treatment (Table 2). The higher $K_a$ values of palmatine also confirmed the above conclusion.

Molecular docking is an effective approach for studying molecular interactions (Pinzi and Rastelli, 2019). Based on the above screening results, the 3D structure of PRAS40 was imported into AutoDock Tools and docked with palmatine and indole (Figures 3A–C). Molecular docking results showed that the binding energy of the PRAS40 to palmatine and indole was −5.06, −4.24 kcal/mol, indicating that the combination of palmatine and the protein is more stable. Among them, ARG76 of PRAS40 interacts with palmatine to form a conventional hydrogen bond interaction; PRO43, ARG70, ALA66, and HIS69 interact with palmatine to form a carbon-hydrogen bond interaction; CYS44 forms a Pi-Alkyl interaction with palmatine while GLY42, TYR46, THR43 and PRO35 generate van der Waals interactions with palmatine (Figures 3D–E). VAL190 of PRAS40 has a hydrogen bond interaction with indole, and CYS44 and HIS69 have a conventional hydrogen bond interaction. In addition, ALA66, ARG70, PRO43, GLY42, and THR73 of the protein have van der Waals interactions with indole (Figures 3F–G). The results of molecular docking are consistent with ITC. Therefore, the pharmacological activity of palmatine *in vitro* and *in vivo* was assessed.

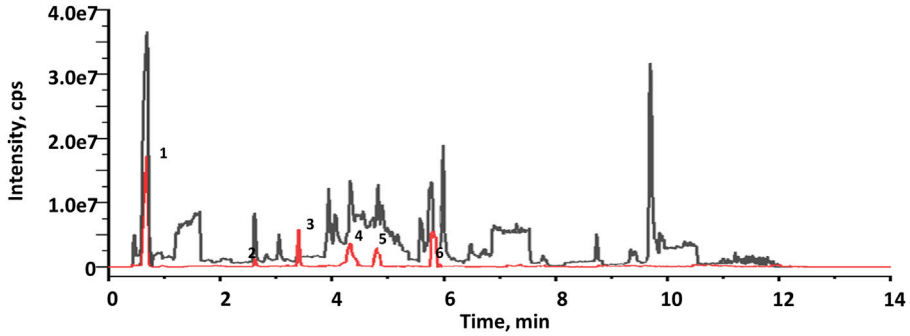


FIGURE 1
Total current ion chromatograms of EXD (black) and collections after screening using immobilized PRAS40 (red).

**TABLE 2** The mass spectral data of the bioactive PRAS40 binding metabolites using HPLC-MSESI-QTOF and MS/MS in positive mode.

| Peak/metabolites | Proposed metabolites | RT(min) | Ionization mode | m/z | Molecular formula | Concentration(%) |
|---|---|---|---|---|---|---|
| 1 | 4-Nitrophenol | 0.68 | $[M + H]^+$ | 140.03 | $C_6H_5NO_3$ | 0.05–0.06 |
| 2 | Indole | 2.61 | $[M + H]^+$ | 117.06 | $C_8H_7N$ | 0.01–0.02 |
| 3 | Terephthalic acid | 3.34 | $[M + H]^+$ | 168.03 | $C_8H_6O_4$ | 0.04–0.05 |
| 4 | Palmatine | 4.32 | $[M]^+$ | 352.15 | $C_{21}H_{22}NO_4$ | 0.08–0.09 |
| 5 | Sinapinaldehyde | 4.83 | $[M + H]^+$ | 208.07 | $C_{11}H_{12}O_4$ | 0.01–0.02 |
| 6 | 3-Chloroaniline | 5.79 | $[M + H]^+$ | 128.03 | $C_6H_6ClN$ | 0.05–0.06 |

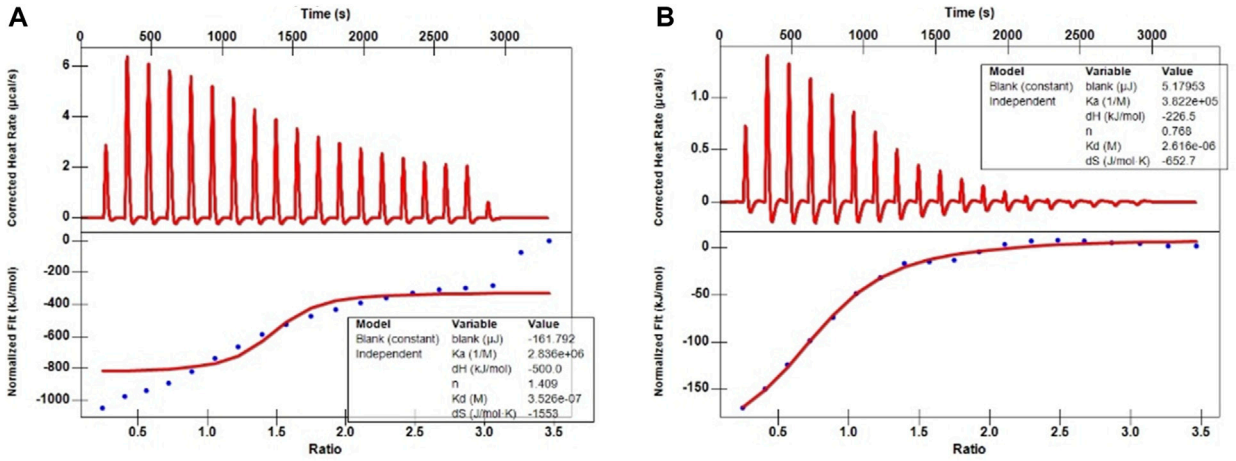


FIGURE 2
ITC traces and binding isotherms between the ligands and PRAS40. **(A)** Palmatine and PRAS40. **(B)** Indole and PRAS40.

**TABLE 3** The ITC data of palmatine and indole binding with PRAS40.

| Metabolites | $K_a$ ($M^{-1}$) | $K_d$ (M) | ΔH (KJ/mol) | ΔS (J/mol·K) | ΔG (KJ/mol) |
|---|---|---|---|---|---|
| Palmatine | $2.84 \times 10^6$ | $3.53 \times 10^{-7}$ | −500 | −1553 | −36.43 |
| Indole | $3.82 \times 10^5$ | $2.62 \times 10^{-6}$ | −226.5 | −625.7 | −31.67 |

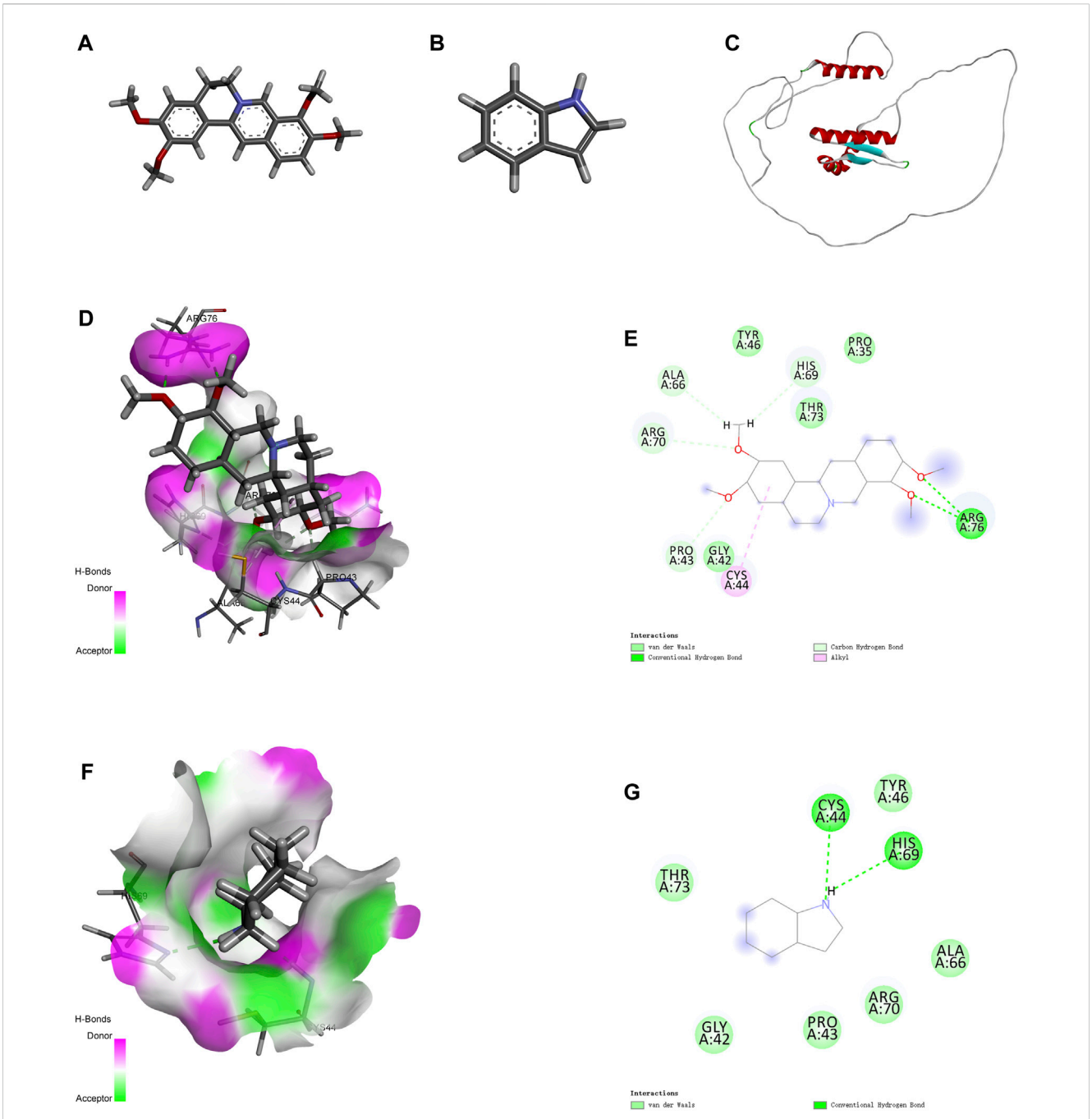


FIGURE 3
Molecular docking. **(A)** 2D structure of palmatine. **(B)** 2D structure of indole. **(C)** 3D structure of PRAS40. **(D)** Docking of PRAS40 to palmatine in 3D view, and **(E)** 2D view. **(F)** Docking of PRAS40 to indole in 3D view, and **(G)** 2D view.

## 3.3 Palmatine inhibits the phosphorylation of PRAS40 and activates autophagic flux in SCI cells model

PC12 cells were stimulated with different $H_2O_2$ concentrations for 24 h to mimic SCI cells, which indicated a dose-dependent (0–300 μM) reduction in cell viability (Figure 4A). Based on this, 200 μM of $H_2O_2$ was selected for SCI construction (viability = 50%). Subsequently, the cells were treated with palmatine (5, 10, and 20 μM concentrations) for 2 h, which revealed a dose-dependent alleviation of the expression level of p-PRAS40, while the level of LC3 was increased (Figures 4B–E). At the same time, the phosphorylation of mTOR, an important target of PRAS40, is also downregulated as the drug concentration increases. Altogether, these data demonstrated that palmatine inhibited the expression of p-mTOR by binding to PRAS40, activating the autophagic flux of PC12 cells.

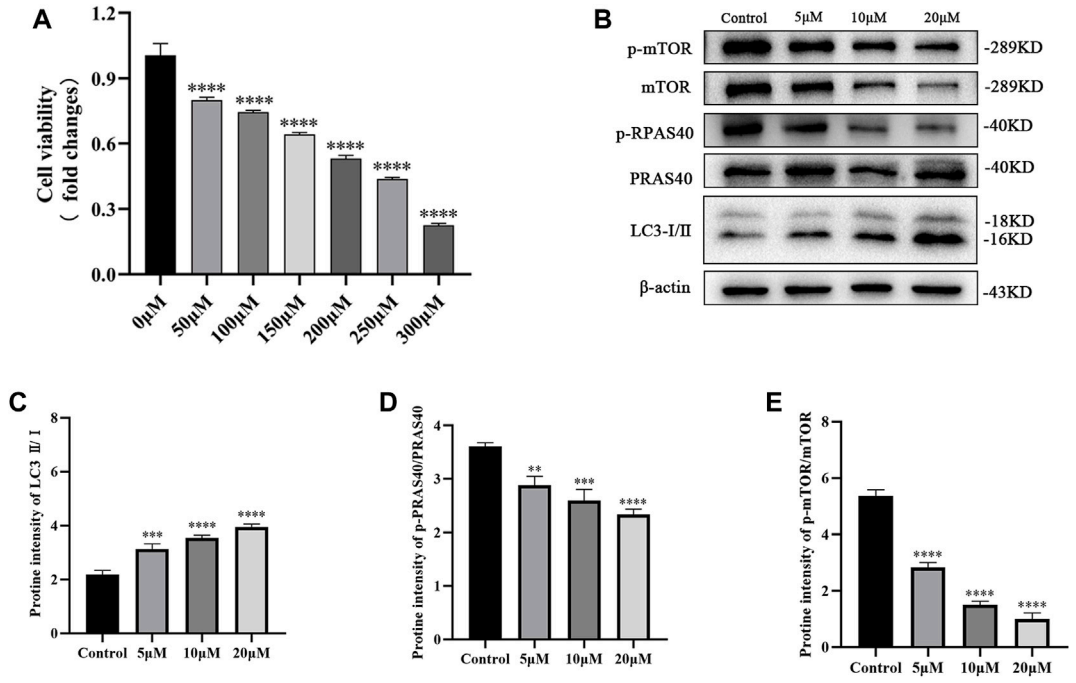


FIGURE 4
**(A)** PC12 cells viability after 24 h treatment with different concentrations of $H_2O_2$. **(B)** Western blot analysis for determining the expression of p-mTOR, mTOR, p-PRAS40, PRAS40, and LC3 (n = 3) **(C)** Quantification of the ratio of LC3-II to LC3-I(***$p < 0.001$, ****$p < 0.0001$), **(D)** p-PRAS40 to PRAS40 (**$p < 0.01$, ***$p < 0.001$, ****$p < 0.0001$), and **(E)** p-mTOR to mTOR(***$p < 0.001$, ****$p < 0.0001$). The data are depicted as the mean ± SEM.

## 3.4 Palmatine can effectively repair motor function after SCI in rats

Furthermore, the *in vivo* assessment was carried out by categorizing rats into five groups (n = 8/group). Following SCI, the treatment groups were injected with palmatine (5, 10, and 20 μM concentrations) in the intrathecal space. The remaining two groups were the sham-operated and negative control groups injected with saline. For each group, BBB scoring was performed during the 7 days treatment period. This score is negatively correlated with the severity of SCI. As illustrated in Figure 5A, palmatine at the two higher doses substantially increased the BBB scores than the control group, indicating a significant improvement in SCI rats. Lastly, the tumor tissue was harvested, and LC3 was quantitated by immunohistochemical staining. The treatment group indicated significantly positive expression of LC3, which was dose-dependently increased after palmatine treatment (Figure 5B). These results indicated the palmatine screened from EXD acts by activating the autophagic flux and could be a potential alternative mechanism explaining EXD used for SCI treatment.

## 3.5 Palmatine activates autophagic flux in SCI cells model by PRAS40/mTOR pathway

To further verify whether palmatine regulates autophagy through the PRAS40/mTOR pathway, PC12 cells were co-incubated with MHY1485 (an agonist of mTOR) and palmatine after treating with $H_2O_2$. The sham group was PC12 cells treated with saline. The results showed that palmatine treatment significantly promoted autophagy in SCI cells (Figure 6B). However, activation of mTOR by MHY1485 attenuated the effect of palmatine. Phosphorylation of PRAS40 can be inhibited by palmatine, as well as decreased p-mTOR levels and increased LC3 levels in the palmatine group compared to the H2O2 group (Figures 6C, D). However, when mTOR is activated, the expression of LC3, which represents the level of autophagy, decreases, indicating that the promotion effect of palmatine on autophagy was reversed.

# 4 Discussion

This investigation aimed to screen PRAS40 binding metabolites from EXD and evaluate the metabolite's efficacy on functional repair after SCI. We first screened out the metabolites in EXD that are affinity with PRAS40 through ligand fishing and analyzed the kinetic parameters and mechanism of their binding to PRAS40 through ITC and molecular docking methods. Finally, we used BBB score, IHC, and WB to verify the effectiveness of the metabolites in treating SCI and it may regulate autophagy through the PRAS40/m-TOR pathway.

SCI refers to damage that causes temporary or permanent functional changes to the spinal cord. It is clinically characterized by high incidence, high cost, and high disability rates (Hu et al., 2023). Over the past few decades, researchers have adopted various strategies to reduce nerve damage and restore nerve function. Due to its long history and rich catalog of medical resources, TCM is also

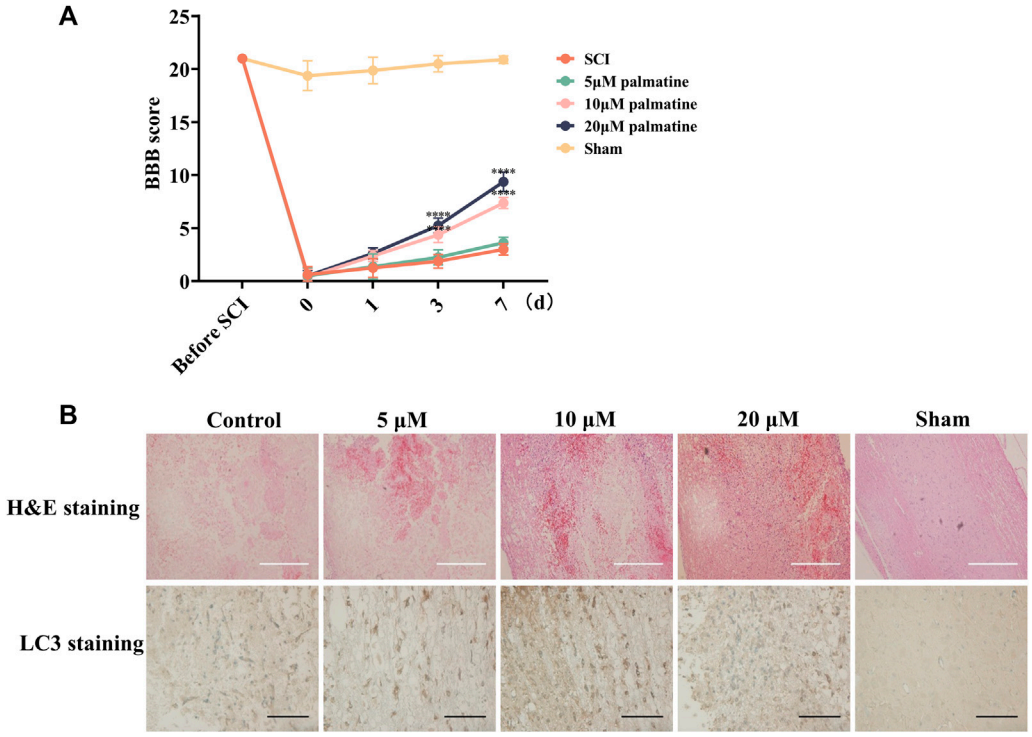


FIGURE 5
**(A)** Rats's BBB scores at different time points (n = 8) ****$p < 0.0001$. **(B)** H&E staining and Immunohistochemistry (IHC) staining using antibodies against LC3 in different groups (n = 3). White scale bar: 500 μm. Black scale bar: 100 μm.

considered to be an effective means of clinical treatment for SCI (Lu et al., 2020). Therefore, studying the impact of TCM and its active extracts on SCI will help advance the treatment of SCI and the development of new clinical drugs. EXD, a famous TCM for the menopausal syndrome, was first introduced by Zhang Bo-Na in the early 1950s (Li et al., 2007). Our previous research showed that EXD can reduce spinal cord edema and improve motor function in SCI rats, suggesting EXD has the potential to treat SCI. In this study, we used the metabolites screened in EXD to treat SCI and improve the motor function of rats with SCI. This further provides support for EXD to be used in the clinical treatment of SCI.

Ligand fishing strategy is a complex system screening strategy based on affinity chromatography theory and using target immobilization technology (Zhuo et al., 2016). Ligand fishing is widely used to screen active compounds in complex samples due to its advantages of rapid and convenient screening (de Moraes et al., 2019; Chen et al., 2022). Finding drug leads from natural products will help subsequent clinical treatments. This study screened PRAS40 inhibitors in EXD by immobilizing PRAS40 and identified six metabolites according to the increased relative concentration (Figure 1; Table 2). By exclusion and screening, palmatine and indole were selected. Their association was determined using ITC and molecular docking. Based on the association constants of palmatine and indole as 2.84 × 106M-1 and 3.82 × 105 M-1, respectively, palmatine is a promising anti-PRAS40 drug candidate for treating SCI (Figure 2; Table 3). And subsequent molecular docking also confirmed these results. Molecular docking results showed that the binding energy of PRAS40 to palmatine and indole was −5.06 and −4.24 kcal/mol, and palmatine interacts with more amino acid residues of PRAS40 in a more abundant binding interaction (Figure 3).

Palmatine, a naturally occurring isoquinoline alkaloid, is a yellow compound found in various Chinese medicines, including *Berberidaceae, Papaveraceae, Ranunculaceae, and Menispermaceae* (Tarabasz and Kukula-Koch, 2020). In Chinese pharmacopeia, palmatine is considered an antibacterial and anti-inflammatory drug mainly used clinically for gynecological inflammation, enteritis, respiratory and urinary tract infections, surgical infections, etc (Johnson-Ajinwo et al., 2019; Ekeuku et al., 2020; Liu et al., 2021). The effects of palmatine on the nervous system have received widespread attention in recent years. Palmatine could pass the blood-brain barrier, improve cognitive impairment in 5xFAD mice after intraperitoneal injection, and alleviate the cerebellum and hippocampus proteome (Kiris et al., 2023). The administration of palmatine could effectively decrease the levels of pro-inflammatory cytokines and increase the levels of anti-inflammatory cytokines in LPS-induced BV2 cells (Wang et al., 2022). This investigation showed that in the SCI cell model palmatine can inhibit the phosphorylation of PRAS40 and increase the expression of LC3, a representative protein of autophagy, and this process is drug concentration-dependent(Figures 4A–D). Furthermore, palmatine significantly improved the BBB scores of SCI rats (Figure 5A). IHC staining of the SCI rat model also indicated that palmatine could treat SCI by regulating autophagy flux (Figure 5B).

Autophagy is an important pathway to maintaining internal balance in organisms, and the inhibition of mTOR physiologically

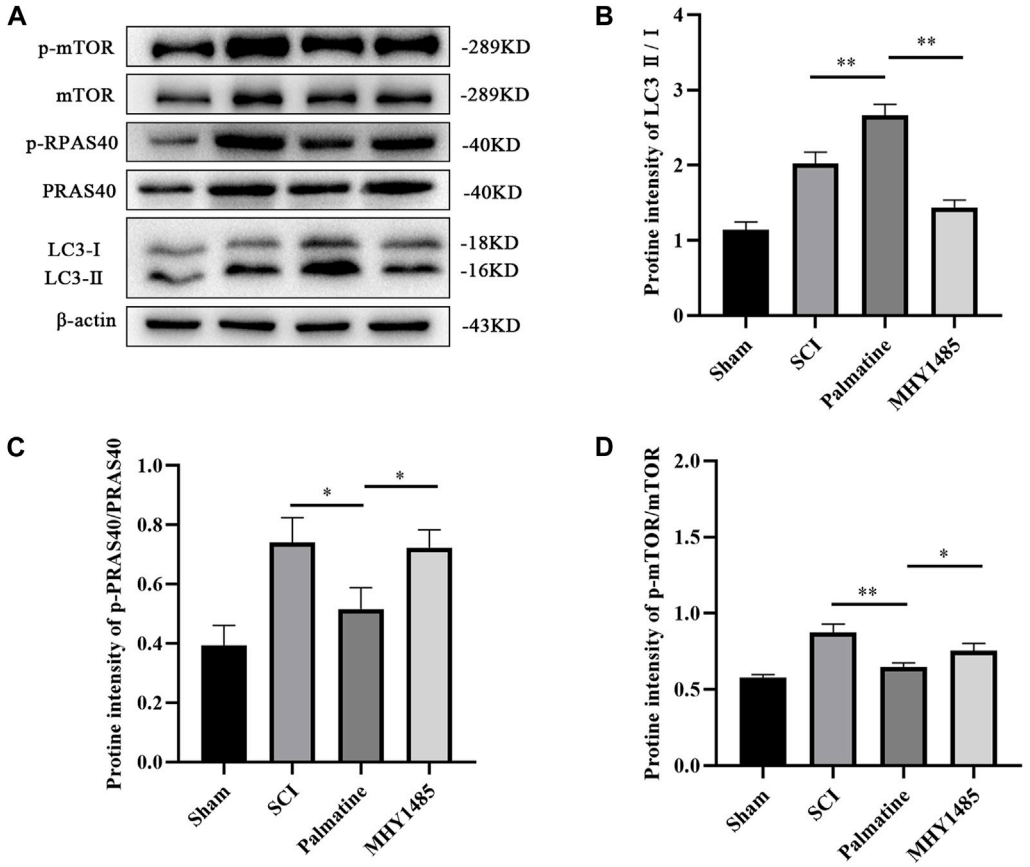


FIGURE 6
Palmatine activates autophagic flux by PRAS40/mTOR pathway. **(A)** Western blot analysis for determining the expression of p-mTOR, mTOR, p-PRAS40, PRAS40, and LC3 (n = 3) **(B)** Quantification of the ratio of LC3-II to LC3-I(**$p < 0.01$), **(C)** p-PRAS40 to PRAS40 (*$p < 0.01$), and **(D)** p-mTOR to mTOR(*$p < 0.01$, ****$p < 0.001$). The data are depicted as the mean ± SEM.

controls the initiation of the autophagy cascade (Klionsky et al., 2021). Currently, there are inhibitors targeting mTOR that regulate the autophagy process. However, these drugs' binding mode and mechanism of action to mTOR still need further study (Chen and Zhou, 2020). Furthermore, research has mainly focused on discovering mTOR ligands, while studies on other protein components that regulate the mTOR kinase domain are lacking. PRAS40 is an insulin-induced PKB/Akt substrate, also called "Akt1s1". Its phosphorylated protein was first observed in the HeLa cell's nuclear extracts (Beausoleil et al., 2004). PRAS40 is located on human chromosome 19q13.33, and its sequence is highly conserved among humans and other mammals (Macias et al., 2002; Wiza et al., 2012). Previous studies have shown that PRAS40 is a crucial inhibitory subunit of mTOR. It can suppress the mTOR kinase activity by binding to Raptor, a component of mTOR, thereby upregulating autophagy (Yamamura et al., 2022). The phosphorylation of PRAS40 leads to the separation of PRAS40 from mTORC1, which reduces the inhibition of mTORC1 (Zhou et al., 2021). In this study, we found that palmatine can regulate the expression of autophagy in SCI cell models. The activation of mTOR through MHY1485, which is an agonist of mTOR, proves that this process is achieved through the PRAS40/mTOR pathway (Figures 6A–D).

## 5 Limitations

However, there are several limitations. First, it was not determined whether other pathways are involved in the effects of palmatine on SCI. Second, The effectiveness and safety of palmatine in SCI treatment require further animal and clinical research support. Finally, The complexity of the EXD composition should be acknowledged, as different metabolites may have synergistic or antagonistic effects.

## 6 Conclusion

In summary, our study screened PRAS40 inhibitor palmatine from EXD. The *in vivo* and *in vitro* assays indicated that palmatine may treat SCI by regulating autophagy. We identified a novel mechanism that palmatine activates autophagy through the PRAS40/mTOR pathway, which also suggests that palmatine may be a new targeting mTOR inhibitor.

## Data availability statement

The raw data supporting the conclusion of this article will be made available by the authors, without undue reservation.

## Ethics statement

The animal study was approved by the Welfare and Ethics Committee of the Laboratory Animal Center of Air Force Military Medical University, China. The study was conducted in accordance with the local legislation and institutional requirements.

## Author contributions

LL: Conceptualization, Formal Analysis, Investigation, Methodology, Writing–original draft, Writing–review and editing. JY: Data curation, Investigation, Methodology, Writing–original draft. JS: Methodology, Software, Writing–original draft. JZ: Methodology, Software, Writing–original draft. BL: Funding acquisition, Project administration, Resources, Supervision, Writing–review and editing.

## Funding

The author(s) declare financial support was received for the research, authorship, and/or publication of this article. We acknowledge the financial support received from the National Natural Science Foundation of China (No. 82174166), Natural Science Basic Research Program of Shaanxi (No. 2023-JC-JQ-70), the Innovation Capability Support Program of Shaanxi (No. 2021TD-45), Program of Development and Innovation of Discipline to Tangdu Hospital (No. 2021LCYJ014).

## Conflict of interest

The authors declare that the research was conducted in the absence of any commercial or financial relationships that could be construed as a potential conflict of interest.

## Publisher's note



## References

Ahn, J. H., Lee, T. K., Kim, B., Lee, J. C., Tae, H. J., Cho, J. H., et al. (2020). Therapeutic hypothermia improves hind limb motor outcome and attenuates oxidative stress and neuronal damage in the lumbar spinal cord following cardiac arrest. *Antioxidants (Basel, Switz.* 9, 38. doi:10.3390/antiox9010038

Author anonymous (2016). Spinal cord injury (SCI) 2016 facts and figures at a glance. *J. spinal cord Med.* 39, 493–494. doi:10.1080/10790268.2016.1210925

Beausoleil, S. A., Jedrychowski, M., Schwartz, D., Elias, J. E., Villén, J., Li, J., et al. (2004). Large-scale characterization of HeLa cell nuclear phosphoproteins. *Proc. Natl. Acad. Sci. U. S. A.* 101, 12130–12135. doi:10.1073/pnas.0404720101

Chen, J. Y., Fu, E. J., Patel, P. R., Hostetler, A. J., Sawan, H. A., Moss, K. A., et al. (2021). Lentiviral interleukin-10 gene therapy preserves fine motor circuitry and function after a cervical spinal cord injury in male and female mice. *Neurother. J. Am. Soc. Exp. Neurother.* 18, 503–514. doi:10.1007/s13311-020-00946-y

Chen, Q., Zhou, W., Huang, Y., Tian, Y., Wong, S. Y., Lam, W. K., et al. (2022). Umbelliferone and scopoletin target tyrosine kinases on fibroblast-like synoviocytes to block NF-κB signaling to combat rheumatoid arthritis. *Front. Pharmacol.* 13, 946210. doi:10.3389/fphar.2022.946210

Chen, X., Li, H., Tian, L., Li, Q., Luo, J., and Zhang, Y. (2020). Analysis of the physicochemical properties of Acaricides based on lipinski's rule of five. *J. Comput. Biol. a J. Comput. Mol. cell Biol.* 27, 1397–1406. doi:10.1089/cmb.2019.0323

Chen, Y., and Zhou, X. (2020). Research progress of mTOR inhibitors. *Eur. J. Med. Chem.* 208, 112820. doi:10.1016/j.ejmech.2020.112820

de Moraes, M. C., Cardoso, C. L., and Cass, Q. B. (2019). Solid-supported proteins in the liquid chromatography domain to probe ligand-target interactions. *Front. Chem.* 7, 752. doi:10.3389/fchem.2019.00752

Ekeuku, S. O., Pang, K. L., and Chin, K. Y. (2020). Palmatine as an agent against metabolic syndrome and its related complications: a review. *Drug Des. Devel Ther.* 14, 4963–4974. doi:10.2147/DDDT.S280520

Greytak, A. B., Abiodun, S. L., Burrell, J. M., Cook, E. N., Jayaweera, N. P., Islam, M. M., et al. (2022). Thermodynamics of nanocrystal-ligand binding through isothermal titration calorimetry. *Chem. Commun. Camb. Engl.* 58, 13037–13058. doi:10.1039/d2cc05012a

Grigalunas, M., Burhop, A., Christoforow, A., and Waldmann, H. (2020). Pseudo-natural products and natural product-inspired methods in chemical biology and drug discovery. *Curr. Opin. Chem. Biol.* 56, 111–118. doi:10.1016/j.cbpa.2019.10.005

Hellenbrand, D. J., Quinn, C. M., Piper, Z. J., Morehouse, C. N., Fixel, J. A., and Hanna, A. S. (2021). Inflammation after spinal cord injury: a review of the critical timeline of signaling cues and cellular infiltration. *J. Neuroinflamm.* 18, 284. doi:10.1186/s12974-021-02337-2

Hou, Y., Luan, J., Huang, T., Deng, T., Li, X., Xiao, Z., et al. (2021). Tauroursodeoxycholic acid alleviates secondary injury in spinal cord injury mice by reducing oxidative stress, apoptosis, and inflammatory response. *J. Neuroinflammation* 18, 216. doi:10.1186/s12974-021-02248-2

Hu, X., Xu, W., Ren, Y., Wang, Z., He, X., Huang, R., et al. (2023). Spinal cord injury: molecular mechanisms and therapeutic interventions. *Signal Transduct. Target. Ther.* 8, 245. doi:10.1038/s41392-023-01477-6

Johnson-Ajinwo, O. R., Richardson, A., and Li, W. W. (2019). Palmatine from unexplored rutidea parviflora showed cytotoxicity and induction of apoptosis in human ovarian cancer cells. *Toxins* 11, 237. doi:10.3390/toxins11040237

Kiris, I., Kukula-Koch, W., Karayel-Basar, M., Gurel, B., Coskun, J., and Baykal, A. T. (2023). Proteomic alterations in the cerebellum and hippocampus in an Alzheimer's disease mouse model: alleviating effect of palmatine. *Biomed. Pharmacother.* 158, 114111. doi:10.1016/j.biopha.2022.114111

Klionsky, D. J., Petroni, G., Amaravadi, R. K., Baehrecke, E. H., Ballabio, A., Boya, P., et al. (2021). Autophagy in major human diseases. *Embo J.* 40, e108863. doi:10.15252/embj.2021108863

Ko, S. H., Apple, E. C., Liu, Z., and Chen, L. (2020). Age-dependent autophagy induction after injury promotes axon regeneration by limiting NOTCH. *Autophagy* 16, 2052–2068. doi:10.1080/15548627.2020.1713645

Kovacina, K. S., Park, G. Y., Bae, S. S., Guzzetta, A. W., Schaefer, E., Birnbaum, M. J., et al. (2003). Identification of a proline-rich Akt substrate as a 14-3-3 binding partner. *J. Biol. Chem.* 278, 10189–10194. doi:10.1074/jbc.M210837200

Li, E., Yan, R., Yan, K., Huang, R., Zhang, R., Wen, Y., et al. (2022). Erxian decoction inhibits apoptosis by activating Akt1 and repairs spinal cord injury in rats. *Heliyon* 8, e11279. doi:10.1016/j.heliyon.2022.e11279

Li, J. J., Li, J. T., and Fu, J. P. (2007). Erxian tang--introduction of a Chinese herbal formula, clinical practice, and experimental studies. *Chin. J. Integr. Med.* 13, 67–73. doi:10.1007/s11655-007-0067-z

Liu, C. S., Xia, T., Luo, Z. Y., Wu, Y. Y., Hu, Y. N., Chen, F. L., et al. (2021). Network pharmacology and pharmacokinetics integrated strategy to investigate the pharmacological mechanism of Xianglian pill on ulcerative colitis. *Phytomedicine Int. J. phytotherapy Phytopharm.* 82, 153458. doi:10.1016/j.phymed.2020.153458

Lu, Y., Yang, J., Wang, X., Ma, Z., Li, S., Liu, Z., et al. (2020). Research progress in use of traditional Chinese medicine for treatment of spinal cord injury. *Biomed. Pharmacother.* 127, 110136. doi:10.1016/j.biopha.2020.110136

Ma, X., Du, W., Wang, W., Luo, L., Huang, M., Wang, H., et al. (2020). Persistent Rheb-induced mTORC1 activation in spinal cord neurons induces hypersensitivity in neuropathic pain. *Cell Death Dis.* 11, 747. doi:10.1038/s41419-020-02966-0

Macias, M. J., Wiesner, S., and Sudol, M. (2002). WW and SH3 domains, two different scaffolds to recognize proline-rich ligands. *FEBS Lett.* 513, 30–37. doi:10.1016/s0014-5793(01)03290-2

Pinzi, L., and Rastelli, G. (2019). Molecular docking: shifting paradigms in drug discovery. *Int. J. Mol. Sci.* 20, 4331. doi:10.3390/ijms20184331

Rong, Y., Liu, W., Wang, J., Fan, J., Luo, Y., Li, L., et al. (2019). Neural stem cell-derived small extracellular vesicles attenuate apoptosis and neuroinflammation after traumatic spinal cord injury by activating autophagy. *Cell Death Dis.* 10, 340. doi:10.1038/s41419-019-1571-8

Szwed, A., Kim, E., and Jacinto, E. (2021). Regulation and metabolic functions of mTORC1 and mTORC2. *Physiol. Rev.* 101, 1371–1426. doi:10.1152/physrev.00026.2020

Tarabasz, D., and Kukula-Koch, W. (2020). Palmatine: a review of pharmacological properties and pharmacokinetics. *Phytotherapy Res. PTR* 34, 33–50. doi:10.1002/ptr.6504

Vargova, I., Machova Urdzikova, L., Karova, K., Smejkalova, B., Sursal, T., Cimermanova, V., et al. (2021). Involvement of mTOR pathways in recovery from spinal cord injury by modulation of autophagy and immune response. *Biomedicines* 9, 593. doi:10.3390/biomedicines9060593

Wang, C., Zhang, L., Ndong, J. C., Hettinghouse, A., Sun, G., Chen, C., et al. (2019). Progranulin deficiency exacerbates spinal cord injury by promoting neuroinflammation and cell apoptosis in mice. *J. Neuroinflammation* 16, 238. doi:10.1186/s12974-019-1630-1

Wang, L., Li, M., Zhu, C., Qin, A., Wang, J., and Wei, X. (2022). The protective effect of Palmatine on depressive like behavior by modulating microglia polarization in LPS-induced mice. *Neurochem. Res.* 47, 3178–3191. doi:10.1007/s11064-022-03672-3

Wiza, C., Nascimento, E. B., and Ouwens, D. M. (2012). Role of PRAS40 in Akt and mTOR signaling in health and disease. *Am. J. physiology. Endocrinol. metabolism* 302, E1453–E1460. doi:10.1152/ajpendo.00660.2011

Xu, S., Wang, J., Zhong, J., Shao, M., Jiang, J., Song, J., et al. (2021). CD73 alleviates GSDMD-mediated microglia pyroptosis in spinal cord injury through PI3K/AKT/Foxo1 signaling. *Clin. Transl. Med.* 11, e269. doi:10.1002/ctm2.269

Yamamura, J., Ma, S., Jia, H., and Kato, H. (2022). Activating transcription factor 4-dependent hsa-miR-663a transcription mediates mTORC1/p70S6K1 signaling underleucine deprivation. *Front. Nutr.* 9, 965771. doi:10.3389/fnut.2022.965771

Zhou, Q., Tang, S., Zhang, X., and Chen, L. (2021). Targeting PRAS40: a novel therapeutic strategy for human diseases. *J. drug Target.* 29, 703–715. doi:10.1080/1061186X.2021.1882470

Zhuo, R., Liu, H., Liu, N., and Wang, Y. (2016). Ligand fishing: a remarkable strategy for discovering bioactive compounds from complex mixture of natural products, *Mol. (Basel, Switz.* 21. doi:10.3390/molecules21111516

frontiers | Frontiers in Pharmacology

TYPE Review
PUBLISHED 08 February 2024
DOI 10.3389/fphar.2024.1348019



OPEN ACCESS

EDITED BY
Peng Sang,
Zhengzhou University, China

REVIEWED BY
Chao Lu,
Jinan University, China
Peng Teng,
Zhejiang University, China

*CORRESPONDENCE
Qin-Ming Yu,
yuqinming2023@126.com

RECEIVED 01 December 2023
ACCEPTED 29 January 2024
PUBLISHED 08 February 2024

CITATION
Yang Y-H, Li C-X, Zhang R-B, Shen Y, Xu X-J and Yu Q-M (2024), A review of the pharmacological action and mechanism of natural plant polysaccharides in depression. *Front. Pharmacol.* 15:1348019. doi: 10.3389/fphar.2024.1348019



# A review of the pharmacological action and mechanism of natural plant polysaccharides in depression

Yu-He Yang[1], Chen-Xue Li[2], Ruo-Bing Zhang[2], Ying Shen[1], Xue-Jiao Xu[1] and Qin-Ming Yu[1]*

[1]Heilongjiang University of Chinese Medicine, Harbin, China, [2]Harbin University of Commerce, Harbin, China

Depression is a prevalent mental disorder. However, clinical treatment options primarily based on chemical drugs have demonstrated varying degrees of adverse reactions and drug resistance, including somnolence, nausea, and cognitive impairment. Therefore, the development of novel antidepressant medications that effectively reduce suffering and side effects has become a prominent area of research. Polysaccharides are bioactive compounds extracted from natural plants that possess diverse pharmacological activities and medicinal values. It has been discovered that polysaccharides can effectively mitigate depression symptoms. This paper provides an overview of the pharmacological action and mechanisms, intervention approaches, and experimental models regarding the antidepressant effects of polysaccharides derived from various natural sources. Additionally, we summarize the roles and potential mechanisms through which these polysaccharides prevent depression by regulating neurotransmitters, HPA axis, neurotrophic factors, neuroinflammation, oxidative stress, tryptophan metabolism, and gut microbiota. Natural plant polysaccharides hold promise as adjunctive antidepressants for prevention, reduction, and treatment of depression by exerting their therapeutic effects through multiple pathways and targets. Therefore, this review aims to provide scientific evidence for developing polysaccharide resources as effective antidepressant drugs.

KEYWORDS

**polysaccharides, natural plant, depression, pharmacological action, mechanism**

## 1 Introduction

Depression, as a common mental disorder, seriously endangers human physical and mental health (Paykel, 2008). People with depression usually show symptoms such as lack of interest, slow thinking, low mood, loss of appetite, insomnia and sleeplessness, and decreased willpower (Thapar et al., 2022). With socio-economic development and incremental pressure on people, the number of people suffering from depression has increased dramatically, bringing serious costs to society and families. Because the severe illness is often accompanied by self-harm, suicidal tendencies and violent tendencies, making depression become the disease with the highest suicide rate in the world. At the same time, the disease can seriously affect or even damage the patient's digestive system, immune system, and nervous system (Fries et al., 2023). The pathogenesis of depression is complex (Guo et al., 2023), and its pathogenic mechanism is not yet clear. Existing studies

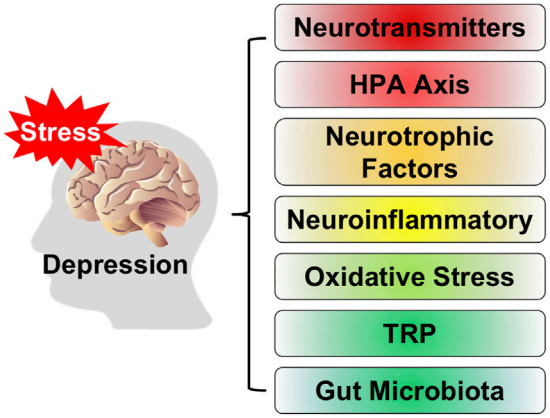


FIGURE 1
The pathogenesis of depression.

have shown that the main features of depression are abnormal neurotransmitter levels in patients, abnormal function of the hypothalamic-pituitary-adrenal (HPA) axis, hormonal imbalance in the organism with inflammation and oxidative stress, neurotrophic factors, tryptophan metabolism, and the occurrence of gut microbiota-related diseases, as shown in Figure 1.

At present, depression is mostly treated with chemical drugs, antipsychotic drugs, which can be divided into first- and second-generation drugs (Rybakowski, 2023). The first-generation drugs are mainly dopamine receptor blockers, which have antipsychotic effects by blocking dopamine receptors in the dopamine pathway of the central nervous system. And their long-term use can cause side effects such as drowsiness and cardiac rhythm disturbances. In response to the problems caused by the first-generation drugs, the second generation of drugs represented by fluoxetine and paroxetine combines therapeutic efficacy and low side effects, which improves depression and relieve anxiety though inhibiting the reuptake of 5-serotonin (5-HT) (Grinchii and Dremencov, 2020). 5-HT, as one of the indole derivatives, is a neurotransmitter with the effects on mood regulation, memory improvement and cognitive enhancement that exerts inhibitory effects in the neuroendocrine system, which is considered to be a messenger of pleasure (Moncrieff et al., 2022). The reduction of its levels is closely correlated with the occurrence of depression and anxiety. However, second-generation drugs tend to have slow onset of action, weak anxiolytic effects and are associated with prolonged cognitive impairment (Barbuti et al., 2023). While these drugs can relieve the symptoms of depression, there is currently no cure for depression. At the same time, antipsychotic drugs are limited by the fact that they can only act at one site or one type of target site. As a result, depression is characterized by low remission rate, high recurrence rate and significant side effects for patients, and only 12.7% of patients received minimal adequate treatment (Grinchii and Dremencov, 2020). Despite the clear target and rapid efficacy of Western clinical antidepressant drugs, they also have the disadvantages of low efficiency, single pathway, and serious adverse effects. Due to the complexity of the pathogenesis of depression, single-target drugs have limited amelioration of depression and serious side effects, the exploitation of new multi-target drugs for the treatment of depression is particularly important.

Therefore, the development of an antidepressant drug, with high efficiency, long-term use, and low side effects, has become a recent research hotspot. Polysaccharides from natural sources have received widespread attention due to their wide range of pharmacological activities and fewer side effects (Song et al., 2021). Polysaccharides are the biologically active macromolecules formed by monosaccharides linked by glycosidic bonds, which are formed by polyhydroxy polymers and their derivatives. They have widespread in natural products of higher plants, animals, microorganisms and algae. Numerous studies have shown that polysaccharides have anti-inflammatory, antioxidant, antiviral, immune regulation, hypoglycemic and hypolipidemic effects, and regulation of gut microbiota (Mu et al., 2021; Ji et al., 2023). Meanwhile, existing studies have demonstrated that the polysaccharide molecules in natural products can effectively alleviate depression, and their mechanism of action has attracted extensive attention from researchers (Yi et al., 2009; Song et al., 2022; Guo et al., 2023). The progress has been reported in the study of the multi-targeted therapeutic effects of polysaccharides in depression. Some researchers have pointed out that the mechanism is achieved through the modulation of brain function, biological and immune barriers. The polysaccharide molecules in natural products can usually be used in multiple targets with significant therapeutic effects and fewer side effects (Wang et al., 2022b). However, there are fewer reports on the relationship between polysaccharides and depression. This review summarizes the recent progress of research on the antidepressant effects of polysaccharides by intervening in different mechanisms in recent years, providing references for further research on the prevention, alleviation and treatment of depression and the development of therapeutic drugs.

## 2 Antidepressant mechanism of natural plant polysaccharides

Polysaccharides in natural plant sources alleviate depression by regulating the expression of neurotransmitters and their receptors, HPA axis, neurotrophic factors, neuroinflammatory, oxidative stress, tryptophan metabolism and gut microbiota. The various plant polysaccharides from different sources can induce antidepressant effects through diverse mechanisms of action, as summarized in Table 1.

### 2.1 Polysaccharides regulate the expression of neurotransmitters and their receptors

The mechanism of action underlying the majority of current antidepressants is predicated upon the hypothesis pertaining to the monoaminergic system. According to the hypothesis of the monoaminergic system, depression is characterized by a reduction in levels of 5-hydroxytryptamine, dopamine (DA), and norepinephrine (NE) within the central nervous system. The pathogenesis of depression is rooted in the dysregulation of 5-HT, DA, and NE neurotransmitter systems. The upregulation of

TABLE 1 Validation models, targeting mechanisms and intervention results of natural plant polysaccharides.

| Name | Polysaccharide source | Monosaccharides composition | Validation model | Administration | Target mechanism | Effect | Positive control | Ref. |
|---|---|---|---|---|---|---|---|---|
| PSP | *Polygonatum sibiricum* Red. | Ara: Glc: GlcA: Gal: GalA: Man: Rha: Rib = 13.7: 82.9: 3.7: 36.2: 4.3: 52.5: 3.3: 1.0 | CUMS-induced ICR mice; | 100–400 mg/kg | Target neurotransmitters; | ↑: 5-HT, DA, NE, ERK1/2, NF-κB, GFAP, Calpastatin, PTEN, SCOP, Nrf2 | Fluoxetine; | Shen et al., 2021 (2022), Wei et al. (2022) |
| | | | LPS and CUMS-induced C57BL/6 mice; | | Target HPA; | ↓: TNF-α, IL-10, TRP, 3-HK, CORT, Caspase-3, GluN2A, GluN2B, Calpain-1, NLRP3, ASC, Iba1, P-ERK, Caspase-1, Cleaved-caspase-1 | Calpeptin; | |
| | | | LPS-induced HT-22 cells; | | Target neuroinflammation; | | MCC | |
| | | | CUMS-induced BALB/c mice | | Target TRP metabolism; | | | |
| | | | | | Target gut microbiota | | | |
| YLSP | *Millettia pulchra* (Benth.) Kurz var. *Laxior* (Dunn) Z. Wei | Ara: Glc = 90.79%:9.21% | UCMS-induced KM mice | 150–600 mg/kg; 1,200 mg/kg | Target neurotransmitters; | ↑: NE, DA, 5-HT, cAMP, BDNF | Fluoxetine | Liang et al., 2010 (2012), Lu et al. (2013) |
| | | | | | Target NTF | | | |
| ASP | *Angelica sinensis* (Oliv.) Diels | NA | CUMS-induced C57BL/6 mice | 20 and 40 mg/kg | Target neurotransmitters | ↑: TPH1, 5-HT, DA, GABA/GLU | Fluoxetine | Ding et al. (2021) |
| SP | *Poria cocos* (Schw.) Wolf | NA | Ovariectomy and CUMS-induced Sprague-Dawley rats | 25, 50, and 100 mg/kg | Target neurotransmitters; | ↑: CREB, BDNF, GluR1, P-GluR1 | NA | Zhang et al. (2019), Zhou and Li (2020) |
| | | | | | Target neuroinflammation | | | |
| PCAP | *Poria cocos* (Schw.) Wolf | NA | CUMS-induced SD rats | 0.1, 0.3, and 0.5 g/kg/d | Target NTF; | ↑: BDNF, 5-HT, 5-HIAA, DA, NE, pro-caspase-1, pro-IL-1β, pro-IL-18 | Fluoxetine | Chen et al. (2021) |
| | | | | | Target neuroinflammation | ↓: GLU, IL-1β, IL-18, TNF-α, ASC, caspase-1, IL-1β, IL-18, NLRP3 | | |
| LNT | *Lentinus edodes* (Berk.) Sing. | NA | CUMS-induced KM mice | 2.5 and 5.0 mg/kg | Target oxidative | ↑: 5-HT1A, SOD | NA | Ma et al. (2015) |
| | | | | | | ↓: MDA, TNF-α, IL-6 | | |
| GLP | *Ganoderma lucidum* (Leyss.ex Fr.) Karst. | Rha: Xyl: Fru: Gal: Man: Glu = 0.793: 0.964: 2.944: 0.167: 0.384: 7.94 | CSDS-induced C57BL/6 mice | 1, 5, and 12.5 mg/kg/d | Target neurotransmitters; | ↓: IL-1β, TNF-α | Imipramine | Cai et al. (2017), Li et al. (2021) |
| | | | | | Target NTF; | ↑: IL-10, BDNF, GluA1 S845, GluA1, GluA2 | | |
| | | | | | Target neuroinflammation | | | |

(Continued on following page)





10.3389/fphar.2024.1348019

TABLE 1 (*Continued*) Validation models, targeting mechanisms and intervention results of natural plant polysaccharides.

| Name | Polysaccharide source | Monosaccharides composition | Validation model | Administration | Target mechanism | Effect | Positive control | Ref. |
|---|---|---|---|---|---|---|---|---|
| LBP | *Lycium barbarum* L. | Rha: Ara: Xyl: Man: Glc: Gal: GalA = 1: 8.34: 1.25: 1.26: 1.91: 7.05: 15.28 | PTSD-induced SD rats; | 25, 50, and 100 mg/kg/d for 3 weeks; | Target neurotransmitters; | ↓: NR2B-Ca MKII, serum CORT, LPO, Bcl-2, PARP | Paroxetine; | Chu, 2019; Zhao et al. (2019), Fu et al. (2021) |
| | | | AS-induced C57BL/6 mice; | 80 mg/kg/d for 4 weeks; | Target oxidative | | Amitriptyline | |
| | | | Reserpine-induced C57BL/6 mice | 5 mg/kg for 28 days | | | | |
| LLP | *Lilium lancifolium* Thunb. | Man: GlcA: NAG: Glc: Gal: Fuc = 1: 0.19: 0.32: 0.46: 0.57: 0.25 | CUMS-induced KM mice | 0.2 g/kg/d | Target neurotransmitters; | ↑: 5-HT, ADCY6, PKA, CREB-1, BDNF | Fluoxetine | Liu et al. (2022b) |
| | | | | | Target HPA; | ↓: ACTH, CORT | | |
| | | | | | Target NTF; | | | |
| APS | *Astragalus membranaceus* (Fisch.) Bge. var. *mongholicus* (Bge.) Hsiao | Man: Rha: GlcUA: GalUA: Glc: Gal = 29.12: 1.89: 4.00: 1.35 : 1: 81.97 | CUMS-induced KM mice; | 200 and 400 mg/kg/d for 4 weeks; | Target neurotransmitters; | ↑: ADCY6, PKA, CREB-1, BDNF, Nrf2, HO-1, SOD, CAT, GSH-Px | Fluoxetine | Wang et al., 2018 (2019a), Liu et al., 2019a (2022b), Su et al. (2021) |
| | | | CUMS-induced Wistar rats; | 0.2 g/kg/day | Target HPA; | ↓: MCAO, MDA; TNF-α, IL-1β, IL-6, NF-κB | | |
| | | | PSD-induced Wistar rats | | Target NTF; | | | |
| | | | | | Target neuroinflammation; | | | |
| | | | | | Target oxidative | | | |
| DOP | *Dendrobium officinale* Kimura et Migo | rhamnose, arabinose, fucose, mannose and glucose, and glycosidic | Ovariectomy and CUMS-induced KM mice; | 50, 150, 300, and 600 mg/kg | Target HPA; | ↓: BDNF–TrkB–CREB, CRH, ACTH, serum CORT | Fluoxetine | Yang et al. (2022), Zhang et al. (2022) |
| | | | CUMS-induced SD rats | | Target NTF; | | | |
| | | | | | Target gut microbiota | | | |
| GEP | *Gastrodia elata* Bl. | NA | LPS-induced C57BL/6 mice | 50, 100, and 200 mg/kg | Target neuroinflammation | ↓: TNF-α, IL-1β | Fluoxetine | Liu et al. (2021) |
| MCP | *Momordica charantia* L. | NA | CSDS-induced C57 mice | 100, 200, and 400 mg/kg/d | Target neuroinflammation | ↓: TNF-α, IL-6, IL-1β, JNK3, c-Jun, P-110β proteins, JNK3/PI3K/AKT | NA | Deng et al. (2019) |
| OP | *Abelmoschus esculentus* (L.) Moecnch | GalA, GlcA, Gal, Ara, Rha = 42.01%, 39.25%, 7.12%、5.51%, 6.11% | CUMS-induced C57BL/6 mice; | 30 μg | Target neuroinflammation; | ↓: TLR4/NF-κB, MAPKs, MAPKs, NO, TNF-α, IL-6, IL-1β | Isotype control antibodies or goat IgG | Brancato et al. (2013), Yan et al. (2020) |
| | | | LPS-induced BV2 cells | | Target gut microbiota | ↑: acetic acid, propionic acid, and butyric acid | | |

(Continued on following page)





10.3389/fphar.2024.1348019

TABLE 1 (*Continued*) Validation models, targeting mechanisms and intervention results of natural plant polysaccharides.

| Name | Polysaccharide source | Monosaccharides composition | Validation model | Administration | Target mechanism | Effect | Positive control | Ref. |
|---|---|---|---|---|---|---|---|---|
| LJP | *Lonicera japonica* Thunb. | GalA: Rha: Gal: Ara: Glc: Man = 8.7%: 8.2%: 16.2%: 19.5%: 26.9%: 20.5% | CUMS-induced KM mice | 100 mg/kg | Target neuroinflammation | ↓: NLRP3, IL-1β, caspase-1 | Fluoxetine | Liu et al. (2019b) |
| APSP | *Acanthopanax senticosus* (Rupr.etMaxim.) Harms | NA | CUMS-induced Wistar rats | 60, 120 mg/kg | Target neuroinflammation; | ↓: IL-1β, IL-6, TNF-α, MDA | Fluoxetine hydrochloride group | Ding et al. (2022) |
| | | | | | Target oxidative | ↑: CAT, SOD, p-PI3K, p-Akt, p-mTOR | | |
| GBP | *Ginkgo biloba* L. | mannose, rhamnose, glucuronic acid, galactose, arabinose | UCMS-induced BALB/c mice | 300 mg/kg | Target gut microbiota | ↑: 5-HT, DA, *Lactobacillus* | Paroxetine | Chen et al. (2019) |
| TG | *Cistanche tubulosa* (Schenk) Wight | NA | CUMS-induced SD rats | 0.26 g/kg | Target TRP metabolism; | ↑: TRP | Imipramine; | Fan et al. (2021) |
| | | | | | Target gut microbiota | ↓: KYN/TRP, IDO1 | Fluoxetine | |
| DPR | *Porphyra haitanensis* Chang et Zheng | NA | LPS-induced C57BL/6 mice | 100, 200, and 400 mg/kg | Target NTF | ↓: NF-κB/NLRP3,TNF-α, IL-6, IL-1β | Fluoxetine | Yi et al. (2021) |
| | | | | | | ↑: BDNF/TrkB/ERK/CREB | | |

Abbreviation: PSP, *Polygonatum sibiricum* polysaccharides; YLSP, *Yulangsan* polysaccharides; ASP, *Angelica sinensis* polysaccharides; SP, sulfated pachymaran; PCAP, *Poria cocos acidic* polysaccharides; LNT, Lentinan; GLP, *Ganoderma lucidum* polysaccharides; LBP, *Lycium barbarum* polysaccharides; LLP, *Lily* polysaccharides; APS, *Astragalus* polysaccharides; DOP, *Dendrobium officinale* polysaccharides; GEP, *Gastrodia elata* polysaccharides; MCP, *Momordica charantia* polysacDOPcharides; OP, Okra polysaccharides; LJP, *Lonicera japonica* polysaccharides; APSP, *Acanthopanax senticosus* polysaccharides; GBP, *Ginkgo biloba* polysaccharides; TG, Total glycosides; DPR, degraded porphyrin.





10.3389/fphar.2024.1348019

type A monoamine oxidase (MAOA) and the downregulation of serotonin (5-hydroxytryptamine, 5-HT) and NE levels in the brain are considered to be the primary etiological factors underlying depression. The MAOA enzyme is responsible for the breakdown of monoamine neurotransmitters, including 5-HT, NE, and DA. It significantly contributes to the pathogenesis, progression, and treatment of various neuropsychiatric conditions. Studies have demonstrated that DA, 5-HT, and other neurotransmitters are crucial in maintaining chemical homeostasis within the brain. An imbalance of these substances, whether it be an excess or deficiency of neurotransmitters, can result in abnormalities within the signaling system of the brain, ultimately leading to the onset and development of depression (Kim et al., 2019).

Serotonin, also known as 5-HT, is a monoamine neurotransmitter that accumulates in nerve endings through the action of the 5-hydroxytryptamine transporter (SERT). This transporter facilitates the uptake of 5-HT into the cytoplasm to replenish synaptic vesicles and terminate its extracellular effects. In addition to regulating behavioral, emotional, and memory processes in the human body, 5-HT also plays a crucial role in the treatment of various psychiatric and neurological disorders and is pivotal in understanding depression's pathogenesis and treatment. In addition, 5-HT exhibits a distinctive form of neuroplasticity that encompasses synaptic plasticity. It has been demonstrated that addressing the deficit in synaptic plasticity caused by neuronal atrophy and cell death can be beneficial in the treatment of depression (Popa et al., 2010). The substance NE is derived from adrenaline by removing the N-methyl group, and it plays a crucial role in regulating the functions of various internal organs, glands, and the immune system. Additionally, NE serves as a vital neurotransmitter within the central nervous system (CNS). NE neurons originate in the locus coeruleus (LC) of the brain and extend their axons through different regions such as the CNS cortex, hypothalamus, amygdala, cerebellum, and spinal cord to reach primary nerve centers or other neurons (Jovanovic et al., 2022). The serotonin and noradrenaline reuptake inhibitor (SNRI) functions as a modulator of NE neurotransmission, making it an effective first-line medication for depression treatment. Its antidepressant effect is attributed to its regulation of NE levels in the body. DA serves as the predominant catecholamine neurotransmitter in the brain and plays a crucial role in transmitting feelings of excitement and happiness, as well as being involved in learning and rewarding activities. It is closely associated with human eroticism and sensation, transmitting pleasure and excitement while participating in learning, motor function, and reward-related processes. Dopaminergic activity is regulated by the ventral inferior colliculus of the hippocampus and basolateral amygdala regions. Studies have demonstrated deficits within the dopaminergic system among patients with depression, suggesting that these deficiencies may originate from dysfunctions within their afferent circuits (Belujon and Grace, 2017). The existing body of evidence strongly indicates an association between dysfunction in the dopaminergic system and depression. The excitatory neurotransmitter glutamate (Glu), which is found in the central nervous system (CNS), functions as an amino acid neurotransmitter and interacts with both ionotropic and metabotropic receptors. The production of Glu in neurons occurs through glucose-derived intermediates of the tricarboxylic acid cycle and branched-chain amino acids. It is subsequently released at synapses in the brain, exerting short-term effects on postsynaptic excitability and longer-term effects on synaptic strength and neural plasticity. This process involves modulation of the second-messenger system, downstream effects on the activity of various membrane-bound receptors, nuclear gene expression, and translation. Abnormalities in the transmission of excitatory or inhibitory neurotransmitters and neuronal plasticity can result in dysfunctions in brain function, while altered levels of Glu and γ-aminobutyric acid (GABA) have been associated with dysfunction of neural networks. Clinical studies conducted on depression have also identified changes in the concentration and activity of Glu and GABA (Duman et al., 2019), suggesting that dysfunctions in excitatory and inhibitory neurotransmitter signaling mechanisms may play a significant role in depression. The findings of other studies have demonstrated that Glu neurotransmission plays a crucial role in the pathophysiology and therapeutic response to depression, leading to a reduction in depressive symptoms (Fond et al., 2014; Newport et al., 2015). The inhibitory neurotransmitter GABA is naturally present in the human nervous system, acting as a non-protein amino acid responsible for precise control and regulation of excitatory transmission. The neurotransmitter GABA is a significant target for 5-HT afferent fibers (Möhler, 2012), and its physiological effects encompass the modulation of synaptic transmission, facilitation of neuronal development, as well as prevention of insomnia and depression.

Currently, the primary focus of clinical depression treatment lies in targeting monoamine neurotransmitters. This is achieved by inhibiting monoamine oxidation and blocking the reuptake of 5-HT and NE, thereby increasing extracellular levels of 5-HT, DA, and NE throughout the brain. Consequently, there is an elevation in synaptic concentrations of these neurotransmitters which enhances excitatory potential transmission at neural synaptic endings to ameliorate depressive symptoms (Yang et al., 2021).

The *Polygonatum sibiricum* is a traditional medicinal and food plant, wherein the *Polygonatum sibiricum* polysaccharide (PSP) serves as one of its primary bioactive constituents. In the acute behavioral despair mouse depression model, PSP (100, 200, and 400 mg/kg) significantly reduced immobility time in tail-hanging and forced-swimming experiments. Moreover, the levels of 5-HT, DA, and NE in the cortex of mice were significantly elevated compared to those in the model group (Wei et al., 2022). In the lipopolysaccharide (LPS) depression mouse model and the chronic unpredictable stress (CUS)-induced depression mouse model, PSP were found to enhance depressive-like behavior in mice and significantly elevate hippocampal 5-HT levels (Shen et al., 2021; Shen et al., 2022). The aforementioned studies suggest that the antidepressant effects of PSP are associated with the modulation of monoamine neurotransmitters in the brain.

The *Yulangsan* polysaccharide (YLSP, 300 and 600 mg/kg) can also exert antidepressant effects by elevating the levels of 5-HT, DA, and NE in brain tissue (Liang et al., 2010). The *Angelica sinensis* polysaccharide (ASP), one of the primary active compounds derived from Angelica sinensis (Hou et al., 2021), has been found to significantly reduce the duration of forced swimming and immobility in mice with hanging tails at a dosage of 40 mg/kg (Ding et al., 2021). Moreover, it enhances sugar-water preference, increases the levels of DA and 5-HT in the hippocampus,

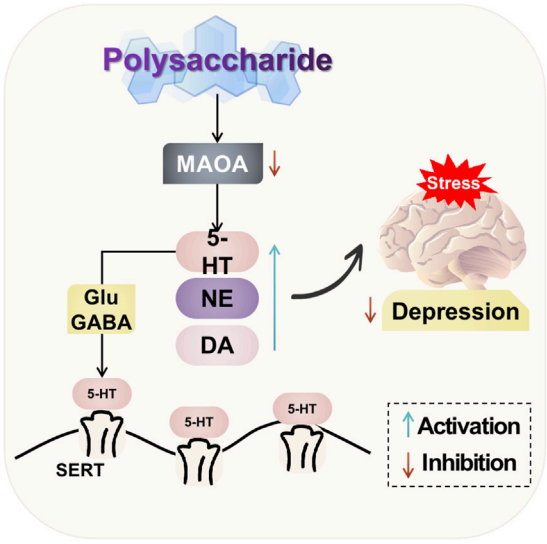


FIGURE 2
Possible antidepressant mechanism of polysaccharide targeted intervention in neurotransmitters and their receptors.

upregulates tryptophan hydroxylase mRNA expression, and elevates the GABA/Glu ratio-an essential rate-limiting enzyme involved in 5-HT synthesis, thereby regulating monoamine neurotransmitter transmission and rectifying excitatory-inhibitory imbalances in mice. The rat depression model was established by (Zhang et al., 2019) through ovarian removal combined with CUS, aiming to explore the correlation between the antidepressant effect of sulfated pachymaran (SP) and AMPA receptors (Zhang et al., 2019). The AMPA receptor, a type of Glu receptor primarily responsible for excitatory synaptic transmission in the brain, is closely associated with the pathogenesis of depression (Shirayama et al., 2022). The administration of SP (50 and 100 mg/kg) for 21 days was found to reduce hippocampal neuronal damage and increase the expression levels of both AMPA receptor Glu R1 and p-Glu R1. However, these anti-inflammatory effects and upregulation of AMPA receptors were completely inhibited by the AMPA receptor inhibitor GYKI52466. These findings suggest that the antidepressant effect of SP may be achieved through the regulation of AMPA receptor Glu R1 expression. *Ganoderma lucidum* polysaccharide (GLP, at doses of 1, 5, and 12.5 mg/kg) also increased the expression levels of p-Glu A1, Glu A1, and Glu A2 in the hippocampus of mice subjected to chronic social frustration stress (Li et al., 2021).

The N-methyl-D-aspartate receptor (NMDAR) is a specific receptor for glutamate, with NR2B being the most important functional subunit. Excessive stress can lead to increased glutamate release and overactivation of NMDAR, resulting in calcium influx and subsequent activation of intracellular signaling pathways that cause neuronal atrophy and death, ultimately leading to mood disorders and depression-like symptoms (Abdoulaye et al., 2021). The administration of *Lycium barbarum* polysaccharide (LBP, 25, 50, and 100 mg/kg) to rats for three consecutive weeks intragastrically was found to effectively inhibit the excessive activation of NR2B in the prefrontal cortex of rats, reduce the expression of calmodulin kinase II (CaMKII), a crucial downstream signaling molecule of NMDAR, and alleviate depressive-like behaviors in rats with PTSD (Chu, 2019).

The natural plant polysaccharides have the ability to modulate neurotransmitters in the brain. They can significantly enhance the levels of 5-HT, DA, and NE; mitigate hippocampal neuronal damage and regulate excitatory synaptic transmission in the brain; as well as exert antidepressant effects. Additionally, natural plant polysaccharides can inhibit excessive activation of NR2B in the prefrontal cortex of rats, reduce expression of the pivotal signaling molecule CaMKII downstream of NMDAR, and ameliorate depressive behaviors induced by post-traumatic stress disorder. The potential mechanism of polysaccharide-targeted intervention in depression through neurotransmitters and their receptors is illustrated in Figure 2.

## 2.2 Polysaccharides regulate the HPA axis

The hypothalamic-pituitary-adrenal (HPA) axis plays a crucial role in stress regulation and serves as a vital component of the neuroendocrine system, which is intricately associated with stress and stimulation (Van Den Eede and Claes, 2004; Mikulska et al., 2021). During prolonged stress and the stress response, corticosterone (CORT) levels remain elevated due to the loss of negative feedback regulation on corticotropin-releasing hormone (CRH) and adrenocorticotropic hormone (ACTH) (Song et al., 2021). This leads to hyperactivity of the HPA axis, increased release of CRH, stimulation of the pituitary gland to release ACTH, and disruption in the normal synthesis, release, and degradation of corticosterone by the adrenal cortex. Consequently, this imbalance results in damage to hippocampal neurons which can trigger or exacerbate depression. In a negative feedback loop, the HPA axis suppresses the feedback signals transmitted by cortisol to the hypothalamus and pituitary gland in order to decrease CRH and ACTH production, thereby regulating its own secretion level for stress response management (Chai et al., 2022). Therefore, implementing strategies to attenuate the release of CORT, CRH, and ACTH while promoting negative feedback regulation of the HPA axis represents efficacious approaches for decelerating the progression of depression.

The administration of Polygonatum sibiricum polysaccharide (PSP) significantly decreased CORT levels in LPS and chronic unpredictable mild stress (CUMS)-induced mice, thereby demonstrating the inhibition of hyperactivity in the HPA axis (Shen et al., 2021). The Lycium barbarum polysaccharide (LBP) significantly downregulated the expression of N-methyl-D-aspartate receptor 2B subunit (NR2B) and calmodulin kinase II (CaMKII) proteins, reduced serum CORT levels, and enhanced the negative feedback regulation of the HPA axis, thereby ameliorating depressive behaviors in rats with post-traumatic stress disorder (PTSD) (Chu, 2019). Liu et al. (2022) discovered that the administration of Lily polysaccharides (LLP), Astragalus polysaccharides (APS), and their combination to CUMS-induced mice for consecutive 28 d significantly ameliorated the depression-like behavior of CUMS mice. The polysaccharides mitigated the pathological damage of neuronal cells in the hippocampal CA1 region to varying extents, and markedly reduced plasma levels of ACTH and CORT. The combined administration of LLP

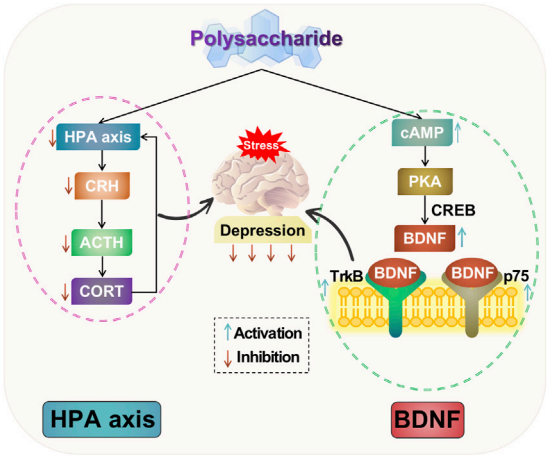


FIGURE 3
Possible antidepressant mechanism of polysaccharide targeted intervention in HPA axis and neurotrophic factors.

and APS exhibited a superior antidepressant effect compared to the individual administration of polysaccharides. The study conducted by Zhang et al. demonstrated that Dendrobium officinale polysaccharide (DOP) effectively reduced the elevated serum levels of CRH, ACTH, and CORT in depression model mice (Zhang et al., 2022). This suggests that DOP restores the HPA axis and mitigates the depressive effects induced by de-virginized and chronic mild stress-induced peri-menopausal syndrome model mice.

In summary, polysaccharides can ameliorate depressive-like behavior by inhibiting hyperactivity of the HPA axis. They have the ability to decrease levels of CRH, ACTH, and CORT, thereby facilitating negative feedback regulation of the HPA axis. Additionally, polysaccharides can mitigate hippocampal neuronal damage, suppress excessive activation of the HPA axis, exerting antidepressant effects. The potential mechanism of polysaccharide-targeted intervention in depression through HPA axis is illustrated in Figure 3.

## 2.3 Polysaccharides regulate the neurotrophic factors

Neurotrophic factors (NTF), also referred to as neurotrophic agents, are a class of substances that exert a supportive influence on neuronal survival and facilitate neuronal regeneration and functional recovery. They are widely employed in the clinical management of Alzheimer's disease, cerebral atrophy, Parkinson's disease, and other neurological disorders (Castrén et al., 2007; PehliVan Karakas et al., 2020). Brain-derived neurotrophic factors (BDNF), the most widely distributed neurotrophic factors in the CNS, plays important roles by activating both the prokinetic myosin-associated kinase (Trk) and p75 receptor. BDNF has become a representative factor in depression research. The blood of patients with persistent and recurrent depression, as well as animal models of depression, have been consistently found to exhibit reduced levels of NTF in numerous studies (Zhao et al., 2021; Zhuang et al., 2022; Joo et al., 2023). The conventional and rapid antidepressants not only rely on the expression of BDNF and its downstream signaling for their efficacy, but they also directly interact with the transmembrane structural domain of the TrkB dimer, leading to the stabilization of a multiprotein complex conformation that facilitates TrkB binding to BDNF. NTF can activate cell signaling pathways through Trk receptors, which in turn regulate various aspects of neuronal function such as cell fate determination, axon growth, dendritic growth and pruning (Dwivedi, 2009).

Neuroplasticity is modulated in individuals with depression, where the ratio of BDNF to pro-BDNF plays a essential role in synaptic plasticity (Vigna et al., 2019). The cyclic AMP (cAMP)/cAMP-response element binding protein (CREB)/BDNF pathway serves as an important antidepressant pathway, as well as a significant route and target for pharmacotherapy in depression. The cAMP/CREB/BDNF is a crucial signaling pathway in regulating hippocampal neuronal regeneration in depression (Yamada et al., 2003). The main mechanism of action of antidepressants is to enhance the concentration of cAMP, thereby inducing alterations in the cAMP signaling cascade and its downstream target, pCREB BDNF (Gao et al., 2022).

The antidepressant effects of *Yulangsan* polysaccharide (YLSP) have been demonstrated in animal models of "behavioral despair" (Liang et al., 2010), exerting a suppressive effect on depression through the upregulation of monoamine neurotransmitters, enhancement of prefrontal cortical adenylate cyclase activity, and increased hippocampal expression of BDNF (Liang et al., 2012). Lu et al. (2013) proposed that the neuroprotective effect of the YLSP group in a chronic stress depression model mice may be attributed to its ability to stimulate the expression of BDNF and its receptor TrkB, thereby activating neuronal protective signaling pathways and CREB activation, which inhibits neuronal death while promoting differentiation and regeneration. The acidic polysaccharides derived from *Poria cocos* were found to enhance the levels of BNDF, 5-HT, 5-HIAA, DA, and NE in the hippocampus while significantly reducing Glu levels. This suggests that these polysaccharides may exert antidepressant effects by modulating relevant trophic factors and neurotransmitters in depressed rats (Chen et al., 2021). Additionally, *Ganoderma lucidum* polysaccharides (GLP) were observed to elevate BDNF expression in the hippocampus of mice subjected to chronic social frustration stress (Li et al., 2021).

The bioactive polysaccharide degraded porphyrin (DPR), extracted from *Porphyra haitanensis*, was utilized by Yi et al. to reverse depressive-like behaviors in LPS-treated mice. This treatment activated the BDNF/TrkB/ERK/CREB signaling pathway in the hippocampus of CUMS mice, offering a potential therapeutic approach for depression (Yi et al., 2021). Yang et al. (2022) discovered that the alcohol-soluble polysaccharides present in *Dendrobium officinale* flowers exhibit additional protective effects against neuronal apoptosis and contribute to the maintenance of the 5-HT system by activating the BDNF/TrkB/CREB pathway. Liu et al. investigated the combined effects of *Lily* polysaccharide (LLP) and *Astragalus* polysaccharide (APS) in a specific ratio on depressive-like behaviors and their modulation of the adenylyl cyclase/cyclic adenosine monophosphate/protein kinase A (AC/cAMP/PKA) signaling pathway in mice subjected to chronic stress (Liu et al., 2022). The findings suggest a significant enhancement in the

antidepressant effect of LLP and APS following their combination, potentially through the modulation of brain 5-HT levels and suppression of HPA axis-induced stress, leading to activation of the AC/cAMP/PKA signaling pathway and upregulation of BDNF levels.

The studies suggest that depression induces neuronal atrophy and loss in limbic regions of the brain, such as the hippocampus, prefrontal lobe, and amygdala, along with a decrease in BDNF expression. Conversely, the administration of antidepressant drugs promotes adult hippocampal neurogenesis and an upregulation of BDNF expression. BDNF and relevant signaling pathways may exert antidepressant effects by modulating neuronal growth, differentiation, injury response, apoptosis, and regulating neuroendocrine networks. Therefore, investigating BDNF and relevant signaling pathway is crucial for studying the pathogenesis of depression. The potential mechanism of polysaccharide-targeted intervention in depression through neurotrophic factors is illustrated in Figure 3.

## 2.4 Polysaccharides regulate the neuroinflammatory

Neuroinflammation is an innate immune response of the nervous system that plays a pivotal role in the pathogenesis of numerous neuropsychiatric disorders (Troubat et al., 2021). Through extensive research on depression, it has been discovered that dysregulated secretion of inflammatory factors can contribute to its onset. The neuroinflammatory response assumes a critical role in mediating depression, as evidenced by elevated levels of pro-inflammatory cytokines within the central nervous system and aberrant activation of astrocytes and microglia (Benedetti et al., 2020). These findings suggest that neuroinflammation can either induce intracerebral lesions or be modulated for repairing intracerebral injuries.

Microglia are specialized cells of the central nervous system that exhibit macrophage-like properties, playing a crucial role in neuroinflammation. In response to stress, infection, trauma, or injury, microglia undergo phenotypic changes known as “microglial activation” and “microglial polarization,” which involve their conversion into pro-inflammatory (M1) and anti-inflammatory (M2) states (Orihuela et al., 2016; Feng et al., 2020; Zhou et al., 2020). The M1 phenotype of microglia is responsible for synthesizing and releasing various cytokines, including prostaglandin E2 (PGE2), CRP, and TNF-alpha, into the bloodstream (Attwells et al., 2020). Maintaining a balanced and stable state of M1/M2 microglia is crucial for normal immune function in the central nervous system. Evidence suggests that an increase in M1 microglia is associated with depression (Guo et al., 2020). The CUS activates microglia and induces depressive behaviors (Xiao et al., 2021), leading Yirmiya et al. to propose that depression can be characterized as “microgliosis” (Yirmiya et al., 2015). These studies indicate that the activation of microglia plays a significant role in the pathogenesis of depression.

Astrocytes and microglia play a crucial role in regulating inflammation within the nervous system through the secretion of various cytokines and inflammatory mediators, such as IL-1, TNF-α, and complement component 1q. The transcriptional responses of astrocytes are induced by the secretion of these molecules from microglia. Additionally, this release of inflammatory mediators leads to a decrease in phagocytosis activity and expression of neurotrophic factors (Linnerbauer et al., 2020). Animal experiments have demonstrated that inhibiting astrocyte activation can improve depressive symptoms (Wang et al., 2019b). However, there is currently limited research investigating the mechanisms underlying astrocyte action in neuroinflammation.

The nucleotide-binding oligomerization structural domain-like receptor protein 3 (NLRP3) inflammatory pathway plays a crucial role in the initiation and progression of depression (Bian et al., 2022). Activated NLRP3 inflammasomes cleave pro-IL-1β into active IL-1β, thereby triggering inflammation and concurrently promoting microglial activation while inhibiting hippocampal neurogenesis (Tastan et al., 2021).

Pro-inflammatory factors such as interleukin-1β (IL-1β), interleukin-6 (IL-6), and tumor necrosis factor-alpha (TNF-α) are regarded as depression biomarkers (Carniel and da Rocha, 2021). The excessive production of pro-inflammatory factors leads to neuronal damage, apoptosis, disruption in neurotransmitter transmission, activation of the HPA axis, alteration in related signaling pathways, and exacerbation of various subtypes of depression. These processes primarily involve the phosphatidylinositol-3-kinase/protein kinase B (PI3K/Akt), nuclear factor-kappa B (NF-kB), NLRP3/ASC/caspase-1, and mitogen-activated protein kinases (MAPKs) signaling pathways.

The *Acanthopanax senticosus* polysaccharides (APSP) demonstrated a reduction in the levels of pro-inflammatory factors IL-1β, IL-6, and TNF-α, while simultaneously increasing the expression of p-PI3K, p-Akt, and p-mTOR proteins induced by chronic mild agnostic stress stimuli in rats (Ding et al., 2022). These findings suggest that the antidepressant effects of spikenard polysaccharides are associated with their modulation of the PI3K/Akt/mTOR pathway and anti-inflammatory properties.

*Ganoderma lucidum* polysaccharides (GLP) significantly mitigated the downregulation of pro-inflammatory cytokines in BV-2 microglia induced by LPS or aβ, while promoting the expression of anti-inflammatory cytokines in both BV-2 and primary microglia (Cai et al., 2017). Furthermore, GLP attenuated inflammation-associated microglial migration, morphological alterations, and phagocytosis potential. Studies have demonstrated that GLP possesses a modulatory effect on LPS and aβ-induced neuroinflammation, suggesting its potential antidepressant effects through modulation of microglial inflammatory and behavioral responses to achieve neuroprotective functions. Other studies have confirmed that GLP possess the ability to alleviate depressive symptoms in mouse models, inhibit microglial activation, and promote astrocyte proliferation (Li et al., 2021). Additionally, it downregulates the expression of pro-inflammatory cytokines IL-1β and TNF-α in the hippocampus of mice while up-regulating the expression of anti-infective cytokines IL-10 and BDNF.

The expression levels of AMPA receptor GluR1 and p-GluR1 were significantly elevated by sulfated pachymaran (SP), whereas the anti-inflammatory and up-regulatory effects of SP on AMPA receptors were completely inhibited by the AMPA receptor inhibitor GYKI 52466 (Zhou and Li, 2020). These findings suggest that the antidepressant effect of SP may be achieved

through its anti-inflammatory properties and regulation of AMPA receptor GluR1 expression. *Poria cocos* acidic polysaccharides (PCAP) significantly reduced the mRNA and protein expression levels of NLRP3, ASC, caspase-1, IL-1β, and IL-18 in the prefrontal cortex of rats in a chronic unpredictable stress model (Chen et al., 2021). Conversely, they significantly increased the mRNA and protein expression levels of pro-caspase-1, pro-IL-1β, and pro-IL-18. These results indicate that PCAP may inhibit the NLRP3 inflammasome pathway and reverse serum levels of inflammatory factors by regulating associated mRNA and protein expression levels related to NLRP3.

*Gastrodia elata* polysaccharides (GEP) exhibited the ability to attenuate the relative mRNA expression of pro-inflammatory cytokines TNF-α and IL-1β in hippocampal tissues of depressed mice, thereby exerting a neuroprotective effect and ameliorating LPS-induced depressive-like behaviors in mice (Liu et al., 2021). *Momordica charantia* polysaccharides (MCP, 200 and 400 mg/kg) also decreased hippocampal levels of IL-1β, IL-6, and TNF-α, alleviating depressive behaviors in mice subjected to chronic social frustration stress (Deng et al., 2019). Additionally, MCP significantly upregulated PI3K activity and Akt phosphorylation in the hippocampus of depressed mice with chronic social frustration stress. Notably, partial inhibition of the antidepressant effects of MCP was observed upon treatment with LY294002, a PI3K inhibitor.

The intervention of *Astragalus* polysaccharide (APS) significantly reduced the levels of hippocampal TNF-α, IL-1β, and IL-6 in rats with CUS-induced depression (Wang et al., 2018; Wang et al., 2019a; Liu et al., 2019). Additionally, it also significantly decreased the levels of NF-κB p65, p-NF-κB p65, p-IκBα, and the DNA-binding activity of NF-κB p65. Notably, p65 is a subunit of NF-κB that plays a crucial role in this process. These findings suggest that the antidepressant effect of APS may be attributed to their ability to inhibit overactivation of NF-κB signaling pathway as well as regulate downstream inflammatory factors. APS intervention also effectively reduced the expression levels of hippocampal ERK1/2, JNK, and p38 along with their phosphorylated forms in LPS-induced depressed rats (Wang et al., 2018). Moreover, it significantly decreased the levels of downstream phosphorylated c-Fos and c-Jun compared to the model group. This indicates that APS can further suppress Activator Protein 1 (AP-1) by inhibiting MAPK signaling pathway to modulate inflammatory responses and thereby ameliorate depressive-like behaviors.

*Polygonatum sibiricum* polysaccharide (PSP) may exert antidepressant effects by inhibiting the activation of NF-κB expression and nuclear translocation in mouse models of depression induced by LPS and CUS (Shen et al., 2021; Shen et al., 2022). Additionally, PSP decreases the expression levels of pro-inflammatory factors IL-1β and TNF-α in hippocampal tissues. Endogenous ligands produced during brain injury activate Toll-like receptor 4 (TLR4), which in turn activates NF-κB through the MyD88-dependent signaling pathway, leading to the transcription of numerous pro-inflammatory factors (Brancato et al., 2013). PSP demonstrated inhibitory effects on the upregulation of NLRP3, ASC, caspase-1, cleaved-caspase-1, and IL-1β in LPS-induced depression model in mice (Shen et al., 2022). Additionally, they downregulated the expression of Iba-1 as a microglial activation marker and GFAP as an astrocyte activation marker, thereby suppressing the activation of microglia and astrocytes. Simultaneously, PSP exhibited potential to ameliorate depressive-like behavior by inhibiting ERK phosphorylation-mediated NF-κB activation and modulating inflammatory responses (Shen et al., 2021).

Yan et al. demonstrated that intervention with Okra polysaccharides (OP) from *Abelmoschus esculentus* (L.) Moecnch suppressed the expression of TLR4, MyD88, and nuclear translocation of NF-κB, suggesting that the TLR4/NF-κB pathway may be involved in the mechanism of action of OP in the brain (Yan et al., 2020). Furthermore, it has been shown that OP can significantly reduce inflammatory factor levels in mice with chronic unpredictable stress-induced depression and concurrently downregulate phosphorylated expression of ERK1/2, JNK, and p38. This suggests that OP may exert their antidepressant effects by modulating inflammatory responses through the MAPKs pathway.

Liu et al. demonstrated that *Lonicera japonica* polysaccharides (LJP) significantly ameliorated depression-like behavior in CUMS model mice (Liu et al., 2019). Furthermore, LJP upregulated the number of hippocampal metameres and protected their structure and arrangement from disruption. There was a significant reduction in the expression of proteins such as NLRP3, Caspase-1, and IL-1β upon treatment with LJP. These findings suggest that LJP may exert an antidepressant effect by inhibiting the NLRP3 inflammatory vesicle-mediated immune-inflammatory response.

In summary, natural plant polysaccharides can modulate the PI3K/AKT and NF-κB signaling pathways, thereby reducing the release of inflammatory factors and decreasing the downstream expression levels of inflammation-related proteins. Additionally, polysaccharides can attenuate the phosphorylated expression of ERK1/2, JNK, and p38 in the MAPKs family, thus influencing neuroinflammatory responses. Moreover, they can inhibit protein expression related to the NLRP3/ASC/caspase-1 signaling pathway, consequently impacting immune inflammation and exerting antidepressant effects. Therefore, polysaccharides play a crucial role in regulating inflammation and their ability to suppress inflammatory responses is an integral part of depression treatment. The potential mechanism of polysaccharide-targeted intervention in depression through neuroinflammatory is illustrated in Figure 4.

## 2.5 Polysaccharides regulate the oxidative stress

The "oxidative stress hypothesis of depression" posits that oxidative stress is accountable for the structural alterations in the brains of individuals with depression. Oxidative stress refers to an imbalance between the oxidizing and antioxidant effects within the body, leading to tissue damage. Elevated levels of oxidative stress result in an excess production of reactive oxygen radicals, known as reactive oxygen species (ROS), and reactive nitrogen radicals, referred to as reactive nitrogen species (RNS), which have potential neurotoxicity (Bhatt et al., 2020). The role of oxidative stress is pivotal in the pathological changes associated with stress-related diseases, and it constitutes a significant component in the pathogenesis of depression (Kim et al., 2016). Clinical studies investigating oxidative stress in depression have demonstrated

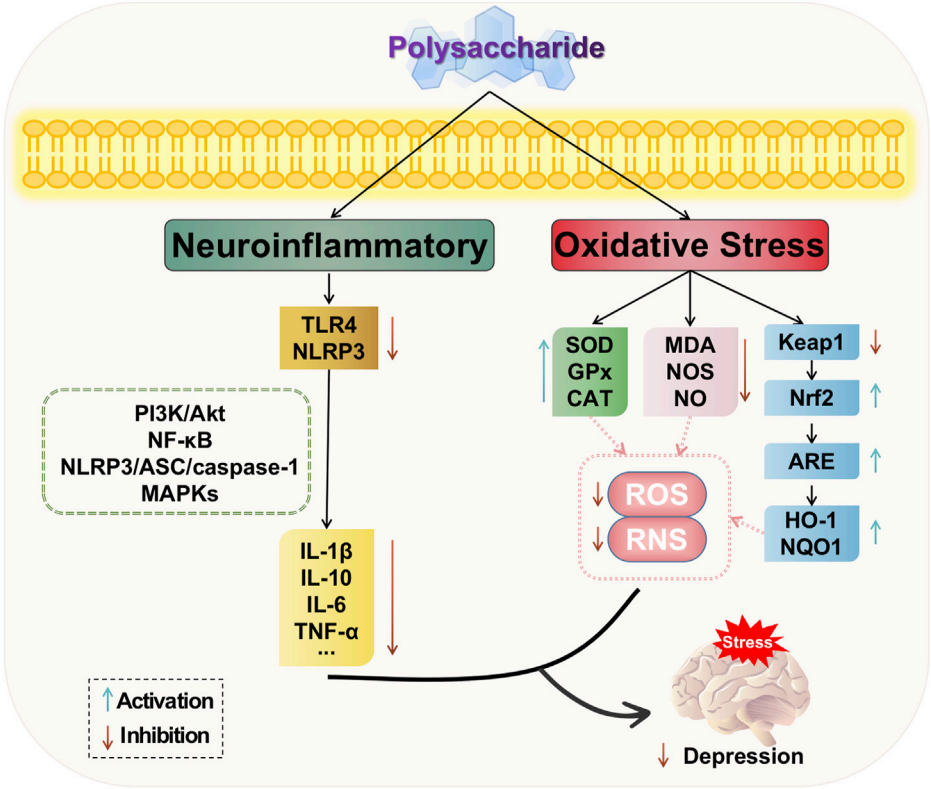


FIGURE 4
Possible antidepressant mechanism of polysaccharide targeted intervention in neuroinflammatory and oxidative stress.

that a key characteristic of oxidative stress in depression is the diminished antioxidant capacity and inadequate blood levels of antioxidant enzymes, such as superoxide dismutase (SOD), glutathione peroxidase (GPx), and catalase (CAT). Conversely, serum levels of lipid markers associated with oxidative stress are elevated, including reactive oxygen species (ROS) and nitrogen species (NS), such as malondialdehyde (MDA), Malondialdehyde (MDA), nitric oxide (NO) and nitric oxide synthase (NOS) (Moylan et al., 2014; Nobis et al., 2020; Manosso et al., 2022). Additionally, there is evidence of protein, DNA, and mitochondrial damage; along with secondary autoimmune responses targeting redox-modified nitrosylated proteins and oxidation-specific epitopes. Therefore, the reduction of oxidative stress damage through elevation of antioxidant levels such as SOD and GSH, along with inhibition of MDA production, contributes to alleviating depressive symptoms in PSD. Moreover, nuclear factor erythroid 2-related factor 2 (Nrf2), a transcription factor, emerges as a pivotal regulator of antioxidant signaling pathways and holds promise as a therapeutic target for depression (Bouvier et al., 2017; Zuo et al., 2022; Luo et al., 2023).

It has been observed that conventional pharmaceutical drugs exhibit limited efficacy in alleviating symptoms and may even induce severe adverse reactions in 30%–60% of patients (Liang et al., 2021). Medicinal plants and their bioactive constituents offer substantial health-promoting advantages, thereby warranting their utilization for the management of various ailments such as cancer, gastrointestinal disorders, and hepatic injury (Cheema and Singh, 2021; Khosravifarsani et al., 2022; Parganiha et al., 2022). Plant-derived polysaccharides represent crucial active components possessing anti-inflammatory, antioxidant, and immunomodulatory properties (Farahani et al., 2015; Wang et al., 2022a; Liaqat et al., 2022b), with notable evidence supporting their potential antidepressant effects.

In recent years, *Polygonatum sibiricum* has been utilized in various formulations for the treatment of depression with promising outcomes (Liu et al., 2022). It encompasses multiple bioactive constituents such as polysaccharides, steroidal saponins, and flavonoids. *Polygonatum sibiricum* polysaccharide (PSP) is a key constituent of PS and exhibits diverse biological activities including antitumor, antioxidant, anti-inflammatory, immunomodulatory effects, as well as regulation of blood glucose and lipids. Shen et al. discovered that the administration of PSP effectively reversed the alterations in reduced SOD levels and increased MDA levels induced by LPS-induced depression model in rats (Shen et al., 2021). PSP may exert its preventive effects on depressive-like behavior through the inhibition of reactive oxygen species (ROS), hyperfunctioning HPA axis, and ERK/NF-κB-mediated inflammatory response. Additionally, Shen et al. employed the LPS and CUMS-induced model to investigate the antidepressant effects of PSP and elucidate its underlying mechanism of action. Their findings revealed that PSP exerts its antidepressant properties by modulating the oxidative stress-calpain-1-NLRP3 signaling axis (Shen et al., 2022). These studies provide experimental foundation for the development of efficacious antidepressant medications.

The *Lycium barbarum* polysaccharide (LBP) is a bioactive compound derived from the *Lycium barbarum* L., which is widely used in traditional Chinese medicine. It possesses various pharmacological properties, including immunomodulatory and anti-aging effects (Xiao et al., 2022). Additionally, LBP exhibits neuroprotective properties that can be attributed to its antioxidant and anti-inflammatory activities (Zhu et al., 2015; Zhao et al., 2017). For instance, studies have demonstrated the protective effects of LBP in models of partial optic dissection injury and focal cerebral ischemic injury (Chu et al., 2013). Recent studies have indicated that LBP may possess therapeutic potential in the treatment of depression (Fu et al., 2021; Li et al., 2022). Zhao et al. conducted an assessment on the antidepressant activity of LBP in rifampicin-induced depressed mice, and proposed a possible mechanism of action whereby LBP attenuates the reduction in apoptosis inhibitors Bcl-2 and PARP by suppressing lipid peroxidation (LPO) production, subsequently leading to a decrease in apoptosis within striatal neurons (Zhao et al., 2019).

The authors hypothesized that *Astragalus* polysaccharide (APS) may exert protective and antidepressant effects on the hippocampus by inhibiting CMUS-induced oxidative stress, which is achieved through APS activation of the Nrf2-ARE pathway in depressed rats (Su et al., 2021). After the study, it was observed that APS intervention significantly upregulated hippocampal Nrf2 gene expression, total Nrf2 protein levels, and nuclear translocation in depressed rats. This finding suggests that APS enhances Nrf2 activation and its subsequent translocation to the nucleus, thereby promoting the antioxidative stress mechanism in rats. Furthermore, APS demonstrated regulatory effects on SOD, GSH-Px, CAT, HO-1 enzymes, indicating its ability to activate the Nrf2-ARE pathway in the hippocampus of depressed rats. Additionally, intervention with *Acanathopanax senticosus* polysaccharides significantly increased CAT and SOD activities while effectively reducing malondialdehyde (MDA) levels in rat hippocampal tissues [69]. The intervention of Lentinan (LNT, 2.5 and 5 mg/kg) also significantly enhanced the activity of superoxide dismutase (SOD) and reduced the levels of malondialdehyde (MDA) in the hippocampus of mice with chronic unpredictable stress-induced depression (Ma et al., 2015).

Based on the aforementioned studies, natural plant polysaccharides exert anti-oxidative stress effects by upregulating the levels of antioxidant enzymes such as superoxide dismutase (SOD), glutathione peroxidase (GSH-Px), and catalase (CAT), while downregulating the levels of malondialdehyde (MDA) as an oxidizing agent. Polysaccharides possess the ability to modulate the oxidative stress response in the depressed hippocampus through multiple pathways, with potential targets including Nrf2-related pathways for polysaccharide-based treatment of depression. The potential mechanism of polysaccharide-targeted intervention in depression through oxidative stress is illustrated in Figure 4.

## 2.6 Polysaccharides regulate the tryptophan metabolism

Tryptophan (TRP) is one of the essential amino acids in the human body and serves as a precursor to 5-HT. Being the sole "raw material" for 5-HT synthesis, it also plays a significant role in the development of depression. Tryptophan undergoes metabolism at three primary sites: the brain, intestine, and liver; among these, the colon stands out as the most crucial site for TRP absorption (O'Mahony et al., 2015; Comai et al., 2020). There are two primary metabolic pathways for tryptophan (Breda et al., 2016; Agus et al., 2018), namely the serotonin pathway and the kynurenine (KNY) pathway (KP). The former involves conversion of tryptophan to 5-HT by tryptophan hydroxylase (TPH), followed by metabolism to 5-hydroxyindoleacetic acid (5-HIAA) via monoamine oxidase in blood. The latter pathway entails generation of kynurenine from tryptophan through the action of indoleamine-2,3-dioxygenase (IDO) or tryptophan-2,3-dioxygenase (TDO). The conversion of tryptophan to kynurenine is catalyzed by the enzyme kynurenine-3-monooxygenase, resulting in the production of 3-hydroxykynurenine (3-HK), which has been implicated in oxidative stress and neurotoxicity. Only a small fraction, less than 5%, of tryptophan is converted to 5-HT, with the majority being metabolized through the KP—the primary route for tryptophan metabolism (Höglund et al., 2019). Studies have demonstrated that acute TRP depletion is associated with the emergence of depressive symptoms, potentially attributed to a significant reduction in 5-HT production (Chen et al., 2022). Simultaneously, an elevation in KYN, another metabolite of TRP, contributes to the development of depressive symptoms through immune dysregulation and induction of neuroinflammation (Schwarcz et al., 2012; Gong et al., 2023). It is evident that there exists a strong correlation between TRP metabolism and depression.

The regulation of key enzyme activities by natural plant polysaccharides can contribute to the modulation and equilibrium of metabolites with specific neuroactive properties, thereby promoting TRP metabolism to 5-HT while inhibiting TRP metabolism to 3-HK (Liaqat et al., 2022a).

Intervention with *Polygonatum sibiricum* polysaccharides (PSP) was found to downregulate TRP and 3-HK levels in the hippocampus of mice in a behavioral despair model (Wei et al., 2022). Furthermore, considering the concurrent increase in 5-HT levels, it is postulated that these polysaccharides may modulate TRP metabolism towards the TRP/5-HT pathway by enhancing TPH enzyme activity and inhibiting IDO enzyme activity. PSP may attenuate kynurenine metabolism and reduce downstream 3-HK levels, thereby exerting their antidepressant effects. The total glycosides (TG) of *Cistanche tubulosa* significantly elevate serum TRP levels in chronically unpredictable stressed rats ($p < 0.05$), while reducing the levels of serum KYN and KYN/TRP ratio ($p < 0.05$) (Fan et al., 2021). Simultaneously, they downregulate the expression of IDO protein in the colon and hippocampus of rats ($p < 0.05$). These findings suggest that these glycosides possess an inhibitory effect on TRP metabolism into KNY, thereby promoting increased conversion of TRP to serotonin and exerting an antidepressant effect. Chen et al. demonstrated the specific protective effect of Tongxieyaofang polysaccharide in mitigating TRP metabolism disorders induced by CUS (Chen et al., 2023). They observed that the administration of polysaccharide solution effectively suppressed the transcriptional activity of IDO1 in the colon, thereby preventing biased TRP metabolism towards the KP. This led to a reduction in serum KYN concentration and KYN/TRP ratio, ultimately resulting in decreased colonic 5-HT levels, increased hippocampal 5-HT levels, and alleviation of depressive symptoms.

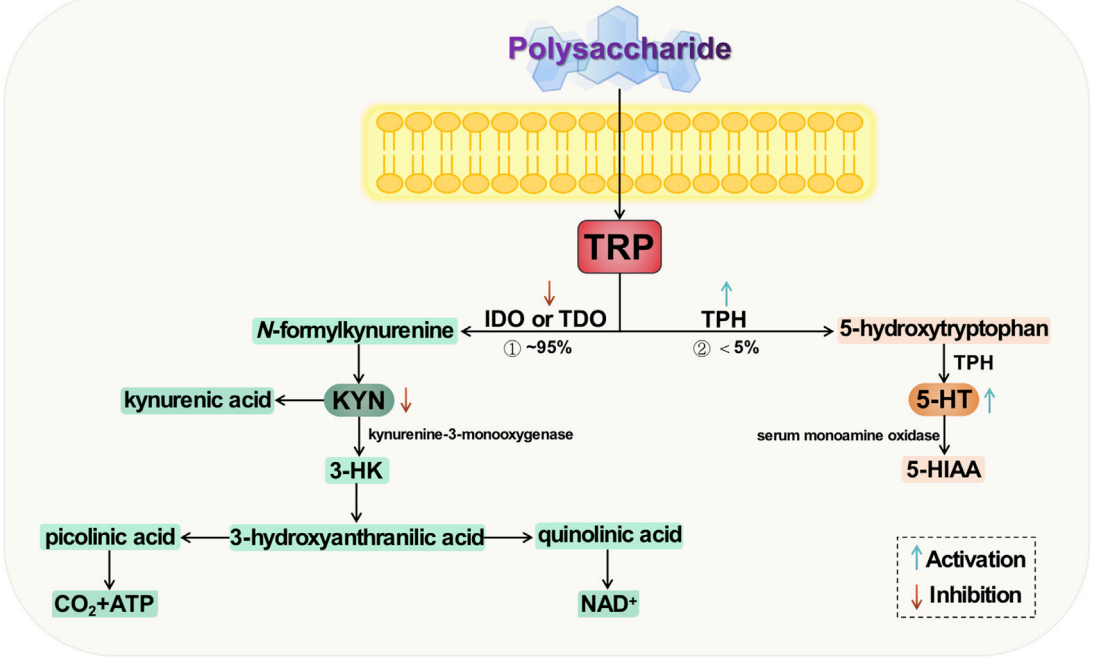


FIGURE 5
Possible antidepressant mechanism of polysaccharide targeted intervention in tryptophan metabolism.

Cheng et al. obtained Tiansi Liquid, formulated with *Morinda officinalis* How polysaccharides and *Cuscuta chinensis* polysaccharides in a 1:1 ratio. After conducting a preliminary investigation, Tiansi liquid exhibits certain effects on monoamine neurotransmission and neuronal morphology in brain tissue by inhibiting the activity of IDO and reducing the expression of its mRNA (Zhou et al., 2015). The activity of IDO is reduced, leading to a decrease in the expression of its mRNA. This results in IDO inhibition, which regulates the TRP/KYN pathway and subsequently impacts monoamine neurotransmitter transmission and neuron morphology in brain tissue, thereby exerting a certain antidepressant effect. Subsequently, the groups investigated the antidepressant mechanism of Tiansi liquid on a hydrocortisone-induced depression rat model (Cheng et al., 2018). The metabolomics results demonstrated that Tiansi liquid effectively downregulated TDO, IDO, and quinoline (QUIN) levels while simultaneously reducing the KYN/TRP ratio. It significantly increased kynurenic acid and 5-HT levels. These findings suggest that Tiansi liquid alleviates depressive symptoms in rats by modulating gut microbiota composition and metabolites within the TRP/KYN pathway.

Tryptophan metabolism is implicated in several hypotheses regarding the pathogenesis of depression. Firstly, under stress conditions, TRP conversion to 5-HT and KYN is affected, leading to decreased expression of TPH and insufficient production of 5-HT, resulting in a deficiency of monoamine transmitters. Secondly, excessive TRP to KYN conversion is closely associated with the body's inflammatory response and overexpression of IDO. Lastly, downstream products of KYN exert excitotoxic effects that can trigger apoptosis through activation of ionotropic glutamate receptors impacting neuroplasticity. The two key enzymes, TPH and IDO, exert control over the direction of TRP metabolism, which is a dynamic factor in depression and various other neuropsychiatric disorders. Consequently, these enzymes may emerge as potential targets for future research on natural plant polysaccharides intervention in depression. The potential mechanism of polysaccharide-targeted intervention in depression through tryptophan metabolism is illustrated in Figure 5.

## 2.7 Polysaccharides regulate the gut microbiota

The gut serves as a habitat for parasitic or commensal bacteria and plays a crucial role in maintaining the homeostasis of the internal milieu (Ji et al., 2020). The gut establishes a bidirectional regulatory mechanism with the brain through the mediation of gut microbiota, known as the microbiota-gut-brain axis (MGBA). This axis encompasses the central nervous system, enteric nervous system, autonomic nervous system, as well as neuroendocrine, enteroendocrine, and neuroimmune systems (Appleton, 2018). The gut microbiota is influenced by stress, leading to changes in its composition and diversity. Disruption of the gastrointestinal microbiota can activate the gut-brain axis, resulting in alterations in mental mood and depressive behaviors (Pferschy-Wenzig et al., 2022). The modulation of the gut-brain axis (MGBA) involves the integration of neural, hormonal, immune signals, and other factors between the gut and brain. This provides a potential pathway for the entry of gut microbiota and its metabolites into the brain. Consequently,

regulating MGBA has emerged as a promising approach for treating psychiatric disorders such as depression (Rathour et al., 2023).

The gut microbiota communicates with the brain by activating the HPA axis, altering neurotransmitters, producing microbial metabolites, influencing neurotrophic factors, modulating immune and inflammatory responses, and engaging vagus nerve pathways to regulate brain function and activity (Han et al., 2022). These interactions subsequently impact the pathogenesis of depression. Dysbiosis of the gut microbiota can lead to hyperactivity of the HPA axis, resulting in elevated levels of ACTH and CORT, as well as reduced BDNF. Conversely, nutritional therapy involving the administration of beneficial bacteria such as Bifidobacteria, *Lactobacillus*, and probiotics can attenuate HPA axis activity, restore normal ACTH, CORT, and BDNF levels, and exert an antidepressant effect (Sun et al., 2022). Dysbiosis of the gut microbiota also leads to dysfunction of specific cellular microbiota (such as enterochromaffin cells and *citrobacter*), thereby impacting the involvement of gut microbiota in the synthesis and secretion of key neurotransmitters and factors, including GABA, Glu, NE, 5-HT, and DA (Rajanala et al., 2021). These dysfunctions contribute to the development of depression. The metabolites produced by the gut microbiota, such as short-chain fatty acids (SCFAs), play a crucial role as signaling molecules that regulate the production of intestinal peptides through enteroendocrine cells (EECs) (Averina et al., 2020). These peptides are responsible for governing the gut-brain axis and stimulating the synthesis of gut-derived 5-HT by enterochromaffin cells (ECs), subsequently influencing hormone communication between the gut and brain (Eicher and Mohajeri, 2022). Thus, a healthy gut microbiota promotes brain development and regulation. Disrupted gut microbiota can impact the expression levels of BNDF, potentially leading to depression (Zhao et al., 2022). Therefore, the treatment of depression may involve regulating the balance of intestinal microbiota, modulating BDNF-related pathways, and promoting both BDNF secretion levels and gene expression. The communication between gut microbiota and the central nervous system (CNS) is facilitated by neuroactive substances produced by the former through the vagus nerve (Tan et al., 2022). Neurotoxic metabolites produced by gut microbiota can be transmitted to the central nervous system (CNS) through the vagus nerve, thereby influencing brain function and inducing depression. Disturbances in gut microbiota may result in the release of bacteria into the bloodstream, leading to excessive production of LPS, which causes oxidative stress and inflammatory responses. These processes can disrupt the blood-brain barrier, allowing inflammatory factors to enter the CNS and subsequently activate neuroglia through various signaling pathways such as NF-κB and cholinergic mechanisms, ultimately promoting the development of depression (Han et al., 2022).

A variety of herbal compounds, monotherapies, and their active ingredients have demonstrated remarkable efficacy in reducing depression symptoms with minimal side effects when utilizing traditional herbal treatments (Bi et al., 2022; Shao et al., 2022). Natural plant polysaccharides can effectively regulate gut microbiota disorders and intervene in the development of depression through MGBA. The intervention of natural plant polysaccharides to improve imbalances in gut microbiota provides a novel target for the prevention and treatment of depression (Sun et al., 2021).

Yan et al. discovered that Okra polysaccharides (OP) from *Abelmoschus esculentus* (L.) Moecnch exhibited significant improvements in depression-like behavior and alterations in the structure and abundance of gut microbiota within a depressed mouse model of CUMS (Yan et al., 2020). Specifically, at the phylum level, there was a notable reduction in the relative abundance of Bacteroidetes and Actinobacteria, accompanied by an increase in the relative abundance of Firmicutes. At the genus level, there was a significant decrease in the relative abundance of Barnesiella and *Bacteroides*, while *Lactobacillus* showed a substantial increase. The relative abundance of *Lactobacillus* was increased, while the levels of Barnesiella and *Bacteroides* were decreased by OP. The antidepressant effects mediated by gut microbiota were further elucidated through fecal microtransplantation technique (FMT). Furthermore, OP significantly reversed the reduction in acetic acid, propionic acid, and butyric acid levels, as well as the elevation in isovaleric acid level within the intestines of CUMS mice. These findings suggest that OP may exert their antidepressant effects by modulating both the composition of gut microbiota and the levels of various metabolites such as SCFAs. Chen et al. discovered that the administration of *Ginkgo biloba* polysaccharides (GBP, 300 mg/kg) for consecutive 28 days effectively mitigated the antidepressant effects induced by chronic stress in mice, while also exerting antidepressant effects through rectifying dysregulated gut homeostasis, elevating brain levels of 5-HT and DA, and enhancing the abundance of *Lactobacillus* in the intestine (Chen et al., 2019). The administration of Total *Cistanche* polysaccharides effectively mitigated the inflammatory response in the colon and ameliorated gut barrier disruption by modulating the dysbiosis of gut microbiota in rats subjected to chronic unpredictable stress, indicating that the antidepressant effect of *Cistanche* polysaccharides is also associated with their regulation on gut microbiota (Fan et al., 2021). The polysaccharides derived from *Polygonum sibiricum* exhibited the ability to suppress depression-like behavior in perimenopausal mice induced by ovariectomy plus chronic mild stress (Zhang et al., 2022). Additionally, they demonstrated the capacity to mitigate the inflammatory response via modulation of the MGBA and inhibit excessive activation of the HPA axis. Zhang and others discovered that *Polygonum sibiricum* polysaccharides (PSP) were capable of elevating serum levels of 5-HT and NE, reducing pro-inflammatory cytokine levels in the hippocampus, as well as inhibiting the PI3K/AKT/TLR4/NF-κB and ERK/CREB/BDNF pathways in mice with depression induced by CUMS (Zhang et al., 2023). The PSP compound exerts antidepressant-like behavior by modulating the MGBA axis.

Based on the aforementioned studies, it can be concluded that natural plant polysaccharides have a significant impact on regulating gut microbiota disorders, improving depressive symptoms through the MGBA axis, and playing a crucial role in modulating host-microbe crosstalk. Current research exploring the relationship between depression and various gut microbiota is still in its preliminary stage. The specific key microbiota responsible for depression has not been identified, leaving ample room for further investigation into utilizing gut microbiota regulation as a broader therapeutic approach to treating depression. Polysaccharide

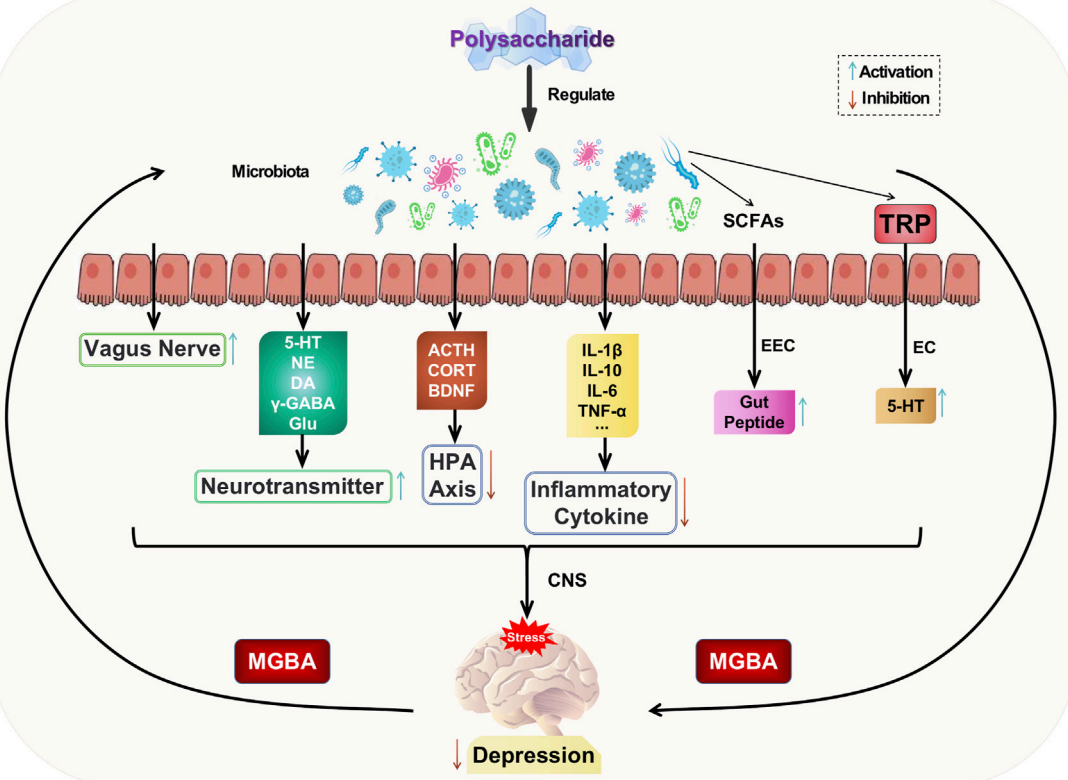


FIGURE 6
Possible antidepressant mechanism of polysaccharide targeted intervention in gut microbiota.

intervention aimed at ameliorating imbalances in gut microbiota offers a novel therapeutic strategy for both preventing and treating depression. The potential mechanism of polysaccharide-targeted intervention in depression through gut microbiota is illustrated in Figure 6.

## 3 Conclusion and prospects

Due to the intricate pathogenesis of depression, the current antidepressants exhibit limited efficacy and are associated with potential toxic side effects. Hence, there is an urgent need to develop drugs that can effectively prevent or treat depression while minimizing adverse reactions. Natural plants derived from diverse sources offer minimal harm to the human body and possess the advantage of being multi-targeted in their actions. Several traditional Chinese medicine polysaccharide drugs, such as *Astragalus* polysaccharide injection, Ginseng polysaccharide injection, and *Poria cocos* acidic polysaccharide oral solution, have been developed for clinical use due to their immunomodulatory effects in improving chemotherapy-induced immune deficiency among tumor patients. The discovery has revealed that natural plant polysaccharides possess the ability to exert antidepressant effects through the regulation of neurotransmitters and their receptors, modulation of the HPA axis, control of inflammatory responses, management of oxidative stress, modulation of neurotrophic factors, regulation of gut microbiota and tryptophan metabolism, as well as other pathways.

In the experimental investigation of natural plant polysaccharide antidepressants, researchers conducted studies using various stress models including chronic unpredictable mild stress, social isolation-induced stress, social defeat stress, post-traumatic stress disorder, and acute behavioral despair depression. It is important to note that many depressed patients also suffer from comorbid psychiatric disorders such as obsessive-compulsive disorder and anxiety disorder. Therefore, future studies should examine the efficacy of polysaccharides in comorbidity models with these factors and explore combination therapy to enhance or optimize depression treatment.

Currently, mice and rats are the most commonly utilized models for depression research and testing of potential depression protective agents. Rodent models offer significant advantages over other mammals due to their metabolic and disease characteristics that closely resemble those of humans. Additionally, their smaller size, docile temperament, and ease of husbandry make them highly suitable for experimental purposes. However, it is important to acknowledge that rodents differ from mammals in terms of brain and neural structural organization; therefore, future studies should pay more attention to the specificities associated with rodent models. The higher complexity of human thinking and emotions compared to other species, as well as the similarity between non-human primate brains and those of humans in comparison to rodents, necessitate further preclinical studies involving higher animals to validate the alleviating and therapeutic effects of polysaccharides on depression.

Ultimately, this will lead to real clinical trials involving human subjects.

Currently, numerous studies have substantiated the antidepressant effects of natural plant polysaccharides and elucidated their mechanisms of action from various perspectives. Furthermore, ongoing research continues to unveil additional insights into the antidepressant mechanisms of natural plant polysaccharides. As one of the primary bioactive constituents found in plants, natural plant polysaccharides exhibit a broad spectrum of biological activities. Therefore, conducting research on the antidepressant effects of natural plant polysaccharides holds immense significance for the development and utilization of natural plant-based polysaccharide antidepressant products.

Recently, there have been advancements in both preclinical and clinical research on the utilization of natural plant polysaccharides for depression treatment. A randomized, double-blind, placebo-controlled trial was conducted by experts to assess the effectiveness of LBP (*Lycium barbarum* polysaccharides, 300 mg/d for 6 weeks) in adolescents with subthreshold depression. The findings demonstrated that LBP effectively alleviated depressive symptoms such as cognitive impairments, retardation, and hopelessness in adolescents with subthreshold depression without any reported adverse events (Li et al., 2022). This experiment serves as a valuable point of reference for the application of natural plant polysaccharides at a human level. We eagerly anticipate further preclinical and clinical trials to validate the efficacy of natural plant polysaccharides in treating depression.

However, there are still numerous issues that require further exploration in the study of the antidepressant effects of natural plant polysaccharides. Firstly, the pathogenesis of depression is diverse and intricate, and natural plant polysaccharides predominantly exert their influence through multiple pathways, thereby rendering the mechanism behind their antidepressant properties even more complex. Although research on the antidepressant effect of polysaccharides has progressed from general observations to molecular-level investigations, our understanding of their signaling pathways and mechanisms remains insufficiently clear and comprehensive. Secondly, while cellular and animal studies on polysaccharides have increased significantly, clinical research in this area is relatively scarce. As research continues to advance, finding ways to extend the study of polysaccharide antidepressant effects to human subjects will remain a crucial point awaiting breakthroughs. Lastly, the physical properties, primary structure, advanced structure, and chemical modification of polysaccharides are closely linked to their biological activity; thus, investigating the conformational relationship between different natural plant polysaccharides with similar efficacy holds great significance for a thorough examination of their biological activity. However, research on the correlation between structure and antidepressant effects of natural plant polysaccharides is still in its early stages. With advancements in current technology for isolating and purifying polysaccharides as well as deepening studies into structural analysis over time, this may become a new avenue for future research on the antidepressant effects of natural plant polysaccharides.

Many active polysaccharides also play a significant role in the treatment of cardiovascular diseases in traditional Chinese medicine. However, most studies on the therapeutic potential of traditional Chinese medicine polysaccharides for depression are limited to animal and cellular models, which may not fully reflect their actual effects in humans. Currently, research on natural plant polysaccharides for depression treatment lacks depth and there is a scarcity of clinical trial studies, hindering widespread implementation in clinical settings and limiting their application within the field of medicine. The mechanism of action and signaling pathways of many natural plant polysaccharides for antidepressants remain unclear due to limitations in research methods, necessitating further investigation. Future studies should delve deeper into the mechanisms underlying natural plant polysaccharides' ability to improve depression, clarifying previously studied but ambiguous mechanisms as well as exploring unreported ones. Additionally, future research should focus on clinical applications of polysaccharides, addressing gaps in knowledge such as tissue distribution and target specificity while also gathering more clinical evidence.

In conclusion, due to their unique advantages, polysaccharides derived from natural resources offer potential for investigating the mechanism of depression and serve as a valuable reference for further research on natural plant polysaccharides. Moreover, this exploration may lay the foundation for clinical applications. Furthermore, the development of antidepressant polysaccharides with minimal adverse reactions and high efficacy holds promise in expanding treatment options for depression.

## Author contributions

Y-HY: Conceptualization, Writing–original draft. C-XL: Investigation, Visualization, Writing–original draft. R-BZ: Project administration, Writing–original draft. YS: Project administration, Writing–review and editing. X-JX: Writing–review and editing. Q-MY: Funding acquisition, Writing–review and editing.

## Funding

The author(s) declare financial support was received for the research, authorship, and/or publication of this article. This work was supported by Education Department of Heilongjiang Provincial Basic research expenses of undergraduate universities (No. 2023-KYYWF-1030), Traditional Chinese medicine research project of Heilongjiang Provincial Administration of Traditional Chinese medicine (No. ZHY2023-198), and Harbin University of Commerce doctoral research support program (No. 22BQ43).

## Acknowledgments

The authors would like to thank the reviewers and authors of all references.

## Conflict of interest

The authors declare that the research was conducted in the absence of any commercial or financial relationships that could be construed as a potential conflict of interest.

## Publisher's note



## References

Abdoulaye, I. A., Wu, S., Chibaatar, E., Yu, D., Le, K., Cao, X., et al. (2021). Ketamine induces lasting antidepressant effects by modulating the NMDAR/CaMKII-mediated synaptic plasticity of the hippocampal dentate gyrus in depressive stroke model. *Neural Plast.* 2021, e6635084. doi:10.1155/2021/6635084

Agus, A., Planchais, J., and Sokol, H. (2018). Gut microbiota regulation of tryptophan metabolism in health and disease. *Cell Host Microbe* 23, 716–724. doi:10.1016/j.chom.2018.05.003

Appleton, J. (2018). The gut-brain axis: influence of microbiota on mood and mental health. *Integr. Med. Clin. J.* 17, 28–32.

Attwells, S., Setiawan, E., Wilson, A. A., Rusjan, P. M., Miler, L., Xu, C., et al. (2020). Replicating predictive serum correlates of greater translocator protein distribution volume in brain. *Neuropsychopharmacology* 45, 925–931. doi:10.1038/s41386-019-0561-y

Averina, O. V., Zorkina, Y. A., Yunes, R. A., Kovtun, A. S., Ushakova, V. M., Morozova, A. Y., et al. (2020). Bacterial metabolites of human gut microbiota correlating with depression. *Int. J. Mol. Sci.* 21, 9234. doi:10.3390/ijms21239234

Barbuti, M., Menculini, G., Verdolini, N., Pacchiarotti, I., Kotzalidis, G. D., Tortorella, A., et al. (2023). A systematic review of manic/hypomanic and depressive switches in patients with bipolar disorder in naturalistic settings: the role of antidepressant and antipsychotic drugs. *Eur. Neuropsychopharmacol.* 73, 1–15. doi:10.1016/j.euroneuro.2023.04.013

Belujon, P., and Grace, A. A. (2017). Dopamine system dysregulation in major depressive disorders. *Int. J. Neuropsychopharmacol.* 20, 1036–1046. doi:10.1093/ijnp/pyx056

Benedetti, F., Aggio, V., Pratesi, M. L., Greco, G., and Furlan, R. (2020). Neuroinflammation in bipolar depression. *Front. Psychiatry* 11, 71. doi:10.3389/fpsyt.2020.00071

Bhatt, S., Nagappa, A. N., and Patil, C. R. (2020). Role of oxidative stress in depression. *Drug Discov. Today* 25, 1270–1276. doi:10.1016/j.drudis.2020.05.001

Bi, C., Guo, S., Hu, S., Chen, J., Ye, M., and Liu, Z. (2022). The microbiota–gut–brain axis and its modulation in the therapy of depression: comparison of efficacy of conventional drugs and traditional Chinese medicine approaches. *Pharmacol. Res.* 183, 106372. doi:10.1016/j.phrs.2022.106372

Bian, H., Yan, F., Li, W., Tu, W., and Ji, X. (2022). Tert-butylhydroquinone prevents neuroinflammation and relieves depression via regulation of NLRP3 signaling in mice. *Int. Immunopharmacol.* 107, 108723. doi:10.1016/j.intimp.2022.108723

Bouvier, E., Brouillard, F., Molet, J., Claverie, D., Cabungcal, J.-H., Cresto, N., et al. (2017). Nrf2-dependent persistent oxidative stress results in stress-induced vulnerability to depression. *Mol. Psychiatry* 22, 1701–1713. doi:10.1038/mp.2016.144

Brancato, S. K., Thomay, A. A., Daley, J. M., Crane, M. J., Reichner, J. S., Sabo, E., et al. (2013). Toll-like receptor 4 signaling regulates the acute local inflammatory response to injury and the fibrosis/neovascularization of sterile wounds. *Wound Repair Regen.* 21, 624–633. doi:10.1111/wrr.12061

Breda, C., Sathyasaikumar, K. V., Sograte Idrissi, S., Notarangelo, F. M., Estranero, J. G., Moore, G. G. L., et al. (2016). Tryptophan-2,3-dioxygenase (TDO) inhibition ameliorates neurodegeneration by modulation of kynurenine pathway metabolites. *Proc. Natl. Acad. Sci.* 113, 5435–5440. doi:10.1073/pnas.1604453113

Cai, Q., Li, Y., and Pei, G. (2017). Polysaccharides from *Ganoderma lucidum* attenuate microglia-mediated neuroinflammation and modulate microglial phagocytosis and behavioural response. *J. Neuroinflammation* 14, 63. doi:10.1186/s12974-017-0839-0

Carniel, B. P., and da Rocha, N. S. (2021). Brain-derived neurotrophic factor (BDNF) and inflammatory markers: perspectives for the management of depression. *Prog. Neuropsychopharmacol. Biol. Psychiatry* 108, 110151. doi:10.1016/j.pnpbp.2020.110151

Castrén, E., Võikar, V., and Rantamäki, T. (2007). Role of neurotrophic factors in depression. *Curr. Opin. Pharmacol.* 7, 18–21. doi:10.1016/j.coph.2006.08.009

Chai, Y., Li, Q., Wang, Y., Tao, E., and Asakawa, T. (2022). The value of HPA axis hormones as biomarkers for screening and early diagnosis of postpartum depression: updated information about methodology. *Front. Endocrinol.* 13, 916611. doi:10.3389/fendo.2022.916611

Cheema, H. S., and Singh, M. P. (2021). The use of medicinal plants in digestive system related disorders: a systematic review. *J. Ayurvedic Herb. Med.* 7, 182–187. doi:10.31254/jahm.2021.7303

Chen, G., Zhou, S., Chen, Q., Liu, M., Dong, M., Hou, J., et al. (2022). Tryptophan-5-HT pathway disorder was uncovered in the olfactory bulb of a depression mice model by metabolomic analysis. *Front. Mol. Neurosci.* 15, 965697. doi:10.3389/fnmol.2022.965697

Chen, H., Kan, Q., Zhao, L., Ye, G., He, X., Tang, H., et al. (2023). Prophylactic effect of Tongxieyaofang polysaccharide on depressive behavior in adolescent male mice with chronic unpredictable stress through the microbiome-gut-brain axis. *Biomed. Pharmacother.* 161, 114525. doi:10.1016/j.biopha.2023.114525

Chen, K., Chen, S., Ren, J., Lin, S., Xiao, M., Cheng, L., et al. (2021). Antidepressant effect of acidic polysaccharides from *Poria* and their regulation of neurotransmitters and NLRP3 pathway. *China J. Chin. Mat. Medica* 46, 5088–5095. doi:10.19540/j.cnki.cjcmm.20210610.705

Chen, P., Hei, M., Kong, L., Liu, Y., Yang, Y., Mu, H., et al. (2019). One water-soluble polysaccharide from *Ginkgo biloba* leaves with antidepressant activities *via* modulation of the gut microbiome. *Food Funct.* 10, 8161–8171. doi:10.1039/C9FO01178A

Cheng, D., Chang, H., Ma, S., Guo, J., She, G., Zhang, F., et al. (2018). Tiansi Liquid modulates gut microbiota composition and tryptophan–kynurenine metabolism in rats with hydrocortisone-induced depression. *Molecules* 23, 2832. doi:10.3390/molecules23112832

Chu, P. H. W., Li, H.-Y., Chin, M.-P., So, K., and Chan, H. H. L. (2013). Effect of *Lycium barbarum* (Wolfberry) polysaccharides on preserving retinal function after partial optic nerve transection. *PLOS ONE* 8, e81339. doi:10.1371/journal.pone.0081339

Chu, S. (2019). Protective effects of *Lycium barbarum* polysaccharide on depression rats with post-traumatic stress disorder. *Mod. Prev. Med.* 46, 2622–2637.

Comai, S., Bertazzo, A., Brughera, M., and Crotti, S. (2020). Tryptophan in health and disease. *Adv. Clin. Chem.* 95, 165–218. doi:10.1016/bs.acc.2019.08.005

Deng, Z., Yuan, C., Yang, J., Peng, Y., Wang, W., Wang, Y., et al. (2019). Behavioral defects induced by chronic social defeat stress are protected by *Momordica charantia* polysaccharides via attenuation of JNK3/PI3K/AKT neuroinflammatory pathway. *Ann. Transl. Med.* 7, 6. doi:10.21037/atm.2018.12.08

Ding, C., Xu, Y., and Ge, Y. (2021). Research on the mechanism and the effects of *Angelica* polysaccharide on the behavior of chronic stress depression mice. *West. J. Tradit. Chin. Med.* 34, 21–27. doi:10.12174/j.issn.2096-9600.2021.06.06

Ding, J., Jiang, C., Yang, L., and Wang, X. (2022). Ameliorative effect of *Acanathopanax senticosus* polysaccharides on depressive behavior in rats by regulating PI3K/Akt/mTOR pathway. *Sci. Technol. Food Ind.* 43, 369–375. doi:10.13386/j.issn1002-0306.2021090141

Duman, R. S., Sanacora, G., and Krystal, J. H. (2019). Altered connectivity in depression: GABA and glutamate neurotransmitter deficits and reversal by novel treatments. *Neuron* 102, 75–90. doi:10.1016/j.neuron.2019.03.013

Dwivedi, Y. (2009). Brain-derived neurotrophic factor: role in depression and suicide. *Neuropsychiatr. Dis. Treat.* 5, 433–449. doi:10.2147/ndt.s5700

Eicher, T. P., and Mohajeri, M. H. (2022). Overlapping mechanisms of action of brain-active bacteria and bacterial metabolites in the pathogenesis of common brain diseases. *Nutrients* 14, 2661. doi:10.3390/nu14132661

Fan, L., Peng, Y., Wang, J., Ma, P., Zhao, L., and Li, X. (2021). Total glycosides from stems of *Cistanche tubulosa* alleviate depression-like behaviors: bidirectional interaction of the phytochemicals and gut microbiota. *Phytomedicine* 83, 153471. doi:10.1016/j.phymed.2021.153471

Farahani, M. S., Bahramsoltani, R., Farzaei, M. H., Abdollahi, M., and Roja, R. (2015). Plant-derived natural medicines for the management of depression: an overview of mechanisms of action. *Rev. Neurosci.* 26, 305–321. doi:10.1515/revneuro-2014-0058

Feng, X., Fan, Y., and Chung, C. Y. (2020). Mefenamic acid can attenuate depressive symptoms by suppressing microglia activation induced upon chronic stress. *Brain Res.* 1740, 146846. doi:10.1016/j.brainres.2020.146846

Fond, G., Loundou, A., Rabu, C., Macgregor, A., Lançon, C., Brittner, M., et al. (2014). Ketamine administration in depressive disorders: a systematic review and meta-analysis. *Psychopharmacol. (Berl.)* 231, 3663–3676. doi:10.1007/s00213-014-3664-5

Fries, G. R., Saldana, V. A., Finnstein, J., and Rein, T. (2023). Molecular pathways of major depressive disorder converge on the synapse. *Mol. Psychiatry* 28, 284–297. doi:10.1038/s41380-022-01806-1

Fu, Y., Peng, Y., Huang, X., Yang, Y., Huang, L., Xi, Y., et al. (2021). *Lycium barbarum* polysaccharide-glycoprotein preventative treatment ameliorates aversive. *Neural Regen. Res.* 16, 543–549. doi:10.4103/1673-5374.293156

Gao, F., Yang, S., Wang, J., and Zhu, G. (2022). cAMP-PKA cascade: an outdated topic for depression? *Biomed. Pharmacother.* 150, 113030. doi:10.1016/j.biopha.2022.113030

Gong, X., Chang, R., Zou, J., Tan, S., and Huang, Z. (2023). The role and mechanism of tryptophan–kynurenine metabolic pathway in depression. *Rev. Neurosci.* 34, 313–324. doi:10.1515/revneuro-2022-0047

Grinchii, D., and Dremencov, E. (2020). Mechanism of action of atypical antipsychotic drugs in mood disorders. *Int. J. Mol. Sci.* 21, 9532. doi:10.3390/ijms21249532

Guo, X., Rao, Y., Mao, R., Cui, L., and Fang, Y. (2020). Common cellular and molecular mechanisms and interactions between microglial activation and aberrant neuroplasticity in depression. *Neuropharmacology* 181, 108336. doi:10.1016/j.neuropharm.2020.108336

Guo, Y., Chen, X., Gong, P., Li, Z., Wu, Y., Zhang, J., et al. (2023). Advances in the mechanisms of polysaccharides in alleviating depression and its complications. *Phytomedicine* 109, 154566. doi:10.1016/j.phymed.2022.154566

Han, W., Wang, N., Han, M., Ban, M., Sun, T., and Xu, J. (2022). Reviewing the role of gut microbiota in the pathogenesis of depression and exploring new therapeutic options. *Front. Neurosci.* 16, 1029495. doi:10.3389/fnins.2022.1029495

Höglund, E., Øverli, Ø., and Winberg, S. (2019). Tryptophan metabolic pathways and brain serotonergic activity: a comparative review. *Front. Endocrinol.* 10, 158. doi:10.3389/fendo.2019.00158

Hou, C., Yin, M., Lan, P., Wang, H., Nie, H., and Ji, X. (2021). Recent progress in the research of *Angelica sinensis* (Oliv.) Diels polysaccharides: extraction, purification, structure and bioactivities. *Chem. Biol. Technol. Agric.* 8, 13. doi:10.1186/s40538-021-00214-x

Ji, X., Guo, J., Cao, T., Zhang, T., Liu, Y., and Yan, Y. (2023). Review on mechanisms and structure-activity relationship of hypoglycemic effects of polysaccharides from natural resources. *Food Sci. Hum. Wellness* 12, 1969–1980. doi:10.1016/j.fshw.2023.03.017

Ji, X., Hou, C., Gao, Y., Xue, Y., Yan, Y., and Guo, X. (2020). Metagenomic analysis of gut microbiota modulatory effects of *Jujube* (Ziziphus jujuba Mill.) polysaccharides in a colorectal cancer mouse model. *Food Funct.* 11, 163–173. doi:10.1039/C9FO02171J

Joo, M.-K., Ma, X., Yoo, J.-W., Shin, Y.-J., Kim, H.-J., and Kim, D.-H. (2023). Patient-derived *Enterococcus mundtii* and its capsular polysaccharides cause depression through the downregulation of NF-κB-involved serotonin and BDNF expression. *Microbes Infect.* 25, 105116. doi:10.1016/j.micinf.2023.105116

Jovanovic, P., Wang, Y., Vit, J.-P., Novinbakht, E., Morones, N., Hogg, E., et al. (2022). Sustained chemogenetic activation of locus coeruleus norepinephrine neurons promotes dopaminergic neuron survival in synucleinopathy. *PLOS ONE* 17, e0263074. doi:10.1371/journal.pone.0263074

Khosravifarsani, M., Tolouian, R., Yadollahifarsani, S., Soleimani, P., Sarazen, M., Mostafizi, P., et al. (2022). Medical plants for lung cancer: an overview of current knowledge. *Immunopathol. Persa* 9, e38455. doi:10.34172/ipp.2022.38455

Kim, Y.-K., Na, K.-S., Myint, A.-M., and Leonard, B. E. (2016). The role of pro-inflammatory cytokines in neuroinflammation, neurogenesis and the neuroendocrine system in major depression. *Prog. Neuropsychopharmacol. Biol. Psychiatry* 64, 277–284. doi:10.1016/j.pnpbp.2015.06.008

Kim, Y.-S., O'Sullivan, D. M., and Shin, S.-K. (2019). Can 24 weeks strength training reduce feelings of depression and increase neurotransmitter in elderly females? *Exp. Gerontol.* 115, 62–68. doi:10.1016/j.exger.2018.11.009

Li, H., Xiao, Y., Han, L., Jia, Y., Luo, S., Zhang, D., et al. (2021). *Ganoderma lucidum* polysaccharides ameliorated depression-like behaviors in the chronic social defeat stress depression model via modulation of Dectin-1 and the innate immune system. *Brain Res. Bull.* 171, 16–24. doi:10.1016/j.brainresbull.2021.03.002

Li, X., Mo, X., Liu, T., Shao, R., Teopiz, K., McIntyre, R., et al. (2022). Efficacy of *Lycium barbarum* polysaccharide in adolescents with subthreshold depression: interim analysis of a randomized controlled study. *Neural Regen. Res.* 17, 1582–1587. doi:10.4103/1673-5374.330618

Liang, S., Huang, R., Lin, X., Huang, J., Huang, Z., and Liu, H. (2012). Effects of *Yulangsan* polysaccharide on monoamine neurotransmitters, adenylate cyclase activity and brain-derived neurotrophic factor expression in a mouse model of depression induced by unpredictable chronic mild stress. *Neural Regen. Res.* 7, 191–196. doi:10.3969/j.issn.1673-5374.2012.03.006

Liang, S., Wang, N., Huang, R., Tan, H., and Fu, S. (2010). Study on anti-depression effect of *Yulangsan* polysaccharides. *Lishizhen Med. Mat. Medica Res.* 21, 241–242.

Liang, X., Wang, X., Zhao, G., Huang, X., Xu, X., and Dong, W. (2021). Research progress of essential oil as a new complementary therapy in the treatment of depression. *Mini Rev. Med. Chem.* 21, 2276–2289. doi:10.2174/1389557521666210219161747

Liaqat, H., Parveen, A., and Kim, S. Y. (2022a). Neuroprotective natural products' regulatory effects on depression *via* gut–brain axis targeting tryptophan. *Nutrients* 14, 3270. doi:10.3390/nu14163270

Liaqat, H., Parveen, A., and Kim, S.-Y. (2022b). Antidepressive effect of natural products and their derivatives targeting BDNF-TrkB in gut–brain axis. *Int. J. Mol. Sci.* 23, 14968. doi:10.3390/ijms232314968

Linnerbauer, M., Wheeler, M. A., and Quintana, F. J. (2020). Astrocyte crosstalk in CNS inflammation. *Neuron* 108, 608–622. doi:10.1016/j.neuron.2020.08.012

Liu, D., Tang, W., Han, C., and Nie, S. (2022a). Advances in *Polygonatum sibiricum* polysaccharides: extraction, purification, structure, biosynthesis, and bioactivity. *Front. Nutr.* 9, 1074671. doi:10.3389/fnut.2022.1074671

Liu, J., Wang, Y., Zhao, H., Shen, Y., Wang, C., Li, S., et al. (2022b). Effect and mechanism of *Lily* polysaccharide combined with *Astragalus* polysaccharide on depressive behavior in chronic stress mice. *Chin. J. Exp. Tradit. Med. Formulae* 24, 62–70. doi:10.13422/j.cnki.syfjx.20220539

Liu, L., Liu, W., Fan, L., and Guo, L. (2019a). Effects of *Astragalus* polysaccharide on post-stroke depression in rats. *China Med. Her.* 16, 11–14.

Liu, M., Zhang, Y., Zhang, Y., Wang, G., and Zhou, B. (2021). Effects and potential mechanisms of *Gastrodia Elata* polysaccharides in LPS-induced depression model mice. *China Pharm.* 24, 2018–2023. doi:10.19962/j.cnki.issn1008-049X.2021.11.011

Liu, P., Bai, X., Zhang, T., Zhou, L., Li, J., and Zhang, L. (2019b). The protective effect of *Lonicera japonica* polysaccharide on mice with depression by inhibiting NLRP3 inflammasome. *Ann. Transl. Med.* 7, 811. doi:10.21037/atm.2019.12.64

Lu, Y., Huang, R., and He, P. (2013). Effects of *Yulangsan* polysaccharides on behavior, structure of hippocampus in mice with chronic stress-induced depression. *Chin. J. Exp. Tradit. Med. Formulae* 19, 220–223. doi:10.13422/j.cnki.syfjx.2013.01.068

Luo, J., Li, J., Shen, Z., Lin, X., Chen, A., Wang, Y., et al. (2023). Advances in health-promoting effects of natural polysaccharides: regulation on Nrf2 antioxidant pathway. *Front. Nutr.* 10, 1102146. doi:10.3389/fnut.2023.1102146

Ma, Q., Pu, Y., Yuan, W., Lv, L., Du, Z., and Li, W. (2015). Antidepressant effect of lentinan in chronically stressed mice and its possible mechanism. *Chin. J. Immunol.* 31, 329–333. doi:10.3969/j.issn.1000-484X.2015.03.009

Manosso, L. M., Camargo, A., Dafre, A. L., and Rodrigues, A. L. S. (2022). Vitamin E for the management of major depressive disorder: possible role of the anti-inflammatory and antioxidant systems. *Nutr. Neurosci.* 25, 1310–1324. doi:10.1080/1028415X.2020.1853417

Mikulska, J., Juszczyk, G., Gawrońska-Grzywacz, M., and Herbet, M. (2021). HPA axis in the pathomechanism of depression and schizophrenia: new therapeutic strategies based on its participation. *Brain Sci.* 11, 1298. doi:10.3390/brainsci11101298

Möhler, H. (2012). The GABA system in anxiety and depression and its therapeutic potential. *Neuropharmacology* 62, 42–53. doi:10.1016/j.neuropharm.2011.08.040

Moncrieff, J., Cooper, R. E., Stockmann, T., Amendola, S., Hengartner, M. P., and Horowitz, M. A. (2022). The serotonin theory of depression: a systematic umbrella review of the evidence. *Mol. Psychiatry.* 28, 3243–3256. doi:10.1038/s41380-022-01661-0

Moylan, S., Berk, M., Dean, O. M., Samuni, Y., Williams, L. J., O'Neil, A., et al. (2014). Oxidative & nitrosative stress in depression: why so much stress? *Neurosci. Biobehav. Rev.* 45, 46–62. doi:10.1016/j.neubiorev.2014.05.007

Mu, S., Yang, W., and Huang, G. (2021). Antioxidant activities and mechanisms of polysaccharides. *Chem. Biol. Drug Des.* 97, 628–632. doi:10.1111/cbdd.13798

Newport, D. J., Carpenter, L. L., McDonald, W. M., Potash, J. B., Tohen, M., Nemeroff, C. B., et al. (2015). Ketamine and other NMDA antagonists: early clinical trials and possible mechanisms in depression. *Am. J. Psychiatry* 172, 950–966. doi:10.1176/appi.ajp.2015.15040465

Nobis, A., Zalewski, D., and Waszkiewicz, N. (2020). Peripheral markers of depression. *J. Clin. Med.* 9, 3793. doi:10.3390/jcm9123793

O'Mahony, S. M., Clarke, G., Borre, Y. E., Dinan, T. G., and Cryan, J. F. (2015). Serotonin, tryptophan metabolism and the brain-gut-microbiome axis. *Behav. Brain Res.* 277, 32–48. doi:10.1016/j.bbr.2014.07.027

Orihuela, R., McPherson, C. A., and Harry, G. J. (2016). Microglial M1/M2 polarization and metabolic states. *Br. J. Pharmacol.* 173, 649–665. doi:10.1111/bph.13139

Parganiha, R., Tripathi, A., Prathyusha, S., Baghel, P., Lanjhiyana, S., Lanjhiyana, S., et al. (2022). A review of plants for hepatic disorders. *J. Complement. Med. Res.* 13, 46. doi:10.5455/jcmr.2022.13.04.10

Paykel, E. S. (2008). Basic concepts of depression. *Dialogues Clin. Neurosci.* 10, 279–289. doi:10.31887/DCNS.2008.10.3/espaykel

PehliVan Karakas, F., Coşkun, H., Soytürk, H., and Bozat, B. G. (2020). Anxiolytic, antioxidant, and neuroprotective effects of goji berry polysaccharides in ovariectomized rats: experimental evidence from behavioral, biochemical, and immunohistochemical analyses. *Turk. J. Biol.* 44, 238–251. doi:10.3906/biy-2003-8

Pferschy-Wenzig, E.-M., Pausan, M. R., Ardjomand-Woelkart, K., Röck, S., Ammar, R. M., Kelber, O., et al. (2022). Medicinal plants and their impact on the gut microbiome in mental health: a systematic review. *Nutrients* 14, 2111. doi:10.3390/nu14102111

Popa, D., Cerdan, J., Repérant, C., Guiard, B. P., Guilloux, J.-P., David, D. J., et al. (2010). A longitudinal study of 5-HT outflow during chronic fluoxetine treatment using a new technique of chronic microdialysis in a highly emotional mouse strain. *Eur. J. Pharmacol.* 628, 83–90. doi:10.1016/j.ejphar.2009.11.037

Rajanala, K., Kumar, N., and Chamallamudi, M. R. (2021). Modulation of gut-brain axis by probiotics: a promising anti-depressant approach. *Curr. Neuropharmacol.* 19, 990–1006. doi:10.2174/1570159X19666201215142520

Rathour, D., Shah, S., Khan, S., Singh, P. K., Srivastava, S., Singh, S. B., et al. (2023). Role of gut microbiota in depression: understanding molecular pathways, recent research, and future direction. *Behav. Brain Res.* 436, 114081. doi:10.1016/j.bbr.2022.114081

Rybakowski, J. K. (2023). Application of antipsychotic drugs in mood disorders. *Brain Sci.* 13, 414. doi:10.3390/brainsci13030414

Schwarcz, R., Bruno, J. P., Muchowski, P. J., and Wu, H.-Q. (2012). Kynurenines in the mammalian brain: when physiology meets pathology. *Nat. Rev. Neurosci.* 13, 465–477. doi:10.1038/nrn3257

Shao, J., Wei, Y., and Wei, X. (2022). A comprehensive review on bioavailability, safety and antidepressant potential of natural bioactive components from tea. *Food Res. Int.* 158, 111540. doi:10.1016/j.foodres.2022.111540

Shen, F., Song, Z., Xie, P., Li, L., Wang, B., Peng, D., et al. (2021). *Polygonatum sibiricum* polysaccharide prevents depression-like behaviors by reducing oxidative stress, inflammation, and cellular and synaptic damage. *J. Ethnopharmacol.* 275, 114164. doi:10.1016/j.jep.2021.114164

Shen, F., Xie, P., Li, C., Bian, Z., Wang, X., Peng, D., et al. (2022). Polysaccharides from *Polygonatum cyrtonema* Hua reduce depression-like behavior in mice by inhibiting oxidative stress-calpain-1-NLRP3 signaling axis. *Oxid. Med. Cell. Longev.* 2022, 2566917–17. doi:10.1155/2022/2566917

Shirayama, Y., Iwata, M., Fujita, Y., Oda, Y., and Hashimoto, K. (2022). The Toll-like receptor 4 antagonist TAK-242 induces antidepressant-like effects in a rat learned helplessness model of depression through BDNF-TrkB signaling and AMPA receptor activation. *Behav. Brain Res.* 423, 113769. doi:10.1016/j.bbr.2022.113769

Song, L., Wu, X., Wang, J., Guan, Y., Zhang, Y., Gong, M., et al. (2021a). Antidepressant effect of catalpol on corticosterone-induced depressive-like behavior involves the inhibition of HPA axis hyperactivity, central inflammation and oxidative damage probably via dual regulation of NF-κB and Nrf2. *Brain Res. Bull.* 177, 81–91. doi:10.1016/j.brainresbull.2021.09.002

Song, Q., Wang, Y., Huang, L., Shen, M., Yu, Y., Yu, Q., et al. (2021b). Review of the relationships among polysaccharides, gut microbiota, and human health. *Food Res. Int.* 140, 109858. doi:10.1016/j.foodres.2020.109858

Song, Z., Cheng, L., Liu, Y., Zhan, S., Wu, Z., and Zhang, X. (2022). Plant-derived bioactive components regulate gut microbiota to prevent depression and depressive-related neurodegenerative diseases: focus on neurotransmitters. *Trends Food Sci. Technol.* 129, 581–590. doi:10.1016/j.tifs.2022.10.019

Su, H., Wang, D., Zhang, T., Zhang, X., Mao, S., and Li, C. (2021). Effects of *Astragalus* polysaccharide on depressive behaviors and hippocampal Nrf2-ARE signaling pathway in rats. *Chin. Pharmacol. Bull.* 37, 839–843. doi:10.3969/j.issn.1001-1978.2021.06.018

Sun, Q., Ho, C.-T., Zhang, X., Liu, Y., Zhang, R., and Wu, Z. (2022). Strategies for circadian rhythm disturbances and related psychiatric disorders: a new cue based on plant polysaccharides and intestinal microbiota. *Food Funct.* 13, 1048–1061. doi:10.1039/D1FO02716F

Sun, Y., Cheng, L., Zeng, X., Zhang, X., Liu, Y., Wu, Z., et al. (2021). The intervention of unique plant polysaccharides-Dietary fiber on depression from the gut-brain axis. *Int. J. Biol. Macromol.* 170, 336–342. doi:10.1016/j.ijbiomac.2020.12.164

Tan, C., Yan, Q., Ma, Y., Fang, J., and Yang, Y. (2022). Recognizing the role of the vagus nerve in depression from microbiota-gut brain axis. *Front. Neurol.* 13, 1015175. doi:10.3389/fneur.2022.1015175

Tastan, B., Arioz, B. I., Tufekci, K. U., Tarakcioglu, E., Gonul, C. P., Genc, K., et al. (2021). Dimethyl fumarate alleviates NLRP3 inflammasome activation in microglia and sickness behavior in LPS-challenged mice. *Front. Immunol.* 12, 737065. doi:10.3389/fimmu.2021.737065

Thapar, A., Eyre, O., Patel, V., and Brent, D. (2022). Depression in young people. *Lancet* 400, 617–631. doi:10.1016/S0140-6736(22)01012-1

Troubat, R., Barone, P., Leman, S., Desmidt, T., Cressant, A., Atanasova, B., et al. (2021). Neuroinflammation and depression: a review. *Eur. J. Neurosci.* 53, 151–171. doi:10.1111/ejn.14720

Van Den Eede, F., and Claes, S. J. (2004). Mechanisms of depression: role of the HPA axis. *Drug Discov. Today Dis. Mech.* 1, 413–418. doi:10.1016/j.ddmec.2004.11.021

Vigna, L., Morelli, F., Agnelli, G. M., Napolitano, F., Ratto, D., Occhinegro, A., et al. (2019). *Hericium erinaceus* improves mood and sleep disorders in patients affected by overweight or obesity: could circulating pro-BDNF and BDNF be potential biomarkers? *Evid. Based Complement. Altern. Med.* 2019, 7861297–7861312. doi:10.1155/2019/7861297

Wang, X., Chen, X., Tang, Y., Wu, J., Qin, D., Yu, L., et al. (2022a). The therapeutic potential of plant polysaccharides in metabolic diseases. *Pharmaceuticals* 15, 1329. doi:10.3390/ph15111329

Wang, X., Cheng, L., Liu, Y., Zhang, R., Wu, Z., Weng, P., et al. (2022b). Polysaccharide regulation of intestinal flora: a viable approach to maintaining normal cognitive performance and treating depression. *Front. Microbiol.* 13, 807076. doi:10.3389/fmicb.2022.807076

Wang, Y., Deng, W., Li, X., and Peng, J. (2019a). Experimental observation on effect of *Astragalus* polysaccharides on learning ability in rats with post-stroke depression. *Lab. Anim. Comp. Med.* 39, 443–448. doi:10.3969/j.issn.1674-5817.2019.06.004

Wang, Y., Li, C., Qu, J., Li, H., Chen, B., Nie, K., et al. (2018). Effects of *Astragalus* polysaccharide on hippocampal NF-κB signaling in rats with depressive behaviors. *Chin. Pharmacol. Bull.* 34, 836–840. doi:10.3969/j.issn.1001-1978.2018.06.019

Wang, Y., Ni, J., Zhai, L., Gao, C., Xie, L., Zhao, L., et al. (2019b). Inhibition of activated astrocyte ameliorates lipopolysaccharide-induced depressive-like behaviors. *J. Affect. Disord.* 242, 52–59. doi:10.1016/j.jad.2018.08.015

Wei, Z., Song, H., An, F., Sun, J., Li, S., Jiang, N., et al. (2022). Protective effects and mechanism of polysaccharide from *Polygonatum sibiricum* on behavioral despair mice. *Sci. Technol. Food Ind.* 43, 351–357. doi:10.13386/j.issn1002-0306.2021060137

Xiao, K., Luo, Y., Liang, X., Tang, J., Wang, J., Xiao, Q., et al. (2021). Beneficial effects of running exercise on hippocampal microglia and neuroinflammation in chronic unpredictable stress-induced depression model rats. *Transl. Psychiatry* 11, 461–512. doi:10.1038/s41398-021-01571-9

Xiao, Z., Deng, Q., Zhou, W., and Zhang, Y. (2022). Immune activities of polysaccharides isolated from *Lycium barbarum* L. What do we know so far? *Pharmacol. Ther.* 229, 107921. doi:10.1016/j.pharmthera.2021.107921

Yamada, S., Yamamoto, M., Ozawa, H., Riederer, P., and Saito, T. (2003). Reduced phosphorylation of cyclic AMP-responsive element binding protein in the postmortem orbitofrontal cortex of patients with major depressive disorder. *J. Neural Transm.* 110, 671–680. doi:10.1007/s00702-002-0810-8

Yan, T., Nian, T., Liao, Z., Xiao, F., Wu, B., Bi, K., et al. (2020). Antidepressant effects of a polysaccharide from okra (*Abelmoschus esculentus* (L) Moench) by anti-inflammation and rebalancing the gut microbiota. *Int. J. Biol. Macromol.* 144, 427–440. doi:10.1016/j.ijbiomac.2019.12.138

Yang, H., Li, M., Zhou, M., Xu, H., Huan, F., Liu, N., et al. (2021). Links between gut dysbiosis and neurotransmitter disturbance in chronic restraint stress-induced depressive behaviours: the role of inflammation. *Inflammation* 44, 2448–2462. doi:10.1007/s10753-021-01514-y

Yang, Y., Fan, L., Peng, Y., Peng, C., and Li, X. (2022). Alcohol–soluble polysaccharides from *Dendrobium officinale* flowers as an antidepressant by regulating the gut–brain axis. *Int. J. Biol. Macromol.* 216, 836–849. doi:10.1016/j.ijbiomac.2022.07.220

Yi, L., Zhang, L., Ding, A., Xu, Q., Zhu, Q., and Kong, L. (2009). Orthogonal array design for antidepressant compatibility of polysaccharides from Banxia-Houpu decoction, a traditional Chinese herb prescription in the mouse models of depression. *Arch. Pharm. Res.* 32, 1417–1423. doi:10.1007/s12272-009-2011-6

Yi, L., Zhang, M., Cheng, J., Wan, H., Li, C., Zhu, J., et al. (2021). Antidepressant-like effects of degraded porphyran isolated from *Porphyra haitanensis*. *Mol. Nutr. Food Res.* 65, 2000869. doi:10.1002/mnfr.202000869

Yirmiya, R., Rimmerman, N., and Reshef, R. (2015). Depression as a microglial disease. *Trends Neurosci.* 38, 637–658. doi:10.1016/j.tins.2015.08.001

Zhang, J., Tang, J., Zhang, Q., Wang, X., and Li, X. (2019). Effects of sulfated pachymaran on AMPA receptor expression in hippocampi of depression model rats. *Chin. J. Clin. Psychol.* 27, 1086–1091. doi:10.16128/j.cnki.1005-3611.2019.06.003

Zhang, Q., Cheng, J., Liu, Q., Xu, G., Li, C., and Yi, L. (2022). *Dendrobium officinale* polysaccharides alleviate depression-like symptoms via regulating gut microbiota-neuroinflammation in perimenopausal mice. *J. Funct. Foods* 88, 104912. doi:10.1016/j.jff.2021.104912

Zhang, Y., Sun, Y., Liu, Y., Liu, J., Sun, J., Liu, X., et al. (2023). *Polygonum sibiricum* polysaccharides exert the antidepressant-like effects in chronic unpredictable mild stress-induced depressive mice by modulating microbiota-gut-brain axis. *Phytother. Res.* 37, 3408–3423. doi:10.1002/ptr.7813

Zhao, K., Yao, M., Zhang, X., Xu, F., Shao, X., Wei, Y., et al. (2022). Flavonoids and intestinal microbes interact to alleviate depression. *J. Sci. Food Agric.* 102, 1311–1318. doi:10.1002/jsfa.11578

Zhao, P., Zhou, R., Zhu, X.-Y., Liu, G., Zhao, Y.-P., Ma, P.-S., et al. (2017). Neuroprotective effects of *Lycium barbarum* polysaccharide on focal cerebral ischemic injury in mice. *Neurochem. Res.* 42, 2798–2813. doi:10.1007/s11064-017-2293-x

Zhao, R., Master, B. Q., Master, B. M., and Cai, Y. (2019). Improving activity of *Lycium Barbarum* polysaccharide on depressive mice induced by reserpine. *Iran. J. Pharm. Res. IJPR* 18, 1556–1565. doi:10.22037/ijpr.2019.1100763

Zhao, S., Rong, C., Gao, Y., Wu, L., Luo, X., Song, S., et al. (2021). Antidepressant-like effect of *Ganoderma lucidum* spore polysaccharide-peptide mediated by upregulation of prefrontal cortex brain-derived neurotrophic factor. *Appl. Microbiol. Biotechnol.* 105, 8675–8688. doi:10.1007/s00253-021-11634-y

Zhou, H., and Li, T. (2020). Antidepressant mechanism of sulfated pachymaran. *J. Wannan Med. Coll.* 39, 209–213. doi:10.3969/j.issn.1002-0217.2020.03.002

Zhou, J., Lu, Y., Xu, X., Zhang, J., Li, H., and Chang, H. (2015). Effect of antidepression and mechanism of regulation on Ido of Tiansi Liquid. *J. Beijing Univ. Tradit. Chin. Med.* 38, 182–185. doi:10.3969/j.issn.1006-2157.2015.03.008

Zhou, S., Chen, S., Xie, W., Guo, X., and Zhao, J. (2020). Microglia polarization of hippocampus is involved in the mechanism of Apelin-13 ameliorating chronic water immersion restraint stress-induced depression-like behavior in rats. *Neuropeptides* 81, 102006. doi:10.1016/j.npep.2020.102006

Zhu, X., Hu, S., Zhu, L., Ding, J., Zhou, Y., and Li, G. (2015). Effects of *Lycium barbarum* polysaccharides on oxidative stress in hyperlipidemic mice following chronic composite psychological stress intervention. *Mol. Med. Rep.* 11, 3445–3450. doi:10.3892/mmr.2014.3128

Zhuang, Y., Zeng, R., Liu, X., Yang, L., and Chan, Z. (2022). Neoagaro-oligosaccharides ameliorate chronic restraint stress-induced depression by increasing 5-HT and BDNF in the brain and remodeling the gut microbiota of mice. *Mar. Drugs* 20, 725. doi:10.3390/md20110725

Zuo, C., Cao, H., Song, Y., Gu, Z., Huang, Y., Yang, Y., et al. (2022). Nrf2: an all-rounder in depression. *Redox Biol.* 58, 102522. doi:10.1016/j.redox.2022.102522

frontiers | Frontiers in Pharmacology

TYPE Original Research
PUBLISHED 07 March 2024
DOI 10.3389/fphar.2024.1346226



OPEN ACCESS

EDITED BY
Junfeng Wang,
Massachusetts General Hospital and Harvard Medical School, United States

REVIEWED BY
Shuang Pan,
Tufts University, United States
Weirong Wang,
Xi'an Jiaotong University, China

*CORRESPONDENCE
Jiaoyan Yu,
969027046@qq.com

†These authors have contributed equally to this work

RECEIVED 29 November 2023
ACCEPTED 19 February 2024
PUBLISHED 07 March 2024

CITATION
Zhang J, Luo L, Guo Y, Liu A, Zhang M, Jiang W, Li X, Liu Q and Yu J (2024), Pharmacological effects and target analysis of Guipi wan in the treatment of cerebral ischemia-reperfusion injury.
*Front. Pharmacol.* 15:1346226.
doi: 10.3389/fphar.2024.1346226



# Pharmacological effects and target analysis of Guipi wan in the treatment of cerebral ischemia-reperfusion injury

Jianfeng Zhang[1†], Li Luo[2†], Yanyan Guo[2], An Liu[2], Mengjia Zhang[3], Wei Jiang[2], Xi Li[2], Qingqing Liu[2] and Jiaoyan Yu[2*]

[1]Department of Pharmacy, Eighth Hospital of Xi'an City, Xi'an, China, [2]Department of Pharmacy, The Second Affiliated Hospital of Air Force Medical University, Xi'an, China, [3]Air Force Medical University, Xi'an, China

Guipi wan (GPW) is a traditional Chinese medicine commonly used in clinical practice, typically to treat neurological diseases such as neurasthenia and traumatic brain injury. It may have positive effects on cerebral ischemia–reperfusion injury (cI/R). This study aimed to assess the effects of GPW in a mouse model of cI/R and find its possible targets. C57BL/6J mice were used to establish the cI/R model, and the laser speckle doppler was used to determine the success of the model. GPW was administered intragastrically for 7 days, brain tissue sections were stained with TTC, HE, and TUNEL, Western blot assay was performed to detect the effect of apoptosis-related proteins. Furthermore, we screened active ingredients from the TCM Database and constructed a compound–target network using the Cytoscape 3.8.0 software. Moreover, we employed protein–protein interaction and component–target–pathway network analyses to determine the potential components of GPW and its target genes, the key target was verified through molecular docking. Finally, we detected the influence of the downstream signaling pathway of the target through Western blot. The results showed that GPW decreased the cerebral infarction area, neurological function scores, and neuronal apoptosis in mice by regulating PI3K/AKT signaling pathway. Network analysis indicated that gamma-aminobutyric acid B receptor 1 (GABBR1) might be a potential target for the treatment of cI/R. Molecular docking indicated that 9 active components in GPW could bind to GABBR1 with desirable binding energy. This study represented the demonstratable effect of GPW in the treatment of cI/R injury and suggested GABBR1 as a potential target using network analysis.

KEYWORDS

**guipi wan, ischemia-reperfusion injury, network analysis, GABBR1, PI3K/AKT**

## 1 Introduction

Ischemic stroke (IS) is the second leading cause of death worldwide and shows a high disability rate (Walter., 2022). It accounts for 70% of all strokes and carries a high risk of long-term recurrence. In 2019, the total number of IS-related deaths reached 3.29 million, accounting for 50.3% of stroke deaths and 17.7% of all cardiovascular disease-related deaths. And research predictive analysis suggested that this number could increase to 4.9 million by 2030 (Fan et al., 2023). Ischemic stroke occurs when blood flow to the brain is blocked due

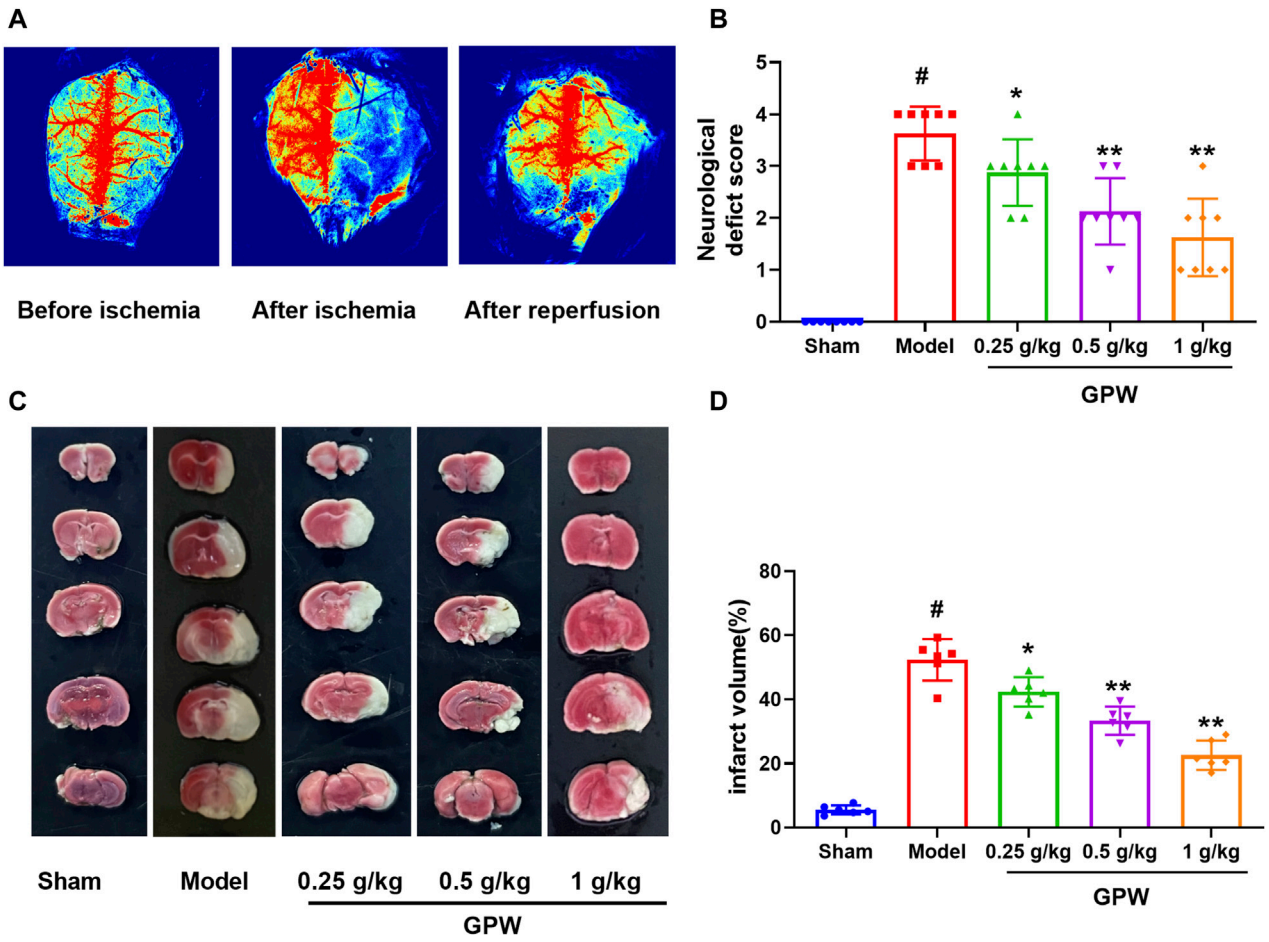


FIGURE 1
GPW reduces the brain damage caused by cerebral ischemia/reperfusion injury (cI/R). **(A)** Laser speckle Doppler shows the success of cI/R induction. **(B)** Neurological function score. $N = 8$ **(C)** Representative images of TTC staining in brain sections from different experimental groups. **(D)** Quantitative assessments of the infarct area from TTC staining. $N = 6$; $^{\#}p < 0.01$ *versus* the sham group; $^{*}p < 0.05$, $^{**}p < 0.01$ compared with the Model group.

to a blocked or ruptured artery, disrupting the brain's energy supply, causing tissue damage, and leading to widespread neuronal death (Tuo et al., 2022). The current treatment for this condition is the use of a recombinant tissue plasminogen activator, which triggers intravenous thrombolysis. However, the window for this treatment is narrow, and patients often face the risk of permanent disability after a stroke (Lin and Lang, 2022). In addition, blood flow restoration can cause more serious cerebral ischemia–reperfusion injury (cI/R) (Campbell and Khatri, 2019). Therefore, a reliable treatment plan is urgently needed to improve the disability and nerve damage caused by reperfusion injury after a stroke.

To date, many drugs have been experimentally shown to have neuroprotective effects, but their clinical application has not yet been confirmed (Tsivgoulis et al., 2023). Specifically, traditional Chinese medicine (TCM) has been used to treat patients during the recovery period after a stroke, and many compound prescriptions have been demonstrated to be effective (Tao et al., 2020). Guipi wan (GPW) is often used to treat neurasthenia and traumatic brain injury, and also to improve the emotional and cognitive dysfunctions that arise after stroke (Li et al., 2020). It mainly comprises 11 traditional Chinese active ingredients, including Codonopsis radix, Atractylodes macrocephala rhizoma, Astragali radix, Glycyrrhizae radix et rhizoma, Poria, Polygalae radix, The seed of Ziziphus jujuba var. Spinos, Longan arillus, Angelicae sinensis radix, Aucklandiae radix and Jujubae fructus. Clinical experimental studies have confirmed that Astragali radix can significantly recover the clinical symptoms of cerebral ischemia, and play anti-atherosclerosis and neuroprotective roles. (Li et al., 2023a). Atractylenolide III in Atractylodes macrocephala Koidz ameliorates cerebral ischemic injury and neuroinflammation associated with inhibiting JAK2/STAT3/Drp1-dependent mitochondrial fission in microglia (Zhou et al., 2019). Several medicinal materials and components of GPW have been reported to improve cerebral ischemia reperfusion injury (Hao et al., 2023). These results suggest that GPW, as a clinical prescription of traditional Chinese medicine, may be effective in treating cerebral ischemia-reperfusion injury, but the underlying pharmacological mechanism remains unclear.

The systemic nature of TCM, which comprises multiple components with numerous downstream targets and complex mechanisms of action, cannot be accurately captured by the principles of Western medical research, which focuses on individual targets and components. Consequently, the Western

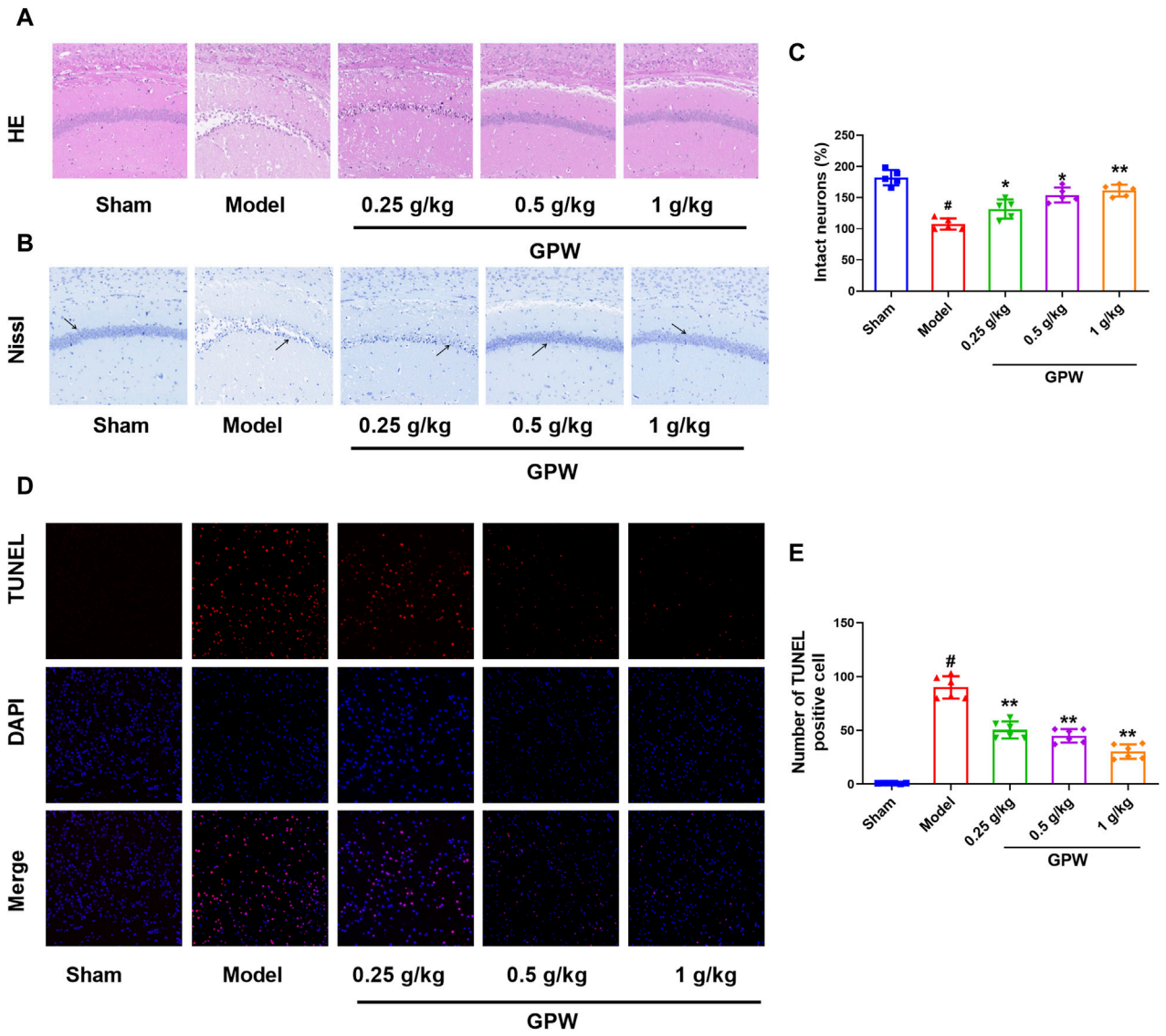


FIGURE 2
GPW alleviates the pathological damage of model mice. **(A)** Hematoxylin and eosin staining results of infarct area (20×). **(B)** Nissl staining results of infarct area (20×), The black arrow shows the Nissl corpuscles. **(C)** Numerical analysis of Nissl staining with ImageJ program. **(D)** TUNEL staining results of brain tissue sections in different experimental groups. **(E)** Statistical analysis of the percentage of intact neurons in the infarct area of mice by TUNEL staining. Scale bar = 75 μm; $N$ = 6 mice per group; $^{\#}p < 0.01$ *versus* the sham group; $^{*}p < 0.05$, $^{**}p < 0.01$ compared with the Model group.

approach has not been satisfactory in elucidating the pharmacodynamics of TCM compound prescriptions (Li et al., 2023b). However, with the advancement of network analysis techniques, more and more studies have begun to use this method to conduct holistic and systematic exploration to explain the mechanism of action of Chinese herbal medicine (Wang et al., 2021a), thus broadening their range of clinical applications. Many studies have successfully used network analysis to explain how effectively these drugs treat various diseases. Therefore, this study intends to combine pharmacological experiments and network analysis techniques to clarify the efficacy and possible targets of GPW in the treatment of cI/R.

This study confirmed that GPW has a significant therapeutic effect on cI/R model mice, in addition, predicted that GABBR1 is an important target for its therapeutic effect, and the downstream signaling pathway was verified, with the intent to elucidate elucidate the therapeutic effect and molecular mechanism of GPW on cI/R injury.

## 2 Materials and methods

### 2.1 Animals and drug administration

Adult male C57BL/6J mice aged 6–8 weeks, weighing 20–25 g, were provided by the Experimental Animal Center of the Fourth Military Medical University. The mice were housed at a constant temperature of 25°C ± 2°C and humidity of 50% ± 10%, with an alternating 12 h light/dark cycle and free access to food and water, they were randomly divided into five groups. Four groups

10.3389/fphar.2024.1346226

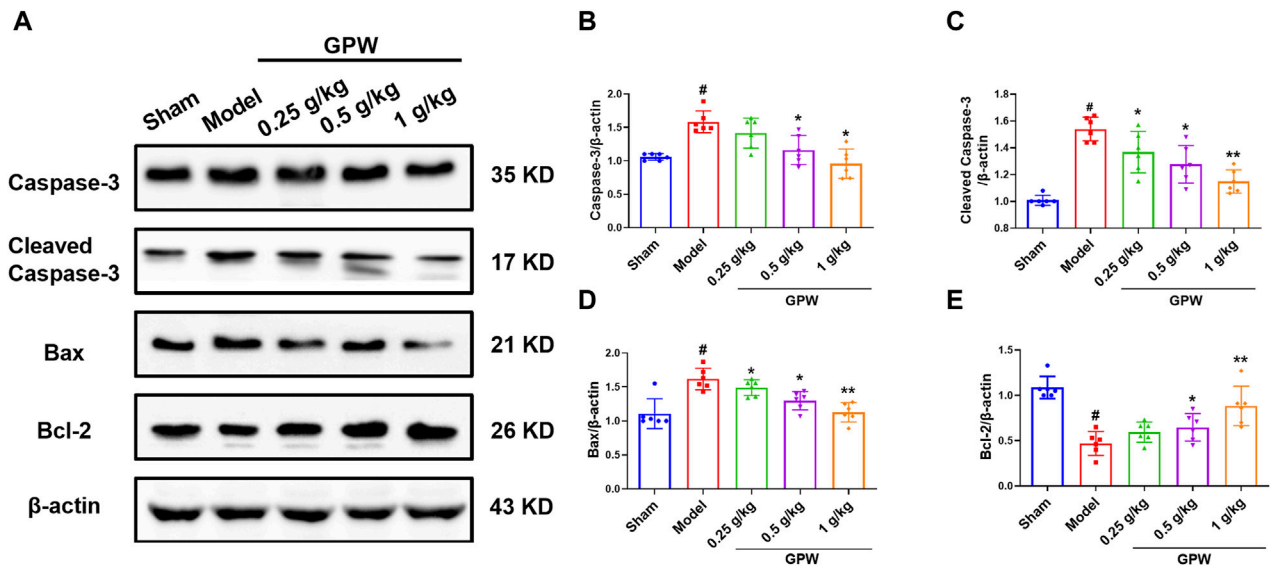


FIGURE 3
Effect of GPW on apoptosis-related proteins. **(A)** Western blot detection of caspase 3, cleaved-caspase 3, Bax, and Bcl-2 bands in the brain tissue of each group of mice. **(B–E)** Statistical analysis of protein expression. *N* = 6 mice per group; $^{\#}p < 0.01$ *versus* the sham group; $^{*}p < 0.05$, $^{**}p < 0.01$ compared with the Model group.

underwent middle cerebral artery occlusion (MCAO) under anesthesia and then were administered a gastric injection with 0.9% saline or GPW extract (Lanzhou Foci Pharmaceutical, Lanzhou, 200,934, China).

GPW extraction process: Codonopsis radix (80 g), Atractylodes macrocephala rhizoma (60 g), Astragali radix (80 g), Glycyrrhizae radix et rhizoma (40 g), Poria (160 g), Polygalae radix (160 g). The seed of Ziziphus jujuba var. Spinosa (80 g), Longan arillus (160 g), Angelicae sinensis radix (160 g), Aucklandiae radix (40 g), Jujubae fructus (40 g), total 1,000 g. Codonopsis radix, Angelicae sinensis radix, Glycyrrhizae radix et rhizoma and Aucklandiae radix were crushed into fine powder, and the other medicinal materials 10 times the volume of water boiled 2 times, for 2 h each time, combined and concentrated into extract, and mixed with fine powder to make pill, weighing about 167 g, that is, 1,000 g of crude drug is equivalent to 167 g of extract, The quality of the extract was identified and the content of astragaloside in the extract detected by HPLC was 0.33 mg/g, which met the extraction requirement of ≥0.1 mg/g in Chinese Pharmacopoeia, as shown in Supplementary Figure S1. During gastric administration, 1 g extract was dissolved in 10 mL normal saline to obtain 6 g crude drug/1g extract/10 mL GPW administration solution.

The clinical dose of drug 15 g crude drug/60 kg used in humans was converted to approximately 3 g crude drug/kg in mouse, with a proportion of 12.3 times based on body surface areas (Reagan-Shaw et al., 2008), this dose was selected as the medium dose group. The low, medium and high doses calculated by the equal ratio of 2 times were 1.5, 3 and 6 crude drugs/kg. These values corresponded to the extract dosage of 0.25, 0.5, 1 g/kg, thereby obtaining the intragastric volume of 2.5 mL/kg, 5 mL/kg, and 10 mL/kg, respectively. The remaining group underwent a sham operation and then received intragastric administration of 0.9% normal saline.

## 2.2 MCAO model

The MCAO model was established with a modified suture method (Barthels and Das, 2020) After intraperitoneal injection of sodium pentobarbital anesthetized, the mouse was fixed in the supine position. Following alcohol disinfection of the neck skin, we incised the midline of the neck, bluntly separating the right common carotid artery (CCA), external carotid artery (ECA), and internal carotid artery (ICA). We threaded the CCA, ICA, and ECA separately. Next, we clamped the proximal end of the CCA and the ICA, and tied the two cords at the proximal end of the ECA to a dead knot, while we tied the cords at the proximal end of the ECA to a slipknot. We cut a small "V" between the two cords at the proximal end of the ECA, inserted the thread plug, and insert the thread. We tightened the proximal end of the ECA line, fixed the line tether, lifted the ECA, and untied the ICA arterial clamp. We then slowly pushed the line tether toward the ICA. When the thread end entered about 1.2 cm, we stopped when we felt some resistance. We then untied the CCA artery clip, at this time. The end of the thread plug was just at the beginning of the middle cerebral artery (MCA), causing an occlusion. After 2 h of ischemia, the thread plug was pulled out to generate the ischemia–reperfusion model.

## 2.3 Laser speckle Doppler

Mice were anesthetized by intraperitoneal injection of 1% sodium pentobarbital solution at 50 μg/kg of body weight. Once anesthetized, the head was fixed on the operating table, the skin was cut along the midline, connective tissue was removed, and brain blood flow images were collected by laser speckle doppler flow imager (RFLSI 111).

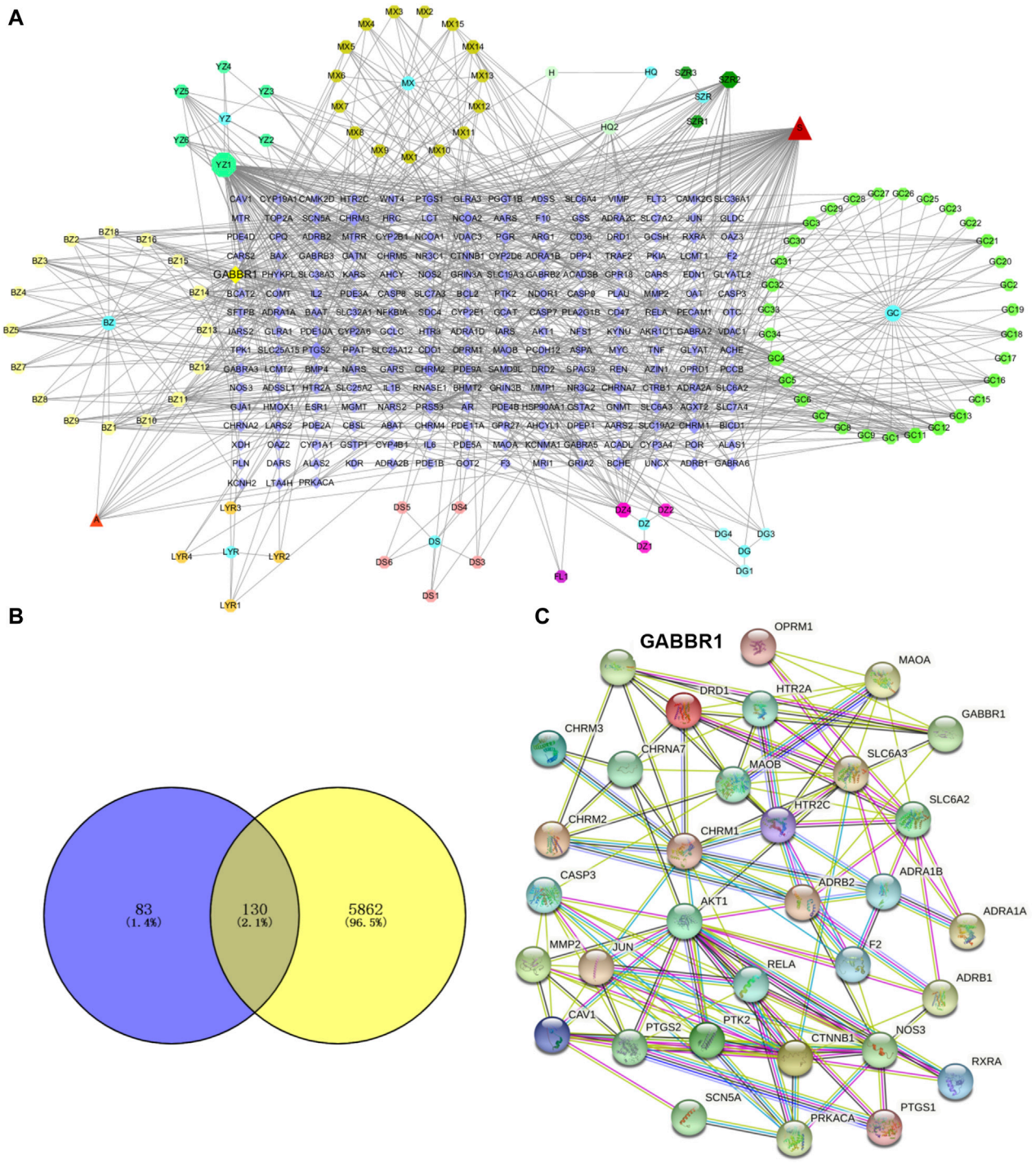


FIGURE 4
GPW component selection and target prediction. **(A)** The active ingredients of GPW and their targets are represented by nodes. The circles represent the plant components of GPW, the number of the corresponding compound is found in Supplementary Table S1, the polygons of different colors represent the main components of each plant, and the purple square represents the relevant target of the component. Edges represent the interaction between the biologically active ingredient and the target. **(B)** The Venn diagram of GPW and cI/R targets. Purple represents component targets, yellow represents disease targets, and the intersection represents common targets. **(C)** Protein–protein interaction network diagram. Nodes represent different proteins, and lines represent interactions.

## 2.4 Neurological scores

After model establishment and drug or saline administration, neurological deficits were assessed with a 5 point scoring system, as previously described (Kuai et al., 2021). According to this method, a score of 0–4 corresponds to no neurological dysfunction, inability to fully extend the left front paw, hovering left, falling left, low level of consciousness and inability to walk autonomously. A score of 5 represents death.

TABLE 1 Compounds screened according to degree value and druggability.

| Molecule name | Degree | Molecule name | Degree |
|---|---|---|---|
| Nuciferine | 31 | Selina-4(14),7(11)-dien-8-one | 11 |
| Atractylone | 19 | (−)-Caryophyllene oxide | 11 |
| Beta-carotene | 19 | 5,6,7,8-Tetrahydro-2,4-dimethylquinoline | 11 |
| 3β-Acetoxyatractylone | 17 | | |
| Benzo [a]carbazole | 16 | Juniper camphor | 10 |
| Coumarin | 14 | Harman | 10 |
| Harmine | 13 | Ermanthin | 9 |
| (+/−)-Isoborneol | 13 | 2-[(2R,5S,6S)-6,10-dimethylspiro [4.5]dec-9-en-2-yl]propan-2-ol | 9 |
| α-Cubebol | | 13 | |
| (5E,9Z)-3,6,10-trimethyl-4,7,8,11-tetrahydrocyclodeca [b]furan | | 11 | |

TABLE 2 The top 20 targets out of 213 possible GPW targets.

| Target name | Degree | Target name | Degree |
|---|---|---|---|
| GABBR1 | 38 | SLC6A2 | 15 |
| PTGS2 | 30 | ADRB2 | 13 |
| CHRM1 | 29 | ADRA1A | 13 |
| CHRM2 | 29 | GABRA3 | 13 |
| CHRM3 | 28 | BCHE | 12 |
| NCOA2 | 21 | GABRA6 | 12 |
| GABRA2 | 20 | ADRA1B | 13 |
| PTGS1 | 18 | SCN5A | 10 |
| PRSS3 | 16 | SLC6A3 | 10 |
| CHRNA7 | 16 | RXRA | 10 |

## 2.5 2,3,5-Triphenyltetrazolium chloride staining

After 24 h, the mice in each group were deeply anesthetized, their brain tissue was removed, and residual blood was washed out with normal saline. Brains were then quickly frozen at −20°C for 20 min and cut into 2 mm slices with a brain slice mold (68,714, RWD Life Science). Sections were stained with 1% 2,3,5-triphenyltetrazolium chloride (TTC, purity >98.0%; Sigma-Aldrich, St Louis, MO, United States) for 30 min at 37°C. ImageJ software (NIH) was used to measure the percentage of tissue affected by cerebral infarction.

## 2.6 Hematoxylin and eosin staining

Brain tissue was immersed in 4% paraformaldehyde for 24 h and then embedded in paraffin. Thereafter, 4-μm-thick sections were prepared for hematoxylin and eosin (HE) staining. After dehydration with a gradient series of ethanol and xylene, the brain tissue structure was observed under an optical microscope (Ts2-FL, Nikon, Tokyo, Japan).

## 2.7 Nissl staining

Paraffin sections were sequentially dehydrated with xylene, and absolute, 95%, 80%, and 70% ethanol. Sections were then washed with distilled water, soaked in 1% tar violet dye for 10 min, washed with distilled water again, and decolorized with gradient ethanol immersion. After becoming transparent, sections were mounted on clear slides with neutral gum, and tissue was observed under an optical microscope.

## 2.8 TUNEL staining

Sections were washed twice for 5 min with xylene. After gradient ethanol immersion, sections were infused with proteinase K to increase cell permeability and incubated at 37°C for 20 min. Next, sections were first incubated with 100 μL of TUNEL (6-Diamidino-2-phenylindole) reaction mixture (ab66110, Abcam) at 37°C for 1 h under dark conditions, and then with 100 μL DAB solution at room temperature for 10 min. Counterstaining with hematoxylin was performed for 3 min and, after rinsing, sections were dehydrated in a graded series of ethanol, made transparent in xylene, and mounted on neutral gum. The number of TUNEL-positive cells was counted under a fluorescence microscope (Ts2-FL, Nikon), and the percentage of TUNEL-positive cells was calculated to calculate the rate of apoptosis.

## 2.9 Western blotting

For Western blotting, 20 mg of brain tissue from the infarct area was lysed in 100 μL RIPA buffer, and homogenized by ultrasonication. Samples were centrifuged at 12,000 rpm for 10 min at 4 °C. The supernatant was removed, and the total

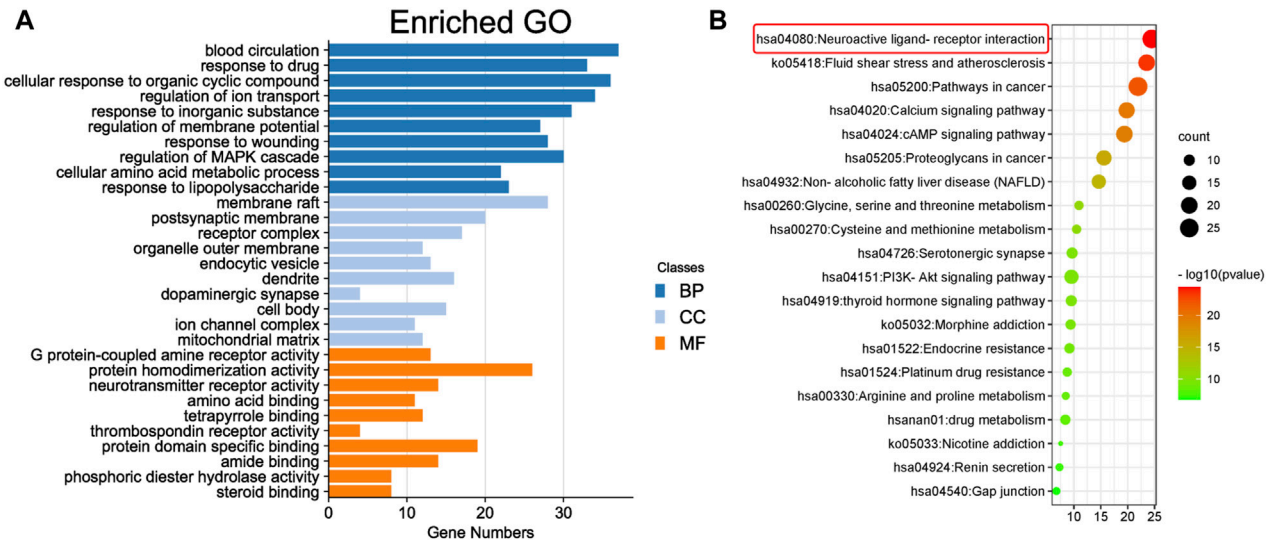


FIGURE 5
Enrichment analysis of core targets. **(A)** The top 10 results for the biological process (BP), cell component (CC), and molecular function (MF) categories in Gene Ontology (GO) annotation analysis. The *y*-axis represents the target-enriched GO, and the *x*-axis represents the gene number in the GO annotation results. **(B)** Top 20 Kyoto Encyclopedia of Genes and Genomes (KEGG) pathway enrichment bubble chart ($p < 0.05$). The *y*-axis represents the name of the enriched pathway, and the *x*-axis represents the enrichment value.

protein concentration in each sample was quantified by bicinchoninic acid assay (Pierce BCA Protein Assay Kit; Thermo Fisher Scientific, Waltham, MA, United States). After heating the samples in the presence of a loading buffer, SDS-PAGE (sodium dodecyl sulphate-polyacrylamide gel electrophoresis) was performed on 8–10% gels. Proteins were later transferred to PVDF membranes, which were blocked in 5% skim milk for 1 h and incubated at 4°C overnight with primary antibodies (1:1,000 dilution) for PI3K (13666S; Cell Signaling Technology, Danvers, MA, United States), AKT (2920ST, Cell Signaling Technology), P-AKT (13038S, Cell Signaling Technology), caspase-3 (9664T, Cell Signaling Technology), cleaved caspase-3 (9664s, Cell Signaling Technology), Bcl-2 (3498s, Cell Signaling Technology), Bax (14796s, Cell Signaling Technology), and β-actin (059M4770v, Sigma-Aldrich). After repeated washing, membranes were incubated with secondary antibodies (1:5,000 dilution) at room temperature for 1 h and subsequently washed. Membranes were then observed and photographed through a gel imager (Bio-Rad, United States). ImageJ was utilized to analyze the relative expression levels of the proteins, with β-actin as a reference.

## 2.10 Target prediction of GPW components

We used the Traditional Chinese Medicine System Pharmacological Analysis Platform (TCMSP, http://tcmspw.com/tcmsp.php) and the Bioinformatics Analysis Tool for Molecular mechanism of Traditional Chinese Medicine (BATMAN-TCM) database (http://bionet.ncpsb.org/batman-tcm) to identify the main active compounds of GPW. The screening conditions were the following: oral bioavailability (OB) ≥ 30%, drug-like activity (DL) ≥ 0.1, and blood–brain barrier (BBB) ≥ 1 (Liu et al., 2020). The information concerning the main active compounds of GPW and their corresponding targets was collected and standardized through the Uniport database (https://www.uniprot.org/), and the gene names of each target were obtained.

## 2.11 Compound-target network construction

Cytoscape 3.8.0 (National Institute of General Medical Sciences, Bethesda, MD, United States) was used to construct a compound-target network for GPW. We also used the GeneCards (https://www.genecards.org/), OMIM (https://omim.org) and DisGeNET (https://www.disgenet.org/) databases with cI/R as the keyword to acquire the key therapeutic targets for cI/R. The downstream targets of GPW and cI/R were imported into the online platform of Venny 2.1.0 for analysis, and Venn diagrams were used to visualize the common targets of GPW and cI/R injury.

## 2.12 Protein-protein interaction network analysis

The common targets were imported into the STRING database (https://string-db.org/), and "multiple proteins" and "*Homo sapiens*" were selected to obtain protein-protein interaction (PPI) data. This information was imported into Cytoscape 3.8.0 to perform a visual analysis by drawing PPI network diagrams. The CytoHubba plug-in was employed for network topology analysis (Athanasios et al., 2017). We selected targets with a degree higher than the average as the key targets in the PPI network.

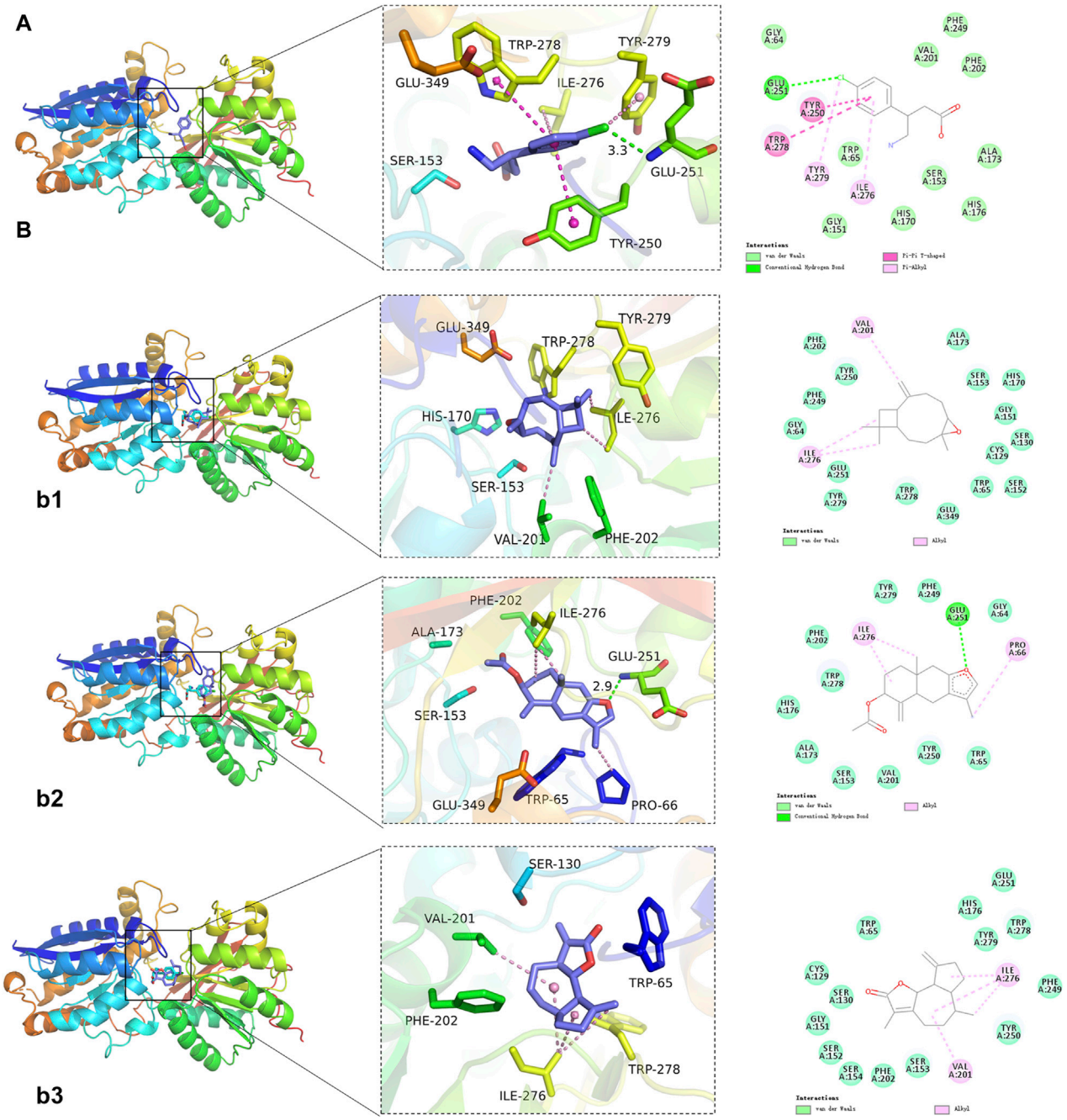


FIGURE 6
Representative results of molecular docking analyses. **(A)** Binding of the positive control baclofen to GABBR1. **(B)** Representative docking results of 3 GPW components. b1: (−)-Caryophylleneoxide; b2: 3β-acetoxyatractylone; b3: Ermanthin.

## 2.13 Gene function annotation and pathway enrichment analysis

To study the potential molecular mechanism through which GPW exerts positive effects on cI/R, the key targets were analyzed by gene function annotation (Gene Ontology, GO), and pathway enrichment analysis (Kyoto Encyclopedia of Genes and Genomes, KEGG). Statistical significance was set at $p < 0.05$. Finally, Cytoscape 3.8.0 was employed to construct a component–target–path (CTP) network to study the reciprocity of components, targets, and paths (Cui et al., 2020). In such a network, the degree value of a node was defined as the number of edges connected to the rest of the network, where each edge corresponds to the interaction between a biologically active ingredient and its target, thus representing the physiological relevance of the node in the network.

TABLE 3 Molecular docking results between ligands and core target receptors.

| Molecule name | Binding energy (kcal/mol) |
|---|---|
| Baclofen (GABBR1 agonist)PTGS2 | −7.0 |
| 3β-acetoxyatractylone | −5.3 |
| (+/−)-Isoborneol | −4.2 |
| α-Cubebol | −5.1 |
| Selina-4(14),7(11)-dien-8-one | −3.4 |
| (−)-Caryophyllene oxide | −6.3 |
| Juniper camphor | −4.8 |
| 2-[(2R,5S,6S)-6,10-dimethylspiro [4.5]dec-9-en-2-yl]propan-2-ol | −5.7 |
| Ermanthin | −5.8 |

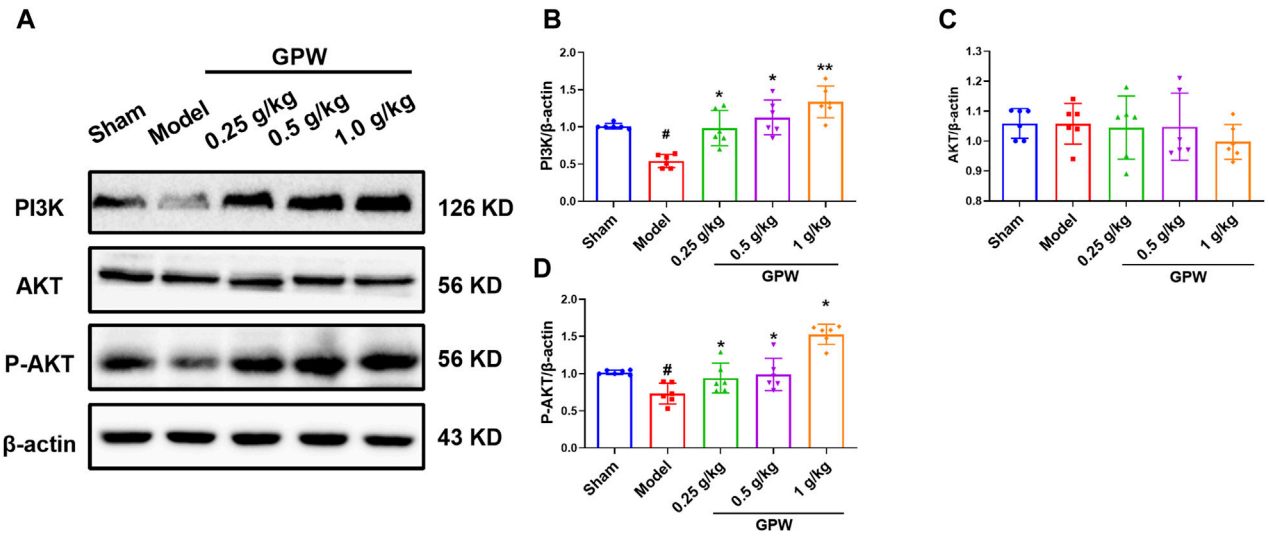


FIGURE 7
Effect of GPW on PI3K/AKT signaling pathways in the infarct area. **(A)** WB representative result chart. **(B)** Statistical analysis results of PI3K expression. **(C)** Quantitative statistical results of AKT expression. **(D)** Quantitative statistical results of the p-AKT expression. *N* = 6 mice per group; $^{\#}p < 0.01$ *versus* the sham group; $^{*}p < 0.05$, $^{**}p < 0.01$ compared with the Model group.

## 2.14 Molecular docking studies

The main chemical components and the core targets obtained from database screening were verified by molecular docking analyses (Taha et al., 2020). The structures of the key components were searched on the PubChem database (http://zinc. docking. org/), optimized, and saved in. mol format (Xia et al., 2020). The Cryo-EM structure of GABBR1 was downloaded from the Protein Data Bank (PDB) and saved in. pdb format. Water molecules and the docking ligand were removed with the PyMOL software (Schrödinger, New York, NY, United States). The obtained protein structures were then imported into AutoDock (Center for Computation Structural Biology, The Scripps Research Institute, La Jolla, CA, United States) to apply pre treatments such as hydrogenation. The active ingredients of GPW and the target proteins were saved as. pdbqt files, and AutoDock was utilized to simulate the docking of each active ingredient and target protein. The data concerning the lowest binding energy resulting from molecular docking was obtained. The lower the binding energy, the stronger the binding force between the active ingredient and the target protein: a drug molecule with binding energy ≤ −5. 0 kJ/mol is considered to have a good binding activity to the target (Li et al., 2021).

## 2.15 Statistical analysis

All data are expressed as mean ± standard deviation (Mean ± SD). SPSS19.0 (IBM, Armonk, NY, United States) and GraphPad 9.0 (GraphPad, La Jolla, CA, United States) were used for statistical analysis and graph plotting. *t*-test was used to compare the means of two samples. A one-way analysis of variance and Tukey's test were employed for comparisons of three or more group means. Statistical significance was set at $p < 0.05$.

# 3 Results

## 3.1 GPW reduced the cerebral infarction area in MCAO mice

The total blood flow on the ischemic side after reperfusion was measured by laser speckle Doppler, and blood flow recovery was greater than 70%, indicating successful induction of cI/R (Figure 1A). Different doses of GPW significantly improved the neurological score of the model mice (Figure 1B). TTC staining showed that GPW significantly reduced the size and volume of the infarct in the model mice compared with that in the sham operation group (Figures 1C, D).

## 3.2 GPW reduced neuronal damage in MCAO mice

HE staining showed that, in the sham group, hippocampal neuronal cell bodies were large and round with obvious nucleoli, and the cells were arranged in multiple well-organized layers. In the model group, the number of cells on the affected side was reduced, the arrangement was sparse, the cell bodies were shrunken, the nuclei were constricted in triangles, and some cell nuclei had disappeared. On the contrary, the proportion of atrophied neurons in the GPW-treated groups was significantly reduced (Figure 2A). Nissl staining showed the same trend. Compared with the sham group, the number of Nissl bodies in the model group was significantly reduced, while that in GPW-treated model groups was significantly increased (Figures 2B, C).

Furthermore, almost no TUNEL-positive cells were observed in the sham group, but their number was significantly increased in the model group. After GPW administration, the number of TUNEL-positive cells in the model mice was reduced in a dose-dependent manner (Figures 2D, E). This further revealed that GPW could reduce neuronal apoptosis of cI/R injury.

## 3.3 GPW decreased the expression of apoptosis-related proteins in MCAO mice

The expression of the pro-apoptotic proteins caspase-3, cleaved caspase-3, and Bax was significantly increased in the model group but significantly decreased after GPW administration (Figure 3A–D). Accordingly, the expression of the anti-apoptotic protein Bcl-2 was significantly reduced in the model group, while the administration of GPW was able to counteract this decrease (Figure 3E). These results indicated that GPW had the potential to inhibit neuronal apoptosis at the molecular level.

## 3.4 Network analysis predicted the main related targets of GPW

The role of GPW in the treatment of cI/R has been determined; further, it is intended to predict its possible targets through network analysis. Through TCMSP, according to the conditions of OB ≥ 30%, DL ≥ 0.1, and BBB ≥1, 95 active components were selected from 11 herbs (Supplementary Table S1). Using the uniprot databases to normalize cI/R targets and delete duplicates, a total of 213 targets were obtained. Then we used cystoscope software to construct the "component-target network" diagram of GPW (Figure 4A). In this diagram, the "degree" is defined as the number of connected edges in the network, representing the importance of the network. We found a total of 29 compounds with a degree value greater than the average value of 8.76. Among these, we further excluded 12 compounds due to a lack of compatibility with Lipinski's rules (Chen et al., 2020); 2) the structure conforming to the characteristics of Pan-Assay Interference Compounds (PAINS), which could indicate positive readouts in biochemical assays via different mechanisms (Grigalunas et al., 2020). Thus, only 17 compounds were selected for the prediction of subsequent targets (Table 1).

To predict the target receptor of GPW for the treatment of cI/R, we performed the analysis from three aspects. First, we list the top 20 targets among the 213 possible action targets selected based on the degree values (Table 2) and found theγ-aminobutyric acid receptor (GABBR1) with the degree value of 38. Second, we selected 130 target receptors that are relevant to the treatment of cI/R with GPW from 5,992 (Figure 4B). After drawing the PPI network structure with the STRING database website, 36 targets with degree values greater than the average were obtained for visualization (Figure 4C). The results showed GABBR1 is included in the main genes that can be exploited for treatment of cI/R. Finally, we employed the GO and KEGG pathway enrichment combined with CTP network analysis. As illustrated in Figure 5A, the top 10 biological process (BP), molecular function (MF), and cellular composition (CC) were represented from 130 potential targets. Furthermore, KEGG analysis revealed that 112 signal pathways are involved in GPW-mediated effects on cI/R injury, among which the top 20 were selected to make a bubble map (Figure 5B). According to the results, GPW mainly acts on cI/R injury through neuroactive ligand–receptor interaction, fluid shear stress, atherosclerosis, calcium signaling pathway, and the cAMP and PI3K/AKT signaling pathways. Interestingly, GABBR1 is a key target in the neuroactive ligand-receptor interaction signaling pathway. Thus, these results, taking three aspects of drug intervention, disease correlation, and pathway enrichment, demonstrated GABBR1 may be an important target for GPW treatment of cI/R.

## 3.5 Molecular docking further confirmed that GABBR1 might be a reliable target for GPW therapy cI/R

To further explore the binding mechanism of GPW on cI/R, we obtained 8 compounds including 3β-acetoxyatractylone, (+/−)-isoborneol, α-cubebol, selina-4(14),7(11)-dien-8-one, (−)-caryophyllene oxide, juniper camphor, 2-[(2R,5S, 6S)-6,10-dimethylspiro [4.5]dec-9-en-2-yl]propan-2-ol, and ermanthin after intersecting the 17 main components of the preliminary screening with 38 components that interact with GABBR1 (Supplementary Figure S2A). Here, we intend to explore the binding mechanism between these active compounds and GABBR1. As illustrated in Figure 6A, taking baclofen as a probe,

we observed baclofen formed one hydrogen bond with Glu251, the alkyl conjugation interactions with Tyr279, and Ile276, and π-π interactions with Tyr250 and Trp278. In addition, the formation of the ligand-receptor complex was also dependent on van der Waals forces with Ser153, Ser131, Trp65, Tyr279, and Phe202. The binding energy of baclofen was −7.0 kcal/mol, indicating the strong binding ability between baclofen and GABBR1.

Next, we performed the molecular docking between these 8 compounds and GABBR1. As illustrated in Figure 6B; Supplementary Figure S2B, we obtained the binding energies ranked −6.3 to −3.4 kcal/mol (Table 3), whereby suggested that these 8 compounds had good binding ability with GABBR1. Similarly, the formation of these 8 ligand-receptor complexes was also based on the hydrogen bond, conjugation interactions, and van der Waals forces formed by 8 compounds with the above-mentioned key amino acid residues in GABBR1. In parallel, these results indicated that the mechanism of the interaction between bioactive compound and GABBR1 was similar to that of clinical drugs, thus proving the promising potential of GPW for cI/R treatment.

### 3.6 GPW affected the expression of PI3K/AKT signaling pathway-related proteins

It has been shown that modulating GABBR1 can inhibit apoptosis of rat hippocampal neurons through the PI3K/Akt pathway in the treatment of refractory epilepsy. We speculate that GPW may affect the PI3K/AKT signaling pathway by activating GABBR1, Therefore, We used Western blotting to evaluate changes in the expression of the related proteins (Figure 7A). Compared with the sham group, the model group had significantly reduced levels of PI3K, whose expression increased after GPW administration (Figure 7B). Also, while the total expression of AKT did not change (Figure 7C), that of phosphorylated AKT (p-AKT) was significantly reduced in the model group; this reduction was restored in GPW-treated mice (Figure 7D). In summary, the results show that GPW can activate the PI3K/AKT signaling pathway.

## 4 Discussion

In this study, we validated the pharmacological effect of GPW in the treatment of cI/R injury. The prevention and treatment of ischemic stroke remain a worldwide challenge. A central issue is the risk of bleeding associated with anticoagulants and antiplatelet drugs (Sandercock et al., 2015). Due to its low side effects, TCM is often sought as an alternative drug therapy for ischemic stroke prevention and rehabilitation intervention in China. Natural medicines in TCM are the origin of many new medicines, such as Salvia miltiorrhiza, which has been used to treat cerebrovascular diseases in China for thousands of years. TCM has been used in humans for more than 2,000 years. The valuable experience provided by this practice can provide powerful guidance for drug discovery (Sun et al., 2015). However, there are still some limitations of TCM, such as the low quality of TCM tests and unclear ingredients and mechanisms. GPW in this study is a classic prescription in TCM, which has been reported to be effective against many neurological diseases. However, its effect and mechanism of action on cI/R injury have not been reported. This study is of great significance for the development of therapeutic drugs for ischemic stroke based on TCM.

Firstly, we used the classical mouse MCAO model to further evaluate the therapeutic effect of GPW (Walter, 2022). The success of the model was verified by laser speckle Doppler, and GPW was found to reduce cerebral infarction size and neural function score and reduce neuronal apoptosis in model mice. Apoptosis is an important pathway leading to neuronal death after stroke, and caspase-3, bax, and blc-2 are apoptosis-related proteins. We further used WB to find that GPW can counteract these changes in stroke levels. The effect of GPW on cI/R was confirmed by experimental pharmacological methods.

Next, the main components and targets of cI/R treatment with GPW were screened and predicted by network analysis. Using the TCMSP database and according to OB, DL, and BBB standards, 96 components of 11 kinds of Chinese herbs in GPW were screened out. Further, the degree values were ranked according to the number of corresponding targets, those less than the average are excluded, and those greater than the average are 29 in total. The druggability of the compound requires compliance with Lipinski's Rule of Five and the PAIN rule, which further excludes some compounds, S-(2-Carboxyethyl)-L-Cysteine and Stigmasterol meet the druggability rules, but there are many targets and poor specificity. Therefore, 17 compounds such as nuciferine, atractylone, β-carotene, and coumarin were obtained. Among these, previous studies have shown that nuciferine was found to significantly improve neurological deficit scores, cerebral edema, and infarction by regulating fat metabolism and inflammatory response (Wu et al., 2020). Similarly, patients with higher serum β-carotene were found to have a significantly lower risk of stroke and death (Huang et al., 2018). Additionally, coumarin is a common oral anticoagulant used for the prevention and treatment of stroke (Cordonnier, 2018). These findings, together with our results, confirm that the core components of GPW can effectively reduce cI/R injury. However, although atractylone, 3β-acetoxyatractylone, and harmine have not been reported to have a therapeutic effect on ischemic stroke, they may play a synergistic role in the treatment of GPW, which needs to be verified by subsequent experiments.

Furthermore, in the results of network analysis, GABBR1 was found to have the highest degree in the target of GPW components. Additionally, combined with the analysis results of PPI, GO, and KEEG analysis found that GABBR1 was closely related to the effect of GPW on cI/R. Combined with the above results, we analyzed and speculated that GABBR1 may be a key target for the treatment of cI/R by GPW. Molecular docking provides further validation and suggests that multiple components in GPW may synergistically act on GABBR1 to produce neuroprotective effects. GABBR1 is the metabolic receptor 1 subtype of the inhibitory neurotransmitter gamma-aminobutyric acid (GABA), It is a G protein-coupled receptor expressed in neurons and glial cells throughout the brain (Cediel et al., 2022). GABBR1 exerts presynaptic and postsynaptic effects to inhibit the release of neurotransmitters and produce a later inhibitory postsynaptic potential, respectively (Gassmann and Bettler, 2012). It has been shown that GABBR1 controls neuronal activity to prevent overexcitation, thereby preventing excitotoxicity

and cell death. Selective continuous activation of GABBR1 can provide neuroprotection *in vitro* and *in vivo* models of cerebral ischemia (Kim et al., 2014). Moreover, studies have shown that the GABBR-mediated PI3K/AKT signaling pathway can reduce oxidative stress and neuronal cell damage in rat models of Alzheimer's disease (Sun et al., 2020). After a stroke, activation of the PI3K/AKT signaling pathway can counteract neuronal apoptosis (Lv et al., 2019). Further, we found that GPW reduced the amount of PI3K protein in cI/R mice and inhibited the phosphorylation of AKT. Our analysis showed that GPW may be mediated by GABBR1 to produce neuroprotective effects in cI/R injury by activating PI3K/AKT signaling.

It is necessary to acknowledge the limitations of this work. First, the composition and target of GPW are statistically obtained from the database, which cannot contain all the compounds and target genes. Second, the effect of GPW on cerebral ischemia-reperfusion injury needs more clinical verification. Finally, in addition to GABBR1, PTGS2, CHRM1, CHRM3, and other targets are also highly correlated. Whether other components of GPW interact with them and participate in the treatment of cerebral ischemia-reperfusion injury is still unclear, and more experiments are needed to verify it.

## 5 Conclusion

In conclusion, this study confirmed the neuroprotective effect of GPW by regulating the PI3K/AKT signaling pathway. In addition, the combination of network analysis and molecular docking predicted that GPW might target GABBR1 for the treatment of cI/R, preliminarily indicating that GPW may be a candidate herb for further research. This work provided a theoretical basis for the clinical application of GPW.

## Data availability statement

The original contributions presented in the study are included in the article/Supplementary Material, further inquiries can be directed to the corresponding author.

## Ethics statement

The animal study was approved by the Animal Experiment Ethics Committee of Air Force Military Medical University. The study was conducted in accordance with the local legislation and institutional requirements.

## Author contributions

JZ: Writing–original draft. LL: Writing–original draft. YG: Writing–original draft. AL: Writing–review and editing. MZ: Writing–review and editing. WJ: Writing–review and editing. XL: Writing–review and editing. QL: Writing–review and editing. JY: Writing–original draft, Writing–review and editing.

## Funding

The author(s) declare financial support was received for the research, authorship, and/or publication of this article. This work was supported by the project of Shaanxi Provincial Administration of Traditional Chinese Medicine (grant number 2021-ZZ-JC030), Tangdu Hospital National Natural Science Foundation Support Program (grant number 2021ZTXM-025).

## Conflict of interest

The authors declare that the research was conducted in the absence of any commercial or financial relationships that could be construed as a potential conflict of interest.

## Publisher's note

All claims expressed in this article are solely those of the authors and do not necessarily represent those of their affiliated organizations, or those of the publisher, the editors and the reviewers. Any product that may be evaluated in this article, or claim that may be made by its manufacturer, is not guaranteed or endorsed by the publisher.

## Supplementary material

The Supplementary Material for this article can be found online at: https://www.frontiersin.org/articles/10.3389/fphar.2024.1346226/full#supplementary-material

## References

Athanasios, A., Charalampos, V., Vasileios, T., and Ashraf, G. M. (2017). Protein-protein interaction (PPI) network: recent advances in drug discovery. *Curr. Drug Metab.* 18 (1), 5–10. doi:10.2174/1389200218011701192048 32

Barthels, D., and Das, H. (2020). Current advances in ischemic stroke research and therapies. *Biochim. Biophys. Acta Mol. Basis Dis.* 1866 (4), 165260. doi:10.1016/j.bbadis.2018.09.012

Campbell, B. C. V., and Khatri, P. (2020). Stroke. *Lancet* 396 (10244), 129–142. doi:10.1016/s0140-6736(20)31179-x

Cediel, M. L., Stawarski, M., Blanc, X., Nosková, L., Magner, M., Platzer, K., et al. (2022). GABBR1 monoallelic *de novo* variants linked to neurodevelopmental delay and epilepsy. *Am. J. Hum. Genet.* 109, 1885–1893. doi:10.1016/j.ajhg.2022.08.010

Chen, X., Li, H., Tian, L., Li, Q., Luo, J., and Zhang, Y. (2020). Analysis of the physicochemical properties of Acaricides based on Lipinski's rule of five. *J. Comput. Biol.* 27, 1397–1406. doi:10.1089/cmb.2019.0323

Cordonnier, C. (2018). Balancing risks versus benefits of anticoagulants in stroke prevention. *Lancet Neurol.* 17, 487–488. doi:10.1016/s1474-4422(18)30164-9

Cui, Q., Zhang, Y. L., Ma, Y. H., Yu, H. Y., Zhao, X. Z., Zhang, L. H., et al. (2020). A network pharmacology approach to investigate the mechanism of Shuxuening injection in the treatment of ischemic stroke. *J. Ethnopharmacol.* 257, 112891. doi:10.1016/j.jep.2020.112891

Fan, J., Li, X., Yu, X., Liu, Z., Jiang, Y., Fang, Y., et al. (2023). Global burden, risk factor analysis, and prediction study of ischemic stroke. *Neurology* 101, 137–150. doi:10.1212/WNL.0000000000207387

Gassmann, M., and Bettler, B. (2012). Regulation of neuronal GABA(B) receptor functions by subunit composition. *Nat. Rev. Neurosci.* 13, 380–394. doi:10.1038/nrn3249

Grigalunas, M., Burhop, A., Christoforow, A., and Waldmann, H. (2020). Pseudo-natural products and natural product-inspired methods in chemical biology and drug discovery. *Curr. Opin. Chem. Biol.* 56, 111–118. doi:10.1016/j.cbpa.2019.10.005

Hao, D. L., Li, J. M., Xie, R., Huo, H. R., Xiong, X. J., Sui, F., et al. (2023). The role of traditional herbal medicine for ischemic stroke: from bench to clinic-A critical review. *Phytomedicine* 109, 154609. doi:10.1016/j.phymed.2022.154609

Huang, J., Weinstein, S. J., Yu, K., Männistö, S., and Albanes, D. (2018). Serum beta carotene and overall and cause-specific mortality. *Circ. Res.* 123 (12), 1339–1349. doi:10.1161/circresaha.118.313409

Kim, J. Y., Ho, H., Kim, N., Liu, J., Tu, C. L., Yenari, M. A., et al. (2014). Calcium-sensing receptor (CaSR) as a novel target for ischemic neuroprotection. *Ann. Clin. Transl. Neurol.* 1, 851–866. doi:10.1002/acn3.118

Kuai, F., Zhou, L., Zhou, J., Sun, X., and Dong, W. (2021). Long non-coding RNA THRIL inhibits miRNA-24-3p to upregulate neuropilin-1 to aggravate cerebral ischemia-reperfusion injury through regulating the nuclear factor κB p65 signaling. *Aging (Albany NY)* 13 (6), 9071–9084. doi:10.18632/aging.202762

Li, M., Lan, R., Wen, Y., Shi, K., and Yang, D. (2020). Guipi decoction for insomnia: systematic review and meta-analysis. *Med. Baltim.* 99 (27), e21031. doi:10.1097/md.0000000000021031

Li, X., Liu, Z., Liao, J., Chen, Q., Lu, X., and Fan, X. (2023a). Network pharmacology approaches for research of Traditional Chinese Medicines. *Chin. J. Nat. Med.* 21, 323–332. doi:10.1016/S1875-5364(23)60429-7

Li, Y., Wang, D., Guo, R., Ma, B., Miao, L., Sun, M., et al. (2023b). Neuroprotective effect of Astragali Radix on cerebral infarction based on proteomics. *Front. Pharmacol.* 14, 1162134. doi:10.3389/fphar.2023.1162134

Li, Z. H., Yu, D., Huang, N. N., Wu, J. K., Du, X. W., and Wang, X. J. (2021). Immunoregulatory mechanism studies of ginseng leaves on lung cancer based on network pharmacology and molecular docking. *Sci. Rep.* 11 (1), 18201. doi:10.1038/s41598-021-97115-8

Lin, K., and Lang, E. (2022). In ischemic stroke upon wakening, IV thrombolysis or EVT improves functional outcome at 90 d. *Ann. Intern Med.* 175, 41. doi:10.7326/J22-0020

Liu, Y., Xue, Q., Li, A., Li, K., and Qin, X. (2020). Mechanisms exploration of herbal pair of HuangQi-DanShen on cerebral ischemia based on metabonomics and network pharmacology. *J. Ethnopharmacol.* 253, 112688. doi:10.1016/j.jep.2020.112688

Lv, Y., Liu, W., Ruan, Z., Xu, Z., and Fu, L. (2019). Myosin IIA regulated tight junction in oxygen glucose-deprived brain endothelial cells via activation of TLR4/PI3K/Akt/JNK1/2/14-3-3ε/NF-κB/MMP9 signal transduction pathway. *Cell. Mol. Neurobiol.* 39, 301–319. doi:10.1007/s10571-019-00654-y

Reagan-Shaw, S., Nihal, M., and Ahmad, N. (2008). Dose translation from animal to human studies revisited. *Faseb J.* 22, 659–661. doi:10.1096/fj.07-9574LSF

Sandercock, P. A., Counsell, C., Kane, E. J., and Signorini, D. (2015). Anticoagulants for acute ischaemic stroke. *Cochrane Database Syst. Rev.* 2015, 1451–1462. doi:10.1002/14651858.CD000024

Sun, K., Fan, J., and Han, J. (2015). Ameliorating effects of traditional Chinese medicine preparation, Chinese materia medica and active compounds on ischemia/reperfusion-induced cerebral microcirculatory disturbances and neuron damage. *Acta Pharm. Sin. B* 5, 8–24. doi:10.1016/j.apsb.2014.11.002

Sun, Z., Sun, L., and Tu, L. (2020). GABAB receptor-mediated PI3K/Akt signaling pathway alleviates oxidative stress and neuronal cell injury in a rat model of Alzheimers disease. *J. Alzheimers Dis.* 76, 1513–1526. doi:10.3233/jad-191032

Taha, K. F., Khalil, M., Abubakr, M. S., and Shawky, E. (2020). Identifying cancer-related molecular targets of Nandina domestica Thunb. by network pharmacology-based analysis in combination with chemical profiling and molecular docking studies. *J. Ethnopharmacol.* 249, 112413. doi:10.1016/j.jep.2019.112413

Tao, T., Liu, M., Chen, M., Luo, Y., Wang, C., Xu, T., et al. (2020). Natural medicine in neuroprotection for ischemic stroke: challenges and prospective. *Pharmacol. Ther.* 216, 107695. doi:10.1016/j.pharmthera.2020.107695

Tsivgoulis, G., Katsanos, A. H., Sandset, E. C., Turc, G., Nguyen, T. N., Bivard, A., et al. (2023). Thrombolysis for acute ischaemic stroke: current status and future perspectives. *Lancet Neurol.* , 22, 418–429. doi:10.1016/S1474-4422(22)00519-1

Tuo, Q. Z., Zhang, S. T., and Lei, P. (2022). Mechanisms of neuronal cell death in ischemic stroke and their therapeutic implications. *Med. Res. Rev.* 42, 259–305. doi:10.1002/med.21817

Walter, K. (2022). What is acute ischemic stroke? *Jama* 327, 885. doi:10.1001/jama.2022.1420

Wang, X., Wang, Z. Y., Zheng, J. H., and Li, S. (2021a). TCM network pharmacology: a new trend towards combining computational, experimental and clinical approaches. *Chin. J. Nat. Med.* 19 (1), 1–11. doi:10.1016/s1875-5364(21)60001-8

Wang, Y., Gai, S., Zhang, W., Huang, X., Ma, S., Huo, Y., et al. (2021b). The GABA(B) receptor mediates neuroprotection by coupling to G(13). *Sci. Signal* 14 (705), eaaz4112. doi:10.1126/scisignal.aaz4112

Wu, L., Chen, C., Li, Y., Guo, C., Fan, Y., Yu, D., et al. (2020). UPLC-Q-TOF/MS-Based serum metabolomics reveals the anti-ischemic stroke mechanism of nuciferine in MCAO rats. *ACS Omega* 5 (51), 33433–33444. doi:10.1021/acsomega.0c05388

Xia, Q. D., Xun, Y., Lu, J. L., Lu, Y. C., Yang, Y. Y., Zhou, P., et al. (2020). Network pharmacology and molecular docking analyses on Lianhua Qingwen capsule indicate Akt1 is a potential target to treat and prevent COVID-19. *Cell. Prolif.* 53 (12), e12949. doi:10.1111/cpr.12949

Zhou, K., Chen, J., Wu, J., Wu, Q., Jia, C., Yang, X. Z. X., et al. (2019). Atractylenolide III ameliorates cerebral ischemic injury and neuroinflammation associated with inhibiting JAK2/STAT3/Drp1-dependent mitochondrial fission in microglia. *Phytomedicine* 59, 152922. doi:10.1016/j.phymed.2019.152922

frontiers | Frontiers in Pharmacology

TYPE Review
PUBLISHED 17 April 2024
DOI 10.3389/fphar.2024.1372110



OPEN ACCESS

EDITED BY
Qi Liang,
Air Force Medical University, China

REVIEWED BY
Jyh-Fei Liao,
National Yang-Ming University, Taiwan
Yuhao Xie,
St. John's University, United States

*CORRESPONDENCE
Binlian Sun,
binlian17@jhun.edu.cn
Yiyuan Xia,
XYY@jhun.edu.cn

†These authors have contributed equally to this work

RECEIVED 17 January 2024
ACCEPTED 02 April 2024
PUBLISHED 17 April 2024

CITATION
Li W, Wan P, Qiao J, Liu Y, Peng Q, Zhang Z, Shu X, Xia Y and Sun B (2024), Current and further outlook on the protective potential of *Antrodia camphorata* against neurological disorders.
*Front. Pharmacol.* 15:1372110.
doi: 10.3389/fphar.2024.1372110



# Current and further outlook on the protective potential of *Antrodia camphorata* against neurological disorders

Weiling Li†, Pin Wan†, Jialu Qiao, Yuchen Liu, Qian Peng, Zehua Zhang, Xiji Shu, Yiyuan Xia* and Binlian Sun*

Hubei Key Laboratory of Cognitive and Affective Disorders, Wuhan Institute of Biomedical Sciences, School of Medicine, Jianghan University, Wuhan, China

Prevalent neurological disorders such as Alzheimer's disease, Parkinson's disease, and stroke are increasingly becoming a global burden as society ages. It is well-known that degeneration and loss of neurons are the fundamental underlying processes, but there are still no effective therapies for these neurological diseases. In recent years, plenty of studies have focused on the pharmacology and feasibility of natural products as new strategies for the development of drugs that target neurological disorders. *Antrodia camphorata* has become one of the most promising candidates, and the crude extracts and some active metabolites of it have been reported to play various pharmacological activities to alleviate neurological symptoms at cellular and molecular levels. This review highlights the current evidence of *Antrodia camphorata* against neurological disorders, including safety evaluation, metabolism, blood-brain barrier penetration, neuroprotective activities, and the potential on regulating the gut-microbiome-brain axis. Furthermore, potential strategies to resolve problematic issues identified in previous studies are also discussed. We aim to provide an overview for the ongoing development and utilization of *Antrodia camphorata* in cerebral neuropathology.

KEYWORDS

***Antrodia camphorata*, neuroprotective activities, CNS disease, secondary metabolite, gut-microbiome-brain axis**

## 1 Introduction

*Antrodia camphorata* (M. Zang & C.H. Su) Sheng H. Wu, Ryvarden & T.T. Chang (AC) also called *Antrodia cinnamomea* or *Taiwanofungus camphoratus* or *Ganoderma camphoratum*, locally known as Niu-Chang-Chih in (Su et al., 2022), is a valuable edible mushroom, with a large potential for biological and medicinal health benefits including anti-cancer, anti-inflammatory, anti-oxidative, hepatoprotective, and neuroprotective properties (Zhang et al., 2022). Naturally, the growth of AC is extremely slow and parasitic on the inner wall of a unique and native tree in Taiwan called *Cinnamomum kanehirai* Hayata on the mountain ranges between 450 to 1200 m higher (Li et al., 2022; Su et al., 2022). AC was first identified in 1990, and was recognized and used as highly beneficial Chinese folk medicine (Chen et al., 2023). As a fungus, AC belongs to the phylum Basidiomycota, the Fomitopsidaceae family, and the *Antrodia* genus (Li et al., 2023). The appearance of fruiting bodies is generally red-orange, but in certain regions of Taiwan,

rarely yellow and white variants also occur. Metabolomic Profiling indicated that red AC possesses relatively higher contents of triterpenoids and diverse metabolites than yellow AC and white AC (Su et al., 2023).

Ever since the spread of AC to the mainland, products like camphor mushroom drop pills and camphor mushroom oral liquid have become popular in the form of healthcare products (Cheng et al., 2005). Wild-grown AC is rare and valuable, but demands have increased in recent years. Therefore, research has been carried out on artificial cultivation including solid state (cutting wood, agar plate medium) culture and liquid culture (submerged fermentation) (Zhang et al., 2019). Although cultured fungus may possess bioactivities similar to those of the naturally occurring fungus, there are several differences in the constituents of ingredients and the content of bioactive metabolites (Du et al., 2012; Tung et al., 2014).

Currently, more than 200 metabolites have been extracted and identified from AC. Many investigations have revealed their pharmacological activities and mechanisms, and some of them are generally recognized by the U.S. Food and Drug Administration (FDA) as potential drugs for clinical trials (Angamuthu et al., 2019). Each stage of the fungal life cycle creates metabolites usually differently. Mycelium, an exponential phase of AC, and polysaccharide is usually produced in this stage (Zhang et al., 2018). It is not easy to artificially cultivate fruiting bodies. The chemical metabolites of the fruiting body are different from the mycelium, and in general, the metabolites of the mycelium are also found in the fruiting body; more secondary metabolites are produced during this mature phase (Chang et al., 2006).

The physiologically active substances in AC can be mainly divided into triterpenoids, polysaccharides, derivatives of ubiquinone, and derivatives of maleic acid and succinic acid (Liu et al., 2023). Triterpenoids are one of the main metabolites of AC, and the content of triterpenoids is approximately 63% in the fruiting body (Geethangili and Tzeng, 2011). Antcins, a typical class of triterpenoids, have high medicinal activity (Kuang et al., 2021). AC polysaccharides are mainly composed of a variety of monosaccharides linked by glycosidic bonds (Lee et al., 2002) and exhibit excellent biological activity of anticancer and anti-inflammatory properties (Yang et al., 2022). Ubiquinones are a class of lipophilic quinones and antroquinonol, probably the most valuable derivatives of ubiquinone in AC, has strong biological activity (Zhang et al., 2017). Maleic acid and succinic acid derivatives also are characteristic active metabolites of AC, mainly antrodin and antrocinnamomin, which are mainly found in the mycelium stage (Nakamura et al., 2004).

Neurological diseases such as Alzheimer's disease (AD), Parkinson's disease (PD), and stroke are becoming serious public health issues, and currently there is still no effective cure or prevention strategies. AD is the most common cause of dementia in older individuals with the pathological hallmarks of amyloid plaques composed of amyloid-β (Aβ) and neurofibrillary tangles consist of phosphorylated tau protein (Kalampokini et al., 2019; Marino et al., 2020). Currently, approved drugs to treat AD are mainly effective in improving the symptoms (Alzheimer's Association, 2023; Yan et al., 2020). PD is the second-most common neurodegenerative disease, the pathological characteristics include the loss of dopaminergic neurons in the substantia nigra and the increase of Lewy body, which is caused by aggregation of α-synuclein in neurons (Beitz, 2014; Breijyeh et al., 2020). Current treatment of PD is limited to symptomatic relief (So et al., 2024). Stroke is one of the primary causes of disability and death worldwide, and ischemic stroke is the most common type (Zhao et al., 2022). Intravascular thrombosis is the primary pathogenic cause of ischemic stroke to result in brain damage, including cerebral tissue lesions and deficiencies in the neurons (Das et al., 2023). Therefore, preventative and improve of neural injuries strategies caused by stroke are of great clinical value.

Although various clinical manifestations are present in neurological disorders, common signaling pathways are shared by AD, PD, and ischemic stroke, including neuronal cell death, inflammation, and oxidative stress (Sun et al., 2022). Figure 1 shows the common signaling pathways in neurological disorders. Hence, research on the inhibition of the common pathway will be useful for the development of new drugs against all neurological disorders. AC has been reported to have excellent neuroprotective effects. In this focused review, we summarize the most recent findings on the neuroprotective properties of the extracts and bioactive metabolites of AC.

## 2 Safety evaluation of AC

Traditionally, AC has been used as a health food, and the historical use of this mushroom as a food supplement supports its safety. Previous studies on genotoxicity, teratotoxicity, and oral toxicity have showed the no-observed-adverse-effect-level (NOAEL) of AC in Sprague–Dawley (SD) rats (Lin et al., 2015). A recent study showed that fruiting body powders of dish-cultured AC did not cause mortality and clinical symptoms of toxicity (Liu et al., 2022). The freeze-dried mycelium of AC can be considered as a novel food by the European Commission, and the European Food Safety Authority (EFSA) Panel on Nutrition, Novel Foods, and Food Allergens has reported no adverse effects at the proposed use level (Turck et al., 2022). In addition to showing an acceptable safety and tolerability profile at doses of up to 2,988 mg/day with no appreciable side effects, a phase I clinical study in healthy adults also raised the possibility that LEAC-102 (a novel botanical drug extracted from AC, major compounds are antcin B, antcin K, and antcin H) may have novel immunomodulatory activities (Liao et al., 2023). Taken together, these findings indicate that crude extracts of AC and its products have no adverse effects on humans within a certain dose range.

The toxicology of metabolites from AC also has been studied. To assess the safety of antroquinonol, a phase I clinic trial was carried out using 50–600 mg daily for 1 month in patients with metastatic non-small-cell lung cancer. Antroquinonol exhibited a mild toxicity profile at all dose levels. Of the five patients with high does at 600 mg, three were evaluable for treatment response, and two achieved stable disease, which was generally considered safe and tolerable without dose-limiting toxicities. Then, the recommended dose for phase II clinic trial is at least 600 mg daily for non-small-cell lung cancer (Lee et al., 2015).

β-glucan (~65% pure) from AC was analyzed in the subchronic toxicity and mutagenicity study in CD (SD) IGS rats (~6 weeks old, 12/sex/group), and a daily dose of 2 g/kg for 3 months of oral

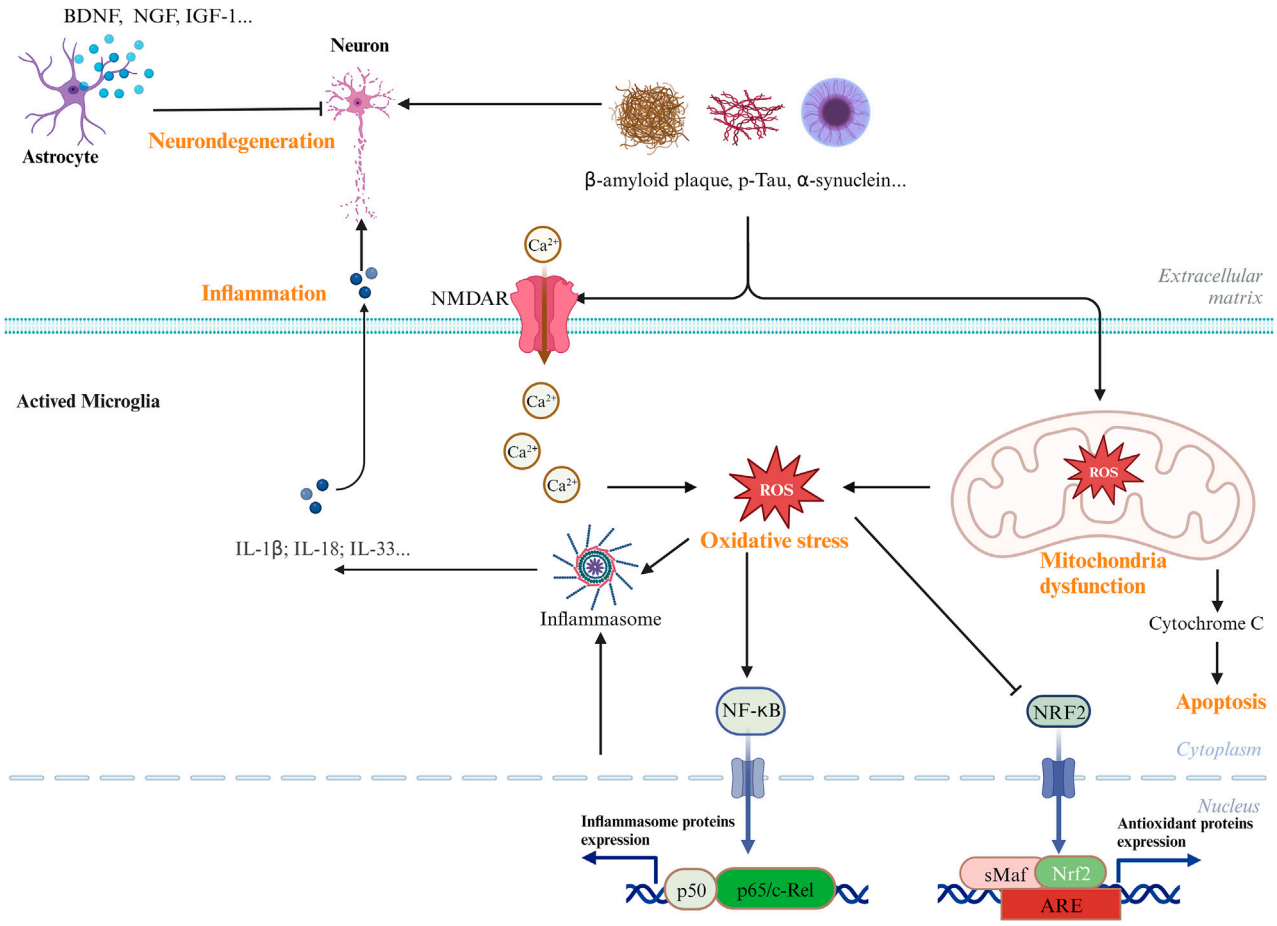


FIGURE 1
Common and major pathways in the CNS diseases. Biological processes, including oxidative stress, neuroinflammatory, and mitochondrial dysfunctions, have been involved in the development and pathogenesis of CNS diseases.

treatment did not show any adverse effects and genotoxicity (Chen et al., 2018). Therefore, AC and some of its bioactive metabolites showed no obvious toxicity within a reasonable dose range.

## 3 Metabolism and blood-brain barrier penetration of AC

As a dietary supplement and adjuvant therapeutic agent, AC is widely used, and the biological activities of different extracts of AC have been thoroughly investigated. Understanding the biological effects and safety of botanical drugs highly depends on preclinical research regarding the metabolism and pharmacokinetics.

To investigate the metabolism of AC *in vivo*, several reports performed mice experiments. A previous study performed oral administration of the ethanol extract of AC in SD rat, only antrodin B and C were detected in plasma (Liu et al., 2010). The metabolism and pharmacokinetics after oral administration of AC in male SD rats were studied (Qiao et al., 2015), and a total of 18 triterpenoids and 8 metabolites were detected in rat plasma after oral administration. Antcins K and H were the major exposure metabolites of AC. While the lanostanes were retained in the plasma at a low concentration for a considerable amount of time, the ergostanes were typically quickly absorbed and removed. Actin H was found in the tumor tissue of ICR mice with xenogra S180 tumor model after oral administration of AC extract (Li et al., 2018). In a Caco-2 cell monolayer model, most ergostanes exhibited high permeability (Wang et al., 2015). In detail, antcin H and antcin B could easily pass through the Caco-2 cell layer; antcins A, B, C, H, and K were absorbed through passive transcellular diffusion; and the permeability of lanostanes was poor, including dehydrosulphurenic acid, 15α-acetyldehydrosulphurenic acid, dehydroeburicoic acid, and eburicoic acid. Components could be absorbed in plasma is the basis for its entry into the brain regions by passing through the blood-brain barrier (BBB) or through the nose-to-brain pathway. The above-mentioned ergostanes in AC may exhibit biological activity for the treatment of neurologic diseases.

Using a SD rat model, the pharmacokinetic properties of ergosterol were investigated (Zhao et al., 2011). After a single oral administration of ergosterol (100 mg/kg) to SD rats, two metabolites (ERG1 and ERG2) were identified in the plasma, urine, and fecal samples. The side-chain was oxidized with β-d-glucopyranoside structure. The peak concentration (Cmax) time was 8.00 ± 1.18 h. Approximately 62.5% of the administered ergosterol was excreted from the feces, while 3.2% was eliminated from the urine. It remains unclear whether ergosterol can transport and metabolism in the brain.

The pharmacokinetics of antroquinonol by administration were evaluated in patients with metastatic non-small-cell lung cancer in a clinical study (Liao et al., 2023). The mean elimination half-life ranged from 1.30 to 4.33 h, regardless of the treatment dose. Four metabolites of antroquinonol were identified by NMR spectroscopic analysis from the male Wistar rats' urine following oral treatment (Chen et al., 2014). These results suggest that antroquinonol has good bioavailability, but the biological activity of four metabolites of antroquinonol was not determined.

The ability of drugs to cross the blood-brain barrier is critical for their neuroprotective function. After oral intake of antroquinonol in mice, no adverse effects were observed, and antroquinonol could penetrate through the blood-brain barrier (Chang et al., 2012). And adenosine from AC can enter brain and the brain efflux index was shown to be capable of reaching 90.1%±1.5% (Isakovic et al., 2004). More reports showed that the extracts and some active metabolites from AC have neuroprotective function, but the ability of them to cross the blood-brain barrier were not be detected. Further investigations need to be performed to clarify the usable of the candidates for neurological diseases.

# 4 Neuroprotection potential of AC

As a rich source of biologically active metabolites, AC exerts excellent effects on a variety of physiological processes and produces various bioactivities. Many other utilizable activities of AC await discovery. Hence, AC has enormous potential for the development of new drugs. The most recent findings on the therapeutic benefits, underlying mechanisms, and active metabolites of AC in the management and avoidance of neurological disorders are thoroughly reviewed in this article.

## 4.1 Neuroprotective activities of AC extracts

There is increasing evidence that AC is an encouraging candidate for various neurological disorders (Wang et al., 2019). Here, we have summarized the effects of AC in chronic neurodegenerative diseases including AD, PD, and other acute neurodegenerative diseases, mainly stroke.

### 4.1.1 Alzheimer's disease

Neuroinflammation, the production of free radicals in the brain, amyloidogenic processing, and the ensuing Aβ cascade-triggered neuronal dysfunction and death are the pathological hallmarks of AD and other forms of dementia, which are the potential targets for AD treatment (Simpson and Oliver, 2020). Pharmacological therapy for neurodegenerative diseases provides only temporary symptomatic relief; hence, more effective drugs need to be developed (Passeri et al., 2022). Natural products with diverse structure and excellent activity are the main sources of new drugs.

The accumulation of Aβ in the brain may directly contribute to the degeneration of neurons during the pathogenesis of AD. Several isoforms of Aβ peptide have been isolated *in vivo* including Aβ1–38, Aβ1–39, Aβ1–40, Aβ1–42, and Aβ1–43. Aβ1–40 is the predominant sequence isolated from cerebrospinal fluid, while Aβ1–42 is the predominant component of senile plaques in parenchyma (Miyashita et al., 2009). Meanwhile, Aβ1-40, which is more abundantly produced by the cells than Aβ1-42, is commonly colocalized with Aβ1-42 in the plaque. Likewise, Aβ25-35 fragment can also induce aggregation and toxicity, similar to Aβ1-42. Aβ peptide is with important applications in the establishment of AD cell model. Methanol extract (10–50 μg/mL) from the wild fruiting body could suppress the inflammation induced by Aβ25-35 in EOC13.31 microglia at a dose-dependent manner, indicating that AC might be useful for the prevention of inflammation in the neurodegenerative brain (Liu et al., 2007). A study was conducted to evaluate the effect of AC fruiting body and mycelium on alleviating neurotoxicity induced by Aβ1-40 in the PC12 cell model and AD animal model (Wang et al., 2012). The results showed that AC can improve the memory and learning abilities by inhibiting several AD risk factors, including reactive oxygen species (ROS), p-tau, and BACE expression, as well as Aβ1-40 accumulation, suggesting that the fruiting body has stronger anti-oxidant and anti-inflammatory abilities to inhibit Aβ1-40-induced neurotoxicity than the mycelium. Another study also reported that AC ethanol extract (ACEE) protected PC12 cells activated by Aβ25-35 via increasing the BcL-2/Bax ratio to resist apoptosis, reducing ROS, and modulating adenosine A1 receptor (ADORA1) to enhance neuroprotective bioactivity and adenosine A2 receptor (ADORA2) to inhibit neurodegeneration. It also prevented the formation of Aβ25-35 fibrils and the production of tumor necrosis factor-alpha (TNF-α), ROS, malondialdehyde (MDA), and NO. Binding the function and the composition determination, it is demonstrated that the high content of triterpenoids, phenolics, and adenosine in ACEE was responsible for the rescue of these detrimental effects (Chang et al., 2012).

### 4.1.2 Parkinson's disease

Typically, PD is mainly caused by intra-cytoplasmic α-synuclein aggregation in the dopaminergic neurons of the substantia nigra compacta, leading to a decrease in the release of dopamine in the striatum. Several hypotheses of the dopaminergic cell death include mitochondrial dysfunction, iron accumulation, and inflammation (Morris et al., 2024). The preference for natural products is attributed to their efficiency and comparably fewer side effects.

1-Methyl-4-phenyl-1,2,3,6-tetrahydropyridine (MPTP) is one of the most used neurotoxins in PD animal models. Recently, an *in vivo* study in a MPTP induced PD mouse model demonstrated the protective role of AC extract administration significantly reduce α-synuclein-positive neuron numbers, and protect the brain from MPTP-induced loss of $TH^+$ neurons, neuroinflammation, and oxidative stress to prevent dopaminergic cell death and glial activation (Lanza et al., 2023). 6-Hydroxydopamine (6-OHDA) is the most sought-after neurotoxin to identify oxidative stress-induced PD model *in vitro and in vivo* because it generates ROS and mimics the neuropathological and biochemical features, which can cause neuronal degradation and apoptosis in the dopaminergic neurons (Hernandez-Baltazar et al., 2017). Among solid-state-cultured mycelium of AC extracts, 11 metabolites belonging to quinone, phenolic acid derivatives, ubiquinone derivatives, alkaloids, and triterpenoid were identified to exhibit potent protective effects against 6-OHDA-induced toxicity to decrease dopaminergic neuronal loss in PC12 cells. The underlying

mechanism likely involved the restoration of morphological changes in the nuclei, the reduction of ROS production and caspase 3 activity (Zou et al., 2022).

#### 4.1.3 Stroke

The most prevalent type of stroke is ischemic stroke, which causes degeneration and death of neurons. The pathology of ischemic stroke is extremely complex, oxidative stress and inflammation are the two major players (Chamorro et al., 2021). Neuroprotection is a promising strategy for stroke treatment. Natural products are reported to have excellent antioxidant and anti-inflammatory activities (Chen et al., 2020).

The activation of JNK and p38 and concurrent inhibition of ERK are critical for induction of apoptosis in both neuronal and non-neuronal cells (Xia et al., 1995). It has been reported that AC could effectively prevent serum-deprived apoptosis of PC12 cells by increasing phosphorylated ERK and decreasing phosphorylated JNK and p38, and by regulating a PKA/CREB-dependent pathway (Huang et al., 2005; Lu et al., 2008). Oral treatment of AC extract provided neuroprotection in rats with thromboembolic stroke by reducing infarct volume, improves neurological outcome (Lee et al., 2014). Furthermore, downregulation of iNOS/HO-1/Bax/caspase-3 and inhibition of hydroxyl radical formation were the main molecular pathways behind the AC neuroprotective activity against cerebral ischemia in rats (Yang et al., 2015). Ethyl acetate crude extract of AC (EtOAc-AC) showed protective effects both in acute ischemic stroke (AIS) injured mice and oxygen-glucose deprivation (OGD) induced Neuro 2A cells by inhibiting inflammation and apoptosis (Wang et al., 2019). Cobalt chloride ($CoCl_2$) acts as hypoxia mimetic agent that increases the ROS production, resulting to the increase of inflammatory mediators such as TNF-α, interleukin 1 beta (IL-1β), inducible nitric oxide synthase (iNOS), and cyclooxygenase-2 (COX-2) (Zhong et al., 2014). In a recent study, the authors found that AC alcohol extracts (AC-AE) reduced cell damage against $CoCl_2$-induced hypoxic toxicity in both C6 neuronal and C6 glial cells, and significantly reduced the stroke infarct size and decreased the level of proinflammatory iNOS and COX-2, and increased anti-inflammatory Nrf2 and HO-1 content in experimental rats, suggesting that AC-AE possesses protective effects in the ischemic stroke model (Kong et al., 2021).

Evidence from the above studies support that the medical benefits of AC can alleviate neuronal disorders. This great potential on the neuroprotective drug development of AC has further encouraged researchers to identify its functional metabolites.

### 4.2 Neuroprotective activities of isolated metabolites

The protective role of AC on neuronal disorders has been demonstrated using *in vitro* and *in vivo* experiments. Common pathways including anti-apoptosis, anti-oxidant, and anti-inflammatory play crucial roles in the degeneration and loss of axons and neurons (Moujalled et al., 2021). The effects of metabolites isolated from AC on neurological disorders are reviewed below.

#### 4.2.1 Anti-apoptotic activities

Extensive neuronal loss was observed in neuronal disorders, and the apoptosis marker activated caspase-3 has been observed in AD, PD, and stroke, which suggested that apoptosis plays crucial roles in the pathological processes (Robertson et al., 2000). A common feature of most neurological diseases is the degeneration of neurons, thus, drugs that inhibit neuronal apoptosis could thus be candidates for therapy of neurodegenerative disorders (D'Mello and Chin, 2005). ADORA2 encodes the G protein-coupled adenosine receptor known as adenosine receptor subtype A2A, which can promote neuronal polarization and axon formation (Alçada-Morais et al., 2021). It is reported that adenosine (ADO) from AC could protect PC12 cells from serum deprivation by activation of the ADORA2 (Lu et al., 2006). Further research showed that adenosine suppressed JNK and p38 activities through a protein kinase A (PKA) pathway in serum-deprived PC12 cells (Lu et al., 2008).

#### 4.2.2 Antioxidant activities

Increasing ROS is demonstrated to be susceptible to neuronal damage and functional deficits, which results in neurological disorders including AD, PD, and ischemic stroke (Teleanu et al., 2022). Brain tissue is characterized by high levels of oxygen consumption and high metabolic demand, but relatively low levels of antioxidant enzymes (HO-1, SOD, CAT, and GPx) and non-enzymatic antioxidants (vitamin A, C, and E) (Halliwell, 1992). Therefore, supplementation of antioxidants represents an effective strategy of prevention and treatment to restore the functionality and survival of neuronal cells against oxidative stress.

Current evidence has shown that AC is a potent scavenger of direct oxygen free radicals that protects cells from oxidative damage. Polysaccharides isolated from AC (ACP) have been found to comprehensively improve the neuroethology of PD mice, including autonomic activity, coordination, motility ability, and cognitive ability. Investigation of the mechanisms showed that ACP can enhance the expression levels of dopamine and dihydroxyphenylacetic acid in the striatum, and significantly decrease the expression of NLRP3 inflammasome and downstream inflammatory factors in a dose-dependent manner (Han et al., 2019). NLRP3 inflammasome can be activated not only by a variety of exogenous pathogens, but also by certain endogenous signals and metabolites. ROS is an upstream signal for NLRP3 activation (Hernandes et al., 2014). Further study demonstrated that ACP intervention can lead to significantly decreased ROS-NLRP3 activation, reduce intracellular ROS, and the apoptotic rate at the cellular and *in vivo* levels (Han et al., 2020).

A recent study in amyloid precursor protein (APP) transgenic mice revealed that antroquinonol, a ubiquinone derivative isolated from AC, might significantly improve memory acquisition, alleviate Aβ plaque pathology, and inflammation, mainly by decreasing histone deacetylase 2 (HDAC2) and increasing Nrf2 levels (Chang et al., 2005). As the catalytic subunit of deacetylase repressor complexes, the increase of HDAC2 level and activity in AD have been linked to the worsening of neuronal and synaptic function (Gonzalez-Zuninga et al., 2014). Further antroquinonol administration studies showed that anxiety-related behavior and cognitive abilities in 3XTgAD mice could be significantly improved; furthermore, inflammatory markers, AD biomarkers, and oxidative

stress markers showed a significant decrease (Francesca et al., 2022). The results are consistent with previously study in the APP transgenic mice, which confirmed the antioxidant capacity of antroquinonol in AD model.

### 4.2.3 Anti-inflammatory activities

The prominent role inflammation plays in various age-related diseases such as AD, PD, and central nervous system (CNS) injury (Khadka et al., 2020). Glial cells and immune cells are associated with the instigation of neuroinflammation. Plenty of potential inflammatory targets for intervention have been proposed (DiSabato et al., 2016).

Several intracellular signaling and transcription factors mediated by the activation of microglia in turn activate the inflammatory pathway in cerebral haemorrhage. The US patent US20180353520 has claimed that the active metabolites dehydroeburicoic acid, dehydrosulphurenic acid, and 4,7-dimethoxy-5-methyl-1,3-benzodioxole from AC can be used for the treatment of stroke (Wu et al., 2018). Their anti-inflammatory bioactivities have been demonstrated by several studies (Shen et al., 2004; Deng et al., 2013; Shie et al., 2016). Oxidative stress is reported to play an important role in the activation of the inflammatory cascade (Fan et al., 2023). Antcin C is a well-known metabolite of AC, which exerts its hepatoprotective and antioxidative activities by modulating the Nrf2 pathway. It is also reported that antcin C treatment in rats with cerebral injury could reduce the oxidative stress parameters and inflammatory cytokine levels via inhibiting the TLR-4 pathway (Ling et al., 2020).

Ergosta-7,9 (11),22-trien-3β-ol (Ergostatrien-3β-ol; EK100), a triterpenoid metabolite abundant in both the fruiting bodies and (Chao et al., 2021), also showed promising medicinal uses in neurological disorders. EK100 and antrodin C effectively improved the autonomous behavior and social ability and alleviated amyloid plaque burden in APP/PS1 mice (Tsay et al., 2021). EK100 from AC improved AD symptoms in a *Drosophila* model with Aβ42 overexpression by preventing the activation of microglial (Liu et al., 2021). EK100 showed a significant anti-inflammatory effect against LPS-induced NO production in BV2 cells, with IC50 values of 18 ± 2 μM, which was almost as potent as the NF-κB inhibitor. In the AIS mouse model, EK100 treatment reduced ischemic brain injury by decreasing the expression of p65 and caspase 3. EK100 also promoted endogenous neurogenesis through GSK-3 inhibition and β-catenin activation by activating PI3K/Akt signaling, suggesting EK100 may have other targets in addition to anti-inflammatory activity and it may act as potent brain protective agent (Wang et al., 2019). In another study, EK100 treatment showed neuroprotective effects on ipsilateral injuries in a mouse model of collagenase-induced intracerebral hemorrhage (ICH) via inhibiting COX-2 and MMP-9; EK100 treatment also exerted significant anti-inflammatory function by downregulating JNK activation in BV-2 cells and ICH mice (Hsueh et al., 2021; Huang et al., 2021). The above reports demonstrated that EK100 isolated from AC showed obvious anti-inflammatory effects through interfering with several pathways and anti-neuropathy *in vivo* and *in vitro*.

Our previous study showed that ergosterol isolated from AC, an isomer of EK100, could suppress the activation of BV2 treated with LPS by inhibiting the NF-κB, MAPK, and AKT signaling pathways (Sun et al., 2023). Further investigation in LPS-treated ICR mice found that ergosterol exhibited anti-neuroinflammatory activity and maintained the synaptic proteins. Another group also reported that ergosterol isolated from *Auricularia polytricha* or *Cordyceps militaris* attenuated neuroinflammation in BV2 cells (Nallathamby et al., 2015; Sillapachaiyaporn et al., 2022a), and exhibited neuroprotective activity in TNF-α-induced HT-22 cells via regulating the expression of N-methyl-D-aspartate receptors (NMDARs) and antioxidant enzyme, and cell survival pathways (Sillapachaiyaporn et al., 2022b). Therefore, ergosterol exerts its neuroprotective effect mainly through its anti-neuroinflammatory property via multiple pathways.

### 4.2.4 Stimulation of neurite regrowth and NGF synthesis

Neurite regrowth promoters were found to be possible therapies for neurological disorders. These neuritogenic substances have the ability to stimulate the growth of neurites in neuronal cells and are expected to be effective in the treatment of nerve injuries (More et al., 2012). Nerve growth factor (NGF), brain derived neurotrophic factor (BDNF), neurotrophin 3 (NT-3), and glia-derived neurotrophic factor (GDNF) are identified as important factors called neurotrophins for the survival and differentiation of neurons as well as neuronal maintenance (Numakawa and Kajihara, 2023). Neurotrophic factors are one of the key mediators of neural plasticity and functional recovery. They have great potential as therapeutic drugs against neurodegenerative diseases.

Some lanostane triterpenoids such as tumulosic acid, polyporenic acid C, 16α-hydroxyeburicoic acid, dehydrotumulosic acid, and pachymic acid are also widely found in medicinal mushrooms other than AC and can induce neurite outgrowth in human astrocytoma 1321N1 and PC12 cells, which might be due to inducing the expression of neurotrophic factors, NGF, and BDNF (Hassan et al., 2022). Further investigation demonstrated that these metabolisms identified as neurotrophins show weak cytotoxic effects on mammalian cells, but they are lacking certain structural features. It is worthwhile to further study these fungi, including their secondary metabolisms, the function structural and so on, which might reveal the interesting chemotaxonomic relationships as well as hitherto unprecedented biological activities of the constituents from AC.

### 4.2.5 Inhibition of beta-amyloid toxicity

Aβ peptide is formed by a cleavage process of APP via beta-cleavage by the secretases beta (BACE1) and gamma-cleavage of gamma secretases. Oligomeric and fibrillar beta-amyloid are both toxic to neurons. Aβ-dependent neuronal death can cause changes in cell membrane fluidity and integrity, leading to ion leakage, disruption of cellular calcium balance, decreased membrane potential, ultimately promoting apoptosis and synaptic loss (Silva et al., 2023).

Five metabolites—19-hydroxylabda-8 (17)-en-16, 15- olide; 3b,19-dihydroxylabda-8 (17), 11E-dien-16,15-olide; 13-epi-3b, 19-dihydroxylabda-8 (17), 11E-dien-16, 15- olide; 19-hydroxylabda-8 (17), 13-dien-16,15-olide, and 14-deoxy-11,

TABLE 1 Summary of the main *in vitro* and preclinical studies on *Antrodia camphorata* and some active metabolites in the CNS diseases.

| Extract/metabolite | Model | Main effects | References |
|---|---|---|---|
| Water and ethanol extract of mycelium and fruiting body | Aβ1-40-induced PC12 cells and Aβ1-40 infusion AD rats | Improved working memory ability | Wang et al. (2012) |
| Ethanolic extract | $A\beta_{25-35}$ induced PC12 cells | Rescued neuronal death by suppressing ROS and modulated ADORA1 and ADORA2A | Chang et al. (2012) |
| Methanol extract of fruiting body | $A\beta_{25-35}$-induced EOC13.31 cells | Inhibited both iNOS and cyclooxygenase-2 (COX-2) expression | Liu et al. (2007) |
| Commercial AC extract | MPTP-induced PD model mice | Increased tyrosine hydroxylase expression, reduced alpha-synuclein-positive neurons number, attenuated the neuroinflammatory state, reduced oxidative stress | Lanza et al. (2023) |
| Solid-state-cultured mycelium | 6-OHDA-induced PC12 cells | Increased cell viability, inhibited cell apoptosis, upregulated tyrosine hydroxylase and dopamine transporter levels, downregulated α-synuclein level | Zou et al. (2022) |
| Ethanolic mycelial extract | Serum deprivation-induced PC12 | Prevented cell apoptosis through MAPK and PKA/CREB pathway | Huang et al. (2005)<br>Lu et al. (2008) |
| Commercial crude extracts | MCAO-induced ischemia rats | Reestablished blood flow, inhibited HO-1, inflammatory responses apoptosis, and free radical formation | Yang et al. (2015)<br>Kong et al. (2021) |
| Alcohol extracts | $CoCl_2$-induced C6/PC12 cells and stroke rat | Reduced cell damage and decreased ROS production, stroke infarct size and MDA level and increased the level of antioxidants | Lee et al. (2014) |
| Ethyl acetate crude extract | Mice AIS model | Activated PI3K/Akt and inhibited GSK-3 to decrease p65NF-κB, caspase 3 and promote neurogenesis | Wang et al. (2019b) |
| ACP | MES23.5 cells and 6-OHDA-induced PD mice | Improved the neurobehavioral behavior, inhibited ROS-NLRP3 signaling | Han et al. (2019)<br>Han et al. (2020) |
| Antcin C | Cerebral injured rats | Reduced the neurological scores and volumes, oxidative stress and cytokine levels; ameliorated TLR-4, IRAK4, and zonula occludens-1 proteins | Ling et al. (2020) |
| Antrodin C | APPswe/PS1dE9 mice | Reduced amyloid deposits and promoted nesting behavior through microglia and perivascular clearance | Tsay et al. (2021) |
| EK100 | Mice AIS model | Activated PI3K/Akt and inhibited GSK-3 to decrease p65NF-κB, caspase 3 and promote neurogenesis | Wang et al. (2019a); Hsueh et al. (2021); Huang et al. (2021); Liu et al. (2021) |
| | Mice ICH model | Inhibited microglial JNK activation, attenuated brain COX-2 expression, MMP-9 activation, inflammatory cytokines and brain injuries | |
| | AD model | Reduced microglia activation, decreased caspase 3 expression; improved the life span, motor function, learning, and memory | |
| Ergosterol | LPS- or BPA-induced BV2 cells | Inhibited the NF-κB, AKT, and MAPK signaling pathways and pro-inflammatory cytokine levels, restored synaptic proteins expression | Nallathamby et al. (2015); Sillapachaiyaporn et al. (2022a); Sillapachaiyaporn et al. (2022b); Sun et al. (2023) |
| | LPS-induced ICR mice | | |
| | TNF-α-induced HT22 cells | Promoted neuronal survival via Akt/GSK-3β signaling | |
| Antroquinonol | APPswe/PS1dE9 mice | Improved learning and memory, reduced hippocampal Aβ levels and astrogliosis, increased Nrf2 and decreased histone deacetylase 2 levels | Chang et al. (2005) |
| | 3XTgAD mice | | Francesca et al. (2022) |

(Continued on following page)

TABLE 1 (*Continued*) Summary of the main *in vitro* and preclinical studies on *Antrodia camphorata* and some active metabolites in the CNS diseases.

| Extract/metabolite | Model | Main effects | References |
|---|---|---|---|
| | | Improved behavior and cognitive abilities, reduced systemic inflammatory markers, AD biomarker levels, oxidative markers | |
| Adenosine | Serum deprivation-induced PC12 | Activated A (2A)-R to prevent cell apoptosis | Lu et al. (2006); Lu et al. (2008) |
| 19-hydroxylabda-8 (17)-en-16,15-olide | $A\beta_{25-35}$-treated Cortical neurons | Protected neuronal viability | Chen et al. (2006) |
| 3â, 19-dihydroxylabda-8 (17), 11E-dien-16,15-olide | | | |
| 13-epi-3â,19-dihydroxylabda-8 (17), 11E-dien-16,15-olide | | | |
| 19-hydroxylabda-8 (17), 13-dien-16,15-olide | | | |
| 14-deoxy-11,12-didehydroandrographolide | | | |
| Tumulosic acid polyporenic acid C 16α-hydroxyeburiconic acid | Rat 1321N1 cells and PC12 cells | Stimulated neurite outgrowth, increased NGF and BDNF levels | Hassan et al. (2022) |

12-didehydroandrographolide—were obtained from the fruiting bodies of AC, and showed neuronal protection against Aβ25–35 damage (Chen et al., 2006). The above-mentioned studies have been demonstrated to be the basic substance of AC for neuroprotection.

Metabolites derived from AC possess potential neuroprotective properties via its various bioactivities. We have summarized the effects of some active metabolites from the AC on CNS diseases in Table 1.

## 5 Potential with the gut-microbiome-brain axis of AC

The gut microbiome plays a key role in human health, such as overall homeostasis maintenance, immune system moderation, and central nervous system regulation. Increasing clinical and preclinical evidence points to the existence of the microbiota-gut-brain axis that forms a bidirectional network between the CNS and the gut (Singh et al., 2016; Sharon et al., 2019). Microbial imbalance is particularly linked to various neurological disorders including AD (Cattaneo et al., 2017), PD (Forsyth et al., 2011), and stroke (Sorboni et al., 2022). Plenty of research has attempted to define the molecular cross-talk between the host and microbiome to provide novel perspectives on promising therapeutic approaches for the management of neurological disorders (Mou et al., 2022).

A previous study in the leptin-induced Caco-2 cells model found that AC had a positive effect on intestinal microflora by repairing intestinal-barrier damage and enhancing the integrity of the intestinal barrier (Tsai et al., 2020). Another study in high-fat diet (HFD)-fed mice demonstrated that AC showed protective effects, maintained the intestinal barrier integrity, reduced the Firmicutes/Bacteroidetes ratio and increased *Akkermansia muciniphila* level (Chang et al., 2018). It is also reported that solid-state cultured AC can reduce hyperglycemia and tend to alleviate metabolic disorder in HFD-induced obese mice, mainly reduce the relative abundance of Firmicutes-to-Bacteroidetes ratio and elevate the relative abundance of *Akkermansia* spp. (Wang et al., 2020). The arrangement of the enterocyte was not disrupted by AC extract treatment, but intactness and denseness of hepatic tissue was elevated by regulating redox and cytoskeleton-related proteins and increasing the abundance of *Akkermansia* spp. in the gut microbiota of C57BL/6 mice (Tsai et al., 2021). *Akkermansia* spp. has reported to improve the situation of AD and PD (He et al., 2022). The above studies demonstrated that AC has neuroprotective potential in the gut microbiome by increasing probiotic bacteria *Akkermansia* spp.

In addition to crude extracts, the functions of AC metabolites on the microbiota-gut-brain axis have also been studied. In LPS-stressed slow-growing broiler breeds model, dietary supplement with 100–400 mg/kg ACP showed beneficial effects on liver damage and the bacterial microbiota species richness and diversity (Ye et al., 2022). Additionally, ACP inhibited the rise of Proteobacteria in LPS-induced group, while restored the beneficial cecal microbiota (typically *Lactobacillus*, *Faecalibacterium*, and Christensenellaceae R-7 group). Thus, ACP enhanced the species richness, and diversity indices might be related to the anti-inflammatory effect. Intragastric administration of exopolysaccharides from AC in lincomycin hydrochloride (LIH)-induced mice greatly reduced serum inflammatory cytokine levels and alleviated immune organs damage, while also regulating the microbial environment via enhancing the relative abundance of beneficial microbiota in the intestine (typically *Lactobacillus*, *Roseburia*, *Ligilactobacillus*, and Lachnospiraceae_NK4A136_group), and reducing the relative abundances of harmful microbes such as *Enterococcus* and *Shigella* (Lu et al., 2022), which were increased in AD subjects (Hou et al., 2021). Antrodin A from AC can alleviate the alcohol-induced metabolic disorders via regulating the composition of intestinal microbiota by decreasing *Clostridium sensu stricto 1*, Lachnospiraceae_NK4A136_group, Prevotellaceae_NK3B31_group, and Prevotellaceae_UCG-001, and increasing the relative abundance of *Lactobacillus* and *Dubosiella* (Yi et al., 2021). Another study demonstrated that the ethyl acetate layer of AC mycelium extract, especially antrodin A, and antroquinonol decreased the abundance of intestinal Helicobacteraceae and increased the relative abundance of Lachnospiraceae and Ruminococcaceae to prevent alcohol-induced oxidative stress and

TABLE 2 Summary of the effects of *Antrodia camphorata* treatment on the GM in different models.

| Model | Treatment | Increased bacteria | Decreased bacteria | References |
|---|---|---|---|---|
| HFD-induced mice | Ethanol extract; 230 mg/kg/day by gavage for 14 weeks | *Akkermansia muciniphila* | *Mucispirillum* and *Blautia* | Chang et al. (2018) |
| | Water extract<br>0.009 and 0.09 g/kg/day for 8 weeks | *Streptococcus* spp., *Eubacterium* spp., *Eggerthella lenta*, *Clostridium methylpentosum*, *A. muciniphila* | Ruminococcaceae and Lachnospiraceae at the family level<br>*Clostridium scindens* and *Clostridium cocleatum* at the species level | Wang et al. (2020) |
| C57BL/6 mice | Solid-state cultivated mycelium; 1.6667 g/kg for 4 weeks | *Alistipes shahii* | | Tsai et al. (2021) |
| ICR mice | Exopolysaccharides<br>0.08, 0.25, 0.75 g/kg 12 days | *Lactobacillus*, *Roseburia*, *Ligilactobacillus*, and Lachnospiraceae_NK4A136_group | *Enterococcus* and *Shigella* | Lu et al. (2022) |
| LPS-induced chicken | ACP; 100, 200, and 400 mg/kg for 21 days | Proteobacteria<br>*Alistipes*, *Ruminiclostridium*, *Megamonas*, [*Ruminococcus*] torques group and *Campylobacter* | Firmicutes, *Lactobacillus*, and *Synergistes* | Ye et al. (2022) |
| Alcoholic liver injury mice | Antrodin A<br>75, 150 mg/kg for 15 days | Firmicutes, *Lactobacillus,* and *Dubosiella* | *Bacteroidetes*, Lachnospiraceae_NK4A136_group, *Prevotellaceae_NK3B31_ group, Prevotellaceae_UCG-001, and Clostridium_ sensu_stricto_1* | Yi et al. (2020); Yi et al. (2021) |
| | Antrodin A; 100, 200 mg/kg/day for 12 days | Muribaculaceae, *Lactobacillus,* Lachnospiraceae<br>Firmicutes, Bacteroidetes<br>Ruminococcaceae | Erysipelotrichaceae, Helicobacteraceae, Proteobacteria | |

inflammation in mice (Yi et al., 2020). The decrease of Ruminococcaceae could act as a predictive marker for the rapidly progressive mild cognitive impairment (Yang et al., 2023). According to these studies, AC metabolites may have the potential to modulate the brain-gut axis.

The composition of the gut microbiota is important for host homeostatic functions. AC and its active metabolites showed prebiotic effects on the gut microbiome to affect the state of the brain and nervous system. AC might show its neuroprotective activity on the gut-microbiota-brain axis. We summarized the effects of AC in the gut microbiome in Table 2. Figure 2 presents the neuroprotective effects of bioactive molecules contained within AC by working on nervous system and gut-microbiota.

# 6 Future perspectives

AC is a valuable and medicinal fungus known widely and has tremendous medicinal properties and nutritional value for brain health. It possesses several health-endorsing properties such as anti-oxidant, anti-apoptosis, and anti-inflammatory and probably improves the gut microbiome in neurologic disorders. In general, the isolated metabolites from AC have not been deeply and systematically studied in neuroscience. There are still metabolites that have not been identified; hence, AC has great potential. For metabolites that have entered clinical evaluation, production should be increased by applying different strategies. Furthermore, in-depth pharmacokinetic studies and modification of AC metabolites are also lacking. The following aspects of AC research could be improved:

## 6.1 Increase the production of the bioactive metabolites in AC

Genomic and transcriptomic analyzes will help to develop strategies to increase the production of useful metabolites (Lu et al., 2014). For tissue-specific metabolites, secondary metabolites biosynthesis pathway genes were enriched, including 14-α-demethylase (CYP51F1) for the conversion of lanosterol to ergosteroidal triterpenes in fruiting bodies, coenzyme Q (COQ) for the synthesis of antroquinonol in mycelia, and polyketide synthase for the synthesis of antrocamphin in fruiting bodies. It was reported that talc enhanced the yield of the bioactive secondary metabolite antioxidant antrodin C in the submerged fermentation of AC by increasing the permeability and fluidity of the cell membrane, upregulating the key genes and then improving the biosynthesis process (Fan J. H. et al., 2023). Another study showed that oxidative stressors supplementation (such as hydrogen peroxide) can increase the yield of antrodin C in submerged fermentation of AC (Hu et al., 2020). For instance, biosynthesis is a strategy to achieve industrial-scale production for the identification of novel metabolites and improvement of the yield of previously known valuable metabolites.

## 6.2 Specific investigation of metabolite pharmacology and pharmacokinetics

As an emerging medicinal fungus, AC has a variety of important biological activities and pharmacological functions, a variety of bioactive metabolites from its fruiting bodies and mycelia that have been isolated and purified, but the underlying mechanism

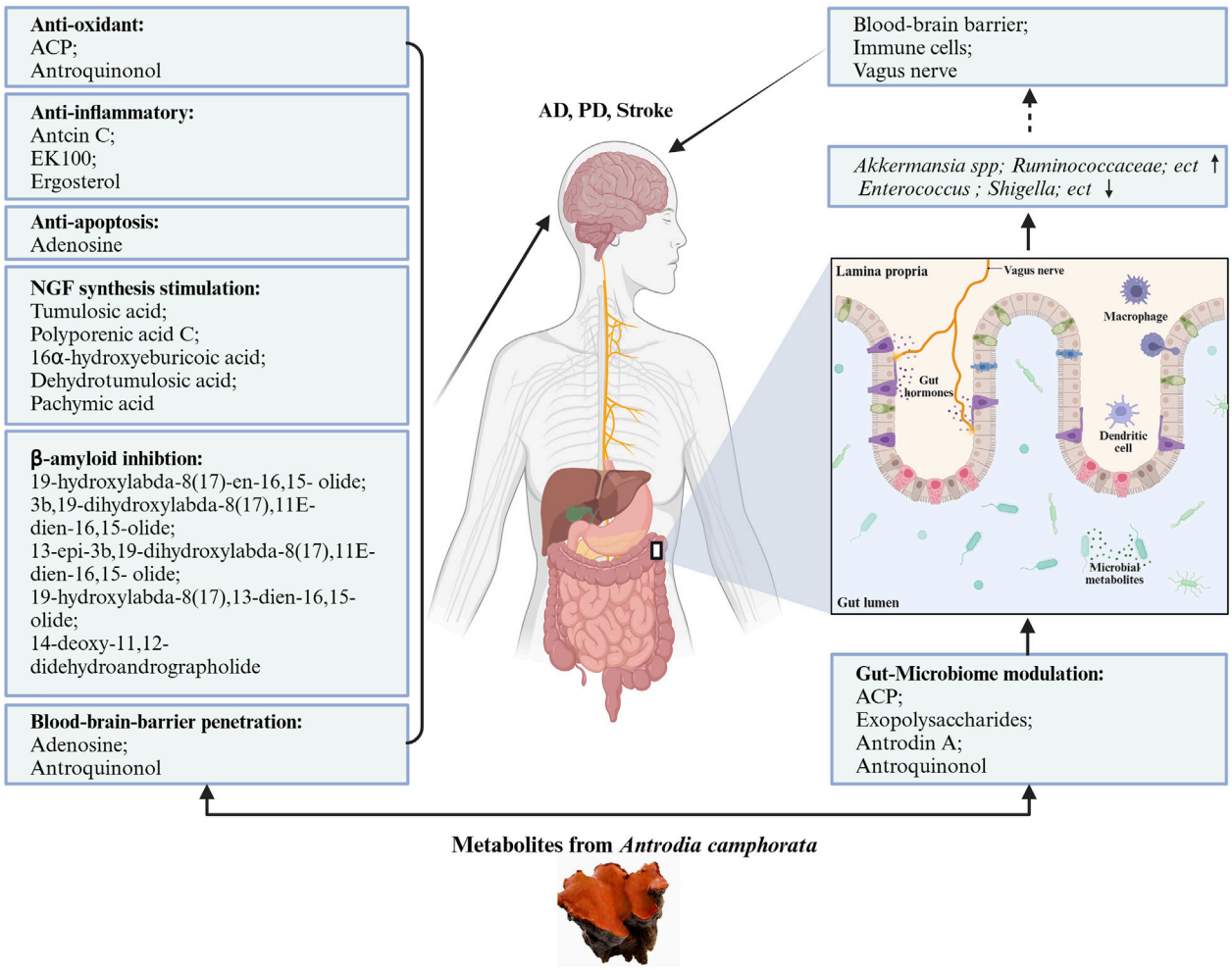


FIGURE 2
Neuroprotective potentials of *Antrodia camphorata*. The bioactive metabolites from AC play neuroprotective function directly by anti-oxidant, anti-inflammatory, anti-apoptotic, stimulation NGF synthesis, and beta-amyloid inhibition pattern, also indirectly by gut-microbiome modulation.

such as the pharmacokinetics and pharmacodynamics remain unclear, which are important for further biochemical research and clinical trials. The establishment of an intracerebral pharmacokinetic research model will truly reflect the process of treatment and action of drugs after entering the brain tissue, ensuring the effective concentration of brain-targeted drugs in the brain and preventing the damage of non-brain-targeted drugs to neurological function, thereby greatly improving the effectiveness and safety. Most pharmacological studies were derived from *in vitro* laboratory investigations; hence, further preclinical studies are necessitated for a full evaluation of these valuable metabolites from AC *in vivo* experiments to promote clinical applications and complete the clinical validation for potential therapeutic benefits.

## 6.3 Strategies for bioavailability improvement of the metabolites from AC

Structure function studies are important for the design of more effective drugs, and many pharmacological actions and its molecular mechanisms are defined. The structures of terpenoids isolated from AC are closely related to the anti-inflammatory activity. The substituents on C15 are crucial to the anti-inflammatory properties of lanostane-type metabolites (Yang et al., 2022).

Chemical modification is necessary to enhance the structural diversity and druggability of natural products. It has been demonstrated that side-chain esterification increased the antitumor activity of *Antrodia* ergosteroids (Li et al., 2020). Furthermore, a number of investigations have shown that amide derivatives of triterpenoids containing nitrogen heterocycles or anilines at the side chain exhibit higher cytotoxicity than the original metabolites (Li et al., 2021). Ergosterol lacks aqueous solubility, but a study found that solubility and bioavailability can be improved by using nanostructured lipid carriers (NLCs). Nanoparticles drug delivery system can also improve the bioavailability of ergosterol following oral administration (Zhang et al., 2016). AC modified the nanocarrier β-cyclodextrin (BCD) inclusion complex could potentially unlock its full potential and attempt to make it suitable for improving skeletal muscle health and possible to develop evidence-based drug (Menon et al., 2022). The blood-brain barrier penetration of potential drugs is a critical issue, and delivery of these neuroprotective metabolites into the brain

requires a tremendous effort, for which nanomedicine has emerged as a promising approach.

## Author contributions

WL: Writing–original draft, Writing–review and editing. PW: Writing–review and editing. JQ: Funding acquisition, Writing–review and editing. YL: Writing–review and editing. QP: Writing–review and editing. ZZ: Funding acquisition, Writing–review and editing. XS: Supervision, Writing–review and editing. YX: Conceptualization, Writing–review and editing. BS: Conceptualization, Writing–review and editing.

## Funding

The author(s) declare financial support was received for the research, authorship, and/or publication of this article. This work was supported by the Research Fund of Jianghan University (grants number: 08190006; 2022SXZX28) and Wuhan Municipal Education Bureau (CXY202204).

## Acknowledgments

The authors acknowledge Biorender that is used to create schematic Figures 1, 2.

## Conflict of interest

The authors declare that the research was conducted in the absence of any commercial or financial relationships that could be construed as a potential conflict of interest.

## Publisher's note



## References

Alçada-Morais, S., Gonçalves, N., Moreno-Juan, V., Andres, B., Ferreira, S., Marques, J. M., et al. (2021). Adenosine A2A receptors contribute to the radial migration of cortical projection neurons through the regulation of neuronal polarization and axon formation. *Cereb. Cortex* 31 (12), 5652–5663. doi:10.1093/cercor/bhab188

Alzheimer's Association (2023). Alzheimer's disease facts and figures. *Alzheimers Dement.* 194, 1598–1695. doi:10.1002/alz.13016

Angamuthu, V., Shanmugavadivu, M., Nagarajan, G., and Velmurugan, B. K. (2019). Pharmacological activities of antroquinonol- Mini review. *Chem. Biol. Interact.* 297, 8–15. doi:10.1016/j.cbi.2018.10.009

Beitz, J. M. (2014). Parkinson's disease: a review. *Front. Biosci. Sch. Ed.* 6 (1), 65–74. doi:10.2741/s415

Breijyeh, Z., and Karaman, R. (2020). Comprehensive review on Alzheimer's disease: causes and treatment. *Molecules* 25 (24), 5789. doi:10.3390/molecules25245789

Cattaneo, A., Cattane, N., Galluzzi, S., Provasi, S., Lopizzo, N., Festari, C., et al. (2017). Association of brain amyloidosis with pro-inflammatory gut bacterial taxa and peripheral inflammation markers in cognitively impaired elderly. *Neurobiol. Aging* 49, 60–68. doi:10.1016/j.neurobiolaging.2016.08.019

Chamorro, Á., Lo, E. H., Renú, A., van Leyen, K., and Lyden, P. D. (2021). The future of neuroprotection in stroke. *J. Neurol. Neurosurg. Psychiatry* 92 (2), 129–135. doi:10.1136/jnnp-2020-324283

Chang, C. H., Wang, H. E., Liaw, P. Y., Peng, C. C., and Peng, R. Y. (2012). Antrodia cinnamomea exhibits a potent neuroprotective effect in the PC12 Cell-Aβ25-35 model - pharmacologically through adenosine receptors and mitochondrial pathway. *Planta Med.* 78 (17), 1813–1823. doi:10.1055/s-0032-1315397

Chang, C. J., Lu, C. C., Lin, C. S., Martel, J., Ko, Y. F., Ojcius, D. M., et al. (2018). Antrodia cinnamomea reduces obesity and modulates the gut microbiota in high-fat diet-fed mice. *Int. J. Obes. (Lond).* 42 (2), 231–243. doi:10.1038/ijo.2017.149

Chang, C. Y., Lee, C. L., and Pan, T. M. (2006). Statistical optimization of medium components for the production of Antrodia cinnamomea AC0623 in submerged cultures. *Appl. Microbiol. Biotechnol.* 72 (4), 654–661. doi:10.1007/s00253-006-0325-6

Chao, T. Y., Hsieh, C. C., Hsu, S. M., Wan, C. H., Lian, G. T., Tseng, Y. H., et al. (2021). Ergostatrien-3β-ol (EK100) from Antrodia camphorata attenuates oxidative stress, inflammation, and liver Injury *in vitro* and *in vivo*. *Prev. Nutr. Food Sci.* 26 (1), 58–66. doi:10.3746/pnf.2021.26.1.58

Chen, C. C., Shiao, Y. J., Lin, R. D., Shao, Y. Y., Lai, M. N., Lin, C. C., et al. (2006). Neuroprotective diterpenes from the fruiting body of Antrodia camphorata. *J. Nat. Prod.* 69 (4), 689–691. doi:10.1021/np0581263

Chen, C. K., Kang, J. J., Wen, W. C., Chiang, H. F., and Lee, S. S. (2014). Metabolites of antroquinonol found in rat urine following oral administration. *J. Nat. Prod.* 77 (4), 1061–1064. doi:10.1021/np400670a

Chen, H., He, Y., Chen, S., Qi, S., and Shen, J. (2020). Therapeutic targets of oxidative/nitrosative stress and neuroinflammation in ischemic stroke: applications for natural product efficacy with omics and systemic biology. *Pharmacol. Res.* 158, 104877. doi:10.1016/j.phrs.2020.104877

Chen, J. J., Zhang, Z., Wang, Y., Yuan, X. L., Wang, J., Yang, Y. M., et al. (2023). Transcriptome analysis of Antrodia cinnamomea mycelia from different wood substrates. *Mycobiology* 51 (1), 49–59. doi:10.1080/12298093.2023.2175434

Chen, S. N., Chang, C. S., Chen, S., and Soni, M. (2018). Subchronic toxicity and genotoxicity studies of Antrodia mushroom β-glucan preparation. *Regul. Toxicol. Pharmacol.* 92, 429–438. doi:10.1016/j.yrtph.2017.12.022

Cheng, J. J., Yang, C. J., Cheng, C. H., Wang, Y. T., Huang, N. K., and Lu, M. K. (2005). Characterization and functional study of Antrodia camphorata lipopolysaccharide. *J. Agric. Food Chem.* 53 (2), 469–474. doi:10.1021/jf049281a

Das, T. K., Ganesh, B. P., and Fatima-Shad, K. (2023). Common signaling pathways involved in Alzheimer's disease and stroke: two faces of the same coin. *J. Alzheimers Dis. Rep.* 7 (1), 381–398. doi:10.3233/ADR-220108

Deng, J. S., Huang, S. S., Lin, T. H., Lee, M. M., Kuo, C. C., Sung, P. J., et al. (2013). Analgesic and anti-inflammatory bioactivities of eburicoic acid and dehydroeburicoic acid isolated from Antrodia camphorata on the inflammatory mediator expression in mice. *J. Agric. Food Chem.* 61 (21), 5064–5071. doi:10.1021/jf303820k

DiSabato, D. J., Quan, N., and Godbout, J. P. (2016). Neuroinflammation: the devil is in the details. *Journal of neurochemistry* 139 (2), 136–153. doi:10.1111/jnc.13607

D'Mello, S. R., and Chin, P. C. (2005). Treating neurodegenerative conditions through the understanding of neuronal apoptosis. *Curr. Drug Targets CNS Neurol. Disord.* 4 (1), 3–23. doi:10.2174/1568007053005118

Du, Y. C., Wu, T. Y., Chang, F. R., Lin, W. Y., Hsu, Y. M., Cheng, F. T., et al. (2012). Chemical profiling of the cytotoxic triterpenoid-concentrating fraction and characterization of ergostane stereo-isomer ingredients from Antrodia camphorata. *J. Pharm. Biomed. Anal.* 58, 182–192. doi:10.1016/j.jpba.2011.09.007

Fan, H., Bai, Q., Yang, Y., Shi, X., Du, G., Yan, J., et al. (2023a). The key roles of reactive oxygen species in microglial inflammatory activation: regulation by endogenous antioxidant system and exogenous sulfur-containing compounds. *Eur. J. Pharmacol.* 956, 175966. doi:10.1016/j.ejphar.2023.175966

Fan, J. H., Lai, K. S., Huang, Y. Y., Chen, H. Y., Xiong, L. Q., Guo, H. K., et al. (2023b). Efficient production of Antrodin C by microparticle-enhanced cultivation of medicinal mushroom Antrodia cinnamomea. *J. Biosci. Bioeng.* 135 (3), 232–237. doi:10.1016/j.jbiosc.2022.12.013

Forsyth, C. B., Shannon, K. M., Kordower, J. H., Voigt, R. M., Shaikh, M., Jaglin, J. A., et al. (2011). Increased intestinal permeability correlates with sigmoid mucosa alpha-synuclein staining and endotoxin exposure markers in early Parkinson's disease. *PloS one* 6 (12), e28032. doi:10.1371/journal.pone.0028032

Francesca, F., Caitlin, A., Sarah, L., and Robyn, G. L. (2022). Antroquinonol administration in animal preclinical studies for Alzheimer's disease (AD): a new avenue for modifying progression of AD pathophysiology. *Brain Behav. Immun. Health* 21, 100435. doi:10.1016/j.bbih.2022.100435

Geethangili, M., and Tzeng, Y. M. (2011). Review of pharmacological effects of Antrodia camphorata and its bioactive compounds. *Evid. Based Complement. Altern. Med.* 2011, 212641. doi:10.1093/ecam/nep108

Gonzalez-Zuñiga, M., Contreras, P. S., Estrada, L. D., Chamorro, D., Villagra, A., Zanlungo, S., et al. (2014). c-Abl stabilizes HDAC2 levels by tyrosine phosphorylation repressing neuronal gene expression in Alzheimer's disease. *Mol. Cell* 56 (1), 163–173. doi:10.1016/j.molcel.2014.08.013

Halliwell, B. (1992). Reactive oxygen species and the central nervous system. *J. Neurochem.* 59, 1609–1623. doi:10.1111/j.1471-4159.1992.tb10990.x

Han, C., Guo, L., Yang, Y., Li, W., Sheng, Y., Wang, J., et al. (2019). Study on Antrodia camphorata polysaccharide in alleviating the neuroethology of PD mice by decreasing the expression of NLRP3 inflammasome. *Phytother. Res.* 33 (9), 2288–2297. doi:10.1002/ptr.6388

Han, C., Shen, H., Yang, Y., Sheng, Y., Wang, J., Li, W., et al. (2020). Antrodia camphorata polysaccharide resists 6-OHDA-induced dopaminergic neuronal damage by inhibiting ROS-NLRP3 activation. *Brain Behav.* 10 (11), e01824. doi:10.1002/brb3.1824

Hassan, K., Matio Kemkuignou, B., Kirchenwitz, M., Wittstein, K., Rascher-Albaghdadi, M., Chepkirui, C., et al. (2022). Neurotrophic and immunomodulatory lanostane triterpenoids from wood-inhabiting Basidiomycota. *Int. J. Mol. Sci.* 23 (21), 13593. doi:10.3390/ijms232113593

He, X., Yan, C., Zhao, S., Zhao, Y., Huang, R., and Li, Y. (2022). The preventive effects of probiotic Akkermansia muciniphila on D-galactose/AlCl3 mediated Alzheimer's disease-like rats. *Exp. Gerontol.* 170, 111959. doi:10.1016/j.exger.2022.111959

Hernandes, M. S., D'Avila, J. C., Trevelin, S. C., Reis, P. A., Kinjo, E. R., Lopes, L. R., et al. (2014). The role of Nox2-derived ROS in the development of cognitive impairment after sepsis. *J. Neuroinflammation* 11, 36. doi:10.1186/1742-2094-11-36

Hernandez-Baltazar, D., Zavala-Flores, L. M., and Villanueva-Olivo, A. (2017). The 6-hydroxydopamine model and parkinsonian pathophysiology: novel findings in an older model. *Neurologia* 32 (8), 533–539. doi:10.1016/j.nrl.2015.06.011

Hou, M., Xu, G., Ran, M., Luo, W., and Wang, H. (2021). APOE-ε4 carrier status and gut microbiota dysbiosis in patients with Alzheimer disease. *Front. Neurosci.* 15, 619051. doi:10.3389/fnins.2021.619051

Hsueh, P. J., Wang, M. H., Hsiao, C. J., Chen, C. K., Lin, F. L., Huang, S. H., et al. (2021). Ergosta-7,9(11),22-trien-3β-ol alleviates intracerebral hemorrhage-induced brain injury and BV-2 microglial activation. *Molecules* 26 (10), 2970. doi:10.3390/molecules26102970

Hu, P. F., Huang, J., Chen, L., Ding, Z., Liu, L., Molnár, I., et al. (2020). Oxidative stress induction is a rational strategy to enhance the productivity of Antrodia cinnamomea fermentations for the antioxidant secondary metabolite Antrodin C. *J. Agric. Food Chem.* 68 (13), 3995–4004. doi:10.1021/acs.jafc.9b07965

Huang, N. K., Cheng, J. J., Lai, W. L., and Lu, M. K. (2005). Antrodia camphorata prevents rat pheochromocytoma cells from serum deprivation-induced apoptosis. *FEMS Microbiol. Lett.* 244 (1), 213–219. doi:10.1016/j.femsle.2005.01.048

Huang, Y. P., Chen, D. R., Lin, W. J., Lin, Y. H., Chen, J. Y., Kuo, Y. H., et al. (2021). Ergosta-7,9(11),22-trien-3β-ol attenuates inflammatory responses via inhibiting MAPK/AP-1 induced IL-6/JAK/STAT pathways and activating Nrf2/HO-1 signaling in LPS-stimulated macrophage-like cells. *Antioxidants* 10 (9), 1430. doi:10.3390/antiox10091430

Isakovic, A. J., Abbott, N. J., and Redzic, Z. B. (2004). Brain to blood efflux transport of adenosine: blood-brain barrier studies in the rat. *J. Neurochem.* 90 (2), 272–286. doi:10.1111/j.1471-4159.2004.02439.x

Kalampokini, S., Becker, A., Fassbender, K., Lyros, E., and Unger, M. M. (2019). Nonpharmacological modulation of chronic inflammation in Parkinson's disease: role of diet interventions. *Park. Dis.* 2019, 7535472. doi:10.1155/2019/7535472

Khadka, B., Lee, J. Y., Park, D. H., Kim, K. T., and Bae, J. S. (2020). The role of natural compounds and their nanocarriers in the treatment of CNS inflammation. *Biomolecules* 10 (10), 1401. doi:10.3390/biom10101401

Kong, Z. L., Hsu, Y. T., Johnson, A., Tsai, T. H., Miao, S., He, J. L., et al. (2021). Protective effects of Antrodia camphorata extract against hypoxic cell injury and ischemic stroke brain damage. *Phytother. Res.* 35 (3), 1609–1620. doi:10.1002/ptr.6928

Kuang, Y., Li, B., Wang, Z., Qiao, X., and Ye, M. (2021). Terpenoids from the medicinal mushroom Antrodia camphorata: chemistry and medicinal potential. *Nat. Prod. Rep.* 38 (1), 83–102. doi:10.1039/d0np00023j

Lanza, M., Cucinotta, L., Casili, G., Filippone, A., Basilotta, R., Capra, A. P., et al. (2023). The transcription factor Nrf2 mediates the effects of Antrodia camphorata extract on neuropathological changes in a mouse model of Parkinson's disease. *Int. J. Mol. Sci.* 24 (11), 9250. doi:10.3390/ijms24119250

Lee, I. H., Huang, R. L., Chen, C. T., Chen, H. C., Hsu, W. C., and Lu, M. K. (2002). Antrodia camphorata polysaccharides exhibit anti-hepatitis B virus effects. *FEMS Microbiol. Lett.* 209 (1), 63–67. doi:10.1111/j.1574-6968.2002.tb11110.x

Lee, Y. C., Ho, C. L., Kao, W. Y., and Chen, Y. M. (2015). A phase I multicenter study of antroquinonol in patients with metastatic non-small-cell lung cancer who have received at least two prior systemic treatment regimens, including one platinum-based chemotherapy regimen. *Mol. Clin. Oncol.* 3 (6), 1375–1380. doi:10.3892/mco.2015.642

Lee, Y. M., Chang, C. Y., Yen, T. L., Geraldine, P., Lan, C. C., Sheu, J. R., et al. (2014). Extract of Antrodia camphorata exerts neuroprotection against embolic stroke in rats without causing the risk of hemorrhagic incidence. *Sci. World J.* 2014, 686109. doi:10.1155/2014/686109

Li, B., Kuang, Y., He, J. B., Tang, R., Xu, L. L., Leung, C. H., et al. (2020). Antcamphorols A-K, cytotoxic and ROS scavenging triterpenoids from Antrodia camphorata. *J. Nat. Prod.* 83 (1), 45–54. doi:10.1021/acs.jnatprod.9b00580

Li, B., Kuang, Y., Yi, Y., Qiao, X., Liang, L., and Ye, M. (2021). Chemical modifications of ergostane-type triterpenoids from Antrodia camphorata and their cytotoxic activities. *Bioorg Med. Chem. Lett.* 43, 128066. doi:10.1016/j.bmcl.2021.128066

Li, H., Dai, J., Shi, Y., Zhu, X., Jia, L., and Yang, Z. (2023). Molecular regulatory mechanism of the iron-ion-promoted asexual sporulation of Antrodia cinnamomea in submerged fermentation revealed by comparative transcriptomics. *J. Fungi (Basel)* 9 (2), 235. doi:10.3390/jof9020235

Li, H. X., Wang, J. J., Lu, C. L., Gao, Y. J., Gao, L., and Yang, Z. Q. (2022). Review of bioactivity, isolation, and identification of active compounds from Antrodia cinnamomea. *Bioeng. (Basel)* 9 (10), 494. doi:10.3390/bioengineering9100494

Li, Z. W., Ji, S., Li, B., Wang, S., Tzeng, Y. M., Qiao, X., et al. (2018). Metabolites identification and quantification of antcin H in mice tumors after oral administration of the anticancer mushroom Antrodia camphorata. *TMR Mod. Herb. Med.* 1, 40. doi:10.53388/tmrmhm2017a15

Liao, Y. T., Huang, K. W., Chen, W. J., and Lai, T. H. (2023). A botanical drug extracted from Antrodia cinnamomea: a first-in-human phase I study in healthy volunteers. *J. Am. Nutr. Assoc.* 42 (3), 274–284. doi:10.1080/07315724.2022.2032868

Lin, C. C., Kumar, K. J. S., Liao, J. W., Kuo, Y. H., and Wang, S. Y. (2015). Genotoxic, teratotoxic and oral toxic assessments of Antrodia cinnamomea health food product (Leader Deluxe Antrodia cinnamomea®). *Toxicol. Rep.* 2, 1409–1417. doi:10.1016/j.toxrep.2015.10.007

Ling, W., Cui, Y., Gao, J., Li, R., Jiang, X., Tian, Y., et al. (2020). Antcin C ameliorates neuronal inflammation due to cerebral haemorrhage by inhibiting the TLR-4 pathway. *Folia Neuropathol.* 58, 317–323. doi:10.5114/fn.2020.102434

Liu, D. Z., Liang, H. J., Chen, C. H., Su, C. H., Lee, T. H., Huang, C. T., et al. (2007). Comparative anti-inflammatory characterization of wild fruiting body, liquid-state fermentation, and solid-state culture of Taiwanofungus camphoratus in microglia and the mechanism of its action. *J. Ethnopharmacol.* 113, 45–53. doi:10.1016/j.jep.2007.03.037

Liu, H. P., Kuo, Y. H., Cheng, J., Chang, L. Z., Chang, M. S., Su, L. W., et al. (2021). Ergosta-7,9(11),22-trien-3β-ol rescues AD deficits by modulating microglia activation but not oxidative stress. *Molecules* 26, 5338. doi:10.3390/molecules26175338

Liu, S. C., Wu, T. Y., Hsu, T. H., Lai, M. N., Wu, Y. C., and Ng, L. T. (2022). Chemical composition and chronic toxicity of disc-cultured Antrodia cinnamomea fruiting bodies. *Toxics* 10, 587. doi:10.3390/toxics10100587

Liu, X., Yu, S., Zhang, Y., Zhang, W., Zhong, H., Lu, X., et al. (2023). A review on the protective effect of active components in Antrodia camphorata against alcoholic liver injury. *J. Ethnopharmacol.* 300, 115740. doi:10.1016/j.jep.2022.115740

Liu, Y., Di, X., Liu, X., Shen, W., and Leung, K. S. (2010). Development of a LC-MS/MS method for the determination of antrodin B and antrodin C from Antrodia camphorata extract in rat plasma for pharmacokinetic study. *J. Pharm. Biomed. Anal.* 53, 781–784. doi:10.1016/j.jpba.2010.05.017

Lu, C. L., Lee, B. H., Ren, Y. L., Ji, D., Rao, S. Q., Li, H. X., et al. (2022). Effects of exopolysaccharides from Antrodia cinnamomea on inflammation and intestinal microbiota disturbance induced by antibiotics in mice. *Food Biosci.* 50, 102116. doi:10.1016/j.fbio.2022.102116

Lu, M. K., Cheng, J. J., Lai, W. L., Lin, Y. J., and Huang, N. K. (2008). Fermented Antrodia cinnamomea extract protects rat PC12 cells from serum deprivation-induced apoptosis: the role of the MAPK family. *J. Agric. Food Chem.* 56, 865–874. doi:10.1021/jf072828b

Lu, M. K., Cheng, J. J., Lai, W. L., Lin, Y. R., and Huang, N. K. (2006). Adenosine as an active component of Antrodia cinnamomea that prevents rat PC12 cells from serum deprivation-induced apoptosis through the activation of adenosine A(2A) receptors. *Life Sci.* 79, 252–258. doi:10.1016/j.lfs.2005.12.042

Lu, M. Y., Fan, W. L., Wang, W. F., Chen, T., Tang, Y. C., Chu, F. H., et al. (2014). Genomic and transcriptomic analyses of the medicinal fungus Antrodia cinnamomea for its metabolite biosynthesis and sexual development. *Proc. Natl. Acad. Sci. U. S. A.* 111, E4743–E4752. doi:10.1073/pnas.1417570111

Marino, B. L. B., de Souza, L. R., Sousa, K. P. A., Ferreira, J. V., Padilha, E. C., da Silva, C. H. T. P., et al. (2020). Parkinson's disease: a review from pathophysiology to treatment. *Mini Rev. Med. Chem.* 20, 754–767. doi:10.2174/1389557519666191104110908

Menon, M. P., Chien, Y. H., Thomas, J., Yu, Y. H., Chang, C. T., and Hua, K. F. (2022). Nano modification of Antrodia cinnamomea exhibits anti-inflammatory action and improves the migratory potential of myogenic progenitors. *Cells* 11, 2512. doi:10.3390/cells11162512

Miyashita, N., Straub, J. E., and Thirumalai, D. (2009). Structures of beta-amyloid peptide 1-40, 1-42, and 1-55-the 672-726 fragment of APP-in a membrane environment with implications for interactions with gamma-secretase. *J. Am. Chem. Soc.* 131 (49), 17843–17852. doi:10.1021/ja905457d

More, S. V., Koppula, S., Kim, I. S., Kumar, H., Kim, B. W., and Choi, D. K. (2012). The role of bioactive compounds on the promotion of neurite outgrowth. *Molecules* 17 (6), 6728–6753. doi:10.3390/molecules17066728

Morris, H. R., Spillantini, M. G., Sue, C. M., and Williams-Gray, C. H. (2024). The pathogenesis of Parkinson's disease. *Lancet* 403 (10423), 293–304. doi:10.1016/S0140-6736(23)01478-2

Mou, Y., Du, Y., Zhou, L., Yue, J., Hu, X., Liu, Y., et al. (2022). Gut microbiota interact with the brain through systemic chronic inflammation: implications on neuroinflammation, neurodegeneration, and aging. *Front. Immunol.* 13, 796288. doi:10.3389/fimmu.2022.796288

Moujalled, D., Strasser, A., and Liddell, J. R. (2021). Molecular mechanisms of cell death in neurological diseases. *Cell Death Differ.* 28 (7), 2029–2044. doi:10.1038/s41418-021-00814-y

Nakamura, N., Hirakawa, A., Gao, J. J., Kakuda, H., Shiro, M., Komatsu, Y., et al. (2004). Five new maleic and succinic acid derivatives from the mycelium of Antrodia camphorata and their cytotoxic effects on LLC tumor cell line. *J. Nat. Prod.* 67, 46–48. doi:10.1021/np030293k

Nallathamby, N., Guan-Serm, L., Vidyadaran, S., Abd Malek, S. N., Raman, J., and Sabaratnam, V. (2015). Ergosterol of Cordyceps militaris attenuates LPS induced inflammation in BV2 microglia cells. *Nat. Prod. Commun.* 10, 1934578X1501000–886. doi:10.1177/1934578x1501000623

Numakawa, T., and Kajihara, R. (2023). Neurotrophins and other growth factors in the pathogenesis of Alzheimer's disease. *Life (Basel)* 13, 647. doi:10.3390/life13030647

Passeri, E., Elkhoury, K., Morsink, M., Broersen, K., Linder, M., Tamayol, A., et al. (2022). Alzheimer's disease: treatment strategies and their limitations. *Int. J. Mol. Sci.* 23 (22), 13954. doi:10.3390/ijms232213954

Qiao, X., Wang, Q., Ji, S., Huang, Y., Liu, K. D., Zhang, Z. X., et al. (2015). Metabolites identification and multi-component pharmacokinetics of ergostane and lanostane triterpenoids in the anticancer mushroom Antrodia cinnamomea. *J. Pharm. Biomed. Anal.* 111, 266–276. doi:10.1016/j.jpba.2015.04.010

Robertson, G. S., Crocker, S. J., Nicholson, D. W., and Schulz, J. B. (2000). Neuroprotection by the inhibition of apoptosis. *Brain Pathol.* 10, 283–292. doi:10.1111/j.1750-3639.2000.tb00262.x

Sharon, G., Cruz, N. J., Kang, D. W., Gandal, M. J., Wang, B., Kim, Y. M., et al. (2019). Human gut microbiota from autism spectrum disorder promote behavioral symptoms in mice. *Cell* 177, 1600–1618. doi:10.1016/j.cell.2019.05.004

Shen, Y. C., Chou, C. J., Wang, Y. H., Chen, C. F., Chou, Y. C., and Lu, M. K. (2004). Anti-inflammatory activity of the extracts from mycelia of Antrodia camphorata cultured with water-soluble fractions from five different Cinnamomum species. *FEMS Microbiol. Lett.* 231, 137–143. doi:10.1016/S0378-1097(03)00953-4

Shie, P. H., Wang, S. Y., Lay, H. L., and Huang, G. J. (2016). 4,7-Dimethoxy-5-methyl-1,3-benzodioxole from Antrodia camphorata inhibits LPS-induced inflammation via suppression of NF-κB and induction HO-1 in RAW264.7 cells. *Int. Immunopharmacol.* 31, 186–194. doi:10.1016/j.intimp.2015.12.030

Sillapachaiyaporn, C., Chuchawankul, S., Nilkhet, S., Moungkote, N., Sarachana, T., Ung, A. T., et al. (2022a). Ergosterol isolated from cloud ear mushroom (Auricularia polytricha) attenuates bisphenol A-induced BV2 microglial cell inflammation. *Food Res. Int.* 157, 111433. doi:10.1016/j.foodres.2022.111433

Sillapachaiyaporn, C., Mongkolpobsin, K., Chuchawankul, S., Tencomnao, T., and Baek, S. J. (2022b). Neuroprotective effects of ergosterol against TNF-α-induced HT-22 hippocampal cell injury. *Biomed. Pharmacother.* 154, 113596. doi:10.1016/j.biopha.2022.113596

Silva, A. M., Preto, M., Grosso, C., Vieira, M., Delerue-Matos, C., Vasconcelos, V., et al. (2023). Tracing the path between mushrooms and Alzheimer's disease-a literature review. *Molecules* 28, 5614. doi:10.3390/molecules28145614

Simpson, D. S. A., and Oliver, P. L. (2020). ROS generation in microglia: understanding oxidative stress and inflammation in neurodegenerative disease. *Antioxidants (Basel)* 9 (8), 743. doi:10.3390/antiox9080743

Singh, V., Roth, S., Llovera, G., Sadler, R., Garzetti, D., Stecher, B., et al. (2016). Microbiota dysbiosis controls the neuroinflammatory response after stroke. *J. Neurosci.* 36, 7428–7440. doi:10.1523/JNEUROSCI.1114-16.2016

So, Y. J., Lee, J. U., Yang, G. S., Yang, G., Kim, S. W., Lee, J. H., et al. (2024). The potentiality of natural products and herbal medicine as novel medications for Parkinson's disease: a promising therapeutic approach. *Int. J. Mol. Sci.* 25 (2), 1071. doi:10.3390/ijms25021071

Sorboni, S. G., Moghaddam, H. S., Jafarzadeh-Esfehani, R., and Soleimanpour, S. (2022). A comprehensive review on the role of the gut microbiome in human neurological disorders. *Clin. Microbiol. Rev.* 35, e0033820. doi:10.1128/CMR.00338-20

Su, C. H. (2002). *Health guardian angel: Antrodia camphorata*. 1st edition. Taipei, Taiwan: EKS Book Publishing.

Su, C. H., Hsieh, Y. C., Chng, J. Y., Lai, M. N., and Ng, L. T. (2023). Metabolomic profiling of different Antrodia cinnamomea phenotypes. *J. Fungi (Basel)* 9, 97. doi:10.3390/jof9010097

Su, R. C., Leu, J. G., Chen, Y. H., Chen, C. Y., Yang, Y. F., Yen, C. C., et al. (2022). Topical application of Antrodia cinnamomea ointment in diabetic wound healing. *Life (Basel)* 12 (4), 507. doi:10.3390/life12040507

Sun, P., Li, W., Guo, J., Peng, Q., Ye, X., Hu, S., et al. (2023). Ergosterol isolated from Antrodia camphorata suppresses LPS-induced neuroinflammatory responses in microglia cells and ICR mice. *Molecules* 28, 2406. doi:10.3390/molecules28052406

Sun, Y., Yang, Y., Liu, S., Yang, S., Chen, C., Lin, M., et al. (2022). New therapeutic approaches to and mechanisms of ginsenoside Rg1 against neurological diseases. *Cells* 11, 2529. doi:10.3390/cells11162529

Teleanu, D. M., Niculescu, A. G., Lungu, I. I., Radu, C. I., Vladâcenco, O., Roza, E., et al. (2022). An overview of oxidative stress, neuroinflammation, and neurodegenerative diseases. *Int. J. Mol. Sci.* 23, 5938. doi:10.3390/ijms23115938

Tsai, Y. T., Ruan, J. W., Chang, C. S., Ko, M. L., Chou, H. C., Lin, C. C., et al. (2020). Antrodia cinnamomea confers obesity resistance and restores intestinal barrier integrity in leptin-deficient obese mice. *Nutrients* 12, 726. doi:10.3390/nu12030726

Tsai, Y. T., Ruan, J. W., Chang, C. S., Ko, M. L., Chou, H. C., Lin, C. C., et al. (2021). Proteomic and microbial assessments on the effect of Antrodia cinnamomea in C57BL/6 mice. *Arch. Biochem. Biophys.* 713, 109058. doi:10.1016/j.abb.2021.109058

Tsay, H. J., Liu, H. K., Kuo, Y. H., Chiu, C. S., Liang, C. C., Chung, C. W., et al. (2021). EK100 and antrodin C improve brain amyloid pathology in APP/PS1 transgenic mice by promoting microglial and perivascular clearance pathways. *Int. J. Mol. Sci.* 22, 10413. doi:10.3390/ijms221910413

Tung, Y. T., Tsai, T. C., Kuo, Y. H., Yen, C. C., Sun, J. Y., Chang, W. H., et al. (2014). Comparison of solid-state-cultured and wood-cultured Antrodia camphorata in anti-inflammatory effects using NF-κB/luciferase inducible transgenic mice. *Phytomedicine* 21, 1708–1716. doi:10.1016/j.phymed.2014.08.011

Turck, D., Bohn, T., Castenmiller, J., De Henauw, S., Hirsch-Ernst, K. I., Maciuk, A., et al. (2022). Safety of freeze-dried mycelia of Antrodia camphorata as a novel food pursuant to regulation (EU) 2015/2283. *EFSA J.* 20, e07380. doi:10.2903/j.efsa.2022.7380

Wang, C., Zhang, W., Wong, J. H., Ng, T., and Ye, X. (2019a). Diversity of potentially exploitable pharmacological activities of the highly prized edible medicinal fungus Antrodia camphorata. *Appl. Microbiol. Biotechnol.* 103 (19), 7843–7867. doi:10.1007/s00253-019-10016-9

Wang, L. C., Wang, S. E., Wang, J. J., Tsai, T. Y., Lin, C. H., Pan, T. M., et al. (2012). *In vitro* and *in vivo* comparisons of the effects of the fruiting body and mycelium of Antrodia camphorata against amyloid β-protein-induced neurotoxicity and memory impairment. *Appl. Microbiol. Biotechnol.* 94, 1505–1519. doi:10.1007/s00253-012-3941-3

Wang, Q., Qiao, X., Qian, Y., Li, Z. W., Tzeng, Y. M., Zhou, D. M., et al. (2015). Intestinal absorption of ergostane and lanostane triterpenoids from Antrodia cinnamomea using Caco-2 cell monolayer model. *Nat. Prod. Bioprospect* 5, 237–246. doi:10.1007/s13659-015-0072-4

Wang, Y. H., Chern, C. M., Liou, K. T., Kuo, Y. H., and Shen, Y. C. (2019b). Ergostatrien-7,9(11),22-trien-3β-ol from Antrodia camphorata ameliorates ischemic stroke brain injury via downregulation of p65NF-κ-B and caspase 3, and activation of Akt/GSK3/catenin-associated neurogenesis. *Food Funct.* 10, 4725–4738. doi:10.1039/c9fo00908f

Wang, Y. Y., Hsieh, Y. H., Kumar, K. J. S., Hsieh, H. W., Lin, C. C., and Wang, S. Y. (2020). The regulatory effects of a formulation of Cinnamomum osmophloeum Kaneh and Taiwanofungus camphoratus on metabolic syndrome and the gut microbiome. *Plants (Basel)* 9, 383. doi:10.3390/plants9030383

Wu, Y., Lo, J., Shih, Y., and Liang, H. J. (2018). *Method for treating stroke or reducing nerve injury*. US20180353520. U.S. Patent.

Xia, Z., Dickens, M., Raingeaud, J., Davis, R. J., and Greenberg, M. E. (1995). Opposing effects of ERK and JNK-p38 MAP kinases on apoptosis. *Science* 270 (5240), 1326–1331. doi:10.1126/science.270.5240.1326

Yan, Y., Yang, H., Xie, Y., Ding, Y., Kong, D., and Yu, H. (2020). Research progress on Alzheimer's disease and resveratrol. *Neurochem. Res.* 45, 989–1006. doi:10.1007/s11064-020-03007-0

Yang, J., Wang, L., Liu, H., Xu, H., Liu, F., Song, H., et al. (2023). Dysregulation of Ruminococcaceae and Megamonas could be predictive markers for rapid progression of mild cognitive impairment. *Microb. Pathog.* 183, 106272. doi:10.1016/j.micpath.2023.106272

Yang, P. S., Lin, P. Y., Chang, C. C., Yu, M. C., Yen, T. L., Lan, C. C., et al. (2015). Antrodia camphorata potentiates neuroprotection against cerebral ischemia in rats via downregulation of iNOS/HO-1/Bax and activated caspase-3 and inhibition of hydroxyl radical formation. *Evid. Based Complement. Altern. Med.* 2015, 232789. doi:10.1155/2015/232789

Yang, X., Wang, X., Lin, J., Lim, S., Cao, Y., Chen, S., et al. (2022a). Structure and anti-inflammatory activity relationship of ergostanes and lanostanes in Antrodia cinnamomea. *Foods* 11, 1831. doi:10.3390/foods11131831

Yang, Y., Han, C., Sheng, Y., Wang, J., Li, W., Zhou, X., et al. (2022b). Antrodia camphorata polysaccharide improves inflammatory response in liver injury via the ROS/TLR4/NF-κB signal. *J. Cell Mol. Med.* 26, 2706–2716. doi:10.1111/jcmm.17283

Ye, J., Zhang, C., Fan, Q., Lin, X., Wang, Y., Azzam, M., et al. (2022). Antrodia cinnamomea polysaccharide improves liver antioxidant, anti-inflammatory capacity,

and cecal flora structure of slow-growing broiler breeds challenged with lipopolysaccharide. *Front. Vet. Sci.* 9, 994782. doi:10.3389/fvets.2022.994782

Yi, Z., Liu, X., Liang, L., Wang, G., Xiong, Z., Zhang, H., et al. (2021). Antrodin A from Antrodia camphorata modulates the gut microbiome and liver metabolome in mice exposed to acute alcohol intake. *Food Funct.* 12, 2925–2937. doi:10.1039/d0fo03345f

Yi, Z. W., Xia, Y. J., Liu, X. F., Wang, G. Q., Xiong, Z. Q., and Ai, L. Z. (2020). Antrodin A from mycelium of Antrodia camphorata alleviates acute alcoholic liver injury and modulates intestinal flora dysbiosis in mice. *J. Ethnopharmacol.* 254, 112681. doi:10.1016/j.jep.2020.112681

Zhang, B. B., Guan, Y. Y., Hu, P. F., Chen, L., Xu, G. R., Liu, L., et al. (2019). Production of bioactive metabolites by submerged fermentation of the medicinal mushroom Antrodia cinnamomea: recent advances and future development. *Crit. Rev. Biotechnol.* 39, 541–554. doi:10.1080/07388551.2019.1577798

Zhang, B. B., Hu, P. F., Huang, J., Hu, Y. D., Chen, L., and Xu, G. R. (2017). Current advances on the structure, bioactivity, synthesis, and metabolic regulation of novel ubiquinone derivatives in the edible and medicinal mushroom Antrodia cinnamomea. *J. Agric. Food Chem.* 65, 10395–10405. doi:10.1021/acs.jafc.7b04206

Zhang, H. Y., Firempong, C. K., Wang, Y. W., Xu, W. Q., Wang, M. M., Cao, X., et al. (2016). Ergosterol-loaded poly(lactide-co-glycolide) nanoparticles with enhanced *in vitro* antitumor activity and oral bioavailability. *Acta Pharmacol.* 37, 834–844. doi:10.1038/aps.2016.37

Zhang, Y., Lv, P., Ma, J., Chen, N., Guo, H., Chen, Y., et al. (2022). Antrodia cinnamomea exerts an anti-hepatoma effect by targeting PI3K/AKT-mediated cell cycle progression *in vitro* and *in vivo*. *Acta Pharm. Sin. B* 12 (2), 890–906. doi:10.1016/j.apsb.2021.07.010

Zhang, Y., Wang, Z., Li, D., Zang, W., Zhu, H., Wu, P., et al. (2018). A polysaccharide from Antrodia cinnamomea mycelia exerts antitumor activity through blocking of TOP1/TDP1-mediated DNA repair pathway. *Int. J. Biol. Macromol.* 120, 1551–1560. doi:10.1016/j.ijbiomac.2018.09.162

Zhao, Y., Zhang, X., Chen, X., and Wei, Y. (2022). Neuronal injuries in cerebral infarction and ischemic stroke: from mechanisms to treatment (Review). *Int. J. Mol. Med.* 49, 15. doi:10.3892/ijmm.2021.5070

Zhao, Y. Y., Cheng, X. L., Liu, R., Ho, C. C., Wei, F., Yan, S. H., et al. (2011). Pharmacokinetics of ergosterol in rats using rapid resolution liquid chromatography-atmospheric pressure chemical ionization multi-stage tandem mass spectrometry and rapid resolution liquid chromatography/tandem mass spectrometry. *J. Chromatogr. B Anal. Technol. Biomed. Life Sci.* 879, 1945–1953. doi:10.1016/j.jchromb.2011.05.025

Zhong, X., Lin, R., Li, Z., Mao, J., and Chen, L. (2014). Effects of Salidroside on cobalt chloride-induced hypoxia damage and mTOR signaling repression in PC12 cells. *Biol. Pharm. Bull.* 37 (7), 1199–1206. doi:10.1248/bpb.b14-00100

Zou, X. G., Xu, M. T., Dong, X. L., Ying, Y. M., Guan, R. F., Wu, W. C., et al. (2022). Solid-state-cultured mycelium of Antrodia camphorata exerts potential neuroprotective activities against 6-hydroxydopamine-induced toxicity in PC12 cells. *J. Food Biochem.* 46, e14208. doi:10.1111/jfbc.14208

## Glossary

| | |
|---|---|
| **6-OHDA** | 6-Hydroxydopamine |
| **Aβ** | amyloid-β |
| **AC** | Antrodia camphorate |
| **ACEE** | Ethanol extract of AC |
| **ACP** | polysaccharides isolated from AC |
| **AD** | Alzheimer's disease |
| **ADO** | adenosine |
| **ADORA1** | adenosine A1 receptor |
| **ADORA2** | adenosine A2 receptor |
| **AIS** | acute ischemic stroke |
| **APP** | amyloid precursor protein |
| **BACE1** | beta-cleavage by the secretases beta |
| **BCD** | β-cyclodextrin |
| **BDNF** | brain derived neurotrophic factor |
| **Cmax** | peak concentration |
| **CNS** | central nervous system |
| **CoCl2** | Cobalt chloride |
| **COQ** | coenzyme Q |
| **COX-2** | cyclooxygenase-2 |
| **CYP51F1** | 14-α-demethylase |
| **EFSA** | European Food Safety Authority |
| **EK100** | Ergosta-7,9 (11),22-trien-3β-ol |
| **EtOAc-AC** | Ethyl acetate crude extract of AC |
| **FDA** | Food and Drug Administration |
| **GDNF** | glia-derived neurotrophic factor |
| **HFD** | high-fat diet |
| **HIF-1a** | hypoxia-inducible transcription factor-1a |
| **ICH** | intracerebral hemorrhage |
| **IL-1β** | interleukin 1 beta |
| **iNOS** | inducible nitric oxide synthase |
| **LIH** | lincomycin hydrochloride |
| **MDA** | Malondialdehyde |
| **MPTP** | 1-Methyl-4-phenyl-1,2,3,6-tetrahydropyridine |
| **NGF** | Nerve growth factor |
| **NLCs** | nanostructured lipid carriers |
| **NMDARs** | N-methyl-D-aspartate receptors |
| **NOAEL** | no-observed-adverse-effect-level |
| **NT-3** | neurotrophin 3 |
| **OGD** | oxygen-glucose deprivation |
| **PD** | Parkinson's disease |
| **PKA** | protein kinase A |
| **ROS** | Reactive oxygen species |
| **SD rats** | Sprague–Dawley rats |
| **TNF-α** | tumor necrosis factor-alpha |

frontiers | Frontiers in Pharmacology

TYPE Original Research
PUBLISHED 30 April 2024
DOI 10.3389/fphar.2024.1362301



OPEN ACCESS

EDITED BY
Qi Liang,
Air Force Medical University, China

REVIEWED BY
Shih-Heng Chen,
National Institute of Environmental Health Sciences (NIH), United States
Yu-Xi Huang,
Peking University, China

*CORRESPONDENCE
Dexi Zhao,
zdx02@163.com
Xu Wang,
20202701164@stu.ccucm.edu.cn
Jinhua Li,
jinhua1@jlu.edu.cn

RECEIVED 28 December 2023
ACCEPTED 10 April 2024
PUBLISHED 30 April 2024

CITATION
Ping N, Zuo K, Cai J, Rong C, Yu Z, Zhang X, Wang G, Ma C, Yang H, Li J, Wang X and Zhao D (2024), Apigenin protects against ischemic stroke by increasing DNA repair.
*Front. Pharmacol.* 15:1362301.
doi: 10.3389/fphar.2024.1362301



# Apigenin protects against ischemic stroke by increasing DNA repair

Niu Ping[1], Kuiyang Zuo[2], Jiahan Cai[3], Chunshu Rong[1], Ziqiao Yu[4], Xu Zhang[2], Gaihua Wang[2], Chunyu Ma[1], Huirong Yang[1], Jinhua Li[2]*, Xu Wang[1,2,4]* and Dexi Zhao[4]*

[1]Department of Encephalopathy, Hospital of Changchun University of Chinese Medicine, Changchun, Jilin, China, [2]School of Public Health, Jilin University, Changchun, Jilin, China, [3]Traditional Chinese Medicine College, Guangdong Pharmaceutical University, Guangzhou, Guangdong, China, [4]College of Traditional Chinese Medicine, Changchun University of Chinese Medicine, Changchun, Jilin, China

**Background and Objective:** Oxidative stress is an important pathological process in ischemic stroke (IS). Apigenin (APG) is a natural product with favorable antioxidative effects, and some studies have already demonstrated the antioxidative mechanism of APG in the treatment of IS. However, the mechanism of APG on DNA damage and repair after IS is not clear. The aim of this study was to investigate the mechanism of APG on DNA repair after IS.

**Methods:** Male Sprague-Dawley rats were used to establish a model of permanent middle cerebral artery occlusion (pMCAO) on one side, and were pre-treated with gavage of APG (30, 60, or 120 mg/kg) for 7 days. One day after pMCAO, the brain tissues were collected. Cerebral infarct volume, brain water content, HE staining and antioxidant index were analyzed to evaluated the brain damage. Molecular Docking, molecular dynamics (MD) simulation, immunohistochemistry, and Western blot were used to explore the potential proteins related to DNA damage repair.

**Results:** APG has a low binding score with DNA repair-related proteins. APG treatment has improved the volume of cerebral infarction and neurological deficits, reduced brain edema, and decreased parthanatos and apoptosis by inhibiting PARP1/AIF pathway. In addition, APG improved the antioxidative capacity through reducing reactive oxygen species and malondialdehyde, and increasing glutathione and superoxide dismutase. Also, APG has reduced DNA damage- and cell death-related proteins such as PARP1, γH2A.X, 53BP1, AIF, cleaved caspase3, Cytochrome c, and increased DNA repair by BRCA1 and RAD51 through homologous recombination repair, and reduced non-homologous end link repair by KU70.

**Conclusion:** APG can improve nerve damage after IS, and these protective effects were realized by reducing oxidative stress and DNA damage, and improving DNA repair.

KEYWORDS

**Apigenin, ischemic stroke, parthanatos, homologous recombination repair, non-homologous end link repair**

# 1 Introduction

Stroke is a common disease with high morbidity and disability worldwide and is also one of the leading causes of death worldwide. Currently, about 80 million people suffer from stroke globally, and the burden of stroke has become the second highest in the world (Feigin et al., 2022). Strokes are divided into hemorrhagic stroke and ischemic stroke (IS), with IS accounting for about 80% of all stroke. However, the availability of drugs for the treatment of IS is very limited. The only approved medication of IS by US Food and Drug Administration is recombinant tissue plasminogen activator, but a strict contraindication (hemorrhagic transformation) and time window has limited its use. In addition, the intense oxidative stress induced by ischemia-reperfusion underlies the pathology leading to severe complications.

Oxidative stress plays an important role in the pathological process of IS. After the onset of IS, large amounts of ROS are released, leading to oxidative DNA damage, which is a serious consequence of oxidative stress (Wang et al., 2006), and can lead to DNA double-strand breaks (DSBs) and finally lead to neuronal cell death through a variety of mechanisms (Martin, 2008). In the face of DNA damage, there exists a well-established cellular response mechanism called the DNA damage response, including homologous recombination (HR) and non-homologous end-joining (NHEJ) to repair these damage (Mao et al., 2008; Shrivastav et al., 2008). Among them, P53-binding protein 1 (53BP1) (Lu et al., 2019) plays a key regulatory role in DSB repair signaling selection, which is involved in the regulation of HR and NHEJ-related proteins ATP-dependent DNA helicase ku70 (KU70) (Kim et al., 2014), Breast cancer type 1 susceptibility protein (BRCA1) (Lou et al., 2003), DNA repair protein RAD51 homolog 1 (RAD51) (Raderschall et al., 2002) and so on. Additionally, poly (ADP-ribose) polymerase 1 (PARP1), which accounts for more than 90% of the PARPs superfamily, is closely related to DNA repair signaling and cell death (Pieper et al., 1999). Increased PARP-1 expression after IS triggers the nuclear translocation of apoptosis inducing factor (AIF), which subsequently induces chromatin lysis and caspase-independent cell death through interaction with histone variant H2AX (Yu et al., 2006; Artus et al., 2010). This caspase-independent cell death mediated by the PARP/AIF pathway has been named parthanatos. Ischemia-induced neuronal DNA damage during oxidative stress is closely associated with parthanatos.

As a DNA damage receptor, about 90% of polyADP ribose (PAR) is produced in response to DNA damage or oxidative stress (Liu S. Q. et al., 2022). DNA damage is a response to cerebral ischemia, including active and passive DNA damage after ischemic brain injury. Active DNA damage is mediated by DNA endonucleases, also known as endonuclease-mediated DNA damage. The most studied active DNA damage is apoptotic DNA fragmentation, which is characterized by DNA double-strand breaks (DSBs) (Chen et al., 1997). DNA fragmentation involves a cascade of cellular self-destruction that is often irreversible. Two endonucleases, caspase-activated deoxyribonucleases and apoptosis inducing factor (AIF), are considered to be the major endonucleases during DNA fragmentation (Li et al., 2011). However, recent findings suggest that at least two pathways upstream of AIF release are involved: one dependent on upstream bcl-2 family proteins such as Bax and caspases, and the other on PARP-1 (Cregan et al., 2004). Translocation of AIF from the mitochondria to the nucleus was identified as a critical step during PARP-1 cell death (Cho and Toledo-Pereyra, 2008). PARP1 inhibition attenuated AIF migration from mitochondria to the nucleus and protected neurons from death after ischemic stroke (Beneke, 2008).

Apigenin (APG) is a natural product widely distributed in nature (green celery heart, Chinese celery), and has the best antioxidative effect among the ten flavonoids (Shrivastav et al., 2008). In a previous study, we have reviewed the therapeutic mechanisms of APG against IS (Wang et al., 2022). The protective effects of APG on IS include anti-inflammation, anti-oxidation and anti-apoptosis. However, whether the antioxidative protection of APG against IS is *via* DNA repair remains unclear. During post-ischemic oxidative stress, we hypothesized that the neuroprotective effects of APG are related to the regulation of DNA damage repair, parthanatos and apoptosis.

In this study, we have constructed a permanent middle cerebral artery occlusion (pMCAO) model after pretreating rats with APG for 7 days. DNA damage repair, apoptosis, and parthanatos were detected in ischemic brain tissues. We found that the protein expression of DNA repair, parthanatos and apoptosis was increased, and DNA repair-related proteins were decreased in the ischemic semi-dark band brain tissue of pMCAO. This phenomenon was reversed by different doses of APG, especially in the medium dose group (60 mg/kg). In addition, we found that APG was involved in regulating DNA repair to rescue neuronal survival in the ischemic semi-dark band. Our study reveals a novel mechanism of APG in the treatment of IS through antioxidant therapy and increasing DNA repair, which provides a theoretical basis for the clinical translation of APG.

# 2 Materials and methods

## 2.1 Reagents

APG and 2,3,5-Triphenyltetrazolium chloride (TTC) were purchased from Meryer Chemical Technology Co. Ltd (Shanghai), and malondialdehyde (MDA) assay kit, total superoxide dismutase (SOD) assay kit, and glutathione (GSH) assay kit were purchased from Nanjing Jiancheng Bioengineering Institute. Nylon wire with a rounded tip (diameter 0.36 mm) was purchased from BEIJING CINONTECH CO.

## 2.2 Experiment animals

Adult male Sprague-Dawley (SD) rats (250 ± 30 g) were purchased from Liaoning Changsheng biotechnology Co. Ltd. The rats were housed in the Animal Experiment Center, School of Public Health, Jilin University, China. All operations of rats were complied with the National Institutes of Health Guide for the Care and National Research Council of the National Academies. Rats were kept under stable conditions with temperature around 23°C ± 1°C, 12 h light/12 h dark cycle, free access to food and water, and air

humidity at 60%–70%. This experiment was approved and supervised by the Animal Experimentation Committee of Changchun University of Traditional Chinese Medicine (ID: 2023158).

## 2.3 Establishment of pMCAO model and animal grouping

The rats were randomly divided into five groups, including the sham operation group (Control group), the model group (pMCAO group), the APG low-dose group (30 mg/kg, L group), the APG medium-dose group (60 mg/kg, M group), and the APG high-dose group (120 mg/kg, H group). The dosage of APG was determined based on previous studies (Wang et al., 2022). The treatment group was pretreated with APG through gavage for 7 days consecutively, and the control and model groups were given equal amounts of sterile saline. All animals were given free access to food and water in an appropriate environment. Rats were weighed and anesthetized by intraperitoneal injection of sodium pentobarbital (2%, 2 mL/kg), and then fixed in the ventral recumbent position, with a warming pad to maintain the core temperature at approximately 37.0°C throughout the operation. The Longa's method was used to establish pMCAO model. The skin was incised along the midline of the neck to expose the common carotid artery (CCA), external carotid artery (ECA) and internal carotid artery (ICA). The CCA and ECA were ligated, and the ICA was gently inserted using a round-tipped nylon wire until slight resistance was felt. The rats were executed 24 h later. Rats in the control group underwent the same surgical exposure steps as the model group except for the insertion of nylon wires.

## 2.4 Neurological deficit score

The Longa method was used to score the neurological function of rats in each group at 24 h after the pMCAO model. The scoring criteria were as follows: 0 point, normal neurological function; 1 point, rats were unable to fully extend the contralateral forepaw; 2 points, rats walked in a circle toward the hemiplegic side; 3 points, rats were prone toward the hemiplegic side at rest; 4 points, rats lost consciousness and were unable to walk on their own (Longa et al., 1989).

## 2.5 Analysis of cerebral infarct volume, brain water content and antioxidant index

After 24 h of modeling, the rats were anesthetized and executed by severing the head, and the brain tissues were taken and frozen at -20°C for 15 min, and then the brain tissues were cut into 2 mm-thick coronal sections and stained with 2% TTC solution at 37°C for 20 min, and images were taken and analyzed by ImageJ software.

Ischemic hemisphere of cerebral edema was determined using the wet/dry method. The formula for the calculation is [(wet weight - dry weight)/wet weight] × 100%.

Brain tissues from the ischemic semi-dark zone were collected as test samples. ROS were detected by probes, and MDA, GSH and SOD were detected by kits according to the manufacturer's procedure. Briefly, 10% tissue homogenate was first prepared, protein concentration was determined and experiment followed with the instructions.

## 2.6 Pathological and immunohistochemical detection of brain tissue

HE staining was performed for histologic examination. Briefly, brain tissues of each group were collected and fixed in 10% paraformaldehyde. Tissue sections were dehydrated, processed in an automated tissue processor and immersed in paraffin. 4 μm paraffin sections were made. HE staining was performed after dewaxing and hydration. Sections were scanned with a scanner.

Immunohistochemical staining was performed on paraformaldehyde-fixed, paraffin-embedded brain tissue sections. Brain sections of 3–4 μ m thickness were incubated with anti-γH2A.X antibody. The primary antibody was incubated at 37 °C for 1 h. Subsequently, the brain slices were incubated with horseradish peroxidase-conjugated secondary antibody at 37 °C for 30 min, and the color reaction was carried out using diaminobenzidine as the chromogen. The final sections were restrained with hematoxylin, dehydrated with graded ethanol and xylene, and images of ischemic semi-dark bands were taken under a light microscope. The integral optical density values of positive cells were analyzed using ImageJ software.

## 2.7 Verification of molecular docking and molecular dynamics (MD) simulation

The 3D conformations of APG were downloaded from PubChem (https://pubchem.ncbi.nlm.nih.gov/), energy minimized using Chem3D software, and saved in pdb format. AIF (PDBID: 1M6I), MIF (PDBID:1CA7), H2AX (PDBID:6K1I), PARP1 (PDBID:4L6S), BRCA1 (PDBID:4IFI), RAD51 (PDBID. 7EJC), KU70 (PDBID:1JEY), KU80 (PDBID:6ERH), CASP3 (PDBID: 1NMS) and other protein conformations were obtained from RCSB PDB database. The receptor and ligands were pre-processed using Pymol and Autodock tool, and docked using AutodockVina 1.2.3 to screen the best binding conformations based on binding energy.

As the conformations of ligand and receptor are constantly changing during the binding process, the conformational situation of semi-flexible docking is still somewhat different from the actual situation. Therefore, we further used molecular dynamics simulations to explore the stability of the binding between APG and nine proteins. All-atom molecular dynamics simulations were performed using the classical molecular dynamics simulation program GROMACS 2020.3, simulations of protein-ligand complexes were performed based on the Amber 99SB-ILDN force field, and ligand molecular topology files were generated using the programs Antechamber and Acpype. Saline solvation boxes of cubic (cubic) were selected, the closest distance between the system boundary and the complex was set to 1.2 nm, and $Na^+$ or $Cl^-$ was randomly added to neutralize the system charge. The energy of each system was minimized using a most rapid descent

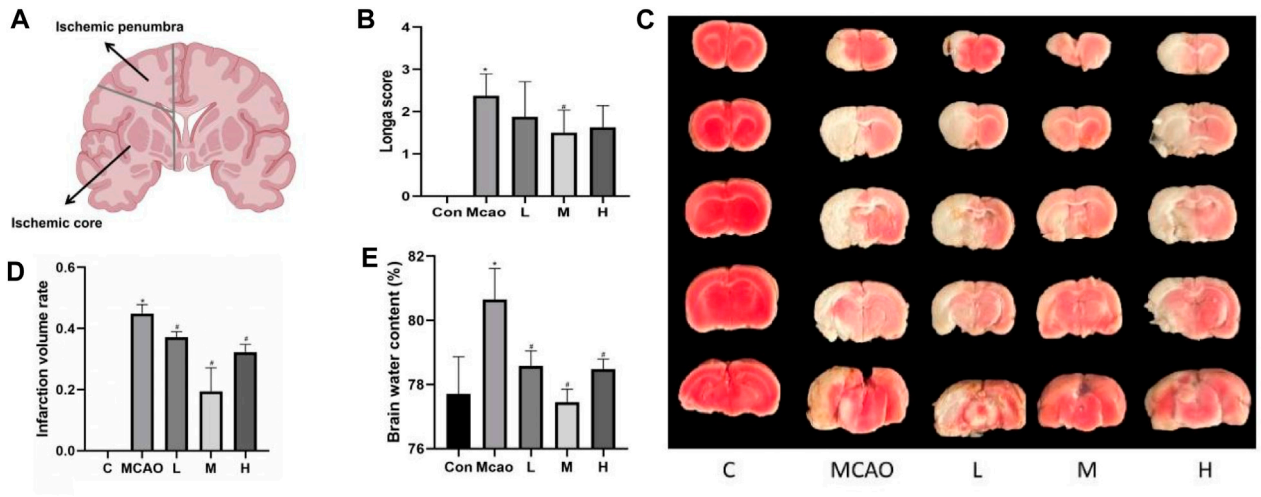


FIGURE 1
Effect of APG treatment on cerebral infarct, neurological function, and brain edema. **(A)** Diagram of ischemic penumbra and ischemic core. **(B)** Statistical graph of neurological deficit score after 1 day pMCAO. Data are expressed as mean ± SD (n = 10). **(C)** Representative TTC staining of rat brain. **(D)** Infarct volumes (%). Data are expressed as mean ± SD (n = 3). **(E)** Statistical graph of the brain water content. Data are expressed as mean ± SD (n = 4). *$p < 0.05$, compared with Con; #$p < 0.05$, compared with pMCAO.

algorithm with a maximum of 50,000 steps. Subsequently, the system was warmed up to 310.15 K with a 100 ps simulation under the normal-variance tether (NVT) and a continuous 100 ps simulation under the isothermal-isobaric tether (NPT). After the system reaches equilibrium, the system bond lengths and bond-forming interactions are constrained with the LINCS algorithm, free dynamics simulations are performed for 50 ns, and finally the trajectories are analyzed using the GROMACS tool and VMD.

## 2.8 Western blot analysis

The brain tissues of the ischemic penumbra (Figure 1A). Brain tissue was crushed under liquid nitrogen, RIPA lysate was added, and protease inhibitors were added. After lysis on ice for 30min, the samples were centrifuged at 12000 rpm for 10 min, the supernatant was removed, and the precipitate was discarded. The supernatant was removed to measure the protein concentration using the BCA method. Loading buffer was added to unify the protein concentration at 95°–100° and boiled for 10 min 30 μg of protein samples were separated by sodium dodecyl sulfate–polyacrylamide gel electrophoresis (SDS-PAGE) and transferred to polyvinylidene difluoride (PVDF) membrane. Subsequently, the membranes were closed with 5% BSA for 60 min at room temperature and then incubated overnight at 4°C with anti-γH2A.X (1:1000, CST: #7631), anti-PARP1 (1:1000, CST: #94885 and abcam: ab227244), anti-AIF (1:1000, CST: #5318 and Proteintech: 67791-1-Ig), anti-GAPDH (1: 10,000, CST: #2118), anti 53BP1 (1:1000, ZEN-BIOSCIENCE: 381816), anti Caspase3 (1:1000, CST: #9661), anti-Cytochrome c (1:1000, CST: #4272), anti-KU70 (1:1000, CST: #4588), anti-BRCA1 (1:1000, abcam: ab238983), and anti-RAD51 (1:1000, CST: #8875). Subsequently, the membranes were washed with TBST and then incubated with horseradish peroxidase-conjugated secondary antibody for 60 min. Blots were visualized using ECL reagent (GE Healthcare, Piscataway, NJ, United States). ImageJ software was applied to analyze the band densities.

## 2.9 Statistical analysis

All experimental data passed Shapiro-Wilk normality test by SPSS 22.0. Data were analyzed using GraphPad Prism. All data were expressed as mean ± standard deviation (SD) and analyzed by one-way analysis of variance (ANOVA) followed by Tukey's test. Differences were considered statistically significant at $p < 0.05$.

# 3 Results

## 3.1 APG improves neurological deficits, reduces cerebral infarct volume and cerebral water content after pMCAO

As shown in Figure 1A, the rats in the pMCAO group showed significant neurological deficits compared with the control group ($p < 0.05$), and the pretreatment with medium-dose APG was effective in improving the neurological deficits compared with the pMCAO group ($p < 0.05$). Compared with the control group, the cerebral infarct volume (Figures 1B, C) and cerebral edema (Figure 1D) was significantly increased in the pMCAO group ($p < 0.05$), and the infarct volume was significantly reduced in APG treatment groups ($p < 0.05$), with the medium-dose group being the most significant. Compared with the control group, the water content of the left cerebral hemisphere of the rats in the pMCAO group was significantly increased, whereas brain edema was reduced in APG treatment groups compared with the pMCAO group, with the medium-dose APG being the most significant (Figure 1E).

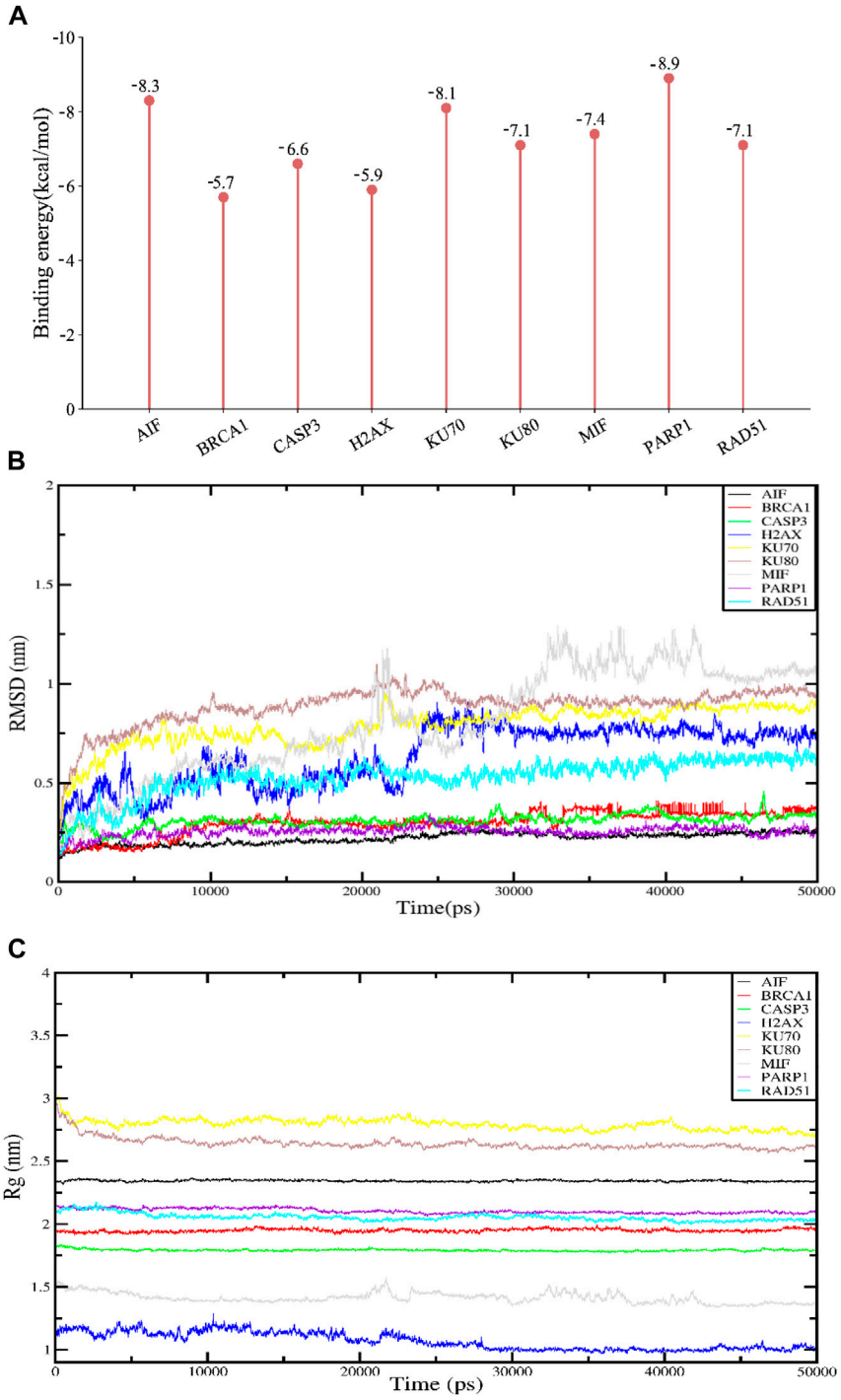


FIGURE 2
Molecular docking and molecular dynamics simulation results. APG has high binding fractions and stability with all docked proteins. **(A)** Molecular docking binding scores of APG to proteins associated with DNA damage, repair and programmed cell death. **(B)** RMSD results for APG molecular dynamics. **(C)** Rg results for APG molecular dynamics.

## 3.2 APG has high binding energy and stable binding to the proteins-related to DNA damage repair and parthanatos

By calculating the binding fraction, the molecular docking result of APG with proteins-related to DNA damage repair and parthanatos was predicted to be less than −5.0 kcal/mol, indicating that APG has a strong binding with these proteins. In other words, the lower the binding fraction of the ligand to the receptor, the more stable the binding conformation. As can be seen from Figure 2A, the binding affinity of all the docking results was below - 5 kcal/mol. The free binding scores of the docking results

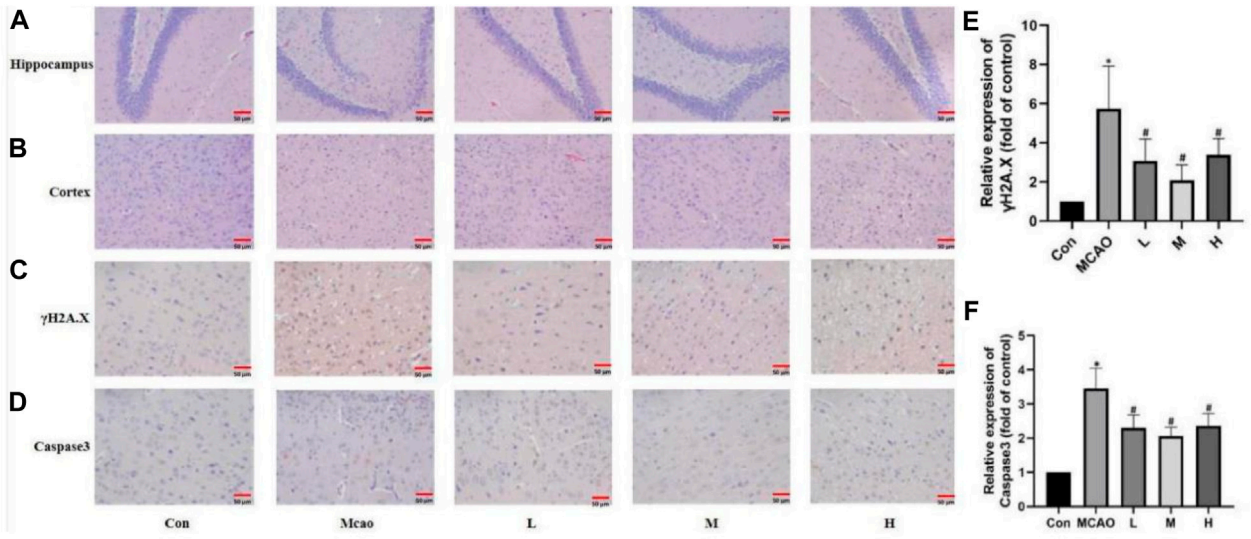


FIGURE 3
APG on pathological changes after pMCAO. **(A,B)** Representative pathological images of the ischemic penumbra (Hippocampus and cortex). Bar = 50 μm. **(C–F)** Immunostaining photomicrographs of γH2A.X, Caspase3 and quantitative analysis of the integrated optical density. Bar = 50 μm. Data are expressed as mean ± SD (n = 5). *$p < 0.05$, compared with Con; #$p < 0.05$, compared with pMCAO.

ranged from −5.7 ~ −8.9 kcal/mol, indicating that APG binds stably to these targets. The lowest binding scores were observed for PARP1 with APG. The Root Mean Square Deviation (RMSD) curve can reflect the degree of fluctuation of the system conformation. As shown in Figure 2B, the RMSD values of the complexed systems of APG and each protein showed some fluctuation and increase in the early stage, which indicated that the conformation changed to some extent relative to the docking initial conformation. However, the RMSD values of the complexes stabilized after a certain period, which indicated that the conformations of the APG-protein complexes did not change significantly, and the APG-protein complexes were able to maintain stable binding. Radius of Gyration (Rg) can characterize the compactness of the system structure. As shown in Figure 2C, the complexes of APG and nine proteins have relatively stable radius of gyration, suggesting that the complexes are conformationally stable and compact, and is in agreement with the results of RMSD. Thus, the molecular dynamics results demonstrated that the relevant proteins have a stable binding conformation with APG.

## 3.3 APG improves histopathology, reduces DNA damage and promotes neuronal survival

HE staining showed edema, structural vacuolization, nuclear consolidation and increased eosinophils in the ischemic semidarktic band of rats in the pMCAO group, which was effectively improved by APG in all dose groups (Figures 3A, B). Immunohistochemical analysis of γH2A.X staining was performed to observe the DNA damage of neurons in the ischemic semi-dark band. Immunohistochemical results showed that DNA damage was reduced in the APG group compared with the control group, especially in the medium-dose group (Figure 3C, $p < 0.05$).

## 3.4 Anti-oxidative stress and inhibition of DNA damage by APG

The ROS and MDA contents were significantly upregulated and SOD and GSH activities were significantly downregulated in the ischemic penumbra tissue of pMCAO group compared with the control group ($p < 0.05$). The above changes were reversed in the APG treatment groups ($p < 0.05$) (Figures 4A–D). Meanwhile, Western blot results showed that γH2A.X, which is the most important DNA damage marker, was decreased in the APG treatment group especially in the medium dose group ($p < 0.05$) (Figures 4E, F). In addition, APG treatment has effectively downregulated 53BP1 (a key protein regulating NHEJ) protein expression compared with the pMCAO group ($p < 0.05$, Figure 4G).

## 3.5 APG inhibits PARP1-mediated parthanatos and apoptosis

The expression of parthanatos- and apoptosis-related proteins was shown in Figure 5A. PARP1 hyperactivation induced by severe DNA damage triggered the initiation of parthanatos in the pMCAO group. pMCAO group showed significantly higher PARP1 expression than the control group ($p < 0.05$) (Figure 5B), and this phenomenon could be effectively reversed by different concentrations of APG treatment ($p < 0.05$). Meanwhile, AIF (67Kda) was significantly decreased in the pMCAO group ($p < 0.05$) than the control group (Figure 5C), and this phenomenon was reversed by medium and high doses of APG. On the contrary, the total content of AIF (57Kda) was significantly higher in the pMCAO group than in the control group ($p < 0.05$, Figure 5D), while the expression of AIF (57Kda) was significantly downregulated in the APG treatment groups ($p < 0.05$). Ratio of AIF 57 kda to AIF 67 kda

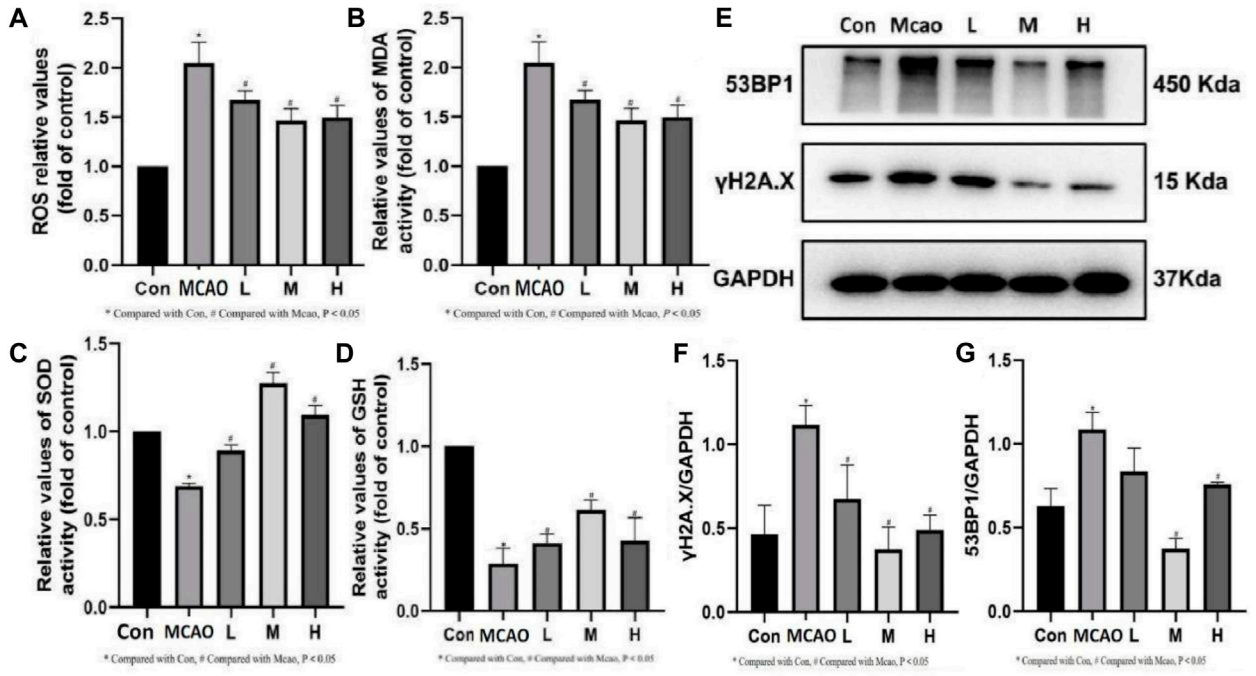


FIGURE 4
Effect of APG on oxidative stress index and DNA damage. **(A–D)** Statistical graph of ROS, MDA, SOD, and GSH. **(E)** Representative images of Western blot, including 53BP1 and γH2A.X. Data are expressed as mean ± SD (n = 3). **(F,G)** The relative band densities of the target proteins were normalized with GAPDH and normalized to control group, and data are expressed as mean ± SD (n = 3). *$p < 0.05$, compared with Con; #$p < 0.05$, compared with pMCAO.

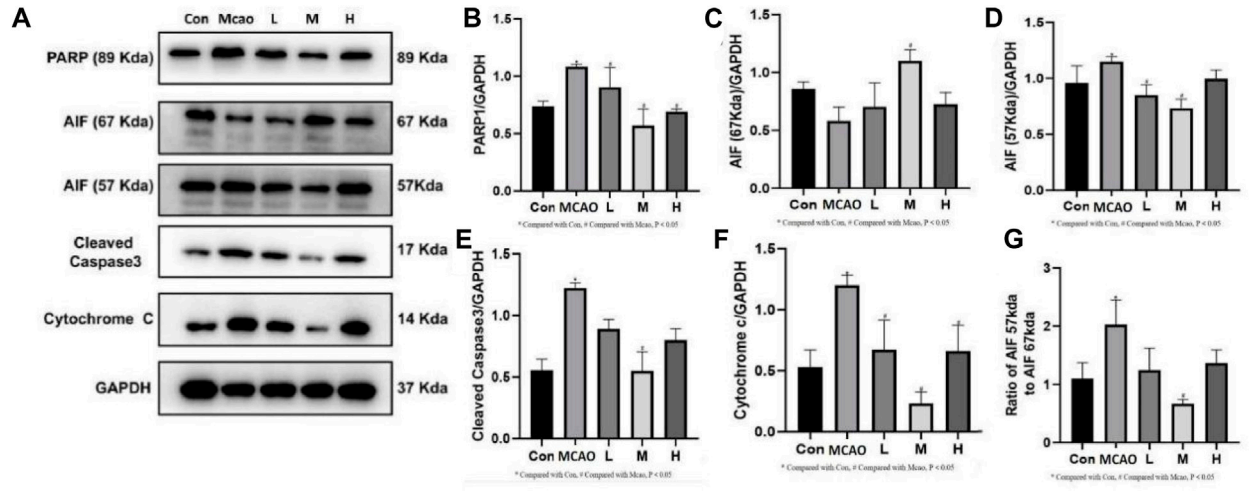


FIGURE 5
Expression of programmed cell death-related proteins determined by Western blot. **(A)** Representative images of Western blot, including PARP1, AIF, Caspase3 and Cyt c. **(B–F)** The relative band densities of the target proteins were normalized with GAPDH, and data are expressed as mean ± SD (n = 3). **(G)**. Ratio of AIF 57 kda to AIF 67 kda. *$p < 0.05$, compared with Con; #$p < 0.05$, compared with pMCAO.

as shown in Figure 5G. This suggests that APG can reduce apoptosis by inhibiting the entry of AIF into the nucleus. Apoptosis, as the most common mode of cell death, was also examined (Figures 5E, F). Cleaved caspase3 and Cytochrome c expression was significantly increased in pMCAO group in comparison with control group. Both cleaved caspase3 and Cyt c expression were downregulated in the ischemic penumbra brain tissue of the pMCAO model after treatment with different concentrations of APG. This phenomenon was particularly evident in the medium-dose APG group.

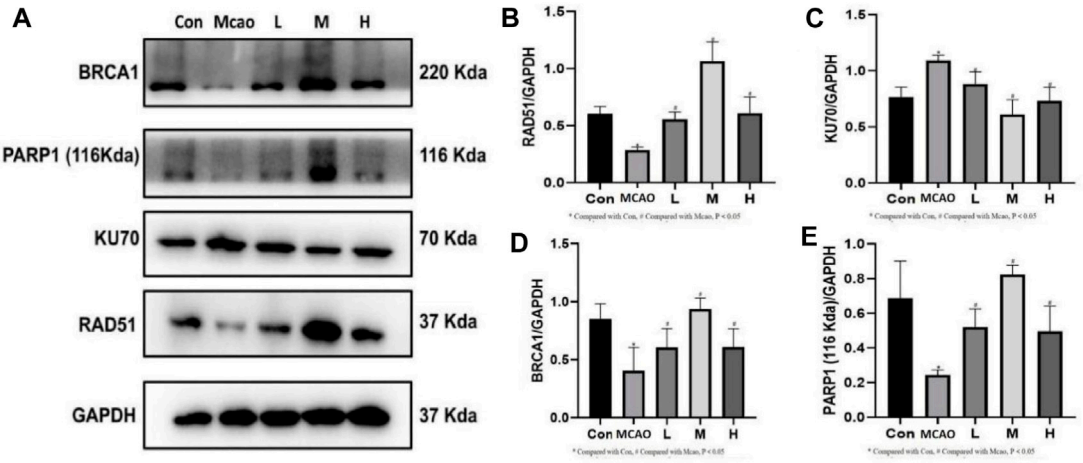


FIGURE 6
DNA repair-related protein expression determined by Western blot. **(A)** Representative images of WB, including BRCA1, PARP1, KU70 and RAD51. **(B–E)** The relative band densities of the target proteins were normalized with GAPDH, and data are expressed as mean ± SD (n = 3). *$p < 0.05$, compared with Con; #$p < 0.05$, compared with pMCAO.

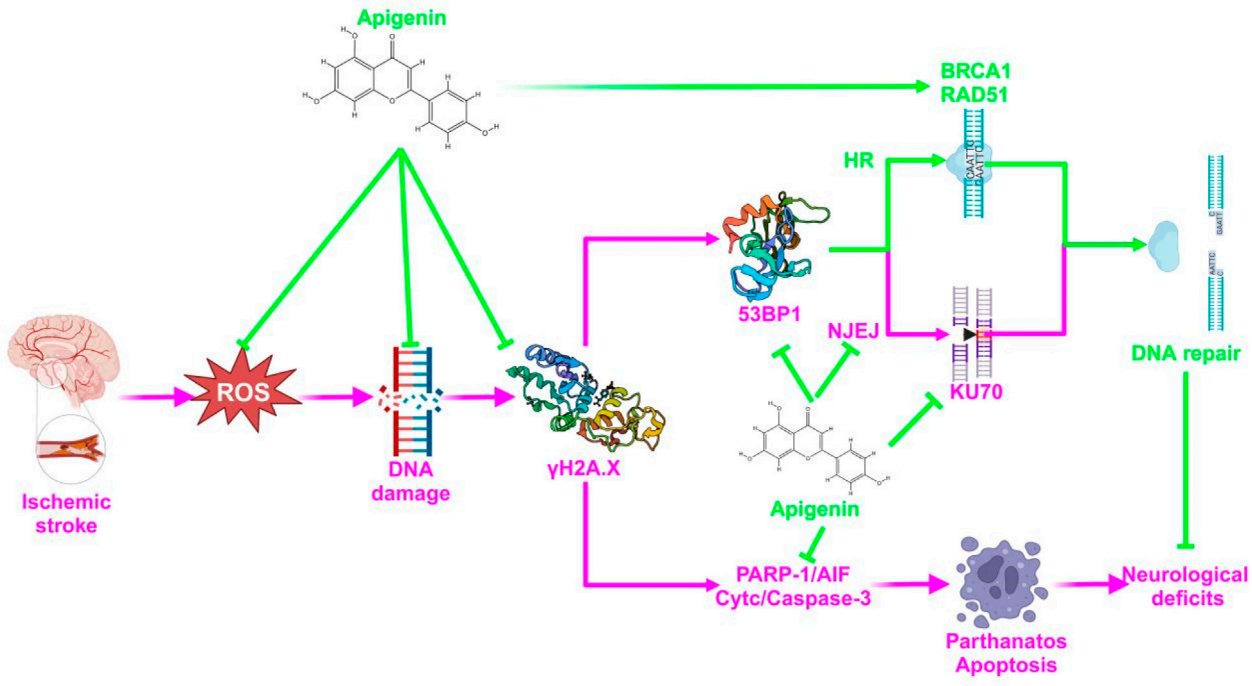


FIGURE 7
A diagrammatic sketch showing the protective effect of APG on pMCAO. The green color represents the therapeutic effect and the pink color represents the mechanism of the pathology.

## 3.6 APG promotes homologous recombination repair but not non-homologous end linkage

The expression of DNA repair-related proteins was shown in Figure 6A. DNA damage-induced activation of PARP1 triggers DNA repair and promotes the survival of damaged cells. pMCAO group showed significantly lower PARP1 expression than the control group ($p < 0.05$, Figure 6B), suggesting that the DNA repair was reduced, which could be effectively reversed by treatment with different concentrations of APG ($p < 0.05$). The repair of NHEJ is prone to errors, causing gene mutations and even cell death. kU70 protein expression was increased in the pMCAO group compared with the control group ($p < 0.05$, Figure 6C). KU70 expression decreased after APG treatment at different concentrations, especially in the medium-dose group ($p < 0.05$).

On the contrary, the expression of HR repair-related proteins BRCA1 and RAD51 was increased after APG treatment ($p < 0.05$, Figures 6D,E).

## 4 Discussion

IS is one of the leading causes of death worldwide and the second largest global burden of disease (Feigin et al., 2022). Oxidative stress is one of the important pathological mechanisms of IS. APG possesses the best ROS scavenging function among 10 flavonoids (Guo et al., 2014). However, the molecular mechanism of APG in treating IS through antioxidant therapy remains unclear. In this study, we firstly performed molecular docking and MD simulations of APG with DNA repair- and parthanatos-related proteins. The molecular docking and MD results showed that these proteins have low binding scores and stable binding conformations with APG. These proteins were subsequently validated in our *in vivo* experiments. Our study revealed elevated ROS level, MDA content, and protein expression of PARP1, γH2A.X, 53BP1, AIF, cleaved caspase3, Cytochrome c, and KU70, as well as decreased GSH content, SOD activity and protein expression of BRCA1 and RAD51 in pMCAO group. This phenomenon was reversed by pretreatment with different concentrations of APG and was most pronounced in the medium concentration of APG (60 mg/kg). APG treatment improved neurological deficits, cerebral infarct area, and cerebral water content in rats after pMCAO.

The brain is more susceptible to oxidative damage than other tissues because it has a higher oxygen-consuming and lipid content (Wang et al., 2023). In addition, there is virtually no low-energy reserves in brain, and its energy expenditure is entirely dependent on a continuous vascular supply of oxygen and glucose (Salim, 2017; Bailey, 2019). Increased ROS and MDA and decreased SOD and GSH in ischemic penumbra brain tissue after pMCAO lead to a disruption of antioxidant homeostasis (Elsayed et al., 2020). DNA damage is a serious consequence of oxidative stress and can cause neuronal cell death (Martin, 2008). The most severe case of DNA damage is DSB (Argunhan et al., 2021), where the serine 139 of histone H2AX is rapidly phosphorylated to produce phosphorylated H2AX, which is γH2A.X (Zeng et al., 2021). Both Western blot and immunohistochemistry results confirmed the increased γH2A.X expression after pMCAO. While, the expression of γH2A.X and PARP1 decreased after APG treatment, suggesting that APG attenuated DNA damage, which might in turn reduce parthanatos. APG reduces DNA damage in the ischemic penumbra of the brain through antioxidant.

PARP1 is the most abundant and representative enzyme of the PARP family and is important in repairing DNA damage and maintaining energy homeostasis (Liu S. Q. et al., 2022; Pinton et al., 2023). The first function of PARP1 is to mediate parthanatos (Huang et al., 2022). In many cells, the AIF 67 kDa precursor protein is the predominant form of AIF present. After entering the mitochondrial membrane space it becomes the mature 57 kDa AIF. Parthanatos is mediated by PARP1 for AIF entry into the nucleus and synergizes with macrophage migration inhibitory factor (MIF) to cleave DNA (Wang et al., 2016), i.e., the PARP1/AIF pathway (Liu L. B. et al., 2022). APG reversed the increased expression of PARP1 and AIF after pMCAO. Thus, APG protects against IS in part by inhibiting the PARP1/AIF pathway and improvement of the 67 kda and 57 kda ratios of the AIF. Similarly, APG also decreased the expression of apoptosis-related proteins cleaved caspase 3 and Cyt c, which was higher in the pMCAO group. Therefore, APG protects IS mainly by inhibiting parthanatos and apoptosis.

The second function of PARP1 is to mediate DSB repair (Yang et al., 2023), including NHEJ and HR. Expression of DNA repair proteins after DNA damage can determine the cellular outcomes (Singh et al., 2014). The NHEJ repair pathway is fast and non-precise, while the HR repair pathway is complex and precise (Radhakrishnan et al., 2014). We found that DNA repair protein PARP1 was decreased and 53BP1 expression was increased after pMCAO. 53BP1 promoted DSB repair through NHEJ (Lee et al., 2009). In contrast, 53BP1 expression was decreased in ischemic penumbra brain tissue after APG treatment. This suggests that APG may be involved in DNA repair through HR. Western blot detection of HR repair-related proteins BRCA1 and RAD51 showed both proteins significantly increased after APG treatment. On the contrary, the expression of NHEJ repair-related protein KU70 was decreased. KU70 is the representative protein of NHEJ (Zhu et al., 2014). These results suggest that APG involvement in DSB repair may be more dependent on HR than NHEJ. This needs to be further verified in future rescue experiment.

The above results suggest that APG bi-directionally regulates PARP1 to reduce nerve damage caused by pMCAO. On one hand, APG reduced PARP1 (89Kda) to inhibit PARP1/AIF pathway, DNA damage, and apoptosis to reduce neural cell death. On the other hand, APG increased PARP1 (116Kda) to improve DNA repair, and this repair may be more in favor of HR repair rather than NHEJ repair. The specific mechanism of APG against IS was proposed and shown in Figure 7. Inevitably, our study has some drawbacks, such as a short pMCAO time and lacks of rescue experiment. In addition, 120 mg/kg of APG may carry a risk of false-positive results.

## 5 Conclusion

In summary, the present study confirmed the novel mechanism of APG in the treatment of IS through antioxidative effects. Moreover, this protective effect of IS is achieved through DNA repair. The future needs more experiments to find the APG through DNA repair mechanisms. This study provides new insights into the mechanism of APG in the treatment of IS. Therefore, APG has the potential to be used as a therapeutic agent for IS. Our study provides a theoretical basis for the clinical translation of APG.

## Data availability statement

The original contributions presented in the study are included in the article/supplementary material, further inquiries can be directed to the corresponding authors.

## Ethics statement

The animal study was approved by the Changchun University of Chinese Medicine. The study was conducted in accordance with the local legislation and institutional requirements.

## Author contributions

NP: Writing–original draft. KZ: Writing–original draft. JC: Formal Analysis, Software, Writing–original draft. CR: Data curation, Formal Analysis, Writing–original draft. ZY: Writing–original draft, Methodology, Supervision. XZ: Validation, Writing–original draft, Data curation. GW: Validation, Writing–original draft, Project administration. CM: Writing–original draft, Validation, Visualization. HY: Writing–original draft, Investigation, Software, Supervision. JL: Conceptualization, Writing–review and editing, Funding acquisition, Writing–original draft. DZ: Writing–review and editing, Conceptualization, Funding acquisition. XW: Conceptualization, Data curation, Supervision, Visualization, Writing–original draft, Writing–review and editing.

## Funding

The author(s) declare that financial support was received for the research, authorship, and/or publication of this article. This study was supported by the grants from Jilin Scientific and Technological Development Program (20220505042ZP), Health Commission of Jilin Province (2022GW016), and Graduate Innovation Fund of Jilin University (2024CX253).

## Conflict of interest

The authors declare that the research was conducted in the absence of any commercial or financial relationships that could be construed as a potential conflict of interest.

## Publisher's note

All claims expressed in this article are solely those of the authors and do not necessarily represent those of their affiliated organizations, or those of the publisher, the editors and the reviewers. Any product that may be evaluated in this article, or claim that may be made by its manufacturer, is not guaranteed or endorsed by the publisher.

## References

Argunhan, B., Iwasaki, H., and Tsubouchi, H. (2021). Post-translational modification of factors involved in homologous recombination. *DNA Repair* 104, 103114. doi:10.1016/j.dnarep.2021.103114

Artus, C., Boujrad, H., Bouharrour, A., Brunelle, M. N., Hoos, S., Yuste, V. J., et al. (2010). AIF promotes chromatinolysis and caspase-independent programmed necrosis by interacting with histone H2AX. *Embo J.* 29, 1585–1599. doi:10.1038/emboj.2010.43

Bailey, D. M. (2019). Oxygen and brain death; back from the brink. *Exp. Physiol.* 104, 1769–1779. doi:10.1113/ep088005

Beneke, S. (2008). Poly(ADP-ribose) polymerase activity in different pathologies - the link to inflammation and infarction. *Exp. Gerontol.* 43, 605–614. doi:10.1016/j.exger.2008.04.008

Chen, J., Jin, K. L., Chen, M. Z., Pei, W., Kawaguchi, K., Greenberg, D. A., et al. (1997). Early detection of DNA strand breaks in the brain after transient focal ischemia: implications for the role of DNA damage in apoptosis and neuronal cell death. *J. Neurochem.* 69, 232–245. doi:10.1046/j.1471-4159.1997.69010232.x

Cho, B. B., and Toledo-Pereyra, L. H. (2008). Caspase-independent programmed cell death following ischemic stroke. *J. Investigative Surg.* 21, 141–147. doi:10.1080/08941930802029945

Cregan, S. P., Dawson, V. L., and Slack, R. S. (2004). Role of AIF in caspase-dependent and caspase-independent cell death. *Oncogene* 23, 2785–2796. doi:10.1038/sj.onc.1207517

Elsayed, W. M., Abdel-Gawad, E. H. A., Mesallam, D. I. A., and El-Serafy, T. S. (2020). The relationship between oxidative stress and acute ischemic stroke severity and functional outcome. *Egypt. J. Neurology Psychiatry Neurosurg.* 56, 74. doi:10.1186/s41983-020-00206-y

Feigin, V. L., Brainin, M., Norrving, B., Martins, S., Sacco, R. L., Hacke, W., et al. (2022). World stroke organization (WSO): global stroke fact sheet 2022. *Int. J. Stroke* 17, 18–29. doi:10.1177/17474930211065917

Guo, H. Z., Kong, S. Z., Chen, W. M., Dai, Z. H., Lin, T. X., Su, J. Y., et al. (2014). Apigenin mediated protection of OGD-evoked neuron-like injury in differentiated PC12 cells. *Neurochem. Res.* 39, 2197–2210. doi:10.1007/s11064-014-1421-0

Huang, P., Chen, G. W., Jin, W. F., Mao, K. J., Wan, H. T., and He, Y. (2022). Molecular mechanisms of parthanatos and its role in diverse diseases. *Int. J. Mol. Sci.* 23, 7292. doi:10.3390/ijms23137292

Kim, K. B., Kim, D. W., Park, J. W., Jeon, Y. J., Kim, D., Rhee, S., et al. (2014). Inhibition of Ku70 acetylation by INHAT subunit SET/TAF-Iβ regulates Ku70-mediated DNA damage response. *Cell. Mol. Life Sci.* 71, 2731–2745. doi:10.1007/s00018-013-1525-8

Lee, J. H., Cheong, H. M., Kang, M. Y., Kim, S. Y., and Kang, Y. (2009). Ser1778 of 53BP1 plays a role in DNA double-strand break repairs. *Korean J. Physiology Pharmacol.* 13, 343–348. doi:10.4196/kjpp.2009.13.5.343

Li, P. Y., Hu, X. M., Gan, Y., Gao, Y. Q., Liang, W. M., and Chen, J. (2011). Mechanistic insight into DNA damage and repair in ischemic stroke: exploiting the base excision repair pathway as a model of neuroprotection. *Antioxidants Redox Signal.* 14, 1905–1918. doi:10.1089/ars.2010.3451

Liu, L. B., Li, J. X., Ke, Y. S., Zeng, X. L., Gao, J. M., Ba, X. Q., et al. (2022b). The key players of parthanatos: opportunities for targeting multiple levels in the therapy of parthanatos-based pathogenesis. *Cell. Mol. Life Sci.* 79, 60. doi:10.1007/s00018-021-04109-w

Liu, S. Q., Luo, W. B., and Wang, Y. F. (2022a). Emerging role of PARP-1 and PARthanatos in ischemic stroke. *J. Neurochem.* 160, 74–87. doi:10.1111/jnc.15464

Longa, E. Z., Weinstein, P. R., Carlson, S., and Cummins, R. (1989). REVERSIBLE MIDDLE CEREBRAL-ARTERY OCCLUSION WITHOUT CRANIECTOMY IN RATS. *Stroke* 20, 84–91. doi:10.1161/01.Str.20.1.84

Lou, Z. K., Chini, C. C. S., Minter-Dykhouse, K., and Chen, J. J. (2003). Mediator of DNA damage checkpoint protein 1 regulates BRCA1 localization and phosphorylation in DNA damage checkpoint control. *J. Biol. Chem.* 278, 13599–13602. doi:10.1074/jbc.C300060200

Lu, X. P., Tang, M., Zhu, Q., Yang, Q. Y., Li, Z. M., Bao, Y. T., et al. (2019). GLP-catalyzed H4K16me1 promotes 53BP1 recruitment to permit DNA damage repair and cell survival. *Nucleic Acids Res.* 47, 10977–10993. doi:10.1093/nar/gkz897

Mao, Z. Y., Bozzella, M., Seluanov, A., and Gorbunova, V. (2008). Comparison of nonhomologous end joining and homologous recombination in human cells. *DNA Repair* 7, 1765–1771. doi:10.1016/j.dnarep.2008.06.018

Martin, L. J. (2008). DNA damage and repair: relevance to mechanisms of neurodegeneration. *J. Neuropathology Exp. Neurology* 67, 377–387. doi:10.1097/NEN.0b013e31816ff780

Pieper, A. A., Verma, A., Zhang, J., and Snyder, S. H. (1999). Poly (ADP-ribose) polymerase, nitric oxide and cell death. *Trends Pharmacol. Sci.* 20, 171–181. doi:10.1016/s0165-6147(99)01292-4

Pinton, G., Boumya, S., Ciriolo, M. R., and Ciccarone, F. (2023). Epigenetic insights on PARP-1 activity in cancer therapy. *Cancers* 15, 6. doi:10.3390/cancers15010006

Raderschall, E., Bazarov, A., Cao, J. P., Lurz, R., Smith, A., Mann, W., et al. (2002). Formation of higher-order nuclear Rad51 structures is functionally linked to p21 expression and protection from DNA damage-induced apoptosis. *J. Cell Sci.* 115, 153–164. doi:10.1242/jcs.115.1.153

Radhakrishnan, S. K., Jette, N., and Lees-Miller, S. P. (2014). Non-homologous end joining: emerging themes and unanswered questions. *DNA Repair* 17, 2–8. doi:10.1016/j.dnarep.2014.01.009

Salim, S. (2017). Oxidative stress and the central nervous system. *J. Pharmacol. Exp. Ther.* 360, 201–205. doi:10.1124/jpet.116.237503

Shrivastav, M., De Haro, L. P., and Nickoloff, J. A. (2008). Regulation of DNA double-strand break repair pathway choice. *Cell Res.* 18, 134–147. doi:10.1038/cr.2007.111

Singh, S. S., Sarma, J., Narasu, L., Dayam, R., Xu, S. L., and Neamati, N. (2014). A review on PARP1 inhibitors: pharmacophore modeling, virtual and biological screening

studies to identify novel PARP1 inhibitors. *Curr. Top. Med. Chem.* 14, 2020–2030. doi:10.2174/1568026614666140929152123

Wang, Q., Tompkins, K. D., Simonyi, A., Korthuis, R. J., Sun, A. Y., and Sun, G. Y. (2006). Apocynin protects against global cerebral ischemia-reperfusion-induced oxidative stress and injury in the gerbil hippocampus. *Brain Res.* 1090, 182–189. doi:10.1016/j.brainres.2006.03.060

Wang, X., Li, J. J., Zhao, D. X., and Li, J. H. (2022). |Therapeutic and preventive effects of apigenin in cerebral ischemia: a review. *Food and Funct.* 13, 11425–11437. doi:10.1039/d2fo02599j

Wang, X., Yu, Z. Q., Dong, F. X., Li, J. J., Niu, P., Ta, Q., et al. (2023). Clarifying the mechanism of apigenin against blood-brain barrier disruption in ischemic stroke using systems pharmacology. *Mol. Divers.* doi:10.1007/s11030-023-10607-9

Wang, Y. F., An, R., Umanah, G. K., Park, H., Nambiar, K., Eacker, S. M., et al. (2016). A nuclease that mediates cell death induced by DNA damage and poly(ADP-ribose) polymerase-1. *Science* 354, aad6872. doi:10.1126/science.aad6872

Yang, S., Hwang, S., Kim, B., Shin, S., Kim, M., and Jeong, S. M. (2023). Fatty acid oxidation facilitates DNA double-strand break repair by promoting PARP1 acetylation. *Cell Death Dis.* 14, 435. doi:10.1038/s41419-023-05968-w

Yu, S. W., Andrabi, S. A., Wang, H., Kim, N. S., Poirier, G. G., Dawson, T. M., et al. (2006). Apoptosis-inducing factor mediates poly(ADP-ribose) (PAR) polymer-induced cell death. *Proc. Natl. Acad. Sci. U. S. A.* 103, 18314–18319. doi:10.1073/pnas.0606528103

Zeng, M. L., Zhou, H. F., He, Y., Wang, Z. X., Shao, C. Y., Yin, J. J., et al. (2021). Danhong injection alleviates cerebral ischemia/reperfusion injury by improving intracellular energy metabolism coupling in the ischemic penumbra. *Biomed. Pharmacother.* 140, 111771. doi:10.1016/j.biopha.2021.111771

Zhu, F., Liu, J. L., Li, J. P., Xiao, F., Zhang, Z. X., and Zhang, L. (2014). MicroRNA-124 (miR-124) regulates Ku70 expression and is correlated with neuronal death induced by ischemia/reperfusion. *J. Mol. Neurosci.* 52, 148–155. doi:10.1007/s12031-013-0155-9

frontiers | Frontiers in Pharmacology

TYPE Systematic Review
PUBLISHED 05 June 2024
DOI 10.3389/fphar.2024.1411026



OPEN ACCESS

EDITED BY
Junfeng Wang,
Massachusetts General Hospital and Harvard Medical School, United States

REVIEWED BY
Luo Qiang,
Children's Hospital of Chongqing Medical University, China
Yinhui Yao,
Affiliated Hospital of Chengde Medical University, China

*CORRESPONDENCE
Yongkang Sun,
sunyongkang00@126.com
Xinzhi Wang,
znqznq@163.com

†These authors have contributed equally to this work and share first authorship

RECEIVED 02 April 2024
ACCEPTED 08 May 2024
PUBLISHED 05 June 2024

CITATION
Song Y, Xu F, Li S, Sun Y and Wang X (2024), Efficacy and safety of Xingnaojing injection for post-operative patients of intracerebral haemorrhage: a meta-analysis and systematic review.
*Front. Pharmacol.* 15:1411026.
doi: 10.3389/fphar.2024.1411026



# Efficacy and safety of Xingnaojing injection for post-operative patients of intracerebral haemorrhage: a meta-analysis and systematic review

Yanbo Song[1,2†], Fangbiao Xu[1,2†], Shuliang Li[1,2], Yongkang Sun[1*] and Xinzhi Wang[1*]

[1]Center of Encephalopathy, The First Affiliated Hospital of Henan University of Chinese Medicine, Zhengzhou, Henan, China, [2]First Clinical Medical College, Henan University of Chinese Medicine, Zhengzhou, Henan, China

**Background:** Intracerebral haemorrhage (ICH) is the deadliest subtype of stroke. Surgery remains a vital measure for life-saving in emergency situations, however, the recovery of post-operative patients is not optimistic. This study aimed to evaluate the evidence of the efficacy and safety of Xingnaojing injection (XNJ) for post-operative patients of ICH.

**Methods:** From inception to 31 January 2024, we searched eight representative databases for randomized controlled trials on post-operative patients of ICH treated with XNJ. A meta-analysis was conducted using R4.2.2, and the quality of the evidence was evaluated by GRADE criteria.

**Results:** The results indicated that the combination of XNJ with conventional western medicine therapy improved the total efficiency rate (RR = 1.26; 95% CI [1.21 to 1.32]; $p < 0.0001$), reduced the all-cause mortality within 15 days (RR = 0.45; 95% CI [0.30 to 0.67]; $p < 0.0001$), decreased the volume of hematoma (MD = −4.72; 95% CI [-7.43 to −2.01]; $p = 0.0006$) and perihematomal edema (MD = −4.11; 95% CI [-8.11 to −0.11]; $p = 0.0441$), reduced the TNF-α levels (SMD = −1.61, 95% CI [−2.23 to −0.99], $p < 0.0001$), decreased neurological impairment (SMD = −1.44; 95% CI [-1.78 to −1.11]; $p < 0.0001$), improved the activities of daily living (SMD = 1.22; 95% CI [0.78 to 1.66]; $p < 0.0001$), and enhanced the consciousness level (MD = 2.08, 95% CI [1.22 to 2.93], $p < 0.0001$). In addition, the complications of the combination therapy group were lower (RR = 0.43; 95% CI [0.35 to 0.54]; $p < 0.0001$) and the adverse drug reactions were comparable to the control group (RR = 0.89; 95% CI [0.55 to 1.45]; $p = 0.6521$). The trial sequential analysis results showed that the sample size is sufficient.

**Conclusion:** Current evidence indicates that XNJ can enhance the efficiency, reduce mortality, and lower the incidence of complications, while demonstrating good tolerability of post-operative patients of ICH. However, the level of evidence from existing studies is relatively weak, and only prove short-term effects, and high-quality RCTs are needed to further verify the accuracy of these conclusions.

**Systematic Review Registration:** identifier (PROSPERO 2024 CRD42024503006). https://www.crd.york.ac.uk/prospero/display_record.php?ID=CRD42024503006, Identifier CRD42024503006.

KEYWORDS

Xingnaojing injection, traditional Chinese medicine, Chinese patent medicine, injection, intracerebral haemorrhage, post-operative patients, meta-analysis

# 1 Introduction

Intracerebral haemorrhage (ICH) refers to non-traumatic spontaneous intracerebral haemorrhage (NBCMA and CDGNBCMA, 2019), which falls under the category of hemorrhagic stroke in Traditional Chinese Medicine (TCM) (Wang and Gao, 2008). China has the highest number of stroke cases in the world (Wang L. D. et al., 2022). Data from the Global burden of disease study (GBD, 2019 Diseases and Injuries Collaborators, 2020) indicates that stroke is the leading cause of death and disability among adults in China, with an ICH prevalence rate of 306 per 100,000 in 2019. Data from 1,672 public tertiary hospitals in the hospital quality monitoring system showed that ICH cases accounted for 14.2% of all stroke cases admitted for treatment in China in 2019 (Wang Y. J. et al., 2022). It is evident that ICH poses a serious threat to public health and impacts economic and social development. Currently, the primary treatment for ICH still focuses on symptomatic relief (Tang et al., 2018). Surgery may improve neurological recovery after ICH, but the presence of perihematomal edema post-surgery and potential secondary damage caused by the operation may limit its therapeutic effectiveness (Thompson et al., 2015).

Excitingly, TCM has accumulated a wealth of clinical experience in the treatment of ICH. With the approval of the National Medical Products Administration of China, Xingnaojing injection (XNJ), a derivative of Angong Niuhuang pill which have been used clinically for over 200 years, is a representative injectable drug in TCM used for the treatment of stroke, and it possesses the effects of clearing heat and detoxifying, cooling the blood and promoting circulation, as well as consciousness-restoring (Deng et al., 2010; Yue et al., 2019), Its formulation of Chinese botanical drugs comprises *Dryobalanops aromatica C.F.Gaertn* [Dipterocarpaceae; Borneolum], *Curcuma aromatica* Salisb. [Zingiberaceae; Curcumae Radix], *Gardenia jasminoides* J. Ellis [Rubiaceae; Gardeniae Fructus], *Moschus berezovskii Flerov, M. sifanicus* Przewalski, or *M. moschiferus* Linnaeus [Cervidae; Moschus], and it is produced using steam distillation to extract the water-soluble or volatile metabolites from the botanical drugs conveniently and effectively, resulting in an intravenous injection (Deng et al., 2010; Yue et al., 2019).

In China, XNJ is produced by three pharmaceutical companies (Wuxi Jiyu Shanhe Pharmaceutical Co., Ltd, Henan Tiandi Pharmaceutical Co., Ltd, and Dali Pharmaceutical Co., Ltd). The production processes and quality standards of all the three companies adhere to the National Drug Standards WS3-B-3353-98-2003 of China. In the preparation process, 30 g of Curcumae Radix and 30 g of Gardeniae Fructus are initially distilled with 1,500 mL of water, yielding 1,000 mL of distillate; subsequently, 7.5 g of Moschus and 250 mL of distilled water are introduced to the aforementioned distillate, followed by the collection of another 1,000 mL of distillate for later use. Next, 1 g of Borneolum and 8 g of polysorbate 80 are pulverized and combined with the distillate. Finally, 8 g of sodium chloride is incorporated, and the mixture is stirred, blended, left to settle overnight in a refrigerated environment, filtered, transferred to containers, and sterilized. Regarding the identified active components, borneol, which is traditionally utilized to monitor the quality of XNJ, should meet a minimum concentration of 0.7 g/L as stipulated by the drug standards set forth by the National Medical Products Administration of China (Pharmacopoeia Commission of the Ministry of Public Health of the People's Republic of China, 1998; China Food and Drug Administration, 2003). Moreover, by using gas chromatography–mass spectrometry (GC-MS), high performance liquid chromatography (HPLC), network pharmacology, and molecular docking technology, researchers recently found that the representative active metabolites of XNJ also include muscone, camphor, eucarvone, isophorone, 4-methylene-isophorone, curcumenone, curcumenol, curdione, curzerenone, furanodienone, curcumol, germacrone, geniposide, etc. (Yang et al., 2016; Fang et al., 2017; Huang et al., 2017; Wu et al., 2021). A previous study has analyzed the 27 possible metabolites of XNJ, and found that among them, the camphor, borneol, and muscone account for more than 85% of the peak area of GC-MS (Zhang et al., 2004).

Numerous systematic reviews and meta-analyses have demonstrated the efficacy and safety of XNJ in the treatment of acute ICH (Peng et al., 2014; Wu et al., 2016; Yu et al., 2016; Xu et al., 2018; Ma et al., 2020; Wang et al., 2021). Many guidelines and consensus in China also recommend the use of XNJ for the emergency treatment of ICH (Gao, 2016; Ni et al., 2020; Gao and Zhao, 2023), but did not specify the recommendations and treatment advantages of XNJ application after the surgery of ICH. The results of one meta-analysis showed that for patients after ICH surgery, the addition of proprietary Chinese patent medicine (Naoxueshu oral liquid) had better clinical efficacy (Yu et al., 2023). Another network meta-analysis (Ren et al., 2022) found that compared with ICH patients who underwent surgery plus conventional western medicine (CWM) treatment, the addition of Chinese herbal injections on this basis could increase the total efficiency rate, lower National Institutes of Health Stroke Scale (NIHSS) scores, and improve Glasgow Coma Scale (GCS) scores, with good safety, and XNJ was ranked first in lowering NIHSS scores. Sadly, this study did not report mortality, perihematomal edema volume, or activities of daily living (ADL) ability, and did not specifically analyze and report the results of the traditional meta-analysis. Thus, there is currently a lack of systematic reviews and meta-analyses for the use of XNJ

treatment in post-operative patients of ICH. Consequently, we used R 4.2.2 to invoke the meta package to perform a meta-analysis on the efficacy and safety of XNJ treatment after surgery of ICH, to provide evidence-based support for the application of it in this field.

# 2 Materials and methods

We performed this meta-analysis in strict accordance with the Preferred Reporting Items for Systematic Reviews and Meta-analyses (PRISMA) 2020 statement (Page et al., 2021). The protocol was already registered in PROSPERO (CRD42 024503006).

## 2.1 Search strategy

Comprehensively searched the published RCTs included in PubMed, Cochrane Library, Embase, Web of Science, China National Knowledge Infrastructure (CNKI), VIP database, Wanfang Database, and SinoMed. Search period: from the inception of the databases to 31 January 2024. Languages: Chinese and English. Search method: using both Medical Subject Headings (MeSH) terms and free-text keywords. The search strategy was appropriately adjusted according to the individual features of each database. The detailed search strategies are provided in the Supplementary Material S1.

## 2.2 Eligibility criteria

### 2.2.1 Inclusion criteria

(1) Study type: Randomized Controlled Trials (RCTs).
(2) Study subjects: Post-operative adult patients of ICH (as diagnosed by a clinician, or using any recognized diagnostic criteria). And surgical treatments including soft/hard channel puncture hematoma aspiration/fragmentation and drainage surgery, ventricular drainage surgery, neuroendoscopic hematoma evacuation surgery, craniotomy for hematoma removal, etc.
(3) Interventions: Both groups received CWM treatments (including hemostasis, dehydration, intracranial pressure reduction, blood pressure reduction, neural nutrition, cerebral cell activation, hyperbaric oxygen therapy, anti-infection, gastric acid suppression, etc.) as the foundation; the experimental group received additional intravenous injections of XNJ, with no restrictions on dosage or course of treatment.
(4) Outcome indicators: The study included at least one of the following outcomes: total efficiency rate; all-cause mortality; neurological impairment, assessed by NIHSS, European Stroke Scale (ESS), Chinese Stroke Scale (CSS), etc.; ability of ADL, assessed by Barthel Index (BI), modified Barthel Index (mBI), etc.; level of consciousness, assessed by GCS, etc.; volume of intracerebral hematoma; volume of perihematomal edema; levels of inflammatory indicator TNF- α, and safety indicators (including adverse drug reactions and incidence of complications).

### 2.2.2 Exclusion criteria

(1) Study that was grouped by incorrect random methods such as the order of admission or treatment method.
(2) Intervention measures include other therapies, in addition to XNJ (intravenous injection) and CWM treatment.
(3) Study with statistical errors where the data cannot be aggregated.
(4) For the same literature published repeatedly, one with complete data was reserved, and the rest were excluded.
(5) For studies with completely duplicated data but different authors, the latest published studies were excluded.

## 2.3 Study selection and data extraction

Two researchers independently screened and extracted information from the literature according to the inclusion and exclusion criteria set forth in the study. In cases where there was disagreement, a discussion was initiated; if disagreements persisted, a third party would consider the different viewpoints and make a decision. The extracted information by preformulated data collection form included the first author, publication year, sample size, gender, age, interventions, duration of treatment, outcome indicators, and their respective data.

## 2.4 Assessment of risk of bias

The quality of the studies was assessed using the Risk of Bias assessment tool (ROB2.0) in the Cochrane Handbook (v6.4) (Higgins et al., 2023). The assessment was cross-checked by two researchers, and any discrepancies were resolved through discussion. If consensus could not be reached, a third researcher was consulted to make a decision. The assessment covered the following domains: randomization process, deviations from intended interventions, missing outcome data, measurement of the outcome, selection of the reported result, and overall risk of bias. Each domain encompassed one to seven specific questions. The results were classified as “low risk of bias”, “some concerns” and “high risk of bias".

## 2.5 Statistical analysis

Meta-analysis was carried out using R 4.2.2. The effect size for dichotomous variables was expressed as relative risks (RR) with their 95% confidence intervals (CI), and a continuity correction of 0.5 was added to each side when there were studies with 0 cells.

For continuous variables, when the outcomes were in the same unit, the weighted mean difference (WMD) with its 95% CI was calculated using the noStandard method; when the units varied or the scales different for the same outcome in different studies, the standardized mean difference (SMD) with its 95% CI was computed using Hedges’ method.

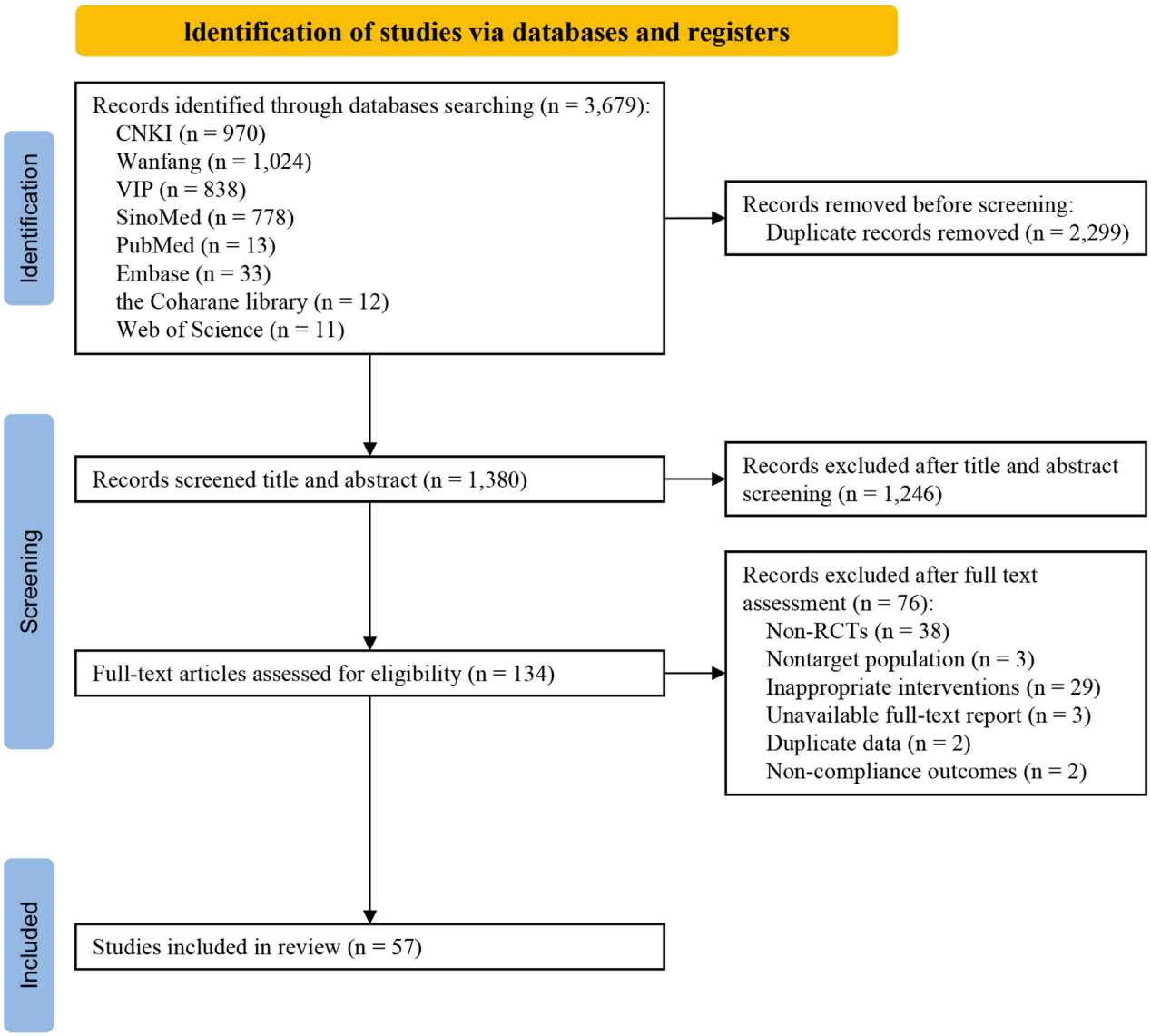


FIGURE 1
Flow chart of the study selection process.

Before combining effect sizes, an assessment ($\chi^2$ and $I^2$ test) for heterogeneity was conducted, and a fixed-effect model was used if $p \geq 0.10$ and $I^2 < 50\%$; otherwise, a random-effects model was employed, and subgroup analyses were undertaken to explore the sources of heterogeneity. Sensitivity analysis was also used to investigate the stability of study results and the sources of heterogeneity. Potential publication bias was explored using Begg's test and Egger's test. It was considered statistically significant when $p < 0.05$.

## 2.6 Trial sequential analysis (TSA) and quality of evidence

Trial sequential analysis (TSA) was performed using TSA 0.9.5.10 Beta (Thorlund et al., 2017). And calculated the Required Information Size (RIS) to determine the possibility of false negative results. The quality of evidence was graded using the web-based development tool of GRADEpro GDT (https://www.gradepro.org/). Based on the GRADE methodology applied in systematic reviews (Guyatt et al., 2011), three upgrading factors (potential confounders, dose-response relationship, large magnitude of effect) and five downgrading factors (publication bias, indirectness, heterogeneity, imprecision, and risk of bias) were thoroughly considered to classify the quality of evidence into four levels: very low, low, moderate, and high. If more than one downgrading factor was present, the quality of evidence would be downgraded, resulting in the formation of an evidence profile.

# 3 Results

## 3.1 Literature search

In this study, a total of 3,679 studies were retrieved, including 3,610 Chinese studies and 69 English studies. The retrieved study

TABLE 1 Characteristics of the included trials.

| Study | Type of ICH | Sample size | | Sex (M/F) | | Age (range/mean) (years) | | Intervention (T) | | Time of surgery (range/mean) | | Duration | Outcomes |
|---|---|---|---|---|---|---|---|---|---|---|---|---|---|
| | | T | C | T | C | T | C | XNJ | Surgery | T | C | | |
| Hao et al. (2024) | ICH | 50 | 50 | 25/25 | 24/26 | 45-80/62.51 ± 7.51 | 45-79/62.48 ± 7.04 | 20 mL qd | Unclear | - | - | 2w | ③⑤⑨ |
| Sun et al. (2022) | HICH | 61 | 61 | 30/31 | 31/30 | 67-81 | 66-82 | 30 mL qd | NES | 2–18 h | 3–19 h | 1w | ①③④⑥⑧⑨ |
| Xiao and Wu (2021) | ICH | 30 | 30 | 15/15 | 14/16 | ≥60/65.87 ± 3.80 | ≥60/66.47 ± 3.55 | 10–20 mL qd | Mix | - | | 2w | ①③④⑧⑨ |
| Deng et al. (2021) | HICH | 50 | 50 | 30/20 | 33/17 | 45-69/50.72 ± 3.00 | 46-69/50.98 ± 3.33 | 20 mL qd | SCPADS | ≤24 h | | 2w | ① |
| Chen (2021) | ICH | 29 | 29 | 12/17 | 16/13 | 45-70/57.1 ± 5.6 | 42-71/57.3 ± 5.4 | 20 mL qd | Unclear | - | | 2w | ③④⑥ |
| Liang and Qin (2020) | HICH | 24 | 24 | 14/10 | 15/9 | 56-78/65.38 ± 4.26 | 58-75/65.80 ± 4.15 | 20 mL qd | HCPADS | ≤36 h | | 2w | ①③⑤ |
| Xu (2020) | HICH | 55 | 55 | 33/22 | 35/20 | 73.79 ± 7.46 | 75.57 ± 8.52 | 20 mL qd | HCPADS | ≤6 h | | 1w | ③⑥ |
| Shu (2020) | HICH | 41 | 41 | 27/14 | 28/13 | 51-74/62.53 ± 1.25 | 51-75/62.58 ± 1.21 | 20 mL qd | HCPADS | <48/14.17 ± 5.36 h | <48/14.20 ± 5.31 h | 30d | ①③⑤ |
| Zhang (2019) | ICH | 40 | 40 | 18/12 | 29/11 | 38-67/51.95 ± 9.93 | 30-70/51.42 ± 7.46 | 10–20 mL qd | HCPADS | - | | 2w | ①⑦ |
| Li (2019) | HICH | 45 | 45 | 48/42 | | 51-72/64.2 ± 6.3 | | 30 mL qd | SCPADS | 5–7 h | | 2w | ⑤ |
| Wang (2019) | HICH | 59 | 59 | 32/27 | 33/26 | 57.24 ± 8.02 | 58.09 ± 7.65 | 20 mL qd | HCPADS | ≤48/14.02 ± 8.95 h | ≤48/13.97 ± 9.02 h | 4w | ①③⑧⑨ |
| You (2019) | HICH | 37 | 37 | 25/12 | 24/13 | 42-70/49.2 ± 5.3 | 39-68/48.8 ± 5.9 | 10–20 mL bid | Unclear | - | | 20d | ①②⑤⑨ |
| Li et al. (2018) | ICH | 51 | 51 | 30/21 | 29/22 | 42-74/54.8 ± 8.4 | 41-76/52.7 ± 7.1 | 20 mL qd | SCPADS | ≤72 h | | 6w | ③④ |
| Jiang and Xiao (2018) | HICH | 25 | 25 | 16/9 | 14/11 | 55-74/66.5 ± 5.2 | 55-75/66.1 ± 5.3 | 10–20 mL qd | SCPADS | - | | 2w | ①⑤⑥ |
| Cheng (2018) | HICH | 20 | 20 | 12/8 | 11/9 | 28-66/56.3 ± 6.2 | 29-67/56.8 ± 6.1 | 20 mL qd | SCPADS | 1.0-21.7/8.7 ± 2.5 h | 0.8-21.3/8.8 ± 2.4 h | 2w | ①③⑤⑦ |
| Jin and Wang (2018) | HICH | 42 | 42 | 28/14 | 29/13 | 62.3 ± 5.1 | 61.6 ± 4.8 | 20 mL qd | HCPADS | - | | 4w | ①②③⑧⑨ |
| Shuang et al. (2017) | HICH | 54 | 54 | 56/52 | | 43-74/63.1 ± 10.2 | | 20 mL qd | NES | 1-36/10.3 ± 3.4 h | | 4w | ①③⑧ |
| Gu and Zhang (2017) | HICH | 44 | 44 | 26/18 | 24/20 | 24-78/56.01 ± 6.05 | 25-80/55.68 ± 5.98 | 20 mL qd | SCPADS | - | | 2w | ①③⑥⑨ |
| Zhou and Sun (2017) | HICH | 50 | 50 | 26/24 | 28/22 | 38-72/51.8 ± 3.2 | 36-71/46.8 ± 2.5 | 30 mL qd | Mix | - | | 30d | ①⑨ |
| Zhang et al. (2016) | HICH | 37 | 37 | 27/10 | 25/12 | 52-70/61.5 ± 4.9 | 53-72/61.8 ± 4.6 | 20 mL qd | HCPFAS | 6-20/12.5 ± 4.1 h | 5-19/12.8 ± 3.7 h | 2w | ①②⑧ |
| Xia et al. (2016) | HICH | 44 | 44 | 29/15 | 30/14 | 35-78/60.1 ± 3.5 | 38-76/59.6 ± 3.6 | 40 mL qd | HCPFAS | - | | 2w | ①③⑤⑥ |
| Ren (2016) | HICH | 53 | 53 | 65/41 | | 35-77/63.6 ± 5.6 | | 4 mL qd | HCPADS | 5.3 ± 1.7 h | | 2w | ③ |
| Liu et al. (2016) | ICH | 49 | 49 | 65/53 | | 52-78/65.8 ± 4.6 | | 20–30 mL qd | Unclear | - | | 4w | ①②③ |
| Lian (2016) | ICH | 80 | 80 | 47/33 | 48/32 | 44-80/58 ± 6 | 45-80/54 ± 8 | 30 mL qd | HCPADS | 12–72 h | | 3w | ③④⑨ |
| Tong et al. (2016) | HICH | 68 | 72 | 38/30 | 36/36 | 57.12 ± 5.42 | 58.38 ± 6.03 | 30 mL qd | Mix | - | | 15d | ①⑨ |
| Zhang et al. (2015) | HICH | 50 | 50 | 54/46 | | 61.2 ± 7.5 | | 30 mL qd | SCPADS | 5–8 h | | 2w | ②③ |
| Xu and Lv (2015) | HICH | 52 | 52 | 29/23 | 27/25 | 44-72/59.12 ± 10.36 | 41-76/58.69 ± 11.02 | 20 mL qd | Mix | - | | 1 m | ① |

(Continued on following page)





10.3389/fphar.2024.1411026

TABLE 1 (*Continued*) Characteristics of the included trials.

| Study | Type of ICH | Sample size | | Sex (M/F) | | Age (range/mean) (years) | | Intervention (T) | | Time of surgery (range/mean) | | Duration | Outcomes |
|---|---|---|---|---|---|---|---|---|---|---|---|---|---|
| | | T | C | T | C | T | C | XNJ | Surgery | T | C | | |
| Tang (2015) | ICH | 50 | 50 | 30/20 | 29/21 | 53-76/65.2 | 51-77/64.9 | 30 mL qd | HCPADS | - | | - | ①③④ |
| He et al. (2015) | HICH | 40 | 40 | 23/17 | 25/15 | 52-75/62.4 ± 8.0 | 50-71/61.8 ± 7.2 | 20 mL qd | HCPFAS | 6-47/15.2 ± 11.9 h | 4-41/14.8 ± 10.2 h | 2w | ①③ |
| Guo (2015) | HICH | 40 | 40 | - | | - | | 20 mL qd | PADS | - | | 3w | ① |
| Dai et al. (2015) | HICH | 30 | 30 | 22/8 | 24/6 | 29-61/51.95 ± 7.93 | 28-68/52.83 ± 7.52 | 20 mL qd | HCPADS | - | | 2w | ①⑦ |
| Cheng (2015) | HICH | 60 | 59 | 37/23 | 36/24 | 49-76/58.92 ± 7.48 | 50-78/60.05 ± 8.36 | 20 mL bid | Unclear | - | | 2w | ①②③⑤⑨ |
| Chen and Li (2015) | HICH | 46 | 44 | 26/20 | 23/21 | 52-76/65.2 ± 6.5 | | 30 mL qd | SCPADS | - | | 2w | ①②③⑤ |
| Zhou (2015) | HICH | 97 | 86 | 53/44 | 51/35 | 42-75 | 40-75 | 20 mL qd | HCPFAS | 1–36 h | 0.5–34 h | 2w | ① |
| Zhou (2014) | HICH | 48 | 48 | 25/23 | 26/22 | 38-78/58.14 ± 7.98 | 39-80/60.02 ± 7.05 | 20 mL bid | HCPFAS | 48 h | | 2w | ① |
| Guo and Wen (2014) | ICH | 61 | 61 | 41/20 | 41/20 | 52-78/65.23 ± 3.49 | 51-79/65.52 ± 3.51 | 30 mL qd | PADS | 9-58/17.63 ± 2.94 h | 8-63/17.72 ± 2.89 h | 2w | ①③④ |
| Huang and Guo (2014) | HICH | 52 | 50 | 68/34 | | 47-79/57.1 ± 6.2 | | 20 mL bid | NES | - | | 15d | ①②③ |
| Xin (2013) | HICH | 42 | 42 | 22/20 | 24/18 | 41-78/58.6 ± 8.4 | 43-79/57.2 ± 9.4 | 40 mL qd | HCPFAS | 4-15/8.5 ± 4.4 h | 3-17/8.4 ± 3.9 h | 2w | ①②③ |
| Tao et al. (2013) | HICH | 42 | 38 | 23/19 | 18/20 | 49-64/55.4 ± 4.6 | 56.7 ± 5.4 | 30 mL qd | SCPADS | - | | 2w | ①③⑦ |
| Sun and Zhong (2013) | HICH | 30 | 30 | - | | - | | 20 mL qd | HCPADS | - | | 2w | ① |
| Shi et al. (2013) | HICH | 40 | 40 | 48/32 | | 17-82/56 ± 18 | | 40 mL qd | HCPFAS | - | | 2w | ①②⑧ |
| Jin (2013) | ICH | 24 | 26 | 13/11 | 13/13 | 40-75/59.7 ± 8.3 | 42-78/57.4 ± 9.1 | 40 mL qd | Craniotomy | 4.5-14/8.2 ± 4.6 h | 2.5-16/8.1 ± 3.8 h | 2w | ① |
| Li and Zhou (2012) | HICH | 21 | 20 | 11/10 | 10/10 | 56-75/65 ± 4.8 | 56-74/65.2 ± 4.9 | 20–30 mL qd | HCPFAS | 4-21/9.6–1.26 h | | 2w | ①②④ |
| Li (2012) | HICH | 25 | 20 | 15/10 | 11/9 | 35-79/53.2 ± 8.3 | 34-81/53.7 ± 5.9 | 20 mL qd | SCPADS | 6–72 h | | 1 m | ①②⑨ |
| Li et al. (2012) | ICH | 28 | 26 | 17/11 | 17/9 | 49-72/57.60 ± 14.9 | 45-70/2.40 ± 11.7 | 20 mL qd | HCPFAS | 6–48 h | | 1w | ③④⑥ |
| Zhao (2011) | ICH | 45 | 45 | 30/15 | 31/14 | 50-75/45-77 | 45-77 | 20–30 mL qd | Unclear | - | | 2w | ①②③ |
| Yang et al. (2011) | HICH | 30 | 30 | 17/13 | 16/14 | 46-78/62.4 | 44-75/61.2 | 20 mL qd | Mix | 5h-5d | 5.5h-6d | 2w | ①②⑨ |
| Wu et al. (2011) | HICH | 20 | 20 | - | | - | | 20 mL qd | Unclear | - | | - | ①② |
| Li et al. (2011) | ICH | 58 | 57 | 33/25 | 34/23 | 53.1 ± 8.4 | 51.8 ± 7.8 | 20 mL qd | HCPADS | 14.9 ± 6.6d | 15.5 ± 4.9d | 2w | ①④ |
| Lu and Tang (2011) | HICH | 54 | 54 | 30/24 | 31/23 | 36-68/58.7 | 35-69/59.1 | 20 mL qd | Unclear | - | | 2w | ①②③ |
| Nie (2010) | HICH | 20 | 20 | 14/6 | 13/7 | 45-75 | | 30 mL qd | Craniotomy | ≤24 h | | 2w | ①④⑨ |
| Lin (2009) | HICH | 24 | 22 | 18/6 | 16/6 | 56.25 ± 4.19 | 57.73 ± 4.47 | 40 mL qd | SCPADS | 6.17 ± 1.19 h | 5.34 ± 0.89 h | 2w | ①④⑤ |
| Tong et al. (2006) | HICH | 42 | 38 | 24/18 | 22/16 | 50-82/64.2 ± 4.9 | 53-78/66.1 ± 3.8 | 20 mL qd | HCPFAS | 5-25/10.6 ± 1.63 h | 4-21/9.6 ± 1.26 h | 2w | ①②⑨ |
| Huang (2005) | HICH | 14 | 15 | 10/4 | 11/4 | 51-78/64.5 | 53-79/65.1 | 10 mL qd | Unclear | 6-19/12.6 h | 7-20/11.2 h | 2w | ③⑦ |

(Continued on following page)





10.3389/fphar.2024.1411026

TABLE 1 (*Continued*) Characteristics of the included trials.

| Study | Type of ICH | Sample size | | Sex (M/F) | | Age (range/mean) (years) | | Intervention (T) | | Time of surgery (range/mean) | | Duration | Outcomes |
|---|---|---|---|---|---|---|---|---|---|---|---|---|---|
| | | T | C | T | C | T | C | XNJ | Surgery | T | C | | |
| Wu and Han (2004) | HICH | 25 | 20 | 14/11 | 12/8 | 40-82 | | 20 mL qd | HCPFAS | 6–72 h | | - | ①②⑨ |
| Lin et al. (2003) | ICH | 37 | 32 | 21/16 | 23/9 | 51-74/59.3 | 54-75/61.2 | 1.0 mL/kg qd | Mix | ≤24 h | | 2w | ①⑥⑨ |
| Wang et al. (2001) | ICH | 60 | 60 | 37/23 | 39/21 | 37-71/60.2 | 36-70/59.2 | 20 mL qd | Mix | 0.5–72 h | 0.5–72 h | 4w | ①③ |

Note: NES, neuroendoscopic hematoma evacuation surgery; Mix, the included patients underwent different surgical measures; SCPADS, soft channel puncture hematoma aspiration and drainage surgery; HCPADS, hard channel puncture hematoma aspiration and drainage surgery; HCPFAS, hard channel puncture hematoma fragmentation and aspiration surgery; PADS, puncture hematoma aspiration and drainage surgery; Unclear, only mentioning minimally invasive surgery; ①, total efficiency rate; ②, all-cause mortality rate; ③, neurological impairment; ④, level of consciousness; ⑤, Activities of daily living (ADL); ⑥, volume of intracerebral hematoma; ⑦, volume of perihematomal edema; ⑧levels of TNF- α, ⑨, safety indicators.

citations were imported into NoteExpress v3.5, and a total of 57 studies (Wang et al., 2001; Lin et al., 2003; Wu and Han, 2004; Huang, 2005; Tong et al., 2006; Lin, 2009; Nie, 2010; Li et al., 2011; Lu and Tang, 2011; Wu et al., 2011; Yang et al., 2011; Zhao, 2011; Li, 2012; Li et al., 2012; Li and Zhou, 2012; Jin, 2013; Shi et al., 2013; Sun and Zhong, 2013; Tao et al., 2013; Xin, 2013; Guo and Wen, 2014; Huang and Guo, 2014; Zhou, 2014; Chen and Li, 2015; Cheng, 2015; Dai et al., 2015; Guo, 2015; He et al., 2015; Tang, 2015; Xu and Lv, 2015; Zhang et al., 2015; Zhou, 2015; Lian, 2016; Liu et al., 2016; Ren, 2016; Tong et al., 2016; Xia et al., 2016; Zhang et al., 2016; Gu and Zhang, 2017; Shuang et al., 2017; Zhou and Sun, 2017; Cheng, 2018; Jiang and Xiao, 2018; Jin and Wang, 2018; Li et al., 2018; Li, 2019; Wang, 2019; You, 2019; Zhang, 2019; Liang and Qin, 2020; Shu, 2020; Xu, 2020; Chen, 2021; Deng et al., 2021; Xiao and Wu, 2021; Sun et al., 2022; Hao et al., 2024) were ultimately included after screening (Figure 1).

## 3.2 Characteristics of the included studies

This study incorporated a total of 57 RCTs, involving 4,852 patients, with 2,445 in the integration of XNJ and CWM therapy group (experimental group) and 2,407 in the CWM treatment group (control group). All studies were conducted in China and were single-center RCTs. The sample sizes ranged from 29 to 183. All RCTs were based on surgery and CWM treatment, with one group receiving additional XNJ (Table 1).

## 3.3 Risk of bias assessment

Regarding the "randomization process", all studies reported comparability of baseline data between the two groups, and with 24 studies (Lin et al., 2003; Lin, 2009; Li, 2012; Tao et al., 2013; Guo and Wen, 2014; Chen and Li, 2015; Dai et al., 2015; Xu and Lv, 2015; Lian, 2016; Ren, 2016; Xia et al., 2016; Zhang et al., 2016; Gu and Zhang, 2017; Cheng, 2018; Jiang and Xiao, 2018; Jin and Wang, 2018; Li et al., 2018; Li, 2019; Wang, 2019; You, 2019; Liang and Qin, 2020; Chen, 2021; Hao et al., 2024) reported specific and correct randomization methods. But only two studies (Lin, 2009; Nie, 2010) of them assessed as "low risk of bias" because they explicitly mentioned the use of opaque envelopes to conceal allocations. In contrast, the remaining studies were assessed as "some concerns" due to the absence of specific randomization strategies or conceal allocations mentioned. For the "deviations from the intended interventions", we assessed it as "low risk of bias". Although only one study (Liu et al., 2016) used a double-blind design, and two studies (Jin, 2013; Tong et al., 2016) administered a placebo treatment (intravenous saline injection) to the control group. However, 14 studies (Lin, 2009; Nie, 2010; Li et al., 2011; Li et al., 2012; Li and Zhou, 2012; Guo and Wen, 2014; He et al., 2015; Tang, 2015; Lian, 2016; Li et al., 2018; Zhang, 2019; Chen, 2021; Xiao and Wu, 2021; Sun et al., 2022) mentioned that all included patients had varying degrees of consciousness impairment, we expect these patients likely did not know which treatment measures they were receiving. There were no instances of patients switching groups due to awareness or unawareness of their treatment modalities. All studies used an intention-to-treat

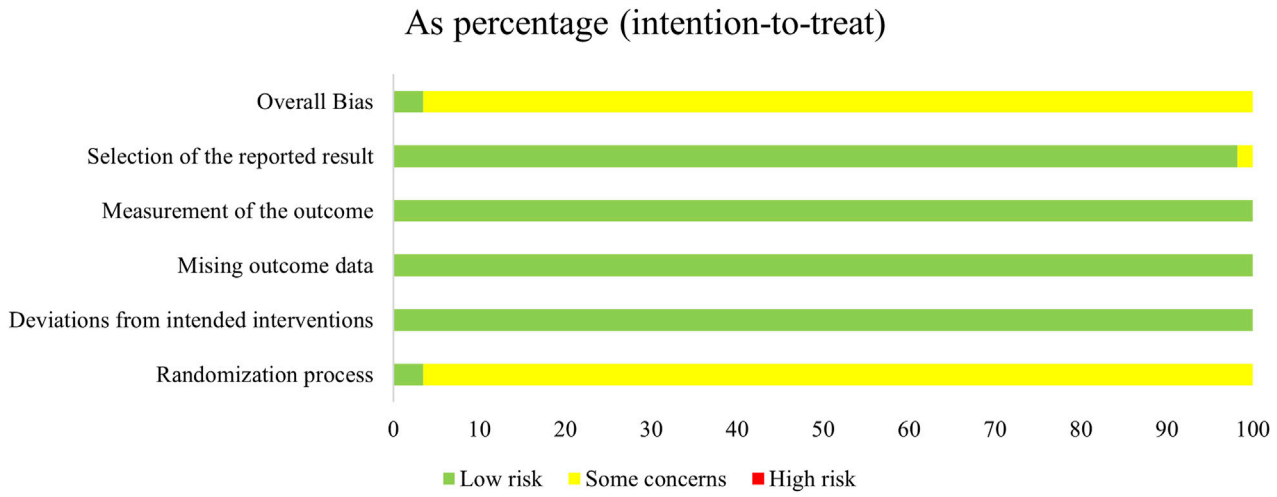


FIGURE 2
Risk of bias graph.

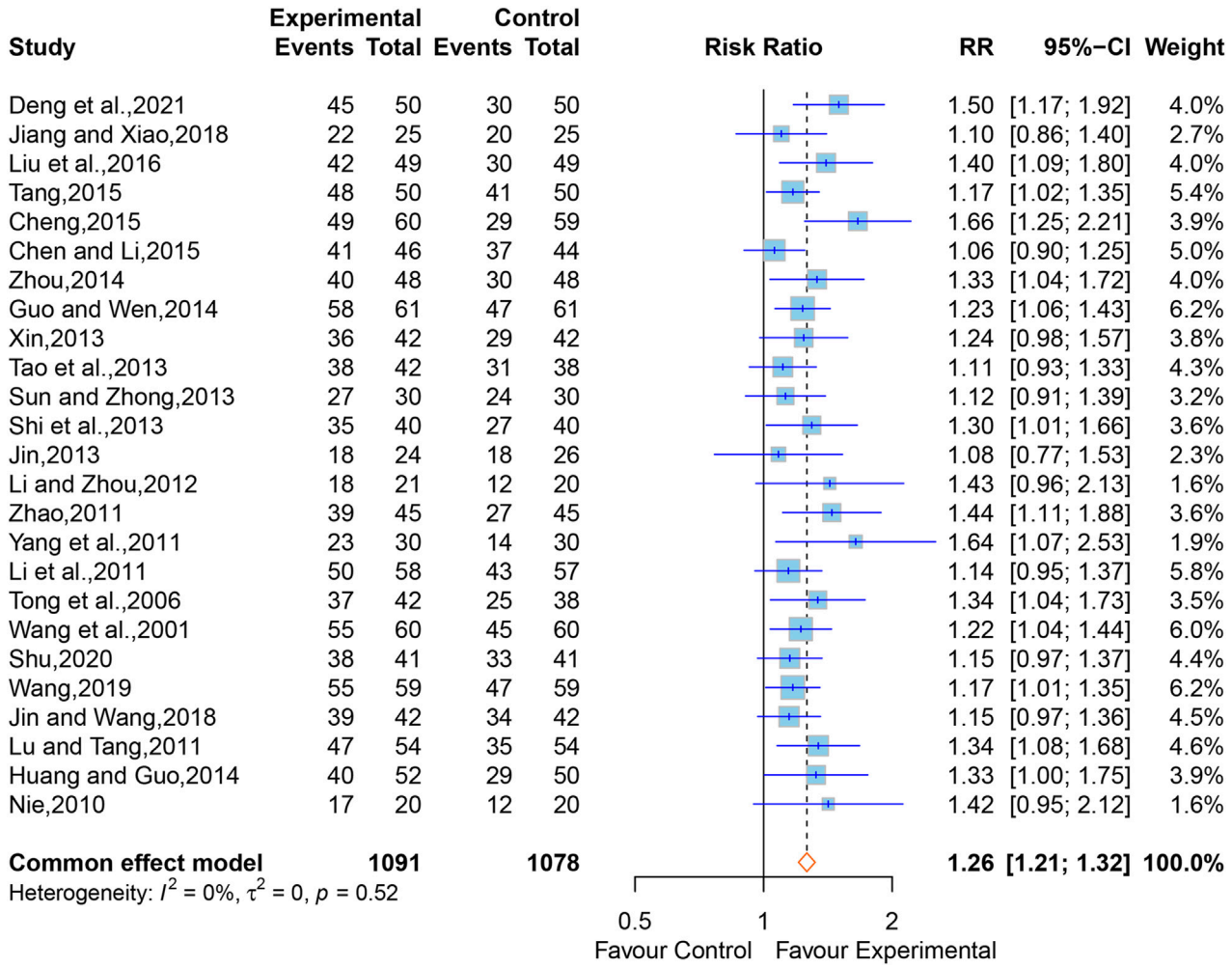


FIGURE 3
Forest plot for the effect of Xingnaojing on the total efficiency rate.

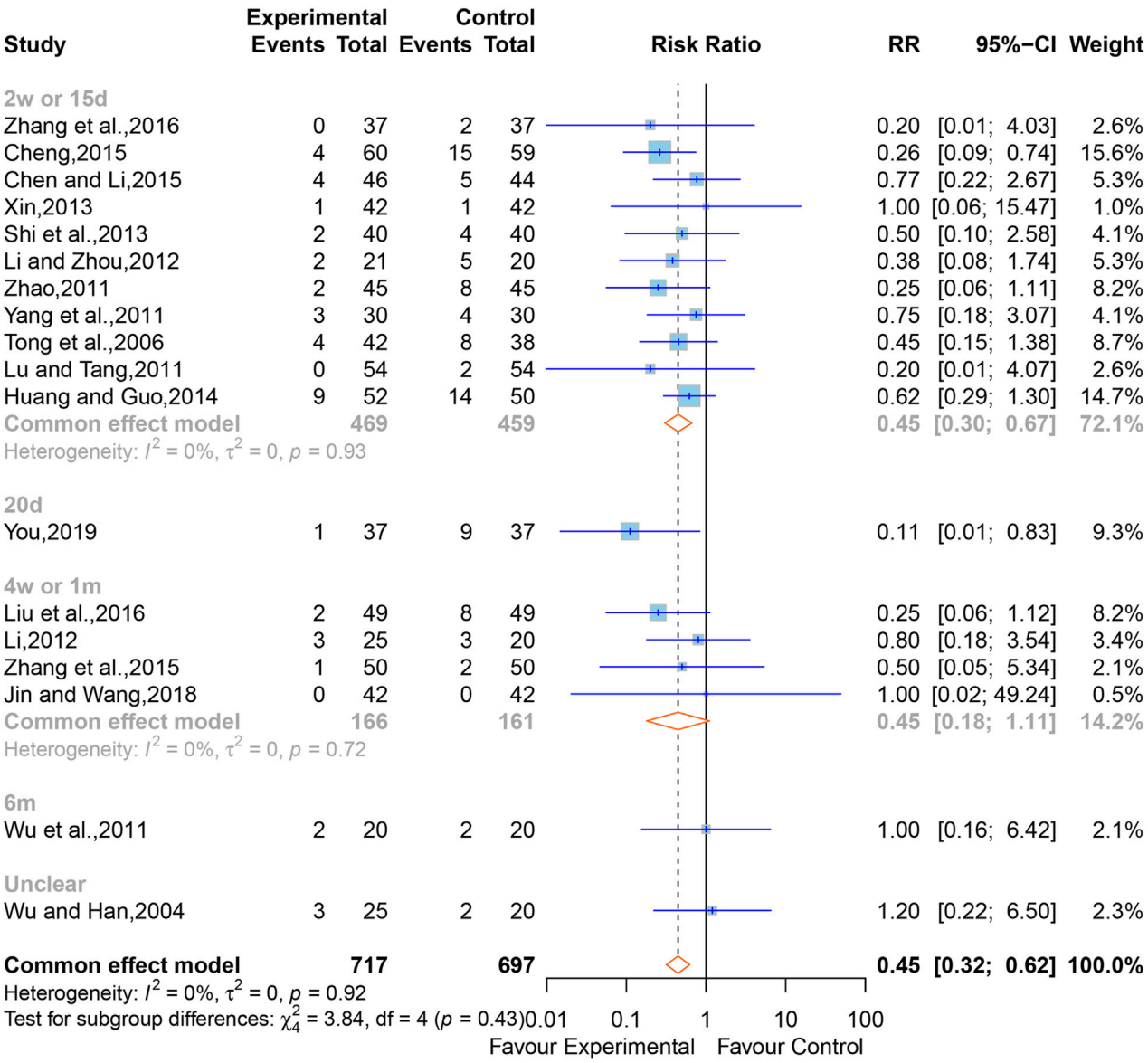


FIGURE 4
Forest plot for the effect of Xingnaojing on the all-cause mortality.

analysis (ITT) to estimate the effects of allocated intervention measures, and were assessed to be at low risk. In addition, we assessed the "missing outcome data" as "low risk" due to no loss to follow-up was reported, or negligible losses to follow-up was founded. The "outcome measurements" were assessed as "low risk" because the criteria for evaluating the outcome indicators between the two groups were reasonable and consistent in all studies. Although they did not mention whether blinding was implemented for the outcome assessors, it is still unclear whether this would affect the judgment of the results, as the outcome assessors' potential preference bias towards the two treatment measures is unknown. Apart from one study (Huang, 2005) (assessed as 'some concerns' due to the safety situation reported only for the experimental group), we assessed all remaining studies as having a "low risk of bias" in the case of "selective reporting" because all of them had clear outcome indicators and comprehensively reported results whether they were statistically significant or not (Figure 2; Supplementary Figure S1).

## 3.4 Primary outcomes

### 3.4.1 Total efficiency rate

A total of 47 studies (Wang et al., 2001; Lin et al., 2003; Wu and Han, 2004; Tong et al., 2006; Lin, 2009; Nie, 2010; Li et al., 2011; Lu and Tang, 2011; Wu et al., 2011; Yang et al., 2011; Zhao, 2011; Li, 2012; Li and Zhou, 2012; Jin, 2013; Shi et al., 2013; Sun and Zhong, 2013; Xin, 2013; Guo and Wen, 2014; Huang and Guo, 2014; Zhou, 2014; Chen and Li, 2015; Cheng, 2015; Dai et al., 2015; Guo, 2015; He et al., 2015; Tang, 2015; Xu and Lv, 2015; Zhou, 2015; Liu et al.,

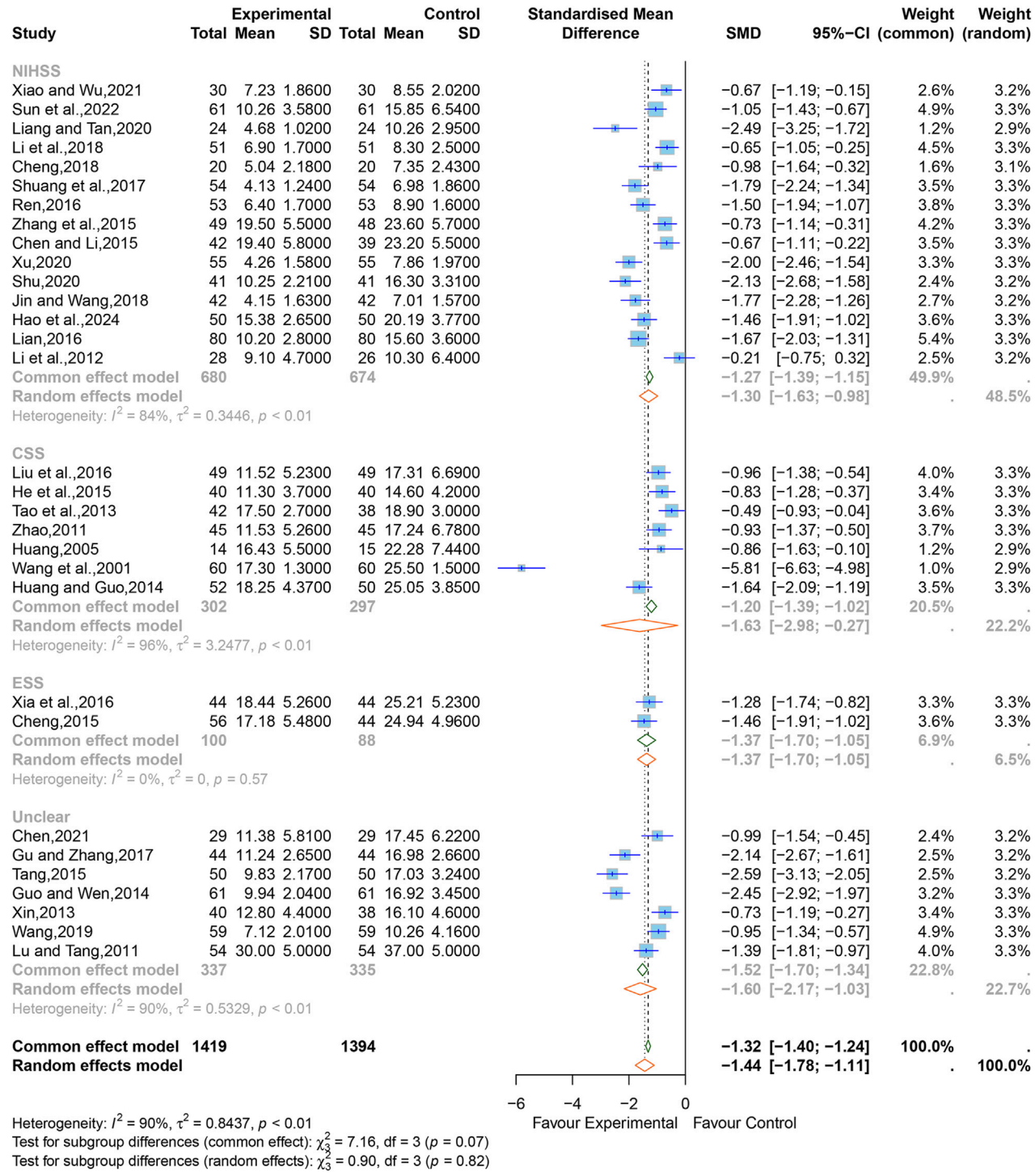


FIGURE 5
Forest plot for the effect of Xingnaojing on neurological impairment.

2016; Tong et al., 2016; Xia et al., 2016; Zhang et al., 2016; Gu and Zhang, 2017; Shuang et al., 2017; Zhou and Sun, 2017; Cheng, 2018; Jiang and Xiao, 2018; Jin and Wang, 2018; Wang, 2019; You, 2019; Zhang, 2019; Liang and Qin, 2020; Shu, 2020; Deng et al., 2021; Xiao and Wu, 2021; Sun et al., 2022) comprising 3,943 participants reported the total efficiency rate. We first conducted a meta-analysis on 25 of the studies (Wang et al., 2001; Tong et al., 2006; Nie, 2010; Li et al., 2011; Lu and Tang, 2011; Yang et al., 2011; Zhao, 2011; Li and Zhou, 2012; Jin, 2013; Shi et al., 2013; Sun and Zhong, 2013; Tao et al., 2013; Xin, 2013; Guo and Wen, 2014; Huang and Guo, 2014; Zhou, 2014; Chen and Li, 2015; Cheng, 2015; Tang, 2015; Liu et al., 2016; Jiang and Xiao, 2018; Jin and Wang, 2018; Wang, 2019; Shu, 2020; Deng et al., 2021) which used "18% reduction in post-treatment neurological impairment scales scores"

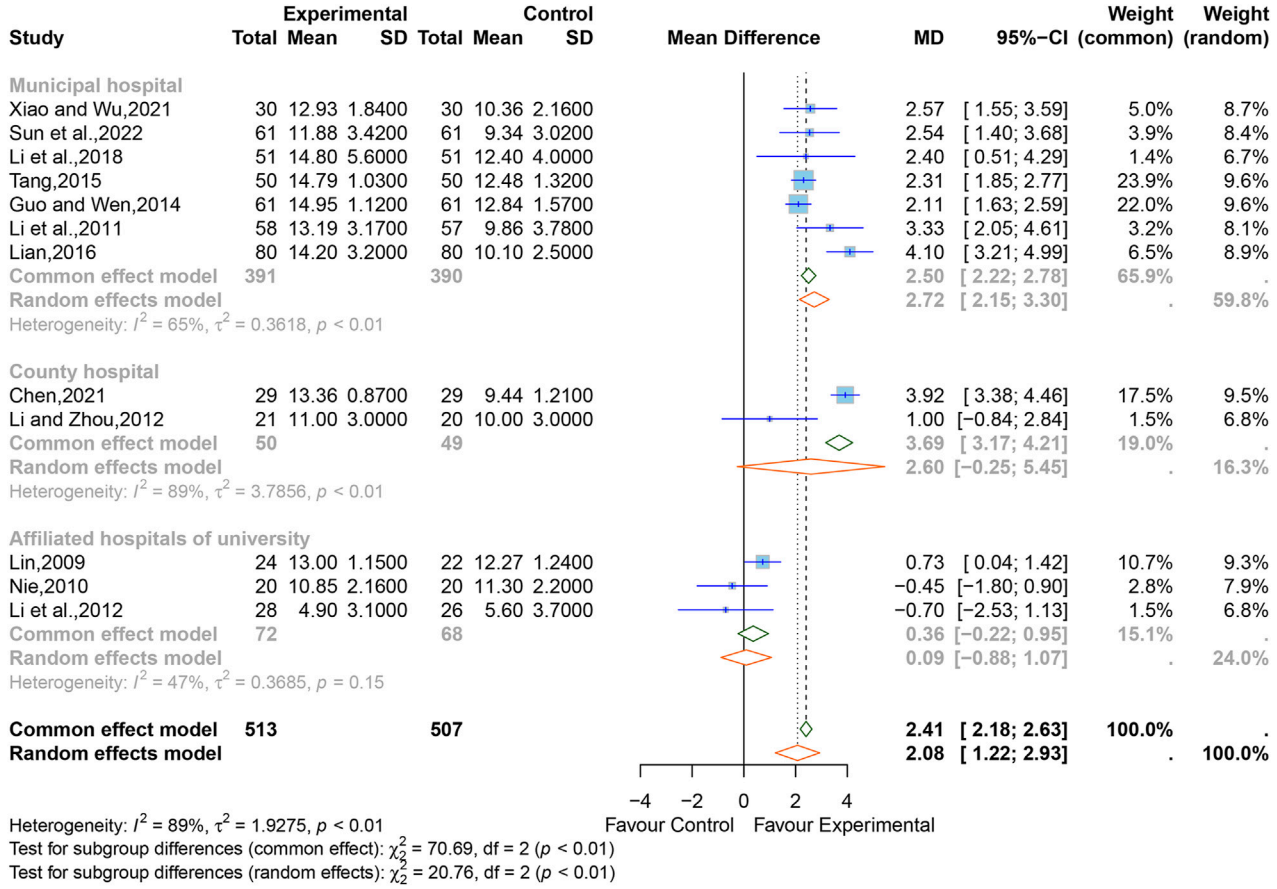


FIGURE 6
Forest plot for the effect of Xingnaojing on the Glasgow coma scale.

as the criterion for total efficiency rate. A fixed-effect model was used due to the low heterogeneity ($I^2$ = 0%, $p$ = 0.52), and the pooled data showed that XNJ significantly improved the total efficiency rate (RR = 1.26; 95% CI [1.21 to 1.32]; $p$ < 0.0001) (Figure 3). Sensitivity analysis clarified that the combined effect size was stable (Supplementary Figure S2).

Considering that different studies have adopted various methods of evaluating therapeutic efficacy, further analyses were then performed, respectively, by different efficacy evaluation criteria. The results indicated that there were no significant differences in treatment efficacy among them ($p$ = 0.58) (Supplementary Figure S12).

## 3.5 Secondary outcomes

### 3.5.1 All-cause mortality

In all, 18 studies (Wu and Han, 2004; Tong et al., 2006; Lu and Tang, 2011; Wu et al., 2011; Yang et al., 2011; Zhao, 2011; Li, 2012; Li and Zhou, 2012; Shi et al., 2013; Xin, 2013; Huang and Guo, 2014; Chen and Li, 2015; Cheng, 2015; Zhang et al., 2015; Liu et al., 2016; Zhang et al., 2016; Jin and Wang, 2018; You, 2019) containing 1,414 cases reported the all-cause mortality. The overall effect of meta-analysis indicated that XNJ reduced the all-cause mortality (RR = 0.45; 95% CI [0.32 to 0.62]; $p$ < 0.0001), and a fixed-effects model was applied due to the low heterogeneity ($I^2$ = 0%, $p$ = 0.92) (Figure 4). Sensitivity analysis indicated that the combined effect size was stable (Supplementary Figure S3).

Subgroup analyses were conducted according to the time point of observation. The outcomes clarified that, compared to the control group, XNJ significantly reduced all-cause mortality after 2 weeks or 15 days of starting treatment. However, at the periods of 4 weeks or 1 month, 6 months, and unclear time for observing the all-cause mortality, the result of the XNJ group was no significant compared with that of the control group. Additionally, for the 20 days, 6 months, and unclear groups, there was only one study each (2w or 15d, RR = 0.45; 95% CI [0.30 to 0.67]; 20d, RR = 0.11; 95% CI [0.01 to 0.83]; 4w or 1m, RR = 0.45; 95% CI [0.18 to 1.11]; 6m, RR = 1.00; 95% CI [0.16 to 6.42]; Unclear, RR = 1.20; 95% CI [0.22 to 6.50]) (Figure 4).

### 3.5.2 Neurological impairment

Regarding neurological impairment, 15 studies (Li et al., 2012; Chen and Li, 2015; Zhang et al., 2015; Lian, 2016; Ren, 2016; Shuang et al., 2017; Cheng, 2018; Jin and Wang, 2018; Li et al., 2018; Liang and Qin, 2020; Shu, 2020; Xu, 2020; Xiao and Wu, 2021; Sun et al., 2022; Hao et al., 2024) containing 1,414 cases reported the grading by NIHSS, seven studies (Wang et al., 2001; Huang, 2005; Zhao, 2011; Li, 2012; Tao et al., 2013; Huang and Guo, 2014; He et al., 2015; Liu et al., 2016) containing 1,414 cases reported the grading by CSS,

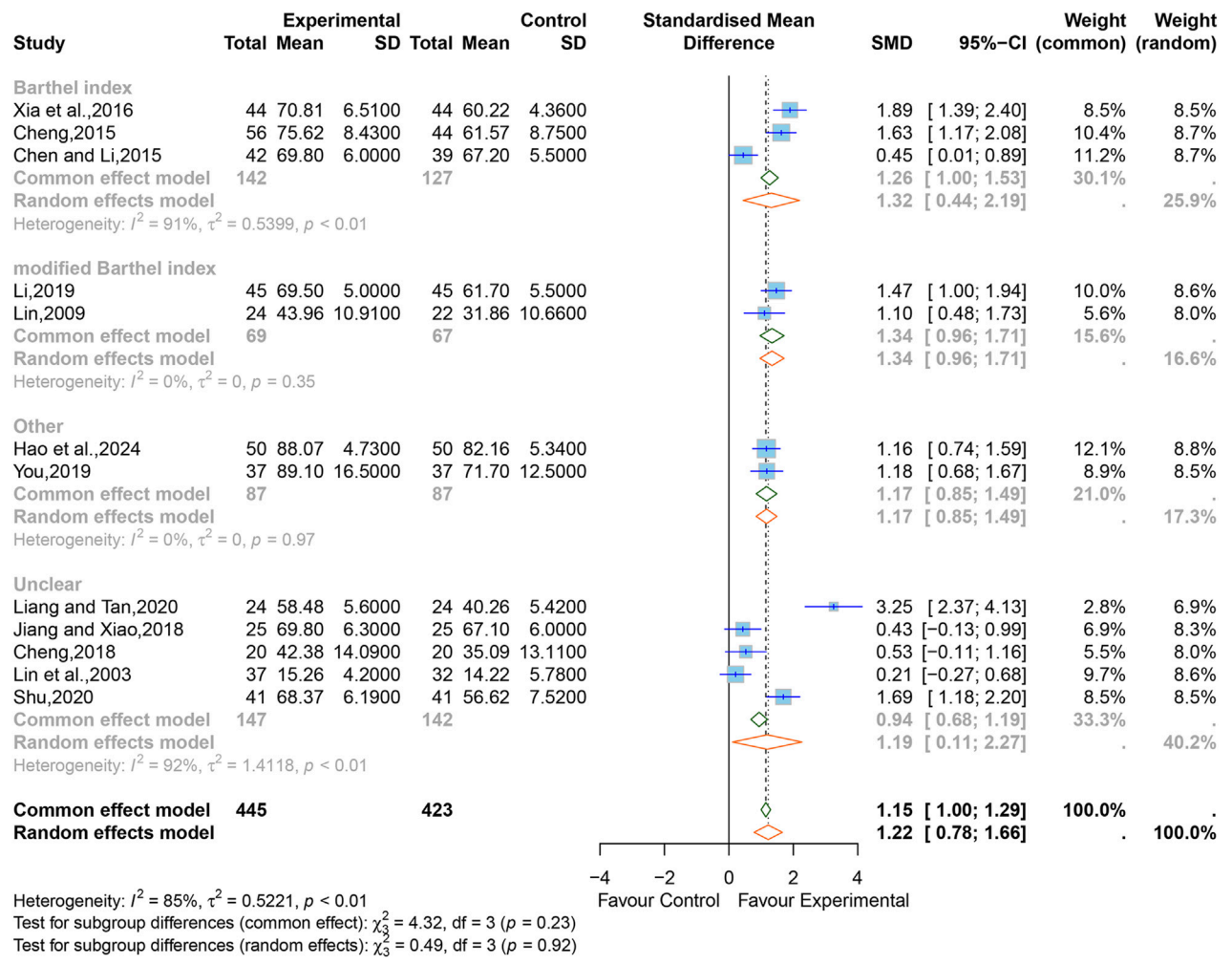


FIGURE 7
Forest plot for the effect of Xingnaojing on the activities of daily living.

two studies (Cheng, 2015; Xia et al., 2016) containing 1,414 cases reported the grading by ESS, and seven studies (Lu and Tang, 2011; Xin, 2013; Guo and Wen, 2014; Tang, 2015; Gu and Zhang, 2017; Wang, 2019; Chen, 2021) did not specify the evaluation scale used.

The SMD was chosen to standardize the effect sizes across studies to counteract the total score differences caused by the use of different scales among the studies. Due to significant heterogeneity among them ($I^2$ = 90%, $p$ < 0.01), a random-effects model was applied. The results indicated that XNJ significantly improved neurological impairment (SMD = −1.44; 95% CI [−1.78 to −1.11]; $p$ < 0.0001) (Figure 5). Sensitivity analysis showed that the results of the combined effect size are stable (Supplementary Figure S4).

Based on the subgroup analyses of different evaluation scales, it can be seen that the heterogeneity of the ESS group was significantly reduced ($I^2$ = 0%, $p$ = 0.57), but the CSS, the NIHSS, and the unclear group were relatively high (NIHSS, $I^2$ = 84%, $p$ < 0.01; CSS, $I^2$ = 96%, $p$ < 0.01; unclear, $I^2$ = 90%, $p$ < 0.01) (Figure 5). The rest of the subgroup analyses are listed in Supplementary Table S1. The overall effect combined by MD showed that there was still statistical significance in each subgroup, which further verified the reliability of the results (NIHSS, MD = −3.56; 95% CI [−4.40 to −2.72]; CSS, MD = −5.26; 95% CI [−7.18 to −3.35]; ESS, MD = −7.30; 95% CI [−8.80 to −5.80]; unclear, MD = −5.65; 95% CI [−6.99 to −4.32]) (Supplementary Figure S13).

### 3.5.3 Consciousness

Of all studies, 12 studies (Lin, 2009; Nie, 2010; Li et al., 2011; Li et al., 2012; Li and Zhou, 2012; Guo and Wen, 2014; Tang, 2015; Lian, 2016; Li et al., 2018; Chen, 2021; Xiao and Wu, 2021; Sun et al., 2022) comprising 1,020 participants reported the state of consciousness of patients after treatment, all evaluated using the GCS. In view of the significant heterogeneity between the studies ($I^2$ = 89%, $p$ < 0.01), thus, a random-effects model was used. The result showed that XNJ significantly improved the GCS scores (MD = 2.08, 95% CI [1.22 to 2.93], $p$ < 0.0001) (Figure 6). Sensitivity analysis indicated that the result was stable (Supplementary Figure S5).

The results of the subgroup analyses based on "hospital" demonstrated that the heterogeneity of the "affiliated hospital of university" group was significantly reduced ($I^2$ = 47%, $p$ = 0.15), the heterogeneity within the other subgroups still remained high (county hospital, $I^2$ = 89%, $p$ < 0.01; municipal hospital, $I^2$ =

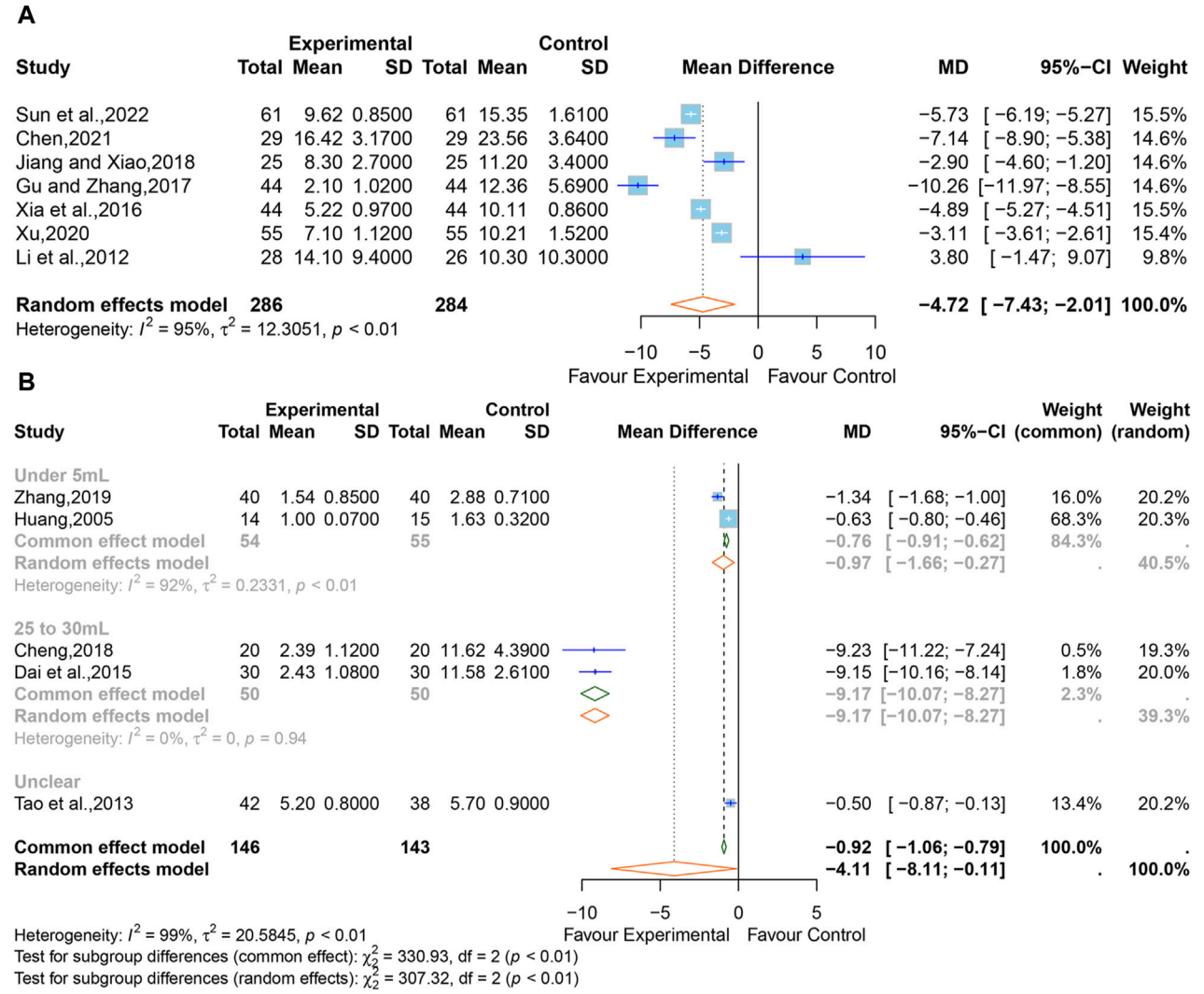


FIGURE 8
**(A)** Forest plot for the effect of Xingnaojing on the volume of intracerebral hematoma. **(B)** Forest plot for the effect of Xingnaojing on the volume of perihematomal edema.

65%, $p$ < 0.01), and the results for both the "affiliated hospital of university" and "county hospital" groups indicated that the GCS scores of the XNJ group was non-significant compared with that of the control group (affiliated hospital of university, MD = 0.36, 95% CI [-0.22 to 0.95]; county hospital, MD = 2.60, 95% CI [-0.25 to 5.45]). However, the results from the "municipal hospital" group showed that there is a statistically significant difference between the two groups (MD = 2.72, 95% CI [2.15 to 3.30]). The rest of the subgroup analyses are listed in Supplementary Table S2.

### 3.5.4 Activities of daily living

After treatment, three studies (Chen and Li, 2015; Cheng, 2015; Xia et al., 2016) containing 269 cases used BI scores to evaluate ADL, two studies (Lin, 2009; Li, 2019) containing 136 cases used mBI, two studies (You, 2019; Hao et al., 2024) containing 174 cases used other scales (SS-QOL, QLQ-C30), and five studies (Lin et al., 2003; Cheng, 2018; Jiang and Xiao, 2018; Liang and Qin, 2020; Shu, 2020) containing 289 cases did not specify the type of scale used.

There was high heterogeneity between the studies ($I^2$ = 85%, $p$ < 0.01), therefore a random-effects model was used with SMD as a summary statistic. The results showed that the difference was statistically significant (SMD = 1.22; 95% CI [0.78 to 1.66]; $p$ < 0.0001) (Figure 7). Sensitivity analysis showed that the overall effect was stable (Supplementary Figure S6).

We performed subgroup analyses, respectively, by the different evaluation scales, and the results indicated that the heterogeneity of the "mBI" and "other scales" groups were significantly reduced (mBI, $I^2$ = 0%, $p$ = 0.35; other scales, $I^2$ = 0%, $p$ = 0.97), the heterogeneity within the other subgroups still remained high (BI, $I^2$ = 91%, $p$ < 0.01; Unclear, $I^2$ = 92%, $p$ < 0.01). The rest of the subgroup analyses are listed in Supplementary Table S3. The results of the combined effect size by MD showed that there was still statistical significance in each subgroup, which further verified the reliability of the results (BI, MD = 9.02; 95% CI [2.39 to 15.64]; mBI, MD = 8.27; 95% CI [6.21 to 10.32]; other, MD = 11.20; 95% CI [-0.03 to 22.42]; unclear, MD = 8.23; 95% CI [1.79 to 14.67]) (Supplementary Figure S14).

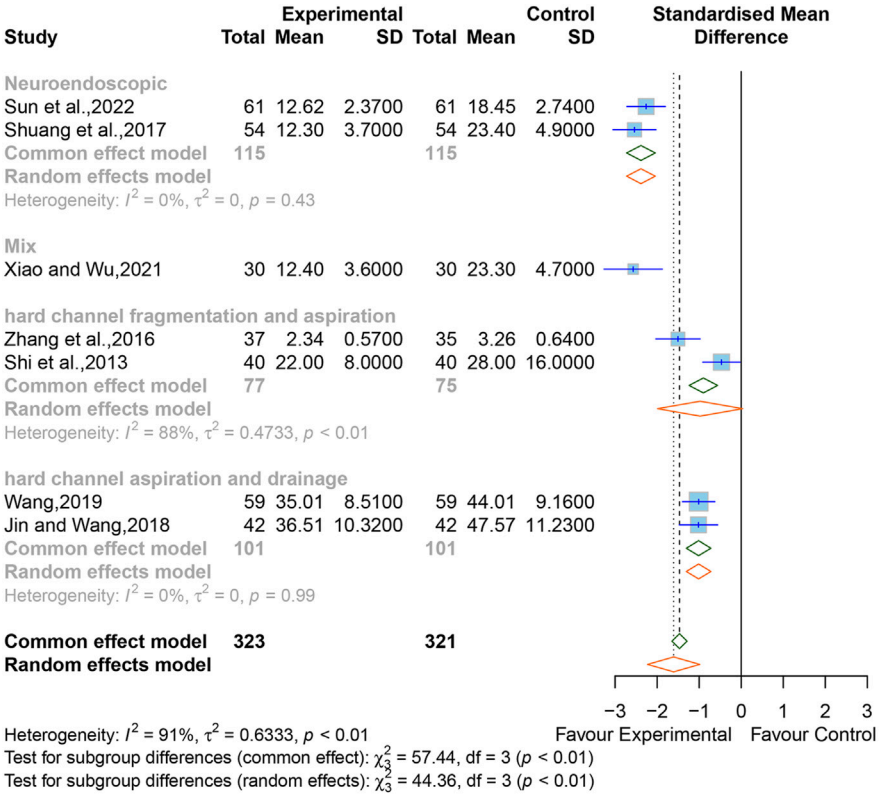


FIGURE 9
Forest plot for the effect of Xingnaojing on the levels of TNF-α.

### 3.5.5 Volume of intracerebral hematoma (mL)

A total of seven studies (Li et al., 2012; Xia et al., 2016; Gu and Zhang, 2017; Jiang and Xiao, 2018; Xu, 2020; Chen, 2021; Sun et al., 2022) comprising 570 participants reported the intracerebral hematoma volume. Considering that high heterogeneity ($I^2$ = 92%, $p$ < 0.01), a random-effects model was adopted, and the pooled data showed that XNJ reduced the hematoma volume (MD = −4.72; 95% CI [-7.43 to −2.01]; $p$ = 0.0006] (Figure 8A). The subgroup analyses could not explain the source of the heterogeneity (Supplementary Table S4). Sensitivity analysis indicated that the combined effect size was stable (Supplementary Figure S7).

### 3.5.6 Volume of perihematomal edema (mL)

Five studies (Huang, 2005; Tao et al., 2013; Dai et al., 2015; Cheng, 2018; Zhang, 2019) reported the volume of perihematomal edema. The pooled results indicated statistically significant differences (MD = −4.11; 95% CI [-8.11 to −0.11]; $p$ = 0.0441) between the XNJ group and the control group and showed large heterogeneity ($I^2$ = 99%, $p$ < 0.01) (Figure 8B).

The subgroup analyses based on "the volume of perihematomal edema before treatment" are shown in Figure 9. It can be seen that the heterogeneity in the group with 25–30 mL of perihematomal edema volume before treatment was significantly reduced ($I^2$ = 0%, $p$ = 0.94), whereas there was considerable heterogeneity in the group with less than 5 mL of perihematomal edema volume before treatment ($I^2$ = 92%, $p$ < 0.01), and one study did not specify the volume of perihematomal edema before treatment. The rest of the subgroup analyses are listed in Supplementary Table S5. Sensitivity analysis indicated that the combined effect size was stable (Supplementary Figure S8).

### 3.5.7 Levels of TNF-α

Seven studies (Shi et al., 2013; Zhang et al., 2016; Shuang et al., 2017; Jiang and Xiao, 2018; Wang, 2019; Xiao and Wu, 2021; Sun et al., 2022) reported the levels of TNF-α. The SMD was used as a summary statistic due to the consistency of the units in these studies being unclear. The outcome showed statistically significant differences (SMD = −1.61, 95% CI [−2.23 to −0.99], $p$ < 0.0001) (Figure 9) between the XNJ and the control group and indicated large heterogeneity ($I^2$ = 91%, $p$ < 0.01). Sensitivity analysis confirmed that the combined effect size was stable (Supplementary Figure S9).

Subgroup analyses based on different surgical techniques revealed that the heterogeneity was significantly reduced in the "neuroendoscopic hematoma evacuation surgery (NES)" group and the "hard channel puncture hematoma aspiration and drainage surgery (HCPADS)" group, while it was still high in the "hard channel puncture hematoma fragmentation and aspiration surgery (HCPFAS)" group (NES, $I^2$ = 0%, $p$ = 0.99; HCPADS, $I^2$ = 0%, $p$ = 0.43; HCPFAS, $I^2$ = 88%, $p$ < 0.01). The "mixed surgery" group (which included patients who underwent different surgical techniques) incorporated only one study. The rest of the subgroup analyses are listed in Supplementary Figure S6.

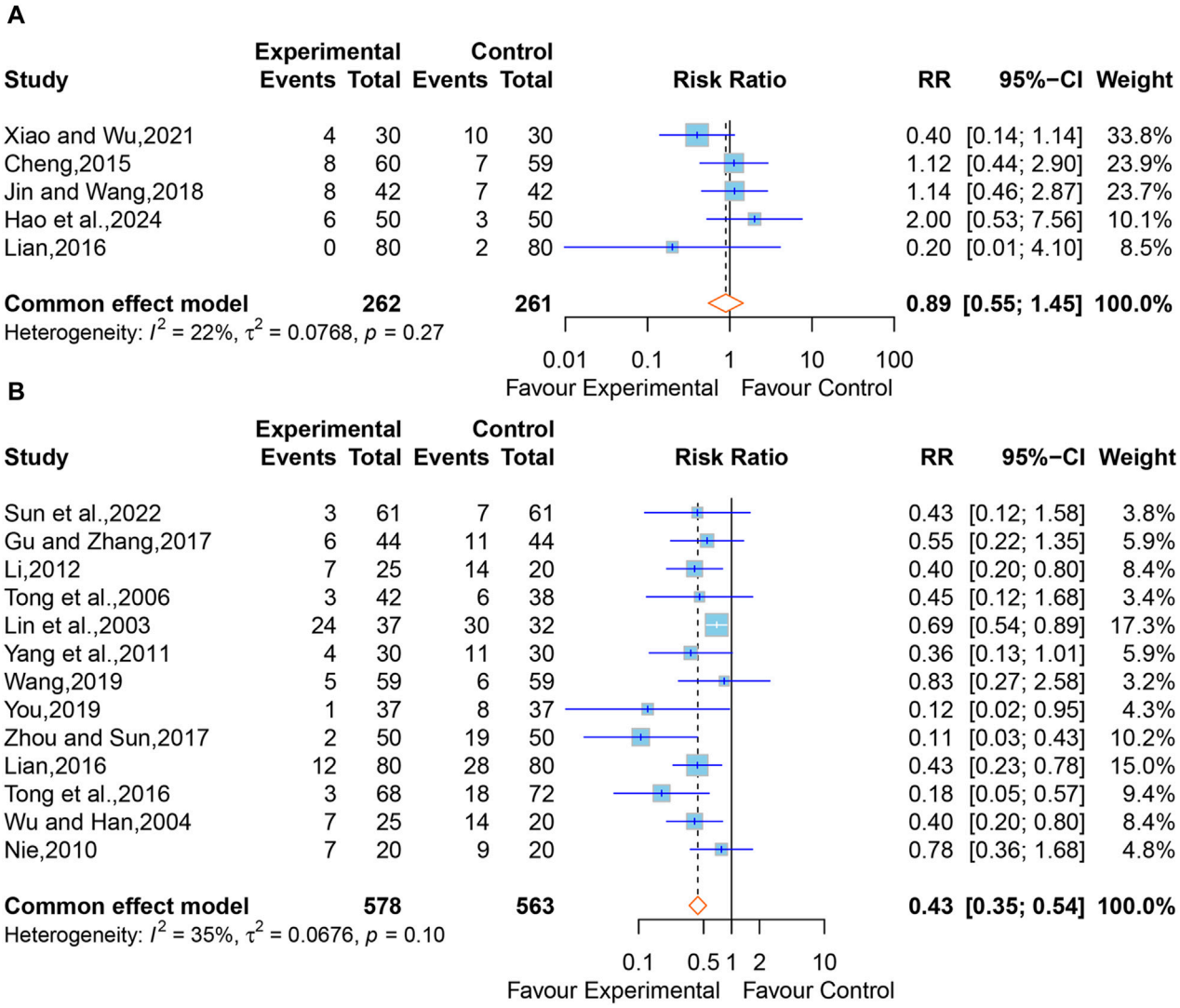


FIGURE 10
**(A)** Forest plot for the effect of Xingnaojing on adverse drug reactions. **(B)** Forest plot for the effect of Xingnaojing on incidence of complications.

### 3.5.8 Safety outcomes (adverse drug reactions, incidence of complications)

In all, six studies reported adverse drug reactions following treatment. However, one study (Huang, 2005) merely stated that no adverse reactions or complications were observed in the XNJ group. We were unable to synthesize this study. The pooled results of the other five studies (Cheng, 2015; Lian, 2016; Jin and Wang, 2018; Xiao and Wu, 2021; Hao et al., 2024) clarified that there was no significant difference between the XNJ group and the control group (RR = 0.89; 95% CI [0.55 to 1.45]; $p$ = 0.6521) (Figure 10A). Meanwhile, No heterogeneity was found ($I^2$ = 22%, $p$ = 0.27); thus, a fixed-effects model was adopted. Sensitivity analysis indicated that the overall effect was stable (Supplementary Figure S10).

Apart from one study (Huang, 2005) that only mentioned no complications in the XNJ group, 15 studies (Lin et al., 2003; Wu and Han, 2004; Tong et al., 2006; Nie, 2010; Yang et al., 2011; Li, 2012; Lian, 2016; Tong et al., 2016; Gu and Zhang, 2017; Zhou and Sun, 2017; Wang, 2019; You, 2019; Sun et al., 2022) reported the postoperative complications in two groups of post-operative patients of ICH. But two of them (Guo, 2015; Xu and Lv, 2015) reported data on the person-time of the outcome, we were unable to synthesize this study. Using the fixed-effect model ($I^2$ = 35%, $p$ = 0.10) for the meta-analysis of the remaining 13 studies, and the results demonstrated that XNJ significantly reduced the incidence of postoperative complications in post-operative patients of ICH (RR = 0.43; 95% CI [0.35 to 0.54]; $p$ < 0.0001) (Figure 10B). Sensitivity analysis indicated that the overall effect was stable (Supplementary Figure S11). Specific adverse drug reactions and incidence of complications mentioned in the studies are listed in Supplementary Tables S7-S8.

## 3.6 Publication bias

The statistical test showed that no obvious publication bias was found in included trials regarding the all-cause mortality (Begg's test, $p$ = 0.8202; Egger's test, $p$ = 0.6864), the GCS score (Begg's test, $p$ =

TABLE 2 Publication bias statistical test by Begg's test and Egger's test.

| Outcomes | No. of studies | *p*-value | |
|---|---|---|---|
| | | Begg's test | Egger's test |
| Total efficiency rate | 25 | 0.0030 | 0.0009 |
| All-cause mortality | 18 | 0.8202 | 0.6864 |
| Neurological impairment | 31 | 0.0351 | 0.0174 |
| Level of consciousness (GCS) | 12 | 0.5371 | 0.4034 |
| Activities of daily living | 12 | 0.5371 | 0.2888 |
| Volume of intracerebral hematoma | 7 | 1.0000 | 0.8659 |
| Volume of perihematomal edema | 5 | 0.2207 | 0.0722 |
| Levels of TNF-α | 7 | 0.1331 | 0.1485 |
| Adverse drug reactions | 5 | 0.8065 | 0.6051 |
| Incidence of complications | 13 | 0.1779 | 0.0069 |

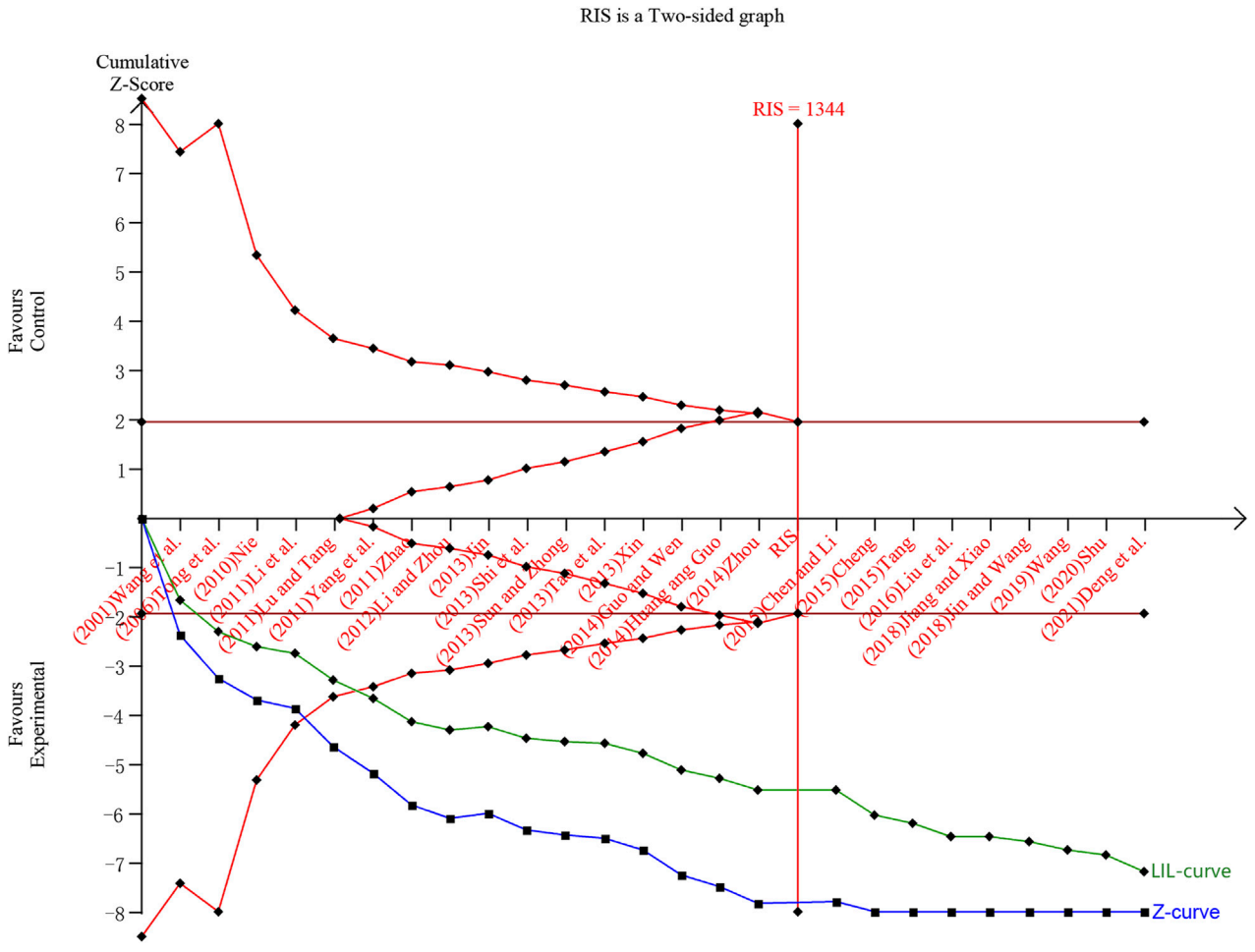


FIGURE 11
Trial sequential analysis and penalty statistics analysis of total efficiency rate. Note: The blue curve is the cumulative Z curve, the green curve (LIL-curve) is the penalized Z curve, the red horizontal line is the traditional threshold, the red curve is the TSA threshold, and the red vertical line is the RIS.

TABLE 3 GRADE evidence profiles.

| Outcomes | Certainty assessment | | | | | | | Effect | | Certainty | Importance |
|---|---|---|---|---|---|---|---|---|---|---|---|
| | No. of studies | Study design | Risk of bias | Inconsistency | Indirectness | Imprecision | Other considerations | Relative (95% CI) | Absolute (95% CI) | | |
| Total efficiency rate | 25 | RCTs | Serious[a] | Not Serious | Not Serious | Not serious | Publication Bias Strongly Suspected[b] | RR 1.26 (1.21–1.32) | 181 more per 1,000 (from 146 more to 222 more) | Low | Critical |
| All-cause mortality within 15 days | 11 | RCTs | Not Serious | Not Serious | Not Serious | Serious[c] | None | RR 0.45 (0.30-0.67) | 81 fewer per 1,000 (from 104 fewer to 49 fewer) | Moderate | Important |
| Neurological impairment | 31 | RCTs | Serious[a] | Serious[d] | Not Serious | Not serious | Publication Bias Strongly Suspected[b] | - | SMD 1.44 SD fewer (1.78 fewer to 1.11 fewer) | Very low | Important |
| Level of consciousness (GCS) | 12 | RCTs | Serious[a] | Serious[d] | Not Serious | Serious[c] | None | - | MD 2.08 higher (1.22 higher to 2.93 higher) | Very low | Important |
| Activities of daily living | 12 | RCTs | Serious[a] | Serious[d] | Not Serious | Not serious | None | - | SMD 1.22 SD higher (0.78 higher to 1.66 higher) | Low | Important |
| Volume of intracerebral hematoma | 7 | RCTs | Not Serious | Serious[d] | Not Serious | Serious[c] | None | - | MD 4.72 lower (7.43 lower to 2.01 lower) | Low | Important |
| Volume of perihematomal edema | 5 | RCTs | Not Serious | Serious[d] | Not Serious | Not serious | None | - | MD 4.11 SD lower (8.11 lower to 0.11 lower) | Moderate | Important |
| Levels of TNF-α | 7 | RCTs | Not serious | Serious[d] | Not serious | Not serious | None | - | SMD 1.61 SD lower (2.23 lower to 0.99 lower) | Moderate | Important |
| Adverse drug reactions | 5 | RCTs | Not Serious | Not Serious | Not Serious | Serious[c] | None | RR 0.89 (0.55–1.45) | 12 fewer per 1,000 (from 50 fewer to 50 more) | Moderate | Important |
| Incidence of complications | 13 | RCTs | Not Serious | Not Serious | Not Serious | Serious[c] | Publication Bias Strongly Suspected[c] | RR 0.43 (0.35–0.54) | 183 fewer per 1,000 (from 209 fewer to 148 fewer) | Low | Important |

[a]Lack of blind method.
[b]Significant publication bias was identified by Begg's test and Egger's test.
[c]Some of the included studies had confidence intervals that crossed the line of equivalence.
[d]There is significant heterogeneity among the included studies.





10.3389/fphar.2024.1411026

0.5371; Egger's test, $p$ = 0.4034), the ADL (Begg's test, $p$ = 0.5371; Egger's test, $p$ = 0.2888), the hematoma volume (Begg's test, $p$ = 1.0000; Egger's test, $p$ = 0.8659), the volume of perihematomal edema (Begg's test, $p$ = 0.2207; Egger's test, $p$ = 0.0722), the TNF-α (Begg's test, $p$ = 0.1331; Egger's test, $p$ = 0.1485), and adverse drug reactions (Begg's test, $p$ = 0.8065; Egger's test, $p$ = 0.6051). However, a publication bias risk was present for the total efficiency rate (Begg's test, $p$ = 0.0030; Egger's test, $p$ = 0.0009), the neurological impairment (Begg's test, $p$ = 0.0351; Egger's test, $p$ = 0.0174), and the incidence of complications (Begg's test, $p$ = 0.1779; Egger's test, $p$ = 0.0069) (Table 2).

## 3.7 Results of TSA

In this study, TSA analysis was performed on 25 studies that reported total effective rates which used "18% reduction in post-treatment neurological impairment scales scores" as the criterion, and the parameters were set according to the user manual for TSA (Thorlund et al., 2017), the type of boundary value was set as two-sided, type I error was defined as $\alpha$ = 0.05, statistical efficacy 1-$\beta$ = 0.8. The results showed that the cumulative $Z$-value crossed the traditional boundary value ($Z$ = 1.96) when included in study 1 (Wang et al., 2001), crossed the TSA boundary value when included in study 5 (Lu and Tang, 2011), and reached the RIS when included in study 17 (Chen and Li, 2015). The penalised $Z$-curve also crossed the traditional boundary value after the inclusion of study 2 (Tong et al., 2006), crossed the TSA boundary value when included study 6 (Yang et al., 2011) and reached the RIS when included in study 17 (Chen and Li, 2015) (Figure 11).

## 3.8 Quality of evidence

The certainty of the evidence of XNJ on all-cause mortality within 15 days, volume of perihematomal edema, levels of TNF-α, and adverse drug reactions was rated as "moderate"; that on total efficiency rate, ADL, intracerebral hematoma volume, and incidence of complications was "low"; and that on neurological impairment and the GCS score was "very low" (Table 3). We judged the quality of evidence as moderate to very low, mainly due to the high risk of bias, imprecision and the severe heterogeneity.

# 4 Discussion

## 4.1 Research significance

Intracerebral haemorrhage (ICH) is the most difficult to treat, the most disabling, and the deadliest type of stroke subtype (Tapia-Pérez et al., 2014; Wilkinson et al., 2018). The mechanisms of pathological damage after ICH primarily involve: the mass effect and mechanical rupture caused by the initial or ongoing bleeding and the expansion of the hematoma, which raise the overall pressure (intracranial pressure) and directly lead to primary brain injury; the physiological response to the hematoma (primarily edema and inflammation), the metabolic effects of thrombotic components, and secondary brain injury caused by toxic biochemicals (Wilkinson et al., 2018). One-third of ICH patients die within a month, and a large number of survivors are left with permanent disabilities (Steiner et al., 2011). Symptomatic treatment has been the primary treatment strategy for ICH to date (Tang et al., 2018). Surgery remains a vital measure for saving lives in emergency situations; however, the most common sites for ICH are deep brain structures, such as the basal ganglia and thalamus. Surgery requires passage through portions of brain tissue, which can lead to iatrogenic injury of healthy brain tissue. In addition, the presence of perihematomal edema after surgery may limit the therapeutic effect (Thompson et al., 2015; de Oliveira Manoel, 2020). Therefore, treatment targeting residual hematoma and cerebral edema post-operatively is a crucial aspect of care (Murthy et al., 2015; Chen et al., 2016).

Results from a systematic pharmacology study (Chen et al., 2018) suggest that XNJ might exert an anti-stroke effect by responding to oxidative stress, regulating blood pressure, calcium signaling pathways, and cell apoptosis among other biological processes and pathways, and Akt1, HIF1a, and ITGB2 may play key roles in the occurrence and regulation of stroke. 1,7-Diphenyl-3-acetoxy-6(E)-hepten, oxycurcumenol and beta-sitosterol may be essential compounds in XNJ and have been reported as effective ingredients for the treatment of stroke. The study also experimentally demonstrated that the oxycurcumenol has a protective effect on PC12 cells against oxidative stress-induced cellular damage. This mechanism does not involve cell cycle-dependent processes but may function through the regulation of autophagy, preliminarily unveiling the potential mechanisms by which XNJ treats stroke systematically. Our research further clarified the clinical efficacy and safety of XNJ in treating post-operative patients with ICH through an evidence-based evaluation, providing support for the clinical application of XNJ from an evidence-based perspective.

## 4.2 Summary of the main results

This meta-analysis included a total of 57 studies involving post-operative patients with ICH. It encompassed 2,445 cases that received a combination of XNJ with CWM treatment and 2,407 cases that received only CWM treatment. This study indicated that in comparison to other outcome indicators, authors of previous studies appeared to prefer to use the total efficiency rate rather than all-cause mortality as an endpoint indicator. And a few studies hold a dialectical perspective toward this phenomenon (Shi et al., 2023). This is due to the fact that the total efficiency rate, as a composite indicator, still lacks a universally accepted standardized evaluation method, and it is an insufficient strategy to evaluate a composite endpoint as if it were a sole primary endpoint (McCoy, 2018). However, we hold a conservative view on this because for patients, efficacy as a positive outcome may be more acceptable than mortality. And the "Clinical neurological impairment scoring standards for stroke patients" (NACCDC, 1996) formed at the fourth Chinese conference on cerebrovascular diseases in 1995 unified the criteria for assessing the "effectiveness" of stroke patient treatment, which was defined as a reduction in neurological impairment score of ≥18% after

treatment. The results of this study showed that most of the previous studies used the aforementioned assessment method to evaluate the total efficiency rate. However, many studies also used different efficacy assessment criteria, and we found through subgroup analyses that there was no significant difference between results using different criteria, and there was low heterogeneity in the overall effect of the meta-analysis.

As for the outcome indicators of neurological impairment and ADL, there were similar issues, especially regarding the assessment of ADL. Some studies only mentioned the use of ADL scales but did not specify the names and criteria of the scales used. In fact, there were many scales commonly used to assess ADL, such as the BI and mBI, etc. We merged the effect sizes of all the studies included in the outcome indicators of neurological impairment and ADL through SMD and compared them with results obtained by merging effect sizes using MD. The results showed that XNJ could significantly reduce neurological impairment and improve ADL after treatment. In contrast, regarding the consciousness state, all studies used GCS for evaluation, and results showed that XNJ significantly improved GCS scores after treatment, but there was also obvious heterogeneity between studies.

Compared with the above subjective outcome indicators, this study also included some objective outcome indicators, and the results showed that XNJ significantly reduced all-cause mortality, hematoma volume, perihematomal edema, and the inflammatory marker TNF-α after treatment. However, subgroup analyses indicated that XNJ had a significant effect on reducing all-cause mortality at 2 weeks or 15 days after starting treatment, but could not reduce all-cause mortality at 4 weeks or 1 month, and even longer time points by pooling a few corresponding data, although there is still a lack of sufficient research to prove its therapeutic effect on 6-month mortality. Despite this, the outcome is still encouraging, as so far, no intervention has demonstrated improved outcomes. Additionally, we conducted specific analyses on safety indicators. Although some studies mentioned adverse reactions, we found that they include two situations: drug adverse reactions and postoperative complications. Our specific analysis showed that XNJ could significantly reduce the incidence of postoperative complications after the surgery of ICH without increasing drug adverse reactions.

Due to the influence of many confounding factors such as surgical methods, geographical regions, age, and methods of outcome evaluation, significant heterogeneity existed among studies included for outcome indicators other than the overall efficacy rate, all-cause mortality, and safety metrics. Despite conducting subgroup and sensitivity analyses, we still cannot completely rule out the impact of confounding factors on the results. Subgroup analyses revealed that the heterogeneity was significantly reduced in the ESS group for the outcome of neurological impairment and in the mBI group for the outcome of ADL. The Subgroup analyses regarding GCS found lower heterogeneity among studies conducted in major affiliated hospitals of the university but yielded negative results, which may be due to the fact that the included patients were those with complex or more severe conditions due to the higher hospital level, thus limiting the treatment effect. The subgroup analyses on perihematomal edema volume showed higher heterogeneity in the group with postoperative edema volume of less than 5 mL, which may be related to the larger measurement errors associated with lower edema volumes. The subgroup analyses targeting TNF-α found that the NES group and the HCPADS group had lower heterogeneity and that the NES group achieved better therapeutic effects. The sources of heterogeneity in the remaining subgroup analyses could not be well explained. Moreover, the results of TSA showed that the cumulative Z-value and the penalised Z-curve crossed both the traditional boundaries and the TSA boundaries, reached the RIS, led to a positive conclusion and excluding the possibility of false positives. Unfortunately, due to the high level of heterogeneity and the absence of blinding in subjective outcome indicators, the level of evidence for the study results is generally low, and our findings according to the current studies should be considered carefully in the clinic.

## 4.3 Strengths and limitations

Compared to the previous network meta-analysis concerning post-operative patients with ICH (Ren et al., 2022), this meta-analysis included the latest RCTs. Past network meta-analyses only focused on the total efficiency rate, NIHSS, and intracerebral hematoma volume. However, we attempted to investigate whether XNJ could reduce all-cause mortality, perihematomal edema volume, TNF-α, and improve the ADL, which are more objective and important for post-operative patients with ICH. We comprehensively collected and assessed existing research data for each outcome indicator, despite that they adopted different evaluation methods for the same outcome indicator. Moreover, we conducted subgroup analyses for different evaluation methods and displayed the results for the convenience of clinical specialists and other researchers' access. In addition, this study performed more comprehensive subgroup analyses for outcome indicators with high heterogeneity, to interpret sources of the heterogeneity and the efficacy results, and explored the stability of the results through sensitivity analyses, etc. Previously, there have been no conventional meta-analysis studies published that specifically involve the use of TCM injections in post-operative patients with ICH.

This study also has certain limitations: the included 57 studies were mostly single-center and small-sample research; some studies only mentioned random allocation without specifying the exact methods; the surgical methods, efficacy evaluation criteria, and outcome indicators varied among the studies; the studies reported only short-term mortality rates, lacking long-term prognosis follow-up, etc. At the same time, the presence of significant publication bias might also affect the reliability of the results.

In view of the above limitations, future research should strengthen the integrity of experimental designs, pay special attention to the accurate application of random methods, allocation concealment, and blinding, clearly define long-term efficacy and safety, and to the extent possible choose widely recognized, unified outcome indicators (Liu et al., 2018), etc. Considering these limitations, the results of this study still await further high-quality RCT research to provide more reliable evidence-based support.

## 5 Conclusion

In conclusion, the present meta-analysis and systematic review of 57 RCTs indicates that the administration of XNJ for post-operative patients with ICH is associated with favorable short-term outcomes (within 1 moth). And it can improve total efficiency rate, level of consciousness, and activities of daily living; alleviate neurological impairment; reduce all-cause mortality, volume of cerebral hematoma, volume of perihematomal edema, levels of TNF- α, incidence of complications, and has good tolerability. However, The current evidence base is insufficient and requires substantiation from further high-quality studies. Methodological shortcomings and a substantial risk of bias have curtailed the positive effects, undermining confidence in the synthesis of evidence. Given the preliminary nature of the evidence and that XNJ has enormous potential as a therapeutic agent for ICH, it is imperative to conduct more stringent RCTs to validate the efficacy of XNJ in post-operative patients with ICH.

## Data availability statement

The original contributions presented in the study are included in the article/Supplementary Material, further inquiries can be directed to the corresponding authors.

## Author contributions

YS: Data curation, Formal Analysis, Methodology, Project administration, Software, Visualization, Writing–original draft, Writing–review and editing. FX: Data curation, Project administration, Software, Visualization, Writing–original draft, Writing–review and editing. SL: Data curation, Software, Visualization, Writing–review and editing. YS: Conceptualization, Funding acquisition, Supervision, Validation, Writing–review and editing. XW: Conceptualization, Funding acquisition, Methodology, Supervision, Validation, Writing–review and editing.

## Funding

The author(s) declare that financial support was received for the research, authorship, and/or publication of this article. This work was supported by the Chinese Medicine Heritage and Innovation "Hundred-Thousand-Ten Thousand" Talent Project-National Chinese Medicine Leading Talent Support Program (No. (2018) 284), Special Project on Traditional Chinese Medicine Scientific Research for the Establishment of "Double First-Class" Disciplines in Henan Province (HSRP-DFCTCM-2023-5-07), and the Henan University of Chinese Medicine 2023 Graduate Student Research and Innovation Program (2023KYCX035).

## Conflict of interest

The authors declare that the research was conducted in the absence of any commercial or financial relationships that could be construed as a potential conflict of interest.

## Publisher's note



## Supplementary material

The Supplementary Material for this article can be found online at: https://www.frontiersin.org/articles/10.3389/fphar.2024.1411026/full#supplementary-material

## References

Chen, G. F., Ping, L., Zhou, S. K., Liu, W. W., Liu, L. J., Zhang, D. M., et al. (2016). Early prediction of death in acute hypertensive intracerebral hemorrhage. *Exp. Ther. Med.* 11, 83–88. doi:10.3892/etm.2015.2892

Chen, T. (2021). Analysis of the wake-up promoting effect of Xingnaojing on postoperative coma in patients with cerebral hemorrhage. *Chin. Sci. Technol. J. Db. Med.* 12, 74–75.

Chen, Y. H., and Li, X. X. (2015). Xingnaojing injection assisted soft channel puncture drainage for the treatment of 46 cases of hypertensive cerebral hemorrhage. *China. Pharm.* 24, 105–106.

Chen, Y. H., Sun, Y., Li, W. D., Wei, H., Long, T. L., Li, H., et al. (2018). Systems pharmacology dissection of the anti-stroke mechanism for the Chinese traditional medicine Xing-Nao-Jing. *J. Pharmacol. Sci.* 136, 16–25. doi:10.1016/j.jphs.2017.11.005

Cheng, L. (2015). The therapeutic effect of naloxone combined with Xingnaojing on hypertensive intracerebral hemorrhage after minimally invasive hematoma removal surgery and its impact on neurological function. *Chin. J. Pract. Nerv. Dis.* 18, 102–103. doi:10.3969/j.issn.1673-5110.2015.11.070

Cheng, X. J. (2018). Observation on the therapeutic effect of puncture drainage combined with Xingnaojing injection on patients with hypertensive basal ganglia hemorrhage. *Med. J. Chin. People's Health* 30, 31–32. doi:10.3969/j.issn.1672-0369.2018.18.013

China Food and Drug Administration (2003) *National drug standards WS3-B-3353-98-2003*. Beijing, China: China Food and Drug Administration.

Dai, X. J., Dong, S. J., Jia, Y., Liu, J. J., and Chen, L. N. (2015). The effect of Xingnaojing injection on brain edema and inflammatory mediators in patients with hypertensive basal ganglia hemorrhage after minimally invasive puncture drainage surgery. *Chin. J. Pract. Nerv. Dis.* 18, 79–80. doi:10.3969/j.issn.1673-5110.2015.22.053

Deng, L. L., Tian, L., and Wang, H. C. (2010). Research progress on clinical application of Angong niuhuangwan and its derivative prescription. *Chin. J. Exp. Tradit. Med. Formulae.* 16, 215–219. doi:10.13422/j.cnki.syfjx.2010.12.053

Deng, Z. F., Yu, Y. X., Huang, W. H., Chen, W. S., and Jiang, J. Y. (2021). Clinical effect analysis of minimally invasive intracranial hematoma removal surgery combined with Xingnaojing injection in the treatment of hypertensive intracerebral hemorrhage. *J. Front. Med.* 11, 113–114.

de Oliveira Manoel, A. L. (2020). Surgery for spontaneous intracerebral hemorrhage. *Crit. Care.* 24, 45. doi:10.1186/s13054-020-2749-2

Fang, J. Y., Yang, B., Ge, Z. W., Bai, X., and Yan, B. J. (2017). Single standard substance for the determination of nine volatile components in the distillate of Fructus Gardeniae and Radix Curcumae (an intermediate of Xingnaojing Injection). *J. Sep. Sci.* 40, 3946–3957. doi:10.1002/jssc.201700593

Gao, L. (2016). Expert consensus on hypertensive intracerebral hemorrhage in acute stage in diagnosis and treatment combining traditional Chinese medicine and Western medicine. *Chin. Gen. Pract.* 19, 3641–3648. doi:10.3969/j.issn.1007-9572.2016.30.001

Gao, Y., and Zhao, X. Q. (2023) *Guideline for the diagnosis and treatment of intracerebral hemorrhage with integrated traditional Chinese and western medicine*. Beijing, China: Chinese Society of Integrated Traditional Chinese and Western Medicine.

GBD 2019 Diseases and Injuries Collaborators (2020). Global burden of 369 diseases and injuries in 204 countries and territories, 1990-2019: a systematic analysis for the global burden of disease study 2019. *Lancet* 396, 1204–1222. doi:10.1016/s0140-6736(20)30925-9

Gu, H. Q., and Zhang, G. B. (2017). Analysis of the effect of Xingnaojing combined with minimally invasive puncture and drainage surgery on moderate to equal volume hypertensive basal ganglia hemorrhage. *Mod. Diagn. Treat.* 28, 1136–1137. doi:10.3969/j.issn.1001-8174.2017.06.096

Guo, C. H., and Wen, F. (2014). Clinical observation of removal of intracranial hematoma combined with xingnaojing injection on cerebral hemorrhage. *J. Hubei Univ. Chin. Med.* 16, 68–69. doi:10.3969/j.issn.1008-987x.2014.02.25

Guo, L. (2015). Observation on the clinical efficacy of Xingnaojing combined with head hypothermia in the treatment of cerebral hemorrhage after stereotactic hematoma puncture and aspiration surgery. *World Chin. Med.* 10, 2.

Guyatt, G., Oxman, A. D., Akl, E. A., Kunz, R., Vist, G., Brozek, J., et al. (2011). GRADE guidelines: 1. Introduction-GRADE evidence profiles and summary of findings tables. *J. Clin. Epidemiol.* 64, 383–394. doi:10.1016/j.jclinepi.2010.04.026

Hao, S. G., Wang, J. X., Wu, W. X., and Yang, B. G. (2024). Effect of Xingnaojing injection combined with nimodipine injection on intracranial blood flow and rehabilitation effect in patients with cerebral hemorrhage after operation. *Chin. J. Clin. Ration. Drug Use* 17, 11–14. doi:10.15887/j.cnki.13-1389/r.2024.02.004

He, W. G., Pan, S. Q., Zhang, B., Hu, J., Zhou, J. Q., and Jiang, H. Q. (2015). The effect of Xingnaojing injection combined with Western medicine on postoperative neurological function recovery in patients with hypertensive intracerebral hemorrhage. *New Chin. Med.* 47, 37–39. doi:10.13457/j.cnki.jncm.2015.10.017

Higgins, J. P. T., Thomas, J., Chandler, J., Cumpston, M., Li, T., Page, M. J., et al. (2023). *Cochrane Handbook for Systematic Reviews of Interventions version 6.4 (updated August 2023)* (Cochrane).

Huang, B. F. (2005). Xingnaojing injection assisted minimally invasive clearing surgery for 29 cases of intracranial hematoma. *Chin. J. Integr. Tradit. West. Med. Intensive Crit. Care* 12, 253–254. doi:10.3321/j.issn:1008-9691.2005.04.022

Huang, K. Y., Wei, D. N., Fang, J. Y., Li, X. Y., and Yan, B. J. (2017). Rapid determination of nine components in the first extraction process of Xingnaojing injection by using ultraviolet spectroscopy. *China J. Chin. Mater. Med.* 42, 3755–3760. doi:10.19540/j.cnki.cjcmm.20170907.015

Huang, S. M., and Guo, S. Q. (2014). Safety evaluation of xingnaojing combined with naloxone in treatment of hypertensive cerebral hemorrhage. *China Mod. doct.* 52, 115–117.

Jiang, Y. M., and Xiao, W. X. (2018). Observation on efficacy of xingnaojing injection combined with soft-channel minimally invasive hematoma drainage in treatment of hypertensive cerebral hemorrhage. *Eval. Anal. Drug-use Hosp. Chin.* 18, 1495–1496. doi:10.14009/j.issn.1672-2124.2018.11.022

Jin, D., and Wang, J. (2018). Clinical study on Xingnaojing Injection combined with urokinase in treatment of hypertensive cerebral hemorrhage. *Drugs Clin.* 33, 1342–1346. doi:10.7501/j.issn.1674-5515.2018.06.011

Jin, X. G. (2013). Analysis of the therapeutic effect of craniotomy hematoma removal combined with Xingnaojing in the treatment of cerebral hemorrhage. *J. Med. Inf.* 26, 669–670. doi:10.3969/j.issn.1006-1959.2013.12.973

Li, C. L., and Zhou, Z. S. (2012). Observation on the therapeutic effect of Xingnaojing injection combined with minimally invasive removal of intracranial hematoma in the treatment of hypertensive intracerebral hemorrhage. *Clin. J. Tradit. Chin. Med.* 24, 933–934. doi:10.16448/j.cjtcm.2012.10.075

Li, C. Y., Zhang, G. H., and Wang, X. L. (2012). Observation on the therapeutic effect of Xingnaojing on 54 cases of cerebral hemorrhage with consciousness disorders after minimally invasive intracranial hematoma aspiration surgery. *Int. J. Trad. Chin. Med.* 34, 1115–1116. doi:10.3760/cma.j.issn.1673-4246.2012.12.020

Li, Q. P., Zhang, H., Song, L., and Yang, S. (2018). The effect of Xingnaojing injection on the levels of IFN-γand TIM-3 in patients with basal ganglia hemorrhage underwent super early minimally invasive surgery. *J. Guangxi Med. Univ.* 35, 502–505. doi:10.16190/j.cnki.45-1211/r.2018.04.020

Li, X. G. (2012) *Clinical observation on the treatment of severe hypertensive intracerebral hemorrhage with directional drainage of hematoma and Xingnaojing*. Changchun.

Li, X. Y., Li, R., and Zhou, L. M. (2011). Observation on the therapeutic effect of minimally invasive debridement combined with Xingnaojing in the treatment of cerebral hemorrhage. *Mod. J. Integr. Tradit. Chin. West. Med.* 20, 29–30. doi:10.3969/j.issn.1008-8849.2011.01.014

Li, Y. C. (2019). Therapeutic effect of Xingnaojing injection assisted soft-channel puncture drainage on hypertensive intracerebral hemorrhage. *Psychol. Mag.* 14, 120–121. doi:10.19738/j.cnki.psy.2019.02.081

Lian, S. M. (2016). Analysis on the curative effect of Xingnaojing injection in the treatment of secondary brain injury followed by intracerebral hemorrhage. *China Mod. doct.* 54, 81–83.

Liang, L. Z., and Qin, Y. A. (2020). The impact of xingnaojing injection combined with minimally invasive hematoma evacuation on serum S-100β and NSE levels in patients with intracerebral hemorrhage. *Mod. Med. Health Res. Electron. Ed.* 4, 62–63.

Lin, J., Zhang, N., Zhou, W. H., and Lin, L. Y. (2003). Evaluation of the therapeutic effect of Xingnaojing injection on postoperative hypertensive intracerebral hemorrhage. *Chin. J. Integr. Tradit. West. Med.* 23, 389–390. doi:10.3321/j.issn:1003-5370.2003.05.025

Lin, Z. S. (2009) *A clinical research of Xingnaojing injection after Stereotactic operation in the Treatment of Hypertensive intracerebral hemorrhage*. Guangzhou.

Liu, H. R., Wu, H. Q., Xu, L. M., Xin, X. W., and Li, X. J. (2016). Effect of xingnaojing injection on postoperative patients with minimally invasive conical hematoma removal in cerebral hemorrhage. *Strait. Pharm. J.* 28, 181–182. doi:10.3969/j.issn.1006-3765.2016.05.101

Liu, M., Zhang, S. H., and Zhu, Y. C. (2018). Consensus on clinical research standards for acute stroke in China 2018. *Chin. J. Neurol.* 51, 247–255. doi:10.3760/cma.j.issn.1006-7876.2018.04.003

Lu, J., and Tang, H. Q. (2011). Observation on the therapeutic effect of Xingnaojing injection after surgery for hypertensive intracerebral hemorrhage. *Shanxi Med. J.* 40, 1025–1026. doi:10.3969/j.issn.0253-9926.2011.10.042

Ma, X., Wang, T., Wen, J. X., Wang, J., Zeng, N., Zou, W. J., et al. (2020). Role of Xingnaojing Injection in treating acute cerebral hemorrhage: a systematic review and meta-analysis. *Med. Baltim.* 99, e19648. doi:10.1097/MD.0000000000019648

McCoy, C. E. (2018). Understanding the use of composite endpoints in clinical trials. *West. J. Emerg. Med.* 19, 631–634. doi:10.5811/westjem.2018.4.38383

Murthy, S. B., Moradiya, Y., Dawson, J., Lees, K. R., Hanley, D. F., Ziai, W. C., et al. (2015). Perihematomal edema and functional outcomes in intracerebral hemorrhage: influence of hematoma volume and location. *Stroke* 46, 3088–3092. doi:10.1161/STROKEAHA.115.010054

NACCDC (1996). Scoring criteria for clinical neurological impairment in stroke patients (1995). *Chin. J. Neurol.* 29, 381–383.

NBCMA and CDGNBCMA (2019). Chinese guidelines for diagnosis and treatment of acute intracerebral hemorrhage 2019. *Chin. J. Neurol.* 52, 994–1005. doi:10.3760/cma.j.issn.1006-7876.2019.12.003

Ni, X. J., Chen, Y. L., and Cai, Y. F. (2020). Evidence-based practice guideline on integrative medicine for stroke 2019. *Chin. J. Evid-Based. Med.* 20, 901–912. doi:10.7507/1672-2531.202001075

Nie, J. (2010) *Microinvasive surgey within 24 hours combined with western medicine and Xingnaojing Injection for Hypertensive intracerebral hemorrhage*. Shanghai.

Page, M. J., McKenzie, J. E., Bossuyt, P. M., Boutron, I., Hoffmann, T. C., Mulrow, C. D., et al. (2021). The PRISMA 2020 statement: an updated guideline for reporting systematic reviews. *BMJ* 372, n71. doi:10.1136/bmj.n71

Peng, W. J., Yang, J. J., Wang, Y., Wang, W. H., Xu, J. X., Wang, L. X., et al. (2014). Systematic review and meta-analysis of randomized controlled trials of xingnaojing treatment for stroke. *Evid-Based Compl. Alt.* 2014, 210851. doi:10.1155/2014/210851

Pharmacopoeia Commission of the Ministry of Public Health of the People's Republic of China (1998) *Drug standard of Ministry of public health of the People's Republic of China - the 17th volume of Chinese patent drugs (WS3-B-3353-98)*. Beijing, China: China Medical Science Press.

Ren, P., Cao, L., Zhao, X. K., Zhu, B. B., and Liu, K. (2022). Network Meta-analysis of Chinese medicine injections in treatment of hypertensive intracerebral hemorrhage. *China J. Chin. Mater. Med.* 47, 3637–3647. doi:10.19540/j.cnki.cjcmm.20220214.501

Ren, X. (2016). Observation on efficacy of xingnaojing combined with minimally invasive operation in treatment of hypertensive cerebral hemorrhage. *Eval. Anal. Drug-use Hosp. China* 16, 463–465. doi:10.14009/j.issn.1672-2124.2016.04.013

Shi, D. J., Cheng, Z. P., and Zeng, L. W. (2013). Effect of xingnaojing injection on serum cytokines after minimally invasive surgery crashing and aspirating hematoma in hypertensive cerebral hemorrhage. *China Pharm.* 22, 5–6. doi:10.3969/j.issn.1006-4931.2013.13.002

Shi, X. Y., Feng, L. D., Li, Y. X., Qin, M. Z., Li, T. T., Cheng, Z. X., et al. (2023). Efficacy and safety of Panax notoginseng saponins (Xuesaitong) for patients with acute ischemic stroke: a systematic review and meta-analysis of randomized controlled trials. *Front. Pharmacol.* 14, 1280559. doi:10.3389/fphar.2023.1280559

Shu, W. H. (2020). The effect of piracetam combined with Xingnaojing on the neurological function and daily living ability of patients with hypertensive intracerebral hemorrhage. *Jiangxi Med. J.* 55, 1629–1630. doi:10.3969/j.issn.1006-2238.2020.11.026

Shuang, Y. H., Mao, Z. L., and Yu, L. (2017). Observation on the application effect of xingnaojing injection in postoperative rehabilitation of minimally invasive hematoma removal in patients with hypertensive cerebral hemorrhage. *Shandong Med. J.* 57, 93–95. doi:10.3969/j.issn.1002-266X.2017.12.032

Steiner, T., Petersson, J., Al-Shahi Salman, R., Christensen, H., Cordonnier, C., Csiba, L., et al. (2011). European research priorities for intracerebral haemorrhage. *Cerebrovasc. Dis.* 32, 409–419. doi:10.1159/000330653

Sun, G. L., and Zhong, B. (2013). Xingnaojing injection combined with stereotactic hematoma puncture aspiration for the treatment of 30 cases of hypertensive intracerebral hemorrhage. *Chin. Med. Mod. Distance Educ. China* 11, 44–45. doi:10.3969/j.issn.1672-2779.2013.15.032

Sun, Y. H., Liu, H. R., Zhang, S. N., and Liu, C. L. (2022). Clinical efficacy of neuroendoscopic hematoma removal combined with Xingnaojing injection in the treatment of hypertensive intracerebral hemorrhage. *Chin. Sci. Technol. J. Db. Cit. Ed. Med. Health* 13, 139–142.

Tang, T. D. (2015). Evaluation of the value of intracranial hematoma removal surgery combined with Xingnaojing injection in the treatment of cerebral hemorrhage. *Chin. J. Mod. Drug. Appl.* 9, 172–173. doi:10.14164/j.cnki.cn11-5581/r.2015.21.128

Tang, Y. P., Yin, F. Q., Fu, D. L., Gao, X. H., Lv, Z. C., and Li, X. T. (2018). Efficacy and safety of minimal invasive surgery treatment in hypertensive intracerebral hemorrhage: a systematic review and meta-analysis. *Bmc. Neurol.* 18, 136. doi:10.1186/s12883-018-1138-9

Tao, Y. Q., Li, Z. Y., Xu, F., Wen, L., Zhang, Y. Q., and Jiang, W. (2013). Clinical efficacy of stereotactic aspiration combined with xingnaojing injection in treatment of hypertensive cerebral hemorrhage study. *J. Liaoning Univ. Tradit. Chin. Med.* 15, 215–217. doi:10.13194/j.issn.1673-842x.2013.11.101

Tapia-Pérez, J. H., Gehring, S., Zilke, R., and Schneider, T. (2014). Effect of increased glucose levels on short-term outcome in hypertensive spontaneous intracerebral hemorrhage. *Clin. Neurol. Neurosurg.* 118, 37–43. doi:10.1016/j.clineuro.2013.12.018

Thompson, B. G., Brown, R. D., Amin-Hanjani, S., Broderick, J. P., Cockroft, K. M., Connolly, E. S., et al. (2015). Guidelines for the management of patients with unruptured intracranial aneurysms: a guideline for healthcare professionals from the American heart association/American stroke association. *Stroke* 46, 2368–2400. doi:10.1161/STR.0000000000000070

Thorlund, K., Engstrøm, J., Wetterslev, J., Brok, J., Imberger, J., and Gluud, C. (2017) *User manual for trial sequential analysis (TSA)*. 2nd ed. Copenhagen: Copenhagen Trial Unit, 1–119.

Tong, H. G., Ke, J. Q., Gan, S. X., Lin, P. M., and Zhang, Z. F. (2006). Clinical observation of Xingnaojing injection assisted with hematoma clearance surgery in the treatment of hypertensive intracerebral hemorrhage. *Zhejiang Pract. Med.* 11, 389–390. doi:10.3969/j.issn.1007-3299.2006.06.005

Tong, M. F., Liu, J. H., and Dai, H. B. (2016). Effect of Xingnaojing Injection on nitric oxide,insulin-like growth factor-1 and macrophage inhibitory factor of hypertensive patients with intracerebral hemorrhage. *Chin. J. Clin. Pharmacol.* 32, 399–401. doi:10.13699/j.cnki.1001-6821.2016.05.005

Wang, L. D., Peng, B., Zhang, H. Q., Wang, Y. L., Liu, M., Shan, C. L., et al. (2022a). Brief report on stroke prevention and treatment in China, 2020. *Chin. J. Cerebrovasc. Dis.* 19, 136–144. doi:10.3969/j.issn.1672-5921.2022.02.011

Wang, L. X., Liu, G. H., Wang, G. S., Yan, R. P., and Cao, J. W. (2001). The effect of early combining Xingnao Jing on nervous function and lipoprotein of patients with acute cerebral haemorrhage. *Chin. Gen. Pract.* 4, 189–190. doi:10.3969/j.issn.1007-9572.2001.03.012

Wang, M., Jia, M., Du, W. Q., Zhang, X. Y., Jiao, W. W., Chen, Q., et al. (2021). Overview of systematic reviews/Meta-analysis of Xingnaojing Injection in treatment of intracerebral hemorrhage. *China J. Chin. Mater. Med.* 46, 4633–4643. doi:10.19540/j.cnki.cjcmm.20210622.501

Wang, Y. J., Li, Z. X., Gu, H. Q., Zhai, Y., Zhou, Q., Jiang, Y., et al. (2022b). China stroke statistics: an update on the 2019 report from the national center for healthcare quality management in neurological diseases, China national clinical research center for neurological diseases, the Chinese stroke association, national center for chronic and non-communicable disease control and prevention, Chinese center for disease control and prevention and institute for global neuroscience and stroke collaborations. *Stroke Vasc. Neurol.* 7, 415–450. doi:10.1136/svn-2021-001374

Wang, Y. L. (2019). Effects of Xingnaojing injection on inflammatory factors and nerve function in patients with hypertensive intracerebral hemorrhage. *Hebei Med. J.* 41, 3291–3294. doi:10.3969/j.issn.1002-7386.2019.21.022

Wang, Y. Y., and Gao, Y. (2008) *Diagnosis and treatment guidelines for common diseases in traditional Chinese medicine: stroke*. Beijing, China: China Press of Traditional Chinese Medicine, 56–62.

Wilkinson, D. A., Pandey, A. S., Thompson, B. G., Keep, R. F., Hua, Y., and Xi, G. (2018). Injury mechanisms in acute intracerebral hemorrhage. *Neuropharmacology* 134, 240–248. doi:10.1016/j.neuropharm.2017.09.033

Wu, C. J., and Han, J. G. (2004). Minimally invasive puncture and intracranial hematoma pulverization combined with Xingnaojing injection for the treatment of hypertensive intracerebral hemorrhage. *Chin. J. Clin.* 32, 31–33. doi:10.3969/j.issn.1008-1089.2004.03.022

Wu, J. N., Liu, R. M., Xu, D. N., Li, Y. X., Chang, Z. M., Hao, J. X., et al. (2021). Anti-cerebral ischemia mechanisms of brain absorption components of Xingnaojing Injection based on GC-MS and network pharmacology. *Chin. Tradit. Herb. Drugs* 52, 808–820. doi:10.7501/j.issn.0253-2670.2021.03.024

Wu, L. J., Zhang, H., Xing, Y. W., Gao, Y. H., Li, Y. D., Ren, X. M., et al. (2016). Meta-analysis of the effects of xingnaojing injection on consciousness disturbance. *Med. Baltim.* 95, e2875. doi:10.1097/MD.0000000000002875

Wu, R., Li, R. H., and Shi, H. P. (2011). Clinical application of Xingnaojing injection combined with local mild hypothermia in the early postoperative stage of hypertensive intracerebral hemorrhage. *Chin. J. Pract. Nerv. Dis.* 14, 78–79. doi:10.3969/j.issn.1673-5110.2011.09.048

Xia, Z. Q., Du, Y. T., Du, G. Y., Gao, L., Zhang, W., Li, T., et al. (2016). Observation on the therapeutic effect of Xingnaojing injection in the treatment of hypertensive intracerebral hemorrhage after puncture aspiration surgery. *J. Clin. Res.* 33, 2051–2053. doi:10.3969/j.issn.1671-7171.2016.10.062

Xiao, F., and Wu, J. B. (2021). The effect of Xingnao Jingdong Diphosphate Choline on postoperative efficacy in patients with cerebral hemorrhage. *Chin. J. Gerontol.* 41, 5508–5510. doi:10.3969/j.issn.1005-9202.2021.24.008

Xin, H. B. (2013). Clinical experience of Xingnaojing combined with intracranial hematoma removal surgery in the treatment of cerebral hemorrhage. *China Pract. Med.* 8, 155–156. doi:10.3969/j.issn.1673-7555.2013.06.119

Xu, S. B. (2020). Clinical value analysis of Xingnaojing injection combined with urokinase in the treatment of hypertensive intracerebral hemorrhage. *J. Hubei Univ. Sci. Technol. Med. Sci.* 34, 18–20. doi:10.16751/j.cnki.2095-4646.2020.01.0018

Xu, W. B., and Lv, J. G. (2015). Observation on the short-term therapeutic effect of Xingnaojing injection after surgery for hypertensive intracerebral hemorrhage. *Med. Forum.* 19, 47–48.

Xu, Y. M., Wang, X. C., Zhang, S. J., Xu, T. T., Li, H. Y., Hei, S. Y., et al. (2018). Role of Xingnaojing combined with naloxone in treating intracerebral haemorrhage: a systematic review and meta-analysis of randomized controlled trials. *Med. Baltim.* 97, e12967. doi:10.1097/MD.0000000000012967

Yang, D. J., Liu, Y. F., Ye, D. J., and Wu, Y. (2011). Craniopuncture scavenging technique and xingnaojing to treat hypertensive intracerebral hemorrhage. *Chin. J. Hemorheol.* 21, 611–613. doi:10.3969/j.issn.1009-881X.2011.04.015

Yang, L. X., Feng, W. H., Xia, B. H., Lin, L. M., Liu, W. W., Miao, W. Q., et al. (2016). HPLC specific chromatograms of Xingnaojing injection. *China J. Chin. Mater. Med.* 41, 1640–1645. doi:10.4268/cjcmm20160912

You, H. F. (2019). Effect of Xingnaojing combined with fasudil Hydrochloride on postoperative hypertensive intracerebral Hemorrhage. *Contemp. Med.* 25, 55–57. doi:10.3969/j.issn.1009-4393.2019.13.019

Yu, J. G., Li, R., Liang, W., Zhu, L. J., and Yao, Y. S. (2016). Effects of Xingnaojing on hypertensive cerebral hemorrhage: a Meta-analysis. *Chin. J. Clin. Pharmacol. Ther.* 21, 417–424.

Yu, M., Zhang, L. N., Ding, W., and Zhang, G. M. (2023). The effect and safety of minimally invasive surgery combined with Naoxueshu oral liquid on spontaneous cerebral hemorrhage: meta-analysis and quality evaluation. *J. Hainan Med. Univ.* 2023, 1–16. doi:10.13210/j.cnki.jhmu.20230728.003

Yue, M. X., Li, L., Lu, C. Z., and Jiang, L. Y. (2019). Expert consensus on the clinical application of Xingnaojing injection in the treatment of acute and critical diseases (symptom). *Chin. J. Hyg. Rescue (Electron. Ed.)* 5, 65–70. doi:10.3877/cma.j.issn.2095-9133.2019.02.001

Zhang, J. L., Wang, L. P., Yuan, S. S., and Liu, Y. M. (2004). Headspace solid-phase microextraction gas chromatography-mass spectrometry study on the fingerprint of Xingnaojing injection. *China J. Chin. Mater. Med.* 29, 86–87. doi:10.3321/j.issn:1001-5302.2004.05.027

Zhang, K. W., Liu, Y. P., Liu, C. Q., Bai, J. L., Lu, L. J., and Zhou, J. F. (2015). Observation on the therapeutic effect of soft channel puncture and drainage surgery on hypertensive intracerebral hemorrhage. *Health Prot. promot.* B, 146. doi:10.3969/j.issn.1671-0223.2015.06.133

Zhang, S. C. (2019). Clinical efficacy of Xingnaojing injection combined with puncture and drainage in the treatment of moderate cerebral hemorrhage in the basal ganglia region. *Chin. J. Integr. Med. Cardio-Cerebrovasc. Dis.* 17, 639–640. doi:10.12102/j.issn.1672-1349.2019.04.050

Zhang, S. P., Gao, Y. S., Hu, C. X., Luo, X. M., Guo, H. W., and Chai, C. (2016). Observation on the therapeutic effect of Xingnaojing injection combined with puncture aspiration for the treatment of hypertensive intracerebral hemorrhage. *Chin. J. Pract. Nerv. Dis.* 19, 121–122. doi:10.3969/j.issn.1673-5110.2016.13.079

Zhao, X. P. (2011). Effect of Xingnaojing injection on patients with cerebral hemorrhage minimally invasive cranial hematoma. *Hebei J. Tradit. Chin. Med.* 33, 1845–1847. doi:10.3969/j.issn.1002-2619.2011.12.047

Zhou, L. L., and Sun, M. F. (2017). Analysis on the effect of Xingnaojing injection on clinical indexes of patients with hypertensive intracerebral hemorrhage. *China Mod. doct.* 55, 116–118.

Zhou, R. Z. (2014). Observation on the therapeutic effect of minimally invasive intracranial hematoma removal surgery combined with Xingnaojing injection in the treatment of hypertensive intracerebral hemorrhage. *Med. Inf.* 27, 95. doi:10.3969/j.issn.1006-1959.2014.13.104

Zhou, X. (2015). Observation on the therapeutic effect of minimally invasive intracranial hematoma removal surgery combined with Xingnaojing injection in the treatment of hypertensive intracerebral hemorrhage. *Chin. J. Clin. Ration. Drug Use* 8, 147. doi:10.15887/j.cnki.13-1389/r.2015.02.108

frontiers | Frontiers in Pharmacology

TYPE Original Research
PUBLISHED 03 July 2024
DOI 10.3389/fphar.2024.1404119



OPEN ACCESS

EDITED BY
Junfeng Wang,
Massachusetts General Hospital and Harvard Medical School, United States

REVIEWED BY
Muyun Xu,
Cambrex, United States
Yasuhiro Kosuge,
Nihon University, Japan
Agustina Alaimo,
National Scientific and Technical Research Council (CONICET), Argentina

*CORRESPONDENCE
Kin Chiu,
datwai@hku.hk
Jiantao Wang,
wangjiantao65@126.com
Lan Ma,
pmalan@sz.tsinghua.edu.cn

†These authors have contributed equally to this work and share first authorship

RECEIVED 20 March 2024
ACCEPTED 11 June 2024
PUBLISHED 03 July 2024

CITATION
Liu J, Zhou L, Wu X, Chen Z, Zheng X, Wang H, So KF, Ma L, Wang J and Chiu K (2024), Lycium ruthenicum water extract preserves retinal ganglion cells in chronic ocular hypertension mouse models.
*Front. Pharmacol.* 15:1404119.
doi: 10.3389/fphar.2024.1404119



# Lycium ruthenicum water extract preserves retinal ganglion cells in chronic ocular hypertension mouse models

Jinfeng Liu[1,2†], Lina Zhou[3†], Xueping Wu[4†], Zihang Chen[5], Xiaofei Zheng[5], Huajun Wang[5], Kwok Fai So[2,6,7,8], Lan Ma[9,10,11*†], Jiantao Wang[1*†] and Kin Chiu[2,6,7*†]

[1]Shenzhen Eye Hospital, Shenzhen Eye Institute, Jinan University, Shenzhen, China, [2]Department of Ophthalmology, LKS Faculty of Medicine, The University of Hong Kong, Pokfulam, Hong Kong SAR, China, [3]Department of Laboratory Medicine, Peking University Shenzhen Hospital, Shenzhen, China, [4]Jinzhou Medical University, Jinzhou, China, [5]Department of Sports Medicine, The First Affiliated Hospital, Guangdong Provincial Key Laboratory of Speed Capability, The Guangzhou Key Laboratory of Precision Orthopedics and Regenerative Medicine, Jinan University, Guangzhou, China, [6]State Key Laboratory of Brain and Cognitive Sciences, The University of Hong Kong, Pokfulam, Hong Kong SAR, China, [7]Department of Psychology, The University of Hong Kong, Pokfulam, Hong Kong SAR, China, [8]Guangdong-Hongkong-Macau Institute of CNS Regeneration, Jinan University, Guangzhou, China, [9]Institute of Biopharmaceutical and Health Engineering, Tsinghua University Shenzhen Graduate School, Tsinghua University, Shenzhen, China, [10]Institute of Biomedical Health Technology and Engineering, Shenzhen Bay Laboratory, Shenzhen, China, [11]State Key Laboratory of Chemical Oncogenomics, Tsinghua Shenzhen International Graduate School, Tsinghua University, Shenzhen, China

*Lycium ruthenicum* Murray (LR), known as "black goji berry" or "black wolfberry", is widely utilized in chinese herbal medicine. LR fruit showed its antioxidant and/or anti-inflammation activity in treating cardiac injury, experimental colitis, nonalcoholic fatty liver disease, fatigue, and aging. Glaucoma is the leading cause of irreversible blindness. Besides elevated intraocular pressure (IOP), oxidative stress and neuroinflammation were recognized to contribute to the pathogenesis of glaucoma. This study investigated the treatment effects of LR water extract (LRE) on retinal ganglion cells (RGCs) threatened by sustained IOP elevation in a laser-induced chronic ocular hypertension (COH) mouse model and the DBA/2J mouse strain. The antioxidation and anti-inflammation effects of LRE were further tested in the $H_2O_2$-challenged immortalized microglial (IMG) cell line *in vitro*. LRE oral feeding (2 g/kg) preserved the function of RGCs and promoted their survival in both models mimicking glaucoma. LRE decreased 8-hydroxyguanosine (oxidative stress marker) expression in the retina. LRE reduced the number of Iba-1+ microglia in the retina of COH mice, but not in the DBA/2J mice. At the mRNA level, LRE reversed the COH induced HO-1 and SOD-2 overexpressions in the retina of COH mice. Further *in vitro* study demonstrated that LRE pretreatment to IMG cells could significantly reduce H2O2 induced oxidative stress through upregulation of GPX-4, Prdx-5, HO-1, and SOD-2. Our work demonstrated that daily oral intake of LRE can be used as a preventative/treatment agent to protect RGCs under high IOP stress probably through reducing oxidative stress and inhibiting microglial activation in the retina.

KEYWORDS

**Lycium ruthenicum murray, glaucoma, retinal ganglion cell, oxidative stress, microglia**

# 1 Introduction

*Lycium ruthenicum* Murray (LR), also called "black goji berry", or "black wolfberry", has traditionally been utilized in medical practices to address conditions such as abnormal menopause, menstruation, and hypertension (Liu et al., 2020). LR fruit contains a rich assortment of compounds, such as anthocyanins, phenolic acids, polysaccharides, carotenoids, alkaloids, essential oils, and fatty acids. LR fruit has multifaceted functions including antioxidant, anti-fatigue, immune-enhancement, and anti-aging properties (Wang et al., 2018). LR extract (LRE) decreased the contents of lipid peroxidation and malondialdehyde (MDA) in serum and brain, accompanied by increased activities of superoxide dismutase (SOD) and glutathione peroxidase (GPX), in D-galactose induced aging mice (Cui et al., 2023). Polyphenols in LRE had neuroprotective effects against acrylamide-induced neurotoxicity (Pang et al., 2023). Polysaccharides in LRE protected cortical neurons against oxygen-glucose deprivation/reperfusion in neonatal hypoxic-ischemic encephalopathy (Deng et al., 2020).

Glaucoma is a leading cause of irreversible blindness, affecting an estimated 111.8 million people worldwide by 2040 (Allison et al., 2020). Progressive degeneration of retinal ganglion cells (RGCs) and subsequent visual field loss is the main symptom of glaucoma (Jayaram et al., 2023). Besides elevated intraocular pressure (IOP), mounting evidence suggests that additional mechanisms, such as oxidative stress and neuroinflammation, contribute to the pathogenesis and progression of glaucoma (Baudouin et al., 2021). In glaucoma, compromised retinal blood flow could trigger the generation of reactive oxygen species (ROS) in the retina (McMonnies, 2018; Wang et al., 2023). Elevated IOP can compress the optic nerve fiber and then reduce retrograde neurotrophin support for RGC axons, further contributing to ROS production in RGCs (McMonnies, 2018). Excessive ROS in RGCs directly induces their degeneration in glaucoma (Fernández-Albarral et al., 2024). ROS can also mediate microglial activation-related inflammation and neurotoxicity, which is a significant contributor to the pathogenesis of glaucoma (Baudouin et al., 2021). The interaction between oxidative stress and inflammatory response in microglia is known to contribute to its activation, playing a role in neurodegenerative diseases including glaucoma (Simpson and Oliver, 2020).

In this study, we investigated the effects of LRE on the retina in 2 mouse models mimicking glaucoma: a laser-induced chronic ocular hypertension (COH) mouse model and the DBA/2J mouse strain. Our primary objectives were to evaluate the impact of LRE on the function and survival of RGCs and to assess its ability to modulate oxidative stress and microglial activation under high IOP mimicking glaucoma.

# 2 Materials and methods

## 2.1 Preparation of *Lycium ruthenicum* water extract

*Lycium ruthenicum* water extract (LRE) was provided by Eu Yan Sang (HK) Ltd. LR from Qinghai, the People's Republic of China, was used for this study. To prepare the LRE, 500 g dried LR was separated into 10 equal portions. Then, one portion of LR was put into 250 mL de-ionized water at 50°C–60°C for 15 min. Subsequently, LR was removed, and the extract was filtered. The filtrate was added with de-ionized water to make up to a final volume of 250 mL. This 250 mL filtrate was used to extract the next portion of LR as above procedures until all 10 portions were processed. Each milliliter of the final LRE contained 2 g of the crude drug. The LRE was stored in a refrigerator at 4°C.

## 2.2 Detection of anthocyanins and anthocyanidins in LRE

To test the anthocyanins and anthocyanidins contents, 39 g LRE was subjected to high-performance liquid chromatography (HPLC) (conducted by Eurofins Food Testing HK Ltd). The contents of anthocyanins and anthocyanidins are listed in Table 1. There were 0.0313% (w/w) anthocyanins and 0.0103% (w/w) anthocyanidins in the LRE. Delphinidine 3 glucoside was the major ingredient which was 0.027% (w/w) in the LRE and used as the standard for quality control.

## 2.3 Animals

CX3CR-1$^{GFP}$ knock-in/knock-out mice (Jackson Laboratory, stock No. 005582), DBA/2J mice (Jackson Laboratory, stock No. 000671), and C57BL/6J mice were obtained from the Laboratory Animal Unit of the University of Hong Kong. The mice were housed in a controlled environment with a 12-h light/dark cycle, maintaining a pathogen-free setting. All animal procedures were conducted in accordance with the ARRIVE guidelines and approved by the Committee on the Use of Live Animals in Teaching and Research of the University of Hong Kong.

## 2.4 Laser photocoagulation induced COH mouse model

COH mouse model was constructed by laser photocoagulation on the corneal limbus according to an optimized protocol (Feng et al., 2013). Briefly, female CX3CR1$^{+/GFP}$ mice at the age of 6 months were anesthetized by intraperitoneal injection with a mixture of ketamine (80 mg/kg) and xylazine (8 mg/kg). The right eyes were applied with 1% cyclopentolate hydrochloride (Mydriacyl, Alcon Labs, Inc., Fort Worth, TX, USA) for pupil dilation followed by proparacaine hydrochloride (0.5% alcaine, Alcon) for topical anesthesia. The anterior chamber was punctured with a 30 G syringe needle to drain the aqueous humor. Subsequently, 60–80 consecutive laser spots (Size, 500 μm; power, 800 mW; pulse duration, 50 msec) were delivered perpendicularly to the limbus surface, while sparing the nasal area, using a 532 nm laser (Lumenis Novus Spectra, Yokneam, Israel). About 10% of mice eyes exhibiting anterior chamber hemorrhage, cataract, or corneal ulcer following the induction of IOP elevation were excluded from the study.

TABLE 1 Identification of anthocyanins and anthocyanidins in LRE by HPLC.

| Compound identity | Results | Unit |
|---|---|---|
| Delphinidin 3 galactoside | Not Detected | % (w/w) |
| Delphinidin 3 glucoside | 0.027 | % (ww) |
| Cyanidin 3 galactoside | Not Detected | % (ww) |
| Delphinidin 3 arabinoside | Not Detected | % (w/w) |
| Cyanidin 3 glucoside | Not Detected | % (w/w) |
| Petunidin 3 galactoside | Not Detected | % (ww) |
| Cyanidin 3 arabinoside | 0.00165 | % (w/w) |
| Petunidin 3 glucoside | Not Detected | % (w/w) |
| Delphinidin | Not Detected | % (w/w) |
| Peonidin 3 galactoside | Not Detected | % (w/w) |
| Petunidin 3 arabinoside | 0.0019 | % (ww) |
| Peonidin 3 glucoside | Not Detected | % (ww) |
| Malvidin 3 galactoside | Not Detected | % (w/w) |
| Peonidin 3 arabinoside | Unable to determine due to interference | % (w/w) |
| Malvidin 3 glucoside | Not Detected | % (ww) |
| Cyanidin | 0.00934 | % (w/w) |
| Malvidin 3 arabinoside | 0.000773 | % (w/w) |
| Petunidin | 0.000647 | % (w/w) |
| Peonidin | 0.000141 | % (w/w) |
| Malvidin | 0.000131 | % (ww) |
| Total anthocyanins | 0.0313 | % (w/w) |
| Total anthocyanidins | 0.0103 | % (w/w) |
| Total anthocyanins and anthocyanidins | 0.0416 | % (w/w) |

## 2.5 Measurement of IOP

The IOP of mouse eyes was measured using a rebound tonometer (Icare®TonoLab, Colonial Medical Supply, Franconia, NH). In the laser-induced COH model, IOP measurements were performed on awake mice without any eye drops, whereas measurements were conducted on general anesthetized DBA/2J mice under local corneal anesthesia. Each IOP value was determined by averaging six consecutive measurements and the IOP level of the mouse eye was represented by the average of three such values.

## 2.6 Animal feeding and grouping

The dose of LRE oral feeding at 2 g/kg body weight was chosen according to the previous LRE dose-response study in mice suffered radiation injury (Duan et al., 2015). For the laser-induced COH mice, daily LRE oral feeding started at 7 days before laser photocoagulation till 30 days after the induction of COH. Distilled water was fed as a placebo control. At the end of the experiment, there were 22 normal control eyes, 20 eyes with COH fed with water, and 22 eyes with COH fed with LRE for data analysis. For DBA/2J mice, daily LRE feeding started at 6 months of age for 4 months and ended at 10 months of age. C57BL/6J mice at 10 months of age were used as wild-type controls. There were 10 mice in each group, both eyes of the DBA/2J and C57BL/6J mice were used for analysis.

## 2.7 Flash electroretinography (ERG)

The function of RGCs was evaluated using flash ERG, following the standard protocol of the International Society for Clinical Electrophysiology of Vision. Following general anesthesia, 1% cyclopentolate hydrochloride (Mydriacyl, Alcon) was applied to the eyes to dilate the pupil and then proparacaine hydrochloride (0.5% alcaine, Alcon) was applied as topical anesthesia for 5 min. Afterward, ERG signals were recorded using an ERG system (Espion E2 Electrophysiology System, Diagnosys LLC, USA). Full-field flash ERG test was conducted at a photopic intensity of 3.0 and 10.0 cd $s.m^{-2}$ to detect the photopic negative response (PhNR) which represents the RGCs activity. The acquired data were

analyzed using Axon pCLAMP 10 software (Molecular Devices Corp., Sunnyvale, CA, USA).

## 2.8 Retinal ganglion cell counting on flat-mounted retina

In the COH mice study, the RGC survival was evaluated by counting the number of Brn-3a+ cells on the flat-mounted retina. Mice were euthanized, and the eyeballs were enucleated and fixed in 4% paraformaldehyde (PFA) for 1 h. Subsequently, the retina was dissected from the sclera and flat mounted with the RGC layer faceup under a stereo microscope. To stain the RGCs, the retinas were rinsed with PBS, followed by blocking with a solution containing 10% normal donkey serum and 0.1% Triton X-100 in PBS. The retinas were then incubated overnight at 4°C with goat anti-Brn-3a (1:500, Santa Cruz, Dallas, USA). After thorough washing, the retinas were incubated with a secondary antibody, Alexa-568 fluorescent-conjugated donkey anti goat IgG secondary antibody (1:500; Thermo Fisher Scientific, Waltham, MA, USA), for 2 h at room temperature. To visualize cell nuclei, the retinas were counterstained with 4',6-Diamidino-2- phenylindole (DAPI) (1: 1000). Confocal images were acquired using a ZEISS LSM 800 confocal microscope (Carl Zeiss Microscopy GmbH, Germany), and the number of Brn-3a+ cells was quantified using ImageJ software (National Institutes of Health, Bethesda, Maryland, USA).

## 2.9 Retinal section histological analysis

In the DBA/2J mice study, the RGC survival was evaluated by counting the nuclei in the RGC layer. After standard eyeball fixation, dehydration, and paraffin embedding, retinal cross sections containing optic nerve were collected for further analysis. These sections were stained with hematoxylin and eosin (H&E) and mounted using DPX mounting medium. Images were captured using an optical microscope (Nikon Eclipse 80i, Tokyo, Japan). The number of nuclei in the RGC layer was quantified using ImageJ software.

## 2.10 Immunohistochemical staining

The eye sections were deparaffinized and subjected to antigen retrieval by immersing them into 95 °C citric acid buffer for 15 min. Subsequently, the sections were blocked with 10% normal goat serum in PBS and then incubated overnight at 4°C with primary antibodies, including rabbit anti-Iba-1 (1:500, WAKO, Chou-ku, Osaka, Japan), rabbit anti-8-hydroxyguanosine (8-OHdG) (1:500, Abcam, Cambridge, UK), and rabbit anti-caspase3 (1:500, Abcam). Following that, the sections were incubated with Alexa-568 or 488 fluorescent-conjugated goat anti rabbit IgG secondary antibodies (1:500; Thermo Fisher Scientific) for 1 h and then counterstained with DAPI (1:1000) at room temperature. Images were captured using a ZEISS LSM 800 confocal microscope. The number of positive cells and fluorescence intensity were quantified using ImageJ software.

## 2.11 Cell culture and treatment

The immortalized microglial (IMG) cell line (Cat. SCC134, Sigma-Aldrich, Burlington, MA, USA) was cultured in Dulbecco's Modified Eagle Medium (DMEM) with high glucose (Thermo Fisher Scientific) supplemented with 10% fetal bovine serum (FBS) (Invitrogen, Carlsbad, CA, USA). The cells were maintained at 37°C in a humidified atmosphere containing 95% air and 5% CO2. To prevent contamination, 1% Penicillin-Streptomycin (Thermo Fisher Scientific) was added to the medium.

For the experiments, IMG cells were seeded in 96-well plates ($1 \times 10^4$ cells/well) or 12-well plates ($1.5 \times 10^5$ cells/well) in DMEM with high glucose supplemented with 1% FBS and allowed to incubate overnight before the treatments. To test the dose-response cytotoxicity (LDH test) induced by H2O2 or LRE, cells were treated with 50, 100, 200, 300, 400, and 800 μM of H2O2 (Merck Millipore, Burlington, MA, USA) or 100, 200, 400, and 800 μg/mL of LRE for 24 h followed by LDH test. The antioxidant effect of LRE was first evaluated in the pretreatment test. The IMG cells were incubated with LRE for 2 h at 10, 50, 100, and 200 μg/mL before 300 μM H2O2 stress. In the further experiments, the timing for 200 μg/mL LRE to be applied were evaluated 2 h before (pretreatment), at the same time (simultaneous), or 2 h after (post-treatment) the H2O2 stimulation in the IMG cells. To explore the mechanism of LRE antioxidative effect, the expressions of H2O2 decomposition related enzymes including catalase, GPX-1, GPX-4, peroxiredoxin (Prdx)-1, Prdx-2, Prdx-3, Prdx-4, Prdx-5, and Prdx-6 were detected at 2 h after 200 μg/mL LRE treatment in IMG cells. Furthermore, LRE pretreatment effect on the antioxidant genes such as heme oxygenase (HO)-1 and SOD-2 were evaluated. Untreated cells were applied as controls. Each experiment was repeated three times.

## 2.12 Cytotoxicity assay

The cytotoxicity of IMG cells was assessed using a Pierce LDH Cytotoxicity Assay Kit (Cat. 88953, Thermo Fisher Scientific). Cells were seeded in a 96-well plate. After 24 h of treatment with H2O2 and/or LRE, the cell culture supernatant was collected and mixed with LDH assay buffer in a new 96-well plate. After incubation for 30 min, the reaction was stopped by adding the stop solution to the sample wells. The absorbance at 490 nm and 680 nm was measured using a spectrometry (EnSpire Multimode Plate Reader, PerkinElmer, Waltham, MA, USA). The LDH activity was determined by subtracting the absorbance at 680 nm from the absorbance at 490 nm.

## 2.13 Quantitative reverse transcription polymerase chain reaction

Total RNA from mouse retinas or IMG cell samples was extracted using an RNA extraction kit (Cat. 74106, QIAGEN, Hilden, Germany). Subsequently, the RNA was reverse transcribed into cDNA using a reverse transcription kit (Cat. 205413, QIAGEN). The resulting cDNA samples were then subjected to real-time PCR analysis using an SYBR Green PCR Kit (Cat. 208056, QIAGEN). The amplification process consisted of an initial incubation at 95 °C for

TABLE 2 Primer sequences used for real-time PCR.

| Gene | Forward primer (5′-3′) | Reverse primer (5′-3′) | Reference |
|---|---|---|---|
| β-actin | GTGACGTTGACATCCGTAAAGA | GCCGGACTCATCGTACTCC | NM_007393 |
| IL-1β | CTGTGACTCATGGGATGATGATG | CGGAGCCTGTAGTGCAGTTG | NM_008361 |
| IL-6 | CTGCAAGAGACTTCCATCCAG | AGTGGTATAGACAGGTCTGTTGG | NM_031168 |
| IL-10 | CTTACTGACTGGCATGAGGATCA | GCAGCTCTAGGAGCATGTGG | NM_010548 |
| CX3CR1 | GAGTATGACGATTCTGCTGAGG | CAGACCGAACGTGAAGACGAG | NM_009987 |
| HO-1 | GATAGAGCGCAACAAGCAGAA | CAGTGAGGCCCATACCAGAAG | NM_010442 |
| SOD-2 | CAGACCTGCCTTACGACTATGG | CTCGGTGGCGTTGAGATTGTT | NM_013671 |
| Catalase | AGCGACCAGATGAAGCAGTG | TCCGCTCTCTGTCAAAGTGTG | NM_009804 |
| GPX-1 | AATGTCGCGTCTCTCTGAGG | TCCGAACTGATTGCACGGG | NM_008160 |
| GPX-4 | GATGGAGCCCATTCCTGAACC | CCCTGTACTTATCCAGGCAGA | NM_008162 |
| Prdx-1 | AATGCAAAAATTGGGTATCCTGC | CGTGGGACACACAAAAGTAAAGT | NM_011034 |
| Prdx-2 | CACCTGGCGTGGATCAATACC | GACCCCTGTAAGCAATGCCC | NM_011563 |
| Prdx-3 | GGTTGCTCGTCATGCAAGTG | CCACAGTATGTCTGTCAAACAGG | NM_007452 |
| Prdx-4 | CTCAAACTGACTGACTATCGTGG | CGATCCCCAAAAGCGATGATTTC | NM_016764 |
| Prdx-5 | GGCTGTTCTAAGACCCACCTG | GGAGCCGAACCTTGCCTTC | NM_012021 |
| Prdx-6 | CGCCAGAGTTTGCCAAGAG | TCCGTGGGTGTTTCACCATTG | NM_007453 |

GPX, glutathione peroxidase; HO-1, heme oxygenase 1; Prdx, peroxiredoxin; SOD-2, superoxide dismutase 2

2 min, followed by 40 cycles of denaturation at 95 °C for 5 s and annealing at 60 °C for 15 s. Melting curve analysis was performed to ensure amplification specificity. The primer sequences of the tested genes are listed in Table 2. The gene expression levels of target genes were normalized to housekeeping gene β-actin. The $2^{-\Delta\Delta CT}$ formula was applied for calculation purposes.

## 2.14 Statistical analysis

GraphPad Prism 8.0 software (GraphPad software, San Diego, California, USA) was utilized to create statistical graphs. Data analysis was performed using SPSS software for Windows (version 20.0; SPSS, Inc., IL, USA). To compare multiple groups, a one-way ANOVA was conducted, followed by Fisher's Least Significant Difference (LSD) test for multiple comparisons or Dunnett's test when the variances of all groups were not equal. When comparing two groups, two-tailed Student's t-tests were employed. The data was presented as mean ± SD, and a significance level of $^{*}p < 0.05$ was considered statistically significant.

# 3 Results

## 3.1 LRE preserved retinal function under sustained IOP elevation

Daily feeding of LRE (2 g/kg) was kept till 30 days after COH induction and started from 6 months till 10 months of age in the DBA/2J mice (Figure 1A). At 30 days after COH induction, the awake IOP in the normal control mice was 20.05 ± 0.64 mmHg. There was significant IOP elevation in both water-fed (24.40 ± 0.44 mmHg, $^{***}p < 0.001$) and LRE-fed (24.52 ± 0.56 mmHg, $^{***}p < 0.001$) COH eyes. There was no significant IOP change between LRE- and water-fed groups (Figure 1B). In the DBA/2J study, the IOP in C57BL/6J mice was 8.26 ± 1.53 mmHg under general anesthesia at 10 months of age. There was significant IOP elevation in the DBA/2J mice reaching about 26 mmHg ($^{***}p < 0.001$, Figure 1C). There was no significant change between the water- (26.89 ± 7.36 mmHg) and LRE-fed (26.17 ± 9.85 mmHg) eyes.

Retinal function was evaluated by the photopic ERG test, there was a significant reduction in the PhNR amplitude in the COH eyes. At photopic 3.0 cd s.m$^{-2}$, it reduced from 30.86 ± 10.50 (normal) to 17.84 ± 3.61 μV ($^{*}p = 0.044$, Figures 1D,H). At photopic 10 cd s.m$^{-2}$, it reduced from 34.85 ± 7.88 (normal) to 7.67 ± 2.60 μV ($^{***}p < 0.001$, Figure 1E, I). LRE oral feeding significantly increased the PhNR amplitude in the COH eyes to 20.12 ± 10.92 μV ($^{**}p = 0.007$ vs. water feeding) at photopic 10 cd s.m$^{-2}$ (Figure 1E, I). In the DBA/2J mice at age of 10 months, the PhNR amplitude significantly reduced from 32.33 ± 5.62 (C57BL/6J) to 25.62 ± 8.31 μV at photopic 3.0 ($^{*}p = 0.037$, Figure 1F, J), and from 39.29 ± 4.56 (C57BL/6J) to 18.16 ± 8.67 μV ($^{***}p < 0.001$, Figure 1G, K) at photopic 10.0 cd s.m$^{-2}$. Unlike in the COH model, the significantly increased PhNR amplitude was detected at the photopic intensity of 3.0 cd s.m$^{-2}$, reaching 33.03 ± 7.06 μV ($^{*}p = 0.022$ vs. water feeding) after 4 months of LRE oral feeding (Figure 1F, J).

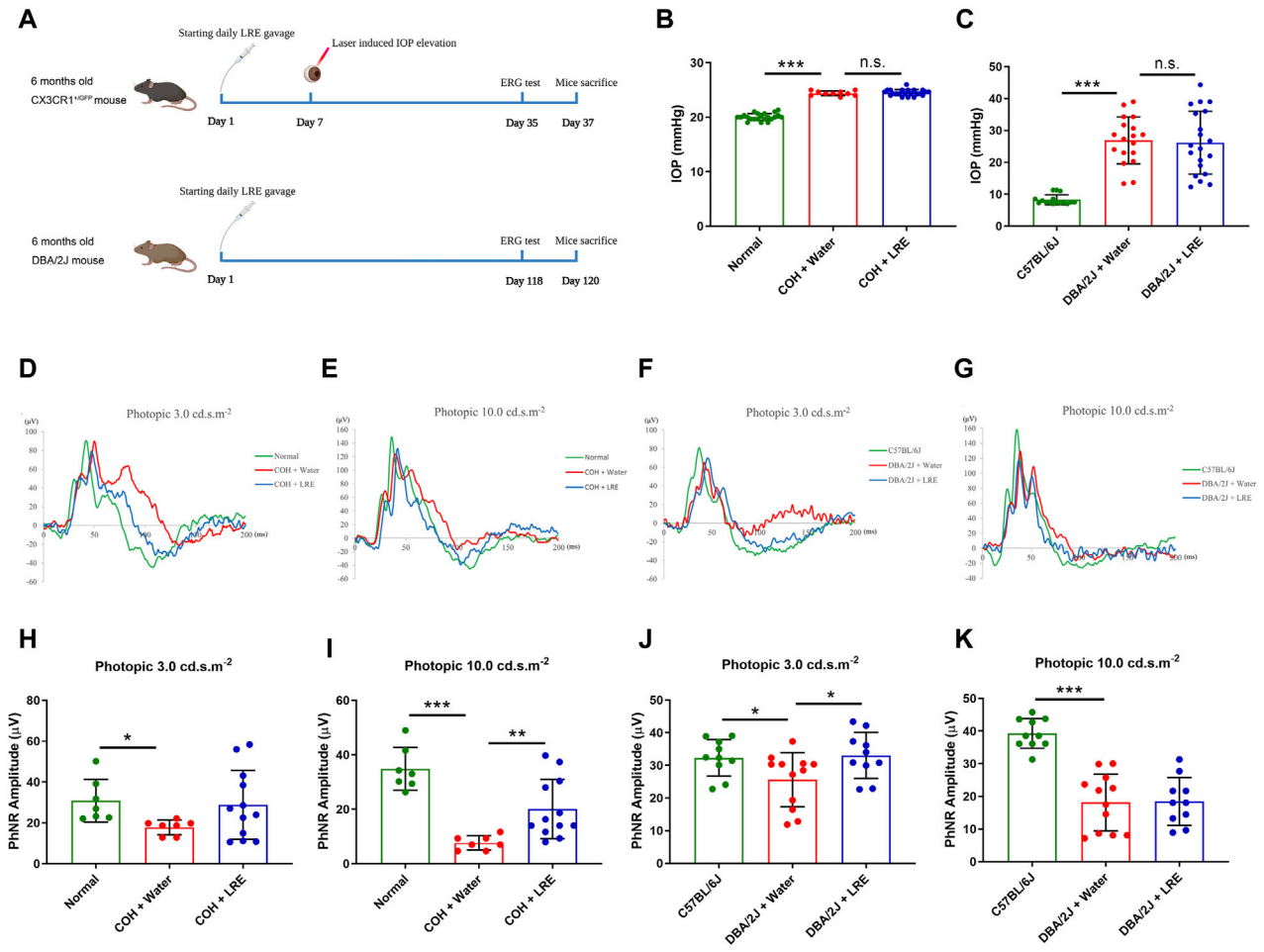


FIGURE 1
LRE preserved RGC function in the eyes of the laser-induced COH and DBA/2J mice without affecting the elevated IOP. **(A)** A schematic representation of the experimental flows in the laser-induced COH mouse model (upper lane) and the DBA/2J mouse strain (lower lane) (Diagram is created in BioRender.com). **(B)** IOP measurement on the awake mice in the laser-induced COH mice after 30 days of laser photocoagulation. **(C)** IOP measurement on the anesthetized C57BL/6J and DBA/2J mice at the age of 10 months. **(D–G)** Representative ERG waves were shown on the assessment of RGC function using a photopic ERG test with flash strengths of 3.0 and 10.0 cd s.m$^{-2}$ in the laser-induced COH, DBA/2J, and control eyes after LRE treatment. **(H–K)** Bar chart figures demonstrated that LRE oral feeding significantly increased the PhNR amplitudes in the COH eyes at photopic 10.0 cd s.m$^{-2}$ and in the DBA/2J mice eyes at photopic 3.0 cd s.m$^{-2}$. *, $p < 0.05$; **, $p < 0.01$; ***, $p < 0.001$; n. s., not significant.

## 3.2 LRE prevented RGC loss induced by sustained IOP elevation

In the COH study, the RGC survival was evaluated by counting the Brn-3a+ cells in the flat-mounted retina (Figure 2A). 30 days of elevated IOP induced significant loss of RGC survival (**$p = 0.004$), it reduced from 4,530 ± 203 in the normal control eyes to 4,008 ± 456 cells/mm$^2$ in the water-fed COH mice at the central retina. There was even severer RGC loss at the peripheral retina, it reduced from 3,592 ± 412 to 2,815 ± 457 cells/mm$^2$ (**$p$ = 0.001, normal vs. water-fed COH mice) (Figure 2B). The LRE oral feeding started 7 days before laser induced IOP elevation till 30 days after COH established. LRE significantly reduced the RGC loss, the RGC number reached 4,621 ± 200 (**$p$ = 0.002) in the central retina and 3,377 ± 368 cells/mm$^2$ (*$p$ = 0.02) in the peripheral retina (Figure 2B). The apoptotic cell marker, Caspase-3, was detected in the retinal cross sections (Figure 3A). In the RGC layer, Caspase-3 positive cell number significantly increased in water-fed COH mice (29 ± 6 cells/mm, ***$p < 0.001$) comparing to the controls (10 ± 6 cells/mm) and LRE significantly reduced it to 10 ± 3 cells/mm (***$p < 0.001$ vs. water feeding, Figure 3B).

This neuroprotective effect of LRE was further proved in the congenital glaucoma model, DBA/2J mice. In the retinal cross sections (Figure 2C), the number of cells in the RGC layer markedly reduced from 96 ± 5 (C57BL/6J mice) to 68 ± 15/mm (**$p$ = 0.001, Figure 2D) in the DBA/2J mice with water feeding at the central retina. 4 months of LRE treatment significantly preserved cells to a density of 83 ± 11/mm (*$p$ = 0.046, LRE vs. water feeding). A similar trend was observed in the peripheral retina, cells reduced from 63 ± 7 (C57BL/6J mice) to 45 ± 11/mm (*$p$ = 0.027, Figure 2D) in the water-fed and then increased to 65 ± 13/mm (**$p$ = 0.009, LRE vs. water feeding) in the LRE-fed DBA/2J mice. The apoptotic caspase-3+ cell number was significantly increased in the RGC layer in DBA/2J mice (26 ± 14 cells/mm) compared to the C57BL/6J controls (5 ± 1 cells/mm, *$p$ = 0.019, Figure 3C, D).

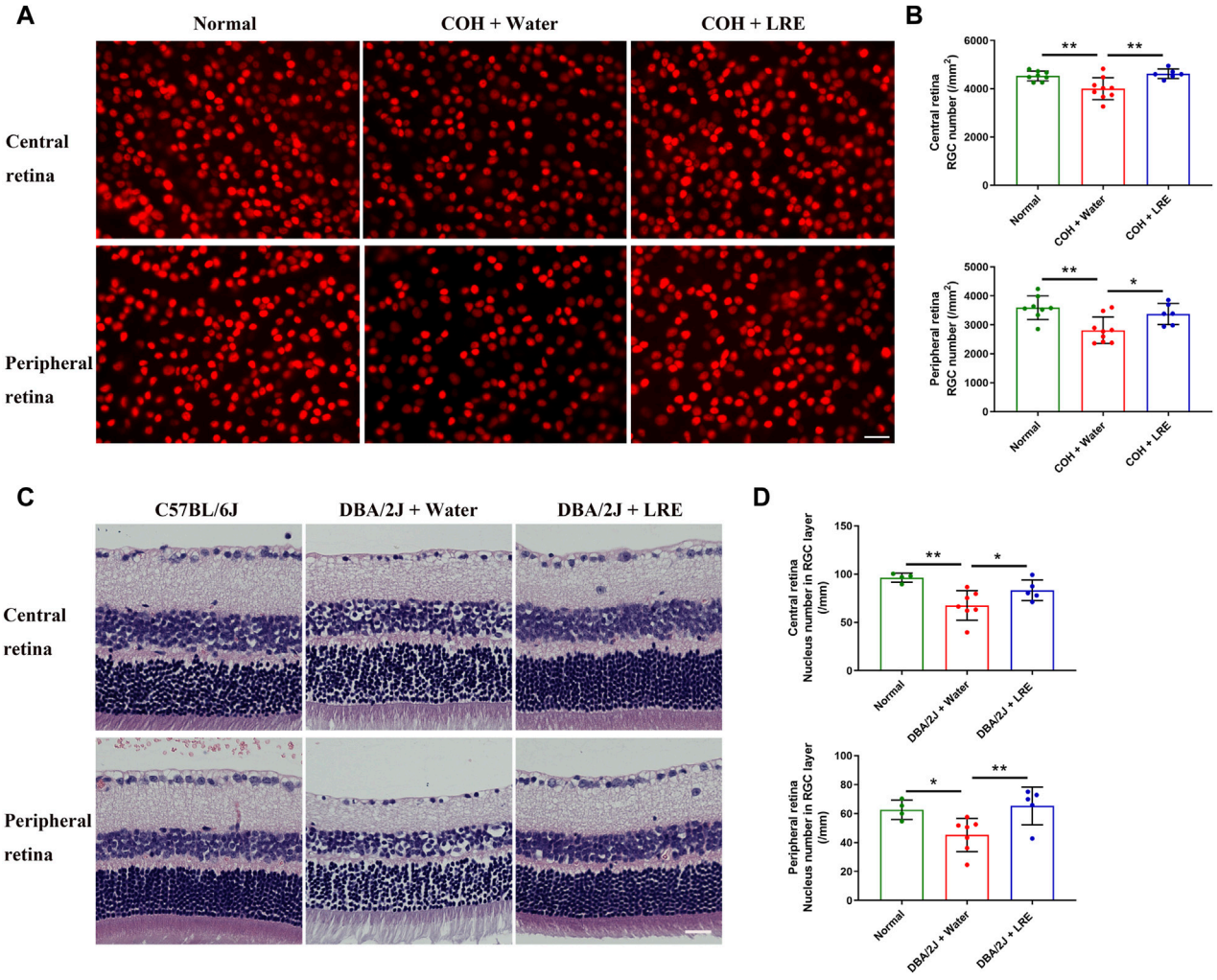


FIGURE 2
LRE promoted RGC survival in the eyes of the laser-induced COH and DBA/2J mice. **(A)** Representative central retina (upper lane) and peripheral retina (lower lane) images of Brn-3a stained RGCs (red) in the retinal flat-mounts from the normal, water-fed, and LRE-fed COH mice. The density of RGCs markedly reduced in the water-fed COH eyes (middle column). Scale bar, 25 μm. **(B)** 30 days of LRE oral feeding significantly increased the RGC number in the central and peripheral retina of the COH eyes. **(C)** Representative images of H&E-stained retinal sections from the C57BL/6J control, water-fed, and LRE-fed DBA/2J mice. There were fewer cells in the RGC layer in the water-fed DBA/2J mice both at the central and peripheral retina. Scale bar, 25 μm. **(D)** 4 months of LRE oral feeding significantly increased nucleus density in the RGC layer of both the central and peripheral retina of the DBA/2J mice. *, $p < 0.05$; **, $p < 0.01$.

LRE significantly reduced the apoptotic cell number to 8 ± 7 cells/mm (*$p$ = 0.043, LRE vs. water feeding, Figure 3D).

## 3.3 LRE reduced oxidative stress in the mouse retina exposed to sustained IOP elevation

Guanine in DNA is converted to 8-OHdG upon free radical attack under oxidative stress (Andrés et al., 2023). Compared to control retinas, the fluorescent intensity of the 8-OHdG markedly increased in water-fed COH eyes in the inner retina including RGC layer and the inner nuclear layer (INL), and slightly upregulated in the outer nuclear layer (ONL) (Figure 4A). Semi-quantitative analysis demonstrated a significant increase in 8-OHdG level in the retina of water-fed COH mice (*$p$ = 0.018 vs. normal), which was effectively reduced by LRE treatment (**$p$ = 0.002, Figure 4B). Furthermore, the gene expressions of HO-1, SOD-2, and GPX-4 significantly increased by 1.51 ± 0.46 (*$p$ = 0.049), 1.10 ± 0.07 (*$p$ = 0.017), and 1.83 ± 0.33 folds (*$p$ = 0.033), respectively, in the retina of COH mice (Figure 4C). LRE mitigated the tissue response to oxidative stress in the retina of the COH eyes. LRE oral feeding reduced the changes of HO-1, SOD-2, and GPX-4 to 1.03 ± 0.34 (*$p$ = 0.044 vs. water feeding), 0.95 ± 0.06 (***$p$ < 0.001 vs. water feeding), and 1.35 ± 0.57 folds ($p$ = 0.108 vs. water feeding), respectively in the COH eyes.

The antioxidant properties of LRE treatment were further investigated in DBA/2J mice. Similar to the changes in COH eyes, there was increased 8-OHdG expression in the inner retina of water-fed DBA/2J eyes (Figure 4D). Semi-quantification revealed a significant increase in 8-OHdG expression in the retina of water-fed DBA/2J mice compared to the C57BL/6J mice (***$p$ < 0.001,

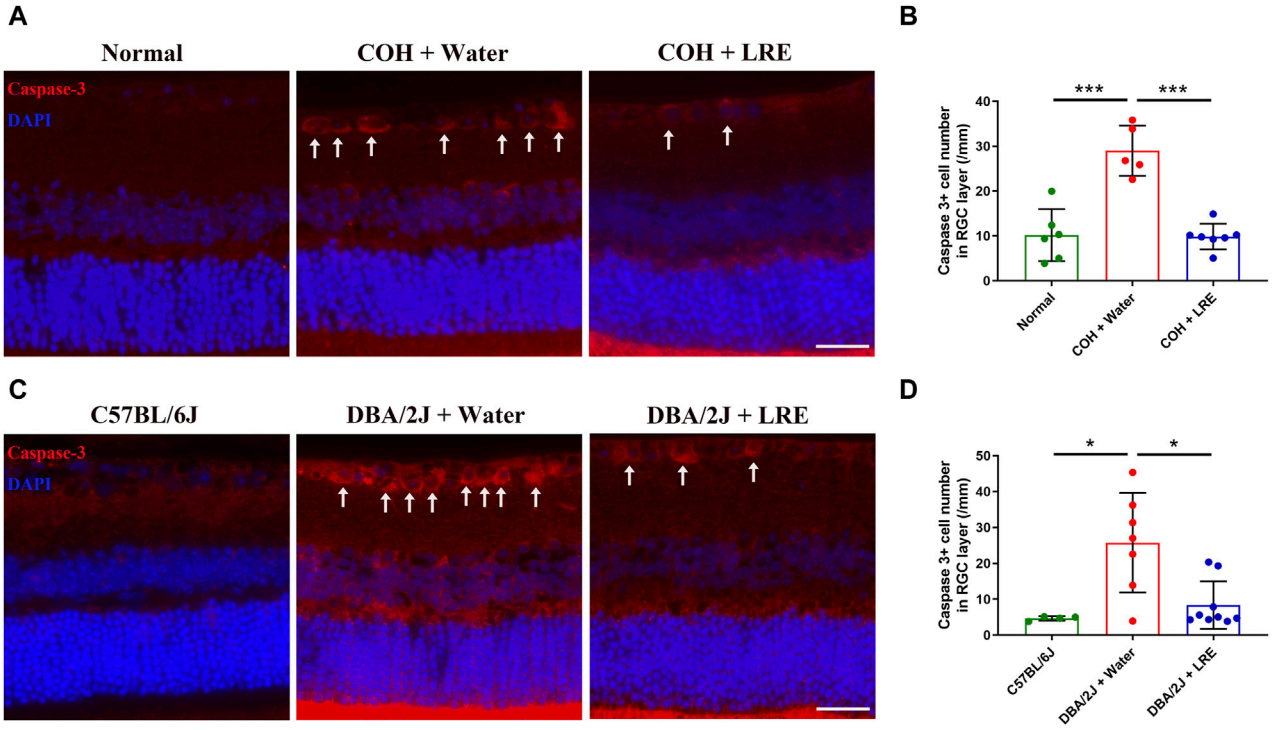


FIGURE 3
LRE inhibited apoptosis in the RGC layer of the laser-induced COH and DBA/2J mice. **(A)** Representative images of caspase-3 positive cells (red, arrows) in the retinal sections from the normal, water-fed, and LRE-fed COH mice. Scale bar, 25 μm. **(B)** LRE significantly decreased the number of caspase-3 positive cells in the RGC layer of the COH eyes. **(C)** Representative images of caspase-3 positive cells (red, arrows) in the retinal sections from the C57BL/6J control, water-fed, and LRE-fed DBA/2J mice. Scale bar, 25 μm. **(D)** LRE significantly decreased the number of caspase-3 positive cells in the RGC layer of the DBA/2J mice. *, $p < 0.05$; ***, $p < 0.001$.

Figure 4E), whereas LRE oral feeding significantly reduced 8-OHdG level in the retina of DBA/2J mice (***$p < 0.001$, Figure 4E).

## 3.4 LRE inhibited microglial activation in the mouse retina under sustained IOP elevation

Microglial activation in the retina of laser-induced COH mice was evaluated by quantifying the number of Iba-1+ microglia in the retinal sections. The microglial number was significantly increased from 14 ± 4 (normal) to 30 ± 4 cells/mm$^2$ (***$p < 0.001$) in the retina of water-fed COH mice (Figure 5A, B). LRE treatment significantly reduced the microglial number to 15 ± 4 cells/mm$^2$ (***$p < 0.001$ vs. water feeding) (Figures 5A, B). The gene expressions of IL-1β, IL-6, IL-10, and CX3CR1 in the water-fed COH mice retina was increased by 1.30 ± 0.23, 1.27 ± 0.24, 1.42 ± 0.51, and 1.59 ± 0.43 folds (vs. normal), respectively. There was significant elevation in IL-1β (*$p = 0.025$) and CX3CR1 (**$p = 0.003$, Figure 5C) in the water-fed COH eyes comparing to normal eyes. LRE oral feeding reduced COH elevated IL-1β, IL-6, IL-10, and CX3CR1 levels without reaching statistical significance (Figure 5C).

In the retina of 10 months old water-fed DBA/2J mice, the Iba-1+ microglial number was significantly increased to 46 ± 13 cells/mm$^2$ (vs. C57BL/6J, ***$p < 0.001$). 4 months of LRE oral feeding did not significantly affect the microglial number (54 ± 17 cells/mm$^2$) in the retina (Figure 5D, E).

## 3.5 LRE upregulated antioxidant enzymes in microglial cells under H2O2 stress

The antioxidation mechanisms of LRE were investigated by adding LRE to H2O2-treated IMG cells *in vitro*. H2O2 induced significant cytotoxicity in IMG cells in a concentration-dependent manner, starting from 200 μM. H2O2 at 300 μM increased cytotoxicity to IMG by 2.12 ± 0.28 folds than control (***$p < 0.001$, Figure 6A). Therefore, 300 μM was chosen to be the oxidative stress stimulator in the following experiments. LRE can also be a stressor to IMG cells. Below 200 μg/mL, there was no significant difference between LRE and no treatment control. However, when the LRE concentration increased to 400 and 800 μg/mL, there was significant cytotoxicity in IMG cells (Figure 6B). The protective effect of LRE was first evaluated by pretreating IMG cells with LRE from 10 to 200 μg/mL for 2 h and then challenging the cells with 300 μM H2O2. LRE significantly prevented H2O2 induced cytotoxicity in IMG cells in a concentration-dependent manner. 200 μg/mL LRE maintained IMG cell's reaction at a level similar to no treatment control (Figure 6C). Following this, the best time for LRE application was further evaluated. 200 μg/mL LRE treatment at 2 h before H2O2 stimulation (pretreatment) significantly reduced the cytotoxicity to 0.85 ± 0.09 folds (***$p < 0.001$ vs. H2O2) and simultaneous administration of LRE with H2O2 also had a protective effect (**$p = 0.003$ vs. H2O2, Figure 6D). But when

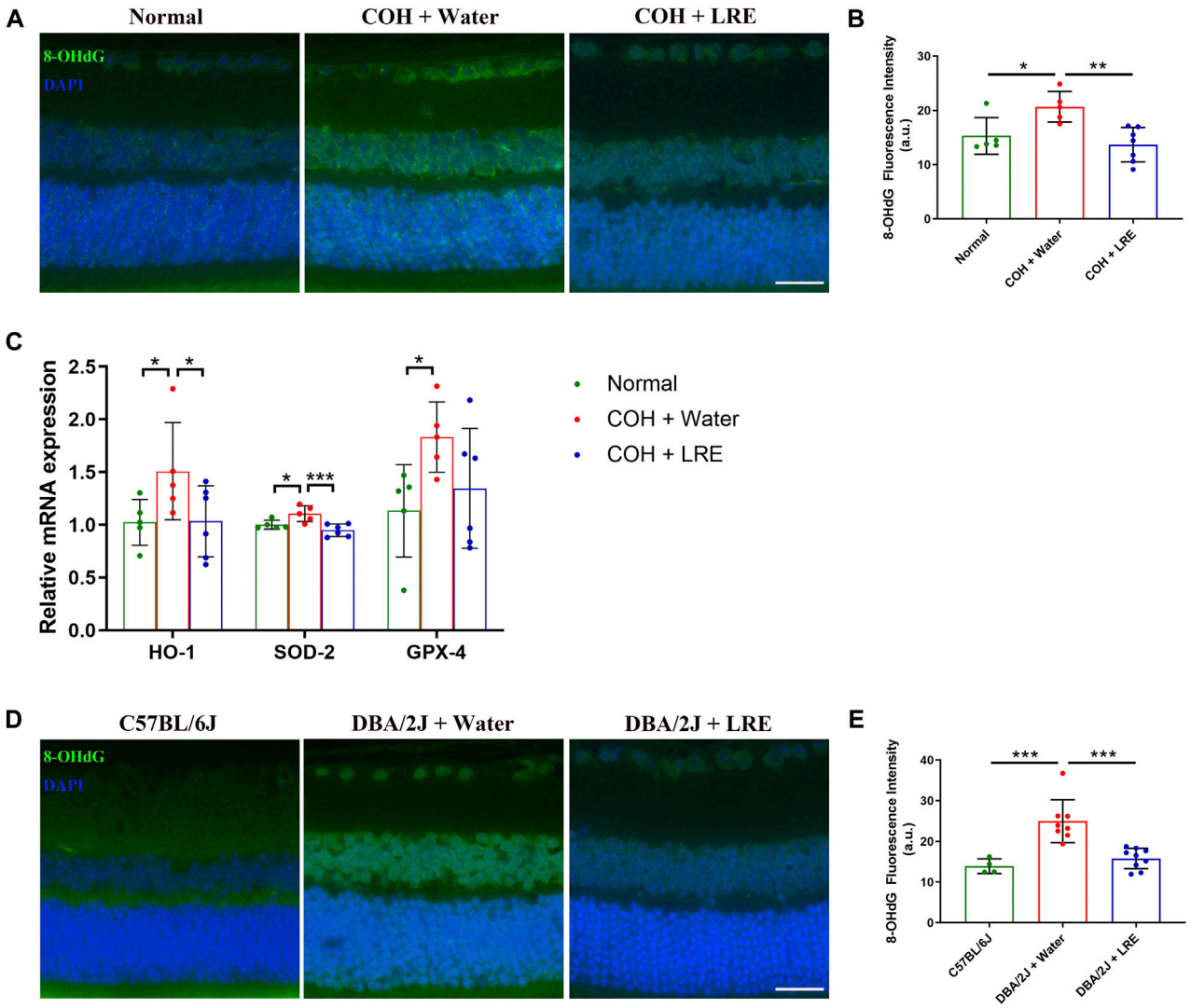


FIGURE 4
LRE mitigated oxidative stress in the retina of the laser-induced COH and the DBA/2J mice. **(A)** Representative images of 8-OHdG stained retinal sections from normal, water-fed, and LRE-fed COH mice. Scale bar, 25 μm. **(B)** LRE significantly reduced the fluorescence intensity of 8-OHdG in the retina of the COH eyes. **(C)** The gene expressions of HO-1, SOD-2, and GPX-4 in the retina of the normal, water-fed, and LRE-fed COH eyes. **(D)** Representative images of 8-OHdG stained retinal sections from the C57BL/6J control, water-fed, and LRE-fed DBA/2J mice. Scale bar, 25 μm. **(E)** LRE significantly reduced the fluorescence intensity of 8-OHdG in the retina of the DBA/2J mice. *, $p < 0.05$; **, $p < 0.01$; ***, $p < 0.001$.

LRE was applied at 2 h after H2O2 stimulation (post-treatment), there was no protective effect.

The fact that pre- and simultaneous LRE treatment protected IMG cells from H2O2-induced oxidative stress, prompted the inquiry of whether LRE pretreatment can effectively prime microglial cells into an antioxidative status by enhancing enzymes involved in H2O2 decomposition, thereby enabling efficient cytoplasmic H2O2 elimination. Among the eight enzymes involved in H2O2 decomposition, GPX-4 and Prdx-5 were significantly increased to 1.44 ± 0.05 (vs. control, ***$p < 0.001$) and 1.33 ± 0.06 (vs. control, ***$p < 0.001$) folds, respectively, following LRE treatment for 2 h (Figure 6E). Furthermore, LRE pretreatment effects on the antioxidant genes HO-1 and SOD-2 were evaluated. While H2O2 demonstrated similar expression levels on these two genes to the control, 200 μg/mL LRE significantly increased the levels of HO-1 and SOD-2 to 6.43 ± 3.20 (vs. control, **$p = 0.002$) and 3.92 ± 0.61 folds (vs. control, ***$p < 0.001$), respectively. There was an accumulation effect of LRE pretreatment to H2O2 as shown in Figure 6F. The levels of HO-1 and SOD-2 raised to 8.80 ± 2.19 (vs. control, ***$p < 0.001$) and 4.73 ± 0.54 folds (vs. control, ***$p < 0.001$).

## 4 Discussion

Neuroprotection, antioxidation, and anti-inflammation effects of LR were summarized by Lee and Choi (2023). Our study investigated the effects of LRE in alleviating RGC degeneration in mouse models mimicking glaucoma. Daily LRE oral feeding significantly preserved RGC function, reduced apoptosis, and promoted RGC survival in the laser-induced COH mouse model

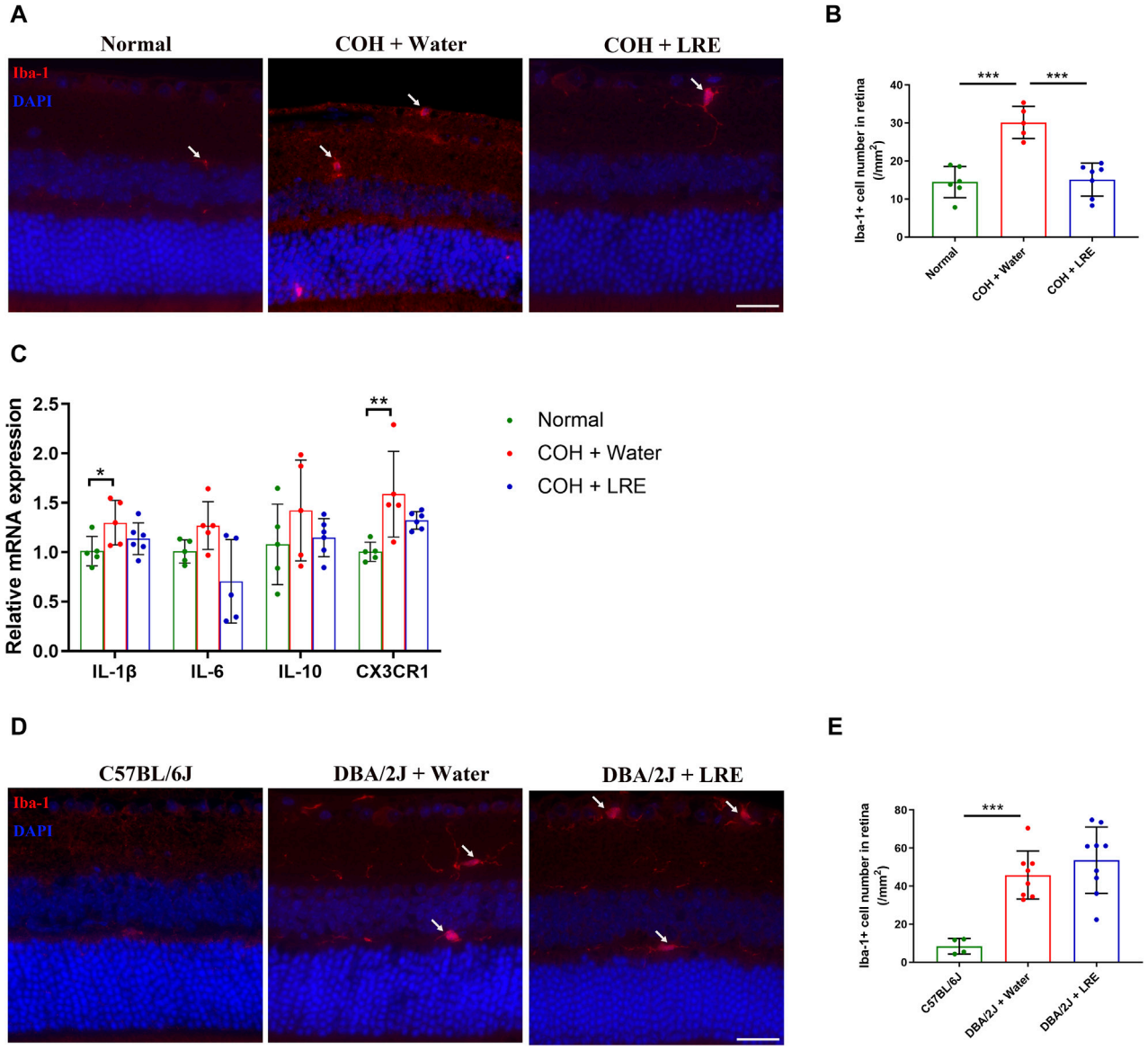


FIGURE 5
LRE affected microglial activation in the retina of the laser-induced COH eyes. **(A)** Representative images of Iba-1 positive cells (red, arrows) in the retinal sections from the normal, water-fed, and LRE-fed COH mice. Scale bar, 25 μm. **(B)** LRE significantly decreased the number of Iba-1 positive microglia in the retina of COH eyes. **(C)** The gene expressions of IL-1β, IL-6, IL-10, and CX3CR1 in the retina of normal, water-fed, and LRE-fed COH eyes. **(D)** Representative images of Iba-1 positive cells (red, arrows) in the retinal sections from the C57BL/6J, water-fed, and LRE-fed DBA/2J mice. Scale bar, 25 μm. **(E)** LRE did not change the Iba-1 positive microglial cell number in the retina of DBA/2J mice. *, $p < 0.05$; **, $p < 0.01$; ***, $p < 0.001$.

and the DBA/2J mouse strain. LRE treatment lowered oxidative DNA damage of the retinal neurons especially in the RGC layer and the INL, as evidenced by reduced 8-OHdG expression. LRE reversed the increase of HO-1 and SOD-2 expressions in the retina of COH mice. Further *in vitro* study demonstrated that LRE pretreatment to IMG cells could significantly reduce H2O2 induced oxidative stress through upregulation of GPX-4, Prdx-5, HO-1 and SOD-2. Retinal microglial activation under sustained IOP elevation was reversed in the COH eyes but not the DBA/2J eyes.

Glaucoma is characterized by progressive RGC loss which leads to irreversible blindness. Current glaucoma treatment relies primarily on IOP lowering surgery/medication, however, was not enough to halt the disease progression (Saifi et al., 2023). Previous studies investigating the pathogenesis of glaucoma highlighted the critical contributions of oxidative stress and microglial activation (Wei et al., 2019; Fan Gaskin et al., 2021). IOP-independent neuroprotective treatments thus are warranted for the future development of glaucoma therapies (Jayaram et al., 2023). Neuroprotective treatments in conjunction with IOP lowering methods might slow down the disease progression especially if the diagnosis is confirmed at early stage. Two mouse models mimicking glaucoma were used in this study with different LRE treatment starting time. In the laser-induced COH model, the LRE oral feeding started at 7 days before the IOP increase. LRE was used as a preventative supplement aiming to

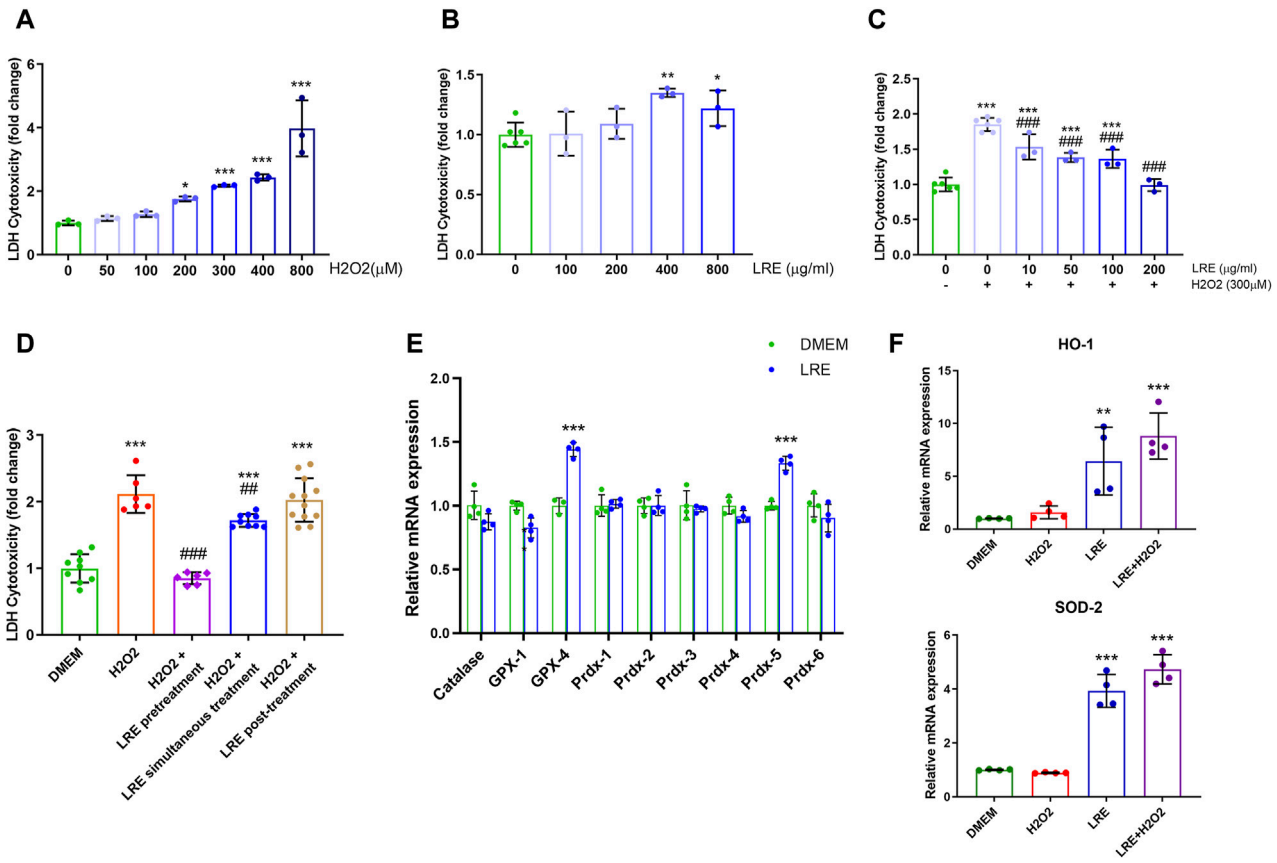


FIGURE 6
LRE protected IMG cells from oxidative stress by enhancing the expressions of antioxidant enzyme related genes. **(A)** Cytotoxicity assay of IMG cells treated by H2O2 at various concentrations, including 50, 100, 200, 300, 400, and 800 μM. **(B)** Cytotoxicity assay of IMG cells treated by LRE at various concentrations, including 100, 200, 400, and 800 μg/mL. **(C)** The effects of 2 h of pretreatment with LRE at 10, 50, 100, and 200 μg/mL on the cytotoxicity induced by 300 μM H2O2 in the IMG cells. **(D)** Pretreatment and simultaneous treatment but not post-treatment with 200 μg/mL LRE significantly reduced 300 μM H2O2-induced cytotoxicity in the IMG cells. **(E)** 2 h of 200 μg/mL LRE treatment on the IMG cells significantly upregulated the gene expressions of GPX-4 and Prdx-5. **(F)** Pretreatment with 200 μg/mL LRE significantly upregulated HO-1 and SOD-2 gene expressions in the IMG cells with or without the 300 μM H2O2 stimulation. *, $p < 0.05$; **, $p < 0.01$; ***, $p < 0.001$ vs. DMEM control. ##, $p < 0.01$; ###, $p < 0.001$ vs. H2O2 stimulation.

potentiate the retinal resilience against high IOP. In the DBA/2J mice, the pigment dispersion in the anterior chamber was detectable from 5–6 months of age and became prominent at 9 months of age (Libby et al., 2005). The dispersed iris pigment obstructs the trabecular meshwork, resulting in secondary IOP elevation in DBA/2J eyes. Libby et al. (2005) found that IOP in DBA/2J eyes started to increase from 6 months of age, reached the highest level at 10 months of age, and then declined at 12 months of age. In this DBA/2J mice, oral feeding of the LRE started at 6 months of age indicating early interference in glaucoma. Oral taking of LRE at a dose of 2 g/kg improved the RGC function and survival without affecting the IOP elevation in both the COH and the DBA/2J mouse models.

LRE showed its antioxidant and anti-inflammatory effects in dextran sulfate sodium induced murine experimental colitis, exhaustive exercise-induced cardiac injury, high-fat diet-induced nonalcoholic fatty liver disease, and radiation injury (Duan et al., 2015; Lin et al., 2015; Hou et al., 2019; Lu et al., 2020; Zong et al., 2020). LRE administration was indicated to enhance the expressions of antioxidant enzymes such as SOD, GPX, and catalase in affected tissues, countering oxidative stress. In fact, anthocyanins, polyphenols, and polysaccharide from LR could activate the Nrf2/HO-1 signaling pathway which regulates a host of antioxidant enzymes (Deng et al., 2020; Tian et al., 2021; Gao et al., 2022). The anthocyanins and anthocyanidins in the LRE might be the key bioactive agents for the protective effect on RGCs under high IOP, they occupied 0.0416% (w/w). LRE oral feeding ameliorated the oxidative stress marked by 8-OHdG increase dominantly in the inner retina of the COH and the DBA/2J eyes. LRE pretreatment of IMG for 2 h successfully upregulated the H2O2 decomposition related enzyme GPX-4 and Prdx-1 gene expression. When H2O2 was added to the LRE primed IMG cells, antioxidant genes (HO-1 and SOD-2) expression increased even higher than the LRE treatment control group. Upregulated GPX-4, Prdx-1, HO-1, and SOD-2 in the LRE pretreatment group successfully prevented the H2O2 induced LDH increase to a level similar to the control group. While this *in vitro* finding is consistent with the reports in other systems, the finding in the COH model that HO-1 and SOD-2 returned to normal levels with LRE oral feeding was unexpected. We postulated that retinal tissue upregulated the antioxidant genes to combat oxidative stress induced by IOP elevation. Daily LRE intake, on the other hand, potentiated the

antioxidant ability of retinal tissue, reducing ROS levels and restoring the retinal microenvironment to normalcy, obviating the need for further antioxidant gene increase. The inconsistency between our *in vivo* findings and others may stem from variations in pathological conditions and their temporal dynamics, which necessitates validation by further investigations.

The anti-inflammatory effect of LRE in the glaucoma models was evaluated by counting the Iba-1 positive cells in the retina. Elevated IOP caused significantly increased microglial activation. LRE as a pretreatment agent decreased Iba-1 positive cells in the COH eyes. In the IMG cell culture, the cytotoxicity of H2O2 can be prevented when LRE was applied as pre- or simultaneous but not post-treatment. In the DBA/2J mice, the RGC function started to be impaired from 3 months of age when the IOP remained at a normal level (Saleh et al., 2007; Harazny et al., 2009). Activation of retinal microglia in the DBA/2J mice is much earlier than 6 months when the LRE oral feeding started. LRE as a post-treatment did not reduce Iba-1 positive cells in the DBA/2J eyes. This differential effect of LRE on microglial activation under high IOP in COH and DBA/2J mice could be induced by the intricate genetic background and the considerable variation in disease progression (Turner et al., 2017).

We demonstrated that daily LRE feeding preserved the function of RGCs and enhanced their survival under the threat of sustained IOP elevation using two chronic glaucoma mouse models. This protective effect was likely attributed to reduced oxidative stress in the retinal neurons by LRE treatment, while inhibition of microglial activation could also contribute. *In vitro* study found that LRE pretreatment protected IMG cells from H2O2 induced damage by priming these microglial cells into an antioxidative status with upregulated GPX-4, Prdx-5, HO-1, and SOD-2. LRE may also confer neuroprotection to other retinal diseases such as retinitis pigmentosa and age-related macular degeneration in which oxidative stress in the ONL was featured (Murakami et al., 2020; Jabbehdari and Handa, 2021). LRE contains various bioactive components, such as anthocyanins, polyphenols, and polysaccharides. Future studies investigating the roles of specific LRE components in treating glaucoma would enhance the translation of LRE treatment to patients.

## 5 Conclusion

LRE oral feeding provided antioxidative effect, preserving the RGCs function and survival as a neuroprotective measure for glaucoma. The 4 months continuous oral feeding in DBA/2J mice that ended at 10 months of age is a precious indication for clinical application of LRE as a supplement to the current glaucoma treatment strategies which focus on IOP control.

## Data availability statement

The original contributions presented in the study are included in the article/Supplementary Material, further inquiries can be directed to the corresponding authors.

## Ethics statement

The animal study was approved by the Committee on the Use of Live Animals in Teaching and Research of the University of Hong Kong. The study was conducted in accordance with the local legislation and institutional requirements.

## Author contributions

JL: Writing–original draft, Conceptualization, Data curation, Formal Analysis, Methodology. LZ: Data curation, Formal Analysis, Methodology, Writing–original draft. XW: Data curation, Formal Analysis, Methodology, Writing–original draft. ZC: Methodology, Writing–original draft. XZ: Data curation, Formal Analysis, Writing–original draft. HW: Data curation, Formal Analysis, Writing–original draft. KS: Validation, Writing–review and editing. LM: Conceptualization, Supervision, Writing–review and editing. JW: Conceptualization, Supervision, Writing–review and editing. KC: Conceptualization, Funding acquisition, Resources, Supervision, Writing–review and editing.

## Funding

The author(s) declare that financial support was received for the research, authorship, and/or publication of this article. This project was supported by Midstream Research Program for Universities (MRP, Project No: MRP-092-17X) in Hong Kong to KC.

## Conflict of interest

The authors declare that the research was conducted in the absence of any commercial or financial relationships that could be construed as a potential conflict of interest.

## Publisher's note



## Supplementary material

The Supplementary Material for this article can be found online at: https://www.frontiersin.org/articles/10.3389/fphar.2024.1404119/full#supplementary-material

# References

Allison, K., Patel, D., and Alabi, O. (2020). Epidemiology of glaucoma: the past, present, and predictions for the future. *Cureus* 12 (11), e11686. doi:10.7759/cureus.11686

Andrés, C. M. C., Lastra, J. M. P., Juan, C. A., Plou, F. J., and Pérez-Lebeña, E. (2023). Chemical insights into oxidative and nitrative modifications of DNA. *Int. J. Mol. Sci.* 24 (20), 15240. doi:10.3390/ijms242015240

Baudouin, C., Kolko, M., Melik-Parsadaniantz, S., and Messmer, E. M. (2021). Inflammation in Glaucoma: from the back to the front of the eye, and beyond. *Prog. Retin Eye Res.* 83, 100916. doi:10.1016/j.preteyeres.2020.100916

Cui, B., Liu, L., Shi, T., Yin, M., Feng, X., and Shan, Y. (2023). The ethanolic extract of Lycium ruthenicum ameliorates age-related physiological damage in mice. *Molecules* 28 (22), 7615. doi:10.3390/molecules28227615

Deng, K., Li, Y., Xiao, M., Wang, F., Zhou, P., Zhang, W., et al. (2020). Lycium ruthenicum Murr polysaccharide protects cortical neurons against oxygen-glucose deprivation/reperfusion in neonatal hypoxic-ischemic encephalopathy. *Int. J. Biol. Macromol.* 158, 562–568. doi:10.1016/j.ijbiomac.2020.04.122

Duan, Y., Chen, F., Yao, X., Zhu, J., Wang, C., Zhang, J., et al. (2015). Protective effect of Lycium ruthenicum murr. Against radiation injury in mice. *Int. J. Environ. Res. Public Health* 12 (7), 8332–8347. doi:10.3390/ijerph120708332

Fan Gaskin, J. C., Shah, M. H., and Chan, E. C. (2021). Oxidative stress and the role of NADPH oxidase in glaucoma. *Antioxidants (Basel)* 10 (2), 238. doi:10.3390/antiox10020238

Feng, L., Chen, H., Suyeoka, G., and Liu, X. (2013). A laser-induced mouse model of chronic ocular hypertension to characterize visual defects. *J. Vis. Exp.* 78, 50440. doi:10.3791/50440

Fernández-Albarral, J. A., Ramírez, A. I., de Hoz, R., Matamoros, J. A., Salobrar-García, E., Elvira-Hurtado, L., et al. (2024). Glaucoma: from pathogenic mechanisms to retinal glial cell response to damage. *Front. Cell Neurosci.* 18, 1354569. doi:10.3389/fncel.2024.1354569

Gao, H., Xue, Y., Wu, L., Huo, J., Pang, Y., Chen, J., et al. (2022). Protective effect of Lycium ruthenicum polyphenols on oxidative stress against acrylamide induced liver injury in rats. *Molecules* 27 (13), 4100. doi:10.3390/molecules27134100

Harazny, J., Scholz, M., Buder, T., Lausen, B., and Kremers, J. (2009). Electrophysiological deficits in the retina of the DBA/2J mouse. *Doc. Ophthalmol.* 119 (3), 181–197. doi:10.1007/s10633-009-9194-5

Hou, C. W., Chen, I. C., Shu, F. R., Feng, C. H., and Hung, C. T. (2019). Protective effect of supplementation with Lycium ruthenicum Murray extract from exhaustive exercise-induced cardiac injury in rats. *Chin. Med. J. Engl.* 132 (8), 1005–1006. doi:10.1097/CM9.0000000000000185

Jabbehdari, S., and Handa, J. T. (2021). Oxidative stress as a therapeutic target for the prevention and treatment of early age-related macular degeneration. *Surv. Ophthalmol.* 66 (3), 423–440. doi:10.1016/j.survophthal.2020.09.002

Jayaram, H., Kolko, M., Friedman, D. S., and Gazzard, G. (2023). Glaucoma: now and beyond. *Lancet* 402 (10414), 1788–1801. doi:10.1016/S0140-6736(23)01289-8

Lee, H. S., and Choi, C. I. (2023). Black goji berry (Lycium ruthenicum Murray): a review of its pharmacological activity. *Nutrients* 15 (19), 4181. doi:10.3390/nu15194181

Libby, R. T., Anderson, M. G., Pang, I. H., Robinson, Z. H., Savinova, O. V., Cosma, I. M., et al. (2005). Inherited glaucoma in DBA/2J mice: pertinent disease features for studying the neurodegeneration. *Vis. Neurosci.* 22 (5), 637–648. doi:10.1017/S0952523805225130

Lin, J., Zhang, Y., Wang, X., and Wang, W. (2015). Lycium ruthenicum extract alleviates high-fat diet-induced nonalcoholic fatty liver disease via enhancing the AMPK signaling pathway. *Mol. Med. Rep.* 12 (3), 3835–3840. doi:10.3892/mmr.2015.3840

Liu, Z., Tang, X., Liu, C., Dong, B., Shao, Y., Liu, B., et al. (2020). Ultrasonic extraction of anthocyanins from Lycium ruthenicum Murr. and its antioxidant activity. *Food Sci. Nutr.* 8 (6), 2642–2651. doi:10.1002/fsn3.1542

Lu, K., Wang, J., Yu, Y., Wu, Y., and He, Z. (2020). Lycium ruthenicum Murr. alleviates nonalcoholic fatty liver in mice. *Food Sci. Nutr.* 8 (6), 2588–2597. doi:10.1002/fsn3.1445

McMonnies, C. (2018). Reactive oxygen species, oxidative stress, glaucoma and hyperbaric oxygen therapy. *J. Optom.* 11 (1), 3–9. doi:10.1016/j.optom.2017.06.002

Murakami, Y., Nakabeppu, Y., and Sonoda, K. H. (2020). Oxidative stress and microglial response in retinitis pigmentosa. *Int. J. Mol. Sci.* 21 (19), 7170. doi:10.3390/ijms21197170

Pang, Y., Chen, J., Yang, J., Xue, Y., Gao, H., and Gao, Q. (2023). Protective effect and mechanism of Lycium ruthenicum polyphenols against acrylamide-induced neurotoxicity. *Food Funct.* 14 (10), 4552–4568. doi:10.1039/d3fo00623a

Saifi, A. I., Nagrale, P., Ansari, K. K., Saifi, I., and Chaurasia, S. (2023). Advancement in understanding glaucoma: a comprehensive review. *Cureus* 15 (9), e46254. doi:10.7759/cureus.46254

Saleh, M., Nagaraju, M., and Porciatti, V. (2007). Longitudinal evaluation of retinal ganglion cell function and IOP in the DBA/2J mouse model of glaucoma. *Invest. Ophthalmol. Vis. Sci.* 48 (10), 4564–4572. doi:10.1167/iovs.07-0483

Simpson, D. S. A., and Oliver, P. L. (2020). ROS generation in microglia: understanding oxidative stress and inflammation in neurodegenerative disease. *Antioxidants (Basel)* 9 (8), 743. doi:10.3390/antiox9080743

Tian, B., Zhao, J., Xie, X., Chen, T., Yin, Y., Zhai, R., et al. (2021). Anthocyanins from the fruits of Lycium ruthenicum Murray improve high-fat diet-induced insulin resistance by ameliorating inflammation and oxidative stress in mice. *Food Funct.* 12 (9), 3855–3871. doi:10.1039/d0fo02936j

Turner, A. J., Vander Wall, R., Gupta, V., Klistorner, A., and Graham, S. L. (2017). DBA/2J mouse model for experimental glaucoma: pitfalls and problems. *Clin. Exp. Ophthalmol.* 45 (9), 911–922. doi:10.1111/ceo.12992

Wang, H., Li, J., Tao, W., Zhang, X., Gao, X., Yong, J., et al. (2018). Lycium ruthenicum studies: molecular biology, Phytochemistry and pharmacology. *Food Chem.* 240, 759–766. doi:10.1016/j.foodchem.2017.08.026

Wang, X., Wang, M., Liu, H., Mercieca, K., Prinz, J., Feng, Y., et al. (2023). The association between vascular abnormalities and glaucoma-what comes first? *Int. J. Mol. Sci.* 24 (17), 13211. doi:10.3390/ijms241713211

Wei, X., Cho, K. S., Thee, E. F., Jager, M. J., and Chen, D. F. (2019). Neuroinflammation and microglia in glaucoma: time for a paradigm shift. *J. Neurosci. Res.* 97 (1), 70–76. doi:10.1002/jnr.24256

Zong, S., Yang, L., Park, H. J., and Li, J. (2020). Dietary intake of Lycium ruthenicum Murray ethanol extract inhibits colonic inflammation in dextran sulfate sodium-induced murine experimental colitis. *Food Funct.* 11 (4), 2924–2937. doi:10.1039/d0fo00172d

frontiers | Frontiers in Pharmacology

TYPE Mini Review
PUBLISHED 31 July 2024
DOI 10.3389/fphar.2024.1436481



OPEN ACCESS

EDITED BY
Qi Liang,
Air Force Medical University, China

REVIEWED BY
Guozheng Huang,
Anhui University of Technology, China

*CORRESPONDENCE
Leilei Chen,
leileichen2019@qdu.edu.cn
Yingjuan Liu,
liuyingjuan829@163.com
Junxia Xie,
jxiaxie@163.com
jxiaxie@public.qd.sd.cn

RECEIVED 22 May 2024
ACCEPTED 15 July 2024
PUBLISHED 31 July 2024

CITATION
Chen L, Liu Y and Xie J (2024), The beneficial pharmacological effects of *Uncaria rhynchophylla* in neurodegenerative diseases: focus on alkaloids.
*Front. Pharmacol.* 15:1436481.
doi: 10.3389/fphar.2024.1436481



# The beneficial pharmacological effects of *Uncaria rhynchophylla* in neurodegenerative diseases: focus on alkaloids

Leilei Chen[1,2,3]*, Yingjuan Liu[1,2,3]* and Junxia Xie[1,2,3]*

[1]Institute of Brain Science and Disease, Qingdao University, Qingdao, Shandong, China, [2]Shandong Provincial Collaborative Innovation Center for Neurodegenerative Disorders, Qingdao University, Qingdao, Shandong, China, [3]Shandong Provincial Key Laboratory of Pathogenesis and Prevention of Neurological Disorders, Qingdao University, Qingdao, Shandong, China

With the intensification of aging population, the prevention or treatment of neurodegenerative diseases, such as Parkinson's disease and Alzheimer's disease, has drawn more and more attention. As a long used traditional Chinese medicine, *Uncaria rhynchophylla* (Miq.) Jacks., named Gouteng in Chinese, has been reported to have an effective neuroprotective role in neurodegenerative diseases. In this review, the beneficial pharmacological effects and signaling pathways of herbal formulas containing *U. rhynchophylla,* especially major compounds identified from *U. rhynchophylla*, such as corynoxine B, corynoxine, rhynchophylline, and isorhynchophylline, in neurodegenerative diseases, were summarized, which not only provide an overview of *U. rhynchophylla* for the prevention or treatment of neurodegenerative diseases but also give some perspective to the development of new drugs from traditional Chinese medicine.

KEYWORDS

***Uncaria rhynchophylla*, alkaloids, Parkinson's disease, Alzheimer's disease, neuroprotection**

## Introduction

Neurodegenerative disease refers to mitochondrial defects, autophagic–lysosomal pathway dysfunctions, synaptic toxicity, and liquid-phase transitions in pathological protein aggregation with neuroinflammation that targets different brain regions in the central nervous system (CNS), accompanied by a progressive loss of neurons in the affected regions (Gan et al., 2018; Peng et al., 2020). As the second leading cause of morbidity and mortality worldwide, neurological diseases have drawn much attention, and the related pharmacological and nonpharmacological interventions to improve the symptoms of neurodegenerative disease have been investigated. Traditional Chinese medicines have long been used in the treatment of neurodegenerative diseases. One of the good examples is *U. rhynchophylla* (Miq.) Jacks., named Gouteng in Chinese. *U. rhynchophylla (Uncaria rhynchophylla)* possesses many medicinal values, such as arresting convulsions, treating gastric problems, reducing the body heat, and suppressing liver hyperfunction in traditional Chinese medicine. Clinically, it has a role in treating hypertension, dizziness, epilepsy, and cardiovascular diseases (Yang et al., 2020). In recent years, *U. rhynchophylla* formulas and its major chemical compounds have shown protective effects on different models of CNS (Ndagijimana et al., 2013; Zhang et al., 2015; Kim et al., 2022).

## U. rhynchophylla

*Uncaria rhynchophylla* can play antineurodegenerative roles in compatibility with many Chinese herbs. Baichanting Compound (BCT), a combination of *U. rhynchophylla* (Miq.) Miq. ex Havil, *Acanthopanax senticosus* (Rupr. and Maxim.) Harms, and *Paeonia lactiflora* Pall, mitigates the development of Parkinson's disease (PD) in alpha-synuclein transgenic mice by regulating the composition and metabolism of the gut microbiota and inhibiting oxidative stress (Lu et al., 2024). Yi-Gan-San, a traditional prescription consisting of *U. rhynchophylla* (Miq.) Miq. ex Havil., *Bupleurum chinense* DC., *Angelica sinensis* (Oliv.) Diels, *Ligusticum wallichii* Franch., and *Poria cocos* (Schw.) Wolf, can improve various behavioral and psychological symptoms of dementia and also showed neuroprotective effects on many neurodegenerative disorders (Yang et al., 2023). Goutengsan, a Chinese herbal formula containing *U. rhynchophylla*, has shown a protective role against Aβ-induced cell damage, and the major compounds identified from the Goutensan extraction, including rhynchophylline, isorhynchophylline, corynoxeine, and isocorynoxeine, also showed a protective role (Huang et al., 2017). This extraction has shown a neuroprotective role in Alzheimer's disease (AD) with evidences of significant inhibition of Aβ aggregation and accumulation in the cortex and subiculum, alleviating synaptic and neuronal loss and improving impaired hippocampal neurogenesis in the 5 × FAD mice (Shin et al., 2018). Extracts containing rhynchophylline and isorhynchophylline improved cognitive function in mice with Alzheimer's-like symptoms and can inhibit the formation and destabilize the preformed fibrils of Aβ protein (Guo et al., 2014). Moreover, intracellular calcium overloading and tau protein hyperphosphorylation in PC12 cells can also be inhibited by rhynchophylline and isorhynchophylline (Xian Y.-F. et al., 2012). Furthermore, the inhibitory effect of *U. rhynchophylla* on the aggregation of both Aβ and tau was confirmed in 3 × Tg mice with both Aβ and tau pathology (Kim et al., 2022). It is reported that *U. rhynchophylla* is an effective anxiolytic agent and acts via the serotonergic nervous system (Jung et al., 2006).

The medicinal uses of *Uncaria* species have resulted in the identification of more than 200 chemical compounds, including flavonoids, indole alkaloids, phenylpropanoids, and triterpenes. Tetracyclic oxindole alkaloids are regarded as the main bioactive constituents acting on the CNS (Zhang et al., 2015). Based on a network pharmacology analysis, 90 anti-AD targets related to alkaloids were identified, of which 28 were significantly correlated with Aβ and tau pathology. KEGG pathway enrichment analysis revealed that the enrichment of AD (hsa05010) was the most significant in alkaloids against AD. Moreover, the dopaminergic synapse (hsa04728) and the cholinergic synapse (hsa04725) pathways were also significantly enriched, suggesting UR alkaloids targeting multiple pathological processes exert AD-resistant effects (Zeng et al., 2021). Combined ingredients target the AD target–pathway network characterized by UHPLC-Q-Exactive Orbitrap MS; many targets of *U. rhynchophylla* were found to be significantly bound up with tau, Aβ, or Aβ and tau. The neuroprotective roles were verified by its reversal of the hyperphosphorylation of tau induced by okadaic acid in SH-SY5Y cells (Jiang et al., 2023).

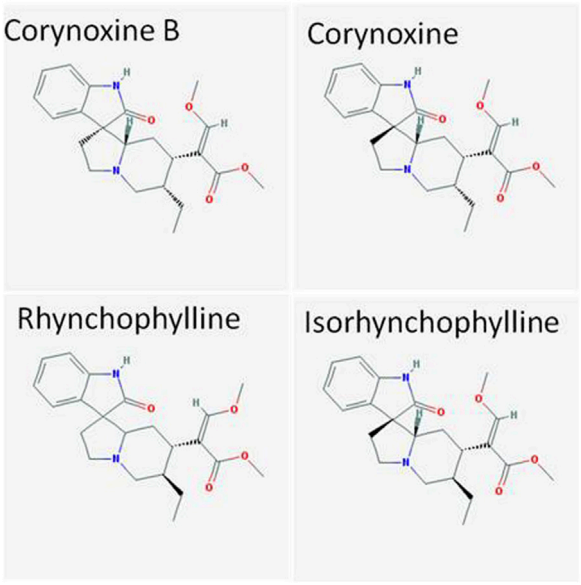


FIGURE 1
Structures of corynoxine B, corynoxine, rhynchophylline, and isorhynchophylline from PubMed.

## Alkaloids

Alkaloids with the blood–brain barrier permeability are the main active pharmacological components of *U. rhynchophylla*. In this review, we summarize the studies about alkaloids against neurodegenerative diseases, focusing on corynoxine B, corynoxine, rhynchophylline, and isorhynchophylline (Figure 1).

## Corynoxine B

Autophagy is a major pathway to promote the clearance of misfolded pathological proteins, and an autophagy inducer has been suggested to be a potential therapeutic strategy for neurodegenerative diseases. Corynoxine B is the first identified alkaloid extracted from *U. rhynchophylla* with the effect of autophagy induction. Both Beclin-1 and HMGB 1/2 are required for corynoxine BF02Dinduced autophagy. Although corynoxine B did affect the protein level of Beclin-1, however, corynoxine B-induced autophagy was completely inhibited after knockdown of Beclin-1 (Lu et al., 2012). Furthermore, corynoxine B was found to improve the impaired cytosolic translocation of HMGB 1 induced by α-synuclein and block the interaction between α-synuclein and HMGB 1, thereby restoring the autophagy flux (Song et al., 2014). In the SH-SY5Y cells with manganese exposure, corynoxine B also showed a neuroprotective effect by restoring the deficient autophagy and disturbing the HMGB 1-α–synuclein interaction (Yan et al., 2019). Recently, corynoxine B was found to directly bind with HMGB 1/2 near the C106 site, enhancing the interaction between Beclin-1 and HMGB 1/2, thereby inducing autophagy and promoting the clearance of α-synuclein in both *Drosophila* and mice PD transgenic models with overexpression of α-synuclein (Zhu et al., 2023). Due to the relatively low brain permeability and

bioavailability, the application prospects of corynoxine B in the PD or AD prevention or treatment will be limited. Therefore, modifications of corynoxine B were performed. CB6 is a derivative of corynoxine B with an N-propyl group modification and is brain-permeable. CB6 induced autophagy through activation of the PIK3C3 complex and promoting PI3P production, which exerted neuroprotective roles in both $MPP^+$-induced cell model and MPTP-induced mice with PD (Zhu et al., 2022). Considering the advantages of exosomes, which could be modified with target-specific receptor ligands on the surface, to cross the blood–brain barrier and then be uptaken by autologous cells, corynoxine B was carried by the Fe65-engineered HT22 hippocampus neuron cell-derived exosomes and delivered to the APP-overexpressed neuron cells in the brain of AD mice, where corynoxine B blocked the interaction between Fe65 and APP and induced autophagy, thereby ameliorating cognitive decline and pathogenesis in AD mice (Iyaswamy et al., 2023).

## Corynoxine

Corynoxine is an enantiomer of corynoxine B, which could also induce autophagy in neuronal cells and promote the clearance of both wild-type and A53T mutant α-synuclein in inducible PC12 cells (Chen et al., 2014). However, the manners of these two oxindole alkaloids to induce autophagy are different. Corynoxine induces autophagy through the Akt/mTOR pathway, while corynoxine B induces autophagy in a Beclin-1-dependent manner (Lu et al., 2012; Chen et al., 2014). In order to identify the key regulator in the processes of corynoxine- or corynoxine B-induced autophagy, we developed a novel network-based algorithm which was named *in silico* Kinome Activity Profiling (iKAP) and found that MAP2K2/MEK2 (mitogen-activated protein kinase 2) and PLK1 (polo-like kinase 1) were significantly upregulated by corynoxine, but not corynoxine B, and the effects of corynoxine in the clearance of APP or α-synuclein were diminished after inhibiting the activity of MAP2K2 and PLK1 (Chen et al., 2017; Chen and Xie, 2018). Furthermore, MAP2K2 was validated to be essential for the induction of autophagy, while PLK1 is involved in the maturation of autophagosomes (Chen et al., 2017; Chen and Xie, 2018). In addition to cell models, the effects of corynoxine on the PD or AD animal models were also evaluated. In both the rotenone-induced rat model of PD with acute toxicity and rotenone-induced mice model of PD with chromic toxicity, corynoxine has been proved to not only decrease α-synuclein aggregates through mTOR-mediated autophagy but also diminish neuroinflammation (Chen et al., 2021). Corynoxine could activate TFEB/TFE3 through inhibiting the signaling pathway of Akt/mTOR and induce neuronal autophagy that promotes the clearance of APP-CTFs and improves the learning and memory function in the 5×FAD mice model; however, the process of corynoxine-induced APP-CTF clearance was abolished by knockdown of TFEB/TFE3 (Guan et al., 2024). Corynoxine also exerts antitumor effects in pancreatic cancer through ROS-p38-mediated cytostatic effects (Wen et al., 2022) and in the non-small cell lung cancer through the AKT-mTOR/GSK3β pathway (Hou et al., 2024). Recently, together with isorhynchophylline and corynoxine, two new oxindole alkaloids, which were named macrophyllines C and D, were isolated from *Uncaria macrophylla*, and macrophyllines D, isorhynchophylline, and corynoxine have showed anti-HIV activities with $EC_{50}$ values of 11.31 ± 3.29 μM, 18.77 ± 6.14 μM, and 30.02 ± 3.73 μM, respectively (Liang et al., 2023).

## Rhynchophylline

Rhynchophylline, a tetracyclic oxindole alkaloid component isolated from *U. rhynchophylla* (Miq.) Jacks., shows efficacy against CNS disorders such as epilepsy, drug addiction, neurodegenerative disease, cerebral ischemia, and vascular dementia, by modulating neurotransmitters, suppressing calcium channels, and inhibiting inflammation (Tognolini et al., 2014; Zhang et al., 2019). Rhynchophylline has exhibited neuroprotective effects in both cell and animal models of PD. Rhynchophylline prevented neurotoxicity and apoptosis caused by 1-methyl-4-phenylpyridinium ion ($MPP^+$) in primary cerebellar granule neurons. The transcription factor myocyte enhancer factor 2D (MEF2D) was identified as the target through the luciferase reporter gene assay, possibly via the inhibition of the PI3-K/Akt/GSK3β cascade (Hu et al., 2018). In 1-methyl-4-phenyl-1,2,3,6-tetrahydropyridine hydrochloride (MPTP)-induced mice, rhynchophylline presented neuroprotective roles through reducing the loss of dopaminergic neurons and reversing the secretion of inflammatory cytokines. Based on a mass spectrometry-based metabolomic strategy, retinol metabolism, arachidonic acid metabolism, glycerophospholipid metabolism, and purine metabolism were recognized as the main targets to ameliorate metabolic disorders in PD (Zhang et al., 2023). Due to the blood–brain barrier (BBB), more than 98% drugs cannot penetrate it, which significantly hampers their effectiveness for PD patients. Lin et al. designed a thermosensitive gel for brain targeted delivery of rhynchophylline through intranasal administration. The cross-linked gel with good adhesion and sustained release properties showed remarkable bioavailability and brain targeting than those of oral administration. Sustained drug delivery of rhynchophylline after nasal administration effectively alleviated the symptoms of PD (Lin et al., 2023).

Rhynchophylline, as an inhibitor of ephrin type A receptor 4 precursor (EphA4) tyrosine kinase, was found to rescue the impairment of synaptic plasticity in the hippocampus and improve cognitive dysfunctions in a mouse model of AD known as APP/PS1 transgenic mice (Fu et al., 2014). Furthermore, rhynchophylline not only ameliorates amyloid plaque burden but also reduces inflammation, mainly by regulating the ubiquitin proteasome system, angiogenesis, and microglial functional states (Fu et al., 2021). Excessive activation of microglial cells has been implicated in neuroinflammation of the progression of neurodegeneration. In lipopolysaccharide (LPS)-stimulated primary microglia, rhynchophylline markedly suppresses inflammatory responses by reducing the production of proinflammatory factors, such as nitric oxide (NO), tumor necrosis factor-α (TNF-α), interleukin-1β (IL-1β), and prostaglandins E2 (PGE2), and down-regulating the mitogen-activated protein kinases (MAPK)/NF-κB signaling pathways (Song et al., 2012). However, the application of rhynchophylline for AD treatment is limited by the low water solubility and bioavailability in brain tissue. The efficiency was improved by

loading rhynchophylline to mPEG-PLGA nanoparticles, which coupled with Tween 80 further for brain targeting delivery (T80-NPS-RIN). According to the pharmacokinetic effects, the nanoparticle delivery system exhibited good biocompatibility and increased the effect of rhynchophylline *in vivo* without hemolysis (Xu et al., 2020). In addition, intraperitoneal administration of rhynchophylline ameliorated Aβ1–42-induced cognitive impairment by improving ARE promoter activity. Rhynchophylline also restored the expression of Nrf2 and its downstream proteins in the frontal cortex and hippocampus of Aβ1–42-treated mice, suggesting rhynchophylline as a potential agent against AD via Nrf2–ARE activation (Jiang et al., 2021).

## Isorhynchophylline

Isorhynchophylline is the steric isomer of rhynchophylline at spiro C7-position of the oxindole moiety. (Yuan et al., 2009). It showed similar inhibitory activity for NO production by LPS-activated rat primary cortical microglia (Yuan et al., 2008). However, in LPS-activated mouse N9 microglial cells, isorhynchophylline showed more potent inhibition of microglial activation. In addition, the modulatory mechanism in activated microglia showed a slight difference. Isorhynchophylline had a better effect on ERK phosphorylation and IκBα degradation, while isorhynchophylline was more potent in inhibiting p38 MAPK phosphorylation. The different data suggest that different microglial cells may show various sensitivities to the C-7 configuration of rhynchophylline (Yuan et al., 2009). Isorhynchophylline has been demonstrated to exert distinct anti-AD effects on several models of AD. Isorhynchophylline inhibited A*β*(25–35)-induced neurotoxicity in PC12 cells via inhibiting oxidative stress and suppressing the mitochondrial pathway of cellular apoptosis (Xian Y. F. et al., 2012). Further study demonstrated that the protective effects of isorhynchophylline against A*β*25–35-induced injury in PC12 cells were related to the enhancement of p-CREB expression via the PI3K/Akt/GSK-3*β* signaling pathway (Xian et al., 2013). In addition, isorhynchophylline administration ameliorated the cognitive deficits and neuronal apoptosis in the hippocampus induced by Aβ25-35 in the rats. Isorhynchophylline suppressed tau protein hyperphosphorylation at the Ser396, Ser404, and Thr205 sites. PI3K/Akt/GSK-3β signaling pathways are intimately involved in the neuroprotection of isorhynchophylline (Xian et al., 2014). In TgCRND8 mice, isorhynchophylline was proven to ameliorate cognitive deficits and amyloid pathology. Isorhynchophylline not only reduced the levels of Aβ40, Aβ42, and inflammatory factors but also modulated the amyloid precursor protein (APP) processing and phosphorylation by decreasing the level of β-site APP cleaving enzyme-1 (BACE-1) and increasing the level of insulin degrading enzyme (IDE), a major Aβ-degrading enzyme. It also inhibited the phosphorylation of tau at the sites of Thr205 and Ser396. Furthermore, isorhynchophylline markedly inhibited the Aβ-induced JNK signaling pathway in primary hippocampus neurons (Li et al., 2019). There was no difference in the extent of protection against the neuronal damage between rhynchophylline and isorhynchophylline treatment in *in vitro* ischemia-induced neuronal damage in the hippocampus (Kang et al., 2004). In addition, rhynchophylline has a noncompetitive antagonistic effect on the NMDA-type ionotropic glutamate receptor on *in vitro* ischemia-induced neuronal damage in the hippocampus in a receptor expression model of *Xenopus* oocytes (Kang et al., 2004).

## Prospects

In addition to alkaloids, other active compounds isolated from the *U. rhynchophylla* also showed potential neuroprotection in AD. Hirsuteine and four uncarialins, identified from *U. rhynchophylla*, showed distinct agonistic effects against the 5-HT1A receptor with the methods of molecular docking and site-directed amino acid mutation (Liang et al., 2019; Yu et al., 2021). BACE-1 is a type-1 membrane-anchored aspartyl protease, which is involved in the production of Aβ peptide species by cutting the amyloid precursor protein (APP) to release the C99 fragment for subsequent γ-secretase cleavage (Maia and Sousa, 2019). By phytochemicals using *in silico* drug discovery analysis, 3F061-dihydro-cadambine was testified as novel inhibitors against BACE-1 (Arif et al., 2020). Molecular docking and proteinF02Dligand interaction analysis displayed catechin in *U. rhynchophylla* as a potent inhibitor of acetylcholinesterase (AChE) for the treatment of AD (Chen et al., 2016). Uncarinic acid C was identified as a specific inhibitor of the nucleation phase of Aβ42 aggregation that is present in *U. rhynchophylla* (Yoshioka et al., 2016). All these evidences have proven the beneficial pharmacological effects of *U. rhynchophylla* in AD or PD, and further investigations that focus on the modifications of active compounds from *U. rhynchophylla* to promote the brain permeability might increase their bioavailability. In addition, chemical synthesis or modification based on these compounds may be a promising drug development strategy for the prevention or treatment of neurodegenerative diseases.

## Author contributions

LC: conceptualization, supervision, writing–original draft, and writing–review and editing. YL: writing–original draft and writing–review and editing. JX: writing–review and editing.

## Funding

The author(s) declare that financial support was received for the research, authorship, and/or publication of this article. This work was supported by grants from the National Natural Science Foundation of China (32170984; 32200802) and the Natural Science Foundation of Shandong Province (ZR2020YQ23).

## Conflict of interest

The authors declare that the research was conducted in the absence of any commercial or financial relationships that could be construed as a potential conflict of interest.

## Publisher's note



## References

Arif, N., Subhani, A., Hussain, W., and Rasool, N. (2020). In Silico inhibition of BACE-1 by selective phytochemicals as novel potential inhibitors: molecular docking and DFT studies. *Curr. Drug Discov. Technol.* 17, 397–411. doi:10.2174/1570163816666190214161825

Chen, L., Huang, Y., Yu, X., Lu, J., Jia, W., Song, J., et al. (2021). Corynoxine protects dopaminergic neurons through inducing autophagy and diminishing neuroinflammation in rotenone-induced animal models of Parkinson's disease. *Front. Pharmacol.* 12, 642900–642910. doi:10.3389/fphar.2021.642900

Chen, L. L., Song, J. X., Lu, J. H., Yuan, Z. W., Liu, L. F., Durairajan, S. S., et al. (2014). Corynoxine, a natural autophagy enhancer, promotes the clearance of alpha-synuclein via Akt/mTOR pathway. *J. Neuroimmune Pharmacol.* 9, 380–387. doi:10.1007/s11481-014-9528-2

Chen, L. L., Wang, Y. B., Song, J. X., Deng, W. K., Lu, J. H., Ma, L. L., et al. (2017). Phosphoproteome-based kinase activity profiling reveals the critical role of MAP2K2 and PLK1 in neuronal autophagy. *Autophagy* 13, 1969–1980. doi:10.1080/15548627.2017.1371393

Chen, L. L., and Xie, J. X. (2018). Identification of neuronal autophagy regulators: combined use of iKAP and THANATOS. *Mov. Disord.* 33, 580–581. doi:10.1002/mds.27354

Chen, Y.-X., Li, G.-Z., Zhang, B. I. N., Xia, Z.-Y., and Zhang, M. E. I. (2016). Molecular evaluation of herbal compounds as potent inhibitors of acetylcholinesterase for the treatment of Alzheimer's disease. *Mol. Med. Rep.* 14, 446–452. doi:10.3892/mmr.2016.5244

Fu, A. K. Y., Hung, K.-W., Huang, H., Gu, S., Shen, Y., Cheng, E. Y. L., et al. (2014). Blockade of EphA4 signaling ameliorates hippocampal synaptic dysfunctions in mouse models of Alzheimer's disease. *Proc. Natl. Acad. Sci.* 111, 9959–9964. doi:10.1073/pnas.1405803111

Fu, W.-Y., Hung, K.-W., Lau, S.-F., Butt, B., Yuen, V.W.-H., Fu, G., et al. (2021). Rhynchophylline administration ameliorates amyloid-β pathology and inflammation in an Alzheimer's disease transgenic mouse model. *ACS Chem. Neurosci.* 12, 4249–4256. doi:10.1021/acschemneuro.1c00600

Gan, L., Cookson, M. R., Petrucelli, L., and La Spada, A. R. (2018). Converging pathways in neurodegeneration, from genetics to mechanisms. *Nat. Neurosci.* 21, 1300–1309. doi:10.1038/s41593-018-0237-7

Guan, X. J., Deng, Z. Q., Liu, J., Su, C. F., Tong, B. C., Zhu, Z., et al. (2024). Corynoxine promotes TFEB/TFE3-mediated autophagy and alleviates Aβ pathology in Alzheimer's disease models. *Acta Pharmacol. Sin.* 45, 900–913. doi:10.1038/s41401-023-01197-1

Guo, Q., Ma, X., Wei, S., Qiu, D., Wilson, I. W., Wu, P., et al. (2014). *De novo* transcriptome sequencing and digital gene expression analysis predict biosynthetic pathway of rhynchophylline and isorhynchophylline from Uncaria rhynchophylla, a non-model plant with potent anti-alzheimer's properties. *BMC Genomics* 15, 676. doi:10.1186/1471-2164-15-676

Hou, G., Hu, W., Sang, Y., Gan, X., Xu, H., Hu, Q., et al. (2024). Corynoxine triggers cell death via activating PP2A and regulating AKT-mTOR/GSK3β axes in NSCLC. *Biochem. Pharmacol.* 222, 116110. doi:10.1016/j.bcp.2024.116110

Hu, S., Mak, S., Zuo, X., Li, H., Wang, Y., and Han, Y. (2018). Neuroprotection against MPP+-Induced cytotoxicity through the activation of PI3-K/Akt/GSK3β/MEF2D signaling pathway by rhynchophylline, the major tetracyclic oxindole alkaloid isolated from Uncaria rhynchophylla. *Front. Pharmacol.* 9, 768. doi:10.3389/fphar.2018.00768

Huang, H. C., Wang, C. F., Gu, J. F., Chen, J., Hou, X. F., Zhong, R. L., et al. (2017). Components of goutengsan in rat plasma by microdialysis sampling and its protection on Aβ1-42-induced PC12 cells injury. *Evid. Based Complement. Altern. Med.* 2017, 7593027. doi:10.1155/2017/7593027

Iyaswamy, A., Thakur, A., Guan, X. J., Krishnamoorthi, S., Fung, T. Y., Lu, K., et al. (2023). Fe65-engineered neuronal exosomes encapsulating corynoxine-B ameliorate cognition and pathology of Alzheimer's disease. *Signal Transduct. Target Ther.* 8, 404. doi:10.1038/s41392-023-01657-4

Jiang, P., Chen, L., Xu, J., Liu, W., Feng, F., and Qu, W. (2021). Neuroprotective effects of rhynchophylline against $A\beta_{1-42}$-induced oxidative stress, neurodegeneration, and memory impairment via Nrf2-ARE activation. *Neurochem. Res.* 46, 2439–2450. doi:10.1007/s11064-021-03343-9

Jiang, S., Borjigin, G., Sun, J., Li, Q., Wang, Q., Mu, Y., et al. (2023). Identification of Uncaria rhynchophylla in the potential treatment of Alzheimer's disease by integrating virtual screening and *in vitro* validation. *Int. J. Mol. Sci.* 24, 15457. doi:10.3390/ijms242015457

Jung, J. W., Ahn, N. Y., Oh, H. R., Lee, B. K., Lee, K. J., Kim, S. Y., et al. (2006). Anxiolytic effects of the aqueous extract of Uncaria rhynchophylla. *J. Ethnopharmacol.* 108, 193–197. doi:10.1016/j.jep.2006.05.019

Kang, T. H., Murakami, Y., Takayama, H., Kitajima, M., Aimi, N., Watanabe, H., et al. (2004). Protective effect of rhynchophylline and isorhynchophylline on *in vitro* ischemia-induced neuronal damage in the hippocampus: putative neurotransmitter receptors involved in their action. *Life Sci.* 76, 331–343. doi:10.1016/j.lfs.2004.08.012

Kim, S., Nam, Y., Shin, S. J., Prajapati, R., Shin, S. M., Kim, M.-J., et al. (2022). Dual modulators of aggregation and dissociation of amyloid beta and tau: *in vitro*, *in vivo*, and *in silico* studies of Uncaria rhynchophylla and its bioactive components. *Biomed. Pharmacother.* 156, 113865. doi:10.1016/j.biopha.2022.113865

Li, H. Q., Ip, S. P., Yuan, Q. J., Zheng, G. Q., Tsim, K. K. W., Dong, T. T. X., et al. (2019). Isorhynchophylline ameliorates cognitive impairment via modulating amyloid pathology, tau hyperphosphorylation and neuroinflammation: studies in a transgenic mouse model of Alzheimer's disease. *Brain Behav. Immun.* 82, 264–278. doi:10.1016/j.bbi.2019.08.194

Liang, J.-H., Luan, Z.-L., Tian, X.-G., Zhao, W.-Y., Wang, Y.-L., Sun, C.-P., et al. (2019). Uncarialins A–I, monoterpenoid indole alkaloids from Uncaria rhynchophylla as natural agonists of the 5-HT1A receptor. *J. Nat. Prod.* 82, 3302–3310. doi:10.1021/acs.jnatprod.9b00532

Liang, X. X., Yang, J. X., Li, J. M., Huang, J. B., Yang, L. M., Sun, T. T., et al. (2023). A pair of new oxindole alkaloids isolated from Uncaria macrophylla. *Nat. Prod. Res.* 37, 1258–1264. doi:10.1080/14786419.2021.2000982

Lin, H., Xie, L., Lv, L., Chen, J., Feng, F., Liu, W., et al. (2023). Intranasally administered thermosensitive gel for brain-targeted delivery of rhynchophylline to treat Parkinson's disease. *Colloids Surfaces B Biointerfaces* 222, 113065. doi:10.1016/j.colsurfb.2022.113065

Lu, J. H., Tan, J. Q., Durairajan, S. S., Liu, L. F., Zhang, Z. H., Ma, L., et al. (2012). Isorhynchophylline, a natural alkaloid, promotes the degradation of alpha-synuclein in neuronal cells via inducing autophagy. *Autophagy* 8, 98–108. doi:10.4161/auto.8.1.18313

Lu, Y., Gao, X., Mohammed, S. a.D., Wang, T., Fu, J., Wang, Y., et al. (2024). Efficacy and mechanism study of Baichanting compound, a combination of Acanthopanax senticosus (Rupr. and Maxim.) Harms, Paeonia lactiflora Pall and Uncaria rhynchophylla (Miq.) Miq. ex Havil, on Parkinson's disease based on metagenomics and metabolomics. *J. Ethnopharmacol.* 319, 117182. doi:10.1016/j.jep.2023.117182

Maia, M., and Sousa, E. (2019). BACE-1 and γ-secretase as therapeutic targets for Alzheimer's disease. *Pharmaceuticals* 12, 41. doi:10.3390/ph12010041

Ndagijimana, A., Wang, X., Pan, G., Zhang, F., Feng, H., and Olaleye, O. (2013). A review on indole alkaloids isolated from Uncaria rhynchophylla and their pharmacological studies. *Fitoterapia* 86, 35–47. doi:10.1016/j.fitote.2013.01.018

Peng, C., Trojanowski, J. Q., and Lee, V. M. Y. (2020). Protein transmission in neurodegenerative disease. *Nat. Rev. Neurol.* 16, 199–212. doi:10.1038/s41582-020-0333-7

Shin, S. J., Jeong, Y., Jeon, S. G., Kim, S., Lee, S. K., Choi, H. S., et al. (2018). Uncaria rhynchophylla ameliorates amyloid beta deposition and amyloid beta-mediated pathology in 5XFAD mice. *Neurochem. Int.* 121, 114–124. doi:10.1016/j.neuint.2018.10.003

Song, J. X., Lu, J. H., Liu, L. F., Chen, L. L., Durairajan, S. S., Yue, Z., et al. (2014). HMGB1 is involved in autophagy inhibition caused by SNCA/α-synuclein overexpression: a process modulated by the natural autophagy inducer corynoxine B. *Autophagy* 10, 144–154. doi:10.4161/auto.26751

Song, Y., Qu, R., Zhu, S., Zhang, R., and Ma, S. (2012). Rhynchophylline attenuates LPS-induced pro-inflammatory responses through down-regulation of MAPK/NF-κB signaling pathways in primary microglia. *Phytotherapy Res.* 26, 1528–1533. doi:10.1002/ptr.4614

Tognolini, M., Incerti, M., and Lodola, A. (2014). Are we using the right pharmacological tools to target EphA4? *ACS Chem. Neurosci.* 5, 1146–1147. doi:10.1021/cn500285h

Wen, C., Ruan, Q., Li, Z., Zhou, X., Yang, X., Xu, P., et al. (2022). Corynoxine suppresses pancreatic cancer growth primarily via ROS-p38 mediated cytostatic effects. *Br. J. Cancer* 127, 2108–2117. doi:10.1038/s41416-022-02002-2

Xian, Y. F., Lin, Z. X., Mao, Q. Q., Chen, J. N., Su, Z. R., Lai, X. P., et al. (2013). Isorhynchophylline protects PC12 cells against beta-amyloid-induced apoptosis via PI3K/Akt signaling pathway. *Evid. Based Complement. Altern. Med.* 2013, 163057. doi:10.1155/2013/163057

Xian, Y.-F., Lin, Z.-X., Mao, Q.-Q., Hu, Z., Zhao, M., Che, C.-T., et al. (2012a). Bioassay-guided isolation of neuroprotective compounds fromUncaria rhynchophyllaagainst beta-amyloid-induced neurotoxicity. *Evidence-Based Complementary Altern. Med.* 2012, 802625–802628. doi:10.1155/2012/802625

Xian, Y. F., Lin, Z. X., Mao, Q. Q., Ip, S. P., Su, Z. R., and Lai, X. P. (2012b). Protective effect of isorhynchophylline against β-amyloid-induced neurotoxicity in PC12 cells. *Cell Mol. Neurobiol.* 32, 353–360. doi:10.1007/s10571-011-9763-5

Xian, Y. F., Mao, Q. Q., Wu, J. C., Su, Z. R., Chen, J. N., Lai, X. P., et al. (2014). Isorhynchophylline treatment improves the amyloid-β-induced cognitive impairment in rats via inhibition of neuronal apoptosis and tau protein hyperphosphorylation. *J. Alzheimers Dis.* 39, 331–346. doi:10.3233/JAD-131457

Xu, R., Wang, J., Xu, J., Song, X., Huang, H., Feng, Y., et al. (2020). Rhynchophylline loaded-mPEG-PLGA nanoparticles coated with tween-80 for preliminary study in alzheimer's disease. *Int. J. Nanomedicine* 15, 1149–1160. doi:10.2147/IJN.S236922

Yan, D., Ma, Z., Liu, C., Wang, C., Deng, Y., Liu, W., et al. (2019). Corynoxine B ameliorates HMGB1-dependent autophagy dysfunction during manganese exposure in SH-SY5Y human neuroblastoma cells. *Food Chem. Toxicol.* 124, 336–348. doi:10.1016/j.fct.2018.12.027

Yang, S.-Y., Lin, Z.-X., Xian, Y.-F., Zhang, H.-M., and Xu, H.-X. (2023). Traditional uses, chemical compounds, pharmacological activities and clinical studies on the traditional Chinese prescription Yi-Gan San. *J. Ethnopharmacol.* 302, 115859. doi:10.1016/j.jep.2022.115859

Yang, W., Ip, S.-P., Liu, L., Xian, Y.-F., and Lin, Z.-X. (2020). Uncaria rhynchophylla and its major constituents on central nervous system: a review on their pharmacological actions. *Curr. Vasc. Pharmacol.* 18, 346–357. doi:10.2174/1570161117666190704092841

Yoshioka, T., Murakami, K., Ido, K., Hanaki, M., Yamaguchi, K., Midorikawa, S., et al. (2016). Semisynthesis and structure-activity studies of uncarinic acid C isolated from Uncaria rhynchophylla as a specific inhibitor of the nucleation phase in amyloid β42 aggregation. *J. Nat. Prod.* 79, 2521–2529. doi:10.1021/acs.jnatprod.6b00392

Yu, Z. L., Bai, R., Zhou, J. J., Huang, H. L., Zhao, W. Y., Huo, X. K., et al. (2021). Uncarialins J—M from *Uncaria rhynchophylla* and their anti-depression mechanism in unpredictable chronic mild stress-induced mice *via* activating 5-HT1A receptor. *Chin. J. Chem.* 39, 1331–1343. doi:10.1002/cjoc.202000652

Yuan, D., Ma, B., Wu, C., Yang, J., Zhang, L., Liu, S., et al. (2008). Alkaloids from the leaves of Uncaria rhynchophylla and their inhibitory activity on NO production in lipopolysaccharide-activated microglia. *J. Nat. Prod.* 71, 1271–1274. doi:10.1021/np8000305

Yuan, D., Ma, B., Yang, J.-Y., Xie, Y.-Y., Wang, L., Zhang, L.-J., et al. (2009). Anti-inflammatory effects of rhynchophylline and isorhynchophylline in mouse N9 microglial cells and the molecular mechanism. *Int. Immunopharmacol.* 9, 1549–1554. doi:10.1016/j.intimp.2009.09.010

Zeng, P., Wang, X.-M., Ye, C.-Y., Su, H.-F., and Tian, Q. (2021). The main alkaloids in Uncaria rhynchophylla and their anti-alzheimer's disease mechanism determined by a network pharmacology approach. *Int. J. Mol. Sci.* 22, 3612. doi:10.3390/ijms22073612

Zhang, C., Xue, Z., Zhu, L., Zhou, J., Zhuo, L., Zhang, J., et al. (2023). Rhynchophylline alleviates neuroinflammation and regulates metabolic disorders in a mouse model of Parkinson's disease. *Food and Funct.* 14, 3208–3219. doi:10.1039/d2fo02939a

Zhang, Q., Zhao, J. J., Xu, J., Feng, F., and Qu, W. (2015). Medicinal uses, phytochemistry and pharmacology of the genus Uncaria. *J. Ethnopharmacol.* 173, 48–80. doi:10.1016/j.jep.2015.06.011

Zhang, Z., Zhang, W., Kang, F., Ip, F. C. F., Ip, N. Y., and Tong, R. (2019). Asymmetric total syntheses of rhynchophylline and isorhynchophylline. *J. Org. Chem.* 84, 11359–11365. doi:10.1021/acs.joc.9b01977

Zhu, Q., Song, J., Chen, J. Y., Yuan, Z., Liu, L., Xie, L. M., et al. (2023). Corynoxine B targets at HMGB1/2 to enhance autophagy for α-synuclein clearance in fly and rodent models of Parkinson's disease. *Acta Pharm. Sin. B* 13, 2701–2714. doi:10.1016/j.apsb.2023.03.011

Zhu, Z., Liu, L. F., Su, C. F., Liu, J., Tong, B. C., Iyaswamy, A., et al. (2022). Corynoxine B derivative CB6 prevents Parkinsonian toxicity in mice by inducing PIK3C3 complex-dependent autophagy. *Acta Pharmacol. Sin.* 43, 2511–2526. doi:10.1038/s41401-022-00871-0

frontiers | Frontiers in Pharmacology

TYPE Original Research
PUBLISHED 26 August 2024
DOI 10.3389/fphar.2024.1439811



OPEN ACCESS

EDITED BY
Qi Liang,
Air Force Medical University, China

REVIEWED BY
Smith B. Babiaka,
University of Tuebingen, Germany
Gwladys Temkou Ngoupaye,
University of Dschang, Cameroon

*CORRESPONDENCE
Gustavo Provensi,
gustavo.provensi@unifi.it

†These authors have contributed equally to this work

RECEIVED 28 May 2024
ACCEPTED 12 August 2024
PUBLISHED 26 August 2024

CITATION
Costa A, Micheli L, Sordi V, Ciampi C, Lucci J, Passani MB and Provensi G (2024) Preventing social defeat stress-induced behavioural and neurochemical alterations by repeated treatment with a mix of *Centella asiatica*, *Echinacea purpurea* and *Zingiber officinale* standardized extracts.
*Front. Pharmacol.* 15:1439811.
doi: 10.3389/fphar.2024.1439811



# Preventing social defeat stress-induced behavioural and neurochemical alterations by repeated treatment with a mix of *Centella asiatica*, *Echinacea purpurea* and *Zingiber officinale* standardized extracts

Alessia Costa[1†], Laura Micheli[1†], Virginia Sordi[1,2], Clara Ciampi[1], Jacopo Lucci[3,4], Maria Beatrice Passani[5] and Gustavo Provensi[1*]

[1]Section of Pharmacology and Toxicology, Department of Neuroscience, Psychology, Drug Research and Child Health (NEUROFARBA), University of Florence, Florence, Italy, [2]Pharmacology Unit, School of Pharmacy, University of Camerino, Camerino, Italy, [3]Bios-Therapy, Physiological Systems for Health S.p.A., Sansepolcro, Italy, [4]Aboca S.p.A. Società Agricola, Innovation and Medical Science Division, Sansepolcro, Italy, [5]Department of Health Sciences (DSS), University of Florence, Florence, Italy

**Background:** Prolonged exposure to stress is a risk factor for the onset of several disorders. Modern life is burdened by a pervasive prevalence of stress, which represents a major societal challenge requiring new therapeutic strategies. In this context, botanical drug-based therapies can have a paramount importance.

**Methods:** Here we studied the preventive effects of a repeated treatment (p.o. daily, 3 weeks) with a combination of Centella asiatica (200 mg/kg), Echinacea purpurea (20 mg/kg) and Zingiber officinale (150 mg/kg) standardized extracts, on the chronic social defeat stress (CSDS) deleterious outcomes. After 10 days of CSDS exposure, male mice' performances were evaluated in paradigms relevant for social (social interaction test), emotional (tail suspension test), cognitive (novel object recognition) domains as well as for pain perception (cold plate and von Frey tests) and motor skills (rotarod). Mice were then sacrificed, the spinal cords, hippocampi and frontal cortices dissected and processed for RT-PCR analysis.

**Results:** Extracts mix treatment prevented stress-induced social aversion, memory impairment, mechanical and thermal allodynia and reduced behavioural despair independently of stress exposure. The treatment stimulated hippocampal and cortical BDNF and TrkB mRNA levels and counteracted stress-induced alterations in pro- (TNF-α, IL-1β and IL-6) and anti-inflammatory (IL4, IL10) cytokines expression in the same areas. It also modulated expression of pain related genes (GFAP and Slc1a3) in the spinal cord.

**Conclusion:** The treatment with the extracts mix obtained from *C. asiatica*, *E. purpurea* and *Z. officinale* may represent a promising strategy to promote resilience and prevent the deleterious effects induced by extended exposure to psychosocial stress.

KEYWORDS

**chronic social defeat stress, botanical drugs, cognition, pain, neuroinflammation, neurotrophins**

# 1 Introduction

Stress can be defined as a process in which environmental demands strain an organism's adaptive capacity (Cohen et al., 2016). Prolonged exposure to stress leads to a constellation of physiological, endocrine, immunological and behavioural alterations representing a major risk factor for the onset of several diseases, in particular psychiatric disorders such as anxiety and depression (Godoy et al., 2018). Modern day life is burdened by an insidious increasing prevalence of psychological stress, representing a major pervasive societal challenge that urgently requires new therapeutic strategies. Promoting resilience to stress may prevent the development of stress-induced psychiatric disorders, and in this context, therapies based on natural products may acquire paramount importance since they are perceived by the patients as safer alternatives to classical pharmacotherapy (Yeung et al., 2018). Many medicinal plants have long been used in folk medicine for treating central nervous system-related pathologies. The effects of a broad range of plants have been confirmed in animal models and for some of them also in clinical trials (Moragrega and Ríos, 2021; Moragrega and Ríos, 2022). Medicinal plants can offer a valid approach to tackling stress-related disorders since they are characterized by a complex mixture of bioactive metabolites which can antagonize the multifactorial and intricate mechanisms of the disease (Colalto, 2018). *Centella asiatica, Echinacea purpurea* and *Zingiber officinale* are plants rich in bioactive molecules with multiple pharmacological effects.

*Centella asiatica* is a plant traditionally used in Ayurvedic medicine as sedative and anxiolytic (Zhang, 2004). Pharmacological studies confirmed such effects (Chanana and Kumar, 2016) and revealed new ones such as anti-hyperalgesic properties in a rat model of osteoarthritis (Micheli et al., 2020b), and procognitive actions (Sbrini et al., 2020). The most conspicuous group of bioactive metabolites isolated from *C. asiatica,* are the triterpenoids, including madecassoside, asiaticoside, asiatic acid and madecassic acid (Mando et al., 2024). *Echinacea* species are medicinal plants of the Asteraceae family native from United States, Canada, Russia and Australia among which *E. purpurea* is one of best known and used from a medical point of view (Burlou-Nagy et al., 2022). This species is considered a valid source of anti-inflammatory metabolites particularly active to boost the immune system (Li et al., 2020; Sharifi-Rad et al., 2018). *Echinacea purpurea* is traditionally used as pain reliever. Recent pharmacological studies confirmed its analgesic properties, which are related to the presence of alkamides, caffeic acid derivatives and polysaccharides (Barnes et al., 2005; Micheli et al., 2023). Among the botanical drugs with potential neuroprotective and anti-inflammatory properties, much attention has been focused on extracts obtained from the Zingiberaceae family. Pharmacologically speaking, *Z. officinale* extracts, rich in gingerols, paradols, and shogaols, shares similarities with non-steroidal anti-inflammatory drugs in inhibiting the activity of cyclooxygenase-2 (COX-2) and lipoxygenase (LOX) enzymes and prostaglandin synthesis (Grzanna et al., 2005). Consistently, the capacity of *Z. officinale* extracts of reducing the production of inflammatory mediators, such as IL-1β, and TNF-α, were demonstrated in *in vitro* (Shen et al., 2003; Shen et al., 2005) and *in vivo* models (Oliveira et al., 2019; Micheli et al., 2022). Several studies evidenced ginger extracts-induced neuroprotective effects, that seem to be related to their anti-oxidative and anti-inflammatory properties as well as to the upregulation of neurotrophins (ALmohaimeed et al., 2021).

We recently reported the beneficial effects of a treatment with the standardized extracts mix obtained from *C. asiatica, E. purpurea* and *Z. officinale* in a model of lipopolysaccharide (LPS)-induced neuroinflammation in mice (Micheli et al., 2022). Here we aimed to expand these observations by assessing the efficacy of the chronic treatment with the same mix of extracts in preventing the alterations induced by chronic social defeat stress (CSDS) in adult mice. This procedure induces behavioural and neurochemical alterations characterized by social avoidance, memory impairment (Golden et al., 2011; Costa et al., 2022), immune system responses in the brain (Hodes et al., 2014; Shimo et al., 2023), impaired blood brain barrier integrity (Dudek et al., 2020) and may affect pain perception, as reviewed in (Vachon-Presseau, 2018). A series of tests were therefore performed to evaluate the efficacy of extracts mix to prevent CSDS-related behavioural outcomes, along with *ex vivo* assessment of neurotrophins, pro- and anti-inflammatory cytokines and blood-brain barrier integrity markers expression at the transcriptional level in the spinal cord, hippocampus and prefrontal cortex.

# 2 Materials and methods

## 2.1 Animals

Adult male C57bl/6 (20–25 g, 8–9 weeks old, *intruders*) and CD1 mice (35–45 g, 10–13 weeks old, *residents*) purchased from Charles River Laboratories (Milan, Italy) were used in this study. These strains are the most commonly *intruder/submissive:resident/aggressive* pair used in CSDS protocols (Golden et al., 2011). They were housed at the animal facility of the Centro di Servizi per la Stabulazione di Animali da Laboratorio (CeSAL) of the University of Florence, in humidity and temperature-controlled rooms (22°C ± 2°C) with free access to food (4RF21; Mucedola s.r.l., Italy) and water, and kept on a 12-h light/dark cycle (lights start at 8:00 a.m.).

After arrival, animals were allowed 1 week to acclimatize to the housing conditions and human contact before the beginning of the experiments. All the experiments were performed between 9:00 a.m. and 2:00 p.m.

Housing and experimental procedures were conducted in accordance with the Council Directive of the European Community (2010/63/EU) and the Italian Decreto Legislativo 26 (13/03/2014) regarding the protection of animals used for scientific purposes, approved by the Animal Care Committee of the University of Florence and Italian Ministry of Health (678-2021-PR prot. 17E9C.235) and supervised by a veterinarian. Every effort was made to minimize animal suffering and to reduce the number of animals used, complying with the 3R principle. Male mice were used to reduce within-group variability due to hormonal fluctuations during oestrous cycle in female mice.

## 2.2 Plant material, extracts preparation and standardization

The following botanical drugs were used in this study: *C. asiatica* (L.) Urb [Apiaceae, *C. asiatica* (L.). Urb., herba], *E. purpurea* (L.) Moench (Asteraceae, *Echinaceae purpureae herba*) and *Z. officinale* Roescoe (Zingiberaceae; *Zingiber officinale* Roscoe, rhizome). The botanical indentification, extracts production and quantification of main metabolites were performed at Aboca S.p.A. (Sansepolcro, Italy). The extracts were prepared following the protocols described previously (Micheli et al., 2020b; Micheli et al., 2022). The preparation and characterization of the extracts studied in our manuscript fulfill all the requirements established by the Consensus-based reporting guidelines for Phytochemical Characterisation of Medicinal Plant extracts (ConPhyMP) (see Supplementary Tables). Briefly, dried *Z. officinale* rhizoma was subjected to extraction by using 30% ethanol (ethanol: water, 30: 70 v/v) for 8 h at 50°C and filtered to remove solid exhausted material. The resulting clarified extract was concentrated by ethanol evaporation under vacuum, until reaching the concentration ratio of 10:1 (v:v, initial alcoholic extract volume compared to the volume after the evaporation step), and then freeze-dried for 72 h. Final drug-extract ratio (DER) = 10.85. Dried flowering tops of *E. purpurea* were subjected to extraction by using 45% ethanol (ethanol: water, 45:55 v/v) for 8 h at 50°C and filtered to remove solid exhausted material. The resulting clarified extract was concentrated by ethanol evaporation under vacuum, until reaching the concentration ratio of 8:1 (v:v, initial volume of alcoholic extract compared to the volume after evaporation step), and then freeze-dried for 72 h. DER = 6.3. Dried *C. asiatica* leaves were subjected to extraction with ethanol 70% (ethanol:water 70: 30 v/v) for 8 h at 50°C and filtered to remove solid exhausted material. The resulting clarified extract was concentrated by ethanol evaporation under vacuum, until reaching the concentration ratio of 7:1 (v:v, initial alcoholic extract volume compared to the volume after the evaporation step), then freeze-dried for 72 h. DER = 4.3. The resulting extracts were stored at 4°C until use, away from light and humidity. The characterization of all extracts was also performed by Aboca S.p.A. following the USP Pharmacopoeia Monographies using different previously reported chromatographic methods (Micheli et al., 2020b; Micheli et al., 2022). *Centella asiatica* extract: Triterpenes, total, 5.01% (Asiatic Acid, 0.09%; Madecassic Acid, 0.66%; Asiaticoside, 1.96%, Madecassoside, 2.30%); *E. purpurea* extract: Phenols, total 5.95% (Chlorogenic acid 0.04%, Caftaric acid, 2.08%, Cicoric acid 3.83%); *Z.officinale* extract: Gingerols, totals 3.107% (6-Gingerol, 2.539%; 8-Gingerol 0.339%, 10-Gingerol 0.229%), Shogaols, totals, 0.647%.

## 2.3 Treatments

The combination of extracts obtained from *C. asiatica* (200 mg/kg), *E. purpurea* (20 mg/kg) and *Z. officinale* (150 mg/kg) were suspended in 1% carboxymethylcellulose sodium salt (CMC; Sigma-Aldrich, Milan, Italy) and orally administered (by gavage) once daily. The doses were chosen based on our previous study reporting their efficacy in an LPS-induced neuroinflammation mouse model (Micheli et al., 2022). To evaluate a potential preventive effect induced by extracts mix, treatments started 21 days before stress exposure and lasted until the end of behavioural experiments on day 37. Control animals received an equal volume of vehicle. Both vehicle and extracts solutions were freshly prepared on each test day and administered during the light-phase (between 4:00 and 6:00 p.m.) to avoid confounding factors regarding putative acute effects on the behavioural tests (performed between 9:00 a.m. and 2:00 p.m.).

## 2.4 Experimental design

C57BL/6J experimental mice were randomly assigned to the following experimental groups (6–8 animals by group): a control group of non-stressed animals treated with vehicle (NS-Vehicle), a group of non-stressed animals treated with the extracts mix (NS-Extracts Mix), a group of stressed mice treated with vehicle (CSDS-Vehicle) and finally, a group of stressed animals receiving the extracts mix daily (CSDS-Extracts Mix). CSDS procedure started on the 21st day of treatment and lasted for 10 days. To evaluate CSDS-related outcomes, animals' behavioural repertoire was assessed using a battery of tests comprehensive of several domains potentially affected by stress. Behavioural assessment was conducted from day 31 to 37. The tasks were performed in separated days, starting with the least stressful/invasive procedure, in the following sequence: social interaction test, open field, novel object recognition, rotarod, von Frey test, cold plate test and tail suspension test. Twenty-four hours after the last behavioural test, animals were sacrificed, and the tissues were collected and stored at −80°C for the *ex vivo* analyses. An overview of the experimental design is shown in Figure 1.

## 2.5 Chronic social defeat stress (CSDS)

The CSDS paradigm was performed as previously described (Rani et al., 2021; Costa et al., 2022). Prior to the experiments, CD1 mice were singly housed and screened for aggressive behaviour according to (Golden et al., 2011). Only those reaching the criterion, defined by demonstrating at least one successful act of aggression during two consecutive days toward another CD1 intruder mouse, were selected

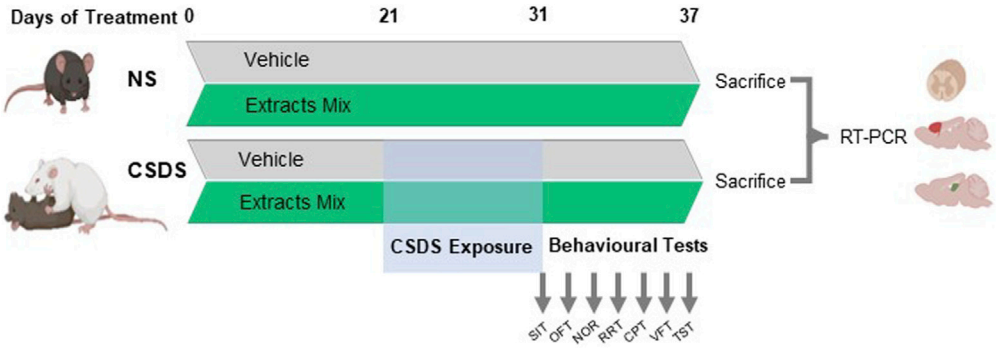


FIGURE 1
Experimental timeline. C57BL/6 mice were treated with vehicle or the combination of extracts obtained from *Centella asiatica* (200 mg/kg, p.o.), *Echinacea purpurea* (20 mg/kg, p.o.) and *Zingiber officinale* (150 mg/kg, p.o.) once daily. After 21 days of treatment, mice were submitted to a 10-days chronic social defeat stress protocol (CSDS). Immediately after the end of stress exposure, animals' behaviour was evaluated using a battery of tests in the following order: social interaction test (SIT), open field (OFT), novel object recognition (NOR), rotarod test (RRT), cold plate test (CPT), von Frey test (VFT) and tail suspension test (TST). The day following the last test, animals were sacrificed, the spinal cord, hippocampi and frontal cortices were dissected and processed for gene expression analysis at transcriptional level by real-time polymerase chain reaction (RT-PCR).

as aggressive-residents and used in the CSDS paradigm. C57BL/6 mice randomly allocated to the experimental stressed groups were singly housed for 4 days prior to the stress exposure. Briefly, the CSDS procedure consisted in the introduction of an experimental C57BL/6 mouse in the home cage of a CD1 aggressor until the occurrence of an aggression. Mice were then separated by a transparent, perforated Plexiglas separator wall allowing visual and olfactory exposure for 2 h. After that the separator was removed, allowing a second attack occurring within 1 min. The procedure was repeated daily for 10 consecutive days (days 21–30), at different timing during the day and changing the CD1 aggressor every day to avoid habituation. The stress protocol included overcrowding sessions that consisted of 8 experimental mice placed together in a standard holding cage (33 cm × 15 cm × 13 cm) for 24 h (days 23–24, 28–29) with diet and water available *ad libitum*. Non-stressed mice were left undisturbed in their home cages housed with other non-stressed mice (four mice per cage) being manipulated only for gavage treatment and body-weight measurement.

## 2.6 Social interaction test (SIT)

SITs were conducted 24 h after the last social defeat session, in an acrylic Plexiglass arena (41 cm × 32 cm x 40 cm) adopting the protocol described in (Golden et al., 2011; Rani et al., 2021; Costa et al., 2022). The SIT protocol is articulated in two sessions: target absent (−) and target present (+) lasting 150s each, with an inter-trial interval of 60s between sessions. In the first session (−) C57BL/6 subject mice were gently placed in the centre of the arena containing an empty wire-mesh box (7.5 cm length, 9.5 cm width) and left free to explore. During the second session (+) C57BL/6 mice were placed in the same arena, this time with a CD1 aggressive mouse inside a wire-mesh container and were again allowed to explore freely. During the inter-trial interval, experimental C57BL/6 mice were placed back in their home-cages. After each session, the arena and the box were cleaned with an ethanol solution (30% v/v) to prevent odour/taste bias. The trials were videotaped, and the time C57BL/6 mice spent in the interaction zone (5 cm around the wire mesh cage) actively exploring the box, was recorded offline by an experienced observer blinded to the experimental groups assignment. Exploration was defined as sniffing or touching the cage with the nose and/or forepaws. A social interaction index was calculated as the ratio between the time spent in the interaction zone during − and + sessions, following the equation:

$$\textit{Social Interaction Ratio (SI ratio)} = \frac{\textit{time exploring SI zone during + session } (t+)}{\textit{time exploring SI zone during − session } (t-)}$$

## 2.7 Open field test (OFT)

Mice locomotor activity was assessed in an open field arena (44 × 44 × 30 cm) constructed in grey Plexiglass. Each C57BL/6 mouse was placed in the centre of the arena and allowed to freely explore it for 10 min. The arena was cleaned with a solution of 30% ethanol (v/v) between trials to remove possible scent cues left by the animals. The experiments were recorded with a camera located on the ceiling above the arena. Using the ANY-Maze (version 7.13, SoeltingCo®) video tracking system software a virtual zone (22 cm × 22 cm) was delimited in the centre of the arena and the distance travelled by each animal in either central and peripheral zones were registered (Rani et al., 2021; Costa et al., 2022).

## 2.8 Novel object recognition test (NOR)

The NOR was performed following the detailed experimental procedure previously published (Rani et al., 2021; Costa et al., 2022; Provensi et al., 2022). The protocol involved three sessions: habituation, acquisition and retention test. Habituation consisted of a 10 min session where the animals were left to freely explore the empty arena (44 cm × 44 cm × 30 cm) constructed in grey Plexiglass. Twenty-four hours later, each C57BL/6 mouse was placed in the same position facing the same direction into the test arena in the presence of two identical objects (plastic shapes such as cubes, cylinders or pyramids 8 cm high) and allowed to explore it for 5 min. To evaluate the impact of stress and

treatments on short-term memory, the retention test session was performed 1 h later. During this session, mice were again placed in the test arena for 5 min in the presence of one familiar object and a novel one. The position of the new object (left/right) was randomized to prevent bias from order or place preference. Animals' behaviour during all sessions was videotaped and the time spent actively exploring each object was recorded by an experienced researcher unaware of the experimental groups. Exploration was defined as sniffing or touching the objects with the nose and/or forepaws. Sitting on or turning around the objects was not considered exploratory behaviour. Each animal was subjected to the procedure separately and care was taken to remove any olfactory/taste cues by cleaning carefully the arena and test objects between trials with an ethanol solution (30% v/v). Mice were placed in their home cages between trials. The final data is expressed as the percentage of time exploring the familiar and new objects during the retention test. The raw exploration data at the retention test was also used to calculate individual discrimination indexes (DIs) according to the follow equation:

$$Discrimination\ Index\ (DI) = \frac{time\ es ploring\ novel\ (tN) - time\ ex ploring\ f amiliar\ (tF)}{total\ ex ploration\ time\ (tN + tF)}$$

## 2.9 Tail suspension test (TST)

The TST, which is widely used to assess drug-induced antidepressant-like effects, was carried out as previously described (Munari et al., 2015; Costa et al., 2018). Briefly, each C57BL/6 mouse was suspended by the tail to a horizontal bar at approximately 30 cm above the floor using adhesive tape (approximately 2 cm from the tip of the tail) for 6 min. The sessions were videotaped and analysed by an experimenter unaware of the experimental groups. The parameter recorded was the number of seconds animals spent immobile during the last 4 min of each session. Mice were considered immobile only when they hung passively and completely motionless.

## 2.10 Cold plate test

Thermal allodynia was assessed using the cold plate test (Ugo Basile, Varese, Italy). With minimal animal–handler interaction, mice were taken from home cages and placed onto the surface of the cold plate maintained at a constant temperature of 4°C ± 1°C. Ambulation was restricted by a cylindrical Plexiglas chamber (diameter, 10 cm; height, 15 cm) with an open top. A timer controlled by a foot peddle was used to monitor timing response latency from the moment the mouse was placed onto the cold plate. Pain-related behaviour (licking of the hind paw) was observed, and the time (seconds) of the first sign was recorded. The cutoff time of paw lifting or licking latency was set at 30 s (Micheli et al., 2022; Micheli et al., 2020a).

## 2.11 von Frey test

An electronic von Frey hair unit (Ugo Basile, Varese, Italy) was used to test mechanical allodynia. The animals were placed in 20 cm × 20 cm Plexiglas boxes equipped with a metallic mesh floor, 20 cm above the bench. A habituation of 15 min was allowed before the test. The withdrawal threshold was evaluated by applying force ranging from 0 to 5 g with a 0.2 g accuracy. Punctuate stimulus was applied to the mid-plantar area of each anterior paw from below the meshy floor through a plastic tip, and the withdrawal threshold was automatically displayed on the screen. The paw sensitivity threshold was defined as the minimum pressure required to elicit a robust and immediate withdrawal reflex of the paw. Voluntary movements associated with locomotion were not taken as a withdrawal response. Stimuli were applied on each anterior paw with an interval of 5 s. The measurement was repeated five times, and the final value was obtained by averaging the five measures (Micheli et al., 2022; Micheli et al., 2021).

## 2.12 Rotarod test

The apparatus consisted of a base platform and a rotating rod with a diameter of 3 cm and a non-slippery surface. The rod was placed at a height of 15 cm from the base. The rod, 30 cm in length, was divided into five equal sections by six disks. Thus, up to five mice were tested simultaneously on the apparatus, with the rotating speed of the rod at 16 revolutions per minute. The integrity of motor coordination was assessed based on the number of falls from the rod in 10 min (Micheli et al., 2022).

## 2.13 Real-time PCR of gene expression in the spinal cord, hippocampus and frontal cortex

The hippocampi, frontal cortices and thoracic portions of the spinal cord were rapidly removed and stored at −80°C. RNA was extracted using TRIzol reagent (Invitrogen, Life Technologies™ Italia). RNA concentrations were determined using a Nanodrop ND-1000 (Labtech, Inc.). cDNA was synthesized with Reliance Select cDNA Synthesis Kit (Bio-Rad Laboratories, Inc.) according to the manufacturer's instructions. Briefly, 1 µg of total RNA mixed with DNase Buffer and DNase (both from Bio-Rad Laboratories, Inc.) was incubated at 25°C for 5 min and at 75°C for 5 min 4 µL Reliance Buffer, 2 µL Random Primer mix and 1 µL of Reliance Reverse Trascriptase were added to each sample and incubated at 50°C for 20 min and at 95°C for 1 min. All RNA samples were synchronously reverse transcribed to minimize interassay variations related to the reverse transcription reaction.

RT-PCR was performed using SsoAdvanced Universal SYBR® Green Supermix (Bio-Rad Laboratories, Inc.) following the default thermocycler program: 2 min of preincubation at 95°C followed by 40 cycles for 5 s at 95°C, 30 s at 60°C and 5 s/step at 65°C–95°C with a 0.5°C increments. RT-PCR reactions were carried out in 10 µL volumes in a 96-well plate (Applied Biosystems™, London, United Kingdom) containing 2 µL RNAse-free water, 1 µL of primer (Bio-Rad Laboratories, Inc.), and 5 µL Universal SYBR® Green Supermix (Bio-Rad Laboratories, Inc.) plus 2 µL of cDNA sample (10 ng/µL).

The following validated primers purchased from Bio-Rad Laboratories, Inc., were used to detect *Bdnf* (qMmuCED0050333), *Ntrk2* (qMmuCID0016820), *Tnf* (qMmuCED0004141), *Il1b* (qMmuCID0005641), *Il6* (qMmuCID0005613), *Il4*

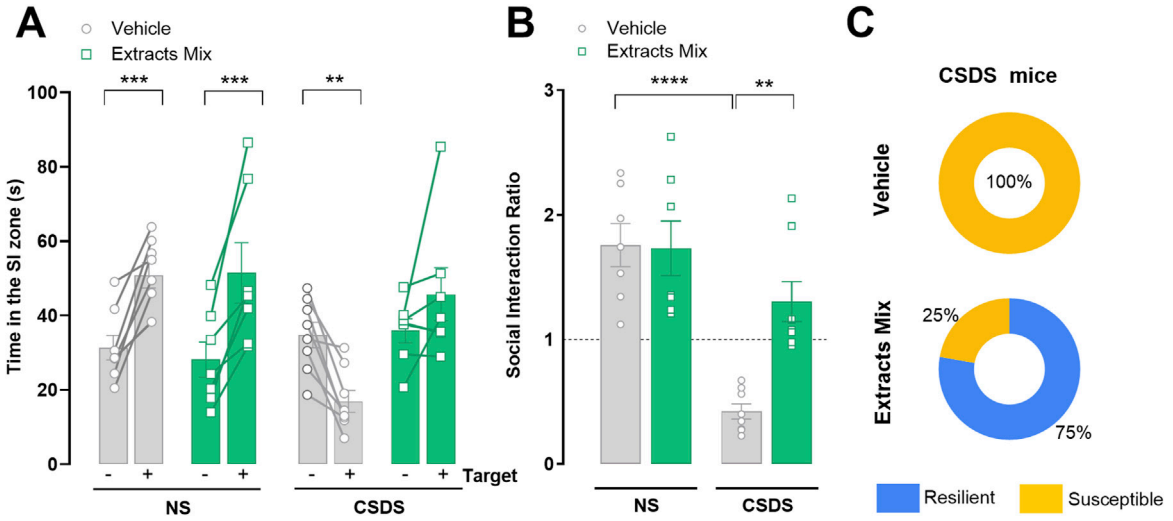


FIGURE 2
Effect of chronic treatment with extracts mix on stress-induced social avoidance. **(A)** Time spent in the social interaction (SI) zone during target absent (–) and target present (+) sessions. $^{**}P < 0.01$ $^{***}P < 0.001$, Three-Way ANOVA and Bonferroni's test. **(B)** SI Ratios calculated for each animal. $^{**}P < 0.01$ $^{****}P < 0.0001$, Two-Way ANOVA and Bonferroni's test **(C)** Percentage of animals exposed to CSDS classified as susceptible (SI Ratio <1) or resilient (SI Ratio >1). N = 7–8 animals per experimental group.

(qMmuCID0006552), *Il10* (qMmuCID0015452), *Aif1* (qMmuCED0025128), *Gfap* (qMmuCIP0032231), *Serpina3n* (qMmuCID0024737), *Scl1a2* (qMmuCIP0031555), *Scl1a3* (qMmuCIP0030473), *Ocln* (qMmuCID0005446), *Cldn5* (qMmuCED0001017), *Marveld2* (qMmuCID0008476), *Tjp1* (qMmuCID0005277), *Cdh5* (qMmuCID0005343), and *Pecam1* (qMmuCID0005317). The differential expression of the transcripts was normalized on the housekeeping gene *Gapdh* (QT01658692, QIAGEN Sciences, LLC). The data of real time PCR are expressed as Fold Change Quantification, each experiment was repeated in triplicate, and quantitative PCR analysis was analyzed with $2^{-\Delta\Delta Ct}$-method (Livak and Schmittgen, 2001).

## 2.14 Statistical analysis

The data were analysed using Graphpad Software (version 10.2.1). Statistical significance was determined using a Two-way or Three-way ANOVA, as appropriate for the variables analysed in each experimental set, followed by Bonferroni's multiple comparison *post hoc* test. The level of significance was set to $P < 0.05$. Outliers were identified and excluded from each experimental set using the ROUT method (Motulsky and Brown, 2006). Data shown in figures are expressed as individual points for each animal (aligned dot plot). Bar graphs represent means ± standard error of the mean (S.E.M).

# 3 Results

## 3.1 Chronic treatment with extracts mix prevented CSDS-induced social avoidance

Following 10 days of CSDS exposure, animals' susceptibility to stress was evaluated by comparing the time spent in the interaction zone during target absent (–) and target present (+) sessions of the SIT (Figure 2). As expected, non-stressed animals spent more time in the interaction zone when the target was present, independently of the treatment ($P < 0.001$). Vehicle-treated stressed animals, instead, spent less time in the interaction zone during the (+) session ($P < 0.01$). Treatment with extracts mix prevented such effect, as revealed by the longer time spent by the animals in the interaction zone when a CD1 mouse was present (Figure 2A). In keeping with these results, a significant reduction of SI ratios emerged for the group of stressed animals treated with vehicle ($P < 0.0001$), which was prevented by the chronic treatment with the extracts mix ($P < 0.01$) (Figure 2B). Analysing SI ratios individually (Figure 2C), we found that all animals allocated to the CSDS-Vehicle group showed a SI <1, confirming that our CSDS protocol was sufficient to generate a large population of stress-susceptible mice. Regarding the group of stressed animals treated with extracts mix, 6 out of 8 stressed animals had a SI ratio >1 (corresponding to 75% of the group), a phenotype classified as stress resilient. For the two remaining animals, the calculated SI ratios were 0.98 and 0.94, very close, but still below the unit, therefore they were classified as stress-susceptible phenotypes (Golden et al., 2011).

## 3.2 Chronic treatment with extracts mix attenuated behavioural despair and prevented stress-induced memory impairment

As shown in Figure 3A chronic treatment with extracts mix significantly decreased the immobility time measured in the tail suspension test, of both stressed ($P < 0.01$) and non-stressed ($P < 0.001$) mice. Next, the impact of stress and treatments on cognition was evaluated with the NOR test. Non-stressed animals, regardless of treatment, recognized the familiar object

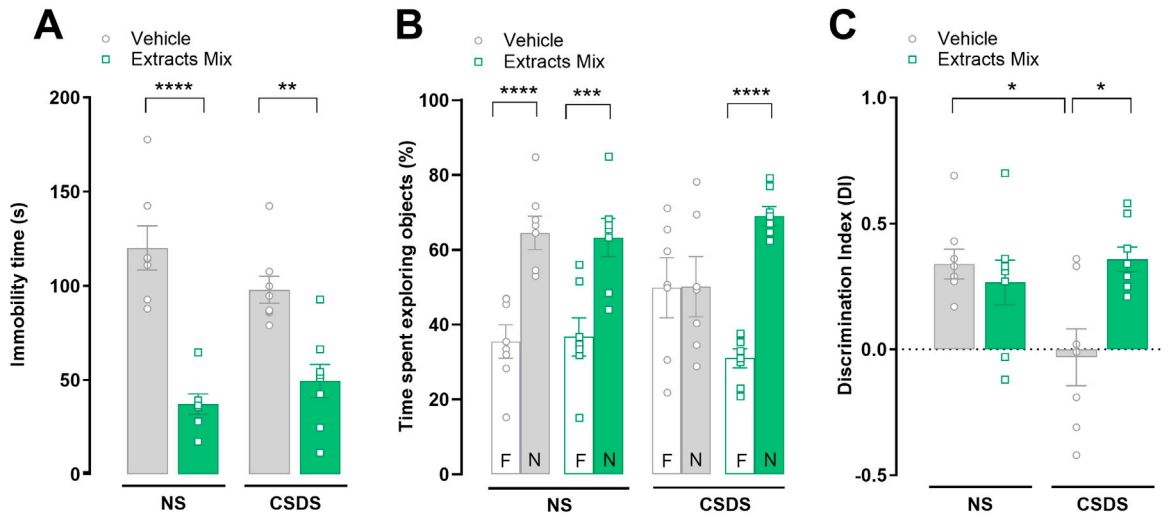


FIGURE 3
Effect of chronic treatment with extracts mix on behavioural despair and stress-induced short-term memory impairment. **(A)** Immobility time, measured in seconds, in the tail suspension test. $^{**}P < 0.01$ $^{****}P < 0.0001$, Two-Way ANOVA and Bonferroni's test. **(B)** Percentage of time spent exploring the familiar (F) or novel (N) objects during the retention test, measured 1 h after acquisition, in the novel object recognition paradigm. $^{***}P < 0.001$, $^{****}P < 0.0001$, Three-Way ANOVA and Bonferroni's test. N = 7–8 animals per experimental group. **(C)** Discrimination Index (DI) calculated following the equation DI = (time spent exploring N−time exploring F)/total time spent exploring objects. $^{*}P < 0.05$ Two-Way ANOVA and Bonferroni's test. N = 7–8 animals per experimental group.

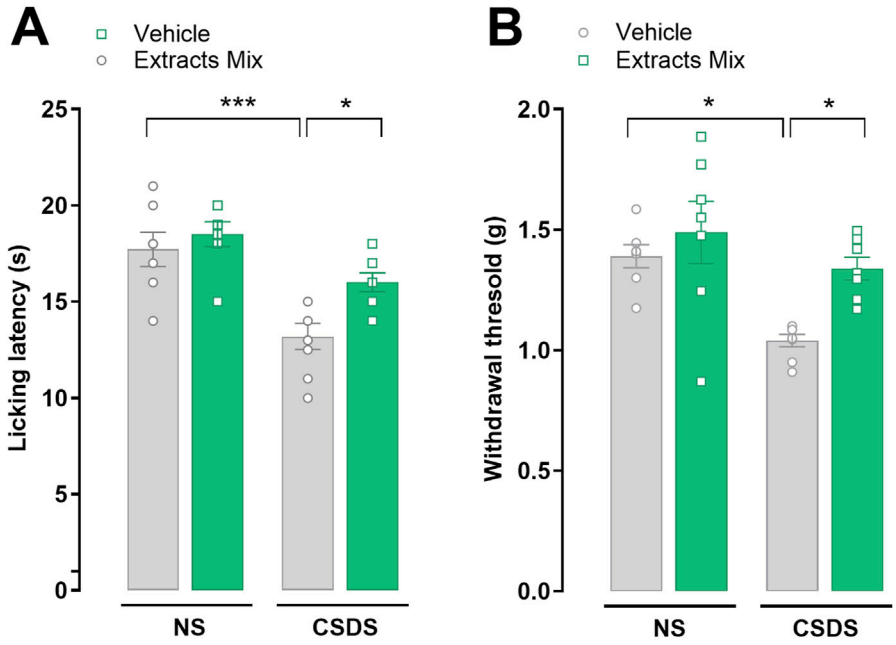


FIGURE 4
Effects of chronic treatment with extracts on stress-induced thermal and mechanical allodynia. Pain threshold alterations evoked by a thermal and mechanical non-noxious stimuli were evaluated using the **(A)** cold plate and **(B)** the von Frey tests, respectively. $^{*}P < 0.05$ $^{***}P < 0.001$, Two-Way ANOVA and Bonferroni's test. N = 6–8 animals per experimental group.

and thus explored the new object for a longer time ($P < 0.001$). Exposure to CSDS had a detrimental effect on recognition memory in vehicle-treated mice, as they did not discriminate between the two objects, confirmed by the significantly lower DI as compared to the NS-Veh group (Figure 3C, $P < 0.005$). Chronic treatment with extracts mix prevented stress-induced amnesic effects as revealed by the increased time mice spent exploring the new object (Figure 3B, $P < 0.001$), as well as by the DI which was significantly higher than the value observed in CSDS-Veh animals (Figure 3C, $P < 0.005$).

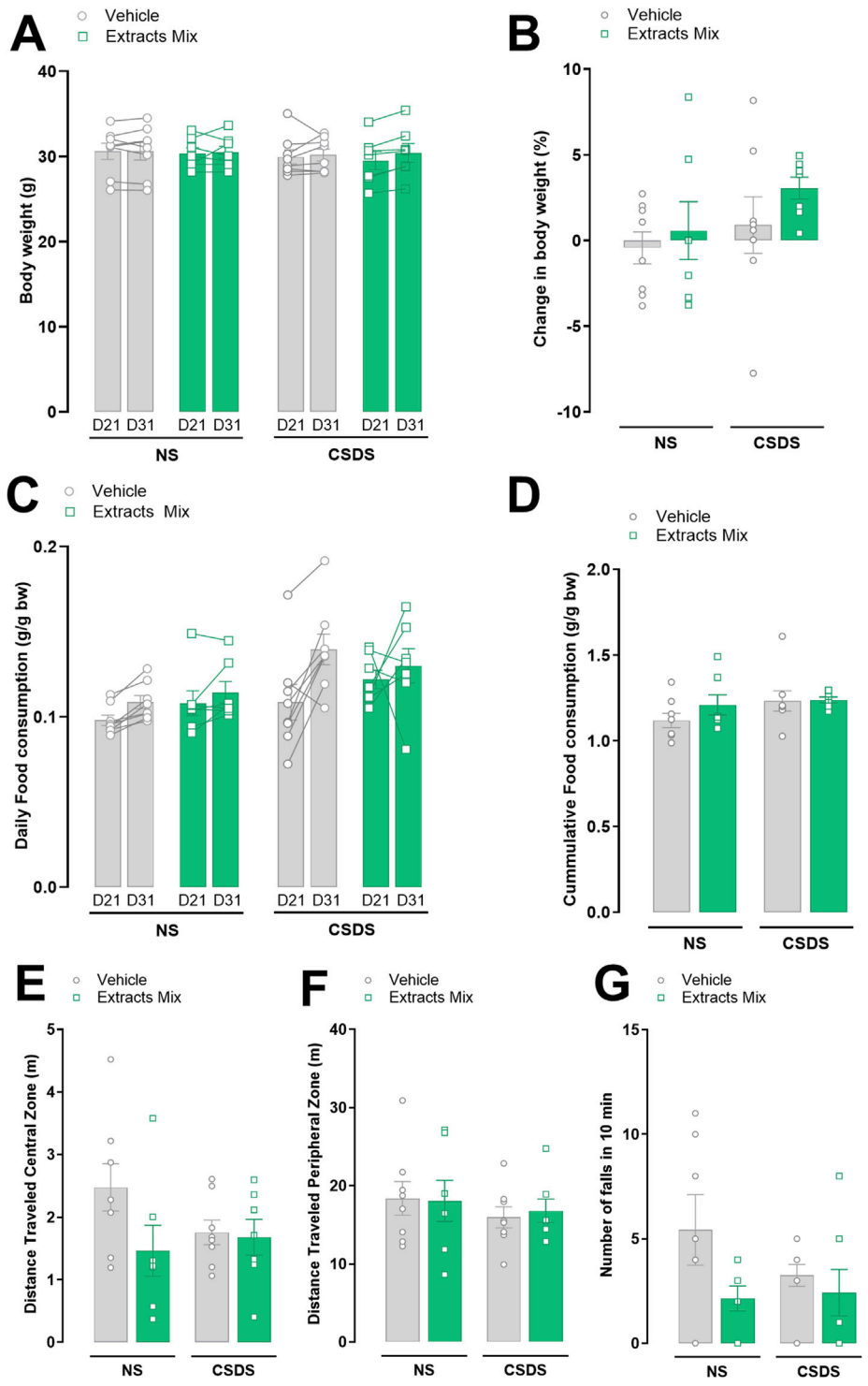


FIGURE 5
Effects of stress and chronic treatment with extracts mix on food consumption, body weight and locomotor activity. Body weight **(A,B)** and food consumption **(C,D)** measured before (D21) and after (D31) stress exposure. Distance travelled in the center **(E)** and periphery **(F)** of an Open Field arena in a 10 min test. Number of falls **(G)** registered in the rotarod during a 10 min session. No differences between groups were detected using Two-Way ANOVA and Bonferroni's test. N = 6–8 animals per experimental group.

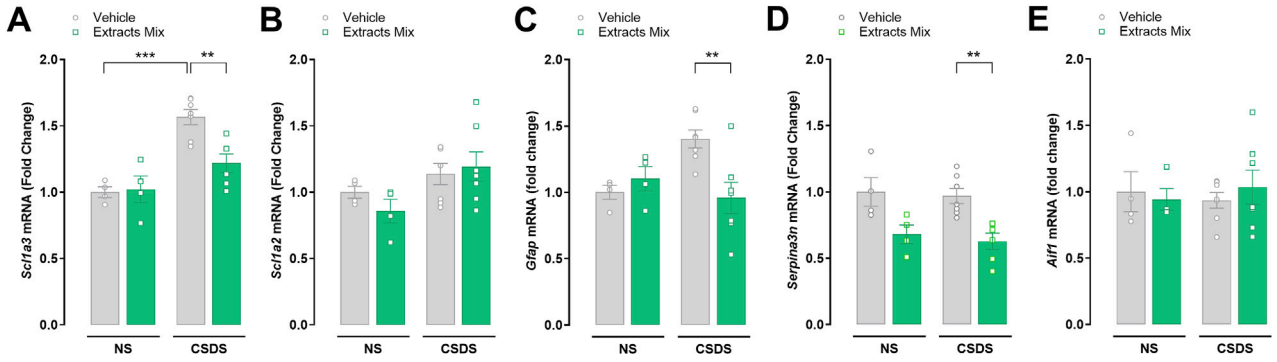


FIGURE 6
Effects of treatment with extracts mix on transcription of pain-related markers in the spinal cord. Fold changes in mRNA expression of *Scl1a3* **(A)**, *Scl1a2* **(B)**, *Gfap* **(C)**, *Serpina3n* **(D)** and *Aif1* **(E)** genes relative to the control group determined by RT-PCR. $^{**}P < 0.01$ $^{***}P < 0.001$, Two-Way ANOVA and Bonferroni's test. N = 4–7 animals per experimental group.

## 3.3 Chronic treatment with extracts mix reduced stress-induced thermal and mechanical allodynia

Pain threshold alterations were evaluated using the cold plate and the von Frey tests. As illustrated in Figure 4A 10 days of CSDS exposure significantly reduced mice licking latency in comparison to non-stressed animals ($P < 0.001$) in the cold plate test. Chronic treatment with the extracts mix significantly increased the time spent by the animals on the cold surface ($P < 0.05$) demonstrating that the extracts mix protected against CSDS-induced thermal allodynia. Similar results were obtained when mice were challenged using a non-noxious mechanical stimulus (von Frey test; Figure 4B). Chronic treatment with extracts mix prevented the development of mechanical allodynia evoked by stress exposure ($P < 0.05$) as it increased paw withdrawal threshold up to the values recorded in the non-stressed group. To note, the repeated administration of the extracts mix to non-stressed mice did not affect pain threshold (Figure 4).

## 3.4 Effects of CSDS and extracts mix on food intake, body weight gain and locomotor activity

Locomotion, measured as the distance travelled in both the central and peripheral zones of an open field arena, was not different between experimental groups (Figures 5E, F). No differences emerged also regarding the number of falls in a 10 min rotarod session (Figure 5G). These data indicate that the effects observed in the previous sessions (stress and treatment) cannot be ascribed to locomotor alterations or motor incoordination.

Food consumption and body weight were measured daily. Figures 5A–D shows the data after 21st and 31st days of treatment with extracts mix or vehicle, i.e., before and after animals' exposure to the 10-day CSDS. Neither stress nor chronic treatment with extracts mix altered the amount of eaten food (Figures 5C, D) and body weight gain (Figures 5A, B).

## 3.5 Chronic treatment with extracts reduced mRNA expression of pain-related markers altered by stress in the spinal cord

The expression of pain-related genes was evaluated by RT-PCR analysis in spinal cord samples of non-stressed and stressed animals treated with the extracts mix or vehicle (Figure 6). CSDS exposure significantly increased the mRNA expression of *Scl1a3* ($P < 0.001$) in comparison to non-stressed animals and we observed a trend increase in *Gfap* expression ($P = 0.0827$), which did not reach statistical significance. The daily repeated treatment with the extracts mix prevented these changes ($P < 0.01$) without modifying the expression of the same genes in non-stressed animals (Figures 6A, C). Moreover, the extracts mix significantly down-modulated the expression of *Serpina3n* ($P < 0.01$; Figure 6D) in comparison to the CSDS-Veh group without affecting the mRNA expression of non-stressed mice. Spinal cord mRNA expression of *Scl1a2* (Figure 6B) and *Aif1* (Figure 6E) were not significantly altered by CSDS exposure nor by the extracts mix treatment.

## 3.6 Chronic treatment with extracts mix prevented CSDS-induced neuroinflammation

The alterations in the expression of several inflammatory mediators were determined at the transcriptional level by RT-PCR. Significant differences emerged among groups when analysing mRNA expression in hippocampal samples (Figures 7A–E). Specifically, CSDS exposure significantly increased the hippocampal expression of the pro-inflammatory cytokines TNF-α (Figure 7A, $P < 0.01$), IL-1β (Figure 7B, $P < 0.05$) and IL-6 (Figure 7C, $P < 0.0001$), which was completely prevented by chronic treatment with extracts mix (Figures 7A–C, $P < 0.05$, $P < 0.05$ and $P < 0.0001$, respectively). Regarding the anti-inflammatory cytokines, IL-4 mRNA expression was increased following extracts treatment reaching statistical significance only in the group of non-stressed animals (Figure 7D, $P > 0.05$), whereas a significant increase of IL-10 mRNA levels (Figure 7E, $P < 0.05$) was

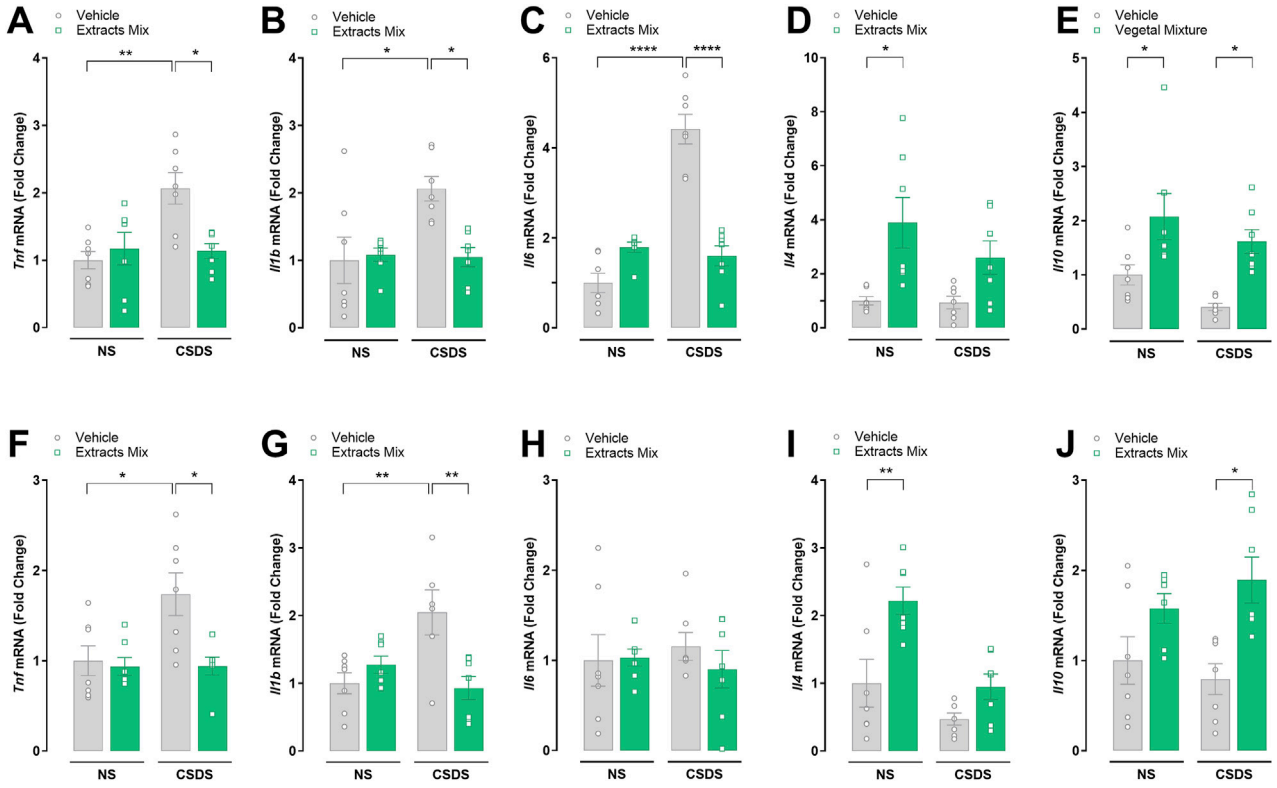


FIGURE 7
Effects of chronic treatment with extracts mix on stress-induced alterations in hippocampal **(A–E)** and cortical **(F–J)** cytokines mRNA expression. Fold changes in mRNA expression of *Tnf* **(A, F)**, *Il1b* **(B, G)**, *Il6* **(C, H)**, *Il4* **(D, I)** and *Il10* **(E, J)** genes relative to the control group determined by RT-PCR. $^{*}P < 0.05$ $^{**}P < 0.01$ $^{****}P < 0.0001$, Two-Way ANOVA and Bonferroni's test. N = 7–8 animals per experimental group.

observed in animals chronically treated with the extracts mix, independently of the stress exposure.

The results emerging from the analysis of cytokines mRNA expression in cortical samples (Figures 7F–J) are largely similar to those observed in the hippocampus, except for the lack of IL-6 increase in the stressed *vs* non-stressed animals treated with vehicle, and IL-10 expression in NS-Extracts mix group compared to NS-Veh group, that did not reach statistical significance.

## 3.7 Effects of CSDS and extracts mix on mRNA expression of BBB integrity-related markers

We determined the expression, at the transcriptional level, of a series of tight junction and adherens proteins (paracellular proteins) in hippocampal (Figures 8A–F) and cortical (Figures 8G–L) samples. Significant increases in the mRNA transcripts for *Ocln* ($P < 0.05$), *Cldn5* ($P < 0.05$), *Marveld2* ($P < 0.05$), *Tjp1* ($P < 0.05$), *Cdh5* ($P < 0.05$) and *Pecam1* ($P < 0.05$) were found in the frontal cortex of stressed animals treated with extracts mix when compared to stressed animals receiving vehicle. No differences among groups were detected in hippocampal samples.

## 3.8 Chronic treatment with extracts mix increased hippocampal and cortical BDNF and TrkB mRNA expression

Next, we studied whether stress and the extracts mix treatment influenced the transcription of the growth factor BDNF and its receptor TrkB in hippocampal and cortical samples (Figure 9). Chronic treatment with extracts mix stimulated *Bdnf* mRNA expression in the hippocampus of both stressed ($P < 0.01$) and non-stressed ($P < 0.05$) mice (Figure 9A). The same trend was observed in cortical samples; however, the increase did not reach statistical significance in non-stressed animals (Figure 9C).

Regarding *Trkb* mRNA expression, a significant increase was found in cortical samples obtained from animals treated with the extracts mix, independently of CSDS exposure (Figure 9D, $P < 0.05$ vs NS-Veh and $P < 0.001$ vs CSDS-Veh). A similar effect was detected in the hippocampus of stressed mice receiving the same treatment ($P < 0.05$), whereas in the non-stressed animals the small increase did not reach statistical significance (Figure 9B).

# 4 Discussion

The CSDS is a widely adopted stress protocol relying on the social conflict between congeners in which a rodent is introduced

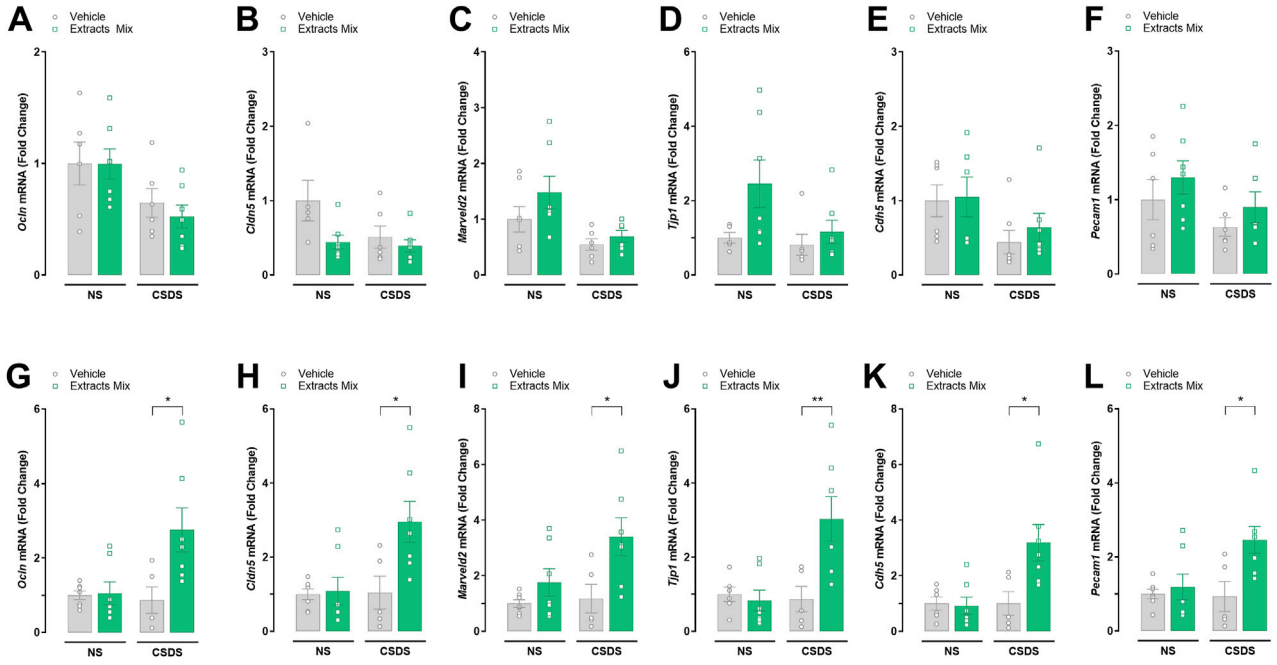


FIGURE 8
Effects of treatment with extracts mix on transcription of blood-brain barrier integrity-related markers in hippocampal **(A–F)** and cortical **(G–L)** samples. Fold changes in mRNA expression of *Ocln* **(A, G)**, *Cldn5* **(B, H)**, *Marveld2* **(C, I)**, Tjp1 **(D, J)**, *Cdn5* **(E, K)** and *Pecam1* **(F, L)** genes relative to the control group determined by RT-PCR. *$P < 0.05$, Two-Way ANOVA and Bonferroni's test. N = 6–8 animals per experimental group.

into the home cage of an older, aggressive, dominant animal which quickly attacks the intruder forcing it to subordination. Subsequently, animals are physically separated to avoid harm, but the visual and olfactory exposure to the stressor remains. The combination of physical and emotional aspects causes long-lasting consequences on animals' behaviour without signs of habituation (Henriques-Alves and Queiroz, 2015). Moreover, the CSDS protocol shows also an important translational value, as the pattern of repetitive attacks inflicted by the dominant mouse on their congeners closely resembles human bullying. In fact, bullies often have intentional, repetitive, and persistent aggressive behaviours towards individuals perceived as less powerful, generating on them a negative emotional state (Rani et al., 2021; Costa et al., 2022; Björkqvist, 2001). Consequently, victims of bullying tend to have poor academic and work performance and increased risk for developing psychiatric disorders (Catone et al., 2017; Wolke and Lereya, 2015). In keeping with earlier reports (Golden et al., 2011; Rani et al., 2021; Costa et al., 2022), we found that mice treated with vehicle and exposed to 10-days of CSDS spent less time interacting with a social target, which is considered a maladaptive response modelling social withdrawal, because defeated mice avoid all mice, including those derived from their own background (Berton et al., 2006). Interestingly, repeated daily treatment with *C. asiatica*, *E. purpurea* and *Z. officinale* standardized extracts largely prevented such effect. In fact, in our study, only 25% of the treated animals exposed to the CSDS protocol exhibited the social avoidance behaviour, indicating that botanical drugs extracts treatment help animals to cope with enduring stress exposure and thus promotes a pro-resilient phenotype. Next we assessed other domains known to be markedly affected by chronic stress exposure, such as pain (Sawicki et al., 2019; Pagliusi et al., 2018), cognition (Monleón et al., 2016; Rani et al., 2021; Costa et al., 2022) and mood (Iñiguez et al., 2016).

Chronic treatment with the mix of botanical drugs extracts counteracted CSDS-induced mechanical and thermal allodynia as well as the increased expression of pain-related genes as *Scl1a3* (Sung et al., 2003; Weng et al., 2006) and *Gfap* (Sweitzer et al., 2001; Ridet et al., 1997) in the spinal cord. We observed that the same treatment also prevented the stress-induced cognitive deficits. These data are in line with our previous evidence showing the anti-hypersensitivity and procognitive effects of this treatment in a mouse model of neuroinflammation (Micheli et al., 2022). Moreover, there are several studies reporting the analgesic properties of purified metabolites obtained from the species used here, such as 8-shogaol and zingiberene from *Z. officinale* (Cheng et al., 2024; Borgonetti et al., 2023), alkylamides and polyphenols from *E. purpurea* (Micheli et al., 2023) and asiatic acid from *C. asiatica* (Huang et al., 2011). The procognitive properties of these species are also abundantly reported in the literature, in particular for *C. asiatica*, whose memory enhancing properties have been described in adult (Sbrini et al., 2020) and aged animals (Gray et al., 2018), as well as in animal models of Alzheimer's disease (Veerendra Kumar and Gupta, 2003). The presence of these metabolites in our extract mix may have contributed to the effects observed in our experiments preventing short-term memory recognition memory deficits.

Behavioural despair models, such as the forced swimming and tail suspension tests, are widely used to assess potential antidepressant-like effects. Their principle is similar: mice are exposed to an inescapable, short-duration, moderately stressful condition, and the time they spend

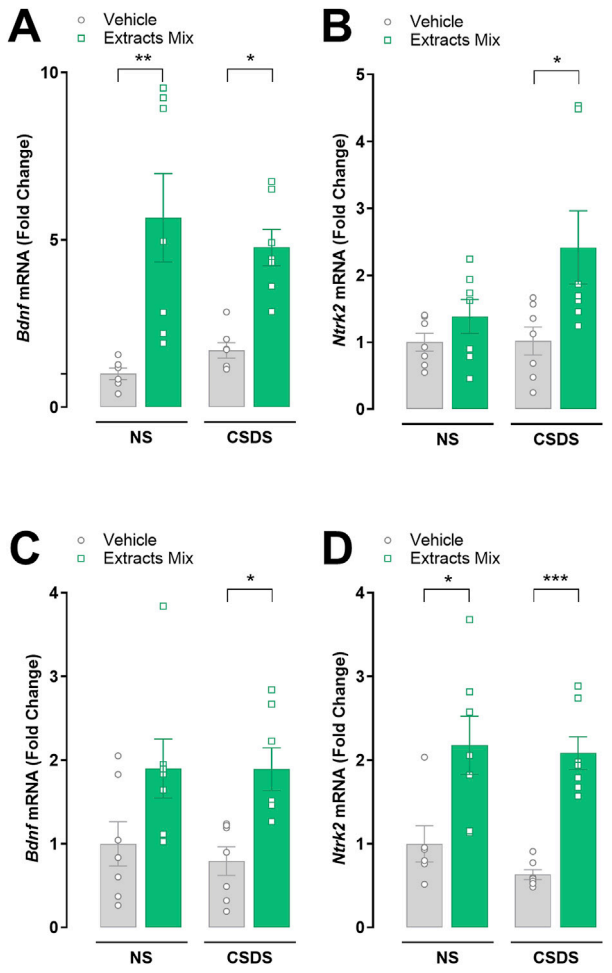


FIGURE 9
Effects of chronic treatment with extracts mix on BDNF and TrkB transcriptional expression in hippocampal **(A, B)** and cortical **(C, D)** samples. Fold changes in mRNA expression of *Bdnf* **(A, C)**, *Ntrk2* **(B, D)** genes relative to the control group determined by RT-PCR. *$P$ < 0.05 **$P$ < 0.01 ***$P$ < 0.001, Two-Way ANOVA and Bonferroni's test. N = 7–8 animals per experimental group.

responding actively (escape-related behaviours) vs. passively (immobility) is measured as an index of behavioural despair/helplessness. Treatment with antidepressant-like drugs stimulates escape-related behaviours consequently reducing the time animals spend immobile (Cryan et al., 2005; Nestler and Hyman, 2010; Castagné et al., 2011). Interestingly, we found that the chronic treatment with the mix of extracts reduced the time the animals spent immobile in the tail suspension test. Such effect was observed in both stressed and non-stressed groups. Therefore, our results suggest that the extract mix possesses antidepressant-like effects independently of stress exposure. The results obtained during the behavioural evaluations fit well with the *ex vivo* analysis, as the treatment with the extracts mix stimulated cortical and hippocampal translational expression of BDNF and its receptor TrkB. BDNF is a member of the neurotrophin family most abundantly expressed in the CNS and by binding and activating the TrkB receptor, it acts as a key regulator of neuronal growth and survival, as well as of neuronal plasticity required to adapt to life events (Colucci-D'Amato et al., 2020). In our study, CSDS did not affect BDNF/TrkB brain expression as reported for other stress protocols (Huang et al., 2022; Miao et al., 2020). Nonetheless the treatment with extract mix augmented BDNF/TrkB mRNA, independently of stress exposure, a result that may explain the potential antidepressant-like effects observed in our experiments. Increased BDNF production and signalling through TrkB has a major role in mood-improving actions of classical antidepressants including classical tricyclic, monoamine oxidase inhibitors, serotonin-selective reuptake inhibitors and others (Casarotto et al., 2021; Castrén and Monteggia, 2021). More recently it was discovered that several antidepressants can directly bind TrkB and allosterically stimulate TrkB signaling (Casarotto et al., 2021), which have been hypothesized as the mechanism underpinning the effects of fast-acting antidepressants such as ketamine, lysergic acid diethylamide (LSD) and psilocin (Moliner et al., 2023; Kim et al., 2024). In this regard, previous studies demonstrated that treatment with bioactive metabolites present in the extracts mix such as chicoric acid and echinacoside from *E. purpurea* (Chuang et al., 2022; Kour and Bani, 2011), asiaticoside and asiatic acid from *C. asiatica* (Lin et al., 2013; Wang et al., 2020) and 6-shoagoal from *Z. officinale* (Afzal et al., 2022) elicits antidepressant effects and modulates brain BNDF levels.

Another important finding of this study is that the treatment with extracts mix attenuated the neuroinflammatory profile observed following CSDS exposure. The CNS and peripheral immune system are in constant communication and influence how each other respond to a challenge. Stressors, particularly of a social nature, are well known for their ability to impact the immune system. Transient neuroinflammation induced by bouts of social stress is not inherently detrimental, but adaptive in the acute phase (Hollis et al., 2022). However, prolonged or severe stress exposure causes elevated and sustained proinflammatory signalling in the CNS which is supposedly linked with stress-related psychiatric disorders (Weber et al., 2017). We found that mice exposed to CSDS show a neuroinflammatory profile in stress-sensitive brain regions, such as hippocampus and frontal cortex characterized by increased proinflammatory (IL-1β, TNF-α, IL-6) and reduced anti-inflammatory (IL-4 and IL-10) cytokines gene expression. Another evidence of the strong association between neuroinflammation and stress susceptibility is that CSDS-induced deleterious effects can be blocked or reversed by inhibiting the inflammatory system with different approaches, such as infusion of the IL-1β receptor antagonist (Wood et al., 2015; Li et al., 2023), IL-6 neutralizing antibodies (Hodes et al., 2014), or minocycline, a robust inhibitor of microglial activation (McKim et al., 2016). Chronic treatment with the extracts mix normalized the alterations induced by stress, suggesting that modulating neuroinflammation related processes may play a key role on the observed effects. These results are in line with previous publications in which anti-inflammatory properties of the extracts and of the isolated metabolites have been discussed (Cheng et al., 2024; Grzanna et al., 2005; Micheli et al., 2022; Sasmita et al., 2018).

Another stress-induced alteration closely associated with neuroinflammation, is the impairment of the blood-brain barrier (BBB) integrity. It is reported that the accumulation of proinflammatory cytokines causes BBB leakage, promoting the infiltration of different immune cells, further potentiating

neuroinflammation which in turn profoundly affects behaviour (Takata et al., 2021). In our hands, no significant differences emerged between non-stressed and stressed animals treated with vehicle. However, in animals chronically treated with extracts mix and submitted to CSDS protocol we found increased mRNA levels of a series of markers related to the BBB integrity in cortical samples. Further investigation is required to understand the implication of these observations on the preventive effects induced by the extracts mix.

One limitation of our study is the lack of comprehensive safety/tolerability data, which are particularly relevant for long-term treatment with botanical drugs preparations (Izzo et al., 2016). Even though we did not specifically address toxicological aspects, no evidence of malaise was observed during the experiments, as confirmed by no differences among experimental groups in terms of food consumption and body weight gain. Moreover, no differences in terms of distance travelled or number of falls were observed in the open field and rotarod tests, respectively, suggesting that neither stress nor the treatment had a major impact on motor activity and coordination. *Zingiber officinale, C. asiatica,* and *E. purpurea* extracts have been used in traditional medicine for a long time, and phyto-pharmaceutical preparations containing extracts of these plants are currently used in clinics to treat different ailments. Consistently, phase I and II clinical trials demonstrate that extracts obtained from these plants are well tolerated (Martins et al., 2019; Wright et al., 2022; Ogal et al., 2021). However, extrapolating such safety conclusions to the present report must be done prudently since here we evaluated the effects of co-administration of the extracts. Such limitations highlight the importance of further research aiming at evaluating the tolerability and toxicological aspects associated with extract mix treatment within the dose range employed in our study to provide more robust considerations relative to their use as a therapeutic strategy.

## 5 Conclusion

Prolonged exposure to stress causes a constellation of alterations which increases the risk for the onset of several diseases. In this study, we demonstrated that repeated daily treatment with the combination of standardized extracts obtained from *C. asiatica* (200 mg/kg, i.p.), *E. purpurea* (20 mg/kg, i.p.) and *Z. officinale* (150 mg/kg, i.p.) had two main effects overall: it prevented the maladaptive responses induced by chronic stress (social avoidance, short-term recognition memory impairment and reduced thermal and mechanical allodynia) and provided potential efficacy as antidepressant independently of stress exposure. *Ex vivo* gene expression analysis suggests that the modulation of neurotrophins, cytokines and pain related markers in the hippocampus, frontal cortex and spinal cord may be the mechanisms underpinning the extracts-induced effects. The extracts mix used is rich in bioactive metabolites acting at multiple targets and holding intrinsic pharmacological properties that potentially contributed to the overall observed effects. Taken together these results suggest that standardized botanical drug extracts may be a promising strategy to promote resilience preventing the deleterious effects related to prolonged stress exposure.

## Data availability statement

The raw data supporting the conclusions of this article will be made available by the authors, without undue reservation.

## Ethics statement

The animal study was approved by the Animal Care Committee of the University of Florence and Italian Ministry of Health (678-2021-PR prot. 17E9C.235) and supervised by a veterinarian. Housing and experimental procedures were conducted in accordance with the Council Directive of the European Community (2010/63/EU) and the Italian Decreto Legislativo 26 (13/03/2014) regarding the protection of animals used for scientific purposes. Every effort was made to minimize animal suffering and to reduce the number of animals used, complying with the 3R principle. The study was conducted in accordance with the local legislation and institutional requirements.

## Author contributions

AC: Formal Analysis, Investigation, Methodology, Project administration, Writing–review and editing. LM: Formal Analysis, Investigation, Methodology, Resources, Writing–review and editing. VS: Formal Analysis, Investigation, Writing–review and editing. CC: Formal Analysis, Investigation, Writing–review and editing. JL: Resources, Writing–review and editing. MP: Writing–review and editing. GP: Conceptualization, Formal Analysis, Funding acquisition, Supervision, Writing–original draft.

## Funding

The author(s) declare that financial support was received for the research, authorship, and/or publication of this article. This research was supported by the Italian Ministry of Universities and Research trough the Programmi di Ricerca di Rilevante Interesse Nazionale (PRIN D.D. n. 104 del 2/2/2022) Grant 2022 (MUR: 2022BYZPFE, CUP: B53D23018540006 U-GOV: PRIN 2022_PROVENSI) and by the University of Florence, Bando per progetti competitivi per Ricercatori a Tempo Determinato (RTD) 2022-2023 (TRAPPOLA project). The funders had no role in study design, data collection, data analysis, interpretation or writing of the report.

## Acknowledgments

We thank Antonio Parrotta for his assistance in the RT-PCR analysis, and Aboca S p A. for kindly providing the standardized extracts.

## Conflict of interest

Author JL was employed by Bios-Therapy, Physiological Systems for Health S.p.A. and Aboca S.p.A. Società Agricola.

The remaining authors declare that the research was conducted in the absence of any commercial or financial relationships that could be construed as a potential conflict of interest.

The author(s) declared that they were an editorial board member of Frontiers, at the time of submission. This had no impact on the peer review process and the final decision.

## Publisher's note

All claims expressed in this article are solely those of the authors and do not necessarily represent those of their affiliated organizations, or those of the publisher, the editors and the reviewers. Any product that may be evaluated in this article, or claim that may be made by its manufacturer, is not guaranteed or endorsed by the publisher.

## Supplementary material

The Supplementary Material for this article can be found online at: https://www.frontiersin.org/articles/10.3389/fphar.2024.1439811/full#supplementary-material

## References


Afzal, M., Kazmi, I., Quazi, A. M., Khan, S. A., Zafar, A., AL-Abbasi, F. A., et al. (2022). 6-Shogaol attenuates traumatic brain injury-induced anxiety/depression-like behavior via inhibition of oxidative stress-influenced expressions of inflammatory mediators TNF-α, IL-1β, and BDNF: insight into the mechanism. *ACS Omega* 7, 140–148. doi:10.1021/acsomega.1c04155

Almohaimeed, H. M., Mohammedsaleh, Z. M., Batawi, A. H., Balgoon, M. J., Ramadan, O. I., Baz, H. A., et al. (2021). Synergistic anti-inflammatory and neuroprotective effects of *Cinnamomum cassia* and *Zingiber officinale* alleviate diabetes-induced hippocampal changes in male albino rats: structural and molecular evidence. *Front. Cell Dev. Biol.* 9, 727049. doi:10.3389/fcell.2021.727049

Barnes, J., Anderson, L. A., Gibbons, S., and Phillipson, J. D. (2005). *Echinacea* species (*Echinacea angustifolia* (DC.) Hell., *Echinacea pallida* (Nutt.) Nutt.,*Echinacea purpurea* (L.) Moench): a review of their chemistry, pharmacology and clinical properties. *J. Pharm. Pharmacol.* 57, 929–954. doi:10.1211/0022357056127

Berton, O., Mcclung, C. A., Dileone, R. J., Krishnan, V., Renthal, W., Russo, S. J., et al. (2006). Essential role of BDNF in the mesolimbic dopamine pathway in social defeat stress. *Science* 311, 864–868. doi:10.1126/science.1120972

Björkqvist, K. (2001). Social defeat as a stressor in humans. *Physiol. Behav.* 73, 435–442. doi:10.1016/s0031-9384(01)00490-5

Borgonetti, V., Governa, P., Manetti, F., and Galeotti, N. (2023). Zingiberene, a non-zinc-binding class I HDAC inhibitor: a novel strategy for the management of neuropathic pain. *Phytomedicine* 111, 154670. doi:10.1016/j.phymed.2023.154670

Burlou-Nagy, C., Bănică, F., Jurca, T., Vicaş, L. G., Marian, E., Muresan, M. E., et al. (2022). *Echinacea purpurea* (L.) Moench: biological and pharmacological properties. A review. *A Rev. Plants (Basel)* 11, 1244. doi:10.3390/plants11091244

Casarotto, P. C., Girych, M., Fred, S. M., Kovaleva, V., Moliner, R., Enkavi, G., et al. (2021). Antidepressant drugs act by directly binding to TRKB neurotrophin receptors. *Cell* 184, 1299–1313.e19. doi:10.1016/j.cell.2021.01.034

Castagné, V., Moser, P., Roux, S., and Porsolt, R. D. (2011). Rodent models of depression: forced swim and tail suspension behavioral despair tests in rats and mice. *Curr. Protoc. Neurosci.* Chapter 8, Unit 8.10A. Chapter 8, Unit 8.10A. doi:10.1002/0471142301.ns0810as55

Castrén, E., and Monteggia, L. M. (2021). Brain-Derived Neurotrophic Factor signaling in depression and antidepressant action. *Biol. Psychiatry* 90, 128–136. doi:10.1016/j.biopsych.2021.05.008

Catone, G., Marotta, R., Pisano, S., Lennox, B., Carotenuto, M., Gritti, A., et al. (2017). Psychotic-like experiences in help-seeking adolescents: dimensional exploration and association with different forms of bullying victimization - a developmental social psychiatry perspective. *Int. J. Soc. Psychiatry* 63, 752–762. doi:10.1177/0020764017733765

Chanana, P., and Kumar, A. (2016). Possible Involvement of Nitric Oxide Modulatory Mechanisms in the neuroprotective effect of *Centella asiatica* against sleep deprivation induced anxiety like behaviour, oxidative damage and neuroinflammation. *Phytother. Res.* 30, 671–680. doi:10.1002/ptr.5582

Cheng, X. L., Ruan, Y. L., Dai, J. Y., Fan, H. Z., Ling, J. Y., Chen, J., et al. (2024). 8-shogaol derived from dietary ginger alleviated acute and inflammatory pain by targeting TRPV1. *Phytomedicine* 128, 155500. doi:10.1016/j.phymed.2024.155500

Chuang, H. W., Wang, T. Y., Huang, C. C., and Wei, I. H. (2022). Echinacoside exhibits antidepressant-like effects through AMPAR-Akt/ERK-mTOR pathway stimulation and BDNF expression in mice. *Chin. Med.* 17, 9. doi:10.1186/s13020-021-00549-5

Cohen, S., Gianaros, P. J., and Manuck, S. B. (2016). A stage model of stress and disease. *Perspect. Psychol. Sci.* 11, 456–463. doi:10.1177/1745691616646305

Colalto, C. (2018). What phytotherapy needs: evidence-based guidelines for better clinical practice. *Phytother. Res.* 32, 413–425. doi:10.1002/ptr.5977

Colucci-D'Amato, L., Speranza, L., and Volpicelli, F. (2020). Neurotrophic factor BDNF, physiological functions and therapeutic potential in depression, neurodegeneration and brain cancer. *Int. J. Mol. Sci.* 21, 7777. doi:10.3390/ijms21207777

Costa, A., Cristiano, C., Cassano, T., Gallelli, C. A., Gaetani, S., Ghelardini, C., et al. (2018). Histamine-deficient mice do not respond to the antidepressant-like effects of oleoylethanolamide. *Neuropharmacology* 135, 234–241. doi:10.1016/j.neuropharm.2018.03.033

Costa, A., Rani, B., Bastiaanssen, T. F. S., Bonfiglio, F., Gunnigle, E., Provensi, G., et al. (2022). Diet prevents social stress-induced maladaptive neurobehavioural and gut microbiota changes in a histamine-dependent manner. *Int. J. Mol. Sci.* 23, 862. doi:10.3390/ijms23020862

Cryan, J. F., Mombereau, C., and Vassout, A. (2005). The tail suspension test as a model for assessing antidepressant activity: review of pharmacological and genetic studies in mice. *Neurosci. Biobehav Rev.* 29, 571–625. doi:10.1016/j.neubiorev.2005.03.009

Dudek, K. A., Dion-Albert, L., Lebel, M., Leclair, K., Labrecque, S., Tuck, E., et al. (2020). Molecular adaptations of the blood-brain barrier promote stress resilience vs. depression. *Proc. Natl. Acad. Sci. U. S. A.* 117, 3326–3336. doi:10.1073/pnas.1914655117

Godoy, L. D., Rossignoli, M. T., Delfino-Pereira, P., Garcia-Cairasco, N., and DE Lima Umeoka, E. H. (2018). A Comprehensive overview on stress neurobiology: basic concepts and clinical implications. *Front. Behav. Neurosci.* 12, 127. doi:10.3389/fnbeh.2018.00127

Golden, S. A., Covington, H. E., Berton, O., and Russo, S. J. (2011). A standardized protocol for repeated social defeat stress in mice. *Nat. Protoc.* 6, 1183–1191. doi:10.1038/nprot.2011.361

Gray, N. E., Zweig, J. A., Caruso, M., Martin, M. D., Zhu, J. Y., Quinn, J. F., et al. (2018). *Centella asiatica* increases hippocampal synaptic density and improves memory and executive function in aged mice. *Brain Behav.* 8, e01024. doi:10.1002/brb3.1024

Grzanna, R., Lindmark, L., and Frondoza, C. G. (2005). Ginger-an herbal medicinal product with broad anti-inflammatory actions. *J. Med. Food* 8, 125–132. doi:10.1089/jmf.2005.8.125

Henriques-Alves, A. M., and Queiroz, C. M. (2015). Ethological evaluation of the effects of social defeat stress in mice: beyond the social interaction ratio. *Front. Behav. Neurosci.* 9, 364. doi:10.3389/fnbeh.2015.00364

Hodes, G. E., Pfau, M. L., Leboeuf, M., Golden, S. A., Christoffel, D. J., Bregman, D., et al. (2014). Individual differences in the peripheral immune system promote resilience versus susceptibility to social stress. *Proc. Natl. Acad. Sci. U. S. A.* 111, 16136–16141. doi:10.1073/pnas.1415191111

Hollis, F., Pope, B. S., Gorman-Sandler, E., and Wood, S. K. (2022). Neuroinflammation and mitochondrial dysfunction link social stress to depression. *Curr. Top. Behav. Neurosci.* 54, 59–93. doi:10.1007/7854_2021_300

Huang, S. S., Chiu, C. S., Chen, H. J., Hou, W. C., Sheu, M. J., Lin, Y. C., et al. (2011). Antinociceptive activities and the mechanisms of anti-inflammation of asiatic acid in mice. *Evid. Based Complement. Altern. Med.* 2011, 895857. doi:10.1155/2011/895857

Huang, L., He, L., Ma, R., Ding, W., Zhou, C., Lin, S., et al. (2022). The role of MeCP2 and the BDNF/TrkB signaling pathway in the stress resilience of mice subjected to CSDS. *Psychopharmacol. Berl.* 239, 2921–2929. doi:10.1007/s00213-022-06176-8

Iñiguez, S. D., Aubry, A., Riggs, L. M., Alipio, J. B., Zanca, R. M., Flores-Ramirez, F. J., et al. (2016). Social defeat stress induces depression-like behavior and alters spine morphology in the hippocampus of adolescent male C57BL/6 mice. *Neurobiol. Stress* 5, 54–64. doi:10.1016/j.ynstr.2016.07.001

Izzo, A. A., Hoon-Kim, S., Radhakrishnan, R., and Williamson, E. M. (2016). A critical approach to evaluating clinical efficacy, adverse events and drug interactions of herbal remedies. *Phytother. Res.* 30, 691–700. doi:10.1002/ptr.5591

Kim, J., He, M. J., Widmann, A. K., and Lee, F. S. (2024). The role of neurotrophic factors in novel, rapid psychiatric treatments. *Neuropsychopharmacology* 49, 227–245. doi:10.1038/s41386-023-01717-x

Kour, K., and Bani, S. (2011). Chicoric acid regulates behavioral and biochemical alterations induced by chronic stress in experimental Swiss albino mice. *Pharmacol. Biochem. Behav.* 99, 342–348. doi:10.1016/j.pbb.2011.05.008

Lin, X., Huang, R., Zhang, S., Wei, L., Zhuo, L., Wu, X., et al. (2013). Beneficial effects of asiaticoside on cognitive deficits in senescence-accelerated mice. *Fitoterapia* 87, 69–77. doi:10.1016/j.fitote.2013.03.023

Li, Q., Yang, F., Hou, R., Huang, T., and Hao, Z. (2020). Post-screening characterization of an acidic polysaccharide from *Echinacea purpurea* with potent anti-inflammatory properties *in vivo*. *Food Funct.* 11, 7576–7583. doi:10.1039/d0fo01367f

Livak, K. J., and Schmittgen, T. D. (2001). Analysis of relative gene expression data using real-time quantitative PCR and the 2(-Delta Delta C(T)) Method. *Methods* 25, 402–408. doi:10.1006/meth.2001.1262

Mando, Z., Mando, H., Afzan, A., Shaari, K., Hassan, Z., Mohamad Taib, M. N. A., et al. (2024). Biomarker triterpenoids of *Centella asiatica* as potential antidepressant agents: combining *in vivo* and *in silico* studies. *Behav. Brain Res.* 466, 114976. doi:10.1016/j.bbr.2024.114976

Martins, L. B., Rodrigues, A. M. D. S., Rodrigues, D. F., Dos Santos, L. C., Teixeira, A. L., and Ferreira, A. V. M. (2019). Double-blind placebo-controlled randomized clinical trial of ginger (*Zingiber officinale* Rosc.) addition in migraine acute treatment. *Cephalalgia* 39, 68–76. doi:10.1177/0333102418776016

Mckim, D. B., Niraula, A., Tarr, A. J., Wohleb, E. S., Sheridan, J. F., and Godbout, J. P. (2016). Neuroinflammatory dynamics underlie memory impairments after repeated social defeat. *J. Neurosci.* 36, 2590–2604. doi:10.1523/JNEUROSCI.2394-15.2016

Miao, Z., Wang, Y., and Sun, Z. (2020). The relationships between stress, mental disorders, and epigenetic regulation of BDNF. *Int. J. Mol. Sci.* 21, 1375. doi:10.3390/ijms21041375

Micheli, L., DI Cesare Mannelli, L., Del Bello, F., Giannella, M., Piergentili, A., Quaglia, W., et al. (2020a). The use of the selective imidazoline I 1 receptor agonist carbophenyline as a strategy for neuropathic pain relief: preclinical evaluation in a mouse model of oxaliplatin-induced neurotoxicity. *Neurotherapeutics* 17, 1005–1015. doi:10.1007/s13311-020-00873-y

Micheli, L., DI Cesare Mannelli, L., Mattoli, L., Tamimi, S., Flamini, E., Garetto, S., et al. (2020b). Intra-articular route for the system of molecules 14G1862 from *Centella asiatica*: pain relieving and protective effects in a rat model of osteoarthritis. *Nutrients* 12, 1618. doi:10.3390/nu12061618

Micheli, L., Durante, M., Lucarini, E., Sgambellone, S., Lucarini, L., DI Cesare Mannelli, L., et al. (2021). The histamine H4 receptor participates in the anti-neuropathic effect of the adenosine A 3 receptor agonist IB-MECA: role of CD4 + T Cells. *Biomolecules* 11, 1447. doi:10.3390/biom11101447

Micheli, L., Maggini, V., Ciampi, C., Gallo, E., Bogani, P., Fani, R., et al. (2023). *Echinacea purpurea* against neuropathic pain: alkamides versus polyphenols efficacy. *Phytother. Res.* 37, 1911–1923. doi:10.1002/ptr.7709

Micheli, L., Toti, A., Lucarini, E., Ferrara, V., Ciampi, C., Olivero, G., et al. (2022). Efficacy of a vegetal mixture composed of *Zingiber officinale, Echinacea purpurea*, and *Centella asiatica* in a mouse model of neuroinflammation: *in vivo* and *ex vivo* analysis. *Front. Nutr.* 9, 887378. doi:10.3389/fnut.2022.887378

Moliner, R., Girych, M., Brunello, C. A., Kovaleva, V., Biojone, C., Enkavi, G., et al. (2023). Psychedelics promote plasticity by directly binding to BDNF receptor TrkB. *Nat. Neurosci.* 26, 1032–1041. doi:10.1038/s41593-023-01316-5

Monleón, S., Duque, A., and Vinader-Caerols, C. (2016). Effects of several degrees of chronic social defeat stress on emotional and spatial memory in CD1 mice. *Behav. Process.* 124, 23–31. doi:10.1016/j.beproc.2015.12.002

Moragrega, I., and Ríos, J. L. (2021). Medicinal plants in the treatment of depression: evidence from preclinical studies. *Planta Med.* 87, 656–685. doi:10.1055/a-1338-1011

Moragrega, I., and Ríos, J. L. (2022). Medicinal plants in the treatment of depression. II: evidence from clinical trials. *Planta Med.* 88, 1092–1110. doi:10.1055/a-1517-6882

Motulsky, H. J., and Brown, R. E. (2006). Detecting outliers when fitting data with nonlinear regression - a new method based on robust nonlinear regression and the false discovery rate. *BMC Bioinforma.* 7, 123. doi:10.1186/1471-2105-7-123

Munari, L., Provensi, G., Passani, M. B., Galeotti, N., Cassano, T., Benetti, F., et al. (2015). Brain histamine is crucial for selective serotonin reuptake inhibitors' behavioral and neurochemical effects. *Int. J. Neuropsychopharmacol.* 18, pyv045. doi:10.1093/ijnp/pyv045

Nestler, E. J., and Hyman, S. E. (2010). Animal models of neuropsychiatric disorders. *Nat. Neurosci.* 13, 1161–1169. doi:10.1038/nn.2647

Ogal, M., Johnston, S. L., Klein, P., and Schoop, R. (2021). Echinacea reduces antibiotic usage in children through respiratory tract infection prevention: a randomized, blinded, controlled clinical trial. *Eur. J. Med. Res.* 26, 33. doi:10.1186/s40001-021-00499-6

Oliveira, C. T., Lacerda, D. R., Zicker, M. C., Martins, L. B., Teixeira, M. M., DE Araujo, R. L. B., et al. (2019). Ginger (*Zingiber officinale* Rosc.) ameliorated metabolic and inflammatory dysfunction induced by high-refined carbohydrate-containing diet in mice. *J. Med. Food* 22, 38–45. doi:10.1089/jmf.2018.0062

Pagliusi, M. O. F., Bonet, I. J. M., Dias, E. V., Vieira, A. S., Tambeli, C. H., Parada, C. A., et al. (2018). Social defeat stress induces hyperalgesia and increases truncated BDNF isoforms in the nucleus accumbens regardless of the depressive-like behavior induction in mice. *Eur. J. Neurosci.* 48, 1635–1646. doi:10.1111/ejn.13994

Provensi, G., Costa, A., Rani, B., Becagli, M. V., Vaiano, F., Passani, M. B., et al. (2022). New β-arylchalcogeno amines with procognitive properties targeting carbonic anhydrases and monoamine oxidases. *Eur. J. Med. Chem.* 244, 114828. doi:10.1016/j.ejmech.2022.114828

Rani, B., Santangelo, A., Romano, A., Koczwara, J. B., Friuli, M., Provensi, G., et al. (2021). Brain histamine and oleoylethanolamide restore behavioral deficits induced by chronic social defeat stress in mice. *Neurobiol. Stress* 14, 100317. doi:10.1016/j.ynstr.2021.100317

Ridet, J. L., Malhotra, S. K., Privat, A., and Gage, F. H. (1997). Reactive astrocytes: cellular and molecular cues to biological function. *Trends Neurosci.* 20, 570–577. doi:10.1016/s0166-2236(97)01139-9

Sasmita, A. O., Ling, A. P. K., Voon, K. G. L., Koh, R. Y., and Wong, Y. P. (2018). Madecassoside activates anti-neuroinflammatory mechanisms by inhibiting lipopolysaccharide-induced microglial inflammation. *Int. J. Mol. Med.* 41, 3033–3040. doi:10.3892/ijmm.2018.3479

Sawicki, C. M., Kim, J. K., Weber, M. D., Faw, T. D., Mckim, D. B., Madalena, K. M., et al. (2019). Microglia promote increased pain behavior through enhanced inflammation in the spinal cord during repeated social defeat stress. *J. Neurosci.* 39, 1139–1149. doi:10.1523/JNEUROSCI.2785-18.2018

Sbrini, G., Brivio, P., Fumagalli, M., Giavarini, F., Caruso, D., Racagni, G., et al. (2020). *Centella asiatica* L. Phytosome improves cognitive performance by promoting Bdnf expression in rat prefrontal cortex. *Nutrients* 12, 355. doi:10.3390/nu12020355

Sharifi-Rad, M., Mnayer, D., Morais-Braga, M. F. B., Carneiro, J. N. P., Bezerra, C. F., Coutinho, H. D. M., et al. (2018). Echinacea plants as antioxidant and antibacterial agents: from traditional medicine to biotechnological applications. *Phytother. Res.* 32, 1653–1663. doi:10.1002/ptr.6101

Shen, C. L., Hong, K. J., and Kim, S. W. (2003). Effects of ginger (*Zingiber officinale* Rosc.) on decreasing the production of inflammatory mediators in sow osteoarthrotic cartilage explants. *J. Med. Food* 6, 323–328. doi:10.1089/109662003772519877

Shen, C. L., Hong, K. J., and Kim, S. W. (2005). Comparative effects of ginger root (*Zingiber officinale* Rosc.) on the production of inflammatory mediators in normal and osteoarthrotic sow chondrocytes. *J. Med. Food* 8, 149–153. doi:10.1089/jmf.2005.8.149

Shimo, Y., Cathomas, F., Lin, H. Y., Chan, K. L., Parise, L. F., Li, L., et al. (2023). Social stress induces autoimmune responses against the brain. *Proc. Natl. Acad. Sci. U. S. A.* 120, e2305778120. doi:10.1073/pnas.2305778120

Sung, B., Lim, G., and Mao, J. (2003). Altered expression and uptake activity of spinal glutamate transporters after nerve injury contribute to the pathogenesis of neuropathic pain in rats. *J. Neurosci.* 23, 2899–2910. doi:10.1523/JNEUROSCI.23-07-02899.2003

Sweitzer, S. M., Schubert, P., and Deleo, J. A. (2001). Propentofylline, a glial modulating agent, exhibits antiallodynic properties in a rat model of neuropathic pain. *J. Pharmacol. Exp. Ther.* 297, 1210–1217.

Takata, F., Nakagawa, S., Matsumoto, J., and Dohgu, S. (2021). Blood-Brain Barrier Dysfunction amplifies the development of neuroinflammation: understanding of cellular events in brain microvascular endothelial cells for prevention and treatment of BBB dysfunction. *Front. Cell Neurosci.* 15, 661838. doi:10.3389/fncel.2021.661838

Vachon-Presseau, E. (2018). Effects of stress on the corticolimbic system: implications for chronic pain. *Prog. Neuropsychopharmacol. Biol. Psychiatry* 87, 216–223. doi:10.1016/j.pnpbp.2017.10.014

Veerendra Kumar, M. H., and Gupta, Y. K. (2003). Effect of *Centella asiatica* on cognition and oxidative stress in an intracerebroventricular streptozotocin model of Alzheimer's disease in rats. *Clin. Exp. Pharmacol. Physiol.* 30, 336–342. doi:10.1046/j.1440-1681.2003.03842.x

Wang, L., Guo, T., Guo, Y., and Xu, Y. (2020). Asiaticoside produces an antidepressant-like effect in a chronic unpredictable mild stress model of depression in mice, involving reversion of inflammation and the PKA/pCREB/BDNF signaling pathway. *Mol. Med. Rep.* 22, 2364–2372. doi:10.3892/mmr.2020.11305

Weber, M. D., Godbout, J. P., and Sheridan, J. F. (2017). Repeated social defeat, neuroinflammation, and behavior: monocytes carry the signal. *Neuropsychopharmacology* 42, 46–61. doi:10.1038/npp.2016.102

Weng, H. R., Chen, J. H., and Cata, J. P. (2006). Inhibition of glutamate uptake in the spinal cord induces hyperalgesia and increased responses of spinal dorsal horn neurons to peripheral afferent stimulation. *Neuroscience* 138, 1351–1360. doi:10.1016/j.neuroscience.2005.11.061

Wolke, D., and Lereya, S. T. (2015). Long-term effects of bullying. *Arch. Dis. Child.* 100, 879–885. doi:10.1136/archdischild-2014-306667

Wood, S. K., Wood, C. S., Lombard, C. M., Lee, C. S., Zhang, X. Y., Finnell, J. E., et al. (2015). Inflammatory factors mediate vulnerability to a social stress-induced depressive-like phenotype in passive coping rats. *Biol. Psychiatry* 78, 38–48. doi:10.1016/j.biopsych.2014.10.026

Wright, K. M., Bollen, M., David, J., Speers, A. B., Brandes, M. S., Gray, N. E., et al. (2022). Pharmacokinetics and pharmacodynamics of key components of a standardized *Centella asiatica* product in cognitively impaired older adults: a phase 1, double-blind, randomized clinical trial. *Antioxidants (Basel)* 11, 215. doi:10.3390/antiox11020215

Yeung, K. S., Hernandez, M., Mao, J. J., Haviland, I., and Gubili, J. (2018). Herbal medicine for depression and anxiety: a systematic review with assessment of potential psycho-oncologic relevance. *Phytother. Res.* 32, 865–891. doi:10.1002/ptr.6033

Zhang, Z. J. (2004). Therapeutic effects of herbal extracts and constituents in animal models of psychiatric disorders. *Life Sci.* 75, 1659–1699. doi:10.1016/j.lfs.2004.04.014

frontiers | Frontiers in Pharmacology

TYPE Review
PUBLISHED 26 August 2024
DOI 10.3389/fphar.2024.1426769



OPEN ACCESS

EDITED BY
Qi Liang,
Air Force Medical University, China

REVIEWED BY
Wenzhi Hao,
Jinan University, China
Dang Chun,
Sichuan University, China

*CORRESPONDENCE
Yanyan Sai,
50041450@qq.com

RECEIVED 03 May 2024
ACCEPTED 06 August 2024
PUBLISHED 26 August 2024

CITATION
Lv S, Yang N, Lu Y, Zhang G, Zhong X, Cui Y, Huang Y, Teng J and Sai Y (2024) The therapeutic potential of traditional Chinese medicine in depression: focused on the modulation of neuroplasticity.
*Front. Pharmacol.* 15:1426769.
doi: 10.3389/fphar.2024.1426769



# The therapeutic potential of traditional Chinese medicine in depression: focused on the modulation of neuroplasticity

Shimeng Lv[1], Ni Yang[1], Yitong Lu[1], Guangheng Zhang[1], Xia Zhong[2], Yaru Cui[3], Yufei Huang[4], Jing Teng[1] and Yanyan Sai[5]*

[1]Department of First Clinical Medical College, Shandong University of Traditional Chinese Medicine, Jinan, China, [2]Institute of Child and Adolescent Health, School of Public Health, Peking University, Beijing, China, [3]Innovative Institute of Chinese Medicine and Pharmacy, Shandong University of Traditional Chinese Medicine, Jinan, China, [4]Ruijin Hospital Affiliated to Shanghai Jiaotong University School of Medicine, Shanghai, China, [5]University Town Hospital, Afiliated Hospital of Shandong University of Traditional Chinese Medicine, Jinan, China

Depression, a mood disorder characterized by a persistent low mood and lack of enjoyment, is considered the leading cause of non-fatal health losses worldwide. Neuroplasticity refers to the brain's ability to adapt to external or internal stimuli, resulting in functional and structural changes. This process plays a crucial role in the development of depression. Traditional Chinese Medicine (TCM) shows significant potential as a complementary and alternative therapy for neurological diseases, including depression. However, there has been no systematic summary of the role of neuroplasticity in the pathological development of depression and TCM Interventions currently. This review systematically summarized recent literature on changes in neuroplasticity in depression and analyzed the regulatory mechanisms of active metabolites in TCM and TCM formulas on neuroplasticity in antidepressant treatment. Additionally, this review discussed the limitations of current research and the application prospects of TCM in regulating neuroplasticity in antidepressant research.

KEYWORDS

**depression, major depressive disorder, antidepressant, traditional Chinese medicine, neuroplasticity**

## 1 Introduction

Depression is a mood illness marked by enduring feelings of sadness and lack of enjoyment. The global average incidence rate is about 4.4%. By 2030, depression is expected to become the leading cause of disease burden worldwide, being the primary contributor to non-fatal health loss globally (Rehm and Shield, 2019; Bayes et al., 2020). Selective serotonin reuptake inhibitors (SSRIs) and other Western medicine therapies are the mainstays of treatment; however, most medications have delayed effects, high rates of non-responsiveness, and significant side effects such as headaches, nausea, weight gain, and chronic dysfunction (Wang et al., 2019; Qu et al., 2021; Wei et al., 2022).

Therefore, developing more effective and safer antidepressant drugs has become an urgent problem to be solved. Traditional Chinese Medicine (TCM) has a long history of understanding and treating depression. TCM is known for its multi metabolite, multi target,

multi link, and multi pathway characteristics, which can act on multiple aspects of the disease and have high efficacy and low toxicity. This highlights the advantages and good prospects of TCM in treating depression. Importantly, compared to Western medicine, they have the advantages of easy use, good therapeutic effects, minimal dosage, and fewer side effects. Due to the shortcomings of existing antidepressants and the urgent market demand, research on the antidepressant mechanism of TCM has attracted much attention (Zhuang et al., 2023).

Neuroplasticity refers to the brain's ability to respond to external or internal stimuli from the environment or organs, resulting in functional and structural changes (Vints et al., 2022). Neuroplasticity is closely related to depression (Tartt et al., 2022), and is a significant focus for the development of future antidepressant drugs (Duman et al., 2016). However, there remains a notable lack of a systematic overview regarding the role of neuroplasticity in the pathological development of depression and the intervention of TCM.

Based on the above findings, this review systematically summarized the changes in neuroplasticity observed in clinical and preclinical studies of depression by searching relevant literature from recent years. Furthermore, it explored into the pharmacological mechanisms through which TCM modulated neuroplasticity to treat depression, providing scientific basis for subsequent basic research and clinical applications.

# 2 Review methodology

To investigate how TCM exerted antidepressant effects by regulating neuroplasticity, we conducted a comprehensive search of articles in PubMed, Embase, Web of Science, and ScienceDirect databases. The search keywords included "Traditional Chinese Medicine," "Chinese herbal medicine," "herb," "Traditional Chinese Medicine formulas," "Traditional Chinese Medicine metabolites," "depression," "major depressive disorder," "syntactic plasticity," and "neuroplasticity." The retrieved articles were reviewed by two independent reviewers based on their titles, abstracts, and full texts, adhering to specific inclusion and exclusion criteria. The inclusion criteria were: 1) Original articles written in English; 2) Articles that examined the relevant mechanisms of TCM in regulating neuroplasticity for the treatment of depression. Exclusion criteria were as follows: 1) Articles written in any language other than English; 2) Gray literature; 3) Editorials; 4) Review articles; 5) Duplicate publications.

# 3 Overview of neuroplasticity

## 3.1 Definition of neuroplasticity

Neuroplasticity is a crucial concept in life sciences, describing how the brain changes and adapts to environmental changes by continually forming new neural connections (Price and Duman, 2020). It represents the adaptability of the nervous system, enabling it to adjust to learning, memory, environmental changes, and rehabilitation following brain injury. The main mechanisms include the regulation of synaptic strength, structural remodeling, and the regulation of intrinsic neuronal properties. These processes are dynamic, involving changes in the number of brain nuclei and structures, various functions, and numerous interactions (Xing and Bai, 2020; Dzyubenko and Hermann, 2023). Neuroplasticity is essential for understanding brain development, learning, and the regulation of homeostasis in the central nervous system (CNS).

## 3.2 Classification of neuroplasticity

Neuroplasticity includes two primary types: structural plasticity and functional plasticity. Structural plasticity refers to changes in mechanisms that promote neurogenesis, the formation of dendritic spines, and the growth and repair of axons. It includes changes in the number and connectivity of synapses, the density of dendritic spines, and modifications in neural processes like axons and dendrites, as well as variations in the number of neuronal cells (De Paola et al., 2006; Knott et al., 2006). On the other hand, functional plasticity involves synaptic changes between neurons without modifying their physical structure, such as long-term potentiation (LTP) and long-term depression (LTD) effects (Castillo, 2012; Marsden, 2013; Diering and Huganir, 2018). LTP and LTD are crucial mechanisms that affect cognitive and emotional functions in depression patients. Intense and sustained stimulation leads to an increase in neuronal discharge, which in turn enhances the strength of synapses. This process facilitates learning and memory, thereby promoting LTP. In contrast, LTD is characterized by a decrease in the efficacy and connectivity of neuronal synapses (Figure 1 showed a schematic diagram of neurogenesis).

Neuroplasticity is regulated by several key mechanisms, one of which is the brain-derived neurotrophic factor (BDNF)/tyrosine kinase receptor B (TrkB) signaling pathway. The synthesis of BDNF is triggered by the activation of cyclic adenosine monophosphate (cAMP) responsive element binding protein (CREB). CREB is pivotal in facilitating LTP and synaptic plasticity. When BDNF binds to TrkB receptors, it triggers various signaling cascades, such as the mitogen-activated protein kinase/extracellular signal-regulated kinase (MAPK/ERK), phosphoinositide 3-kinase (PI3K), and mammalian target of rapamycin (mTOR) pathways, which are responsible for spine enlargement and increased glutamate sensitivity (Figure 2 showed the regulatory mechanism) (Bourtchuladze et al., 1994; Tanaka et al., 2008; Tejeda and Díaz-Guerra, 2017).

# 4 Neuroplasticity and depression

## 4.1 Changes in neuroplasticity in depression

### 4.1.1 Clinical studies

Meta-analysis is a prominent method for evaluating the effectiveness of public health interventions (Tanner-Smith and Grant, 2018). In the pathophysiology of depression, impaired neuroplasticity plays a crucial role, as indicated by a meta-analysis conducted on the cerebrospinal fluid of individuals with unipolar depression (Mousten et al., 2022). Studies have shown that the increase in motor evoked potential amplitude, induced by paired associative stimulation, weakens during severe depressive episodes

and normalizes during remission. It suggests the presence of LTP deficits in individuals with depression (Player et al., 2013; Kuhn et al., 2016). Furthermore, compared to healthy subjects, patients with depression, particularly those with refractory depression, exhibit impaired neuroplasticity in the dorsolateral prefrontal cortex. Female patients with depression also demonstrate persistent LTD-like plasticity deficits (Noda et al., 2018; Yu et al., 2020; Kaneko et al., 2024). Abnormal changes in neuroplasticity-related proteins have been observed in depression patients (Hidese et al., 2020). The ratio of BDNF to leptin levels has been associated with treatment responses in depression and may also be related to the neuroplasticity of depression, as evidenced by a 12-week follow-up study (An et al., 2019).

### 4.1.2 Preclinical studies

#### 4.1.2.1 Depression model induced by stress

Stress is recognized as a normal physiological and psychological response to both positive and negative situations. Chronic stress, in particular, plays a key role in the development of mental illnesses such as depression (Ray et al., 2017; Beurel et al., 2020; Monroe and Harkness, 2022). Prolonged exposure to chronic stress exacerbates the phagocytosis of synaptic elements and results in defects in neuroplasticity (Kokkosis et al., 2024). Synaptic pruning, as a developmental process, is closely related to synaptic plasticity. In models of depression induced by chronic unpredictable mild stress (CUMS), excessive activation of microglia leads to exaggerated synaptic pruning (Zhang et al., 2022a), accompanied by impairments in synaptic plasticity (Li et al., 2021a; Yan et al., 2021). Early-life stress increases susceptibility to depression in adolescent mice by regulating the miR-34c-5p/synaptotagmin-1 (SYT1) axis and disrupting hippocampal neuroplasticity (Yu et al., 2024). In a combined model, adult female rats subjected to maternal-infant separation (MS) and CUMS exhibited more severe depressive and anxiety-like behaviors, potentially linked to compromised synaptic plasticity (Huang et al., 2021). In a depression model where insomnia was induced by CUMS combined with sleep deprivation, dendritic spines in the hippocampal dentate gyrus (DG) region were damaged, neural networks were disrupted, and neuroplasticity was inhibited (Li et al., 2022). Studies have also demonstrated that the absence of bombesin receptor-activated protein homologous protein affects hippocampal synaptic plasticity and exacerbates CUMS-mediated behavioral changes (Yao et al., 2023). Mechanistic research has revealed that CUMS alters synaptic plasticity in the nucleus accumbens (NAc) by influencing Kv4.2 channels through glycogen synthase kinase 3β (GSK3β)-dependent mechanisms (Aceto et al., 2020). Additionally, CUMS can disrupt the synaptic plasticity of regenerating neurons in the hippocampus of ischemic rats via astrocytic glutamate transporter-1 (Yu et al., 2019).

#### 4.1.2.2 Depression model induced by social isolation

Social isolation can induce fatigue, behavioral changes, substance abuse, and various mental illnesses. These effects can be sustained and irreversible, impacting both humans and animals and increasing the risk of developing mental illness (Jaremka et al., 2014; Hueston et al., 2017). Neuroplasticity-related signals play a crucial role in the impact of induced isolation on sexual and neurological behavioral deficits (Liu et al., 2020). Animals subjected to chronic social isolation (CSIS) displayed depressive-like behavior (Perić et al., 2021), accompanied by proteomic findings showing dysregulated expression of synaptic plasticity-related proteins (Filipović et al., 2023). Moreover, animals raised in isolation exhibited immature dendritic spines that appear small and thin, with impaired neuroplasticity observed through LTP testing (Medendorp et al., 2018). However, treatment with fluoxetine has been shown to alleviate depressive-like behavior induced by CSIS and regulate neuroplasticity-related proteins (Filipović et al., 2022).

#### 4.1.2.3 Depression mode induced by corticosterone

The hypothalamic-pituitary-adrenal (HPA) axis is a vital metabolite of the neuroendocrine system. When active, the anterior pituitary gland releases adrenocorticotropin (ACTH) into the bloodstream. This signal is received by the paraventricular nucleus of the hypothalamus, which then produces corticotropin-releasing hormone. ACTH, in turn, stimulates the adrenal cortex to release cortisol (CORT) (Frankiensztajn et al., 2020). Excessive activation of the HPA axis correlates significantly with sustained elevation of CORT levels and depression. Elevated CORT levels observed in individuals with depression closely correlate with the severity of depressive symptoms and poor treatment outcomes (Karin et al., 2020). Chronic exposure to CORT reduces the structural plasticity of astrocytes in the hippocampus of mice, leading to hippocampal atrophy (Zhang et al., 2015). Mice treated with CORT exhibit depressive-like behavior accompanied by changes in synaptic plasticity (Crupi et al., 2013; Freitas et al., 2016). Mechanistic studies have shown that CORT reduces synaptic density and vesicle recycling by downregulating BNIP3 like (BNIP3L)/NIX, thereby inhibiting mitochondrial autophagy (Choi et al., 2021).

#### 4.1.2.4 Lipopolysaccharide (LPS) induced depression model

LPS can be found in the outer wall of Gram-negative bacterial cells, consisting of lipids and polysaccharides. Mouse models induced with LPS to mimic depression-like symptoms are commonly used to study the mechanisms of inflammation-related depression and the therapeutic effects of various drugs (Yin et al., 2023). Early reports indicated that LPS administration could induce LTP and depression in the hippocampal CA1 area (Jo et al., 2001). Recent studies have found that LPS mediates depressive-like behavior by promoting neuroinflammation in the basolateral amygdala (BLA), enhancing glutamatergic synaptic transmission, and increasing the intrinsic excitability of BLA projection neurons (Zheng et al., 2021). Wu et al. (2019), through a combination of proteomics and metabolomics, found that LPS intervention in mice disrupts glutamatergic transmission and Ephrin receptor signaling, potentially leading to impaired hypothalamic synaptic plasticity and depressive-like behavior.

## 4.2 Impact of antidepressant treatment on neuroplasticity

### 4.2.1 Chemicals acting on the CNS

Fluoxetine, a widely used SSRI in clinical practice, exerts its antidepressant effects by enhancing synaptic plasticity (Qian et al., 2024). It alos modified mood behaviors and hippocampal neuroplasticity by disrupting the nNOS-CAPON interaction that links postsynaptic 5-HT1AR activation (Shi et al., 2022). Additionally, fluoxetine enhances hippocampal neuroplasticity by promoting axonal formation induced by growth-associated protein

TABLE 1 Regulation of antidepressant chemicals on neuroplasticity.

| Chemical | Molecular formula | CAS NO. | Main mechanism of action | Reference |
|---|---|---|---|---|
| Fluoxetine | $C_{17}H_{18}F_3NO$ | 5410-89-3 | Enhanced synaptic plasticity | Qian et al. (2024) |
| | | | Modified mood behaviors and hippocampal neuroplasticity by disrupting the nNOS-CAPON interaction that links postsynaptic 5-HT1AR activation | Shi et al. (2022) |
| | | | Enhanced hippocampal neuroplasticity by promoting axonal formation induced by GAP-43 | Zavvari et al. (2020) |
| | | | Preventing LTD and spatial memory deficits caused by stress | Han et al. (2015) |
| Citalopram | $C_{20}H_{21}FN_2O$ | 59729-33-8 | Combined use with *Punica granatum* can alleviate damage to dendritic spines in the DG region of the hippocampus | Vega-Rivera et al. (2023) |
| Agomelatine | $C_{15}H_{17}NO_2$ | 138112-76-2 | Modulating BDNF signaling, synaptic plasticity, and epigenetic remodeling | Martin et al. (2017) |
| | | | Restored the activity of hippocampal neurons affected by stress and promotes adult hippocampal neurogenesis | Dagyte et al. (2010) |
| Ketamine | $C_{13}H_{16}ClNO$ | 6740-88-1 | Modulating neuroplasticity | Clarke et al. (2017) |
| | | | Inducing postsynaptic enhancement in the hippocampal CA1 region | Kim and Monteggia (2020) |
| | | | Increased neural plasticity, including synaptic interactions | Kopelman et al. (2023) |
| | | | Prevent the loss of critical neural circuit connections caused by stress | Aleksandrova et al. (2020) |
| Metformin | $C_4H_{11}N_5$ | 657-24-9 | Upregulation of the expression of plasticity markers such as synaptic proteins, deacetylase-1, AMP activated protein kinase, and BDNF | Muñoz-Arenas et al. (2020) |
| | | | Improved the survival rate of hippocampal NeuN positive cells and increase the number of BDNF positive cells stimulated by fluoxetine, thereby enhancing its effect on neural plasticity | Mendonça et al. (2022) |
| | | | Improving synaptic plasticity damage | Zhou et al. (2021) |
| | | | Improving the expression of synaptic plasticity markers | Lv et al. (2023) |
| $H_2S$ | $H_2S$ | 7783-06-4 | Improving synaptic plasticity in hippocampus | Liu et al. (2024) |

43 (GAP-43) (Zavvari et al., 2020). Pre-treatment with fluoxetine has been shown to prevent stress-induced LTD and spatial memory deficits in the hippocampus of rats (Han et al., 2015). Citalopram, another SSRI, is composed of two enantiomers, R-citalopram and S-citalopram, which inhibit serotonin (5-HT) reuptake in the brain, thereby exerting an antidepressant effect (Yan et al., 2023a). When combined with *Punica granatum*, citalopram can alleviate damage to dendritic spines in the hippocampal DG region (Vega-Rivera et al., 2023).

Agomelatine, a synthetic analogue of melatonin, exerts its antidepressant effects by stimulating melatonin receptors (MT1 and MT2) and antagonizing 5-HT2C receptors (Maddukuri et al., 2021). Research indicates that agomelatine improves pathological behavior in stressed mice by modulating BDNF signaling, synaptic plasticity, and epigenetic remodeling (Martin et al., 2017). It also demonstrates beneficial effects in mitigating stress-induced brain damage, as it restores the activity of hippocampal neurons affected by stress and promotes adult hippocampal neurogenesis (Dagyte et al., 2010).

Ketamine, a non-competitive N-methyl-D-aspartate receptor (NMDAR) antagonist, specifically inhibits GluN2B-containing NMDARs on inhibitory GABAergic interneurons (Sato et al., 2022). Its antidepressant mechanism involves modulating neuroplasticity (Clarke et al., 2017), and low concentrations of ketamine (20 μM) can induce postsynaptic enhancement in the hippocampal CA1 (Kim and Monteggia, 2020). Its antidepressant effects are mediated by increased neuroplasticity, including synaptic actions (Kopelman et al., 2023), and it can "reset the system" by participating in synaptic plasticity processes to reverse stress-induced loss of key neural circuit connections (Aleksandrova et al., 2020). In animal models with chronic pain and depression, TIAM1-mediated synaptic plasticity is a crucial factor in the antidepressant effect of ketamine (Ru et al., 2022). Ketamine may also exert rapid antidepressant effects by enhancing neuroplasticity, triggering autophagy, and preventing ferroptosis in the nucleus (Zhang et al., 2022b). Studies have found that ketamine-induced hippocampal synaptic plasticity during antidepressant treatment depends on 4E binding proteins (Aguilar-Valles et al., 2021).

### 4.2.2 Other types of chemicals

Metformin is the first-line treatment for type 2 diabetes, primarily acting by reducing liver gluconeogenesis and enhancing glucose metabolism. It also exhibits pleiotropic effects (LaMoia and Shulman, 2021). Beyond its antidiabetic role, metformin has been investigated for its potential in treating depression. Studies indicate that compared to other oral hypoglycemic drugs, metformin is associated with a lower risk of depression and demonstrates pleiotropic effects in depression management (Yu et al., 2022).

Additionally, metformin can upregulate the expression of plasticity markers such as synapsin, sirtuin-1, AMP-activated protein kinase, and BDNF (Muñoz-Arenas et al., 2020). When combined with fluoxetine, metformin enhances the survival of NeuN-positive cells in the hippocampus and increases the number of BDNF-positive cells stimulated by fluoxetine, thereby enhancing its impact on neuroplasticity (Mendonça et al., 2022). Furthermore, metformin has been shown to mitigate synaptic plasticity damage induced by LPS in rats (Zhou et al., 2021) and improve the expression of synaptic plasticity markers [anti-microtubule-associated protein 2, synaptophysin (SYP), postsynaptic density protein 95], thereby alleviating depressive-like behavior in mice with allergic rhinitis (AR) (Lv et al., 2023). Hydrogen sulfide ($H_2S$) is recognized as the third endogenous gas transmitter and can be produced in mammals through four enzyme pathways (Wu et al., 2018). $H_2S$ has been found to improve hippocampal synaptic plasticity in a Warburg-dependent manner, alleviating depression related to Parkinson's disease (PD) (Liu et al., 2024) (Table 1).

In summary, neuroplasticity undergoes alterations in patients with depression and is also impaired in stress-induced, social isolation-induced, CORT-induced, and LPS-induced depression models. Substances like fluoxetine, ketamine, and metformin can mitigate depressive symptoms by modulating neuroplasticity, suggesting that targeted manipulation of neuroplasticity offers potential for treating depression. However, fluoxetine carries specific adverse effects in therapeutic contexts, including the potential for hallucinations, hepatotoxicity, neurotoxicity, and addiction, which may restrict its clinical application.

# 5 Pharmacological mechanisms of TCM

At present, the treatment of depression is a major issue in the medical field, and neuroplasticity is closely related to depression. Regulation based on neuroplasticity is one of the potential important measures for the treatment of depression. However, the current Western medicine for treating depression is mainly developed based on the "monoamine neurotransmitter hypothesis" of depression, but drug dependence and withdrawal reactions are common. Therefore, the development of new antidepressant drugs has become a hot topic at present. TCM has unique advantages in preventing and treating depression, including its overall concept, syndrome differentiation, and treatment methods, as well as the specific characteristics of its multiple components and targets, which are beneficial to the overall internal environment while treating depression (Zhuang et al., 2023). Numerous studies have shown that the active metabolites and herbal formulas in TCM are involved in regulating neuroplasticity during the process of antidepressant treatment.

## 5.1 Active metabolites of TCM

### 5.1.1 Flavonoids

Engeletin, a flavonoid metabolite initially extracted from the leaves of *Astragalus mongholicus* Bunge (Huang et al., 2011), is a potent natural metabolite with antioxidant and anti-inflammatory properties (Fang et al., 2023). Recent research has shown that Engeletin exerts antidepressant effects by activating the BDNF/TrkB/mTORC1 signaling pathway and enhancing synaptic plasticity in the prefrontal cortex (Xu et al., 2023). Baicalein, an important flavonoid found in the roots *Scutellaria baicalensis* Georgi, is frequently used in Chinese medicine and herbal tea preparations to promote wellbeing (Chandrashekar and Pandi, 2022). In preclinical studies of antidepressant effects, baicalein has been found to activate the BDNF/TrkB/CREB signaling pathway and protect against synaptic plasticity damage in mice with depression related to PD (Zhao et al., 2021). It also increases the ratio of mature BDNF (mBDNF) to proBDNF, regulates neuronal survival and synaptic plasticity, and suppresses neuroinflammation, effectively alleviating LPS-induced depressive symptoms in mice (Liu et al., 2022). Baicalin, extracted from *S. baicalensis* Georgi, has significant biological activity, including anti-inflammatory properties (Guo et al., 2019). Its antidepressant effect involves regulating the expression of synaptophysin (SYP), PSD95, BDNF, and TrkB, activating the Rac1-cofilin pathway, and enhancing synaptic plasticity (Lu et al., 2019).

Quercitrin, a naturally occurring flavonoid found in various fruits and vegetables, is commonly used as a dietary metabolite and supplement (Chen et al., 2022a). In mice with LPS-induced depression, quercitrin intervention could improve hippocampal damage, restore the abnormal expression of the pCREB/BDNF/PSD95/Synapsin1 pathway, regulates the PI3K/AKT/NF-κB signaling pathway, and enhances neuroplasticity (Sun et al., 2021). Luteolin, another natural flavonoid found in plants such as *Chrysanthemum indicum* L., *Capsicum annuum* L., and *Perilla frutescens* (L.) Britton has been studied for its pharmacological mechanism in treating late-onset depression, involving the regulation of neuroplasticity-related proteins (Li et al., 2021b; Liu et al., 2023; Rauf et al., 2024).

Soy isoflavones (SI), essential metabolites of *Glycine max* (L.) Merr., have different biological functions. SI can upregulate the expression of phosphorylated SYP (p-SYP) and PSD95 in the hippocampus of mice, inhibit neuroinflammation, regulate tryptophan metabolism, and reverse LPS-induced depressive behavior (Lu et al., 2022). Additionally, S-equol, a metabolite of dietary soy isoflavones, has demonstrated antidepressant effects by increasing synaptic plasticity proteins and inhibiting neuroinflammation (Lu et al., 2021). Silibinin, a polymorphic flavonoid extracted from milk thistle [*Silybum marianum* (L.) Gaertn.] (Ma et al., 2023), exerts its antidepressant effects by improving neuroplasticity and increasing neurotransmitter levels (Yan et al., 2015).

### 5.1.2 Polyphenols

Polyphenols, metabolites widely distributed in a variety of plants, have garnered significant interest for their potential pharmacological actions, particularly their immune-stimulating and anticancer activities (Wang et al., 2022a). These metabolites have been found to enhance brain function by directly influencing cells and processes in the CNS (Grabska-Kobyłecka et al., 2023). Curcumin,a primary bioactive polyphenolic metabolite extracted from the rhizomes of *Curcuma longa* L., has been extensively studied for its therapeutic properties. In an ovariectomy-induced depression model, Curcumin was found to be a safe and effective regulator of 5-

TABLE 2 Information on the action of active metabolites in TCM.

| Category | Active metabolites | Source information | *In vivo*/ *in vitro* | Modeling method | Dosage | Behavioral testing evaluation | Main pharmacological mechanisms | References |
|---|---|---|---|---|---|---|---|---|
| Flavonoids | Engeletin | *Astragalus mongholicus Bunge* | *In vivo* | CRS | 2.5, 5, 10, 20 mg/kg | FST, TST, OFT, SPT | Activation of BDNF/TrkB/mTORC1 signaling pathway and regulation of PFC synaptic plasticity | Xu et al. (2023) |
| | Baicalein | *Scutellaria baicalensis* Georgi | *In vivo* | Rotenone | 300 mg/kg | TST, SPT, OFT, Rotarod test | Activating the BDNF/TrkB/CREB signaling pathway to improve neural plasticity | Zhao et al. (2021) |
| | | | *In vivo* and *in vitro* | LPS | *In vivo*: 3 mg/kg | FST, TST | Increase the proportion of mBDNF/proBDNF to regulate neuronal survival and synaptic plasticity | Liu et al. (2022) |
| | Baicalin | *Scutellaria baicalensis* Georgi | *In vivo* | CMS | 25, 50, 100 mg/kg | OFT, FST, SPT | Promote the expression of BDNF and CREB, regulate neuronal survival and synaptic plasticity | Lu et al. (2019) |
| | Quercitrin | Multiple fruits and vegetables | *In vivo* | LPS | 10, 20, 30 mg/kg | FST, TST, OFT, SPT | Inhibiting Neuroinflammation PI3K/AKT/NF-κB Signal Transduction and Improving Damaged CREB/BDNF Neuroplastic Signal Transduction | Sun et al. (2021) |
| | luteolin | *Chrysanthemum indicum L.*, *Capsicum annuum L.*, and *Perilla frutescens (L.) Britton* | *In vivo* | CUMS | 25 mg/kg | SPT, OFT, FST, MWM | Regulating Neuroplasticity Related Proteins | Liu et al. (2023) |
| | Soy isoflavones | *soybeans* | *In vivo* | LPS | 10, 20, 40 mg/kg | FST, TST, OFT, SPT | Upregulation of hippocampal SYP phosphorylation and expression of PSD95 | Lu et al. (2022) |
| Polyphenols | Curcumin | *Curcuma longa L* | *In vivo* | Ovariectomised | 100 mg/kg | FST | Regulating neural plasticity | Abd-Rabo et al. (2019) |
| | | | *In vivo* | CUMS | 40 mg/kg | OFT, SPT, FST | Regulating neural plasticity related proteins (PSD95 and SYP) | Zhang et al. (2014) |
| Alkaloids | Berberine | *Coptis chinensis* Franch | *In vivo* | CUMS | 2.5, 5, 10 mg/kg | OFT, FST, Novelty-suppressed feeding test (NSFT) | Promote synaptic plasticity and regulate tryptophan metabolism by inhibiting IDO1 and activating TPH1 | Ge et al. (2023) |
| | | | *In vivo* | CORT | 100, 200 mg/kg | FST, TST, OFT, SPT | Inhibiting the activation of NLRP3 inflammasome to reduce neuroinflammatory response and promote synaptic plasticity and neurogenesis | Qin et al. (2023) |
| Saponins | Saikosaponin C | *Bupleurum chinense DC.* | *In vivo* and *in vitro* | *In vivo*: CSDS *In vitro*: LPS/ATP | *In vivo*: 0.5, 1 mg/kg | Social interaction TEST (SI), SPT, TST, FST, OFT | Inhibiting DNMT1 protein to reduce IL6 methylation, inducing decreased IL6 expression, and promoting synaptic plasticity | Bai et al. (2023) |

(Continued on following page)

TABLE 2 (*Continued*) Information on the action of active metabolites in TCM.

| Category | Active metabolites | Source information | *In vivo*/ *in vitro* | Modeling method | Dosage | Behavioral testing evaluation | Main pharmacological mechanisms | References |
|---|---|---|---|---|---|---|---|---|
| | Ginsenoside Rb1 | *Panax ginseng* C.A.Mey | *In vivo* | CUMS | 20 mg/kg | FST, TST, OFT, SPT | Regulating hippocampal synaptic plasticity through the miR-134 mediated BDNF pathway | Wang et al. (2022b) |
| | | | *In vivo* and *in vitro* | *In vivo*: CUMS *In vitro*: LPS-ATP stimulation | *In vivo*: 10 mg/kg | OFT, FST, SPT | Regulating mitophagy and NF-κB pathway to inhibit astrocyte pyroptosis, thereby inhibiting neuroinflammation and enhancing synaptic plasticity | Li et al. (2023a) |
| | Ginsenoside-Rg1 | *Panax ginseng* C.A.Mey | *In vivo* | LPS | 40 mg/kg | SPT, FST, OFT, EPM, MWM | It has a synergistic effect with volumetric running, with anti-inflammatory and improved neural plasticity functions | Wang et al. (2023a) |
| Terpenoids | Geniposide | *Gardenia jasminoides* J.Ellis | *In vivo* | prenatal restraint stress | 25, 50, 100 mg/kg | SPT, OFT, FST | Regulating the HPA axis and improving the expression of synaptic plasticity related proteins | Ma et al. (2024) |
| | Paeoniflorin | *Paeonia lactiflora Pall* | *In vivo* | CUMS | 20 mg/kg | SPT, FST, TST, MWM | Improving LTP in hippocampal CA1 region and upregulating hippocampal dendritic spine density and expression levels of BDNF and PSD95 | Liu et al. (2019) |
| | Oleanolic acid | *Olea europaea L* | *In vivo* | Maternal separation | 30 mg/kg | OFT, EPM, Splash test, FST | Both OA and UA can upregulate synapsin levels, and OA can also upregulate the expression level of PSD95 | Kong et al. (2023) |
| | Ursolic acid | Exists in various plants | | | | | | |
| Polysaccharides | Polysaccharides from *Polygonatum cyrtonema* Hua | *Polygonatum cyrtonema Hua* | *In vivo* | Single prolonged stress | 200, 400, 800 mg/kg | OFT, EPM, Fear conditioning task | Relieve oxidative stress and neuroinflammation, and act on the Nrf2/HO-1 signaling pathway to improve synaptic damage | Xie et al. (2024) |
| | Inulin | *Inula helenium L* | *In vivo* | CUMS | 0.037 g of inulin/kcal | SPT, FST, OFT, TST, EPM | Enhancing CREB/BDNF signaling to improve neurogenesis and synaptic plasticity | Wang et al. (2023b) |
| | Polysaccharide-rich fraction from *Schisandra chinensis* (Turcz.) Baill | *Schisandra chinensis* (Turcz.) Baill | *In vivo* | Olfactory bulbectomy | 50, 200, 800 mg/kg | FST, TST, Locomotor activity test | Improving abnormal synaptic plasticity (upregulating PSD95 expression), inhibiting excessive HPA axis activity, and regulating gut microbiota | Zhu et al. (2024) |
| Botanical drugs extracts | Saffron Extract (Affron®) | Saffron (*Crocus sativus L.*) | *In vivo* | Unpredictable chronic mild stress | 100, 200 mg/kg | SPT | Adjusting the HPA axis to increase hypothalamic neural plasticity | Kim et al. (2023) |
| | Blueberry Extract | Blueberry (*Vaccinium* spp.) | *In vivo* | LPS | 100, 200 mg/kg | OFT, FST | Downregulation of hippocampal AChE activity, inhibition of neuroinflammation, and potential protection of neuroplasticity | Spohr et al. (2023) |

(Continued on following page)

TABLE 2 (*Continued*) Information on the action of active metabolites in TCM.

| Category | Active metabolites | Source information | *In vivo*/ *in vitro* | Modeling method | Dosage | Behavioral testing evaluation | Main pharmacological mechanisms | References |
|---|---|---|---|---|---|---|---|---|
| Other types | Honokiol | *Magnolia grandiflora L* | *In vivo* and *in vitro* | *In vivo*: CUMS | 10 mg/kg | OFT, SPT | Activate the HIF-1α/ VEGF signaling pathway and upregulate the protein expression levels of SYP 1 and PSD 95 | Fan et al. (2022) |
| | Salidroside | *Rhodiola rosea L* | *In vivo* and *in vitro* | *In vivo*: CORT or LPS *In vitro*: CORT or nigericin | 20, 40 mg/kg | OFT, SPT, FST | Upregulation of BDNF expression, improvement of synaptic plasticity, and inhibition of P2X7/NF-κB/NLRP3 signaling pathway mediated pyroptosis | Chai et al. (2022) |
| | Crocin | *Crocus sativus L* | *In vivo* and *in vitro* | *In vivo*: CUMS | 12.5, 25 mg/kg | SPT, TST, FST, OFT | Regulating the Wnt/β-catenin signaling pathway to promote adult hippocampal neurogenesis | Tao et al. (2023a) |
| | | | *In vivo* | Prenatal stress | 10, 20, 40 mg/kg | OFT, TST, FST, SPT, NSFT | Regulating hippocampal synaptic plasticity related proteins | Wu et al. (2020) |
| | Panaxynol | *Panax ginseng* C.A.Mey | *In vivo* | CUMS | 1.0 mg/kg | OFT, EPM, SPT | Regulating the HPA axis, promoting the release of 5-HT and DA, and improving hippocampal synaptic plasticity | Sun et al. (2020) |

HT, similar to fluoxetine and neurotrophic E2, and was involved in regulating neuroplasticity (Abd-Rabo et al., 2019; Zia et al., 2021). Additionally, in the CUMS model, Curcumin was found to improve depressive-like behavior in animals by regulating the expression of synaptic plasticity proteins (Zhang et al., 2014).

### 5.1.3 Alkaloids

The defining characteristic uniting the diverse class of chemicals known as alkaloids is the presence of a nitrogen atom in a heterocyclic ring (Ziegler and Facchini, 2008). Berberine, an isoquinoline alkaloid derived from the Chinese botanical drug *Coptis chinensis* Franch. and related *Berberis* species, possesses a broad variety of pharmacological effects (Song et al., 2020). Studies have shown that Berberine effectively treats depression by inhibiting neuroinflammation and improving gut microbiota (Zhu et al., 2017; Yang et al., 2023a). Berberine has multi-target and multi-pathway antidepressant characteristics (Gao et al., 2024). Recent research has emphasized the impact of Berberine on neuroplasticity in the context of depression. In mouse models of depression treated with Berberine, an increase in neuronal and synaptic plasticity has been observed. Berberine targets enzymes such as tryptophan 5-hydroxylase one and indoleamine 2,3-dioxygenase one involved in tryptophan metabolism, thereby improving depressive symptoms in CUMS stimulated mice (Ge et al., 2023). Additionally, Berberine's antidepressant effect is accompanied by a reduction in neuroinflammatory responses through the inhibition of NLRP3 inflammasome activation, promoting plasticity and neurogenesis to alleviate neuronal damage (Qin et al., 2023).

### 5.1.4 Saponins

Saponins, naturally occurring substances found in a wide range of plants, have garnered interest for their potential pharmacological properties (Zhang et al., 2023). Saikosaponin C, a metabolite purified from the traditional Chinese botanical drug *Bupleurum chinense* DC., has been studied for its effects on depression. Recent reports indicate that saikosaponin C reduces IL6 levels by inhibiting DNA methyltransferase one protein, leading to a decrease in IL6 expression. This metabolite promotes synaptic plasticity and alleviates depression-like behavior induced by chronic social defeat stress (Pan et al., 2019; Bai et al., 2023).

Ginsenoside Rb1, one of the main ginsenosides found in *Panax ginseng* C.A.Mey., is known for its neuroprotective properties (Ni et al., 2022). Research has shown that ginsenoside Rb1 can alleviate depressive symptoms induced by CUMS by modulating hippocampal synaptic plasticity through the miR-134-mediated BDNF signaling pathway (Wang et al., 2022b). Additionally, ginsenoside Rb1 regulates mitochondrial autophagy and the NF-κB pathway to inhibit astrocyte apoptosis, thereby reducing neuroinflammation and enhancing synaptic plasticity to maintain nervous system homeostasis (Li et al., 2023a). Ginsenoside Rg1, another key metabolite of *P. ginseng* C.A.Mey., has gained attention for its potential in preventing neurological diseases, especially dementia and depression (Yang et al., 2023b). It has been found to synergize with exercise in treating depression by reducing inflammation and improving neuroplasticity (Wang et al., 2023a).

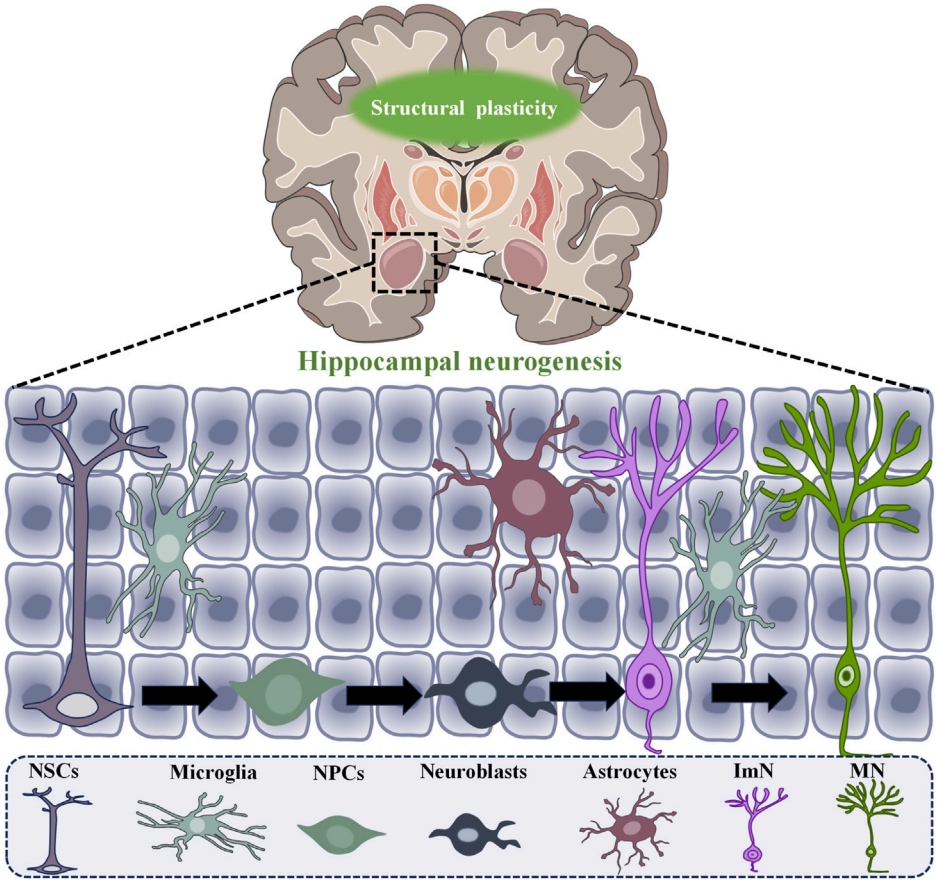


FIGURE 1
Schematic diagram of neurogenesis in structural plasticity.

### 5.1.5 Terpenoids

The largest class of natural products is terpenoids, offering a plethora of potential therapeutic candidates (Huang et al., 2012). *Gardenia jasminoides* J. Ellis contains a type of iridoid glycoside called geniposide, which has various of biological benefits, including anti-neurodegenerative effects (Shen et al., 2020a). In a mouse model of *postpartum* depression, researchers observed excessive activation of the HPA axis and abnormal expression of proteins related to synaptic plasticity. Treatment with geniposide can alleviate these pathological phenomena and improve depressive-like behavior in mice (Ma et al., 2024). Xia et al. (2021) found that iridoids from *Gardeniae fructus* exerted antidepressant-like effects by stimulating AMPAR/mTOR signaling to enhance synaptic plasticity. For over a millennium, *Paeonia lactiflora* Pall. has been used in TCM to address ailments related to pain, inflammation, and the immune system (Zhang and Wei, 2020). *Paeonia lactiflora* Pall. produces a water-soluble monoterpene glycoside known as paeoniflorin (Cao et al., 2023), effectively reversing LTP damage induced by CUMS in the hippocampal CA1 region. Additionally, it can prevent CUMS-induced changes in dendritic spine density in the mouse hippocampus and downregulate BDNF and postsynaptic density protein 95 (PSD95) expression (Liu et al., 2019).

The pentacyclic triterpenoid chemical oleanolic acid (OA) is a naturally occurring substance extracted from various plants, including *Olea europaea* L. (Luo et al., 2024). Ursolic acid (UA) is another naturally occurring pentacyclic triterpenoid found in plants (Li et al., 2023b). Kong et al. (2023) conducted a study comparing the antidepressant effects of OA and UA, and found that in a depression model induced by CMS, OA was more effective than UA at reversing the depressive-like behavior induced by MS. In their mechanistic study, it was found that both OA and UA treatments reversed the decrease in synapsin expression levels caused by MS, but only OA upregulated the expression level of PSD-95 (Kong et al., 2023).

### 5.1.6 Polysaccharides

Polysaccharides are carbohydrate polymers composed of at least ten monosaccharides linked by glycosidic linkages (Yi et al., 2020). They are found in plants, microbes, bacteria, fungi, and seaweed all contain polysaccharides, playing crucial roles in various physiological processes (Chen et al., 2017). Post-traumatic stress disorder (PTSD) is a type of depression syndrome, and Xie et al. (2024) found that polysaccharides from *Polygonatum cyrtonema* Hua can improve PTSD-induced behavioral abnormalities and synaptic damage in mice by reducing oxidative stress and neuroinflammation, and by acting on the Nrf2/HO-1 signaling pathway. Inulin, a non-digestible fructan-type carbohydrate, was originally isolated from the roots of *Inula helenium* L. (Illippangama et al., 2022). Studies suggest that inulin improves neurogenesis and

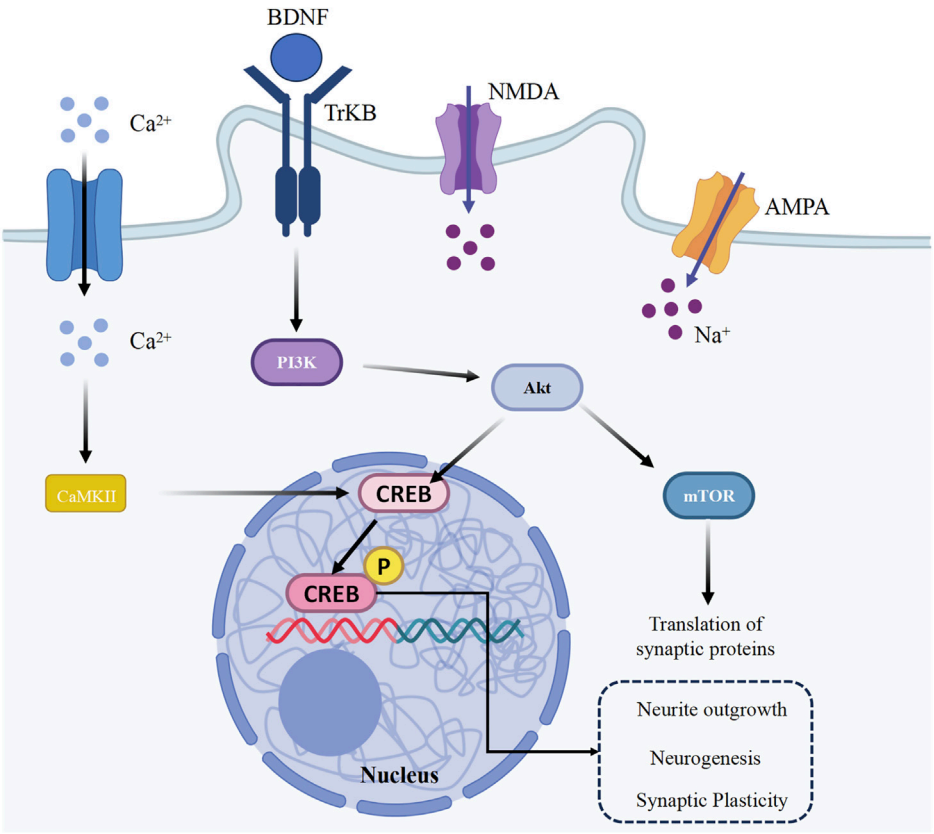


FIGURE 2
Neuroplasticity regulatory mechanisms.

synaptic plasticity by enhancing CREB/BDNF signaling, prevents CUMS-induced reduction in blood-brain barrier permeability, reduces neuroinflammation, preserves intestinal barrier integrity, and promotes the production of short-chain fatty acids (SCFAs) (Wang et al., 2023b). *Schisandra chinensis* (Turcz.) Baill., belonging to the Magnoliaceae family and has been widely used as a medicinal plant in China for centuries. Modern pharmacological research has revealed the anti-inflammatory and anti-aging properties of *S. chinensis* and its active metabolites (Bian et al., 2022). Notably, studies have shown that the polysaccharide-rich fraction from *S. chinensis* (Turcz.) Baill. exhibits antidepressant effects in olfactory bulbectomized mice by enhancing abnormal synaptic plasticity (upregulating PSD95 expression), suppressing excessive activity of the HPA axis, and regulating gut microbiota (Zhu et al., 2024).

### 5.1.7 Botanical drugs extracts

Botanical drugs extracts are considered valuable for their comprehensive active properties, driven by complex biochemical interactions and synergistic effects among their natural metabolites (Pace and Martinelli, 2022). Saffron (*Crocus sativus* L.), a well-known natural product, has long been used to prevent and treat different disorders (Ghaffari and Roshanravan, 2019). In rats exposed to chronic mild stress (CMS), repeated administration of doses of 100 mg/kg and 200 mg/kg doses of Saffron Extract (Affron®) effectively normalized HPA axis dysregulation. Moreover, hypothalamic neuroplasticity showed a significant dose-dependent increase following treatment with Saffron Extract (Affron®) (Kim et al., 2023). Blueberry (*Vaccinium* spp.), a member of the *Vaccinium* genus, is recognized as one of the top five nutritious foods for humans and is often referred to as the "king of fruits." This reputation has fueled considerable interest in the market for plant-based prebiotics (Duan et al., 2022). Blueberry Extract has demonstrated efficacy in alleviating depression-like behavior in LPS-induced mice. It also mitigates the increase in acetylcholinesterase (AChE) activity in the hippocampus induced by LPS and inhibits the mRNA expression of TNF-α, IL-1β, and IL-10 in the cerebral cortex following LPS administration, indicating a potential protective effect on neuroplasticity (Spohr et al., 2023).

### 5.1.8 Other types of active metabolites

Honokiol is a versatile lignan metabolites naturally occurring in plants like *Magnolia grandiflora* L., known for its anti-inflammatory and neuroprotective effects (Rauf et al., 2021; Hu et al., 2023). Fan et al. (2022) found that the antidepressant mechanism of Honokiol involved the activation of the HIF-1α/VEGF signaling pathway and the upregulation of synaptic protein one and PSD 95 expression levels. Salidroside, an active metabolites found in *Rhodiola rosea* L. used in TCM, has various pharmacological effects (Xue et al., 2019). It enhances BDNF expression, improve synaptic plasticity, and inhibits pyroptosis mediated by the P2X7/NF-κB/NLRP3 signaling pathway, thereby providing a treatment for depression (Chai et al., 2022).

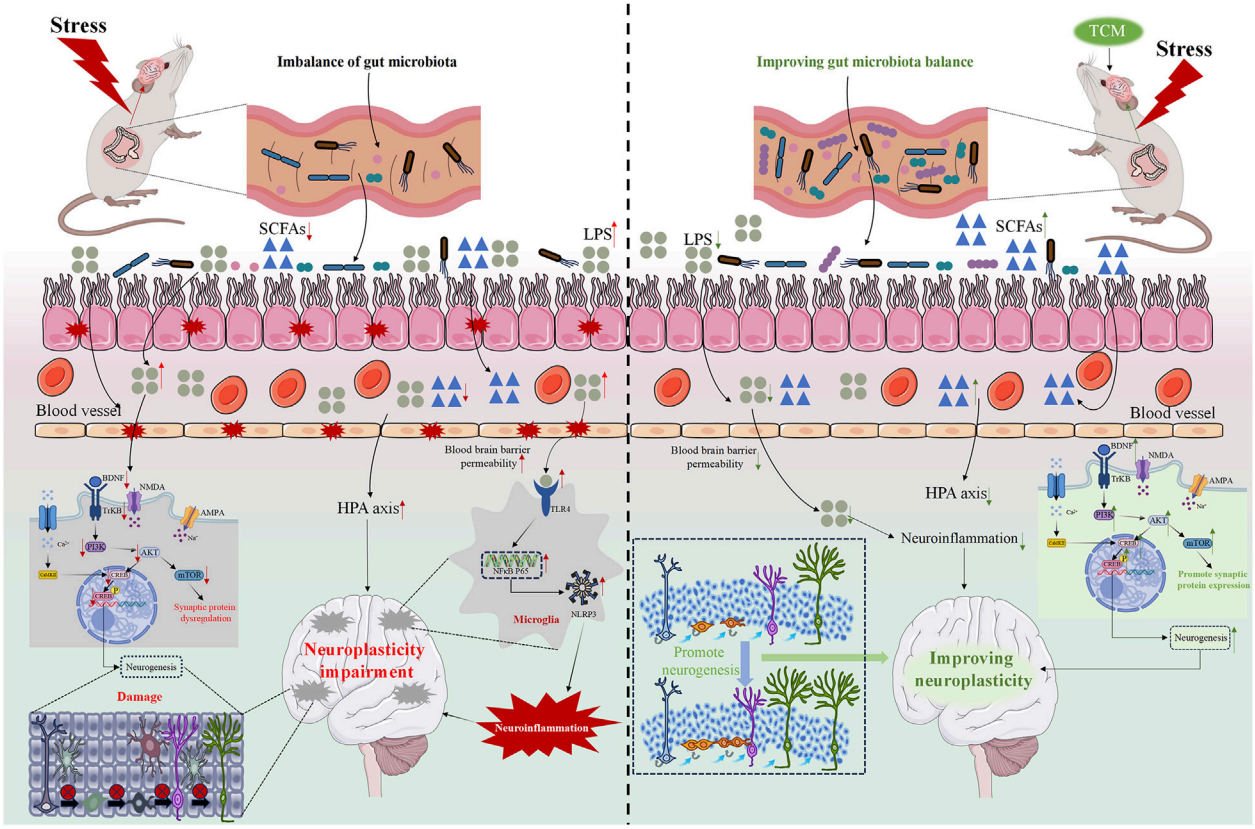


FIGURE 3
The pharmacological mechanism of TCM regulation of neuroplasticity in the treatment of depression. The red arrow indicates changes caused by stress, while the green arrow indicates changes caused by TCM.

Crocin is a hydrophilic carotenoid produced in the blooms of *C. sativus* L., has been associated with promoting new nerve cell generation in the adult hippocampus and exerting antidepressant effects by activating the Wnt/β-catenin signaling pathway (Boozari and Hosseinzadeh, 2022; Tao et al., 2023a), Neurogenesis plays a key role in the physiological mechanism of structural neuroplasticity. Wu et al. (2020) also found that crocin rapidly and persistently induced antidepressant effects in mice subjected to Prenatal stress (PNS), acting through the GHSR-PI3K signaling pathway and modulating the expression of hippocampal synaptic plasticity-related proteins. Panaxynol, commonly found in plants of the *P. ginseng* C.A.Mey., can alleviate HPA axis overactivity induced by CUMS, promote the release of 5-HT and dopamine (DA), enhance hippocampal synaptic plasticity, and improve neurotransmitter effectiveness (Table 2 showed the active metabolites of TCM information) (Sun et al., 2020).

## 5.2 TCM formulas

Zhi-Zi-Chi-Tang (ZZCT) is a potent traditional Chinese herbal remedy with a historical record in the "Shanghan Lun." It consists of the dehydrated mature fruits of *G. jasminoides* J. Ellis and *G. max* (L.) Merr. In a rat depression model induced by CUMS, ZZCT enhances neuroplasticity through the 14–3–3ζ/GSK-3β/CREB/BDNF signaling pathway. It restores the expression of synaptic plasticity-related proteins like MAP2 and PSD95 in the hippocampal CA1 region, enhances LTP induction, and improves neuronal damage caused by CUMS (Tao et al., 2023b).

Zi-Shui-Qing-Gan-Yin (ZSQGY) is another traditional Chinese herbal remedy commonly used in China for depression symptoms. ZSQGY consists of 12 botanical drugs, including *P. ginseng* C.A.Mey et al. In a study conducted both *in vivo* and *in vitro* by Zhu et al. (2023), it was found that ZSQGY significantly improved depression-like behavior induced by monosodium glutamate (MSG) in rats. Further investigations revealed that ZSQGY improved synaptic ultrastructure by upregulating PGC-1α, regulating mitochondrial function, and inhibiting the expression of pro-inflammatory cytokines (Zhu et al., 2023).

The traditional remedy Danggui-Buxue Decoction (DBD), is taken from Li Dongyuan's work on differentiating endogenous and exogenous diseases in the Jin and Yuan Dynasties (Shi et al., 2019). Studies suggest that DBD protects and reshapes hippocampal neurons by regulating the CREB/BDNF/TrkB pathway. It shows promise as a potential metabolite for preventing diabetes mellitus with depression (DD), with ferric acid potentially playing a crucial role in its effects (Wang et al., 2021). The Erzhi formula, composed of *Ligustrum lucidum* W.T.Aiton and *Eclipta prostrata* (L.) L., represents a TCM treatment (Peng et al., 2022). In an *in vitro* depression model, the Erzhi formula revealed the capacity to diminish dexamethasone-induced apoptosis in primary cultured

TABLE 3 Information on the action of TCM formulas.

| TCM formulas | Main composition | *In vivo*/ *in vitro* | Modeling method | Dosage | Behavioral testing evaluation | Main pharmacological mechanisms | References |
|---|---|---|---|---|---|---|---|
| Zhi-Zi-Chi-Tang (ZZCT) | *Gardenia jasminoides* J.Ellis and *Glycine max (L.)* Merr | *In vivo* | CUMS | 3, 6 g/kg | SPT, TST, FST, OFT | Regulating the 14–3–3ζ/GSK-3β/CREB/BDNF signaling pathway to enhance neural plasticity | Tao et al. (2023b) |
| Zi-Shui-Qing-Gan-Yin (ZSQGY) | *Panax ginseng C.A.Mey*, *Dioscorea oppositifolia L*, *Bupleurum chinense DC*, *Paeonia lactiflora Pall*, *Angelica sinensis (Oliv.) Diels*, *Anemarrhena asphodeloides Bunge*, Cornus officinalis Siebold and Zucc, Paeonia × suffruticosa Andrews, *Smilax glabra Roxb*, *Ziziphus jujuba Mill*, *Alisma plantago-aquatica L* and *Gardenia jasminoides* J.Ellis | *In vivo* and *in vitro* | *In vivo*: monosodium glutamate *In vitro*: CORT | 12, 24, 48 g/kg | SFT, SPT, OFT | Upregulation of PGC-1α to improve pathological changes in synaptic ultrastructure, regulate mitochondrial function, and inhibit the expression level of pro-inflammatory cytokines | Zhu et al. (2023) |
| Danggui-Buxue Decoction (DBD) | *Astragalus mongholicus Bunge* and *Angelica sinensis (Oliv.) Diels* | *In vivo* | CUMS | 4, 8 g/kg | FST, OFT, TST | Regulating the CREB/BDNF/TrkB pathway to protect and reshape hippocampal neurons | Wang et al. (2021) |
| Erzhi formula | *Ligustrum lucidum W.T.Aiton* and *Eclipta prostrata (L.) L* | *In vitro* | Dexamethasone | -- | -- | Reduce neuronal apoptosis and improve synaptic damage | Han et al. (2023) |
| Jiawei-Xiaoyao pill (JWX) | *Gardenia jasminoides J.Ellis*, *Paeonia × suffruticosa Andrews*, *Bupleurum chinense DC.* , *Paeonia lactiflora Pall.*, *Angelica sinensis (Oliv.) Diels*, *Atractylodes macrocephala Koidz.*, *Smilax glabra Roxb.*, *Glycyrrhiza glabra L.* and *Mentha canadensis L* | *In vivo* | CORT | 0.7, 1, 1.4, 1.8 g/kg | OFT, TST, FST, SPT | Stimulation of CaMKII signaling pathway, followed by activation of mTOR/BDNF signaling pathway, enhances hippocampal neural plasticity | Zhang et al. (2024a) |
| Modified Xiaoyaosan (MXYS) | *Bupleurum chinense DC.*, *Angelica sinensis (Oliv.) Diels*, *Paeonia lactiflora Pall.*, *Atractylodes macrocephala Koidz.*, *Acorus calamus L.*, *Curcuma aromatica Salisb.*,*Reynoutria multiflora (Thunb.)* Moldenke, *Schisandra chinensis (Turcz.) Baill.*, *Ziziphus jujuba Mill.*, and *Periploca forrestii Schltr* | *In vivo* | CUMS | 0.4 g/kg | SPT, TST, FST | Promote hippocampal neurogenesis and improve BOLD signaling | Gao et al. (2018) |
| SiNiSan (SNS) | *Citrus × aurantium f. Aurantium*, *Paeonia lactiftora Pall.*, *Glycyrrhiza glabra L.*, and *Bupleurum chinense DC* | *In vivo* | Maternal separation and CUMS | 0.25, 0.5, 1 g/mL | SPT, OFT, FST | Activating the CaSR-PKC-ERK signaling pathway | Shen et al. (2020b) |
| | | *In vivo* | Maternal separation | 2.5, 5, 10 g/kg | SPT, OFT, FST | Regulating mitochondrial function, and improving neural plasticity | Deng et al. (2022) |
| Suanzaoren Decoction (SZRD) | *Ziziphus jujuba Mill.*, *Smilax glabra Roxb.*, *Anemarrhena asphodeloides Bunge*, *Oreocome striata (DC.) Pimenov and Kljuykov*, and *Glycyrrhiza glabra L* | *In vivo* and *in vitro* | *In vivo*: CUMS *In vitro*: LPS | 15 g/kg | SPT, FST, OFT | Elevated the expression levels of BDNF, SYP, and PSD95, and inhibited the activation of TLR4/MyD88/NF-κB and Wnt/β-catenin pathways | Du et al. (2024) |
| | | *In vivo* | CUMS | 2.5, 5, 10 g/kg | SPT, OFT | Modulating CaMK signal system | Zhang et al. (2024b) |

(Continued on following page)

TABLE 3 (*Continued*) Information on the action of TCM formulas.

| TCM formulas | Main composition | *In vivo*/ *in vitro* | Modeling method | Dosage | Behavioral testing evaluation | Main pharmacological mechanisms | References |
|---|---|---|---|---|---|---|---|
| Zhi-Zi Hou-Po Decoction (ZZHP) | *Gardenia jasminoides J.Ellis*, *Citrus × aurantium f. Aurantium* and *Magnolia officinalis Rehder and E.H.Wilson* | *In vivo* | CUMS | 0, 30, 40 mg/kg | SPT, TST, FST, OFT | Activating the BDNF/TrkB/CREB pathway protects neuronal synaptic plasticity and promotes hippocampal neurogenesis | Ye et al. (2024) |
| Kaiyu Zhishen Decoction (KZD) | *Paeonia lactiflora Pall.*, *Cyperus rotundus L.*, *Smilax glabra Roxb.*, *Angelica sinensis (Oliv.) Diels.*, *Panax ginseng C.A.Mey.*, *Gardenia jasminoides J.Ellis.*, *Atractylodes macrocephala Koidz.*, *Citrus reticulata Blanco.*, *Glycyrrhiza glabra L.*, and *Bupleurum chinense DC* | *In vivo* and *in vitro* | *In vivo*: CUMS *In vitro*: CORT | 1.579, 4.73, 14.21 g/kg | SPT, FST, TST | Regulating the ERK-CREB-BDNF signaling pathway and enhancing neuronal repair | Chen et al. (2024) |

cortical neurons and repair synaptic damage. Its neuroprotective effects were linked to the 11β-hydroxysteroid dehydrogenase 1 (HSD1)-glucocorticoids (GC)/glucocorticoid receptor (GR) signaling pathway (Han et al., 2023).

Xiaoyaosan, a TCM formula first introduced in the book "Prescriptions of the Bureau of Taiping People's Welfare Pharmacy," has a historical use in treating mental disorders, such as depression (Jiao et al., 2024). The ancient Chinese medicine pharmacopoeia also mentions Jiawei-Xiaoyao pill (JWX), a traditional Chinese medication, for the treatment of a variety of illnesses, including mood disorders. JWX consists of nine botanical drugs, including *G. jasminoides* J. Ellis et al. Studies have shown that JWX stimulates CaMKII signaling, leading to the activation of the mTOR/BDNF signaling pathway, Furthermore, it also enhances hippocampal neuroplasticity and triggering rapid antidepressant effects (Zhang et al., 2024a).

For more precise administration in patients with depression, Gao et al. (2018) introduced an empirical prescription called modified Xiaoshan (MXYS) based on Xiaoshan consisting of *B. chinense* DC et al. In a depression model induced by CUMS, MXYS was found to promote hippocampal neurogenesis and improve brain blood oxygen level-dependent signaling, indicating its potential therapeutic benefits for depression (Gao et al., 2018).

SiNiSan (SNS) is a TCM formula. Originally mentioned in the Treatise on Febrile Diseases for controlling liver qi (Cao et al., 2024), SNS has been shown to regulate neuroplasticity by activating the Calcium sensitive receptor (CaSR)-protein kinase C (PKC)-ERK signaling pathway. It also helps in regulating mitochondrial function and improving neuroplasticity (Shen et al., 2020b; Deng et al., 2022). Suanzaoren Decoction (SZRD), a TCM combination with a history of insomnia treatment (Dong et al., 2021; Yan et al., 2023b). Research by Du et al. (2024) using *in vivo* and *in vitro* experiments demonstrated that SZRD increases the expression levels of BDNF, SYP, and PSD95. It also inhibits the activation of the TLR4/MyD88/NF-κB and Wnt/β-catenin pathways, showing antidepressant effects, and SZRD could also adjust the CaMK signal system (Zhang et al., 2024b; Du et al., 2024).

Zhi-Zi Hou-Po Decoction (ZZHP), a TCM formula widely used in depression treatment (Feng et al., 2022). Studies suggest that ZZHP effectively reverses the decrease of monoamine neurotransmitters in the hippocampus, maintains their homeostasis, activates the BDNF/TrkB/CREB pathway, protects neuronal synaptic plasticity, promotes hippocampal neurogenesis, and alleviates depression-like symptoms in mice caused by CUMS (Ye et al., 2024). Kaiyu Zhishen Decoction (KZD) is composed of botanical drugs such as *P. lactiflora* Pall. Chen et al. (2024) found through network pharmacology and experimental verification that the antidepressant effect of KZD involves regulating the ERK-CREB-BDNF signaling pathway and promoting neuronal repair, potentially regulating neuroplasticity (Figure 3 showed the mechanism of TCM action and Table 3 showed the TCM formulas information).

## 6 Conclusion and prospects

Depression is a common long-lasting mental disorder marked by enduring feelings of sadness, low self-esteem, and potentially dangerous suicidal ideation. Understanding the pathogenesis of depression remains a challenge in modern medicine, and there is a deficiency of therapeutic strategies that may effectively prevent or entirely reverse depression (Chen et al., 2022b; Xia et al., 2023). At now, great progress has been achieved in the study of depression, both at the preclinical level and at the fundamental research level. Multiple chemicals with antidepressant effects have been developed in some clinical treatments, but there are still certain side effects and insufficient efficacy. In addition, there is a lack of suitable and appropriate depression prediction tools in clinical practice. Currently, finding antidepressant drugs with multiple targets, high safety, good efficacy, and minimal adverse reactions is a major task.

In recent years, TCM has received attention and promotion, and has been vigorously developed in various aspects. In the research of antidepressants, TCM has gradually become the focus and hotspot of research. In the treatment of depression, it is crucial to explore

how TCM can complement Western medicine approaches, leveraging the strengths of TCM's multi-target effects and individualized treatments. Research in multi-target antidepressant therapies is essential to achieve outcomes comparable to modern medical "cocktail therapy." TCM offers multiple advantages, including its emphasis on multiple targets and individualized treatment in line with the principles of precision medicine. Active metabolites in TCM, such as flavonoids, polyphenols, alkaloids, saponins, terpenes, polysaccharides, and TCM extracts, along with TCM formulas such as ZZCT, ZSQGY, DBD, Erzhi formula, JWX, MXYS, SNS, SZRD, KZD and ZZHP, play a role in regulating neuroplasticity through various targets and pathways when exerting antidepressant effects.

However, the causes and mechanisms of depression have not been fully elucidated, and there is a lack of unified and relatively authoritative methods for evaluating depression symptoms in clinical practice. There is no clear standard for the specific indicators of depression. More importantly, current research mostly focuses on the *in vivo* or *in vitro* levels, lacking high-quality clinical research on active metabolites and TCM formulas. Most studies only explore the mechanism of drug action, and the connection between TCM theory and neuroplasticity has not been thoroughly investigated. Furthermore, compared to the active metabolites of TCM, research on TCM formulas is relatively weak, and the diversity and depth of neuroplasticity-related signaling pathways explored are insufficient. There is no active substance in the world that not only exerts its pharmacological effects but also has non-specific off-target effects on normal tissues of the body (Guo et al., 2023). In current research on antidepressants, there has been insufficient exploration of the toxicology and side effects of TCM.

In addition, some Chinese herbal medicines lack clear quality control standards, compromising the stability and consistency of their chemical metabolites, limiting their clinical application and complicating the study of their pharmacological mechanisms. Furthermore, certain active metabolites of TCM face challenges such as poor stability, solubility issues, and difficulty in crossing the blood-brain barrier, which need further investigation to ascertain their efficacy in targeting CNS organs. The mechanism of neuroplasticity is complex, involving multiple signaling pathways and cell coordination. While TCM possesses the advantage of targeting multiple pathways, current research predominantly focuses on single signaling pathways with limited detection indicators. This approach fails to comprehensively elucidate the synergistic mechanisms underlying TCM's multi-target and multi-pathway regulation of neuroplasticity.

Therefore, in future research, multicenter, large-sample clinical randomized controlled trials guided by TCM theory should be conducted to explore the efficacy and safety of TCM in treating depression, as well as the regulatory mechanisms of neuroplasticity, aiming to provide deeper insights into how TCM works in antidepressant treatment. Simultaneously, it is essential to enhance the quality control standards for TCM and strengthen the exploration of targeted delivery systems for TCM to increase the concentration and duration of TCM in target organs, thereby improving the therapeutic outcomes. Furthermore, focusing on cutting-edge technologies such as combined single-cell sequencing and spatial transcriptomics is necessary to further reveal the key regulatory targets of TCM and the regulatory mechanisms of neuroplasticity at different time points and cell types. This review systematically elucidated the role of neuroplasticity in the pathological development of depression and the regulatory role of TCM. In conclusion, substantial research efforts are still needed to fully explore the potential of TCM in modulating neuroplasticity for the prevention and treatment of depression.

## Author contributions

SL: Writing–original draft. NY: Writing–review and editing. YL: Writing–review and editing. GZ: Writing–review and editing. XZ: Writing–review and editing. YC: Writing–review and editing. YH: Writing–review and editing. JT: Writing–review and editing. YS: Writing–review and editing.

## Funding

The author(s) declare that financial support was received for the research, authorship, and/or publication of this article. This work was supported by the Shandong Province Special Disease Prevention Project of Integrated Traditional Chinese and Western Medicine (YXH2019ZXY006) and Academic Project for College Students of Shandong Province Youth Education Science Planning Project (24BSH467).

## Conflict of interest

The authors declare that the research was conducted in the absence of any commercial or financial relationships that could be construed as a potential conflict of interest.

## Publisher's note



## References

Abd-Rabo, M. M., Georgy, G. S., Saied, N. M., and Hassan, W. A. (2019). Involvement of the serotonergic system and neuroplasticity in the antidepressant effect of curcumin in ovariectomized rats: comparison with oestradiol and fluoxetine. *Phytother. Res.* 33 (2), 387–396. doi:10.1002/ptr.6232

Aceto, G., Colussi, C., Leone, L., Fusco, S., Rinaudo, M., Scala, F., et al. (2020). Chronic mild stress alters synaptic plasticity in the nucleus accumbens through GSK3β-dependent modulation of Kv4.2 channels. *Proc. Natl. Acad. Sci. U. S. A.* 117 (14), 8143–8153. doi:10.1073/pnas.1917423117

Aguilar-Valles, A., De Gregorio, D., Matta-Camacho, E., Eslamizade, M. J., Khlaifia, A., Skaleka, A., et al. (2021). Antidepressant actions of ketamine engage cell-specific translation via eIF4E. *Nature* 590 (7845), 315–319. doi:10.1038/s41586-020-03047-0

Aleksandrova, L. R., Wang, Y. T., and Phillips, A. G. (2020). Ketamine and its metabolite, (2R,6R)-HNK, restore hippocampal LTP and long-term spatial memory in the Wistar-Kyoto rat model of depression. *Mol. Brain.* 13 (1), 92. doi:10.1186/s13041-020-00627-z

An, J. H., Jang, E. H., Kim, A. Y., Fava, M., Mischoulon, D., Papakostas, G. I., et al. (2019). Ratio of plasma BDNF to leptin levels are associated with treatment response in major depressive disorder but not in panic disorder: a 12-week follow-up study. *J. Affect. Disord.* 259, 349–354. doi:10.1016/j.jad.2019.08.021

Bai, Z., Gao, T., Zhang, R., Lu, Y., Tian, J., Wang, T., et al. (2023). Inhibition of IL-6 methylation by Saikosaponin C regulates neuroinflammation to alleviate depression. *Int. Immunopharmacol.* 118, 110043. doi:10.1016/j.intimp.2023.110043

Bayes, J., Schloss, J., and Sibbritt, D. (2020). Effects of polyphenols in a mediterranean diet on symptoms of depression: a systematic literature review. *Adv. Nutr.* 11 (3), 602–615. doi:10.1093/advances/nmz117

Beurel, E., Toups, M., and Nemeroff, C. B. (2020). The bidirectional relationship of depression and inflammation: double trouble. *Neuron* 107 (2), 234–256. doi:10.1016/j.neuron.2020.06.002

Bian, Z., Qin, Y., Li, L., Su, L., Fei, C., Li, Y., et al. (2022). Schisandra chinensis (Turcz.) Baill. Protects against DSS-induced colitis in mice: involvement of TLR4/NF-κB/NLRP3 inflammasome pathway and gut microbiota. *J. Ethnopharmacol.* 298, 115570. doi:10.1016/j.jep.2022.115570

Boozari, M., and Hosseinzadeh, H. (2022). Crocin molecular signaling pathways at a glance: a comprehensive review. *Phytother. Res.* 36 (10), 3859–3884. doi:10.1002/ptr.7583

Bourtchuladze, R., Frenguelli, B., Blendy, J., Cioffi, D., Schutz, G., and Silva, A. J. (1994). Deficient long-term memory in mice with a targeted mutation of the cAMP-responsive element-binding protein. *Cell.* 79 (1), 59–68. doi:10.1016/0092-8674(94)90400-6

Cao, K., Zhong, J., Wang, S., Shi, Y., Bai, S., Zhao, J., et al. (2024). SiNiSan exerts antidepressant effects by modulating serotonergic/GABAergic neuron activity in the dorsal raphe nucleus region through NMDA receptor in the adolescent depression mouse model. *J. Ethnopharmacol.* 328, 118040. doi:10.1016/j.jep.2024.118040

Cao, Y., Xiong, J., Guan, X., Yin, S., Chen, J., Yuan, S., et al. (2023). Paeoniflorin suppresses kidney inflammation by regulating macrophage polarization via KLF4-mediated mitophagy. *Phytomedicine* 116, 154901. doi:10.1016/j.phymed.2023.154901

Castillo, P. E. (2012). Presynaptic LTP and LTD of excitatory and inhibitory synapses. *Cold. Spring. Harb. Perspect. Biol.* 4 (2), a005728. doi:10.1101/cshperspect.a005728

Chai, Y., Cai, Y., Fu, Y., Wang, Y., Zhang, Y., Zhang, X., et al. (2022). Salidroside ameliorates depression by suppressing NLRP3-mediated pyroptosis via P2X7/NF-κB/NLRP3 signaling pathway. *Front. Pharmacol.* 13, 812362. doi:10.3389/fphar.2022.812362

Chandrashekar, N., and Pandi, A. (2022). Baicalein: a review on its anti-cancer effects and mechanisms in lung carcinoma. *J. Food. Biochem.* 46 (9), e14230. doi:10.1111/jfbc.14230

Chen, J., Lei, C., Li, X., Wu, Q., Liu, C., Ma, Q., et al. (2022b). Research progress on classical traditional Chinese medicine formula xiaoyaosan in the treatment of depression. *Front. Pharmacol.* 13, 925514. doi:10.3389/fphar.2022.925514

Chen, J., Li, G., Sun, C., Peng, F., Yu, L., Chen, Y., et al. (2022a). Chemistry, pharmacokinetics, pharmacological activities, and toxicity of Quercitrin. *Phytother. Res.* 36, 1545–1575. doi:10.1002/ptr.7397

Chen, Q., Shao, X., Ling, P., Liu, F., Han, G., and Wang, F. (2017). Recent advances in polysaccharides for osteoarthritis therapy. *Eur. J. Med. Chem.* 139, 926–935. doi:10.1016/j.ejmech.2017.08.048

Chen, Y., Chen, X., Zhang, J., Wang, D., Lu, N., et al. (2024). Network pharmacology and experimental evidence: ERK/CREB/BDNF signaling pathway is involved in the antidepressive roles of Kaiyu Zhishen decoction. *J. Ethnopharmacol.* 329, 118098. doi:10.1016/j.jep.2024.118098

Choi, G. E., Lee, H. J., Chae, C. W., Cho, J. H., Jung, Y. H., Kim, J. S., et al. (2021). BNIP3L/NIX-mediated mitophagy protects against glucocorticoid-induced synapse defects. *Nat. Commun.* 12 (1), 487. doi:10.1038/s41467-020-20679-y

Clarke, M., Razmjou, S., Prowse, N., Dwyer, Z., Litteljohn, D., Pentz, R., et al. (2017). Ketamine modulates hippocampal neurogenesis and pro-inflammatory cytokines but not stressor induced neurochemical changes. *Neuropharmacology* 112 (Pt A), 210–220. doi:10.1016/j.neuropharm.2016.04.021

Crupi, R., Paterniti, I., Ahmad, A., Campolo, M., Esposito, E., and Cuzzocrea, S. (2013). Effects of palmitoylethanolamide and luteolin in an animal model of anxiety/depression. *CNS. Neurol. Disord. Drug. Targets.* 12 (7), 989–1001. doi:10.2174/18715273113129990084

Dagyte, G., Trentani, A., Postema, F., Luiten, P. G., Den Boer, J. A., Gabriel, C., et al. (2010). The novel antidepressant agomelatine normalizes hippocampal neuronal activity and promotes neurogenesis in chronically stressed rats. *CNS. Neurosci. Ther.* 16 (4), 195–207. doi:10.1111/j.1755-5949.2009.00125.x

Deng, D., Cui, Y., Gan, S., Xie, Z., Cui, S., Cao, K., et al. (2022). Sinisan alleviates depression-like behaviors by regulating mitochondrial function and synaptic plasticity in maternal separation rats. *Phytomedicine* 106, 154395. doi:10.1016/j.phymed.2022.154395

De Paola, V., Holtmaat, A., Knott, G., Song, S., Wilbrecht, L., Caroni, P., et al. (2006). Cell type-specific structural plasticity of axonal branches and boutons in the adult neocortex. *Neuron* 49 (6), 861–875. doi:10.1016/j.neuron.2006.02.017

Diering, G. H., and Huganir, R. L. (2018). The AMPA receptor code of synaptic plasticity. *Neuron* 100 (2), 314–329. doi:10.1016/j.neuron.2018.10.018

Dong, Y. J., Jiang, N. H., Zhan, L. H., Teng, X., Fang, X., Lin, M. Q., et al. (2021). Soporific effect of modified Suanzaoren Decoction on mice models of insomnia by regulating Orexin-A and HPA axis homeostasis. *Biomed. Pharmacother.* 143, 112141. doi:10.1016/j.biopha.2021.112141

Du, Y., Yan, T., Wu, B., He, B., and Jia, Y. (2024). Research on the mechanism of antidepressive effect of Suanzaoren Decoction through TLR4/MyD88/NF-κB pathway and Wnt/β-catenin pathway. *J. Ethnopharmacol.* 319 (Pt 1), 117190. doi:10.1016/j.jep.2023.117190

Duan, Y., Tarafdar, A., Chaurasia, D., Singh, A., Bhargava, P. C., Yang, J., et al. (2022). Blueberry fruit valorization and valuable constituents: a review. *Int. J. Food. Microbiol.* 381, 109890. doi:10.1016/j.ijfoodmicro.2022.109890

Duman, R. S., Aghajanian, G. K., Sanacora, G., and Krystal, J. H. (2016). Synaptic plasticity and depression: new insights from stress and rapid-acting antidepressants. *Nat. Med.* 22 (3), 238–249. doi:10.1038/nm.4050

Dzyubenko, E., and Hermann, D. M. (2023). Role of glia and extracellular matrix in controlling neuroplasticity in the central nervous system. *Semin. Immunopatho.* 45 (3), 377–387. doi:10.1007/s00281-023-00989-1

Fan, X. X., Sun, W. Y., Li, Y., Tang, Q., Li, L. N., Yu, X., et al. (2022). Honokiol improves depression-like behaviors in rats by HIF-1α- VEGF signaling pathway activation. *Front. Pharmacol.* 13, 968124. doi:10.3389/fphar.2022.968124

Fang, Z., Liu, Z., Tao, B., and Jiang, X. (2023). Engeletin mediates antiarrhythmic effects in mice with isoproterenol-induced cardiac remodeling. *Biomed. Pharmacother.* 161, 114439. doi:10.1016/j.biopha.2023.114439

Feng, X., Bi, Y., Wang, J., Li, T., Yu, G., Zhang, T., et al. (2022). Discovery of the potential novel pharmacodynamic substances from zhi-zi-hou-Po decoction based on the concept of Co-decoction reaction and analysis strategy. *Front. Pharmacol.* 12, 830558. doi:10.3389/fphar.2021.830558

Filipović, D., Novak, B., Xiao, J., Yan, Y., Bernardi, R. E., and Turck, C. W. (2023). Chronic fluoxetine treatment in socially-isolated rats modulates the prefrontal cortex synaptoproteome. *J. Proteomics.* 282, 104925. doi:10.1016/j.jprot.2023.104925

Filipović, D., Novak, B., Xiao, J., Yan, Y., Yeoh, K., and Turck, C. W. (2022). Chronic fluoxetine treatment of socially isolated rats modulates prefrontal cortex proteome. *Neuroscience* 501, 52–71. doi:10.1016/j.neuroscience.2022.08.011

Frankiensztajn, L. M., Elliott, E., and Koren, O. (2020). The microbiota and the hypothalamus-pituitary-adrenocortical (HPA) axis, implications for anxiety and stress disorders. *Curr. Opin. Neurobiol.* 62, 76–82. doi:10.1016/j.conb.2019.12.003

Freitas, A. E., Egea, J., Buendia, I., Gómez-Rangel, V., Parada, E., Navarro, E., et al. (2016). Agmatine, by improving neuroplasticity markers and inducing Nrf2, prevents corticosterone-induced depressive-like behavior in mice. *Mol. Neurobiol.* 53 (5), 3030–3045. doi:10.1007/s12035-015-9182-6

Gao, L., Huang, P., Dong, Z., Gao, T., Huang, S., Zhou, C., et al. (2018). Modified xiaoyaosan (MXYS) exerts anti-depressive effects by rectifying the brain blood oxygen level-dependent fMRI signals and improving hippocampal neurogenesis in mice. *Front. Pharmacol.* 9, 1098. doi:10.3389/fphar.2018.01098

Gao, Y., Nie, K., Wang, H., Dong, H., and Tang, Y. (2024). Research progress on antidepressant effects and mechanisms of berberine. *Front. Pharmacol.* 15, 1331440. doi:10.3389/fphar.2024.1331440

Ge, P. Y., Qu, S. Y., Ni, S. J., Yao, Z. Y., Qi, Y. Y., Zhao, X., et al. (2023). Berberine ameliorates depression-like behavior in CUMS mice by activating TPH1 and inhibiting Ido1-associated with tryptophan metabolism. *Phytother. Res.* 37 (1), 342–357. doi:10.1002/ptr.7616

Ghaffari, S., and Roshanravan, N. (2019). Saffron; an updated review on biological properties with special focus on cardiovascular effects. *Biomed. Pharmacother.* 109, 21–27. doi:10.1016/j.biopha.2018.10.031

Grabska-Kobyłecka, I., Szpakowski, P., Król, A., Książek-Winiarek, D., Kobyłecki, A., Głąbiński, A., et al. (2023). Polyphenols and their impact on the prevention of neurodegenerative diseases and development. *Nutrients* 15 (15), 3454. doi:10.3390/nu15153454

Guo, C., Huang, Q., Wang, Y., Yao, Y., Li, J., Chen, J., et al. (2023). Therapeutic application of natural products: $NAD^+$ metabolism as potential target. *Phytomedicine* 114, 154768. doi:10.1016/j.phymed.2023.154768

Guo, L. T., Wang, S. Q., Su, J., Xu, L. X., Ji, Z. Y., Zhang, R. Y., et al. (2019). Baicalin ameliorates neuroinflammation-induced depressive-like behavior through inhibition of toll-like receptor 4 expression via the PI3K/AKT/FoxO1 pathway. *J. Neuroinflammation* 16 (1), 95. doi:10.1186/s12974-019-1474-8

Han, H., Dai, C., and Dong, Z. (2015). Single fluoxetine treatment before but not after stress prevents stress-induced hippocampal long-term depression and spatial memory retrieval impairment in rats. *Sci. Rep.* 5, 12667. doi:10.1038/srep12667

Han, R., Han, G., Yan, Y., Han, L., Li, L., and Zhang, H. (2023). Protective effects and mechanisms of the Erzhi formula on glucocorticoid induced primary cortical neuron injury. *Front. Pharmacol.* 14, 1038492. doi:10.3389/fphar.2023.1038492

Hidese, S., Hattori, K., Sasayama, D., Tsumagari, T., Miyakawa, T., Matsumura, R., et al. (2020). Cerebrospinal fluid neuroplasticity-associated protein levels in patients with psychiatric disorders: a multiplex immunoassay study. *Transl. Psychiatry.* 10 (1), 161. doi:10.1038/s41398-020-0843-5

Hu, M., Jiang, W., Ye, C., Hu, T., Yu, Q., Meng, M., et al. (2023). Honokiol attenuates high glucose-induced peripheral neuropathy via inhibiting ferroptosis and activating AMPK/SIRT1/PGC-1α pathway in Schwann cells. *Phytother. Res.* 37 (12), 5787–5802. doi:10.1002/ptr.7984

Huang, H., Cheng, Z., Shi, H., Xin, W., Wang, T. T., and Yu, L. L. (2011). Isolation and characterization of two flavonoids, engeletin and astilbin, from the leaves of Engelhardia roxburghiana and their potential anti-inflammatory properties. *J. Agric. Food. Chem.* 59 (9), 4562–4569. doi:10.1021/jf2002969

Huang, J., Shen, C., Ye, R., Shi, Y., and Li, W. (2021). The effect of early maternal separation combined with adolescent chronic unpredictable mild stress on behavior and synaptic plasticity in adult female rats. *Front. Psychiatry.* 12, 539299. doi:10.3389/fpsyt.2021.539299

Huang, M., Lu, J. J., Huang, M. Q., Bao, J. L., Chen, X. P., and Wang, Y. T. (2012). Terpenoids: natural products for cancer therapy. *Expert. Opin. Investig. Drugs.* 21 (12), 1801–1818. doi:10.1517/13543784.2012.727395

Hueston, C. M., Cryan, J. F., and Nolan, Y. M. (2017). Adolescent social isolation stress unmasks the combined effects of adolescent exercise and adult inflammation on hippocampal neurogenesis and behavior. *Neuroscience* 365, 226–236. doi:10.1016/j.neuroscience.2017.09.020

Illippangama, A. U., Jayasena, D. D., Jo, C., and Mudannayake, D. C. (2022). Inulin as a functional ingredient and their applications in meat products. *Carbohydr. Polym.* 275, 118706. doi:10.1016/j.carbpol.2021.118706

Jaremka, L. M., Andridge, R. R., Fagundes, C. P., Alfano, C. M., Povoski, S. P., Lipari, A. M., et al. (2014). Pain, depression, and fatigue: loneliness as a longitudinal risk factor. *Health. Psychol.* 33 (9), 948–957. doi:10.1037/a0034012

Jiao, H., Fan, Y., Gong, A., Li, T., Fu, X., and Yan, Z. (2024). Xiaoyaosan ameliorates CUMS-induced depressive-like and anorexia behaviors in mice via necroptosis related cellular senescence in hypothalamus. *J. Ethnopharmacol.* 318 (Pt A), 116938. doi:10.1016/j.jep.2023.116938

Jo, J. H., Park, E. J., Lee, J. K., Jung, M. W., and Lee, C. J. (2001). Lipopolysaccharide inhibits induction of long-term potentiation and depression in the rat hippocampal CA1 area. *Eur. J. Pharmacol.* 422 (1-3), 69–76. doi:10.1016/s0014-2999(01)01075-5

Kaneko, N., Wada, M., Nakajima, S., Takano, M., Taniguchi, K., Honda, S., et al. (2024). Neuroplasticity of the left dorsolateral prefrontal cortex in patients with treatment-resistant depression as indexed with paired associative stimulation: a TMS-EEG study. *Cereb. Cortex* 34 (2), bhad515. doi:10.1093/cercor/bhad515

Karin, O., Raz, M., Tendler, A., Bar, A., Korem Kohanim, Y., Milo, T., et al. (2020). A new model for the HPA axis explains dysregulation of stress hormones on the timescale of weeks. *Mol. Syst. Biol.* 16 (7), e9510. doi:10.15252/msb.20209510

Kim, C. Y., Ko, K., Choi, S. H., Jo, M., Kim, J., Yoon, S., et al. (2023). Effects of Saffron extract (Affron®) with 100 mg/kg and 200 mg/kg on hypothalamic-pituitary-adrenal Axis and stress resilience in chronic mild stress-induced depression in wistar rats. *Nutrients* 15 (23), 4855. doi:10.3390/nu15234855

Kim, J. W., and Monteggia, L. M. (2020). Increasing doses of ketamine curtail antidepressant responses and suppress associated synaptic signaling pathways. *Behav. Brain. Res.* 380, 112378. doi:10.1016/j.bbr.2019.112378

Knott, G. W., Holtmaat, A., Wilbrecht, L., Welker, E., and Svoboda, K. (2006). Spine growth precedes synapse formation in the adult neocortex *in vivo*. *Nat. Neurosci.* 9 (9), 1117–1124. doi:10.1038/nn1747

Kokkosis, A. G., Madeira, M. M., Hage, Z., Valais, K., Koliatsis, D., Resutov, E., et al. (2024). Chronic psychosocial stress triggers microglial-/macrophage-induced inflammatory responses leading to neuronal dysfunction and depressive-related behavior. *Glia* 72 (1), 111–132. doi:10.1002/glia.24464

Kong, C. H., Park, K., Kim, D. Y., Kim, J. Y., Kang, W. C., Jeon, M., et al. (2023). Effects of oleanolic acid and ursolic acid on depression-like behaviors induced by maternal separation in mice. *Eur. J. Pharmacol.* 956, 175954. doi:10.1016/j.ejphar.2023.175954

Kopelman, J., Keller, T. A., Panny, B., Griffo, A., Degutis, M., Spotts, C., et al. (2023). Rapid neuroplasticity changes and response to intravenous ketamine: a randomized controlled trial in treatment-resistant depression. *Transl. Psychiatry.* 13 (1), 159. doi:10.1038/s41398-023-02451-0

Kuhn, M., Mainberger, F., Feige, B., Maier, J. G., Wirminghaus, M., Limbach, L., et al. (2016). State-dependent partial occlusion of cortical LTP-like plasticity in major depression. *Neuropsychopharmacology* 41 (6), 1521–1529. doi:10.1038/npp.2015.310

LaMoia, T. E., and Shulman, G. I. (2021). Cellular and molecular mechanisms of metformin action. *Endocr. Rev.* 42 (1), 77–96. doi:10.1210/endrev/bnaa023

Li, B., Du, P., Du, Y., Zhao, D., Cai, Y., Yang, Q., et al. (2021b). Luteolin alleviates inflammation and modulates gut microbiota in ulcerative colitis rats. *Life. Sci.* 269, 119008. doi:10.1016/j.lfs.2020.119008

Li, J., Tian, S., Wang, H., Wang, Y., Du, C., Fang, J., et al. (2021a). Protection of hUC-MSCs against neuronal complement C3a receptor-mediated NLRP3 activation in CUMS-induced mice. *Neurosci. Lett.* 741, 135485. doi:10.1016/j.neulet.2020.135485

Li, Y., Li, J., Yang, L., Ren, F., Dong, K., Zhao, Z., et al. (2023a). Ginsenoside Rb1 protects hippocampal neurons in depressed rats based on mitophagy-regulated astrocytic pyroptosis. *Phytomedicine* 121, 155083. doi:10.1016/j.phymed.2023.155083

Li, Y., Zhao, L., Zhao, Q., Zhou, Y., Zhou, L., Song, P., et al. (2023b). Ursolic acid nanoparticles for glioblastoma therapy. *Nanomedicine* 50, 102684. doi:10.1016/j.nano.2023.102684

Li, Z. R., Liu, D. G., Xie, S., Wang, Y. H., Han, Y. S., Li, C. Y., et al. (2022). Sleep deprivation leads to further impairment of hippocampal synaptic plasticity by suppressing melatonin secretion in the pineal gland of chronically unpredictable stress rats. *Eur. J. Pharmacol.* 930, 175149. doi:10.1016/j.ejphar.2022.175149

Liu, F., Tian, Q., Tang, H. L., Cheng, X., Zou, W., and Zhang, P. (2024). Hydrogen sulfide attenuates depression-like behaviours in Parkinson's disease model rats by improving synaptic plasticity in a hippocampal Warburg effect-dependent manner. *Pharmacol. Biochem. Behav.* 234, 173677. doi:10.1016/j.pbb.2023.173677

Liu, H. T., Lin, Y. N., Tsai, M. C., Wu, Y. C., and Lee, M. C. (2022). Baicalein exerts therapeutic effects against endotoxin-induced depression-like behavior in mice by decreasing inflammatory cytokines and increasing brain-derived neurotrophic factor levels. *Antioxidants (Basel)* 11 (5), 947. doi:10.3390/antiox11050947

Liu, K., Li, H., Zeng, N., Li, B., Yao, G., Wu, X., et al. (2023). Exploration of the core pathways and potential targets of luteolin treatment on late-onset depression based on cerebrospinal fluid proteomics. *Int. J. Mol. Sci.* 24 (4), 3485. doi:10.3390/ijms24043485

Liu, N., Wang, Y., An, A. Y., Banker, C., Qian, Y. H., and O'Donnell, J. M. (2020). Single housing-induced effects on cognitive impairment and depression-like behavior in male and female mice involve neuroplasticity-related signaling. *Eur. J. Neurosci.* 52 (1), 2694–2704. doi:10.1111/ejn.14565

Liu, S. C., Hu, W. Y., Zhang, W. Y., Yang, L., Li, Y., Xiao, Z. C., et al. (2019). Paeoniflorin attenuates impairment of spatial learning and hippocampal long-term potentiation in mice subjected to chronic unpredictable mild stress. *Psychopharmacol. Berl.* 236 (9), 2823–2834. doi:10.1007/s00213-019-05257-5

Lu, C., Gao, R., Zhang, Y., Jiang, N., Chen, Y., Sun, J., et al. (2021). S-equol, a metabolite of dietary soy isoflavones, alleviates lipopolysaccharide-induced depressive-like behavior in mice by inhibiting neuroinflammation and enhancing synaptic plasticity. *Food. Funct.* 12 (13), 5770–5778. doi:10.1039/d1fo00547b

Lu, C., Wei, Z., Wang, Y., Li, S., Tong, L., Liu, X., et al. (2022). Soy isoflavones alleviate lipopolysaccharide-induced depressive-like behavior by suppressing neuroinflammation, mediating tryptophan metabolism and promoting synaptic plasticity. *Food. Funct.* 13 (18), 9513–9522. doi:10.1039/d2fo01437h

Lu, Y., Sun, G., Yang, F., Guan, Z., Zhang, Z., Zhao, J., et al. (2019). Baicalin regulates depression behavior in mice exposed to chronic mild stress via the Rac/LIMK/cofilin pathway. *Biomed. Pharmacother.* 116, 109054. doi:10.1016/j.biopha.2019.109054

Luo, Q., Wei, Y., Lv, X., Chen, W., Yang, D., and Tuo, Q. (2024). The effect and mechanism of oleanolic acid in the treatment of metabolic syndrome and related cardiovascular diseases. *Molecules* 29 (4), 758. doi:10.3390/molecules29040758

Lv, H., Gao, Z., Wang, Y., Chen, S., Liu, P., Xie, Y., et al. (2023). Metformin improves comorbid depressive symptoms in mice with allergic rhinitis by reducing olfactory bulb damage. *Neurochem. Res.* 48 (12), 3639–3651. doi:10.1007/s11064-023-04012-9

Ma, X., Xie, Y., Gong, Y., Hu, C., Qiu, K., Yang, Y., et al. (2023). Silibinin prevents tgfβ-induced EMT of RPE in proliferative vitreoretinopathy by inhibiting Stat3 and Smad3 phosphorylation. *Invest. Ophthalmol. Vis. Sci.* 64 (13), 47. doi:10.1167/iovs.64.13.47

Ma, Y., Li, S. X., Zhou, R. Y., Deng, L. J., le He, W., Guo, L. L., et al. (2024). Geniposide improves depression-like behavior in prenatal stress male offspring through restoring HPA axis- and glucocorticoid receptor-associated dysfunction. *Life. Sci.* 340, 122434. doi:10.1016/j.lfs.2024.122434

Maddukuri, R. K., Hema, C., Sri Tejaswi, K., Venkata Mounika, M., and Vegesana, B. P. (2021). Antidepressant efficacy of Agomelatine: meta-analysis of placebo controlled and active comparator studies. *Asian. J. Psychiatr.* 65, 102866. doi:10.1016/j.ajp.2021.102866

Marsden, W. N. (2013). Synaptic plasticity in depression: molecular, cellular and functional correlates. *Prog. Neuropsychopharmacol. Biol. Psychiatry* 43, 168–184. doi:10.1016/j.pnpbp.2012.12.012

Martin, V., Allaïli, N., Euvrard, M., Marday, T., Riffaud, A., Franc, B., et al. (2017). Effect of agomelatine on memory deficits and hippocampal gene expression induced by chronic social defeat stress in mice. *Sci. Rep.* 8, 45907. doi:10.1038/srep45907

Medendorp, W. E., Petersen, E. D., Pal, A., Wagner, L. M., Myers, A. R., Hochgeschwender, U., et al. (2018). Altered behavior in mice socially isolated during adolescence corresponds with immature dendritic spine morphology and impaired plasticity in the prefrontal cortex. *Front. Behav. Neurosci.* 12, 87. doi:10.3389/fnbeh.2018.00087

Mendonça, I. P., Paiva, I. H. R., Duarte-Silva, E. P., Melo, M. G., Silva, R. S. D., Oliveira, W. H., et al. (2022). Metformin and fluoxetine improve depressive-like behavior in a murine model of Parkinsońs disease through the modulation of neuroinflammation, neurogenesis and neuroplasticity. *Int. Immunopharmacol.* 102, 108415. doi:10.1016/j.intimp.2021.108415

Monroe, S. M., and Harkness, K. L. (2022). Major depression and its recurrences: life course matters. *Annu. Rev. Clin. Psychol.* 18, 329–357. doi:10.1146/annurev-clinpsy-072220-021440

Mousten, I. V., Sørensen, N. V., Christensen, R. H. B., and Benros, M. E. (2022). Cerebrospinal fluid biomarkers in patients with unipolar depression compared with healthy control individuals: a systematic review and meta-analysis. *JAMA. Psychiatry.* 79 (6), 571–581. doi:10.1001/jamapsychiatry.2022.0645

Muñoz-Arenas, G., Pulido, G., Treviño, S., Vázquez-Roque, R., Flores, G., Moran, C., et al. (2020). Effects of metformin on recognition memory and hippocampal neuroplasticity in rats with metabolic syndrome. *Synapse* 74 (9), e22153. doi:10.1002/syn.22153

Ni, X. C., Wang, H. F., Cai, Y. Y., Yang, D., Alolga, R. N., Liu, B., et al. (2022). Ginsenoside Rb1 inhibits astrocyte activation and promotes transfer of astrocytic mitochondria to neurons against ischemic stroke. *Redox. Biol.* 54, 102363. doi:10.1016/j.redox.2022.102363

Noda, Y., Zomorrodi, R., Vila-Rodriguez, F., Downar, J., Farzan, F., Cash, R. F. H., et al. (2018). Impaired neuroplasticity in the prefrontal cortex in depression indexed through paired associative stimulation. *Depress. Anxiety.* 35 (5), 448–456. doi:10.1002/da.22738

Pace, R., and Martinelli, E. M. (2022). The phytoequivalence of herbal extracts: a critical evaluation. *Fitoterapia* 162, 105262. doi:10.1016/j.fitote.2022.105262

Pan, Y., Ke, Z., Ye, H., Sun, L., Ding, X., Shen, Y., et al. (2019). Saikosaponin C exerts anti-HBV effects by attenuating HNF1α and HNF4α expression to suppress HBV pgRNA synthesis. *Inflamm. Res.* 68 (12), 1025–1034. doi:10.1007/s00011-019-01284-2

Peng, M., Xia, T., Zhong, Y., Zhao, M., Yue, Y., Liang, L., et al. (2022). Integrative pharmacology reveals the mechanisms of Erzhi Pill, a traditional Chinese formulation, against diabetic cardiomyopathy. *J. Ethnopharmacol.* 296, 115474. doi:10.1016/j.jep.2022.115474

Perić, I., Costina, V., Djordjević, S., Gass, P., Findeisen, P., Inta, D., et al. (2021). Tianeptine modulates synaptic vesicle dynamics and favors synaptic mitochondria processes in socially isolated rats. *Sci. Rep.* 11 (1), 17747. doi:10.1038/s41598-021-97186-7

Player, M. J., Taylor, J. L., Weickert, C. S., Alonzo, A., Sachdev, P., Martin, D., et al. (2013). Neuroplasticity in depressed individuals compared with healthy controls. *Neuropsychopharmacology* 38 (11), 2101–2108. doi:10.1038/npp.2013.126

Price, R. B., and Duman, R. (2020). Neuroplasticity in cognitive and psychological mechanisms of depression: an integrative model. *Mol. Psychiatry.* 25 (3), 530–543. doi:10.1038/s41380-019-0615-x

Qian, X., Zhong, Z. D., Zhang, Y., Qiu, L. Q., and Tan, H. J. (2024). Fluoxetine mitigates depressive-like behaviors in mice via anti-inflammation and enhancing neuroplasticity. *Brain. Res.* 1825, 148723. doi:10.1016/j.brainres.2023.148723

Qin, Z., Shi, D. D., Li, W., Cheng, D., Zhang, Y. D., Zhang, S., et al. (2023). Berberine ameliorates depression-like behaviors in mice via inhibiting NLRP3 inflammasome-mediated neuroinflammation and preventing neuroplasticity disruption. *J. Neuroinflammation* 20 (1), 54. doi:10.1186/s12974-023-02744-7

Qu, S. Y., Li, X. Y., Heng, X., Qi, Y. Y., Ge, P. Y., Ni, S. J., et al. (2021). Analysis of antidepressant activity of huang-lianie Jie-du decoction through network pharmacology and metabolomics. *Front. Pharmacol.* 12, 619288. doi:10.3389/fphar.2021.619288

Rauf, A., Olatunde, A., Imran, M., Alhumaydhi, F. A., Aljohani, A. S. M., Khan, S. A., et al. (2021). Honokiol: a review of its pharmacological potential and therapeutic insights. *Phytomedicine* 90, 153647. doi:10.1016/j.phymed.2021.153647

Rauf, A., Wilairatana, P., Joshi, P. B., Ahmad, Z., Olatunde, A., Hafeez, N., et al. (2024). Revisiting luteolin: an updated review on its anticancer potential. *Heliyon* 10 (5), e26701. doi:10.1016/j.heliyon.2024.e26701

Ray, A., Gulati, K., and Rai, N. (2017). Stress, anxiety, and immunomodulation: a pharmacological analysis. *Vitam. Horm.* 103, 1–25. doi:10.1016/bs.vh.2016.09.007

Rehm, J., and Shield, K. D. (2019). Global burden of disease and the impact of mental and addictive disorders. *Curr. Psychiatry. Rep.* 21 (2), 10. doi:10.1007/s11920-019-0997-0

Ru, Q., Lu, Y., Saifullah, A. B., Blanco, F. A., Yao, C., Cata, J. P., et al. (2022). TIAM1-mediated synaptic plasticity underlies comorbid depression-like and ketamine antidepressant-like actions in chronic pain. *J. Clin. Invest.* 132 (24), e158545. doi:10.1172/JCI158545

Sato, S., Bunney, B., Mendoza-Viveros, L., Bunney, W., Borrelli, E., Sassone-Corsi, P., et al. (2022). Rapid-acting antidepressants and the circadian clock. *Neuropsychopharmacology* 47 (4), 805–816. doi:10.1038/s41386-021-01241-w

Shen, B., Feng, H., Cheng, J., Li, Z., Jin, M., Zhao, L., et al. (2020a). Geniposide alleviates non-alcohol fatty liver disease via regulating Nrf2/AMPK/mTOR signalling pathways. *J. Cell. Mol. Med.* 24 (9), 5097–5108. doi:10.1111/jcmm.15139

Shen, C., Cao, K., Cui, S., Cui, Y., Mo, H., Wen, W., et al. (2020b). SiNiSan ameliorates depression-like behavior in rats by enhancing synaptic plasticity via the CaSR-PKC-ERK signaling pathway. *Biomed. Pharmacother.* 124, 109787. doi:10.1016/j.biopha.2019.109787

Shi, H. J., Wu, D. L., Chen, R., Li, N., and Zhu, L. J. (2022). Requirement of hippocampal DG nNOS-CAPON dissociation for the anxiolytic and antidepressant effects of fluoxetine. *Theranostics* 12 (8), 3656–3675. doi:10.7150/thno.70370

Shi, X. Q., Yue, S. J., Tang, Y. P., Chen, Y. Y., Zhou, G. S., Zhang, J., et al. (2019). A network pharmacology approach to investigate the blood enriching mechanism of Danggui buxue Decoction. *J. Ethnopharmacol.* 235, 227–242. doi:10.1016/j.jep.2019.01.027

Song, D., Hao, J., and Fan, D. (2020). Biological properties and clinical applications of berberine. *Front. Med.* 14 (5), 564–582. doi:10.1007/s11684-019-0724-6

Spohr, L., de Aguiar, M. S. S., Bona, N. P., Luduvico, K. P., Alves, A. G., Domingues, W. B., et al. (2023). Blueberry extract modulates brain enzymes activities and reduces neuroinflammation: promising effect on lipopolysaccharide-induced depressive-like behavior. *Neurochem. Res.* 48 (3), 846–861. doi:10.1007/s11064-022-03813-8

Sun, X., Zhang, T., Zhao, Y., Cai, E., Zhu, H., and Liu, S. (2020). Panaxynol attenuates CUMS-induced anxiety and depressive-like behaviors via regulating neurotransmitters, synapses and the HPA axis in mice. *Food. Funct.* 11 (2), 1235–1244. doi:10.1039/c9fo03104a

Sun, Y., Zhang, H., Wu, Z., Yu, X., Yin, Y., Qian, S., et al. (2021). Quercitrin rapidly alleviated depression-like behaviors in lipopolysaccharide-treated mice: the involvement of PI3K/AKT/NF-κB signaling suppression and CREB/BDNF signaling restoration in the Hippocampus. *Acs. Chem. Neurosci.* 12 (18), 3387–3396. doi:10.1021/acschemneuro.1c00371

Tanaka, J., Horiike, Y., Matsuzaki, M., Miyazaki, T., Ellis-Davies, G. C., and Kasai, H. (2008). Protein synthesis and neurotrophin-dependent structural plasticity of single dendritic spines. *Science* 319 (5870), 1683–1687. doi:10.1126/science.1152864

Tanner-Smith, E. E., and Grant, S. (2018). Meta-analysis of complex interventions. *Annu. Rev. Public. Health.* 39, 135–151. doi:10.1146/annurev-publhealth-040617-014112

Tao, W., Ruan, J., Wu, R., Zhao, M., Zhao, T., Qi, M., et al. (2023a). A natural carotenoid crocin exerts antidepressant action by promoting adult hippocampal neurogenesis through Wnt/β-catenin signaling. *J. Adv. Res.* 43, 219–231. doi:10.1016/j.jare.2022.02.015

Tao, W., Yao, G., Yue, Q., Xu, C., Hu, Y., Cheng, X., et al. (2023b). 14-3-3ζ Plays a key role in the modulation of neuroplasticity underlying the antidepressant-like effects of Zhi-Zi-Chi-Tang. *Phytomedicine* 116, 154888. doi:10.1016/j.phymed.2023.154888

Tartt, A. N., Mariani, M. B., Hen, R., Mann, J. J., and Boldrini, M. (2022). Dysregulation of adult hippocampal neuroplasticity in major depression: pathogenesis and therapeutic implications. *Mol. Psychiatry.* 27 (6), 2689–2699. doi:10.1038/s41380-022-01520-y

Tejeda, G. S., and Díaz-Guerra, M. (2017). Integral characterization of defective BDNF/TrkB signalling in neurological and psychiatric disorders leads the way to new therapies. *Int. J. Mol. Sci.* 18 (2), 268. doi:10.3390/ijms18020268

Vega-Rivera, N. M., González-Trujano, M. E., Luna-Angula, A., Sánchez-Chapul, L., and Estrada-Camarena, E. (2023). Antidepressant-like effects of the Punica granatum and citalopram combination are associated with structural changes in dendritic spines of granule cells in the dentate gyrus of rats. *Front. Pharmacol.* 14, 1211663. doi:10.3389/fphar.2023.1211663

Vints, W. A. J., Levin, O., Fujiyama, H., Verbunt, J., and Masiulis, N. (2022). Exerkines and long-term synaptic potentiation: mechanisms of exercise-induced neuroplasticity. *Front. Neuroendocrinol.* 66, 100993. doi:10.1016/j.yfrne.2022.100993

Wang, G., An, T., Lei, C., Zhu, X., Yang, L., Zhang, L., et al. (2022b). Antidepressant-like effect of ginsenoside Rb1 on potentiating synaptic plasticity via the miR-134-mediated BDNF signaling pathway in a mouse model of chronic stress-induced depression. *J. Ginseng. Res.* 46 (3), 376–386. doi:10.1016/j.jgr.2021.03.005

Wang, L., Wang, Z., Lan, Y., Tuo, Y., Ma, S., and Liu, X. (2023b). Inulin attenuates blood-brain barrier permeability and alleviates behavioral disorders by modulating the TLR4/MyD88/NF-κB pathway in mice with chronic stress. *J. Agric. Food. Chem.* 71 (36), 13325–13337. doi:10.1021/acs.jafc.3c03568

Wang, Q., Yang, B., Wang, N., and Gu, J. (2022a). Tumor immunomodulatory effects of polyphenols. *Front. Immunol.* 13, 1041138. doi:10.3389/fimmu.2022.1041138

Wang, W., Wang, L., Wang, L., Li, Y., Lan, T., Wang, C., et al. (2023a). Ginsenoside-Rg1 synergized with voluntary running exercise protects against glial activation and dysregulation of neuronal plasticity in depression. *Food. Funct.* 14 (15), 7222–7239. doi:10.1039/d3fo00496a

Wang, W. K., Zhou, Y., Fan, L., Sun, Y., Ge, F., and Xue, M. (2021). The antidepressant-like effects of Danggui Buxue Decoction in GK rats by activating CREB/BDNF/TrkB signaling pathway. *Phytomedicine* 89, 153600. doi:10.1016/j.phymed.2021.153600

Wang, Y. S., Shen, C. Y., and Jiang, J. G. (2019). Antidepressant active ingredients from herbs and nutraceuticals used in TCM: pharmacological mechanisms and prospects for drug discovery. *Pharmacol. Res.* 150, 104520. doi:10.1016/j.phrs.2019.104520

Wei, Y., Chang, L., and Hashimoto, K. (2022). Molecular mechanisms underlying the antidepressant actions of arketamine: beyond the NMDA receptor. *Mol. Psychiatry*. 27 (1), 559–573. doi:10.1038/s41380-021-01121-1

Wu, D., Wang, H., Teng, T., Duan, S., Ji, A., and Li, Y. (2018). Hydrogen sulfide and autophagy: a double edged sword. *Pharmacol. Res.* 131, 120–127. doi:10.1016/j.phrs.2018.03.002

Wu, R., Xiao, D., Shan, X., Dong, Y., and Tao, W. W. (2020). Rapid and prolonged antidepressant-like effect of crocin is associated with GHSR-mediated hippocampal plasticity-related proteins in mice exposed to prenatal stress. *Acs. Chem. Neurosci.* 11 (8), 1159–1170. doi:10.1021/acschemneuro.0c00022

Wu, Y., Wei, Z., Li, Y., Wei, C., Li, Y., Cheng, P., et al. (2019). Perturbation of Ephrin receptor signaling and glutamatergic transmission in the hypothalamus in depression using proteomics integrated with metabolomics. *Front. Neurosci.* 13, 1359. doi:10.3389/fnins.2019.01359

Xia, B., Huang, X., Sun, G., and Tao, W. (2021). Iridoids from Gardeniae fructus ameliorates depression by enhancing synaptic plasticity via AMPA receptor-mTOR signaling. *J. Ethnopharmacol.* 268, 113665. doi:10.1016/j.jep.2020.113665

Xia, C. Y., Guo, Y. X., Lian, W. W., Yan, Y., Ma, B. Z., Cheng, Y. C., et al. (2023). The NLRP3 inflammasome in depression: potential mechanisms and therapies. *Pharmacol. Res.* 187, 106625. doi:10.1016/j.phrs.2022.106625

Xie, P., Chen, L., Wang, J., Wang, X., Yang, S., and Zhu, G. (2024). Polysaccharides from Polygonatum cyrtonema Hua prevent post-traumatic stress disorder behaviors in mice: mechanisms from the perspective of synaptic injury, oxidative stress, and neuroinflammation. *J. Ethnopharmacol.* 319 (Pt 1), 117165. doi:10.1016/j.jep.2023.117165

Xing, Y., and Bai, Y. (2020). A review of exercise-induced neuroplasticity in ischemic stroke: pathology and mechanisms. *Mol. Neurobiol.* 57 (10), 4218–4231. doi:10.1007/s12035-020-02021-1

Xu, Y., Zhang, J., Yu, L., Zhang, W., Zhang, Y., Shi, Y., et al. (2023). Engeletin alleviates depression-like phenotype by increasing synaptic plasticity via the BDNF-TrkB-mTORC1 signalling pathway. *J. Cell. Mol. Med.* 27 (23), 3928–3938. doi:10.1111/jcmm.17975

Xue, H., Li, P., Luo, Y., Wu, C., Liu, Y., Qin, X., et al. (2019). Salidroside stimulates the Sirt1/PGC-1α axis and ameliorates diabetic nephropathy in mice. *Phytomedicine* 54, 240–247. doi:10.1016/j.phymed.2018.10.031

Yan, L., Ai, Y., Xing, Y., Wang, B., Gao, A., Xu, Q., et al. (2023a). Citalopram in the treatment of elderly chronic heart failure combined with depression: a systematic review and meta-analysis. *Front. Cardiovasc. Med.* 10, 1107672. doi:10.3389/fcvm.2023.1107672

Yan, W. J., Tan, Y. C., Xu, J. C., Tang, X. P., Zhang, C., Zhang, P. B., et al. (2015). Protective effects of silibinin and its possible mechanism of action in mice exposed to chronic unpredictable mild stress. *Biomol. Ther. Seoul.* 23 (3), 245–250. doi:10.4062/biomolther.2014.138

Yan, Y., Li, J., Zhang, Y., Wang, H., Qin, X., Zhai, K., et al. (2023b). Screening the effective components of Suanzaoren decoction on the treatment of chronic restraint stress induced anxiety-like mice by integrated chinmedomics and network pharmacology. *Phytomedicine* 115, 154853. doi:10.1016/j.phymed.2023.154853

Yan, Y., Xu, X., Chen, R., Wu, S., Yang, Z., Wang, H., et al. (2021). Down-regulation of MST1 in hippocampus protects against stress-induced depression-like behaviours and synaptic plasticity impairments. *Brain. Behav. Immun.* 94, 196–209. doi:10.1016/j.bbi.2021.02.007

Yang, L., Huang, Y., Chen, F., Wang, Y., Su, K., Zhao, M., et al. (2023a). Berberine attenuates depression-like behavior by modulating the hippocampal NLRP3 ubiquitination signaling pathway through Trim65. *Int. Immunopharmacol.* 123, 110808. doi:10.1016/j.intimp.2023.110808

Yang, S. J., Wang, J. J., Cheng, P., Chen, L. X., Hu, J. M., and Zhu, G. Q. (2023b). Ginsenoside Rg1 in neurological diseases: from bench to bedside. *Acta. Pharmacol. Sin.* 44 (5), 913–930. doi:10.1038/s41401-022-01022-1

Yao, X., Qin, X., Wang, H., Zheng, J., Peng, Z., Wang, J., et al. (2023). Lack of bombesin receptor-activated protein homologous protein impairs hippocampal synaptic plasticity and promotes chronic unpredictable mild stress induced behavioral changes in mice. *Stress* 26 (1), 1–14. doi:10.1080/10253890.2022.2155513

Ye, Z., Wang, J., Fang, F., Wang, Y., Liu, Z., Shen, C., et al. (2024). Zhi-Zi-Hou-Po decoction alleviates depressive-like behavior and promotes hippocampal neurogenesis in chronic unpredictable mild stress induced mice via activating the BDNF/TrkB/CREB pathway. *J. Ethnopharmacol.* 319 (Pt 3), 117355. doi:10.1016/j.jep.2023.117355

Yi, Y., Xu, W., Wang, H. X., Huang, F., and Wang, L. M. (2020). Natural polysaccharides experience physiochemical and functional changes during preparation: a review. *Carbohydr. Polym.* 234, 115896. doi:10.1016/j.carbpol.2020.115896

Yin, R., Zhang, K., Li, Y., Tang, Z., Zheng, R., Ma, Y., et al. (2023). Lipopolysaccharide-induced depression-like model in mice: meta-analysis and systematic evaluation. *Front. Immunol.* 14, 1181973. doi:10.3389/fimmu.2023.1181973

Yu, C., Li, A., Li, X., Chen, Z., Wang, P., Dong, Z., et al. (2020). Impaired LTD-like motor cortical plasticity in female patients with major depression disorder. *Neuropharmacology* 179, 108268. doi:10.1016/j.neuropharm.2020.108268

Yu, D., Cheng, Z., Ali, A. I., Wang, J., Le, K., Chibaatar, E., et al. (2019). Chronic unexpected mild stress destroys synaptic plasticity of neurons through a glutamate transporter, GLT-1, of astrocytes in the ischemic stroke rat. *Neural. Plast.* 2019, 1615925. doi:10.1155/2019/1615925

Yu, H., Yang, R., Wu, J., Wang, S., Qin, X., Wu, T., et al. (2022). Association of metformin and depression in patients with type 2 diabetes. *J. Affect. Disord.* 318, 380–385. doi:10.1016/j.jad.2022.09.015

Yu, S., Zhao, Y., Luo, Q., Gu, B., Wang, X., Cheng, J., et al. (2024). Early life stress enhances the susceptibility to depression and interferes with neuroplasticity in the hippocampus of adolescent mice via regulating miR-34c-5p/SYT1 axis. *J. Psychiatr. Res.* 170, 262–276. doi:10.1016/j.jpsychires.2023.12.030

Zavvari, F., Nahavandi, A., and Goudarzi, M. (2020). Fluoxetine attenuates stress-induced depressive-like behavior through modulation of hippocampal GAP43 and neurogenesis in male rats. *Jj. Chem. Neuroanat.* 103, 101711. doi:10.1016/j.jchemneu.2019.101711

Zhang, H., Sun, Y., Huang, Z., Wu, Z., Ying, Y., Liu, R., et al. (2024a). Jiawei-Xiaoyao pill elicits a rapid antidepressant effect, dependent on activating CaMKII/mTOR/BDNF signaling pathway in the hippocampus. *J. Ethnopharmacol.* 318 (Pt B), 117016. doi:10.1016/j.jep.2023.117016

Zhang, H., Zhao, Y., and Wang, Z. (2015). Chronic corticosterone exposure reduces hippocampal astrocyte structural plasticity and induces hippocampal atrophy in mice. *Neurosci. Lett.* 592, 76–81. doi:10.1016/j.neulet.2015.03.006

Zhang, L., Luo, J., Zhang, M., Yao, W., Ma, X., and Yu, S. Y. (2014). Effects of curcumin on chronic, unpredictable, mild, stress-induced depressive-like behaviour and structural plasticity in the lateral amygdala of rats. *Int. J. Neuropsychopharmacol.* 17 (5), 793–806. doi:10.1017/S1461145713001661

Zhang, L., and Wei, W. (2020). Anti-inflammatory and immunoregulatory effects of paeoniflorin and total glucosides of paeony. *Pharmacol. Ther.* 207, 107452. doi:10.1016/j.pharmthera.2019.107452

Zhang, M., Lyu, D., Wang, F., Shi, S., Wang, M., Yang, W., et al. (2022b). Ketamine may exert rapid antidepressant effects through modulation of neuroplasticity, autophagy, and ferroptosis in the habenular nucleus. *Neuroscience* 506, 29–37. doi:10.1016/j.neuroscience.2022.10.015

Zhang, M. M., Huo, G. M., Cheng, J., Zhang, Q. P., Li, N. Z., Guo, M. X., et al. (2022a). Gypenoside XVII, an active ingredient from gynostemma pentaphyllum, inhibits C3aR-associated synaptic pruning in stressed mice. *Nutrients* 14 (12), 2418. doi:10.3390/nu14122418

Zhang, R., Zeng, M., Zhang, X., Zheng, Y., Lv, N., Wang, L., et al. (2023). Therapeutic candidates for alzheimer's disease: saponins. *Int. J. Mol. Sci.* 24 (13), 10505. doi:10.3390/ijms241310505

Zhang, X., Guo, J., Zhang, C., Wang, W., Du, S., and Tian, X. (2024b). Suanzaoren decoction exerts its antidepressant effect via the CaMK signaling pathway. *Transl. Neurosci.* 15 (1), 20220341. doi:10.1515/tnsci-2022-0341

Zhao, X., Kong, D., Zhou, Q., Wei, G., Song, J., Liang, Y., et al. (2021). Baicalein alleviates depression-like behavior in rotenone-induced Parkinson's disease model in mice through activating the BDNF/TrkB/CREB pathway. *Biomed. Pharmacother.* 140, 111556. doi:10.1016/j.biopha.2021.111556

Zheng, Z. H., Tu, J. L., Li, X. H., Hua, Q., Liu, W. Z., Liu, Y., et al. (2021). Neuroinflammation induces anxiety- and depressive-like behavior by modulating neuronal plasticity in the basolateral amygdala. *Brain. Behav. Immun.* 91, 505–518. doi:10.1016/j.bbi.2020.11.007

Zhou, C., Peng, B., Qin, Z., Zhu, W., and Guo, C. (2021). Metformin attenuates LPS-induced neuronal injury and cognitive impairments by blocking NF-κB pathway. *Bmc. Neurosci.* 22 (1), 73. doi:10.1186/s12868-021-00678-5

Zhu, S. M., Luo, F. Y., Peng, J., Luo, L. Y., Xue, R., Yang, Y., et al. (2024). The physicochemical characteristics and antidepressant-like effects of a polysaccharide-rich fraction from Schisandra chinensis (Turcz.) Baill in behavioral despair mice and olfactory bulbectomy-induced depression-like mice. *J. Ethnopharmacol.* 320, 117464. doi:10.1016/j.jep.2023.117464

Zhu, W., Zhang, W., Yang, F., Cai, M., Li, X., Xiang, Y., et al. (2023). Role of PGC-1α mediated synaptic plasticity, mitochondrial function, and neuroinflammation in the antidepressant effect of Zi-Shui-Qing-Gan-Yin. *Front. Neurol.* 14, 1108494. doi:10.3389/fneur.2023.1108494

Zhu, X., Sun, Y., Zhang, C., and Liu, H. (2017). Effects of berberine on a rat model of chronic stress and depression via gastrointestinal tract pathology and gastrointestinal flora profile assays. *Mol. Med. Rep.* 15 (5), 3161–3171. doi:10.3892/mmr.2017.6353

Zhuang, W., Liu, S. L., Xi, S. Y., Feng, Y. N., Wang, K., Abduwali, T., et al. (2023). Traditional Chinese medicine decoctions and Chinese patent medicines for the treatment of depression: efficacies and mechanisms. *J. Ethnopharmacol.* 307, 116272. doi:10.1016/j.jep.2023.116272

Zia, A., Farkhondeh, T., Pourbagher-Shahri, A. M., and Samarghandian, S. (2021). The role of curcumin in aging and senescence: molecular mechanisms. *Biomed. Pharmacother.* 134, 111119. doi:10.1016/j.biopha.2020.111119

Ziegler, J., and Facchini, P. J. (2008). Alkaloid biosynthesis: metabolism and trafficking. *Annu. Rev. Plant. Biol.* 59, 735–769. doi:10.1146/annurev.arplant.59.032607.092730

## Glossary

| | |
|---|---|
| **TCM** | Traditional Chinese medicine |
| **MDD** | Major depressive disorder |
| **SSRIs** | Selective serotonin reuptake inhibitors |
| **LTP** | Long-term potentiation |
| **LTD** | long-term depression |
| **BDNF** | Brain-derived neurotrophic factor |
| **TrkB** | Tyrosine kinase receptor B |
| **cAMP** | Cyclic adenosine monophosphate |
| **CREB** | cAMP responsive element binding protein |
| **CUMS** | Chronic unpredictable mild stress |
| **MS** | maternal-infant separation |
| **DG** | Dentate gyrus |
| **CSIS** | Chronic social isolation |
| **HPA** | Hypothalamic-pituitary-adrenal |
| **ACTH** | Adrenocorticotropin |
| **CRH** | Corticotropin-releasing hormone |
| **CORT** | Cortisol |
| **BNIP3L** | BNIP3 like |
| **LPS** | Lipopolysaccharide |
| **PNs** | Projection neurons |
| **CNS** | Central nervous system |
| **BLA** | Basolateral amygdala |
| **nNOS** | neural nitric oxide synthase |
| **GAP-43** | Growth associated protein 43 |
| **5-HT** | Serotonin |
| **NMDAR** | N-methyl-D-aspartate receptor |
| **4E-BPs** | 4E binding proteins |
| **AR** | Allergic rhinitis |
| **$H_2S$** | Hydrogen sulfide |
| **SI** | Soy isoflavones |
| **p-SYP** | Phosphorylated SYP |
| **OA** | Oleanolic acid |
| **PTSD** | Post-traumatic stress disorder |
| **SCFAs** | Short-chain fatty acids |
| **AChE** | Acetylcholinesterase |
| **PNS** | Prenatal stress |
| **DA** | Dopamine |
| **ZZCT** | Zhi-Zi-Chi-Tang |
| **ZSQGY** | Zi-Shui-Qing-Gan-Yin |
| **MSG** | monosodium glutamate |
| **DBD** | Danggui-Buxue Decoction |
| **AR** | *Astragali Radix* |
| **ASR** | *Angelica Sinensis Radix* |
| **DD** | Diabetes mellitus with depression |
| **HSD1** | 11β-hydroxysteroid dehydrogenase 1 |
| **GC** | Glucocorticoids |
| **GR** | Glucocorticoid receptor |
| **JWX** | Jiawei-Xiaoyao pill |
| **MXYS** | Modified Xiaoshan |
| **SNS** | SiNiSan |
| **SZRD** | Suanzaoren Decoction |
| **ZZHP** | Zhi-Zi Hou-Po Decoction |

frontiers | Frontiers in Pharmacology

TYPE Review
PUBLISHED 24 December 2024
DOI 10.3389/fphar.2024.1494277



OPEN ACCESS

EDITED BY
Peng Sang,
Zhengzhou University, China

REVIEWED BY
Zhiyou Yang,
Guangdong Ocean University, China
Smita Kumari,
The Ohio State University, United States

*CORRESPONDENCE
Ping Li,
liping@ccucm.edu.cn

RECEIVED 10 September 2024
ACCEPTED 14 November 2024
PUBLISHED 24 December 2024

CITATION
Shi Z, Zhang Y, Xiao Y, Shi Z, Wei X, Wang B, Yuan Y and Li P (2024) The protective effects of gastrodin on neurological disorders: an update and future perspectives.
*Front. Pharmacol.* 15:1494277.
doi: 10.3389/fphar.2024.1494277



# The protective effects of gastrodin on neurological disorders: an update and future perspectives

Zhouying Shi[1], Yali Zhang[2], Yuhua Xiao[2], Zhoujing Shi[3], Xiaotong Wei[1], Bin Wang[1], Yue Yuan[4] and Ping Li[4]*

[1]College of Traditional Chinese Medicine, Changchun University of Chinese Medicine, Changchun, China, [2]College of Basic Medicine, Changchun University of Chinese Medicine, Changchun, China, [3]College of Basic Medicine, Heilongjiang University of Chinese Medicine, Harbin, China, [4]College of Nursing, Changchun University of Chinese Medicine, Changchun, China

Neurological disorders are characterized by high mortality and disability rates. Furthermore, the burden associated with disability and mortality resulting from neurological disorders has been increasing at an alarming rate. Botanical drugs and their bioactive components have emerged as a prominent area of research, offering a promising avenue for developing novel alternatives for treating neurological diseases. Gastrodin is the principal active component derived from the traditional Chinese medicinal plant *Gastrodia elata* Blume (GEB). Existing literature reveals that gastrodin exerts various pharmacological protective actions against neurological disorders. This review aimed to collate novel literature on gastrodin for treating neurological disorders from Web of Science, PubMed, Embase and CNKI. The pharmacokinetics of gastrodin, its therapeutic role in neurological disorders, the main mechanisms of action and clinical application were addressed. Furthermore, a detailed overview of gastrodin drug delivery systems and physical enhancement methods was presented, offering invaluable insights into potential research and the extensive applications of gastrodin.

KEYWORDS

**gastrodin, neurological disorders, molecular mechanism, pharmacological effects, pharmacokinetics, drug delivery system**

## 1 Introduction

Neurological disorders are the primary reason for disability and the second leading cause of mortality worldwide (Feigin et al., 2020). Smoking, alcohol consumption, and high intake of sugar and salt levels are important risk factors for the development of neurological disorders (Collaborators, 2019). The most common neurological disorders with high rates of mortality and disability are stroke, migraine, vascular dementia (VD), and Alzheimer's disease (AD) (Feigin and Vos, 2019), followed by epilepsy, traumatic brain injury (TBI), Parkinson's disease (PD), peripheral nerve injury (PNI), hypoxic-ischemic brain damage (HIBD), and others (Wei et al., 2023; Min et al., 2020; Liu B. et al., 2018). Currently, the treatment of neurological diseases is mainly focused on symptom management and delaying disease progression, rather than targeting the underlying pathological cause, and treatment with these drugs often has limited efficacy and side effects (Rahimi

Darehbagh et al., 2024). Developing new drugs is a central objective of scientific research in this field.

Compared to modern pharmaceuticals, traditional herbal plants have been successfully used for centuries (Choi et al., 2011). The botanical drug GEB is a perennial plant. In the first century BC, GEB was documented as a superior Chinese medicine agent with a long history of use for treating stroke and epilepsy (Zhan et al., 2016). Modern research has extracted approximately 134 components from GEB, including phenols, polysaccharides, and glycosides (Gong et al., 2024). Gastrodin (GAS) is the principal active component due to its neuropharmacological properties (Kim et al., 2012), which extracted from GEB by reflux extraction, ultrasound-assisted extraction and microwave extraction (Teo et al., 2008). However, due to the low content of GAS in GEB, traditional isolation and purification methods are unable to obtain a high yield, high purity and low cost of GAS. Therefore, GAS used in the current research is mainly produced by chemical and biological synthesis (Dai et al., 2024). The research findings indicate that GAS can reduce inflammation and oxidative stress-induced neurological damage (Xiao et al., 2023). It has been widely used to treat neurological disorders (More et al., 2013; Jangra et al., 2022; Fan et al., 2024). Nevertheless, the extensive application of GAS and its molecular mechanism of action remain significant challenges due to its favorable hydrophilicity, low blood-brain barrier (BBB) permeability, and poor bioavailability (Illum, 2003; Huang et al., 2022; Wang et al., 2021).

A literature review revealed many studies examining the therapeutic potential of GAS in managing neurological disorders. The majority of these studies focused on central nervous system (CNS) disorders He et al. (2024); Liu B. et al. (2018), providing a review of the chemical structure, pharmacokinetics, and pharmacological effects of GAS (Dai et al., 2024). There is a lack of reviews on the studies of GAS in peripheral nervous system disorders, GAS delivery systems, and clinical studies of its monotherapy and combinations on neurological disorders. Consequently, this paper provided a comprehensive review of studies related to GAS in central and peripheral nervous system disorders. In addition, the paper discussed the GAS drug delivery system, physical enhancement methods, their primary mechanisms of action in neurological disorders and clinical application in great detail. Finally, we put forward suggestions regarding future research directions in light of the limitations of current research on GAS and the potential for drug development. Previous literature reviews of the neurological disorders of GAS treatment reported a lack of coverage of these aspects (Xiao et al., 2023; Liu Y. et al., 2018). This review article aimed to overcome these limitations and further contribute to the extensive research and applications of GAS.

# 2 Search strategy and selection criteria

## 2.1 Search strategy

Web of Science, PubMed, Embase and CNKI databases were searched for all relevant articles published in the English language from the database inception until 30 March 2024 using the following terms: “gastrodin”, “gastrodia elata Blume”, “neurological disorders”, “cerebrovascular disease”, “ischemic stroke”, “hemorrhagic stroke”, “vascular dementia”, “Parkinson’s disease ”, “Alzheimer’s disease”, “neurodegenerative disease”, “epilepsy”, “migraine”, “traumatic brain injury”, “peripheral nerve injury”, “hypoxic-ischemic brain damage”, “depression”, “nervous system tumours”, “pharmacokinetics”, “drug delivery systems”, “nanoparticles”, “polyurethane porous membranes”, “solid dispersions”, “*in situ* gelling systems”, “focused ultrasound”, “focused shock wave.”

## 2.2 Selection criteria

The inclusion criteria were as follows: GAS was the study subject; the diseases treated by GAS belonged to the neurological disorders category; and the study results involved the exploration of the mechanisms. The exclusion criteria were: unclear neurological diseases treated by GAS; unclear research object, research method, and mechanism of action in case reports and literature reviews; poor methodology, unreliable results or poor quality; repetitive publication and duplication of research content in the literature.

Two researchers (ZS and YZ) undertook an independent screening and analysis of all the literature during the collation process, thus ensuring the reliability of the study.

# 3 Pharmacokinetics of gastrodin

GAS is a phenolic glucoside active component with good hydrophilicity and the highest systemic exposure compared to other *G. elata* extracts (Dong et al., 2020). GAS is rapidly absorbed in the intestinal tract. A metabolic kinetics study of GAS in SD rats showed that the time to reach peak plasma concentration ($T_{max}$) of GAS administered as a single dose of 100 mg/kg was 0.5 h in both the ingested and fasted states. However, the peak plasma concentration ($C_{max}$) and the area under the curve (AUC) in the fasted state were approximately twice those observed in the ingested state (Jia et al., 2014). The half-life ($t_{1/2}$) of fasting administration was markedly longer than feeding administration, suggesting that fasting may lead to better and faster GAS absorption (Jia et al., 2014). Following oral administration, GAS was rapidly absorbed into the blood and widely distributed throughout the organs and tissues. Moreover, Jiang et al. (2017) observed that GAS is predominantly distributed in the kidneys, with a concentration of 12,584.06 ng/g, followed by the heart (2034.08 ng/g), liver (1592.58 ng/g), and lung (1433.08 ng/g). The lowest distribution was observed in the brain and spleen, which is consistent with results reported by Lin et al. (2007), who observed that the $C_{max}$ of GAS (100 mg/kg i. v.) in the brain and blood of SD rats was 1.4 and 533 μg/mL, respectively. This may be related to the good hydrophilicity and low BBB permeability of GAS (Ji et al., 2015).

GAS is rapidly absorbed and enters the bloodstream, where it undergoes a biotransformation process and is metabolized into various metabolites (Cheng and Deng, 2021). It has been reported that the urinary excretion rate of GAS reaches its peak at the 1-h mark following administration, with a cumulative excretion rate of 53% within 0–48 h, which suggests that urine is the primary route of excretion of GAS (Zhang et al., 2019). However,

Jiang et al. (2017) examined the excretion of GAS in the urine and feces of SD rats following the administration of GEB powder (4 g/kg orally) and GEB extract (0.6 g/kg orally). The results showed that the renal excretion of GAS within 24 h of oral administration was <51.42% (bulk) and <18.13% (extract). The quantity excreted in feces was minimal. In addition, Nepal et al. (2019) confirmed that GAS is readily hydrolyzed by intestinal flora in the intestinal tract and rapidly converted to 4-HBA, which is significantly different from the pharmacokinetics of rats after antibiotic use. This indicates that the absorption and metabolism of GAS in the intestinal tract mainly depend on the intestinal microbiota. It may be concluded that renal and intestinal metabolism are the main metabolic pathways of GAS. Nevertheless, the quantity of GAS excreted in urine and feces is restricted, and GAS may be excreted via alternative metabolic pathways through conversion to other metabolites.

Recent research has found that combining botanical drugs may prolong the activation time of drugs and enhance the absorption of active components (Tang et al., 2022). The combination of *Ligusticum chuanxiong* with GEB represents a well-established approach to treating migraine (Wang et al., 2016). Tetramethylpyrazine (TMP) and ferulic acid (FA) represent the principal active components of *L. chuanxiong*. In their study, Mi et al. (2020a) used a migraine SD rat model of liver yang ascendant hyperactivity, where the $C_{max}$ of SD rats treated with GAS (915 mg/kg. i. g.) alone was 132.95 μg/mL. The $C_{max}$ of SD rats in the group treated with GAS (915 mg/kg. i. g.) in combination with TMP and FA was 314.33 μg/mL. Furthermore, the AUC, mean retention time (MRT), and $t_{1/2}$ were noticeably lower in the combined treatment group than the GAS alone group. The metabolic kinetics of GAS in the brain tissue of migraine model rats exhibited a consistency with the results observed in blood. Also, the $T_{1/2}$ increased with the rising TMP and FA levels (Mi et al., 2020b). The results suggest that adding TMP and FA enhances the permeability of the BBB for GAS, thereby facilitating its absorption and metabolism. Moreover, Mi et al. (2020a) confirmed that GAS and FA exerted bidirectional regulatory effects in the blood-stasis migraine model. It was observed that the $T_{1/2}$, MRT, $C_{max,}$ and AUC in the blood and brain interstitial fluid (BIF) of the SD rats in the group that received GAS exhibited a notable increase compared to the group that did not. Furthermore, the degree of TMP uptake in the blood and BIF was positively correlated with the concentration of GAS. These results suggest that GAS may markedly enhance the bioavailability and prolong the duration of FA by reducing BBB permeability (Mi et al., 2020a). The combination of GAS and other treatments has been demonstrated to reduce neuropathy and modulate pain pathways effectively (Ferrari et al., 2024). These findings offer insights into potentially novel approaches for treating neurological disorders.

# 4 Drug delivery system and physical enhancement methods

The BBB represents a significant obstacle in treating neurological disorders, impeding the delivery of pharmaceutical agents into the brain (Zhang et al., 2021). Hydrophilicity of GAS severely affects the therapeutic efficacy and bioavailability of GAS for neurological disorders (Long et al., 2020). In recent decades, nanoscience, ultrasound science, and natural components have been gradually integrated into medical science research to develop safe, highly biocompatible, and bioavailable drug delivery systems. In light of the growing interest in drug delivery systems, various innovative systems based on GAS have been developed. These include gold nanoparticles (AuNPs), polyurethane (PU) porous film, solid dispersion (SD), and *in situ* gelling systems (ISGS) (Shen et al., 2024; Li et al., 2020; Cai et al., 2014). Furthermore, the combination of physical methods, including focused ultrasound (FUS) and focused shockwaves (FSW), with GAS also improves the delivery of GAS in the brain (Kung et al., 2021) (see Figures 1, 2; Table 1, 2).

## 4.1 Drug delivery system

### 4.1.1 Gold nanoparticles (AuNPs)

AuNPs are made of gold, which has safe and distinctive biomolecular characteristics (Lu et al., 2021). Currently, AuNPs are utilized in several biomedical applications such as drug delivery, cellular imaging, etc. (Arami et al., 2022; Betzer et al., 2017). In particular, these nanoparticles are employed extensively in diagnosing and treating neurodegenerative diseases. E.g., AuNPs can delay the development of Alzheimer's disease (AD) by inducing the polarization of macrophages to the M2 phenotype and attenuating neuroinflammation (Aili et al., 2023). Additionally, AuNPs can target pathological proteins, facilitating early and precise diagnosis by enhancing protein signals (Chiang et al., 2024). Many protein detection sensors based on AuNPs have been developed, e.g., Tau and α-synuclein targeted AuNPs for diagnosing neurodegenerative disorders (Tapia-Arellano et al., 2024). Over the years, AuNPs have become increasingly important as potential tools for diagnosing and treating neurological diseases (Baez et al., 2021).

While AuNPs improve drug penetration across the BBB (Sokolova et al., 2020), the delivery of AuNPs into the brain is constrained by the BBB. Consequently, contemporary researchers have sought to enhance the functionalization of AuNPs to facilitate their delivery by modifying the surface of the AuNPs using carrier materials (Baez et al., 2021). GAS does not readily cross the BBB due to its hydrophilic nature. To enhance the efficacy of GAS on cerebral ischemia-reperfusion injury (CIRI), Huang et al. (2022) employed the physical embedding method to load GAS into a carrier material encapsulated with AuNPs, resulting in the preparation of the GAS-loaded drug delivery system Au-G5. NHAc-PS/GAS with excellent biocompatibility and sustained drug release capabilities. Au-G5. NHAc-PS/GAS significantly reduced and downregulated the production of pro-inflammatory factors compared to GAS alone. The nano drug-carrying system enhanced the penetration ability of the BBB of *Aspergillus* and significantly improved bioavailability (Huang et al., 2022).

### 4.1.2 Polyurethane porous film

Polyurethane (PU) is a polymer with favorable properties, including mechanical properties, biodegradability, and biocompatibility, particularly applicable to biomedical applications (Wendels and Averous, 2021). Due to their straightforward processing, extensive availability, and low cost

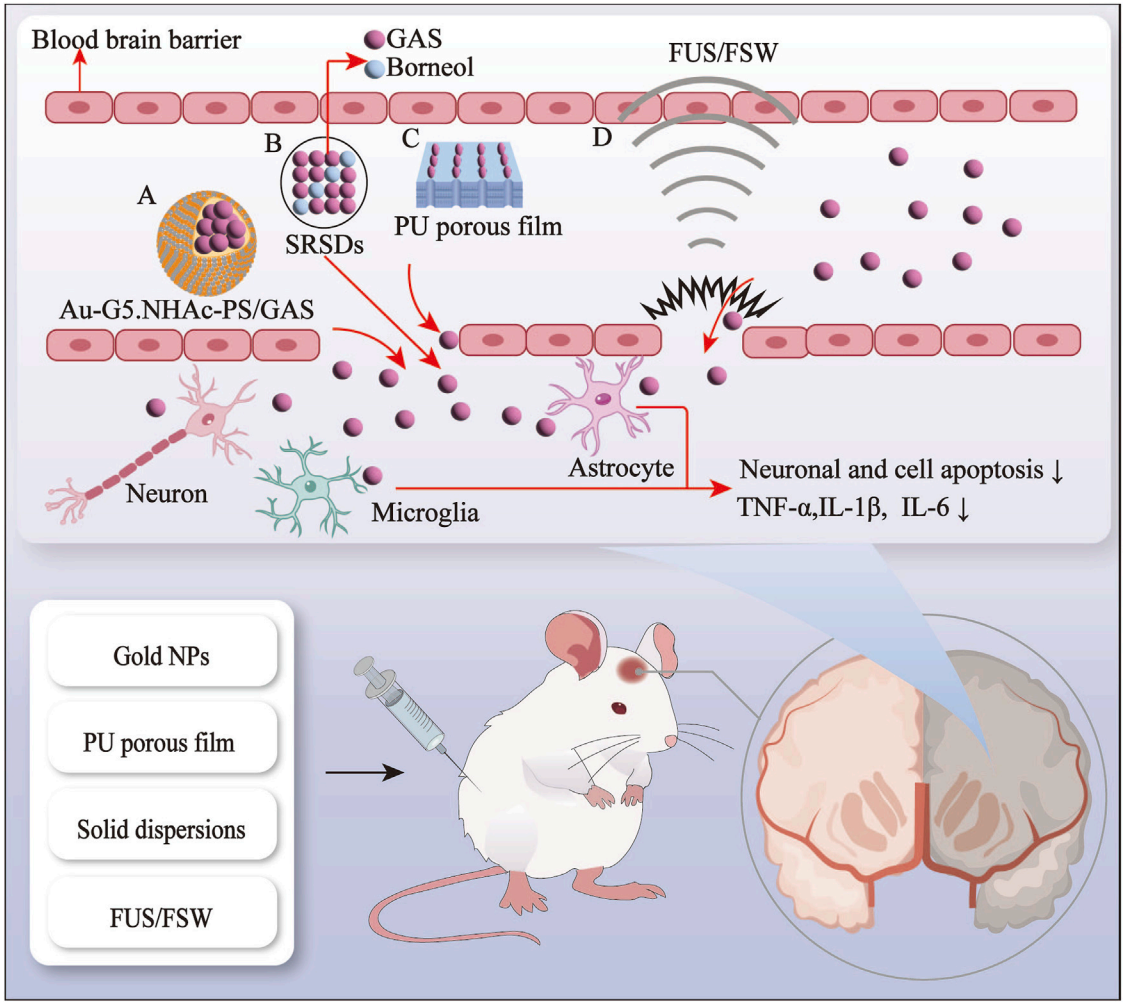


FIGURE 1
The gastrodin drug delivery system and physical enhancement methods via the blood-brain barrier route. A, gold nanopaticles; B, solid dispersions, C, polyurethane porous film; D, focused ultrasound and focused shockwave.

(Uscategui et al., 2019), polyurethanes have been developed into membranes, scaffolds, and gels for pharmaceutical use Arshad et al. (2024). The development of multifunctional membranes utilizing polymers such as polyurethanes has been shown to enhance protein loading capacity and regulate the release of nerve growth factor (Uz et al., 2017).

Several researchers have designed a novel GAS-crosslinking PU elastomer that enhances cellular activity by using the ability of polyurethane to modulate nerve growth factor release. However, this elastomer cannot differentiate nerves (Li et al., 2018). The high interconnectivity and interconnected porous film structure of the material facilitate peripheral nerve regeneration by improving oxygen and protein circulation (Hsu and Ni, 2009). Li et al. (2020) developed an elastomeric PU porous film functionalized with GAS, which has been demonstrated to promote peripheral nerve regeneration. This was achieved by combining GAS and PU porous film, building upon previous research on GAS-crosslinking PU elastomers, which improved the bioavailability of GAS. The potential of PU membranes in treating peripheral nerve injury is significant. However, there is a paucity of clinical or experimental studies on using polyurethane porous membranes in peripheral nervous system diseases or nerve injury-related neurological diseases. Future research should investigate the efficacy of polyurethane porous membranes in treating neurological disorders.

### 4.1.3 Solid dispersion (SD)

SD is the combination of hydrophobic drugs with a hydrophilic carrier, which increases the solubility of the drug by changing its state (Tran and Park, 2021). The $T_{1/2}$, $AUC_{0-t}$, and $AUC_{0-\alpha}$ of andrographolide (50 mg/kg) in the plasma of Wistar rats were found to be 2.6 h, 532 and 608 ng h/mL, respectively. However, when the SD technique was employed, these values increased to 4.0 h, 653 ng/h, and 867 ng/h/mL, respectively (Assim et al., 2024). SD technology significantly reduces the drug clearance of andrographolide. Previous studies have also demonstrated that SDs enhance drug bioavailability by increasing water solubility and maintaining drug release (Gala et al., 2020).

Cai et al. (2014) used SD technology to prepare sustained-release SDs (SRSDs) for co-loading GAS and borneol. Their findings demonstrated that SRSDs markedly diminished gastric irritation,

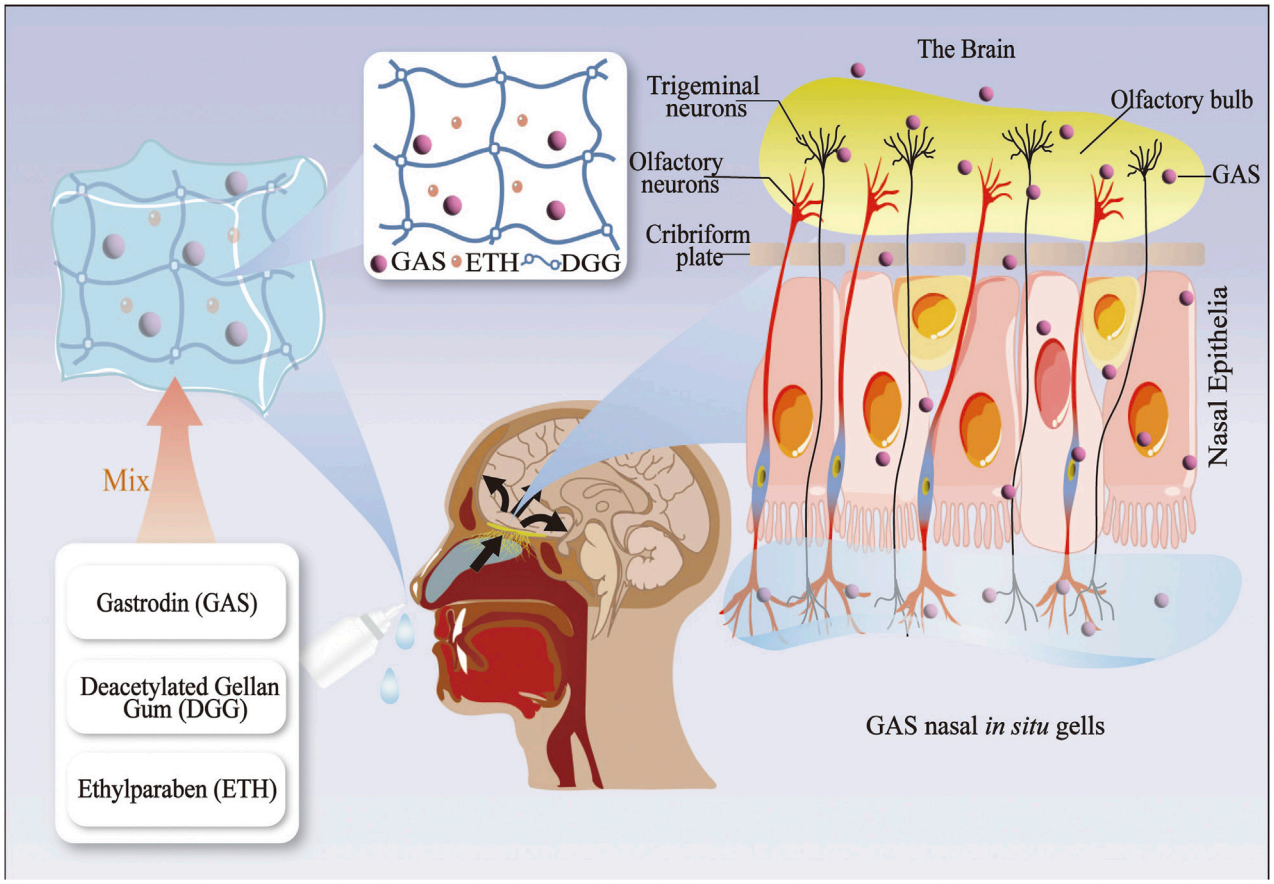


FIGURE 2
The gastrodin drug delivery system via the nose-brain route (GAS nasal *in situ* gelling systems).

**TABLE 1** Improved properties of gastrodin drug delivery system and physical enhancement methods.

| Delivery system | Improved properties | Refs. |
|---|---|---|
| Gold nanoparticles | Improved bioavailability; reduced cytotoxicity; facilitated cellular uptake; prolonged persistence in the blood circulation | Huang et al. (2022) |
| PU porous film | Improved hydrophilicity; excellent biocompatibility; maintains cells with more neurite extension concomitantly | Li et al. (2020) |
| Solid dispersions | Improved bioavailability; reduced stomach irritation; improved and maintained brain targeting | Cai et al. (2014) |
| *In situ* gelling systems | Improved bioavailability; enhanced analgesic and sedative effects | Cai et al. (2011) |
| Focused ultrasound | Increased permeability of blood-brain barrier; increased drug uptake; improved brain targeting | Wang et al. (2022), Luo et al. (2022), Wang et al. (2021) |
| Focused shockwave | Improved brain targeting; increased and prolonged circulation of drugs in the cerebrospinal fluid | Kung et al. (2021) |

Refs., references; PU, Polyurethane.

enhanced bioavailability, and sustained the adequate oral brain-targeted drug delivery capacity of GAS compared to oral GAS alone. Previous studies have demonstrated that the combination of GAS and borneol enhances the absorption of GAS via oral administration and improves the brain targeting of GAS (Yao et al., 2020). SDs have a beneficial impact on both hydrophobic and hydrophilic drugs. In particular, they enhance the absorption of hydrophilic drugs, such as GAS, while reducing adverse drug reactions, thus expanding the potential applications of drugs for neurological diseases.

### 4.1.4 *In Situ* gelling systems

Under normal temperature conditions *in vitro*, the *in situ* gels exist as a liquid and change to a gel state when stimulated by different factors *in vivo* (Kolawole and Cook, 2023). *In situ* gels prolong drug retention time, improve bioavailability, and control release profiles at

TABLE 2 Gastrodin drug delivery system and physical enhancement methods studied in preclinical acute neurological disorders.

| Delivery system | Disease | Experimental model | Targets | Main results | Refs |
|---|---|---|---|---|---|
| Gold nanoparticles | CIRI | *In vivo:* SD rats | *In vivo* and *In vitro*: NA | *In vivo and in vitro:* decreased the apoptosis rate and improved the therapeutic effects of GAS on CIRI. | Huang et al. (2022) |
| | | *In vitro:* astrocytes/hypothalamic neurons | | | |
| PU porous film | PNI | *In vitro:* PC12 cells | *In vitro*: BDNF, GDNF↑ | *In vitro:* promoted the regeneration, proliferation, and differentiation of nerve cells | Li et al. (2020) |
| Focused ultrasound | AD | *In vivo:* Kunming mice | *In vivo*: AQP4, BDNF, SYN, PSD-95↑ | *In vivo:* alleviated memory deficit and neuropathology of the AD-like mouse model | Luo et al. (2022) |
| | | | Aβ, tau, p-tau↓ | | |
| Focused ultrasound | PD | *In vivo:* C57BL/6J mice | *In vivo*: TH, DAT, Bcl-2, BDNF, SYN, PSD-95↑ | *In vivo:* strengthened the protective effect of GAS on dopaminergic neurons through reinforcing the anti-apoptotic activity and the expression of synaptic-related proteins | Wang et al. (2022) |
| | | | caspase-3↓ | | |
| Focused shockwave | Epilepsy | *In vivo:* SD rats | *In vivo*: SOD, CAT, GSH, T-AOC↑ | *In vivo:* epileptiform discharges, inflammation, oxidative stress, and apoptosis were reduced | Kung et al. (2021) |
| | | | IL-1β, MDA↓ | | |

Refs., references; CIRI, cerebral ischemia–reperfusion injury; NA, not applicable; GAS, gastrodin; PU, polyurethane; PNI, peripheral nerve injury; BDNF, brain-derived neurotrophic factor; GDNF, glial cell derived neurotrophic factor; AD, Alzheimer's disease; AQP4, aquaporin-4; SYN, synaptophysin; PSD-95, postsynaptic density protein 95; Aβ, beta-amyloid; tau, tubulin associated unit; p-tau, phosphorylated tau; PD, Parkinson's disease; TH, tyrosine hydroxylase; DAT, dopamine transporter; Bcl-2, B-cell lymphoma 2; SOD, superoxide dismutase; CAT, catalase; GSH, glutathione; T-AOC, total antioxidant capacity; IL-1β, interleukin-1β; MDA, malondialdehyde.

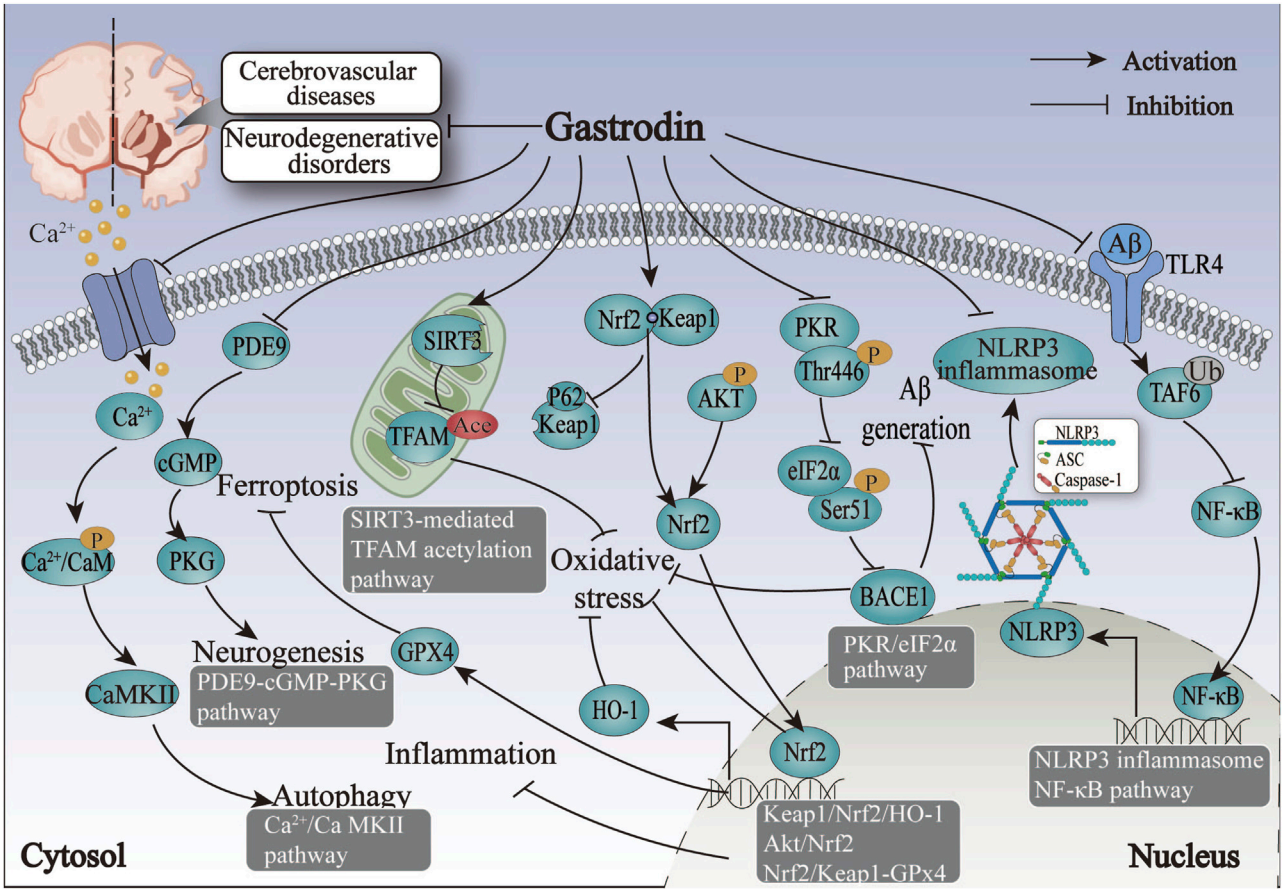


FIGURE 3
The therapeutic mechanism and critical pathways of gastrodin against cerebrovascular diseases and neurodegenerative disorders.

TABLE 3 Summary of the targets/pathways/mechanisms and effects of gastrodin on cerebrovascular diseases.

| Disease | Inducer | Experimental model | Dose | Targets/mechanisms | Effects | Refs. |
|---|---|---|---|---|---|---|
| IS | *In vivo:* NA | *In vivo:* C57BL/6J mice | *In vivo*: 50, 100 mg/kg (i.p. injection) | *In vivo:* cGMP, PKG, BDNF↑ | Promotes hippocampal neuronal regeneration and attenuated neurological damage after cerebral ischemia via the PDE9-cGMP-PKG pathway | Xiao et al. (2021) |
| | | | | activity of PDE9↓ | | |
| | *In vitro:* NA | *In vitro:* Neural stem cells | *In vitro*: 0.01, 0.1, 1 μM/L | *In vitro:* cGMP, PKG, BDNF↑ | | |
| | | | | PDE9↓ | | |
| IS | *In vivo:* NA | *In vivo:* SD rats | *In vivo:* NA | *In vivo:* protein expression levels of NLRP3, NLRC4, IL-18, caspase-1, p-STAT3↓ | Decreases the expression of NLRP3 and NLRC4 inflammasome via inhibition of STAT3 and NF-κB signaling pathway | Sui et al. (2019) |
| | *In vitro:* NA | *In vitro:* TNA2 astrocytes | *In vitro:* 10, 20, 50, 100 μM | *In vitro:* mRNA and protein expression of NLRP3, NLRC4, IL-18, caspase-1↓ | | |
| | | | | protein expression of p-STAT3↓ | | |
| IS | *In vivo:* NA | *In vivo:* SD rats | *In vivo:* 20, 40, 80 mg/kg (i.p. injection) | *In vivo:* PH, $pCO_2$, Glucose↓ | Inhibits $Zn^{2+}$-induced astrocytic cell death by inhibiting the inductions of p67 and PARP-1 | Luo et al. (2018) |
| | | | | $pO_2$↑ | | |
| | *In vitro:* zinc sulfate | *In vitro:* C6 astroglial cells | *In vitro:* 50, 100, 250 μM | *In vitro:* Nrf2, HO-1, GCLM, NAD↑ | | |
| | | | | ROS, p67, PARP-1, PAR↓ | | |
| IS | *In vivo:* NA | *In vivo:* C57BL/6J mice | *In vivo:*10, 50, 100 mg/kg (i.p. injection) | *In vivo:* caspase-3, Bax↓, MDA↓, TNF-α, IL-1β↓ | Activates the Akt/Nrf2 pathway and exerts neuroprotective effects against cerebral ischemia through anti-inflammatory, anti-oxidative, and anti-apoptotic pathways | Peng et al. (2015) |
| | | | | Bcl-2, SOD, Akt, p-Akt, Nrf2, HO-1↑ | | |
| HS | *In vivo:* Collagenase IV | *In vivo:* SD rats | *In vivo:*100 mg/kg (i.p. injection) | *In vivo:* ROS, 8-OHDG, 3-NT, MDA↓ | Activates Keap1/Nrf2/HO-1 signaling pathway to reduce inflammatory and oxidative factors and inhibit neuronal apoptosis. | Liu et al. (2020) |
| | | | | Keap1, Nrf2, HO-1, Bcl-2, GSH-Px, SOD↑ | | |
| | | | | Bax, caspase-3, caspase-9↓ | | |
| | *In vitro:* Hematoma lysate | *In vitro:* Primary cortical neuron | *In vitro*: 0, 10, 100, 300 μM | *In vitro:* cell viability↑, cell apoptosis↓ | | |
| HS | *In vitro:* NA | *In vivo:* SD rats | *In vivo:* 100 mg/kg (i.p. injection) | *In vivo:* Nrf2, HO-1, SOD, p-Akt, Bcl-2↑ | Inhibits microglia and astrocyte activation, oxidative stress, and neuronal apoptosis by reducing glutamate excess-mediated neurotoxicity. | Wang et al. (2019) |
| | | | | IL-1β, TNF-α, GFAP, MDA, 3-NT, 8-OHDG, Bax↓ | | |
| | | | | concentration of Glu, $Ca^{2+}$↓ | | |
| VD | *In vivo:* NA | *In vivo:* SD rats | *In vivo*: 15, 30, 60 mg/kg (i.g.) | *In vivo:* p62, Bcl-2↑ | Attenuates Aβ deposition, inhibiting autophagy and apoptosis via P38 MAPK signaling pathway. | Liu et al., 2018 |
| | | | | p-P38 MAPK, Bax, Beclin-1, LC3-II, $Aβ_{1-40/42}$, APP, BACE1↓ | | |
| VD | *In vivo:* NA | *In vivo:* SD rats | *In vivo*: 25, 50 mg/kg (i.p. injection) | *In vivo:* LC3, p62 and caspase-3↓, p-CaMKIIα↓, | Attenuates autophagic flux dysfunction by inhibiting the $Ca^{2+}$/CaMKII signaling pathway to ameliorate cognitive impairment in VD. | Chen et al. (2021) |
| | | | | LAMP-2↑ | | |
| | *In vitro:* $CoCl_2$ 200 μM | *In vitro:* HT22 cells | *In vitro:* 200 μM | *In vitro:* LC3-II, LC3, p62, p-p62, $Ca^{2+}$, p-CaMKIIα↓ | | |
| | | | | LAMP-2↑ | | |
| VD | *In vivo and In vitro:* NA | *In vivo:* SD rats | *In vivo:* 25, 50 mg/kg (i.p. injection) | *In vivo and In vitro:* GPx4, Nrf2, GSH↑ | Inhibits ferroptosis in hippocampal neurons by activating the Nrf2/Keap1-GPx4 signaling pathway | Li et al. (2022) |
| | | *In vitro:* HT22 cells | *In vitro:* 25, 50, 100 μmol/L | $Fe^{2+}$, MDA, COX2, Keap1↓ | | |

(Continued on following page)

TABLE 3 (*Continued*) Summary of the targets/pathways/mechanisms and effects of gastrodin on cerebrovascular diseases.

| Disease | Inducer | Experimental model | Dose | Targets/mechanisms | Effects | Refs. |
|---|---|---|---|---|---|---|
| VD | *In vivo:* NA | *In vivo:* SD rats | *In vivo:* 25, 50 mg/kg (i.g.) | *In vivo:* $A\beta_{1\text{-}42}$, p-tau396, p-tau217↓ | Enhances neuronal energy metabolism and improves neuronal mitochondrial function | Wu et al. (2023) |
| | *In vitro:* NA | *In vivo:* SD rats | *In vitro:* 12.5, 25, 37.5, 50, 75, 100 μM | *In vitro:* cell viability↑, mitochondrial dysfunction↓ | | |
| VD | *In vivo and In vitro:* NA | *In vivo:* SD rats | *In vivo:* 20, 50 mg/kg (i.p. injection) | *In vivo* and *In vitro:* The contents of ATP, NADH, NDUFB8, SDHB, UQCRC2, MTCO1, ATP5A, GSH↑ | Alleviates mitochondrial dysfunction by attenuating the SIRT3-mediated TFAM acetylation pathway and increasing the production of ATP, GSH, and SOD. | Chen et al. (2024) |
| | | *In vitro:* HT22 cells | *In vitro*: 0, 50, 100, 200 μM | SOD, SIRT3, TFAM, Mfn1/2, HO-1, Prdx1↑ | | |
| | | | | ROS, P53, P21, P16, Fis1, DRP1↓ | | |

IS, ischemic stroke; NA, not applicable; cGMP, cyclic guanosine mono phosphate; PKG, protein kinase G; BDNF, brain-derived neurotrophic factor; PDE9, Phosphodiesterase 9; SD, Sprague-Dawley; NLRP, nod-like receptor protein; IL, interleukin; STAT3, Signal transducer and activator of transcription 3; Nrf2, nuclear factor erythroid 2-related factor 2; HO-1, heme oxygenase-1; GCLM, Glutamate-cysteine ligase modifier; NAD, nicotinamide adenine dinucleotide; ROS, reactive oxygen species; PARP, poly ADP-ribose polymerase; MDA, malondialdehyde; TNF, tumor necrosis factor; SOD, superoxide dismutase; HS, hemorrhagic stroke; Akt, protein kinase B; GFAP, glial fibrillary acidic protein; 3-NT, 3-nitrotyrosine; Bcl-2, B-cell lymphoma-2; Bax, Bcl-2-associated X protein; 8-OHDG, 8-hydroxydeoxyguanosine; VD, vascular dementia; MAPK, mitogen-activated protein kinase; LC3-II, light chain 3-II; Aβ, amyloid β-protein; GSH-Px, antioxidant enzymes glutathione peroxidase; APP, amyloid precursor protein; BACE1, β-site APP, cleaving enzyme 1; CaMKIIα, $Ca^{2+}$-calmodulin stimulated protein kinase IIα; LAMP, lysosomal-associated membrane protein; GSH, glutathione; GPx4, glutathione peroxidase 4; COX2, cyclooxygenase 2; ATP, adenosine triphosphate; NDUFB8, Ubiqui none Oxidoreductase Subunit B8; SDHB, succinate dehydrogenase complex iron sulfur subunit B; UQCRC2, ubiquinol-cytochrome c reductase core protein 2; MTCO1, mitochondrially encoded, cytochrome coxidase subunit 1; TFAM, transcription factor A; Mfn1/2, Mitofusin 1/2; HO-1, heme oxygenase-1; Prdx, Peroxiredoxin; Fis1, Fission 1; DRP1, dynamin-related protein1.

specific body sites (Agrawal et al., 2020). *In situ* gel formulations were initially developed for topical administration. They can be delivered to various parts of the body via the oral, ocular, nasal, and vaginal routes, where they are used to treat oral, ocular, nasal, and vaginal diseases, respectively (Kolawole and Cook, 2023).

Some researchers combined the GAS and nasal *in situ* gel into a GAS nasal ISGS, finding that a GAS (50 mg/kg) nasal *in situ* gel preparation had the same analgesic effect on Kunming strain mice as an oral GAS (100 mg/kg) preparation. Furthermore, mice in the nasal *in situ* gel preparation group had a significantly longer sleep duration than mice in the oral solution group after receiving the same dose of GAS. The nasal ISGS enhanced the bioavailability and brain targeting of GAS while also improving its analgesic and sedative efficacy (Cai et al., 2011). Recent research has corroborated the efficacy of nasal ISGS in treating neurological disorders. This approach improves drug bioavailability by circumventing the BBB through cellular and trans-neural pathways, facilitating direct drug delivery to the brain (Samaridou et al., 2020). At present, the nasal route of drug administration is employed as an alternative means of delivering drugs to the CNS (Patharapankal et al., 2023). Nevertheless, there is a paucity of research on the utilization of nasal ISGS in the context of neurological disorders, whereas there is more literature on ocular ISGS in relation to the optic nerve (Al-Kinani et al., 2018). Accordingly, developing an ophthalmic ISGS based on the eye-brain pathway may be feasible for potential future applications in treating neurological disorders.

## 4.2 Physical enhancement methods

### 4.2.1 Focused ultrasound

The initial application of medical ultrasound in neurology was primarily focused on detecting the brain through Doppler ultrasound diagnosis. Highly focused ultrasound can stimulate a discrete region of the brain, facilitating independent navigation to accurately localize a specific brain area and regulate brain activity (Beisteiner et al., 2023), which is employed for highly focused tissue ablation and clinical neuromodulation brain stimulation. Besides, it has been shown that focused ultrasound can target focal BBB openings and reversibly disclose the localized openings, which are approximately 1 $cm^3$ in volume, without causing damage to brain tissue (Huang et al., 2017). The FUS-mediated opening of the BBB has been increasingly recognized as a potential enhancement method for treating brain diseases (Wang et al., 2022). The combination of FUS and microbubble drug delivery has been demonstrated to facilitate highly targeted delivery of drugs to the brain, opening the BBB and reducing apoptosis (Wang et al., 2021). Research has also shown that combining FUS with intravenous microbubble administration offers significant advantages in treating neurological disorders, particularly neurodegenerative diseases (Gasca-Salas et al., 2021).

Luo et al. (2022) demonstrated that FUS-mediated GAS (100 mg/kg) was more efficacious than the same dose of GAS in ameliorating memory in an amyloid-beta $(A\beta)_{1-42}$ peptide-induced AD mouse model. Another study demonstrated that the intervention of FUS significantly augmented the content of GAS in the sonicated hemisphere of a Parkinson's mouse model and raised the expression of anti-apoptotic and synaptic-related proteins (Wang et al., 2022). The combined application of FUS has been demonstrated to improve the bioavailability and brain targeting of GAS, thereby providing a novel drug delivery route for the effective treatment of neurological diseases. However, the therapeutic effects of distinct, focused ultrasound frequencies on disparate neurological disorders may also vary (Chen et al., 2022; Bachu et al., 2021). Hence, the optimal frequency and safety value of focused ultrasound in relation to adaptive diseases warrant further investigation.

TABLE 4 Summary of the targets/pathways/mechanisms and effects of gastrodin on neurodegenerative disorder.

| Disease | Inducer | Experimental model | Dose | Targets/mechanisms | Effects | Refs |
|---|---|---|---|---|---|---|
| AD | *In vitro:* $A\beta_{1\text{-}42}$ (10 μM) | *In vitro:* hippocampal neurons | *In vitro:* 0, 0.1, 0.3, 1, 3, 10, 30, 100, 300 μM | *In vitro:* mRNA and protein expression of SOD, Nrf2↑ | Protects hippocampal neurons against Aβ (1–42)-induced neurotoxicity by activation of ERK1/2 signaling pathway | Zhao et al. (2012) |
| | | | | The content and mRNA expression of CAT↑ | | |
| | | | | protein expression of ERK1/2, p-ERK1/2↑ | | |
| AD | *In vivo:* NA | *In vivo:* Tg2576 transgenic mice | *In vivo:* 60 mg/kg | *In vivo:* SOD, CAT↑ | Inhibits BACE1 expression under oxidative stress conditions by inhibition of the PKR/eIF2α signaling pathway | Zhang et al. (2016) |
| | | | | MDA, BACE1↓ | | |
| | | | | The ratio of p-$PKR_{Thr446}$/PKR, p-$eIF2\alpha_{Ser51}$/eIF2α↓ | | |
| | *In vitro: NA* | *In vitro:* SH-SY5Y cells | *In vitro:* 25, 50 μM | *In vitro:* P-$PKR_{Thr446}$, P-$eIF2\alpha_{Ser51}$↓ | | |
| AD | *In vitro:* D-galactose | *In vivo:* mice | *In vivo:* 3, 90, 210 mg/kg (i.g.) | *In vivo:* mRNA expression of BDNF↑ | Alleviates neuron inflammation of the AD mouse model via partly targeting the microbiota–gut–brain axis | Fasina et al. (2022) |
| | | | | protein expression of TLR4, p-IκBα↓, LPS, IL-1β, TNF-α, IL-6↓ | | |
| | | | | ZO-1, occludin↑ | | |
| AD | *In vivo:* LPS (2 mg/kg) | *In vivo:* C57BL/6 mice | *In vivo:* 100 mg/kg (i.p. injection) | *In vivo:* protein expression of p-Stat3, p-NF-κBp65, TLR4, TRAF6↓ | Alleviates neuroinflammation in AD model mice through inhibition of the TLR4/TRAF6/NF-κB signaling pathway and activation of microglia and astrocytes | Wang et al. (2024) |
| | | | | levels of Iba1, GFAP↓ | | |
| | | | | mRNA and protein expression of TNF-α, IL-1β↓ | | |
| | | | | mRNA of Arg-1↑ | | |
| AD | *In vitro:* LPS (1 μg/mL) | *In vitro:* BV-2 cells | *In vitro:* 1, 10 μg/mL | *In vitro:* iNOS, CD206↑ | | Wang et al. (2024) |
| | | | | p-Stat3, NF-κBp65↓ | | |
| PD | *In vivo:* rotenone (2 mg/kg/d) | *In vivo:* Wistar rats | *In vivo:* 0.2 g/kg/d (i.g.) | *In vivo:* TH↑ | Exerts a protective effect on dopaminergic neurons by reducing the expression of pro-inflammatory factors | Li et al. (2012) |
| | | | | TNF-α, IL-1β, IL-6↓ | | |

(Continued on following page)





10.3389/fphar.2024.1494277

TABLE 4 (*Continued*) Summary of the targets/pathways/mechanisms and effects of gastrodin on neurodegenerative disorder.

| Disease | Inducer | Experimental model | Dose | Targets/ mechanisms | Effects | Refs |
|---|---|---|---|---|---|---|
| PD | *In vivo:* MPTP (30 mg/kg/day) | *In vivo:* C57BL/6 mice | *In vivo:* 10, 30, 60 mg/kg (i.g.) | *In vivo:* TH, SOD↑ | Restores TH levels and GFAP expression and protects dopamine neurons from neurotoxicity | Kumar et al. (2013) |
| | | | | GFAP, cleavage PARP, caspase-3↓ | | |
| | | | | mRNA expression of Bcl-2↑ | | |
| | | | | mRNA expression of Bax and the ratio of Bax/Bcl-2↓ | | |
| | *In vitro:* MPTP (30 mg/kg/day) | *In vitro:* SH-SY5Y cells | *In vitro:* 1, 5, 25 μM | *In vitro:* cleavage PARP, ROS↓ | | |
| | | | | SOD↑ | | |
| | | | | mRNA expression of HO-1, Bax, Bax/Bcl-2↓ | | |
| | | | | mRNA expression of Bcl-2↑ | | |
| PD | *In vivo:* MPTP | *In vivo:* C57BL/6 mice | *In vivo:* 60 mg/kg (i.p. injection) | *In vivo:* mRNA and protein expression of HO-1, GSH, SOD, Nrf2↑ | Activates the ERK1/2 signaling pathway and promotes nuclear translocation of Nrf2 to play an antioxidant role | Wang et al. (2014) |
| | | | | protein expression of p-ERK1/2↑ | | |
| | | | | protein expression of MDA↓ | | |
| PD | *In vivo:* 6-OHDA (8 μg/2 μL/rat) | *In vivo:* Wistar rats | *In vivo:* 20, 40, 80 μg/3 μL/rat | *In vivo:* The activity of MPO↓ | Reduces peroxidase activity, lipid peroxidation levels, NO production, and restores TAC levels to alleviate PD. | Haddadi et al. (2018) |
| | | | | level of MDA, NO↓ | | |

AD, Alzheimer's disease; Aβ, beta-amyloid; SOD, superoxide dismutase; Nrf2, nuclear factor erythroid 2-related factor 2; CAT, catalase; ERK, extracellular regulated kinase; NA, not applicable; MDA, malondialdehyde; BACE1, β-site APP, cleaving enzyme 1; PKR, protein kinase; eIF2α, eukaryotic initiation factor-2a; BDNF, brain-derived neurotrophic factor; TLR4, toll-like receptor 4; IκBα, Inhibitor of kappa B-α; LPS, lipopolysaccharide; IL, interleukin; TNF-α, tumor necrosis factor-α; ZO-1, zonulin-1; Stat3, signal transducer and activator of transcription 3; NF-κB, nuclear factor-κB; TRAF6, tumor necrosis factor receptor-associated factor 6; GFAP, glial fibrillary acidic protein; Arg-1, arginase-1; iNOS, inducible nitric oxide synthase; PD, Parkinson's disease; TH, tyrosine hydroxylase; MPTP, 1-methyl-4-phenyl-1, 2,3,6-tetrahydropyridine; PARP, poly ADP-ribose polymerase; Bax, Bcl-2-associated X protein; Bcl-2, B-cell lymphoma-2; 6-OHDA, 6-hydroxydopamine; GSH, glutathione; MPO, myeloperoxidase; SD, Sprague-Dawley; NO, nitric oxide.





10.3389/fphar.2024.1494277

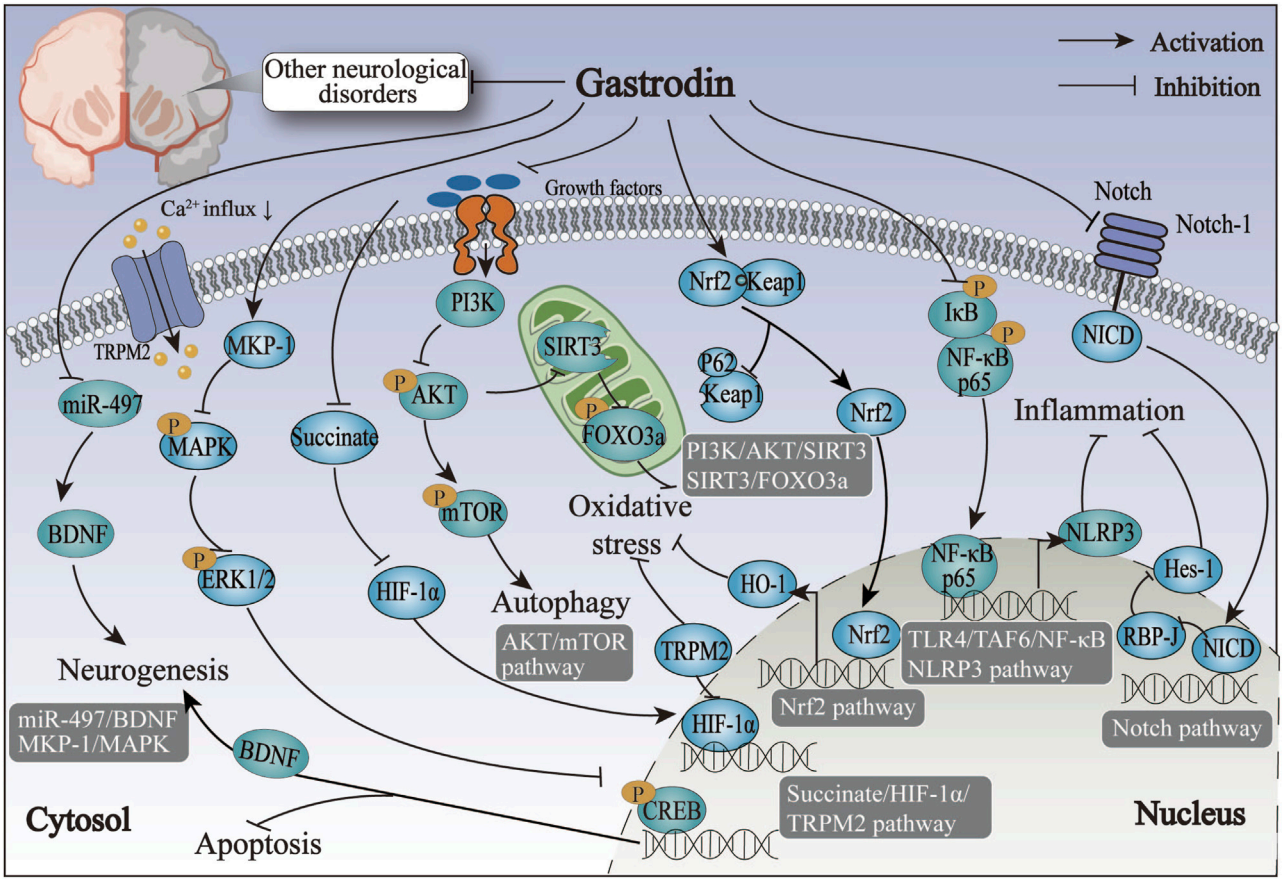


FIGURE 4
The therapeutic mechanism and critical pathways of gastrodin against epileptic neurological disorder, peripheral nerve injury, traumatic brain injury, hypoxic-ischemic brain damage, depression, and nervous system tumors.

### 4.2.2 Focused shockwave

A shock wave is a specific type of sound wave classified according to the characteristics of shock wave energy focusing that can be divided into three main categories, i.e., FSW, radiating shock wave, and plane shock wave. Compared to the latter two, FSWs are more complex to operate; however, they offer precise positioning characteristics and the capacity to treat deep-seated lesions. Similarly to FUS, FSW can open the BBB in a controlled and reversible manner (Kung et al., 2020).

Kung et al. (2021) investigated the effect of FSW on the blood-cerebrospinal fluid barrier (BCB). Their findings revealed that FSW-mediated opening of the BCB substantially increased the level of systemically-administered GAS in the cerebrospinal fluid, accompanied by a prolonged retention time of GAS. Simultaneously, epileptiform discharges, neuroinflammatory responses, and apoptosis in the brain were diminished by the FSW-GAS treatment (Kung et al., 2021), which may be related to the fact that FSW noninvasively and selectively induces the opening of the cerebrospinal fluid barrier in specific brain regions enriched with choroid plexus by disrupting or tightly connecting open channels through acoustic pressure (Kung et al., 2022; Liao et al., 2020). Notably, the choroid plexus is not the same as the capillaries of the BBB. The vessel wall is more permeable, and the blood flow in the choroid plexus is greater. Therefore, compared with the FUS-induced opening of the BBB, FSW facilitates the delivery of drugs to a greater extent and with greater speed by opening the BCB (Kung et al., 2022). Nevertheless, the literature on focused shock waves in neurological disorders primarily includes clinical studies on post-stroke spasticity diseases (Starosta et al., 2024). There is a notable dearth of research on other neurological-related diseases and drug delivery, so further investigation and improvement are required.

In order to promote the bioavailability and the efficacy of treatment with GAS, a range of drug delivery systems and physical enhancement methods for GAS have been investigated to increase its BBB permeability, bioavailability, brain targeting, drug release rate, and *in vivo* retention time. Nevertheless, these novel drug delivery systems and physical enhancement methods have yet to be widely adopted in clinical practice, and there is a limited number of preclinical studies. Further studies are warranted to evaluate their safety and efficacy.

TABLE 5 Summary of the targets/pathways/mechanisms and effects of gastrodin on epileptic neurological disorder.

| Disease | Inducer | Experimental model | Dose | Targets/ mechanisms | Effects | Refs |
|---|---|---|---|---|---|---|
| Epilepsy | *In vivo:* PTZ (5 mM) | *In vivo:* Zebrafish (*Danio rerio*) | *In vivo:* 600, 800, 1,000 μM | *In vivo:* mRNA expression of c-fos, Keap1↓ | Inhibits ROS generation and enhances the antioxidant defense system, and increases SOD and CAT activities | Jin et al. (2018) |
| | | | | mRNA expression of Mn-sod, Cu/Zn-sod, CAT, Gpx1a, Nrf2↑ | | |
| | | | | content of ROS, MDA↓ | | |
| | | | | activities of SOD, CAT↑ | | |
| Epilepsy | *In vivo:* PTZ (90 mg/kg) | *In vivo:* C57BL/6 mice | *In vivo:* 50, 100, 200 mg/kg | *In vivo:* IL-1β, TNF-α, p-ERK1/2, p-JNK, p-p38, CREB, IκB-α↓ | Reduces neuroinflammation and abnormal synchronous discharges by inhibiting the MAPK signaling pathway and IκB-α and CREB phosphorylation | Chen et al. (2017) |
| | | | | IL-10, p-MKP-1↑ | | |
| Epilepsy | *In vivo:*LC (3 mEq/kg), Pamine (25 mg/kg) | *In vivo:* SD rats | *In vivo:* 50 mg/kg (i.p. injection) | *In vivo:* $GABA_A$ receptor α1↑ | Alleviates seizure severity and neuronal excitability by enhancing the transmission of $GABA_A$ receptors | Yang et al. (2021) |
| Migraine | *In vivo:* NA | *In vivo:* SD rats | *In vivo:* 30, 100 mg/kg (i.v.) | *In vivo:* NA | Inhibits nociceptive dural-evoked neuronal firing in the trigeminocervical complex | Zhao et al. (2018) |
| Migraine | *In vivo:* NTG (10 mg/kg) | *In vivo:* C57BL/6 mice | *In vivo:* 200 mg/kg (i.p. injection) | *In vivo:* ROS, HIF-1α↓ | Inhibits TRPM2-dependent $Ca^{2+}$ inward flow by attenuating succinate accumulation and HIF-1α-associated transcriptional regulation, and thereby alleviation of trigeminal neuron cell death and neurotoxicity | Ma et al. (2024) |
| | | | | mRNA expression of IL-1β, IL-6, TNF-α↓ | | |
| | | | | mRNA and protein expression of Trpm2↓ | | |
| | | | | succinate, $Ca^{2+}$ influx↓ | | |

PTZ, pentylenetetrazole; Keap1, kelch like ECH-associated protein 1; Mn-sod, manganese superoxide dismutase; Cu/Zn-sod, copper/zinc superoxide dis mutase; CAT, catalase; Gpx1a, glutathione peroxidase 1a; Nrf2, nuclear erythroid factor 2-related factor 2; ROS, reactive oxygen species; MDA, malondialdehyde; SOD, super oxide dismutase; IL, interleukin; TNF, tumor necrosis factor; ERK1/2, extracellular regulated kinase 1/2; JNK, c-Jun N-terminal kinases; CREB, cyclic adenosine monophosphate-responsive element binding protein; IκB-α, inhibitor of kappa B-α; MKP-1, mitogen-activated protein kinase phosphatase-1; LC, methyl scopolamine; Pamine, methylscopolamine; SD, Sprague-Dawley; $GABA_A$, γ-aminobutyric acid A; NA, not applicable; NTG, nitroglycerin; HIF-1α, hypoxia inducible factor-1α; Trpm 2, transient receptor potential melastatin 2.

# 5 Neuroprotective effects of GAS on neurological disorders

## 5.1 Effects of GAS on cerebrovascular diseases

### 5.1.1 Anti-ischemic stroke (IS) effects

IS is the most prevalent cerebrovascular disease (Hu et al., 2017) and the primary cause of disability and mortality in adults in China (Wu et al., 2019). The primary pathological characteristic of IS is damage to brain tissue, which is caused by neuronal apoptosis and inflammation (Tuo et al., 2022).

In the IS model, GAS might be a novel method to attenuate nerve damage, mainly because GAS inhibits the assembly of the nod-like receptor protein (NLRP) 3 inflammasome and the expression of oxidation factors in astrocytes. Sui et al. (2019) used different concentrations of GAS to treat OGD-exposed TNA2 astrocytes, finding that GAS effectively inhibited the expression of NLRP inflammatory vesicles and inflammatory factors in astrocytes, especially when the concentration of GAS was 20 μM. Also, GAS inhibited the expression levels of NLRP3 and NLRC4 most significantly. The study also found that GAS effectively inhibits signal transducer and activator of transcription (STAT3) in astrocytes of the middle cerebral artery occlusion (MCAO)-induced IS rat model and concluded that GAS suppresses NLRP3 inflammatory vesicles by restraining the NF-κB pathway, thereby attenuating the inflammatory response of IS. Using the same model, Peng et al. (2015) discovered that GAS (100 mg/kg) significantly activates the protein kinase B (AKT)/nuclear factor erythroid 2-related factor 2 (Nrf2) pathway, thereby attenuating neurological injury by inhibiting interleukin (IL)-1β, tumor necrosis factor (TNF)-α and increasing the expression of oxidative factors such as superoxide dismutase (SOD) and heme oxygenase 1 (HO-1). Furthermore, a transient MCAO-induced stroke model also proved that GAS could promote the expression of antioxidant genes in astrocytes by up-regulating Nrf2 and nuclear translocation, as well as significant attenuation of the massive neuronal damage caused by $Zn^{2+}$ overload in late stroke (Luo et al., 2018). It is suggested that the inhibition of GAS on neuronal apoptosis could be related to Nrf2-mediated inflammation and oxidative stress. Another bilateral common carotid artery occlusion (BBCAO)-induced IS model found that GAS facilitated hippocampal neuronal regeneration via the phosphodiesterase 9 (PDE9)-cyclic guanosine monophosphate (cGMP)-protein kinase G (PKG) pathway, demonstrating the neuroprotective effect of GAS on IS(Xiao et al., 2021).

The studies above indicate that regulating nervous function may represent a primary mechanism for treating IS with GAS.

TABLE 6 Summary of the targets/pathways/mechanisms and effects of gastrodin on peripheral nerve injury, traumatic brain injury, and hypoxic-ischemic brain damage.

| Disease | Inducer | Experimental model | Dose | Targets/mechanisms | Effects | Refs. |
|---|---|---|---|---|---|---|
| PNI | *In vivo*: NA | *In vivo*: SD rats | *In vivo*: 20 mg/kg (i.p. injection) | *In vivo*: SOD, CAT, GSH↑ | Alleviates the oxidative stress of SCs and accelerates the axonal growth, myelination, and functional recovery of peripheral nerve after PNI via miR-497/BDNF pathway | Yongguang et al. (2022) |
| | | | | content of MDA↓ | | |
| | | | | mRNA and protein expression of BDNF↑, miR-497↓ | | |
| | *In vitro*: NA | *In vitro*: RSC96, HEK293T cells | *In vitro*: 200 μg/mL | *In vitro*: SOD, CAT, GSH↑ | | |
| | | | | content of MDA↓ | | |
| PNI | *In vitro*: NA | *In vitro*: RSC96 SC cells | *In vitro*: 0, 50, 100, 200 μM | *In vitro*: mRNA expression of GDNF, BDNF, CNTF↑ | Affects SC metabolism through the activation of the PI3K pathway and inhibition of the MAPK pathway | Zuo et al. (2016) |
| | | | | protein expression of p-Akt↑, p-ERK1/2↓ | | |
| TBI | *In vivo*: NA | *In vivo*: SD rats | *In vivo*: 50, 100 mg/kg | *In vivo*: protein expression of Bcl-2, Nrf2, HO-1, NQO-1, SOD, GSH-px, CAT↑ | Activates the Nrf2 signaling pathway, increasing the levels of antioxidant enzymes to enhance antioxidant capacity | Wang and Dong (2021) |
| | | | | Bax, cleaved-caspase-3, MDA↓ | | |
| TBI | *In vivo*: NA | *In vivo*: NA | *In vivo*: 15, 30, 60 mg/kg (i.p. injection) | *In vivo*: TNF-α, IL-1β, IL-18, GSDMD, caspase-1, caspase-11, NLRP3, ASC↓ | Attenuates neurological injury in TBI rats by inhibiting the NLRP3 inflammasome signaling pathway and decreasing the level of pyroptosis | Yang et al. (2022) |
| HIBD | *In vitro*: NA | *In vivo*: SD rats | *In vivo*: 100 mg/kg (i.p. injection) | *In vivo*: Notch-1, NICD, Hes-1, RBP-JK↓ | Inhibits overactivated microglial cells to reduce neuroinflammation by decreasing the expression of key components of the Notch signaling pathway | Guo et al. (2021) |
| | | | | Sirt3↑ | | |
| | *In vitro*: LPS (1 μg/mL) | *In vitro*: BV-2 cells | *In vitro*: 0.17 mM, 0.34 mM | *In vitro*: Notch-1, NICD, Hes-1, RBP-JK, iNOS, TNF-α↓ | | |
| | | | | Sirt3↑ | | |
| HIBD | *In vivo*: NA | *In vivo*: C57BL/6J mice | *In vivo*: 300 mg/kg (i.p. injection) | *In vivo*: P-PI3K, P-AKT, TGF-β1, Arg-1, CD206↑ | Reduces activated microglia apoptosis through the PI3K/AKT signaling pathway | Zuo et al. (2023) |
| | | | | TNF-α, Bax/Bcl-2, CD16/32↓ | | |
| | *In vitro*: LPS (1 μg/mL) | *In vitro*: BV-2 cells | *In vitro*: 0.17mM, 0.34 mM | *In vitro*: TGF-β1, Arg-1, CD206, IL-10, P-FOXO3a, P-PI3K, P-AKT↑ | | |
| | | | | TNF-α, Bax/Bcl-2, CD16/32, ROS↓ | | |
| HIBD | *In vitro*: NA | *In vitro*: TNC1 cells | *In vitro*: 0.17, 0.34, 0.51, 0.68, 0.85, 1.02 mM | *In vitro*: IGF-1, BDNF, Sirt3↑ | Inhibits the expression of pro-inflammatory factors and promotes the expression of neurotrophic factors | Zhang et al. (2021) |
| | | | | TNF-α, IL-1β, Notch-1, NICD, Hes-1, RBP-JK↓ | | |

PNI, peripheral nerve injury; NA, not applicable; SD, Sprague-Dawley; SOD, superoxide dismutase; CAT, catalase; GSH, glutathione; MDA, malondialdehyde; BDNF, brain-derived neurotrophic factor; GDNF, glial cell-derived neurotrophic factor; CNTF, ciliary neurotrophic factor; AKT, protein kinase B; TBI, traumatic brain injury; ERK, extracellular regulated kinase; Bcl-2, B-cell lymphoma-2; Nrf2, nuclear factor erythroid 2-related factor 2; HO-1, heme oxygenase-1; NQO-1, NAD (P)H quinone dehydrogenase 1; GSH, glutathione; TNF, tumor necrosis factor; IL, interleukin; GSDMD, Gasdermin D; NLRP, nod-like receptor protein; ASC, apoptosis-associated speck-like protein; iNOS, inducible nitric oxide synthase; NF-κB, nuclear factor-κB; HIBD, hypoxic-ischemic brain damage; NICD, notch intracellular domain; Hes-1, Transcription factor hairy and enhancer of split-1; RBP-JK, recombining binding protein suppressor of hairless; Sirt3, Sirtuin 3; PI3K, phosphatidylinositol-4, 5-bisphosphate 3-kinase; TGF, transforming growth factor; Arg-1, arginase-1; Bax, Bcl-2-associated X protein; IGF-1, insulin-like growth factor 1.

GAS may exert its neuroprotective effects in IS by modulating the NF-κB, NLRP3, AKT/Nrf2 inflammatory and oxidative stress pathways and promoting neural regeneration by neural-related signaling pathways such as PDE9-cGMP-PKG pathways (Figure 3; Table 3).

### 5.1.2 Anti-hemorrhagic stroke (HS) effects

HS, including cerebral hemorrhage and subarachnoid hemorrhage (Ohashi et al., 2023), is a subtype of stroke with a high mortality and morbidity rate (Keep et al., 2012). The principal pathological mechanisms underlying the secondary injury following

TABLE 7 Summary of the targets/pathways/mechanisms and effects of gastrodin on depression and nervous system tumors.

| Disease | Inducer | Experimental model | Dose | Targets/ mechanisms | Effects | Refs |
|---|---|---|---|---|---|---|
| Depression | *In vivo*: NA | *In vivo*: C57BL/6J mice | *In vivo*: 10, 20 mg/kg | *In vivo*: NE, 5-HT, DA, Bcl-2↑ | Improves depression-like behaviors and nerve cell injury by inhibiting Caspase-3-mediated apoptosis | Pei et al. (2024) |
| | | | | Caspase-3, Bax↓ | | |
| Depression | *In vivo*: NA | *In vivo*: SD rats | *In vivo*: 100 mg/kg (i.g.) | *In vivo*: 5-HT 1A receptor, CRMP2, PFN1↑ | Regulates the expression of cytoskeleton remodeling-related protein in the Slit-Robo pathway and promotes hippocampal neuronal cell plasticity | Chen et al. (2016) |
| | | | | Slit1, RhoA↓ | | |
| | *In vitro*: NA | *In vitro*: Hs 683 cells | *In vitro*: 50, 100, 100 μM | *In vitro*: Slit1↓ | | |
| Depression | *In vivo*: NA | *In vivo*: SD rats | *In vivo*: 50, 100, 200 mg/kg (i.p.) | *In vivo*: GFAP, BDNF↑ | Protects astrocytes and promotes the expression of BDNF through activating ERK1/2 | Zhang et al. (2014) |
| | *In vitro*: NA | *In vitro*: hippocampal astrocytes | *In vitro*: 5, 10, 20, 50, 100 μg/mL | *In vitro*: BDNF, p-ERK1/2↑ | | |
| Depression | *In vivo*: NA | *In vivo*: SD rats | *In vivo*: 50, 100, 200 mg/kg (i.p.) | *In vivo*: p-IκB, NF-κB, IL-1β↓ | Alleviates depressive-like behavior by protecting the hippocampal neural stem cells from the damage of the pro-inflammatory cytokine IL-1β | Wang et al. (2014) |
| | *In vitro*: NA | *In vitro*: hippocampal NSC cells | *In vitro*: 5, 10, 20, 50 μg/mL | *In vitro*: IL-1β↓ | | |
| | | | | The ratio of $BrdU^+/PI^+$ cells, $BrdU^+/PI^+$↑ | | |
| Depression | *In vivo:* LPS 0.25 mg/kg/d | *In vivo:* C57BL/6 mice | *In vivo:* 25, 50, 100 mg/kg/d (i.p.) | *In vivo and In vitro:* mRNA and protein expression of Nrf2, p-Nrf2↑ | Attenuates neuroinflammation in LPS-induced depressed rats by promoting an $Arg\text{-}1^+$ microglia phenotype through the Nrf2 pathway | Zhang et al. (2023) |
| | *In vitro:* LPS 5 μg/mL | *In vitro:* Primary microglia | *In vitro:* 25, 50, 100 μM | mRNA expression of Arg-1, IL-10↑ | | |
| | | | | mRNA expression of iNOS, CD11b, CD86, NLRP3, IL-1β, IL-6↓ | | |
| Nervous system tumors | *In vivo*: NA | *In vivo*: BALB/c nude mice T98 cells | *In vivo*: 40 mg/kg | *In vivo*: HOXD10, ACSL4↑ | Induces the occurrence of glioma ferroptosis by up-regulating HOXD10 and ACSL4 and down-regulating KI67 and PCNA proteins | Cao et al. (2023) |
| | | | | KI67, PCNA↓ | | |
| | *In vitro*: NA | *In vitro*: HT22, C6, LO2, HK2, HPDE, NHA, U251, T98, LN229 and PC12 cells | *In vitro*: 0, 5, 10, 20 μM | *In vitro*: proliferation of the glioma cells↓ | | |
| | | | | mRNA and protein expression of HOXD10↑ | | |
| | | | | ROS, iron, MDA↑ | | |
| | | | | GPX, GSH↓ | | |
| Nervous system tumors | *In vivo*: NA | *In vivo*: NOD-NCG mice | *In vivo*: NA | *In vivo*: NA | Upregulates the expression of SIP1, enhances the ability of CAR11-3 migrating to the homing bone marrow, and crosses the blood–brain barrier to the brain to fight against tumors | Huang et al. (2023) |
| | *In vitro*: NA | *In vitro*: U87 cells, NT, and CAR-T cells | *In vitro*: NA | *In vitro*: mRNA expression of gng8, add2↑ | | |
| | | | | release of IFN-γ↑ | | |
| | | | | percent of perforin, CD107a↓ | | |
| | | | | mRNA and protein expression of S1P1↑ | | |
| Nervous system tumors | *In vitro*: NA | *In vitro*: SH-SY5Y cells | *In vitro*: 0, 1, 2, 3, 4, 5 mM | *In vitro*: cell viability↑ | Exhibits an anti-autophagic effect to inhibit the METH-induced Beclin-1 protein expression via the AKT/mTOR pathway | Yang et al. (2019) |
| | | | | LC3B, Beclin-1, mTOR, p-mTOR, AKT, p-AKT↓ | | |

NE, noradrenaline; 5-HT, serotonin; DA, dopamine; Bcl-2, B-cell lymphoma-2; Bax, Bcl-2-associated X protein; CRMP, 2, dihydropyrimidinase-related protein 2; PFN1, profilin 1; RhoA, Ras homologous member A; GFAP, glial fibrillary acidic protein; BDNF, brain-derived neurotrophic factor; ERK, 1/2, extracellular regulated kinase 1/2; IκB, inhibitor of kappaB; IL, interleukin; Nrf2, nuclear erythroid factor 2-related factor 2; Arg-1, arginase-1; HOXD10, Homeobox D10; iNOS, inducible nitric oxide synthase; NLRP3,nod-like receptor protein; ACSL4, acyl-CoA, synthetase-4; ROS, reactive oxygen species; PCNA, proliferating cell nuclear antigen; GPX, glutathione peroxidase; GSH, glutathione; gng8, Guanine nucleotide binding protein (G protein) gamma 8; IFN-γ, interferon-γ; S1P1, Sphingosine1-phosphate1; LC3B, light chain 3B; mTOR, mammalian target of rapamycin; AKT, protein kinase B.

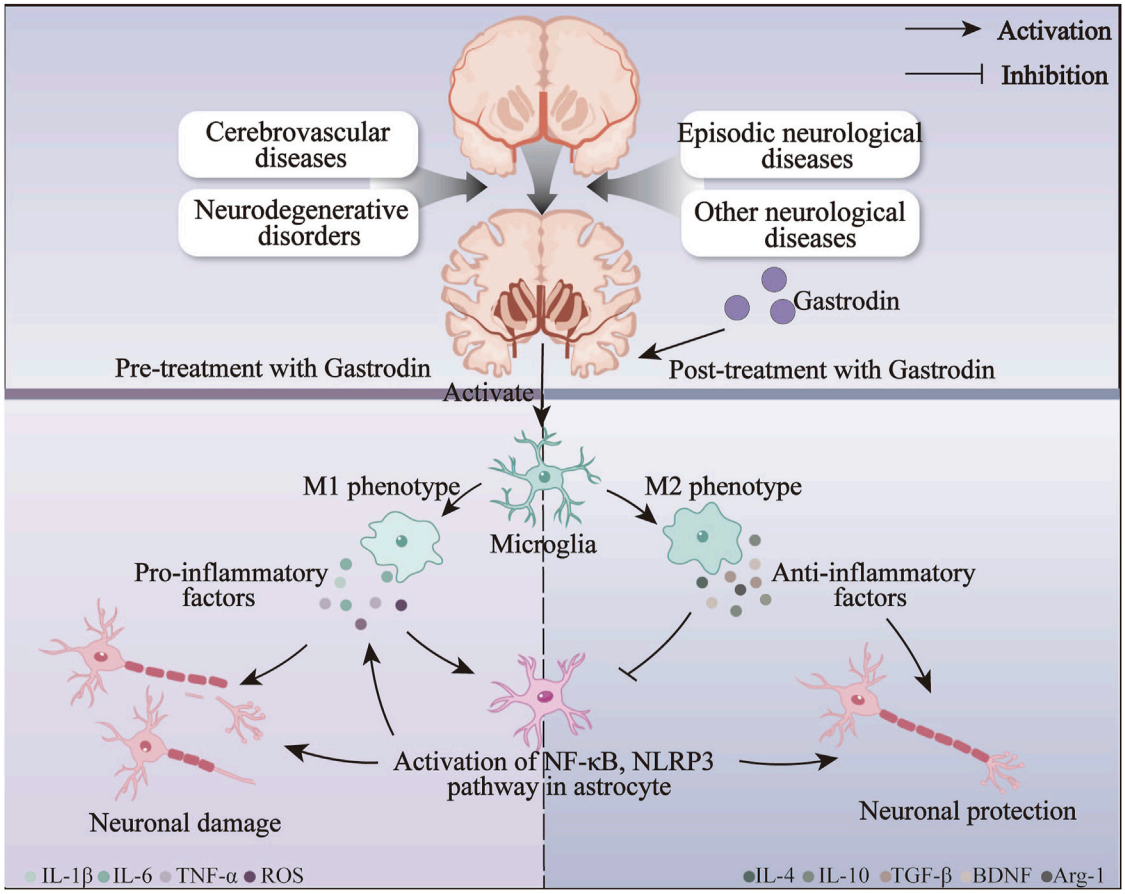


FIGURE 5
The anti-inflammatory mechanisms of gastrodin on neurological disorders via inhibiting the activation of microglia and astrocytes.

HS are inflammation and oxidative stress (Aronowski and Zhao, 2011).

Liu et al. (2020) demonstrated that GAS markedly influenced apoptotic factors and impeded neuronal apoptosis by reducing the expression of TNF-α, IL-1β, malondialdehyde (MDA), 8-hydroxydeoxyguanosine and 3-nitrotyrosine in the vicinity of hematoma following a collagenase-induced HS model in rats with HS. The inhibition of inflammatory and oxidative factors might be associated with the Kelch-like ECH-associated protein 1 (Keap1)/Nrf2/HO-1 pathway (Liu et al., 2020). Furthermore, Wang et al. (2019) proved that GAS (100 mg/kg) reduces glutamate and intracellular $Ca^{2+}$ levels, increases Nrf2, HO-1, and Akt phosphorylation expression, and prevents microglia activation, neuronal apoptosis, and oxidative stress by reducing glutamate excess-mediated neurotoxicity in a rat model of subarachnoid hemorrhage (Li et al., 2011). The maintenance of glutamate homeostasis has been shown to protect against nerve damage caused by subarachnoid hemorrhage.

The protective mechanism of GAS against HS revolves around the processes of inflammation and oxidative stress, primarily through the activation of the Nrf2-mediated Keap1/Nrf2/HO-1 pathway, thus suggesting that Nrf2 may be the target of action of GAS in the treatment of HS (Figure 3; Table 3).

### 5.1.3 Anti-vascular dementia (VD) effects

VD has become the second most prevalent form of dementia, following AD (Ismail et al., 2020). Most patients with VD also have the pathology of amyloid plaque formation and diffuse accumulation of neurofibrillary tangles in AD (van der Flier et al., 2018). Aβ has a significant role in the formation of amyloid plaque.

Chen et al. (2024) demonstrated that GAS (25 and 50 mg/kg, gavage) modulates the sirtuin 3 (Sirt3)-mediated transcription factor acetylation pathway and enhances the generation of adenosine triphosphate, superoxide dismutase (SOD), and glutathione (GSH), thus mitigating BBCAO-induced mitochondrial dysfunction in VD. This molecular mechanism may be related to the reduction of Aβ accumulation. The results of another bilateral common carotid artery ligation (2-VO) model of VD corroborated the significance of Aβ in VD, revealing that the same dose of GAS was efficacious in mitigating neuronal damage in VD rats by inhibiting Aβ production, lowering $Aβ_{1-40/42}$ levels and activating tubulin associated unit (tau). This was also demonstrated *in vitro*, where GAS attenuated mitochondrial respiratory depression and metabolic dysfunction in $H_2O_2$-induced HT-22 cells (Wu et al., 2023). Furthermore, Liu B. et al. (2018) found that oral administration of GAS inhibited autophagy and apoptosis in neurons of a VD rat model by modulating the deposition of Aβ

TABLE 8 Single-agent of gastrodin clinical application in neurological disorders.

| Disease | Study type | Gastrodin form, dose and therapy | Control group | Efficacy and results | Adverse events | Refs |
|---|---|---|---|---|---|---|
| IS | Meta-analysis (12 RCTs) | Gastrodin injection | Compound Danshen injection | Total effective rate↑, neural functional deficit score↓ | No obvious adverse reactions | Zhou (2018) |
| | | | Western medicine treatment | The levels of PV, WBV, Hct, RBC AI and FIB↓, the levels of TC, TG, LDL, HDL↓ | | |
| IS | RCT (n = 106) | Gastrodin injection, 0.6 g (i.v. gtt), once daily for 21 days | Compound Danshen injection | Remission rate (94.3%), GCS scores↑, NIHSS score↓, incidence of adverse reactions↓ | Gastrointestinal symptoms, blood platelet reduce, headache | Xiu-Yun (2020) |
| Migraine | RCT (n = 80) | Gastrodin injection, 0.6 g (i.v.gtt), once daily for 10 days | Flunarizine capsules | Total effective rate (92.5%), VAS score↓, the levels of CGRP, NO and ET↓ | NA | Yang et al. (2017) |
| Post-TBI Syndrome | RCT (n = 90) | Gastrodin sustained-release tablets, 150 mg, twice daily for 4 weeks | Flunarizine capsules | Total effective rate (93.33%), SCL-90 score↓, the levels of IGF-1 and IL-6↓ | No obvious adverse reactions | Xuegong (2015) |
| | | Gastrodin tablets, 100 mg, three daily for 4 weeks | | Total effective rate (73.33%), the levels of IGF-1 and IL-6↓ | | |
| TBI | RCT (n = 60) | Gastrodin injection, 0.6 g, once daily for 2 weeks | Mouse nerve growth factor injection | Abnormal blood pressure, respiration and heart rate were improved; GCS and MMSE score↑, NIHSS score↓ | Rash | Ming (2015) |

IS, ischemic stroke; RCT, randomized controlled trial; PV, plasma viscosity; WBV, whole blood viscosity; Hct, hematocrit; RBC AI, red blood cell aggregation index; FIB, fibrinogen; TC, total cholesterol; TG, triglycerides; LDL, low-density lipoprotein; HDL, high-density lipoprotein; GCS, glasgow coma scale; NIHSS, national institutes of health stroke scale; VAS, visual analogue scale; CGRP, calcitonin gene-related peptide; NO, nitric oxide; ET, endothelin; NA, not applicable; TBI, traumatic brain injury; SCL-90, Symptom Checklist-90; IGF, insulin-like growth factor; IL, interleukin; MMSE, Mini-Mental State Examination.

protein and inhibiting the expression of autophagy-associated proteins Beclin-1 and Light Chain 3 (LC3)-II, as well as the activity of apoptotic factors b-cell lymphoma (Bcl)-2 and p-P38 mitogen-activated protein kinase (MAPK). In another autophagy study (Chen et al., 2021), the investigators administered a 200 μM dose of GAS to $H_2O_2$-induced HT-22 cells, finding that GAS markedly diminished extracellular $Ca^{2+}$influx in HT-22 cells, inhibited the generation of autophagic vesicles, facilitated their degradation, and sustained the equilibrium of autophagic flux via the $Ca^{2+}$/$Ca^{2+}$-calmodulin-stimulated protein kinase II (CaMKII) pathway. On the other hand, Li et al. (2022) found that GAS mitigated cognitive deficits in VD rats by inhibiting ferroptosis and enhancing antioxidant capacity via the activation of the Nrf2/Keap1-glutathione peroxidase 4 (GPx4) pathway.

The above summary demonstrates that regulating Aβ-related proteins by GAS is pivotal in alleviating ischemic hypoxia-induced VD. The alleviation of cognitive deficits after VD by GAS through mitochondrial metabolic disorders, autophagy, and the ferroptosis pathway offers promising avenues for the treatment of neurological disorders with cognitive dysfunction (Figure 3; Table 3).

## 5.2 Effects of GAS on neurodegenerative disorders

### 5.2.1 Improvement of Alzheimer's disease (AD)

AD is a common progressive neurodegenerative disorder. The accumulation of Aβ has been identified as a pathogenic factor of AD, which produces oxidative stress and induces neuroinflammation, thus exerting a considerable influence on the pathogenesis of AD (Zhang et al., 2023).

In their *in vitro* study, Zhao et al. (2012) administered dosages ranging from 1 to 100 μM of GAS to hippocampal neurons with $Aβ_{1-42}$-induced, finding that GAS, particularly at 30 μM, markedly elevated the levels of catalase (CAT), and SOD and regulated active oxygen species, thereby reducing neuronal death. Meanwhile, they also found that GAS can mitigate Aβ-induced oxidative damage in neurons by modulating the ERK1/2-Nrf2 pathway. *In vivo* studies confirmed that GAS (60 mg/kg, gavage) was observed to inhibit the expression of β-site APP cleaving enzyme 1 (BACE1) and the phosphorylation levels of $PKR_{Thr446}$ and $eIF2α_{Ser51}$ by upregulating the expression of SOD, CAT in mice mutant for overexpression of amyloid precursor protein gene (Zhang et al., 2016). Oxidative stress-induced phosphorylation of $eIF2α_{Ser51}$ has been found to increase BACE1 translation and promote Aβ production (O'Connor et al., 2008). These findings suggested that GAS may diminish Aβ production by curbing the oxidative stress-mediated PKR/eIF2α pathway, thus alleviating cognitive impairment in AD mice. In addition, Fasina et al. (2022) found that 90 or 210 mg/kg of GAS inhibited the increase of pro-inflammatory factors in the brain of D-galactose-induced AD model mice and induced the proliferation of beneficial microorganisms in the intestinal tract, thus suggesting that GAS may improve memory deficits in AD model mice by attenuating neuroinflammation through the gut-brain axis. A further study used LPS-stimulated mice to replicate pathological alterations in the initial stages of AD, revealing that GAS (100 mg/kg) suppressed TLR4/TRAF6/NF-κB pathway-related proteins expression, promoted the transformation of microglia from a pro-inflammatory to an anti-inflammatory phenotype, and mitigated neuroinflammation in hippocampal neurons, thereby improving the LPS-induced deficits in memory and learning (Wang et al., 2024).

TABLE 9 Drug combinations of gastrodin clinical application in neurological disorders.

| Disease | Study type | Gastrodin form, dose and therapy | Combination drugs and doses | Efficacy and results | Adverse events | Refs. |
|---|---|---|---|---|---|---|
| IS | RCT (n = 96) | Gastrodin injection, 0.6 g (i.v.gtt), once daily for 21 days | Edaravone injection, 30 mg (i.v.gtt), twice daily for 21 days | Total effective rate (89.58%), the levels of PV, WBV, Hct and FIB↓, the levels of hsCRP, Ang-Ⅱ, MCP-1and sICAM-1↓, NIHSS scores↓ | NA | Feife (2018) |
| IS | Retrospective analysis (n = 110) | Gastrodin injection, 0.6 g (i.v.gtt), once daily for 2 weeks | butylphthalide injection, 25 mg (i.v.gtt), twice daily for 2 weeks | Total effective rate (94.74%), SSA, HAMD, HAMA and NIHSS scores↓, BI↑, the level of sTRAIL, OPG, TNF-α, and IL-8↓ | Epilepsy, gastrointestinal bleeding, pulmonary infection and arrhythmia | Wang and Wang (2023) |
| Migraine | RCT (n = 100) | Gastrodin injection, 0.6 g (i.v.gtt), once daily for 2 weeks | Sodium Valproate, 0.2 g (i.v.gtt), three times a day for 2 weeks | Total effective rate (96%), headache attack frequency, attack duration, headache severity score↓, life quality score↑ | Dizziness, limb numbness, weakness, memory decline | Li (2016) |
| Migraine | RCT (n = 240) | Gastrodin injection, 0.6 g (i.v.gtt), once daily for 2 weeks | Nimodipine, 60 mg (po), three times a day for 2 weeks | Total effective rate (91.67%); headache attack frequency, attack duration, headache severity score↓, the blood flow velocity of MCA and ACA↓, SF-36 score↑ | Nausea, drowsiness, dizziness, diarrhea | Zhang (2020) |
| Migraine | RCT (n = 61) | Gastrodin capsules, 50 g (po), three times a day for 4 weeks | Toutongning capsule, 1.2 g (po), three times a day for 4 weeks | Total effective rate (93.55%); VAS score↓, SF-36 score↑, the levels of PV, Hct and FIB↓ | NA | Ying (2022) |
| Migraine | RCT (n = 82) | Gastrodin capsules, 100 mg (po), three times a day for 8 weeks | Lomerizine, 5 mg (po), twice daily for 8 weeks | Total effective rate (95.12%), headache attack frequency, attack duration, headache severity score↓, VAS score↓, SF-36 score↑, the levels of hsCRP, HCY, LPA, VEGF and SP↓, the blood flow velocity of ACA, MCA, PCA, BA and VA↓ | No obvious adverse reactions | Zhang and Li (2019) |
| Migraine | Meta-analysis (16 RCTs) | Gastrodin injection | Sodium valproate, dexamethasone, flunarizine, nimodipine tablet and others | Increase efficiency; reduce pain scores; improve the duration of migraine; slow down the average blood flow velocity of the middle cerebral artery | Dizziness and lethargy; dry mouth and nausea, limb numbness; weakness; memory decline, diarrhea | Zhou et al. (2022) |
| Trigeminal neuralgia | RCT (n = 100) | Gastrodin capsules, 100 mg (po), three times a day for 4 weeks | Phenytoin sodium, 100 mg (po), three times a day for 4 weeks | Total effective rate (94.00%), headache attack frequency, attack duration, headache severity score↓, VAS score↓, the levels of 5-HT, PGE2, IL-1β↓ and β-EP↑ | Nausea and vomiting, headache, rash, dry mouth | Li Yong-Hua (2021) |
| Cognitive impairment after IS | RCT (n = 102) | Gastrodin injection, 0.3 g (i.m.), twice daily for 4 weeks | Oxiracetam, 0.4 g (i.m.), once daily for 4 weeks | Total effective rate (90.20%), MoCA and ADL scores↑, the levels of NSE, HCY, hs CRP↓ | Skin itch, nausea, sleep disorder, mental excitation | Xiaobo (2020) |
| Epilepsy after stroke | RCT (n = 92) | Gastrodin tablets, 50 mg (po), three times a day for 3 months | Folate, 5 mg (po), once daily for 3 months; vitamin-B12, 25 μg (po), three times a day for 3 months | Total effective rate (95.65%), MoCA score↓, the frequency of seizures↓, the levels of HCY, HMGB-1, IL-2, IL-6↓, FOL, V-B12↑ | NA | Zhou et al. (2017) |
| Post-traumatic syndrome | RCT (n = 78) | Gastrodin tablets, 100 mg (po), three times a day for 2 weeks | Oxiracetam injection, 4 g (i.v.gtt), once daily for 2 weeks | Total effective rate (97.44%), the scores of headaches, dizziness, anxiety, insomnia and depression↓, the levels of IL-6, IGF-1, MCP-1, sICAM-1↓ | No obvious adverse reactions | Wei (2017) |

(Continued on following page)

TABLE 9 (*Continued*) Drug combinations of gastrodin clinical application in neurological disorders.

| Disease | Study type | Gastrodin form, dose and therapy | Combination drugs and doses | Efficacy and results | Adverse events | Refs. |
|---|---|---|---|---|---|---|
| Depression | RCT (n = 90) | Gastrodin injection, 0.6 g (i.v.gtt), once daily for 4 weeks | Paroxetine, 20 mg (po), once daily for 4 weeks | Total effective rate (91.1%), HAMD, SDS, SAS and SCL-90 scores↓ | Nausea, headache, weakness, agrypnia, constipation, dry mouth | Di Jin (2020) |

IS, ischemic stroke; RCT, randomized controlled trial; PV, plasma viscosity; WBV, whole blood viscosity; Hct, hematocrit; FIB, fibrinogen; hsCRP, high-sensitivity C-reactive protein; Ang-II, angiotensin II; MCP-1, monocyte chemoattractant protein-1; sICAM-1, soluble intercellular adhesion molecule-1; NIHSS, national institutes of health stroke scale; NA, not applicable; SSA, Symptom Checklist-90; HAMD, hamilton depression scale; HAMA, hamilton anxiety scale; BI, barthel index; sTRAIL, soluble tumor necrosis factor related apoptosis inducing ligand; OPG, osteoprotectin; TNF-α, tumor necrosis factor-alpha; IL, interleukin; MCA, middle cerebral artery; ACA, anterior cerebral artery; SF-36, Medical Outcomes Study Short Form-36; VAS, visual analogue scale; HCY, homocysteine; LPA, lysophosphatidic acid; VEGF, vascular endothelial growth factor); SP, substance P; PCA, posterior cerebral artery; BA, bilateral artery; VA, vascular access; 5-HT, 5-hydroxy tryptamine; PGE2, Prostaglandin E2; β-EP, β-endorphin; MoCA, montreal cognitive assessment; ADL, activities of daily living; NSE, neuron specific enolase; HMGB1, High mobility group box 1; FOL, folate; V-B12, vitamin B12; IGF, insulin-like growth factor; SDS, Self-rating depression scale; SAS, Self-Rating Anxiety Scale; SCL-90, Symptom Checklist-90.

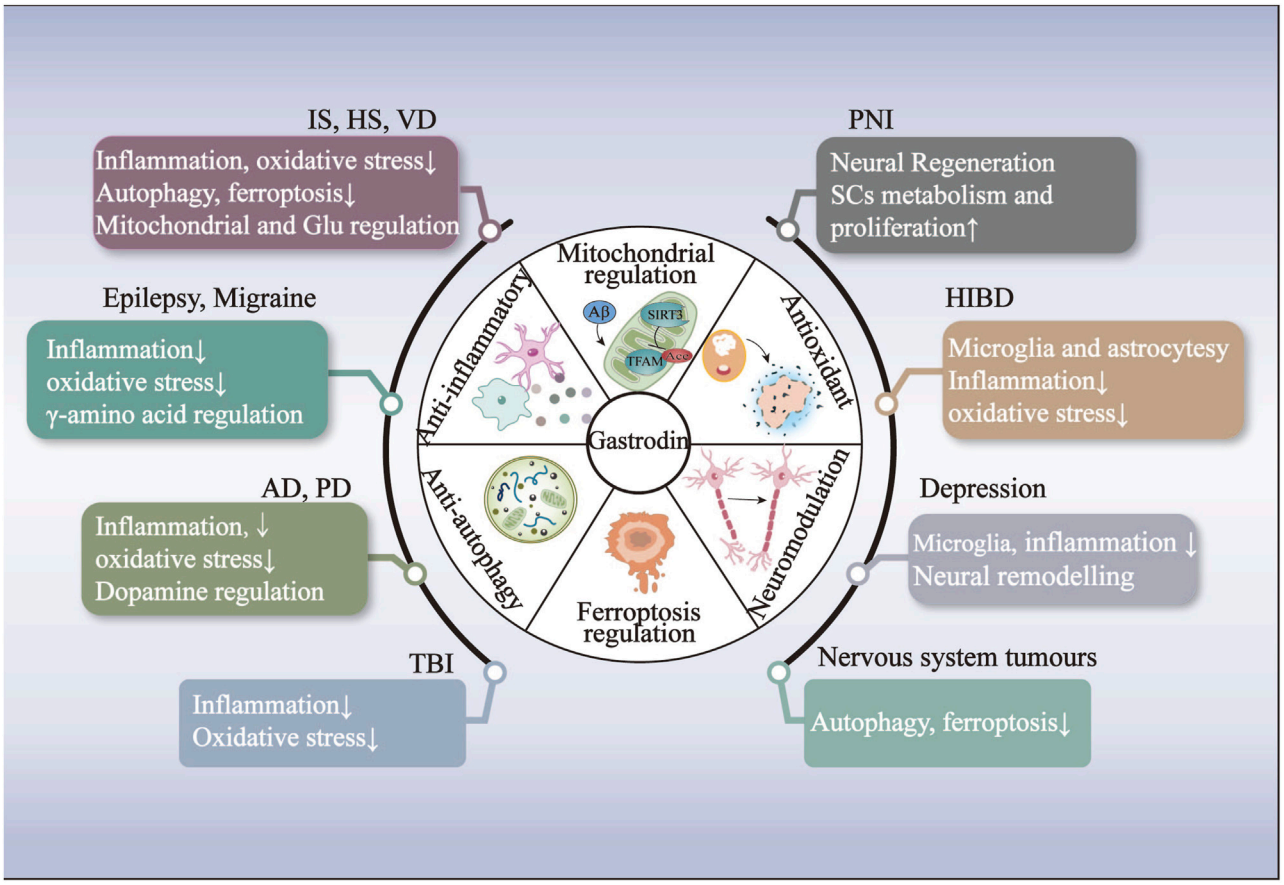


FIGURE 6
A summary of the main mechanism of gastrodin on neurological disorders.

In conclusion, Aβ significantly influences the formation and development of AD. GAS exerts an anti-oxidative stress effect by inhibiting PKR/eIF2α and ERK1/2-Nrf2 pathways. The mitigating effects of GAS on AD are mediated by the TLR4/TRAF6/NF-κB pathway, which involves gut microbes and microglia activation. GAS has a crucial role in AD-induced neurological impairments through suppressing neuroinflammation and oxidative stress (Figure 3; Table 4).

### 5.2.2 Improvement of Parkinson's disease (PD)

PD is the second most common neurodegenerative disorder, whose principal symptoms encompass a spectrum of motor manifestations, including rigidity, tremor, and bradykinesia (Moustafa et al., 2016). Although the etiology of PD has not been clearly defined, epidemiological and genetic studies have indicated that dopamine neuron deficiency, neuroinflammation, and oxidative stress characterize its pathogenesis (Ye et al., 2023).

Kumar et al. (2013) investigated the influence of GAS on dopamine neurons using a PD mouse model induced by 1-methyl-4-phenyl-1,2,5,6-tetrahydropyridine (MPTP). They found that a dose of 5 and 25 μM of GAS led to a restoration of glial fibrillary acidic protein (GFAP) expression and a recovery of tyrosine hydroxylase (TH) levels in a dose-dependent manner. They also noted that GAS treatment could protect dopamine neurons from neurotoxicity. A further fisetin-induced PD rat model verified the Kumar' study data, confirming that GAS exerts a protective effect on dopaminergic neurons by decreasing the expression of pro-inflammatory factors (Li et al., 2012). Moreover, Wang et al. (2014) demonstrated that GAS exerts antioxidant effects in mitigating dyskinesia in MPTP-induced PD model mice through the promotion of Nrf2 nuclear translocation and the activation of the ERK1/2 pathway. Similarly, the same findings were obtained in a 6-hydroxydopamine (OHDA)-induced PD mouse model, which demonstrated that GAS significantly inhibited the severity of catalepsy in PD mice by reducing nitric oxide (NO) production, peroxidase activity and lipid peroxidation levels and restoring total antioxidant capacity levels (Haddadi et al., 2018).

According to the above research, the protective effect of dopamine neurons may represent a crucial mechanism for treating PD by GAS. Nrf2 are significant action targets, and ERK1/2-Nrf2 pathways are essential for GAS to exert anti-inflammatory and antioxidant effects and attenuate dopamine neuron damage and apoptosis (Figure 3; Table 4).

## 5.3 Effects of GAS on episodic neurological diseases

### 5.3.1 Anti-epileptic effects

Epilepsy is a seizure disorder of the nervous system featuring unprovoked seizures and recurrent (Devinsky et al., 2018). Seizures occur due to hypersynchronous abnormal, excessive discharges of neurons in the brain, causing a paroxysmal change in neural function (Stafstrom and Carmant, 2015).

In a study conducted by Chen et al. (2017), pentylenetetrazole (PTZ)-induced seizure mice were administered GAS, which was found to mitigate PTZ-induced microglia activation through the inhibition of the MAPK pathway, cyclic adenosine monophosphate-responsive element binding protein (CREB) phosphorylation, and NF-κB, accompanied by a reduction in TNF-α and IL-1β expression. Additionally, GAS demonstrated the ability to attenuate neuroinflammation within the mouse brain and abnormal synchronous discharges while reducing seizure intensity and prolonging seizure duration. The same drug induction was used by Jin et al. (2018), who discovered that GAS (600, 800, and 1,000 μM) reinforced the antioxidant defense system by inhibiting the production of reactive oxygen species (ROS) and enhancing the activity of SOD and CAT. It was also found that this may assist in protecting zebrafish from further seizures. The mRNA levels of CAT, Mn-SOD, Cu/Zn-SOD, and glutathione peroxidase 1a in PTZ-induced animals were nearly normal at a concentration of 1,000 μM of GAS. GAS attenuated PTZ-induced oxidative stress and alleviated seizures in a concentration-dependent manner. In their study, Yang et al. (2021) used the temporal lobe epilepsy model induced by lithium-pilocarpine, finding that GAS (50 mg/kg) attenuated seizure severity and neuronal excitability by enhancing the γ-aminobutyric acid (GABA) A receptor.

The above overview suggests that MAPK and GABA may be involved in neurotoxicity-induced seizures, such as PTZ-induced and lithium-pilocarpine, through the immune response pathway. Furthermore, GAS may exert its antiepileptic properties by inhibiting inflammatory and oxidant reactions via the MAPK and GABA pathway. However, future *in vitro* and clinical trials are needed to further investigate the specific effects of GAS on other aspects of GABA metabolism (Figure 4; Table 5).

### 5.3.2 Analgesic effects of migraine

Migraine is a pervasive episodic neurological disorder (Gbd et al., 2018). The pathogenesis of migraine attacks remains incompletely understood. Modern research suggests that migraine attacks primarily relate to the trigeminovascular system, consisting of the trigeminal nerve and the intracranial vasculature projected by trigeminal nerve axons (Ashina, 2020).

Zhao et al. (2018) observed that GAS at doses of 30 and 100 mg/kg significantly inhibits dural stimulation-induced pain-related neuronal discharges in the trigeminal cervical complex and that low doses of GAS produced inhibition of persistent spontaneous nerve discharges. Ma et al. (2024) further showed that 200 mg/kg GAS impedes the succinate/hypoxia-inducible factor (HIF)-1α/transient receptor potential melastatin2 (TRPM2) pathway by regulating metabolic inhibition, which leads to a reduction in trigeminal ganglion neuron-dependent $Ca^{2+}$influx after succinate injury and attenuates nitroglycerin-induced migraine-induced trigeminal cell death and neurotoxicity.

From the above summary, our findings suggest that GAS may possess analgesic properties that could potentially alleviate migraine symptoms by inhibiting spontaneous nerve discharges in the trigeminal ganglion. This may be achieved by reducing neurotoxicity and neuronal apoptosis via the succinate/HIF-1α/TRPM2 pathway. Nevertheless, the precise molecular mechanisms remain elusive. Future studies should focus on the mechanisms of migraines and the analgesic mechanism of GAS in treating migraines (Figure 4; Table 5).

## 5.4 Effects of GAS on nerve regeneration post PNI

PNI is a sensory and motor dysfunction resulting from acute compression or trauma to the peripheral nerves (Hussain et al., 2020). Schwann cells (SCs) are responsible for the production and secretion of neurotrophic and nerve regeneration factors, which are the primary regulators of peripheral nerve development (Jessen and Mirsky, 1999; Raphael et al., 2010).

Zuo et al. (2016) demonstrated that GAS induced the metabolism and proliferation of SCs by activating Akt phosphorylation and inhibiting ERK1/2 phosphorylation and that 200 μM was the optimal concentration of GAS for stimulating the proliferation of RSC96 SCs. Their study also revealed that GAS significantly upregulated the gene expression of neurotrophic factors, which reconfirmed that GAS exerts a neurodegenerative role by regulating SCs (Zuo et al., 2016). An *In vivo* study showed

that treatment with GAS (20 mg/kg/d) resulted in a significant increase in the sciatic nerve function index and a reduction in muscle atrophy in rats with a PNI model established by sciatic nerve injury. The expression of myelin basic protein and neurofilament-200 was increased in the sciatic nerve of GAS-treated PNI rats in comparison to the control group (Li et al., 2022), which may be because GAS accelerates peripheral nerve axon growth, myelin formation, and functional recovery by upregulating the activities of SOD, CAT, and GSH in SCs through the miR-497/brain-derived neurotrophic factor (BDNF) pathway (Li et al., 2022).

In conclusion, nerve regeneration is a principal mechanism in treating peripheral nerve injury with GAS. GAS exerts its effects primarily by regulating the miR-497/BDNF and ERK1/2 pathways, with SCs pivotal in promoting peripheral nerve regeneration (Figure 4; Table 6).

## 5.5 Effects of GAS on TBI neuroprotective

Traumatic brain injury (TBI), also referred to as brain damage or head injury, is defined as a head injury caused by impacts such as accidental falls and road traffic accidents (Maas et al., 2022). The principal characteristics of secondary brain damage resulting from TBI are oxidative stress and an inflammatory response (Kaur and Sharma, 2018).

After the induction of TBI in neuronal cells, the Nrf2 pathway gets activated, resulting in elevated levels of the downstream proteins NAD (P)H quinone dehydrogenase 1 and HO-1. These proteins exert neuroprotective effects. A study employing the free-fall method to construct a TBI model demonstrated that GAS (50, 100 mg/kg) protects neuronal cells from TBI-induced injury by activating the Nrf2 signaling pathway, decreasing MDA levels and increasing antioxidant enzyme levels, including GSH-peroxidase, CAT, and SOD (Wang and Dong, 2021). Another study (Yang et al., 2022) employed the same experimental method to establish a TBI model to investigate the mechanism of action of GAS in alleviating TBI injury from the perspective of inflammation. It was found that the GAS (15, 30, and 60 mg/kg, intraperitoneal injection) group could reduce the production of TNF-α, IL-1β and IL-18 and cellular death after TBI by suppressing the NLRP3 inflammasome pathway, in comparison with the TBI group. This effect was more significant when the dose of GAS was 60 mg/kg than 30 mg/kg (Yang et al., 2022), which aligns with the observations of Wang et al. and indicates that GAS has a dose-dependent impact on the management of cerebral injury in TBI.

In conclusion, the modulation of inflammatory factors, oxidative factors, Nrf2, and NLRP3 inflammasome pathways appear to have pivotal roles in regulating TBI by GAS (Figure 4; Table 6). The therapeutic effect of GAS on TBI is dose-dependent. However, further investigation is necessary to ascertain the optimal therapeutic efficacy and safety dose.

## 5.6 Effects of GAS on HIBD microglial activation

Hypoxic-ischemic brain damage (HIBD) mainly results from perinatal asphyxia or some other etiology, resulting in brain damage due to hypoxia and reduced blood perfusion to the brain, accompanied by a high mortality rate (You et al., 2023). Microglial activation is a hallmark of HIBD in neonates (Del and Becker, 1994).

*In vivo* and *in vitro* experiments conducted by Guo et al. (2021) showed that GAS exerts an inhibitory effect on the overactivation of microglia in both LPS-induced BV-2 microglia and HIBD model mice by decreasing the expression of the Notch signaling pathway and its related key proteins. Concurrently, GAS enhances the expression of Sirt3, which reduces the expression of TNF-α, and attenuates neuroinflammation. Zhang et al. (2021) found consistent results in an astrocyte model of hypoxia-ischemia established through oxygen-glucose deprivation. Their findings indicated that GAS significantly improved the pro-inflammatory environment in hypoxia-ischemia-induced TNC1 astrocytes through the Notch and Sirt3 pathways, thereby promoting the secretion of neurotrophic factors and exerting neuroprotective effects. Zuo et al. (2023) further investigated the effect of GAS on the Sirt3 pathway, finding that 300 mg/kg GAS regulated Sirt3 in microglia that 300 mg/kg of GAS regulated Sirt3 in microglia through the phosphatidylinositol-4,5-bisphosphate 3-kinase (PI3K)/AKT pathway, effectively reduced CD16/32, TNF-α levels in HIBD mice, and enhanced transfer growth factor (TGF)-β1, CD206 expression in HIBD mice. Concurrently, GAS inhibited lipopolysaccharide-induced ROS production in BV-2 microglial cells by promoting phosphorylation for forkhead box O3a (FOXO3a). This indicates that GAS may regulate microglia activation through the PI3K/AKT/Sirt3 and Sirt3/FOXO3a pathways, exerting antioxidant and anti-inflammatory effects on HIBD (Zuo et al., 2023).

The above overview indicates that the alleviation of HIBD by GAS is predominantly linked to a microglia-mediated inflammatory response. The underlying molecular mechanisms may be linked to the Notch signaling pathway and Sirt3 (Figure 4; Table 6).

## 5.7 Anti-depressant effects of GAS

Depression is a heterogenous disorder that belongs to the neurological system. It is also a major risk factor for the development of concurrent neurodegenerative disorders, including PD and dementia (Filatova et al., 2021). The current literature suggests that the mechanisms of depression are associated with neuroplasticity, cytokines, and neuro-immune processes (Cui et al., 2024; Hodes et al., 2015).

Previous studies have shown that administration of 100 and 200 mg/kg of GAS alleviated the behavioral symptoms of depression-like in a chronic unpredictable stress (CUS) rat model. This may be achieved by restoring the levels of the GFAP and up-regulating the phosphorylation of ERK1/2 and the levels of BDNF in the hippocampus (Zhang et al., 2014). *In vitro* studies have found that despite not enhancing astrocyte viability, 20 μg/mL of GAS upregulates ERK1/2 phosphorylation and BDNF levels, thereby protecting astrocytes from 72 h serum-free injury and exerting trophic neurological effects. Chen et al. (2016) further revealed that 100 mg/kg of GAS exerted an antidepressant effect in a rat model of depression induced by forced swimming experiments by regulating the expression of proteins related to cytoskeletal remodeling in the Slit-Robo pathway. This may be related to the

fact that GAS acts as a caspase-3 inhibitor and attenuates neuronal cell damage in depression models by blocking caspase-3-mediated apoptosis (Pei et al., 2024). The results suggest that the neuroprotective and remodeling effects of GAS are crucial for the efficacy of antidepressant medications. In addition, some researchers examined the impact of GAS on a depression model developed by CUS from the perspective of inflammatory factors. Their findings demonstrated that GAS (200 mg/kg) reversed the augmented effects of CUS on IL-1β, NF-κB and p-iκB and attenuated depressive-like behaviors by mitigating the damage caused by pro-inflammatory cytokines to hippocampal neural stem cells (Wang et al., 2014). The capacity of GAS to mitigate neuroinflammation by fostering an Arg-1+ microglia phenotype via the Nrf2 pathway was corroborated in the lipopolysaccharide-induced depressed rat model (Zhang et al., 2023).

Above data suggests that the antidepressant effects of GAS are exerted by multiple mechanisms, including reducing neuronal apoptosis and enhancing neuroplasticity and anti-neuroinflammation (Figure 4; Table 7).

## 5.8 Anti-tumor effects of GAS

Nervous system tumors represent the most lethal form of tumor in the United States of America (Miller et al., 2021). Gliomas constitute a specific type of cranial tumor, accounting for approximately one-third of all tumors affecting the CNS and brain (Berger et al., 2022). Gliomas are aggressive and malignant tumors, particularly those found in adults, such as glioblastomas and other aggressive diffuse gliomas, accounting for 54% of all malignant cases (Miller et al., 2021).

Cao et al. (2023) discovered that GAS induced the occurrence of glioma ferroptosis by up-regulating Homeobox D10 (HOXD10) and acyl-CoA synthetase-4 and down-regulating KI67 and PCNA proteins. The silencing of HOXD10 resulted in the attenuation of the suppressive action of GAS on the proliferation of glioma cells, indicating that GAS may exert its anti-glioma effect by inducing the onset of glioma iron death through the HOXD10 pathway. In addition, a separate study on neuroblastoma revealed that GAS (2 and 4 mM) diminished the expression of autophagy-related proteins LC3B and Beclin-1 in methamphetamine-induced human dopamine neuroblastoma SH-SY5Y cells by inhibiting the AKT/mammalian target of rapamycin pathway, thereby exerting anti-autophagic effects (Yang et al., 2019).

Considering the limitations of radiotherapy and chemotherapy for gliomas and their associated adverse effects on the body, researchers have initiated investigations into novel anti-tumor therapies focusing on genes and the immune systems (Xu et al., 2021). Some clinical investigators have observed that IL-13 receptor α2 (Rα2) chimeric antigen receptor T cells elicited an anti-glioma response in patients with recurrent multifocal glioblastoma without the occurrence of treatment-related side effects (Brown et al., 2016). In their recent study, Huang et al. (2023) revealed that GAS enhances the migration of IL-13Rα2 T cells to the brain, thereby facilitating the combat of glioblastoma multiforme. Xu et al. (2022) designated the T cell as CAR11-3. Their team observed that 100 mg/kg GAS affected the expression of sphingosine1-phosphate1 (S1P1), the motility of CAR11-3, and persistently traversed the BBB to the brain, where it combatted glioblastoma (Huang et al., 2023). These findings illustrate that GAS can elicit antitumor effects through an immune response (Figure 4; Table 7).

# 6 Mechanism of action of GAS on neurological disorders

## 6.1 Anti-inflammatory effect

An inflammatory response is one of the most prevalent responses to neurological disorders associated with the pathophysiological processes of numerous neurological disorders (He et al., 2024). Resident immune cells in the CNS, microglia, and astrocytes are the primary glial cells implicated in the induction and regulation of inflammatory processes in neurological diseases (Colonna and Butovsky, 2017). In the event of damage to the nervous system resulting from trauma or hemorrhage, microglia are activated, thereby increasing the production of M1-type pro-inflammatory factors. This, in turn, serves to exacerbate the damage to the nerves (Shields et al., 2020). GAS can induce a transformation of microglia from the M1 pro-inflammatory phenotype to the M2 anti-inflammatory phenotype, which is achieved by the inhibition of various pathways, including those involving TLR4/TRAF6/NF-κB, PI3K/AKT, and Nrf2/STAT3, thereby reducing neuroinflammation and improving neuroinflammatory damage, and exerting an anti-inflammatory effect in neurological disorders such as AD and epilepsy. Furthermore, following the onset of neuroinflammation, activated microglia interact with astrocytes, regulating their immune response to neuroinflammation (Jha et al., 2019). The anti-inflammatory action of GAS on astrocytes is primarily achieved by inhibiting the NF-κB pathway, which prevents the assembly of NLRP3 inflammatory vesicles. At the same time, GAS also exerted neuroprotective effects by significantly improving the pro-inflammatory environment in astrocytes after brain injury through the Notch and Sirt3 pathways. The neuroprotective effect of GAS on neurological disorders may be primarily achieved by inhibiting the activation of astrocytes and microglia against neuroinflammation (Figure 5).

## 6.2 Antioxidant properties

Oxidative stress has been associated with the advancement of numerous neurological disorders, particularly neurodegenerative conditions, which are distinguished by extensive oxidative destruction of lipids, proteins, and other biological molecules (Barnham et al., 2004). In their study, Buendia et al. (2016) identified Nrf2 as a potential pivotal target in the antioxidant stress response associated with emerging neurodegenerative diseases, which is in accordance with the findings of the GAS study in treating neurological disorders. The present study has demonstrated that GAS exerts its antioxidant effects on neurodegenerative disease, primarily through the Nrf2-related pathway. GAS exerts antioxidant effects by promoting Nrf2 nuclear translocation and activating the ERK1/2 pathway, thereby reducing Aβ-induced oxidative damage in neurons and

alleviating dyskinesia in the PD model mice (Wang et al., 2014). Moreover, GAS has been found to confer neuroprotective benefits against IS and TBI through the activation of the Nrf2 pathway and the enhancement of antioxidant factors production (Luo et al., 2018; Wang and Dong, 2021). This indicates that the antioxidant effects of GAS on neurological diseases are primarily mediated by the activation of Nrf2 and its associated pathways.

## 6.3 Neurotransmitter modulation

Neurotransmitters, which serve as vital messengers for transmitting messages between neurons, are crucial in the onset and development of neurological diseases and defense and treatment strategies (Teleanu et al., 2022). Amino acid neurotransmitters are a vital class of chemical messengers within the nervous system (Arumugasamy et al., 2019). Glutamate and γ-aminobutyric acid are the primary amino acid neurotransmitters within the nervous system (Dalangin et al., 2020). Maintaining equilibrium between glutamate and γ-aminobutyric acid is crucial for sustaining brain homeostasis (Wen et al., 2022). Accordingly, regulating the equilibrium between glutamate and γ-aminobutyric acid represents the critical molecular mechanism through which GAS exerts its neuroprotective effects against neurological disorders. GAS can maintain homeostatic balance in the brain and attenuate the nerve damage of seizures and HS by inhibiting glutamate excess-mediated excitatory neurotoxicity and enhancing γ-amino acid A receptor transmission. Furthermore, GAS protects dopamine neurons from neurotoxicity by restoring the expression of GFAP and TH levels, which indicates the regulatory role GAS has regarding neurotransmission.

## 6.4 Neural remodelling and neural regeneration

In neurological diseases, neuronal cells undergo apoptosis due to various factors, including trauma and hemorrhage, which occur through several pathways, including inflammation, pyroptosis, iron death, and autophagy (Moujalled et al., 2021). Consequently, remodeling and regenerating neurons are important for ameliorating brain damage in neurological diseases. Similarly, this is the principal mechanism of GAS action in treating neurological disorders. It has been demonstrated that GAS can facilitate neural remodeling and hippocampal neuron regeneration by regulating the expression of cytoskeletal remodeling-related proteins in the Slit-Robo pathway and neurotrophic factors in the PDE9/cGMP/PKG pathway, which can exert a neuroprotective role (Chen et al., 2016; Xiao et al., 2021). Furthermore, SC cells, which are glial cells in the peripheral nervous system, can produce and secret neurotrophic and regenerative factors. They also exert substantial remodeling and repair effects on peripheral nerve injuries. GAS can improve the metabolism and proliferation of SCs, thereby upregulate the expression of neurotrophic factor through the AKT, ERK1/2, and miR-497/BDNF pathways (Li et al., 2022; Zuo et al., 2016). This promotes the regeneration of peripheral neurons and the improvement of peripheral nerve injury. SCs may represent a pivotal target for GAS in the management of neurodegenerative disorders.

## 6.5 Mitochondrial function regulation

The normal functioning of the brain's regions depends on mitochondrial energy metabolism. Dysfunctions of mitochondrial function, including $Ca^{2+}$ homeostasis, cell death regulation, and mitochondrial dynamics, have emerged as a primary mechanism underlying the development of numerous neurological disorders (Cabral-Costa and Kowaltowski, 2020). The modulation of mitochondrial function represents a novel mechanism through which GAS exerts neuroprotective effects. GAS has been demonstrated to enhance mitochondrial respiration and dynamics and reverse mitochondrial dysfunction in vascular dementia by inhibiting the sirtuin 3 (Sirt3)-mediated transcription factor A acetylation pathway. Mitochondrial dysfunction resulting from altered mitochondrial dynamics in AD has been linked to Aβ accumulation (de la Cueva et al., 2022). Wu et al. (2023) demonstrated that GAS could alleviate mitochondrial respiratory depression and metabolic disturbances in VD model rats by inhibiting Aβ production. This indicates that GAS can potentially alleviate mitochondrial dysfunction by reducing Aβ accumulation, thereby protecting against Aβ-related neurological diseases.

## 6.6 Inhibition of autophagy effect

Autophagy is a precisely regulated cellular degradation pathway, and neuronal quality control is directly correlated with the physiological function of autophagy (Nikoletopoulou et al., 2015). Damage to the neuronal autophagy pathway causes neuronal degeneration, the primary factor affecting cognitive function, leading to cognitive deficits in neurological disorders such as AD and VD (Grosso et al., 2024). The regulation of autophagy has become a focal point of research in treating neurological disorders, especially neurodegenerative diseases (Corti et al., 2020; Nixon and Rubinsztein, 2024). Inhibition of neuronal autophagy represents a crucial mechanism through which GAS exerts its neuroprotective effects against neurological disorders. GAS has been demonstrated to directly inhibit the expression of autophagy-related proteins, such as LC3-II and Beclin-1, in a VD rat model. Additionally, GAS can indirectly reduce $H_2O_2$–induced extracellular $Ca^{2+}$ inward flow in HT-22 cells by inhibiting the $Ca^{2+}$/CaM-CaMKII pathway, thereby promoting the fusion of autophagic vesicles with lysosomes and the degradation of autophagic vesicles. This process maintains the homeostasis of autophagic flow, which benefits cognitive function in neurological disorders.

## 6.7 Ferroptosis bidirectional regulation

Ferroptosis represents a novel form of cell death resulting from the accumulation of iron, which generates substantial quantities of lipid peroxides. These disrupt intracellular redox homeostasis and induce cell death due to lipid peroxidation (Li et al., 2020). It has

been demonstrated that glutathione peroxidase (GPX4) can exert a preventive effect against ferroptosis by catalyzing lipid peroxidation. Consequently, the GPX4 pathway has become essential for regulating the antioxidant defense against ferroptosis (Yan et al., 2021). GAS has been shown to enhance the antioxidant capacity and inhibit ferroptosis through the Nrf2/Keap1-glutathione peroxidase 4 (GPx4) pathway, thus improving cognitive impairment in rats with VD. Conversely, GAS demonstrated its anti-glioma impact by triggering the onset of glioma ferroptosis via the HOXD10 pathway. GAS exhibited antioxidant effects by inhibiting ferroptosis in non-tumor neurological disorders and anti-tumor effects by inducing ferroptosis in tumor neurological disorders, indicating that GAS may have a bi-directional modulating effect on ferroptosis in treating neurological disorders.

# 7 Clinical application of GAS in neurological disorders

## 7.1 Single-agent of GAS clinical application in neurological disorders

Currently, GAS is approved for clinical use in China by the China Drug Administration in various dosage forms, such as injection, tablet and capsule. In clinical practice, GAS injection is the most commonly used form of the drug, and it is primarily employed in the treatment of neurological disorders such as cerebral infarction, migraine, and traumatic brain injury (Table 8).

Zhou (2018) conducted a Meta-analysis of clinical studies on GAS injection for IS and screened 12 randomised controlled trials. The results showed that the improvement of nerve function, blood rheological indexes and blood lipid content of GAS injection was superior to that of Compound Danshen injection. It also demonstrated that 11 of the 12 studies lacked records of adverse reactions, and one result indicated the absence of significant adverse reactions following the administration of the drug (Zhou, 2018). Xiu-Yun (2020) evaluated the efficacy and incidence of adverse reactions associated with GAS injection in a cohort of 106 patients with IS. The analysis revealed that the incidence of adverse reactions such as gastrointestinal reactions and headache was 3.8% in the GAS injection group, while it was 18.9% in the Compound Danshen injection group, which was a statistically significant difference. These findings are inconsistent with those of the previous study. Further investigation is required to ascertain whether the use of GAS has a positive effect on the incidence of adverse reactions.

In addition, another study (Yang et al., 2017) showed that the same dosage of GAS injection was capable of reducing the expression of calcitonin gene-related peptide, NO and endothelin-1 in the peripheral blood of migraine patients. It suggests that GAS may regulate vasoactive factors and inflammatory responses by modulating the vasoactive factors and inflammatory responses. Xuegong (2015) found that both GAS extended-release tablets and GAS tablets were efficacious in reducing reduce serum insulin-like growth factor-1 and IL-6 levels in patients with post-traumatic brain syndrome. In contrast, the control group was administered flunarizine hydrochloride capsules, which demonstrated no significant change. This finding corroborates the anti-inflammatory effect of GAS on neurological diseases.

## 7.2 Drug combinations of GAS clinical application in neurological disorders

In clinical practice, the combination of GAS is more prevalent than GAS alone (Table 9). Li (2016) conducted a randomised controlled trial of 100 cases of migraine patients, the results found that the clinical efficacy of GAS combined with sodium valproate was significantly higher than that of the GAS alone group. And the frequency of headache attacks, duration of attacks, headache degree, and memory of the incidence of adverse reactions were all significantly lower than those observed in the GAS alone group. In a further clinical investigation into the treatment of migraine (Zhang, 2020), it was demonstrated that the combination of GAS and nimodipine was capable of effectively reducing the mean blood flow velocity of the anterior and middle cerebral arteries in patients with migraine. Zhang and Li, 2019 obtained the same results when treating migraine with a combination of GAS and lomerizine, indicating that the association of GAS with calcium channel blockers may exert analgesic effects on migraine by enhancing blood flow velocity.

Furthermore, GAS injection combined with edaravone can reduce plasma viscosity, whole blood viscosity, haematocrit, fibrinogen, and lowered serum high-sensitivity C-reactive protein, angiotensin II, monocyte chemoattractant protein-1, and soluble intercellular adhesion molecule-1, and attenuated neurological deficits in patients with acute IS (Feife, 2018). GAS combined with olanzapine improved MoCA and ADL scores in patients with cognitive dysfunction after IS (Xiaobo, 2020), and reduced serum levels of IL-6, MCP-1 and other inflammatory factors in patients with TBI (Wei, 2017). GAS combined with folic acid and vitamin B12 significantly improves the inflammatory response while effectively controlling seizures (Zhou et al., 2017). It is suggested that the combination of GAS enhances the anti-inflammatory effect of GAS on neurological diseases.

In conclusion, GAS alone and in combination exerts protective effects on neurological diseases mainly through anti-inflammation and improving hemorheology in clinical practice. In the future, the protective mechanism of GAS on the nervous system can be explored from the perspective of vasoactive substances. In addition, the sample size of current clinical research is small, and there is a lack of high-quality, large sample and multi-center clinical research. In the future, the scientific nature of clinical research design should be strengthened.

# 8 Challenges and future perspectives

## 8.1 Challenges and limitations

One of the most significant obstacles to utilizing GAS in managing neurological diseases is the capacity to traverse the BBB. Although drug delivery systems such as AuNPs, SD, nasal ISGS, and physical enhancement methods are available, there is a paucity of clinical studies on applying GAS and its drug delivery

system in neurological disorders. And the current clinical studies of GAS are characterised by small sample sizes, imperfect adverse reaction records and a predominantly observational clinical phase. There is a paucity of multi-centre, large-sample, double-blind and other high-quality clinical studies. Consequently, it is necessary to conduct additional clinical studies to validate the safety and efficacy of this approach. Secondly, the therapeutic dose of GAS varies considerably *in vivo* and *in vitro*, which may be attributable to differences in the disease model, animal species, duration of treatment, route of administration, and time point. Furthermore, GAS has been demonstrated to possess notable vasoprotective, analgesic, anticancer, and neurorestorative effects. However, the current research on GAS for neurological diseases predominantly focuses on VD, AD, and PD, with a comparatively limited investigation into cerebrovascular diseases, neuro tumours, and neurological injury categories such as peripheral nerve injury and TBI. This is particularly evident in the lack of research on peripheral neurological diseases.

## 8.2 Prospects for drug development

Currently, the clinical dosage forms of GAS are primarily injectable and oral. However, the inhalation dosage form, which can reflect the characteristics of GAS absorption through the nose, has yet to be fully explored. The development of nasal ISGS permits the administration of GAS via the naso-cerebral route, thereby circumventing the BBB and enhancing the brain targeting of GAS. It has been proposed that GAS can be used as an inhaled dosage form. Secondly, the ocular ISGS, inspired by the ocular *in situ* gel system via the eye-brain route, is also a potential drug for treating neurological disorders. Ultimately, combining GAS with ligustrazine, FA, and borneol improves the bioavailability of GAS, proposing the combined dosage form of GAS as a new idea for drug development.

## 8.3 Recommendations for future research

A review of the literature on the use of GAS in treating neurological disorders has identified several areas that warrant further investigation. Firstly, there is a need to increase the number of high-quality clinical studies related to applying GAS and its delivery system in neurological disorders. The scientific quality of the clinical study design should be improved by increasing the sample size, utilizing a multicentre approach, and implementing randomized controls. Secondly, preclinical studies should determine the safe and effective doses of GAS for treating different neurological disorders and adjust them accordingly. Thirdly, it is necessary to increase the number of studies on GAS for the treatment of cerebrovascular disease, neurogenic seizure disorders, peripheral nerve injury, and neuro-oncology, starting from the pathways of iron death, autophagy, mitochondria, ubiquitination, and acetylation. Fourthly, to improve the bioavailability of GAS, further research should focus on various nanoscale drug delivery systems, investigating the optimal effective dose of different drug delivery systems developed in different animal models of neurological disorders and their safety issues. Ultimately, the advancement of metagenomics, metabolomics, and other medical technologies is expected to further facilitate investigation into the molecular mechanisms of GAS in the treatment of neurological disorders.

# 9 Conclusion

The permeability of the BBB represents a significant challenge in the current study on the potential of GAS in treating neurological disorders. However, the development of GAS drug-carrying systems and the application of physical enhancement methods have led to a notable improvement in the bioavailability of GAS, which may have a protective role against neurological diseases through a range of mechanisms, including anti-inflammatory, antioxidant, modulation of neurological and mitochondrial functions, inhibition of autophagy, modulation of iron death and other mechanisms of action (Figure 6). This paper represents a novel perspective on the development and utilization of GAS-based drug delivery systems and the potential mechanisms underlying the action of GAS in neurological disorders. It should be noted that this review is not without limitations. In comparison to existing reviews on the use of GAS in the treatment of central nervous system disorders, this review did not include an analysis of less-studied conditions such as perioperative cognitive dysfunction, sleep deprivation, Tourette's syndrome, and diabetic encephalopathy. However, it has expanded the scope of this review to encompass a greater number of peripheral neurological disorders. Furthermore, the synthesis and chemical structure of the GAS sources are incomplete.

# Author contributions

ZYS: Writing–original draft, Conceptualization, Data curation, Formal Analysis, Writing–review and editing. YLZ: Writing–original draft, Conceptualization, Data curation, Formal Analysis. YHX: Writing–review and editing, Visualization. ZJS: Writing–review and editing, Visualization. XTW: Writing–review and editing, Visualization. BW: Writing–review and editing, Visualization. YY: Writing–review and editing, Supervision. PL: Writing–review and editing, Supervision.

# Funding

The author(s) declare that financial support was received for the research, authorship, and/or publication of this article. This work was supported by the Natural Science Foundation of Jilin Province (No. YDZJ202401133ZYTS) and the National Traditional Chinese Medicine Clinical Excellence Talent Advanced Study Program (National Administration of TCM Personnel and Education Letter [2022] No. 239).

# Conflict of interest

The authors declare that the research was conducted in the absence of any commercial or financial relationships that could be construed as a potential conflict of interest.

## Publisher's note



## References

Agrawal, M., Saraf, S., Saraf, S., Dubey, S. K., Puri, A., Gupta, U., et al. (2020). Stimuli-responsive *in situ* gelling system for nose-to-brain drug delivery. *J. Control. Release.* 327, 235–265. doi:10.1016/j.jconrel.2020.07.044

Aili, M., Zhou, K., Zhan, J., Zheng, H., and Luo, F. (2023). Anti-inflammatory role of gold nanoparticles in the prevention and treatment of Alzheimer's disease. *J. Mat. Chem. B* 11 (36), 8605–8621. doi:10.1039/d3tb01023f

Al-Kinani, A. A., Zidan, G., Elsaid, N., Seyfoddin, A., Alani, A., and Alany, R. G. (2018). Ophthalmic gels: past, present and future. *Adv. Drug Deliv. Rev.* 126, 113–126. doi:10.1016/j.addr.2017.12.017

Arami, H., Kananian, S., Khalifehzadeh, L., Patel, C. B., Chang, E., Tanabe, Y., et al. (2022). Remotely controlled near-infrared-triggered photothermal treatment of brain tumours in freely behaving mice using gold nanostars. *Nat. Nanotechnol.* 17 (9), 1015–1022. doi:10.1038/s41565-022-01189-y

Aronowski, J., and Zhao, X. (2011). Molecular pathophysiology of cerebral hemorrhage: secondary brain injury. *Stroke; a J. Cereb. circulation* 42 (6), 1781–1786. doi:10.1161/STROKEAHA.110.596718

Arshad, N., Batool, S. R., Razzaq, S., Arshad, M., Rasheed, A., Ashraf, M., et al. (2024). Recent advancements in polyurethane-based membranes for gas separation. *Environ. Res.* 252 (Pt 3), 118953. doi:10.1016/j.envres.2024.118953

Arumugasamy, S. K., Chellasamy, G., Gopi, S., Govindaraju, S., and Yun, K. (2019). Current advances in the detection of neurotransmitters by nanomaterials: an update. *TrAC Trends Anal. Chem.* 123, 115766. doi:10.1016/j.trac.2019.115766

Ashina, M. (2020). Migraine. *N. Engl. J. Med.* 383 (19), 1866–1876. doi:10.1056/NEJMra1915327

Assim, H. S., Paudwal, G., Banjare, N., Iqbal, A. N., Wazir, P., Nandi, U., et al. (2024). Sustained release polymer and surfactant based solid dispersion of andrographolide exhibited improved solubility, dissolution, pharmacokinetics, and pharmacological activity. *Int. J. Pharm.* 651, 123786. doi:10.1016/j.ijpharm.2024.123786

Bachu, V. S., Kedda, J., Suk, I., Green, J. J., and Tyler, B. (2021). High-intensity focused ultrasound: a review of mechanisms and clinical applications. *Ann. Biomed. Eng.* 49 (9), 1975–1991. doi:10.1007/s10439-021-02833-9

Baez, D. F., Gallardo-Toledo, E., Oyarzun, M. P., Araya, E., and Kogan, M. J. (2021). The influence of size and chemical composition of silver and gold nanoparticles on *in vivo* toxicity with potential applications to central nervous system diseases. *Int. J. Nanomed.* 16, 2187–2201. doi:10.2147/IJN.S260375

Barnham, K. J., Masters, C. L., and Bush, A. I. (2004). Neurodegenerative diseases and oxidative stress. *Nat. Rev. Drug Discov.* 3 (3), 205–214. doi:10.1038/nrd1330

Beisteiner, R., Hallett, M., and Lozano, A. M. (2023). Ultrasound neuromodulation as a new brain therapy. *Adv. Sci.* 10 (14), e2205634. doi:10.1002/advs.202205634

Berger, T. R., Wen, P. Y., Lang-Orsini, M., and Chukwueke, U. N. (2022). World Health organization 2021 classification of central nervous system tumors and implications for therapy for adult-type gliomas A review. *JAMA Oncol.* 8 (10), 1493–1501. doi:10.1001/jamaoncol.2022.2844

Betzer, O., Perets, N., Angel, A., Motiei, M., Sadan, T., Yadid, G., et al. (2017). *In vivo* neuroimaging of exosomes using gold nanoparticles. *ACS Nano* 11 (11), 10883–10893. doi:10.1021/acsnano.7b04495

Brown, C. E., Alizadeh, D., Starr, R., Weng, L., Wagner, J. R., Naranjo, A., et al. (2016). Regression of glioblastoma after chimeric antigen receptor T-cell therapy. *N. Engl. J. Med.* 375 (26), 2561–2569. doi:10.1056/NEJMoa1610497

Buendia, I., Michalska, P., Navarro, E., Gameiro, I., Egea, J., and Leon, R. (2016). Nrf2-ARE pathway: an emerging target against oxidative stress and neuroinflammation in neurodegenerative diseases. *Pharmacol. Ther.* 157, 84–104. doi:10.1016/j.pharmthera.2015.11.003

Cabral-Costa, J. V., and Kowaltowski, A. J. (2020). Neurological disorders and mitochondria. *Mol. Asp. Med.* 71, 100826. doi:10.1016/j.mam.2019.10.003

Cai, Z., Lei, X., Lin, Z., Zhao, J., Wu, F., Yang, Z., et al. (2014). Preparation and evaluation of sustained-release solid dispersions co-loading gastrodin with borneol as an oral brain-targeting enhancer. *Acta Pharm. Sin. B* 4 (1), 86–93. doi:10.1016/j.apsb.2013.12.012

Cai, Z., Song, X., Sun, F., Yang, Z., Hou, S., and Liu, Z. (2011). Formulation and evaluation of *in situ* gelling systems for intranasal administration of gastrodin. *AAPS PharmSciTech* 12 (4), 1102–1109. doi:10.1208/s12249-011-9678-y

Cao, W. P., Lan, J. Z., Zeng, Z. R., Yu, W. F., and Lei, S. (2023). Gastrodin induces ferroptosis of glioma cells via upregulation of Homeobox D10. *Molecules* 28 (24), 8062. doi:10.3390/molecules28248062

Chen, L., Cruz, E., Oikari, L. E., Padmanabhan, P., Song, J., and Gotz, J. (2022). Opportunities and challenges in delivering biologics for Alzheimer's disease by low-intensity ultrasound. *Adv. Drug Deliv. Rev.* 189, 114517. doi:10.1016/j.addr.2022.114517

Chen, L., Liu, X., Wang, H., and Qu, M. (2017). Gastrodin attenuates pentylenetetrazole-induced seizures by modulating the mitogen-activated protein kinase-associated inflammatory responses in mice. *Neurosci. Bull.* 33 (3), 264–272. doi:10.1007/s12264-016-0084-z

Chen, T. T., Zhou, X., Xu, Y. N., Li, Y., Wu, X. Y., Xiang, Q., et al. (2021). Gastrodin ameliorates learning and memory impairment in rats with vascular dementia by promoting autophagy flux via inhibition of the Ca(2+)/CaMKII signal pathway. *Aging (Albany NY)* 13 (7), 9542–9565. doi:10.18632/aging.202667

Chen, W. C., Lai, Y. S., Lin, S. H., Lu, K. H., Lin, Y. E., Panyod, S., et al. (2016). Anti-depressant effects of Gastrodia elata Blume and its compounds gastrodin and 4-hydroxybenzyl alcohol, via the monoaminergic system and neuronal cytoskeletal remodeling. *J. Ethnopharmacol.* 182, 190–199. doi:10.1016/j.jep.2016.02.001

Chen, Y. X., Yang, H., Wang, D. S., Chen, T. T., Qi, X. L., Tao, L., et al. (2024). Gastrodin alleviates mitochondrial dysfunction by regulating SIRT3-mediated TFAM acetylation in vascular dementia. *Phytomedicine* 128, 155369. doi:10.1016/j.phymed.2024.155369

Cheng, L., and Deng, Y. (2021). Characterization by HPLC of p -hydroxybenzyl alcohol biotransformation to gastrodin *in vivo*. *Nat. Prod. Commun.* 16. doi:10.1177/1934578x211035069

Chiang, M. C., Yang, Y. P., Nicol, C., and Wang, C. J. (2024). Gold nanoparticles in neurological diseases: a review of neuroprotection. *Int. J. Mol. Sci.* 25 (4), 2360. doi:10.3390/ijms25042360

Choi, D. K., Koppula, S., and Suk, K. (2011). Inhibitors of microglial neurotoxicity: focus on natural products. *Molecules* 16 (2), 1021–1043. doi:10.3390/molecules16021021

Collaborators, G. S. (2019). Global, regional, and national burden of neurological disorders, 1990-2016: a systematic analysis for the Global Burden of Disease Study 2016. *Lancet Neurol.* 18 (5), 459–480. doi:10.1016/S1474-4422(18)30499-X

Colonna, M., and Butovsky, O. (2017). Microglia function in the central nervous system during Health and neurodegeneration. *Annu. Rev. Immunol.* 35, 441–468. doi:10.1146/annurev-immunol-051116-052358

Corti, O., Blomgren, K., Poletti, A., and Beart, P. M. (2020). Autophagy in neurodegeneration: new insights underpinning therapy for neurological diseases. *J. Neurochem.* 154 (4), 354–371. doi:10.1111/jnc.15002

Cui, L., Li, S., Wang, S., Wu, X., Liu, Y., Yu, W., et al. (2024). Major depressive disorder: hypothesis, mechanism, prevention and treatment. *Signal Transduct. Target. Ther.* 9 (1), 30. doi:10.1038/s41392-024-01738-y

Dai, Y., Ban, W., and Yang, Z. (2024). Gastrodin, a promising natural small molecule for the treatment of central nervous system disorders, and its recent progress in synthesis, pharmacology and pharmacokinetics. *Int. J. Mol. Sci.* 25 (17), 9540. doi:10.3390/ijms25179540

Dalangin, R., Kim, A., and Campbell, R. E. (2020). The role of amino acids in neurotransmission and fluorescent tools for their detection. *Int. J. Mol. Sci.* 21 (17), 6197. doi:10.3390/ijms21176197

Del, B. M., and Becker, L. E. (1994). Microglial aggregation in the dentate gyrus: a marker of mild hypoxic-ischaemic brain insult in human infants. *Neuropathol. Appl. Neurobiol.* 20 (2), 144–151. doi:10.1111/j.1365-2990.1994.tb01173.x

de la Cueva, M., Antequera, D., Ordonez-Gutierrez, L., Wandosell, F., Camins, A., Carro, E., et al. (2022). Amyloid-β impairs mitochondrial dynamics and autophagy in Alzheimer's disease experimental models. *Sci. Rep.* 12 (1), 10092. doi:10.1038/s41598-022-13683-3

Devinsky, O., Vezzani, A., O'Brien, T. J., Jette, N., Scheffer, I. E., de Curtis, M., et al. (2018). Epilepsy. *Nat. Rev. Dis. Prim.* 4, 18024. doi:10.1038/nrdp.2018.24

Di Jin, M. (2020). Observation on curative effect of gastrodin injection combined with paroxetine on depression. *Mod. J. Integr. Traditional Chin. West. Med.* (33), 3654–3657. doi:10.3969/j.issn.1008-8849.020.33.002

Dong, J., Ji, D., Su, L., Zhang, F., Tong, H., Mao, C., et al. (2020). A simplified LCMS/MS approach for simultaneous quantification and pharmacokinetics of five compounds in rats following oral administration of Gastrodia elata extract. *J. Anal. Sci. Technol.* 11 (1), 18–19. doi:10.1186/s40543-020-00211-z

Fan, G., Liu, M., Liu, J., Huang, Y., and Mu, W. (2024). Traditional Chinese medicines treat ischemic stroke and their main bioactive constituents and mechanisms. *Phytother. Res.* 38 (1), 411–453. doi:10.1002/ptr.8033

Fasina, O. B., Wang, J., Mo, J., Osada, H., Ohno, H., Pan, W., et al. (2022). Gastrodin from gastrodia elata enhances cognitive function and neuroprotection of AD mice via the regulation of gut microbiota composition and inhibition of neuron inflammation. *Front. Pharmacol.* 13, 814271. doi:10.3389/fphar.2022.814271

Feife, L. (2018). Effects of edaravone and gastrodin on hemorheology and serum hsCRP, Ang-Ⅱ, MCP-1 and s ICAM-1 in patients with acute cerebral in farction. *Chin. J. Integr. Med. Cardio-Cerebrovascular Dis.* 16 (5), 613–617. doi:10.3969/j.issn.1672-1349.2018.05.027

Feigin, V. L., and Vos, T. (2019). Global burden of neurological disorders: from global burden of disease estimates to actions. *Neuroepidemiology* 52 (1-2), 1–2. doi:10.1159/000495197

Feigin, V. L., Vos, T., Nichols, E., Owolabi, M. O., Carroll, W. M., Dichgans, M., et al. (2020). The global burden of neurological disorders: translating evidence into policy. *Lancet Neurol.* 19 (3), 255–265. doi:10.1016/S1474-4422(19)30411-9

Ferrari, S., Mule, S., Galla, R., Brovero, A., Genovese, G., Molinari, C., et al. (2024). Effects of nutraceutical compositions containing rhizoma gastrodiae or lipoic acid in an *in vitro* induced neuropathic pain model. *Int. J. Mol. Sci.* 25 (4), 2376. doi:10.3390/ijms25042376

Filatova, E. V., Shadrina, M. I., and Slominsky, P. A. (2021). Major depression: one brain, one disease, one set of intertwined processes. *Cells* 10 (6), 1283. doi:10.3390/cells10061283

Gala, U. H., Miller, D. A., and Williams, R. R. (2020). Harnessing the therapeutic potential of anticancer drugs through amorphous solid dispersions. *Biochim. Biophys. Acta-Rev. Cancer* 1873 (1), 188319. doi:10.1016/j.bbcan.2019.188319

Gasca-Salas, C., Fernandez-Rodriguez, B., Pineda-Pardo, J. A., Rodriguez-Rojas, R., Obeso, I., Hernandez-Fernandez, F., et al. (2021). Blood-brain barrier opening with focused ultrasound in Parkinson's disease dementia. *Nat. Commun.* 12 (1), 779. doi:10.1038/s41467-021-21022-9

Gbd, Headache, and Collaborators (2018). Global, regional, and national burden of migraine and tension-type headache, 1990-2016: a systematic analysis for the Global Burden of Disease Study 2016. *Lancet Neurol.* 17, 954–976. doi:10.1016/S1474-4422(18)30322-3

Gong, M. Q., Lai, F. F., Chen, J. Z., Li, X. H., Chen, Y. J., and He, Y. (2024). Traditional uses, phytochemistry, pharmacology, applications, and quality control of Gastrodia elata Blume: a comprehensive review. *J. Ethnopharmacol.* 319 (Pt 1), 117128. doi:10.1016/j.jep.2023.117128

Grosso, J. H., Wasserlein, E. M., Ishola, A., Litt, N., Staniszewski, A., Arancio, O., et al. (2024). Adult-onset deactivation of autophagy leads to loss of synapse homeostasis and cognitive impairment, with implications for alzheimer disease. *Autophagy*, 1–16. doi:10.1080/15548627.2024.2368335

Guo, J., Zhang, X. L., Bao, Z. R., Yang, X. K., Li, L. S., Zi, Y., et al. (2021). Gastrodin regulates the Notch signaling pathway and Sirt3 in activated microglia in cerebral hypoxic-ischemia neonatal rats and in activated BV-2 microglia. *Neuromolecular Med.* 23 (3), 348–362. doi:10.1007/s12017-020-08627-x

Haddadi, R., Poursina, M., Zeraati, F., and Nadi, F. (2018). Gastrodin microinjection suppresses 6-OHDA-induced motor impairments in parkinsonian rats: insights into oxidative balance and microglial activation in SNc. *Inflammopharmacology* 26 (5), 1305–1316. doi:10.1007/s10787-018-0470-4

He, X., Chen, X., Yang, Y., Gu, J., Xie, Y., Liu, Y., et al. (2024). The role of gastrodin in the management of CNS-related diseases: underlying mechanisms to therapeutic perspectives. *Phytother. Res.* 38, 5107–5133. doi:10.1002/ptr.8314

Hodes, G. E., Kana, V., Menard, C., Merad, M., and Russo, S. J. (2015). Neuroimmune mechanisms of depression. *Nat. Neurosci.* 18 (10), 1386–1393. doi:10.1038/nn.4113

Hsu, S. H., and Ni, H. C. (2009). Fabrication of the microgrooved/microporous polylactide substrates as peripheral nerve conduits and *in vivo* evaluation. *Tissue Eng. Part a.* 15 (6), 1381–1390. doi:10.1089/ten.tea.2008.0175

Hu, X., De Silva, T. M., Chen, J., and Faraci, F. M. (2017). Cerebral vascular disease and neurovascular injury in ischemic stroke. *Circ. Res.* 120 (3), 449–471. doi:10.1161/CIRCRESAHA.116.308427

Huang, S., Bai, Y., An, Z. J., Xu, C., Zhang, C., Wang, F., et al. (2023). Gastrodin synergistically increases migration of interleukin-13 receptor a2 chimeric antigen receptor T cell to the brain against glioblastoma multiforme: a preclinical study. *Phytother. Res.* 37 (12), 5947–5957. doi:10.1002/ptr.8007

Huang, W., Wang, L., Zou, Y., Ding, X., Geng, X., Li, J., et al. (2022). Preparation of gastrodin-modified dendrimer-entrapped gold nanoparticles as a drug delivery system for cerebral ischemia-reperfusion injury. *Brain Behav.* 12 (12), e2810. doi:10.1002/brb3.2810

Huang, Y., Alkins, R., Schwartz, M. L., and Hynynen, K. (2017). Opening the blood-brain barrier with MR imaging-guided focused ultrasound: preclinical testing on a trans-human skull porcine model. *Radiology* 282 (1), 123–130. doi:10.1148/radiol.2016152154

Hussain, G., Wang, J., Rasul, A., Anwar, H., Qasim, M., Zafar, S., et al. (2020). Current status of therapeutic approaches against peripheral nerve injuries: a detailed story from injury to recovery. *Int. J. Biol. Sci.* 16 (1), 116–134. doi:10.7150/ijbs.35653

Illum, L. (2003). Nasal drug delivery--possibilities, problems and solutions. *J. Control. Release.* 87 (1-3), 187–198. doi:10.1016/s0168-3659(02)00363-2

Ismail, Z., Black, S. E., Camicioli, R., Chertkow, H., Herrmann, N., Laforce, R. J., et al. (2020). Recommendations of the 5th Canadian Consensus Conference on the diagnosis and treatment of dementia. *Alzheimers. Dement.* 16 (8), 1182–1195. doi:10.1002/alz.12105

Jangra, A., Verma, M., Kumar, D., Rachamalla, M., Dey, A., Dua, K., et al. (2022). Targeting endoplasmic reticulum stress using natural products in neurological disorders. *Neurosci. Biobehav. Rev.* 141, 104818. doi:10.1016/j.neubiorev.2022.104818

Jessen, K. R., and Mirsky, R. (1999). Schwann cells and their precursors emerge as major regulators of nerve development. *Trends Neurosci.* 22 (9), 402–410. doi:10.1016/s0166-2236(98)01391-5

Jha, M. K., Jo, M., Kim, J. H., and Suk, K. (2019). Microglia-astrocyte crosstalk: an intimate molecular conversation. *Neuroscientist* 25 (3), 227–240. doi:10.1177/1073858418783959

Ji, W., Zhang, M., Wang, D., Wang, X., Liu, J., and Huang, L. (2015). Superhydrophilic molecularly imprinted polymers based on a water-soluble functional monomer for the recognition of gastrodin in water media. *J. Chromatogr. A* 1425, 88–96. doi:10.1016/j.chroma.2015.11.053

Jia, Y., Shen, J., Li, X., Xie, H., Wang, J., Luo, J., et al. (2014). Identification and analysis of gastrodin and its five metabolites using ultra fast liquid chromatography electrospray ionization tandem mass spectrometry to investigate influence of multiple-dose and food. *J. Chromatogr. A* 1358, 110–116. doi:10.1016/j.chroma.2014.06.080

Jiang, Z., Zheng, X., Gong, X., Zhao, C., Zhou, X., Zhao, Y., et al. (2017). Relative tissue distribution and excretion studies of gastrodin and parishin from powder and extract of Gastrodiae Rhizoma in rat by UHPLC-ESI-MS/MS. *Biomed. Chromatogr.* 31 (7). doi:10.1002/bmc.3909

Jin, M., He, Q., Zhang, S., Cui, Y., Han, L., and Liu, K. (2018). Gastrodin suppresses pentylenetetrazole-induced seizures progression by modulating oxidative stress in zebrafish. *Neurochem. Res.* 43 (4), 904–917. doi:10.1007/s11064-018-2496-9

Kaur, P., and Sharma, S. (2018). Recent advances in pathophysiology of traumatic brain injury. *Curr. Neuropharmacol.* 16 (8), 1224–1238. doi:10.2174/1570159X15666170613083606

Keep, R. F., Hua, Y., and Xi, G. (2012). Intracerebral haemorrhage: mechanisms of injury and therapeutic targets. *Lancet. Neurol.* 11 (8), 720–731. doi:10.1016/S1474-4422(12)70104-7

Kim, B., Koppula, S., Kim, J., Lim, H., Hwang, J., Kim, I., et al. (2012). Modulation of LPS-stimulated neuroinflammation in BV-2 microglia by Gastrodia elata: 4-Hydroxybenzyl alcohol is the bioactive candidate. *J. Ethnopharmacol.* 139 (2), 549–557. doi:10.1016/j.jep.2011.11.048

Kolawole, O. M., and Cook, M. T. (2023). *In situ* gelling drug delivery systems for topical drug delivery. *Eur. J. Pharm. Biopharm.* 184, 36–49. doi:10.1016/j.ejpb.2023.01.007

Kumar, H., Kim, I. S., More, S. V., Kim, B. W., Bahk, Y. Y., and Choi, D. K. (2013). Gastrodin protects apoptotic dopaminergic neurons in a toxin-induced Parkinson's disease model. *Evid.-based Complement. Altern. Med.* 2013, 514095. doi:10.1155/2013/514095

Kung, Y., Chen, K. Y., Liao, W. H., Hsu, Y. H., Wu, C. H., Hsiao, M. Y., et al. (2022). Facilitating drug delivery in the central nervous system by opening the blood-cerebrospinal fluid barrier with a single low energy shockwave pulse. *Fluids Barriers CNS* 19 (1), 3. doi:10.1186/s12987-021-00303-x

Kung, Y., Hsiao, M. Y., Yang, S. M., Wen, T. Y., Chen, M., Liao, W. H., et al. (2021). A single low-energy shockwave pulse opens blood-cerebrospinal fluid barriers and facilitates gastrodin delivery to alleviate epilepsy. *Ultrason. Sonochem.* 78, 105730. doi:10.1016/j.ultsonch.2021.105730

Kung, Y., Huang, H. Y., Liao, W. H., Huang, A. P., Hsiao, M. Y., Wu, C. H., et al. (2020). A single high-intensity shock wave pulse with microbubbles opens the blood-brain barrier in rats. *Front. Bioeng. Biotechnol.* 8, 402. doi:10.3389/fbioe.2020.00402

Li, C., Chen, X., Zhang, N., Song, Y. W., and Mu, Y. (2012). Gastrodin inhibits neuroinflammation in rotenone-induced Parkinson's disease model rats. *Neural Regen. Res.* 7 (5), 325–331. doi:10.3969/j.issn.1673-5374.2012.05.001

Li, J., Cao, F., Yin, H. L., Huang, Z. J., Wang, G., Mao, N., et al. (2020). Ferroptosis: past, present and future. *Cell Death Dis.* 11 (2), 88. doi:10.1038/s41419-020-2298-2

Li, L., Li, Q., Yang, J., Sun, L., Guo, J., Yao, Y., et al. (2018). Enhancement in mechanical properties and cell activity of polyurethane scaffold derived from gastrodin. *Mater. Lett.* 228 (OCT.1), 435–438. doi:10.1016/j.matlet.2018.06.061

Li, M. H., Inoue, K., Si, H. F., and Xiong, Z. G. (2011). Calcium-permeable ion channels involved in glutamate receptor-independent ischemic brain injury. *Acta Pharmacol. Sin.* 32 (6), 734–740. doi:10.1038/aps.2011.47

Li, Q., Li, L., Yu, M., Zheng, M., Li, Y., Yang, J., et al. (2020). Elastomeric polyurethane porous film functionalized with gastrodin for peripheral nerve regeneration. *J. Biomed. Mater. Res. Part A.* 108 (8), 1713–1725. doi:10.1002/jbm.a.36937

Li, X. X. L. Z. (2016). Clinical effect of sodium valproate combined with gastrodin on migraine. *Pract. J. Cardiac Cereb. Pneumal Vasc. Dis.* 24 (9), 98–100. doi:10.3969/j.issn.1008-5971.2016.09.026

Li, Y., Zhang, E., Yang, H., Chen, Y., Tao, L., Xu, Y., et al. (2022). Gastrodin ameliorates cognitive dysfunction in vascular dementia rats by suppressing

ferroptosis via the regulation of the Nrf2/Keap1-GPx4 signaling pathway. *Molecules* 27 (19), 6311. doi:10.3390/molecules27196311

Li, Y. G., Wang, X. W., Yan, H. C., and Zhang, Y. X. (2022). Gastrodin promotes the regeneration of peripheral nerves by regulating miR-497/BDNF axis. *BMC Complement. Med. Ther.* 22 (1), 45. doi:10.1186/s12906-021-03483-z

Liao, W. H., Hsiao, M. Y., Kung, Y., Liu, H. L., Bera, J. C., Inserra, C., et al. (2020). TRPV4 promotes acoustic wave-mediated BBB opening via Ca(2+)/PKC-delta pathway. *J. Adv. Res.* 26, 15–28. doi:10.1016/j.jare.2020.06.012

Lin, L. C., Chen, Y. F., Tsai, T. R., and Tsai, T. H. (2007). Analysis of brain distribution and biliary excretion of a nutrient supplement, gastrodin, in rat. *Anal. Chim. Acta.* 590 (2), 173–179. doi:10.1016/j.aca.2007.03.035

Liu, B., Gao, J. M., Li, F., Gong, Q. H., and Shi, J. S. (2018a). Gastrodin attenuates bilateral common carotid artery occlusion-induced cognitive deficits via regulating aβ-related proteins and reducing autophagy and apoptosis in rats. *Front. Pharmacol.* 9, 405. doi:10.3389/fphar.2018.00405

Liu, X. C., Wu, C. Z., Hu, X. F., Wang, T. L., Jin, X. P., Ke, S. F., et al. (2020). Gastrodin attenuates neuronal apoptosis and neurological deficits after experimental intracerebral hemorrhage. *J. Stroke Cerebrovasc. Dis.* 29 (1), 104483. doi:10.1016/j.jstrokecerebrovasdis.2019.104483

Liu, Y., Gao, J., Peng, M., Meng, H., Ma, H., Cai, P., et al. (2018b). A review on central nervous system effects of gastrodin. *Front. Pharmacol.* 9, 24. doi:10.3389/fphar.2018.00024

Li Yong-Hua, G. J. W. X. (2021). Clinical study on Gastrodin Capsules combined with phenytoin sodium in treatment of trigeminal neuralgia. *Drugs & Clin.* 36 (1), 50–53. doi:10.7501/j.issn.1674-5515.2021.01.009

Long, Y., Yang, Q., Xiang, Y., Zhang, Y., Peng, W., Liu, S., et al. (2020). Nose to brain drug delivery - a promising strategy for active components from herbal medicine for treating cerebral ischemia reperfusion. *Pharmacol. Res.* 159, 104795. doi:10.1016/j.phrs.2020.104795

Lu, W., Yao, J., Zhu, X., and Qi, Y. (2021). Nanomedicines: redefining traditional medicine. *Biomed. Pharmacother.* 134, 111103. doi:10.1016/j.biopha.2020.111103

Luo, K., Wang, Y., Chen, W. S., Feng, X., Liao, Y., Chen, S., et al. (2022). Treatment combining focused ultrasound with gastrodin alleviates memory deficit and neuropathology in an Alzheimer's disease-like experimental mouse model. *Neural Plast.* 2022, 5241449. doi:10.1155/2022/5241449

Luo, L., Kim, S. W., Lee, H. K., Kim, I. D., Lee, H., and Lee, J. K. (2018). Gastrodin exerts robust neuroprotection in the postischemic brain via its protective effect against $Zn^{2+}$-toxicity and its anti-oxidative effects in astrocytes. *Anim. Cells Syst.* 22 (6), 429–437. doi:10.1080/19768354.2018.1549099

Ma, C., Zhu, C., Zhang, Y., Yu, M., Song, Y., Chong, Y., et al. (2024). Gastrodin alleviates NTG-induced migraine-like pain via inhibiting succinate/HIF-1α/TRPM2 signaling pathway in trigeminal ganglion. *Phytomedicine* 125, 155266. doi:10.1016/j.phymed.2023.155266

Maas, A. I. R., Menon, D. K., Manley, G. T., Abrams, M., Akerlund, C., Andelic, N., et al. (2022). Traumatic brain injury: progress and challenges in prevention, clinical care, and research. *Lancet Neurol.* 21 (11), 1004–1060. doi:10.1016/S1474-4422(22)00309-X

Mi, Y., Guo, S., Cheng, H., Liu, M., Wei, P., Wang, M., et al. (2020a). Pharmacokinetic comparative study of tetramethylpyrazine and ferulic acid and their compatibility with different concentration of gastrodin and gastrodigenin on blood-stasis migraine model by blood-brain microdialysis method. *J. Pharm. Biomed. Anal.* 177, 112885. doi:10.1016/j.jpba.2019.112885

Mi, Y., Wang, M., Liu, M., Cheng, H., and Li, S. (2020b). Pharmacokinetic comparative study of GAS with different concentration of tetramethylpyrazine and ferulic acid on liver-yang hyperactivity migraine model by blood-brain microdialysis method. *J. Pharm. Biomed. Anal.* 191, 113643. doi:10.1016/j.jpba.2020.113643

Miller, K. D., Ostrom, Q. T., Kruchko, C., Patil, N., Tihan, T., Cioffi, G., et al. (2021). Brain and other central nervous system tumor statistics, 2021. *Ca. Cancer. J. Clin.* 71 (5), 381–406. doi:10.3322/caac.21693

Min, Y. J., Ling, E. A., and Li, F. (2020). Immunomodulatory mechanism and potential therapies for perinatal hypoxic-ischemic brain damage. *Front. Pharmacol.* 11, 580428. doi:10.3389/fphar.2020.580428

Ming, Q. F. Z. (2015). Efficacy and safety evaluation of gastrodine injection for craniocerebral injury. *Liaoning J. Traditional Chin. Med.* 42 (1), 111–113. doi:10.13192/j.issn.1000-1719.2015.01.045

More, S. V., Kumar, H., Kang, S., Song, S., Lee, K., and Choi, D. (2013). Advances in neuroprotective ingredients of medicinal herbs by using cellular and animal models of Parkinson ' s disease. *Evid.-based Complement. Altern. Med.* 2013, 957875. doi:10.1155/2013/957875

Moujalled, D., Strasser, A., and Liddell, J. R. (2021). Molecular mechanisms of cell death in neurological diseases. *Cell Death Differ.* 28 (7), 2029–2044. doi:10.1038/s41418-021-00814-y

Moustafa, A. A., Chakravarthy, S., Phillips, J. R., Gupta, A., Keri, S., Polner, B., et al. (2016). Motor symptoms in Parkinson's disease: a unified framework. *Neurosci. Biobehav. Rev.* 68, 727–740. doi:10.1016/j.neubiorev.2016.07.010

Nepal, M. R., Jeong, K. S., Kim, G. H., Cha, D. H., Kang, M. J., Kim, J. S., et al. (2019). Role of intestinal microbiota in metabolism of gastrodin *in vitro* and *in vivo*. *Metabolites* 9 (4), 69. doi:10.3390/metabo9040069

Nikoletopoulou, V., Papandreou, M. E., and Tavernarakis, N. (2015). Autophagy in the physiology and pathology of the central nervous system. *Cell Death & Differ.* 22 (3), 398–407. doi:10.1038/cdd.2014.204

Nixon, R. A., and Rubinsztein, D. C. (2024). Mechanisms of autophagy-lysosome dysfunction in neurodegenerative diseases. *Nat. Rev. Mol. Cell Biol.* 25, 926–946. doi:10.1038/s41580-024-00757-5

O'Connor, T., Sadleir, K. R., Maus, E., Velliquette, R. A., Zhao, J., Cole, S. L., et al. (2008). Phosphorylation of the translation initiation factor eIF2alpha increases BACE1 levels and promotes amyloidogenesis. *Neuron* 60 (6), 988–1009. doi:10.1016/j.neuron.2008.10.047

Ohashi, S. N., Delong, J. H., Kozberg, M. G., Mazur-Hart, D. J., van Veluw, S. J., Alkayed, N. J., et al. (2023). Role of inflammatory processes in hemorrhagic stroke. *Stroke* 54 (2), 605–619. doi:10.1161/STROKEAHA.122.037155

Patharapankal, E. J., Ajiboye, A. L., Mattern, C., and Trivedi, V. (2023). Nose-to-Brain (N2B) delivery: an alternative route for the delivery of biologics in the management and treatment of central nervous system disorders. *Pharmaceutics* 16 (1), 66. doi:10.3390/pharmaceutics16010066

Pei, H., Shen, H., Bi, J., He, Z., and Zhai, L. (2024). Gastrodin improves nerve cell injury and behaviors of depressed mice through Caspase-3-mediated apoptosis. *Ther* 30 (3), e14444. doi:10.1111/cns.14444

Peng, Z. W., Wang, S. Q., Chen, G. J., Cai, M., Liu, R., Deng, J., et al. (2015). Gastrodin alleviates cerebral ischemic damage in mice by improving anti-oxidant and anti-inflammation activities and inhibiting apoptosis pathway. *Neurochem. Res.* 40 (4), 661–673. doi:10.1007/s11064-015-1513-5

Rahimi Darehbagh, R., Seyedoshohadaei, S. A., Ramezani, R., and Rezaei, N. (2024). Stem cell therapies for neurological disorders: current progress, challenges, and future perspectives. *Eur. J. Med. Res.* 29 (1), 386–405. doi:10.1186/s40001-024-01987-1

Raphael, A. R., Perlin, J. R., and Talbot, W. S. (2010). Schwann cells reposition a peripheral nerve to isolate it from postembryonic remodeling of its targets. *Development* 137 (21), 3643–3649. doi:10.1242/dev.057521

Samaridou, E., Walgrave, H., Salta, E., Alvarez, D. M., Castro-Lopez, V., Loza, M., et al. (2020). Nose-to-brain delivery of enveloped RNA - cell permeating peptide nanocomplexes for the treatment of neurodegenerative diseases. *Biomaterials* 230, 119657. doi:10.1016/j.biomaterials.2019.119657

Shen, W., Wu, S., Ge, X., Ao, F., Mao, Y., Hu, J., et al. (2024). Preparation of gastrodin modified P(VDF-TrFE)-Eudragit L100-AuNPs nanofiber membranes with piezoelectric property. *J. Mech. Behav. Biomed. Mater.* 151, 106355. doi:10.1016/j.jmbbm.2023.106355

Shields, D. C., Haque, A., and Banik, N. L. (2020). Neuroinflammatory responses of microglia in central nervous system trauma. *J. Cereb. Blood. Flow. Metab.* 40 (1_Suppl. l), S25-S33–S33. doi:10.1177/0271678X20965786

Sokolova, V., Mekky, G., Meer, S. B. V. D., Seeds, M. C., and Epple, M. (2020). Transport of ultrasmall gold nanoparticles (2 nm) across the blood–brain barrier in a six-cell brain spheroid model. *Sci. Rep.* 10 (1), 18033. doi:10.1038/s41598-020-75125-2

Stafstrom, C. E., and Carmant, L. (2015). Seizures and epilepsy: an overview for neuroscientists. *Cold Spring Harb. Perspect. Med.* 5 (6), a022426. doi:10.1101/cshperspect.a022426

Starosta, M., Marek, K., Redlicka, J., and Miller, E. (2024). Extracorporeal shockwave treatment as additional therapy in patients with post-stroke spasticity of upper limb-A narrative review. *J. Clin. Med.* 13 (7), 2017. doi:10.3390/jcm13072017

Sui, Y., Bian, L., Ai, Q., Yao, Y., Yu, M., Gao, H., et al. (2019). Gastrodin inhibits inflammasome through the STAT3 signal pathways in TNA2 astrocytes and reactive astrocytes in experimentally induced cerebral ischemia in rats. *Neuromolecular Med.* 21 (3), 275–286. doi:10.1007/s12017-019-08544-8

Tang, C., Fang, Z., Chu, D., Zhang, L., Tang, Y., Zhou, J., et al. (2022). Pharmacodynamics, network pharmacology, and pharmacokinetics of Chinese medicine formula 9002A in the treatment of Alzheimer's disease. *Front. Pharmacol.* 13, 849994. doi:10.3389/fphar.2022.849994

Tapia-Arellano, A., Cabrera, P., Cortes-Adasme, E., Riveros, A., Hassan, N., and Kogan, M. J. (2024). Tau- and α-synuclein-targeted gold nanoparticles: applications, opportunities, and future outlooks in the diagnosis and therapy of neurodegenerative diseases. *J. Nanobiotechnology.* 22 (1), 248. doi:10.1186/s12951-024-02526-0

Teleanu, R. I., Niculescu, A. G., Roza, E., Vladacenco, O., Grumezescu, A. M., and Teleanu, D. M. (2022). Neurotransmitters-key factors in neurological and neurodegenerative disorders of the central nervous system. *Int. J. Mol. Sci.* 23 (11), 5954. doi:10.3390/ijms23115954

Teo, C. C., Tan, S. N., Yong, J. W., Hew, C. S., and Ong, E. S. (2008). Evaluation of the extraction efficiency of thermally labile bioactive compounds in Gastrodia elata Blume by pressurized hot water extraction and microwave-assisted extraction. *J. Chromatogr. A* 1182 (1), 34–40. doi:10.1016/j.chroma.2008.01.011

Tran, P., and Park, J. S. (2021). Application of supercritical fluid technology for solid dispersion to enhance solubility and bioavailability of poorly water-soluble drugs. *Int. J. Pharm.* 610, 121247. doi:10.1016/j.ijpharm.2021.121247

Tuo, Q. Z., Zhang, S. T., and Lei, P. (2022). Mechanisms of neuronal cell death in ischemic stroke and their therapeutic implications. *Med. Res. Rev.* 42 (1), 259–305. doi:10.1002/med.21817

Uscategui, Y. L., Diaz, L. E., Gomez-Tejedor, J. A., Valles-Lluch, A., Vilarino-Feltrer, G., Serrano, M. A., et al. (2019). Candidate polyurethanes based on Castor oil (Ricinus communis), with polycaprolactone diol and chitosan additions, for use in biomedical applications. *Molecules* 24 (2), 237. doi:10.3390/molecules24020237

Uz, M., Sharma, A. D., Adhikari, P., Sakaguchi, D. S., and Mallapragada, S. K. (2017). Development of multifunctional films for peripheral nerve regeneration. *Acta Biomater.* 56, 141–152. doi:10.1016/j.actbio.2016.09.039

van der Flier, W. M., Skoog, I., Schneider, J. A., Pantoni, L., Mok, V., Chen, C., et al. (2018). Vascular cognitive impairment. *Nat. Rev. Dis. Prim.* 4, 18003. doi:10.1038/nrdp.2018.3

Wang, D., and Dong, X. Q. (2021). Gastrodin provides neuroprotection in models of traumatic brain injury via Nrf2 signaling pathway. *Qual. Assur. Saf. Crop. Foods* 13 (4), 62–69. doi:10.15586/qas.v13i4.965

Wang, H., and Wang, D. (2023). Effect of butylphthalide injection combined with gastrodin to improve sTRAIL and inflammatory factors in elderly patients with cerebral infarction. *Am. J. Transl. Res.* 15 (4), 2552–2560.

Wang, H. N., Zhang, R. G., Qiao, Y. T., Xue, F., Nie, H., Zhang, Z. J., et al. (2014). Gastrodin ameliorates depression-like behaviors and up-regulates proliferation of hippocampal-derived neural stem cells in rats: involvement of its anti-inflammatory action. *Behav. Brain Res.* 266, 153–160. doi:10.1016/j.bbr.2014.02.046

Wang, J., Li, Z., Pan, M., Fiaz, M., Hao, Y., Yan, Y., et al. (2022). Ultrasound-mediated blood-brain barrier opening: an effective drug delivery system for theranostics of brain diseases. *Adv. Drug Deliv. Rev.* 190, 114539. doi:10.1016/j.addr.2022.114539

Wang, J., Xie, L., Shi, Y., Ao, L., Cai, F., and Yan, F. (2021). Early detection and reversal of cell apoptosis induced by focused ultrasound-mediated blood-brain barrier opening. *ACS Nano* 15 (9), 14509–14521. doi:10.1021/acsnano.1c04029

Wang, Q., Shen, L., Ma, S. Y., Chen, M. W., Lin, X., Hong, Y. L., et al. (2016). Determination of the levels of two types of neurotransmitter and the anti-migraine effects of different dose-ratios of Ligusticum chuanxiong and Gastrodia elata. *J. Food Drug Anal.* 24 (1), 189–198. doi:10.1016/j.jfda.2015.08.005

Wang, W., Wang, Y., Wang, F., Xie, G., Liu, S., Li, Z., et al. (2024). Gastrodin regulates the TLR4/TRAF6/NF-κB pathway to reduce neuroinflammation and microglial activation in an AD model. *Phytomedicine* 128, 155518. doi:10.1016/j.phymed.2024.155518

Wang, X., Li, S., Ma, J., Wang, C., Chen, A., Xin, Z., et al. (2019). Effect of gastrodin on early brain injury and neurological outcome after subarachnoid hemorrhage in rats. *Neurosci. Bull.* 35 (3), 461–470. doi:10.1007/s12264-018-00333-w

Wang, X. L., Xing, G. H., Hong, B., Li, X. M., Zou, Y., Zhang, X. J., et al. (2014). Gastrodin prevents motor deficits and oxidative stress in the MPTP mouse model of Parkinson's disease: involvement of ERK1/2-Nrf2 signaling pathway. *Life Sci.* 114 (2), 77–85. doi:10.1016/j.lfs.2014.08.004

Wang, Y., Luo, K., Li, J., Liao, Y., Liao, C., Chen, W. S., et al. (2022). Focused ultrasound promotes the delivery of gastrodin and enhances the protective effect on dopaminergic neurons in a mouse model of Parkinson's disease. *Front. Cell. Neurosci.* 16, 884788. doi:10.3389/fncel.2022.884788

Wei, C., Wang, J., Yu, J., Tang, Q., Liu, X., Zhang, Y., et al. (2023). Therapy of traumatic brain injury by modern agents and traditional Chinese medicine. *Chin. Med.* 18 (1), 25. doi:10.1186/s13020-023-00731-x

Wei, W. (2017). Clinical study on Gastrodin Tablets combined with oxiracetam in treatment of post-traumatic syndrome. *Drugs & Clin.* 32 (7), 1205–1208. doi:10.7501/j.issn.1674-5515.2017.07.009

Wen, Y., Dong, Z., Liu, J., Axerio-Cilies, P., Du, Y., Li, J., et al. (2022). Glutamate and GABA(A) receptor crosstalk mediates homeostatic regulation of neuronal excitation in the mammalian brain. *Signal Transduct. Target. Ther.* 7 (1), 340. doi:10.1038/s41392-022-01148-y

Wendels, S., and Averous, L. (2021). Biobased polyurethanes for biomedical applications. *Bioact. Mater.* 6 (4), 1083–1106. doi:10.1016/j.bioactmat.2020.10.002

Wu, S., Huang, R., Zhang, R. Q., Xiao, C., Wang, L. L., Luo, M., et al. (2023). Gastrodin and gastrodigenin improve energy metabolism disorders and mitochondrial dysfunction to antagonize vascular dementia. *Molecules* 28 (6), 2598. doi:10.3390/molecules28062598

Wu, S., Wu, B., Liu, M., Chen, Z., Wang, W., Anderson, C. S., et al. (2019). Stroke in China: advances and challenges in epidemiology, prevention, and management. *Lancet Neurol.* 18 (4), 394–405. doi:10.1016/S1474-4422(18)30500-3

Xiao, G., Tang, R., Yang, N., and Chen, Y. (2023). Review on pharmacological effects of gastrodin. *Arch. Pharm. Res.* 46 (9-10), 744–770. doi:10.1007/s12272-023-01463-0

Xiao, H., Jiang, Q. S., Qiu, H. M., Wu, K., Ma, X. J., Yang, J. X., et al. (2021). Gastrodin promotes hippocampal neurogenesis via PDE9-cGMP-PKG pathway in mice following cerebral ischemia. *Neurochem. Int.* 150, 105171. doi:10.1016/j.neuint.2021.105171

Xiaobo, L. W. L. H. (2020). Clinical study of Gastrodin combined with Oxiracetam in the treatment of cognitive impairment in elderly patients with ischemic stroke. *CHINA Med. Her.* 17 (14), 78–81.

Xiu-Yun, Z. (2020). Clinical study of gastrodin injection in the treatment of cerebral infarction. *Syst. Med.* 5 (5), 10–12. doi:10.19368/j.cnki.2096-1782.2020.05.010

Xu, C., Bai, Y., An, Z., Hu, Y., Zhang, C., and Zhong, X. (2022). IL-13Rα2 humanized scFv-based CAR-T cells exhibit therapeutic activity against glioblastoma. *Mol. Ther. Oncolytics.* 24, 443–451. doi:10.1016/j.omto.2022.01.002

Xu, Y., Su, G. H., Ma, D., Xiao, Y., Shao, Z. M., and Jiang, Y. Z. (2021). Technological advances in cancer immunity: from immunogenomics to single-cell analysis and artificial intelligence. *Signal Transduct. Target. Ther.* 6 (1), 312. doi:10.1038/s41392-021-00729-7

Xuegong, L. (2015). Curative effect of gastrodin sustained-release tablets in treatment of post traumatic brain syndrome and its effect on expression of IGF-1,il-6. *J. Hubei Univ. Chin. Med.* 12 (6), 13–16. doi:10.3969/j.issn.1008-987x.2015.06.05

Yan, H. F., Zou, T., Tuo, Q. Z., Xu, S., Lei, P., Belaidi, A. A., et al. (2021). Ferroptosis: mechanisms and links with diseases. *Signal Transduct. Target. Ther.* 6 (1), 49. doi:10.1038/s41392-020-00428-9

Yang, C. S., Chiu, S. C., Liu, P. Y., Wu, S. N., Lai, M. C., and Huang, C. W. (2021). Gastrodin alleviates seizure severity and neuronal excitotoxicities in the rat lithium-pilocarpine model of temporal lobe epilepsy via enhancing GABAergic transmission. *J. Ethnopharmacol.* 269, 113751. doi:10.1016/j.jep.2020.113751

Yang, F., Li, G., Lin, B., and Zhang, K. (2022). Gastrodin suppresses pyroptosis and exerts neuroprotective effect in traumatic brain injury model by inhibiting NLRP3 inflammasome signaling pathway. *J. Integr. Neurosci.* 21 (2), 72. doi:10.31083/j.jin2102072

Yang, G. M., Zeng, X. F., Li, J., Leung, C. W., Zhang, D. X., Hong, S. J., et al. (2019). Protective effect of gastrodin against methamphetamine-induced autophagy in human dopaminergic neuroblastoma SH-SY5Y cells via the AKT/mTOR signaling pathway. *Neurosci. Lett.* 707, 134287. doi:10.1016/j.neulet.2019.134287

Yang, X., Shi, G., Zeng, L., Wang, J., and Jiang, P. (2017). Influences of gastrodin on CGRP, NO and ET1 expression in peripheral blood of migraine patients. *J. Nanjing Univ. traditional Chin. Med.* 33 (1), 23–25. doi:10.14148/j.issn.1672-0482.2017.0023

Yao, Y. Y., Ling, E. A., and Lu, D. (2020). Microglia mediated neuroinflammation - signaling regulation and therapeutic considerations with special reference to some natural compounds. *Histol. Histopathol.* 35 (11), 1229–1250. doi:10.14670/HH-18-239

Ye, H., Robak, L. A., Yu, M., Cykowski, M., and Shulman, J. M. (2023). Genetics and pathogenesis of Parkinson's syndrome. *Annu. Rev. Pathol.* 18, 95–121. doi:10.1146/annurev-pathmechdis-031521-034145

Ying, W. J. G. (2022). Clinical study of toutongning capsule combined with gastrodin capsule in treatment of migraine. *Liaoning J. Traditional Chin. Med.* 49 (11), 138–140. doi:10.13192/jissn.1000-17192022.11036

Yongguang, L., Xiaowei, W., Huichao, Y., and Yanxiang, Z. (2022). Gastrodin promotes the regeneration of peripheral nerves by regulating miR-497/BDNF axis. *BMC Complement. Med. Ther.* 22 (1), 45. doi:10.1186/s12906-021-03483-z

You, Q., Lan, X. B., Liu, N., Du, J., Ma, L., Yang, J. M., et al. (2023). Neuroprotective strategies for neonatal hypoxic-ischemic brain damage: current status and challenges. *Eur. J. Pharmacol.* 957, 176003. doi:10.1016/j.ejphar.2023.176003

Zhan, H. D., Zhou, H. Y., Sui, Y. P., Du, X. L., Wang, W. H., Dai, L., et al. (2016). The rhizome of Gastrodia elata Blume - an ethnopharmacological review. *J. Ethnopharmacol.* 189, 361–385. doi:10.1016/j.jep.2016.06.057

Zhang, H., Wang, L., Lu, B., Qi, W., Jiao, F., Zhang, H., et al. (2019). Metabolite profiling and quantification of phytochemicals of Tianma-Gouteng granule in human and rat urine using ultra high performance liquid chromatography coupled with tandem mass spectrometry. *J. Sep. Sci.* 42 (17), 2762–2770. doi:10.1002/jssc.201900029

Zhang, J., Li, L., Liu, Q., Zhao, Z., Su, D., Xiao, C., et al. (2023). Gastrodin programs an Arg-1+ microglial phenotype in hippocampus to ameliorate depression- and anxiety-like behaviors via the Nrf2 pathway in mice. *Phytomedicine* 113, 154725. doi:10.1016/j.phymed.2023.154725

Zhang, J. S., Zhou, S. F., Wang, Q., Guo, J. N., Liang, H. M., Deng, J. B., et al. (2016). Gastrodin suppresses BACE1 expression under oxidative stress condition via inhibition of the PKR/eIF2α pathway in Alzheimer's disease. *Neuroscience* 325, 1–9. doi:10.1016/j.neuroscience.2016.03.024

Zhang, R. G., Peng, Z. W., Wang, H. H., Xue, F., Chen, Y. H., Wang, Y., et al. (2014). Gastrodin ameliorates depressive-like behaviors and up-regulates the expression of BDNF in the Hippocampus and hippocampal-derived astrocyte of rats. *Neurochem. Res.* 39 (1), 172–179. doi:10.1007/s11064-013-1203-0

Zhang, T., and Li, W. C. (2019). Clinical study on Gastrodin Capsules combined with lomeflozine in treatment of vasculoneurous migraine. *Drugs & Clin.* 34 (2), 327–331. doi:10.7501/j.issn.1674-5515.2019.02.012

Zhang, W., Mehta, A., Tong, Z., Esser, L., and Voelcker, N. H. (2021). Development of polymeric nanoparticles for blood-brain barrier transfer-strategies and challenges. *Adv. Sci.* 8 (10), 2003937. doi:10.1002/advs.202003937

Zhang, X., Yang, X. K., Wu, C. Y., and Yuan, Y. (2021). Gastrodin exerts protective effects in reactive TNC1 astrocytes via regulation of the Notch signaling pathway. *Ann. Transl. Med.* 9 (24), 1754. doi:10.21037/atm-21-5787

Zhang, Y., Chen, H., Li, R., Sterling, K., and Song, W. (2023). Amyloid β-based therapy for Alzheimer's disease: challenges, successes and future. *Signal Transduct. Target. Ther.* 8 (1), 248. doi:10.1038/s41392-023-01484-7

Zhang, Y. (2020). Clinical study of gastrodine for injeetion combined with nimodipine in the treatment of acute migraine. *Chin. J. Pract. Nerv. Dis.* 23 (1), 54–59. doi:10.12083/SYSJ.2020.01.012

Zhao, X., Zou, Y., Xu, H., Fan, L., Guo, H., Li, X., et al. (2012). Gastrodin protect primary cultured rat hippocampal neurons against amyloid-beta peptide-induced neurotoxicity via ERK1/2-Nrf2 pathway. *Brain Res.* 1482, 13–21. doi:10.1016/j.brainres.2012.09.010

Zhao, Y. L., Martins-Oliveira, M., Akerman, S., and Goadsby, P. J. (2018). Comparative effects of traditional Chinese and Western migraine medicines in an animal model of nociceptive trigeminovascular activation. *Cephalalgia* 38 (7), 1215–1224. doi:10.1177/0333102417728245

Zhou, C. (2018). Efficacy and safety of Tianmasu injection in treatment of acute cerebral infaretion: a meta analysis. *China Med.* 13 (11), 1655–1660. doi:10.3760/j.issn.1673-4777.2018.11.015

Zhou, H., Wang, N., Xu, L., Huang, H., and Yu, C. (2017). The efficacy of gastrodin in combination with folate and vitamin B12 on patients with epilepsy after stroke and its effect on HMGB-1, IL-2 and IL-6 serum levels. *Exp. Ther. Med.* 14 (5), 4801–4806. doi:10.3892/etm.2017.5116

Zhou, X., Shao, J., Xie, X., Xu, Y., Shao, T., and Jin, Z. (2022). Effectiveness of gastrodin for migraine: a meta-analysis. *Front. Neurol.* 13, 939401. doi:10.3389/fneur.2022.939401

Zuo, H. J., Wang, P. X., Ren, X. Q., Shi, H. L., Shi, J. S., Guo, T., et al. (2023). Gastrodin regulates PI3K/AKT-Sirt3 signaling pathway and proinflammatory mediators in activated microglia. *Mol. Neurobiol.* 61, 2728–2744. doi:10.1007/s12035-023-03743-8

Zuo, W., Xu, F., Zhang, K., Zheng, L., and Zhao, J. (2016). Proliferation-enhancing effects of gastrodin on RSC96 Schwann cells by regulating ERK1/2 and PI3K signaling pathways. *Biomed. Pharmacother.* 84, 747–753. doi:10.1016/j.biopha.2016.09.106

frontiers | Frontiers in Pharmacology

TYPE Original Research
PUBLISHED 09 January 2025
DOI 10.3389/fphar.2024.1496917



OPEN ACCESS

EDITED BY
Qi Liang,
Air Force Medical University, China

REVIEWED BY
Domenico D'Arca,
University of Modena and Reggio Emilia, Italy
Nebojsa Petar Stilinovic,
University of Novi Sad, Serbia

*CORRESPONDENCE
Changling Sun,
winterc126@sina.com

RECEIVED 15 September 2024
ACCEPTED 24 December 2024
PUBLISHED 09 January 2025

CITATION
Miao Z, Chang D, Du X and Sun C (2025) Berberrubine protects against cisplatin-induced ototoxicity by promoting folate biosynthesis. *Front. Pharmacol.* 15:1496917.
doi: 10.3389/fphar.2024.1496917



# Berberrubine protects against cisplatin-induced ototoxicity by promoting folate biosynthesis

Zhuang Miao, Danyang Chang, Xiaodong Du and Changling Sun*

Department of Otolaryngology-Head and Neck Surgery, Affiliated Hospital of Jiangnan University, Wuxi, Jiangsu, China

**Objective:** This research investigated the possible shielding properties of BB (Berberrubine) against the harmful auditory effects of cisplatin, preliminarily delving into the underlying mechanisms responsible for this protection.

**Methods:** HEI-OC1 cell viability was determined using a Cell Counting Kit-8 (CCK-8). The impact of BB on cochlear hair cells was studied through *in vitro* cochlear explants culture. Apoptosis levels were measured through Annexin V-PI, Cleaved Caspase-3, and TUNEL staining. The level of ROS (reactive oxygen species) was measured through the application of DCFH-DA, MitoSOX, and JC-1 fluorescent dyes for staining. Immunofluorescence analysis of cochlear samples from mice was conducted to quantify the hair cell count, and concurrently, ABR (Auditory Brainstem Response) testing was utilized to evaluate auditory function. The mechanism of action of BB was explored using RNA-Seq and qRT-PCR analysis.

**Results:** BB significantly improved cell survival rates under cisplatin treatment, reduced levels of apoptotic markers (TUNEL, Cleaved Caspase-3, Annexin V-PI), decreased ROS and MitoSOX levels, and improved JC-1 signals in both HEI-OC1 cells and cochlear hair cells in cochlear explants culture. Animal studies demonstrated that treatment with BB enhanced the survival of cochlear hair cells, reduced hearing impairment caused by cisplatin in mice. RNA-seq and qRT-PCR analysis revealed that BB influenced the expression levels of multiple genes (*Ccnd2, Reln, Pgf, Mylk3, Ppplr12c, Thbsl*), by promoting folate biosynthesis for hearing protection.

**Conclusion:** Our findings suggest that BB protects against cisplatin-induced hearing damage by enhancing folate biosynthesis, decreasing intracellular ROS levels, and inhibiting apoptosis.

KEYWORDS

**berberrubine, cisplatin, ototoxicity, hair cells, folate, oxidative stress**

## 1 Introduction

Hearing loss is a widespread global concern that profoundly affects the quality of life. Numerous factors can contribute to it, including genetics, aging, noise exposure, diseases, drug-induced damage, and trauma, among others (Albera et al., 2010; Gong et al., 2018; Liu and Yan, 2007). Among drug-induced cases, hearing loss caused by ototoxicity from cisplatin is commonly observed in clinical environments. Cisplatin, a chemotherapy agent utilized extensively, is potent against several types of cancers such as ovarian, prostate, testicular, lung, nasopharyngeal, esophageal, lymphoma, head

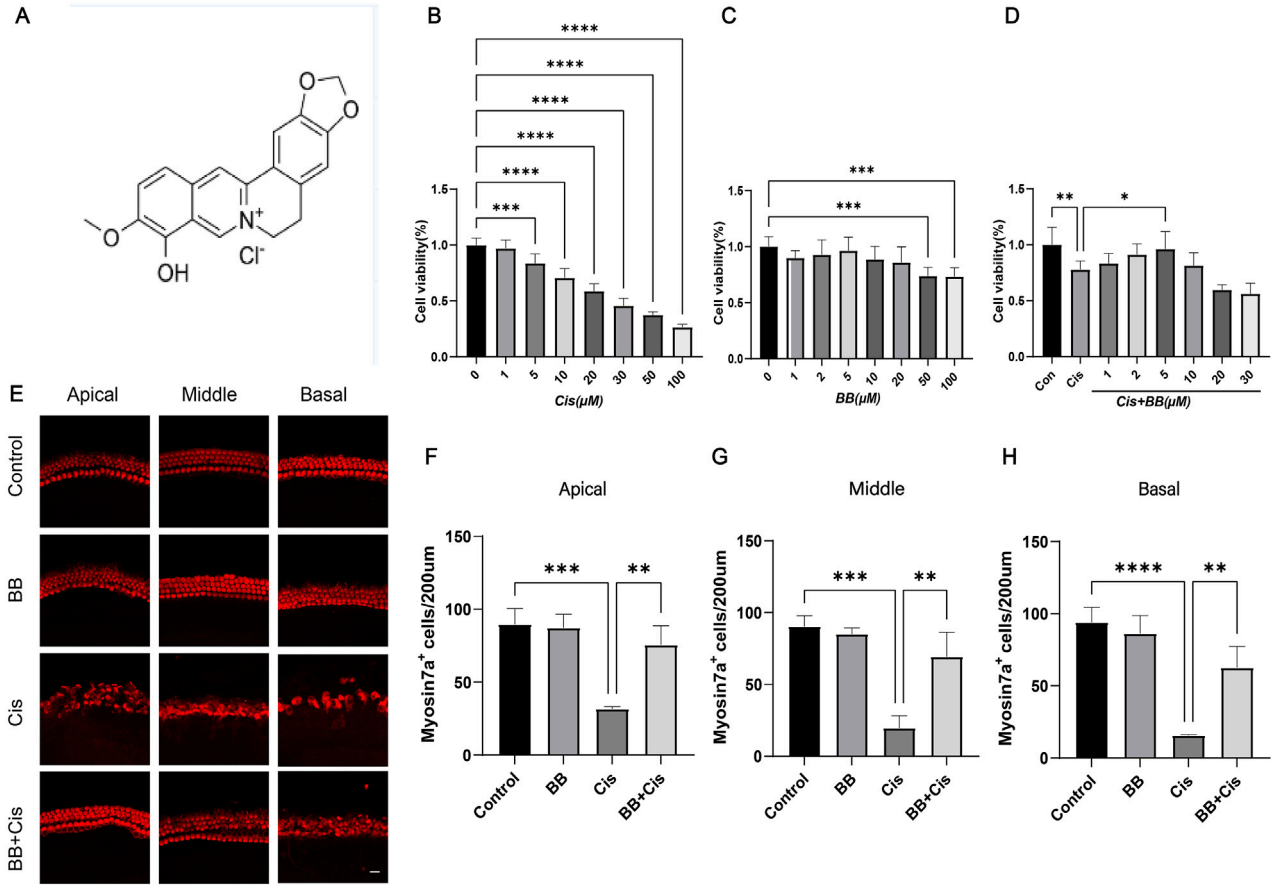


FIGURE 1
BB enhances cell survival in the exposure of cisplatin. **(A)** Chemical structure of BB. **(B)** CCK-8 assay shows cisplatin toxicity in HEI-OC1 cells at various concentrations. **(C)** CCK-8 assay indicates BB toxicity at different dosages. **(D)** CCK-8 assay reveals BB's protective effect on cisplatin-treated HEI-OC1 cells. **(E)** Immunofluorescence of cochlear hair cells labeled with myosin 7a at the cochlea's apex, midsection, and base. **(F–H)** Quantitative assessment of hair cell counts in the cochlea's apex, midsection, and base. *$P < 0.05$, **$P < 0.01$, ***$P < 0.001$, ****$P < 0.0001$. BB: Berberrubine; Cis: Cisplatin.

and neck squamous cell carcinoma, and osteogenic sarcoma (Dasari and Tchounwou, 2014; Makovec, 2019; Romani, 2022; Tang et al., 2024). Although effective, the prevalence of side effects including kidney damage, nerve toxicity, and hearing impairment restricts its widespread use (Boulikas and Vougiouka, 2003; Crona et al., 2017; Fetoni et al., 2022). Techniques to prevent and treat cisplatin-induced nephrotoxicity and neurotoxicity are currently available; however, effective treatments for ototoxicity are still limited. Research indicates that ototoxicity from cisplatin is characterized by progressive, dose-dependent, and bilateral auditory damage (Callejo et al., 2017; Callejo et al., 2015; Guidotti et al., 2023). The suspected mechanisms involve oxidative stress, inflammatory response, apoptosis, and autophagy, which impair critical physiological components such as hair cells, stria vascularis, and spiral ganglia, although the precise details remain unclear (Guo et al., 2018; Kros and Steyger, 2019; Li Y. et al., 2023; Steyger, 2021). Therefore, it is crucial to identify medications or interventions that can offer protection,and investigate the underlying molecular pathways of cisplatin-related hearing damage.

Berberine exhibits potent pharmacological properties. Berberine exhibits antioxidant, anti-inflammatory, antimicrobial, antitumor, and neuroprotective activities (Jin et al., 2016; Song et al., 2020; Wang et al., 2017). Despite these potent effects, the relatively low concentration of berberine found in circulation seems to contrast with its extensive pharmacological influence. Conversely, the substantial presence of Berberrubine (BB, Figure 1A) in the bloodstream, as the predominant metabolite of berberine, suggests that it may significantly contribute to the overall therapeutic impact attributed to berberine. Furthermore, studies have indicated that BB possesses a beneficial ameliorative effect on diseases related to inflammatory-oxidative stress. Given that inflammatory response and oxidative stress are key mechanisms in cisplatin ototoxicity, this suggests that BB theoretically holds potential in preventing cisplatin-induced hearing damage (Li et al., 2010; Sun et al., 2021; Wang et al., 2020). In this research, we examined BB's protective role against cisplatin-induced ototoxicity *via* cellular experiments, cochlear explants culture, and *in vivo* animal studies. Additionally, we investigated the underlying mechanisms of its action, which may offer a potential therapy for cisplatin-induced ototoxicity.

# 2 Materials and methods

## 2.1 Cell culture

HEI-OC1 line were cultivated in 10-cm circular dishes for cell culture, using high-glucose medium (Gibco, 11965092, United States) supplemented with 10% fetal bovine serum (Gibco, A5670701, United States) and 0.1% ampicillin (Beyotime, ST008, China). The cell cultures were maintained at a temperature of 33°C in a controlled atmosphere with 10% CO2 concentration. Due to the unique properties of HEI-OC1 cells, their metabolic state is more stable under 33 °C culture conditions, which can better promote cell proliferation and reduce cell differentiation. Cells were passaged using a solution of 0.25% trypsin with EDTA (Gibco, 25200056, United States) when the cell population in the dish reached approximately 80%–90%.

## 2.2 Cochlear explants culture

Six mice were sterilized using 75% alcohol before undergoing dissecting to extract the cochlea. The isolated cochlea was then immersed in a 6 cm dissecting dish containing Hank's Balanced Salt Solution (HBSS) (Beyotime, C0219, China). Using fine tweezers on a sterile surface, the spiral ligament, cochlear implant, and vascular structure were meticulously removed to isolate the cochlear basement membrane. This membrane was subsequently laid flat on a Cell-Tak-coated circular slide (Corning, 354,240, United States), which was then transferred to a four-hole dish with a six-cm diameter. The cochleas, numbering a total of twelve, were divided into separate experimental groups, control, BB-only, cisplatin-only, and BB combined with cisplatin groups. Each subgroup contained three basement membranes. These specimens were cultured in 3 mL of F12 high-glucose medium (Gibco, 11330–032, United States) along with B27 (Thermo Fisher, 17504044, United States), N2 (Thermo Fisher, 17502001, United States), and ampicillin, and were kept in a 5% carbon dioxide incubator at 37°C. After the attachment phase, Berberrubine (TargetMol, 15401–69–1, United States) was added to both the BB-only and the BB combined with cisplatin groups, achieving a final concentration of 5 μM and subsequently pre-incubated for 12 h. Subsequently, cisplatin was introduced to the groups cisplatin-only and BB combined with cisplatin groups, reaching a final concentration of 50 μM, after which the incubation continued for another 24 h.

## 2.3 Mouse models

Four-week-old male C57BL/6 mice were procured from Nanjing Qinglongshan Animal Co., Ltd., China. The animal studies conducted in strict compliance with the ethical standards of Southeast University, aligning with the national laws and regulations for animal experimentation. A total of twenty-four mice aged P28 were divided into four groups: control, BB gavage, cisplatin injury, and combined BB gavage with cisplatin injury. In the first week, the BB gavage groups and combined BB gavage with cisplatin injury groups received 20 mg/kg of BB (Yuanye, 15401–69–1, China) *via* gavage. The control and cisplatin injury groups were administered 0.9% saline orally. Moving into the second week, the gavage regimen continued for all groups, with the cisplatin-injured and combined BB gavage with cisplatin injury groups receiving an additional daily intraperitoneal injection of 4 mg/kg cisplatin. Similarly, the control group and the BB gavage group received injections of an equal amount of normal saline solution. Following the treatment period, the mice underwent ABR testing and hair cell counting.

## 2.4 Cell viability assay

The measurement of how alive the cells was done using the Cell Counting Kit-8 (CCK-8) (MCE, HY-K0301, United States). To begin with, the HEI-OC1 cells that were grown well were exposed to a 0.25% trypsin solution, and the enzymatic action was stopped by supplementing with an equivalent amount of growth medium. Subsequently, the cells were transferred to 15 mL centrifuge tubes for spinning at a speed of 1,000 rpm over a period of 5 min. The concentration of cells was determined with a cell counting chamber, followed by their seeding into 96-well plates at a density of 5,000 cells per well. Each well was categorized into different groups based on drug concentration, with 6 replicates wells in each group. Post drug treatment, CCK-8 reagent diluted in serum-free culture medium was added to each well and incubated for 1 h. A microplate reader was used to measure the absorbance at 450 nm, which was then utilized to compute the percentage of viable cells based on the obtained optical density readings.

## 2.5 TUNEL staining

To perform TUNEL staining, the 5 X equilibrium solution was first diluted to 1 X. Following dilution, the sample was placed in a four-well dish, and 1X equilibrium solution was added for equilibration for 30 min. Throughout this timeframe, the TUNEL reaction system (Beyotime, C1086, China) was prepared by combining $ddH_2O$, equilibrium solution, a fluorescent dye, and terminal deoxynucleotidyl transferase (TDT). After the equilibration process was finished, the balanced solution was removed, and 50 μL of the TUNEL reagent was added to each well of the 4-well dish. Following that step, the dish was placed in an incubator maintained at a temperature of 37°C for a duration of 1 hour, ensuring it was kept in the dark to prevent light exposure. Upon completion of the incubation period, the TUNEL staining solution was decanted, and DAPI staining solution (from Beyotime, C1002, China) was applied. Subsequently, the samples were subjected to a further incubation period of 1 hour at ambient temperature. Once the incubation was complete, the medium was aspirated off, and the samples underwent three successive rinses using PBS (Beyotime, C0221A, China) for 5 min per wash. The samples were subsequently sealed using nail polish and analyzed using a confocal microscope. Should immunofluorescence staining be necessary, the samples would undergo the appropriate immunofluorescence staining procedure.

## 2.6 Annexin V-PI staining

For Annexin V-PI staining, initially the drug-treated cell samples underwent two washes with pre-cooled PBS. Subsequently, the Annexin V and PI Staining Solution, which was prepared using Binding Buffer (Beyotime, C1062S, China), was introduced to the cell samples. Using a pipette, Annexin V and PI Staining Solution was gently agitated to ensure thorough interaction with the cells. The cells were incubated for 10 min at ambient temperature. The setting was shielded from light. After incubation, the staining solution was aspirated or discarded and DAPI Staining Solution was applied for an additional 10-minute period. Following the DAPI staining procedure, the samples underwent three consecutive washes using PBS to remove any excess stain. To conclude the process, the samples were transferred onto microscope slides, and covered with coverslips, and then analyzed under a confocal scanning microscope.

## 2.7 ROS staining

To conduct ROS staining, had the culture medium removed. DCFH-DA (Beyotime, S0033M, China) was prepared by diluting it in a medium devoid of serum to a concentration ratio of 1:1,000. The diluted DCFH-DA solution was then applied to ensure full coverage of the cells. Following the preparation, The cells were placed in an incubator set to 37°C for 20 min. After the incubation, the cells underwent three washes with serum-free DMEM. This was followed by the removal of the staining solution and incubating the cells with DAPI staining for 10 min at room temperature. After the incubation, the cells underwent three rounds of washing using PBS. The samples were mounted onto slides with coverslips in place and then examined using a confocal microscope for detailed observation.

## 2.8 MitoSOX staining

For MitoSOX staining, begin by removing the drug-treated samples from the culture medium. Prepare a MitoSOX staining solution (Beyotime, S0061S, China), dilute it to a concentration of 5 μM with HBSS. Apply the prepared MitoSOX solution to the samples, then place them in an incubator set to 37°C for a duration of 10 min, to ensure taking care to protect them from light exposure. Following incubation, carefully remove the staining solution and wash the samples three times with pre-warmed HBSS at 37°C, each wash lasting for 5 min. After the washing process, mount the cells onto slides and incubate them with DAPI staining solution at room temperature for 10 min, again protecting them from light. Subsequent washing of the samples should be done three times with PBS. To conclude, the cell samples onto microscope slides secure with coverslips, and then proceed to examine them under a confocal microscope. If immunofluorescence staining is necessary, follow the relevant immunofluorescence staining protocol.

## 2.9 JC-1 mitochondrial membrane potential staining

To stain mitochondrial membrane potential, The working solution of JC-1 was diluted using ultra-pure water initially. Removal of the culture medium from the treated cell samples took place, followed by a single wash with PBS. Subsequently, the working solution of JC-1 (Beyotime, C2006, China) was combined with the culture medium and applied to the cell samples. The cells were then incubated at 37°C for 20 min. The JC-1 staining buffer was prepared using ultra-pure water and stored on ice. After the 20-minutes incubation, elimination of the staining solution and double washing of samples with the staining buffer took place. Lastly, the samples were observed using a confocal microscope.

## 2.10 Immunofluorescence analysis

HEI-OC1 cells, cochlear basement membrane, and cochlea samples underwent fixation in 4% paraformaldehyde. For the adult rat cochlea samples decalcification with EDTA solution was carried out prior to fixation. The cochlear basement membrane was then carefully dissected into three slices representing different turns (apical, middle, and basal) under a microscope post decalcification and fixation. Following the sample processing, the samples were permeabilized with PBST for 5 min, repeated three times. Subsequently, the samples were soaked with an immunofluorescence sealing solution for an hour. Once the blocking step was complete, the primary antibody specific for Myosin7a was introduced to the samples, which were then incubated at a temperature of 4°C in a refrigerator environment protected from light for an extended period overnight. On the following day, the primary antibody solution was aspirated off, the samples were washed extensively with PBST in three rounds of 5-minute intervals. Subsequent steps included the addition of the secondary antibody (goat anti-mouse AlexaFluor Plus 555) and DAPI, followed by an incubation period of 1 h at room temperature in the dark. Subsequently, the secondary antibody solution was eliminated, followed by a rigorous washing of the samples using PBST, which was done in triplicate for durations of 5 minutes per wash. When prepared, the samples were meticulously mounted onto DAKO-brand slides, topped with coverslips, and secured with a layer of clear nail polish to prevent leakage. The slides were left at room temperature for half an hour to allow the nail polish to dry before observation under a confocal microscope. The experiment utilized various primary and secondary antibodies as well as dyes such as goat anti-rabbit Alexa Fluor Plus 488, goat anti-rabbit Alexa Fluor Plus 555, goat anti-mouse AlexaFluor Plus 555 and phalloidin, in addition to DAPI staining solution. This meticulous process ensures the precise visualization and analysis of the cochlear structures and components in the samples, contributing valuable insights to the study of auditory system biology.

## 2.11 Auditory Brainstem Response (ABR) threshold

Mice were administered an isobarbital solution at a dosage rate of 10 mg/kg of body weight, rendered unconscious and then placed on a warming pad maintained at a temperature of 37°C. Judging the effectiveness of anesthesia by finger pinching reflex, if there is no response when pinching the toes of mice, it indicates that anesthesia is complete. Following anesthesia, ABR thresholds were recorded

using a TDT system (Tucker Davies Technologies, Gainesville, FL, United States) at frequencies of 4, 8, 12, 16, 24, and 32 kHz.

## 2.12 RNA sequencing (RNA-Seq)

The HEI-OC1 cells were distributed into two groups and cultured in six-well plates, designating three wells per group for the experiment. One of the groups served as the control, while the other was subjected to BB treatment. Once the cells had adhered, the experimental group received BB at a concentration of 5 μM, which was maintained for a period of 24 h. Following the treatment, RNA was harvested from the cells in each well and then proceeded to RNA sequencing, conducted by Lianchuan Biotechnology Co., Ltd., China. following successful RNA quality control checks.

## 2.13 Quantitative real-time PCR (qRT-PCR)

Total RNA was extracted from lysed cells and reverse-transcribed into cDNA using a cDNA synthesis kit (Vazyme, RC112-01, China). The qRT-PCR reaction was set up with primers and a qRT-PCR master mix (Vazyme, Q511-02, China), The qRT-PCR program started with an initial denaturation at 95°C for 5 min, then 40 cycles of alternating between 95°C for 10 s and 60°C for 30 s. Following the amplification cycles, a melting curve analysis was conducted, which included steps at 95°C for 15 s, 60°C for a minute, and a final step at 95°C for another 15 s. The collected data were analyzed through the comparative Ct (cycle threshold) method, utilizing GAPDH as a housekeeping gene for normalization.

## 2.14 Statistical analysis

The data are expressed as mean values with their accompanying standard deviations (SD). For data that follows a normal distribution, a Student's t-test was employed to assess the differences between two-group comparisons, while analysis of variance (ANOVA) followed by the Dunnett's test was used for the comparison of three or more groups. For data that does not conform to a normal distribution, we use logarithmic transformation to transform it into data that conforms to a normal distribution, and then use the above statistical methods for analysis. Statistical analyses were conducted using Microsoft Excel and GraphPad Prism 9, with results considered statistically significant for $P < 0.05$.

# 3 Results

## 3.1 BB enhances cell survival in the exposure of cisplatin

A range of cisplatin concentrations, spanning from 0 to 100 μM in increments of 1 μM, 5 μM, 10 μM, 20 μM, 30 μM, 50 μM and 100 μM was applied to HEI-OC1 cells for exposure. The study's findings indicated that cisplatin exhibited a lethal impact on approximately 50% of the HEI-OC1 cells within the concentration range of 20–30 μM (Figure 1B). Therefore, we chose 30 μM cisplatin for further investigation. To establish the optimal concentration of BB for treating HEI-OC1 cells before cisplatin treatment, varying doses of BB (1, 2, 5, 10, 20, 50, and 100 μM) were tested. The CCK-8 assay showed no toxic effects at cisplatin concentrations from 1 to 20 μM (Figure 1C). When HEI-OC1 cells were pre-incubated with BB concentrations ranging from 1 to 30 μM for 12 h, followed by concurrent treatment with 30 μM cisplatin and BB for an additional 24 h, it was found that a 5 μM of BB was effective in mitigating the damage caused by cisplatin to the cells (Figure 1D). Additionally, in explants culture models, pre-treatment with 5 μM BB alleviated the hair cell damage caused by cisplatin (Figures 1E–H). In summary, BB alleviates cisplatin-induced cell injury, enhancing cell survival in the exposure of cisplatin.

## 3.2 BB shield mice from hearing impairment caused by cisplatin exposure

By creating mouse models to induce hearing loss with cisplatin (Figure 2A), Our investigation delved into the potential of BB to safeguard against hearing impairment triggered by cisplatin. The ABR results revealed severe hearing impairment in the cisplatin group with significantly elevated thresholds. Conversely, the group treated with BB showed a significant decrease in hearing impairment caused by cisplatin across the tested frequencies, which included 4, 8, 12, 16, and 24 kHz (Figure 2B). The immunofluorescence examination revealed a significant depletion of hair cells across the cochlea apex, midsection, and base in the basilar membrane area. Furthermore, pretreatment with BB mitigated this damage and restored hair cell counts, underscoring its role in safeguarding cochlear hair cells (Figures 2C–F). In conclusion, BB exhibits a protective effect against hearing loss caused by cisplatin in mice, highlighting its potential as a therapeutic agent for mitigating the ototoxic effects of cisplatin.

## 3.3 BB reduces apoptosis of HEI-OC1 cells triggered by cisplatin

We utilized TUNEL and Cleaved Caspase-3 staining to evaluate apoptosis, pretreated HEI-OC1 cells with BB for 12 h before exposing them to cisplatin for 24 h. Compared to the control group, the group treated with cisplatin showed a significant elevation in indicators of apoptosis, such as TUNEL positivity and levels of Cleaved Caspase-3. In contrast, the group pretreated with BB showed a notable decrease in these apoptotic markers (Figures 3A–D). Additionally, the use of Annexin V-PI staining provided an additional method to evaluate the extent of apoptosis. Under the same treatment conditions, cisplatin exposure resulted in higher apoptosis rates than the control group. However, the addition of BB substantially reduced the apoptotic markers (Figures 3E–G). In summary, BB significantly mitigates cisplatin-induced apoptosis in HEI-OC1 cells.

## 3.4 BB mitigates the apoptosis of hair cells in cochlear explants induced by cisplatin

In our study, cochlear explants underwent TUNEL and Cleaved Caspase-3 staining. BB was introduced at a concentration of 5 μM

10.3389/fphar.2024.1496917

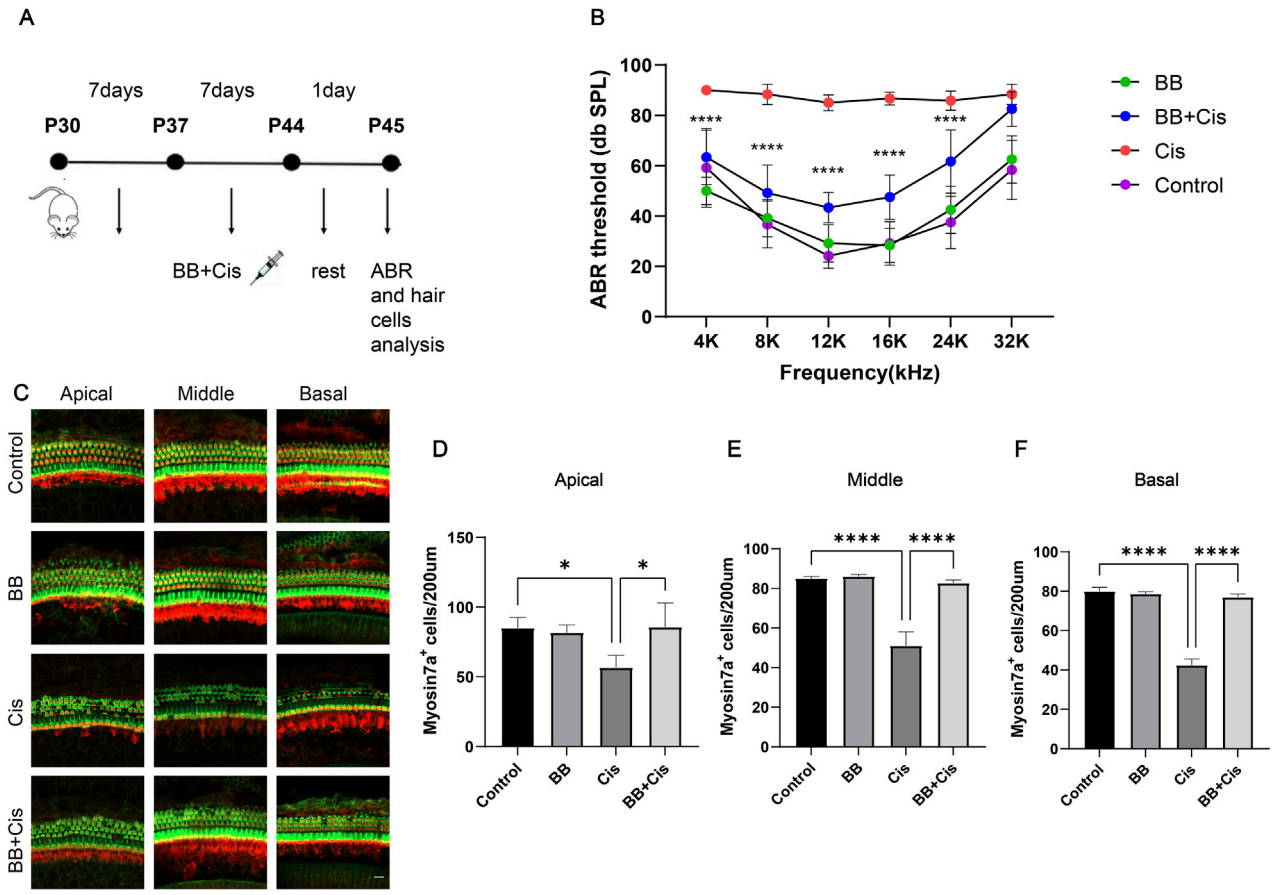


FIGURE 2
BB shield mice from hearing impairment caused by cisplatin exposure. **(A)** Schematic of the cisplatin-induced damage model. **(B)** ABR threshold analysis showing BB's effect on cisplatin-induced hearing loss in C57 mice (n = 6). **(C)** Myosin 7a immunofluorescence visualizes cochlear hair cells across the apex, midsection, and base of the cochlea. Red fluorescence: myosin7a Green fluorescence: Phalloidin **(D–F)** Numerical analysis of cochlear hair cell populations in the apex, midsection, and base (n = 3). *$P < 0.05$, ****$P < 0.0001$. BB: Berberrubine; Cis: Cisplatin.

for 12 h, followed by cisplatin exposure for 24 h. Immunofluorescence analysis revealed that, in the cisplatin-treated group, the count of dual positive cells for TUNEL/myosin 7a and Cleaved Caspase-3/myosin 7a was elevated. Conversely, BB treatment mitigated hair cell damage, substantially reducing the levels of TUNEL and Cleaved Caspase-3, indicative of apoptosis (Figures 4A–D). In conclusion, BB significantly reduced hair cell apoptosis induced by cisplatin in the cochlear basement membrane in cochlear explants.

## 3.5 BB reduces cisplatin-induced oxidative stress response

A significant accumulation of ROS in the mitochondrial compartment is crucial for the onset of hearing loss caused by cisplatin. To investigate ROS levels in HEI-OC1 cells, we utilized DCFH, MitoSOX staining, and JC-1 analysis to assess mitochondrial membrane potential. Following treatment with BB and cisplatin, the cells were stained with DCFH, MitoSOX, and JC-1. Following cisplatin treatment, a noticeable rise in the number of cells staining positively for DCFH, MitoSOX, and JC-1 indicators was detected when compared with the untreated control group. Notably, pre-treatment with BB significantly decreased the number of cells showing positivity for DCFH, MitoSOX, and JC-1 in HEI-OC1 cells (Figures 5A–G). Furthermore, the expression of MitoSOX in cochlear explants was evaluated in a similar fashion. In line with the cell-based results, cisplatin administration led to an elevation in ROS levels in cochlear hair cells, while BB pre-treatment mitigated ROS production (Figures 5H–I). In summary, the findings demonstrate that BB successfully diminishes the production of ROS triggered by cisplatin in both the HEI-OC1 cell line and cochlear explant cultures.

## 3.6 Promoting folate synthesis may be one of the mechanisms by which berberine antagonizes cisplatin ototoxicity

To further investigate how BB antagonizes cisplatin-induced ototoxicity, an RNA sequencing analysis was conducted on HEI-OC1 cells following treatment with BB. The data indicated that treatment with BB led to the upregulation of 226 genes and the downregulation of 65 genes, in contrast to the gene expression levels observed in the control group (Figures 6A–C). Pathway enrichment analysis based on the Kyoto Encyclopedia of Genes and Genomes

10.3389/fphar.2024.1496917

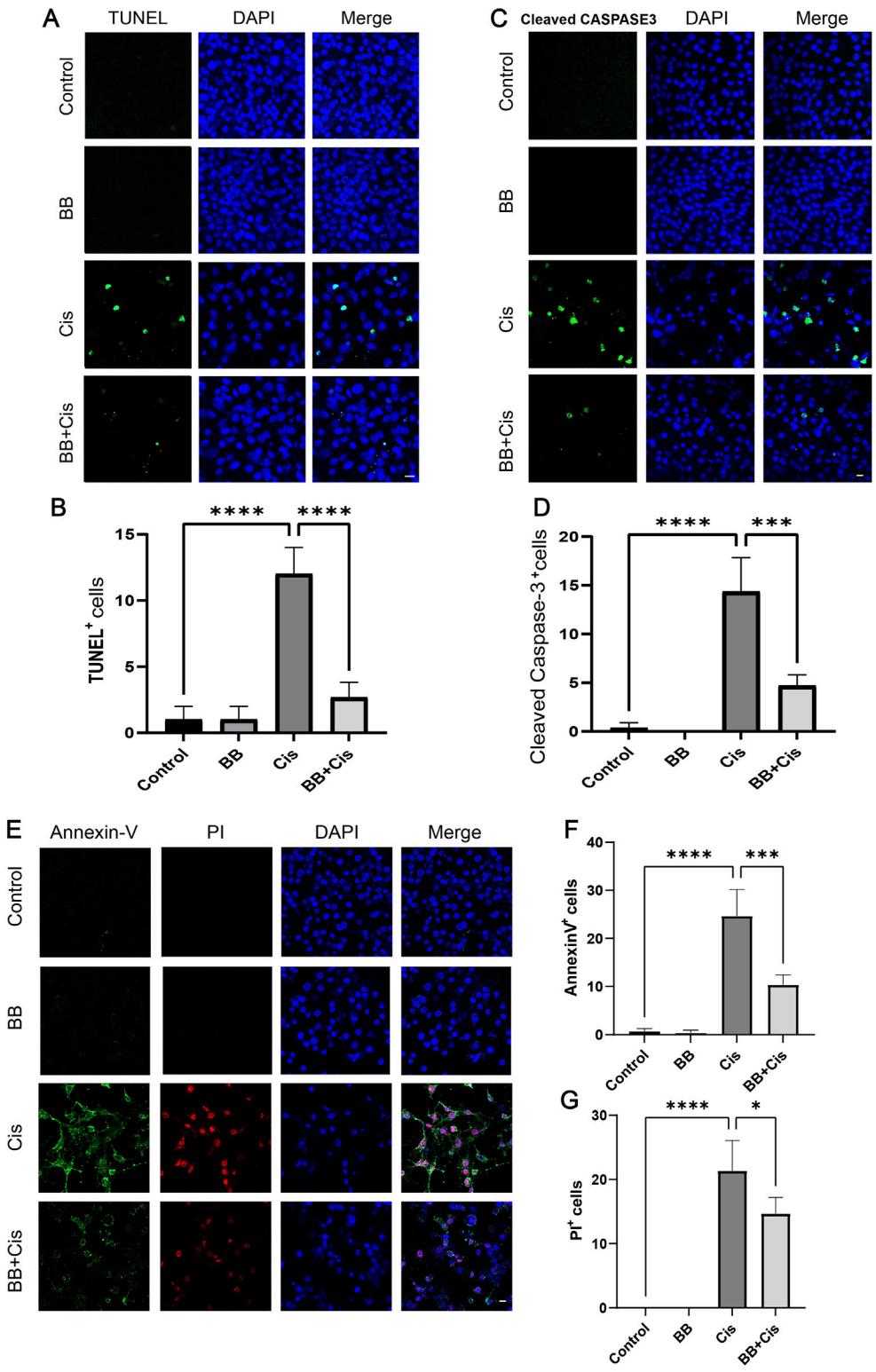


FIGURE 3
BB reduces apoptosis of HEI-OC1 cells triggered by cisplatin. **(A)** TUNEL assay shows BB's influence on apoptosis in cisplatin-treated HEI-OC1 cells. Scale bar: 20 μm. **(B)** Quantification of TUNEL-positive cells in **(A)** (n = 3). **(C)** Cleaved Caspase-3 immunofluorescence indicates BB's modulation of the apoptotic response to cisplatin. Scale bar: 20 μm. **(D)** Numerical count of Cleaved Caspase-3-positive cells in **(C)** (n = 3). **(E)** Annexin V-PI staining highlights BB's effect on apoptosis initiated by cisplatin. Scale bar: 20 μm. **(F, G)** Quantification of Annexin V-positive and PI-positive cells in **(E)** (n = 3). $^{*}P < 0.05$, $^{***}P < 0.001$, $^{****}P < 0.0001$. BB: Berberrubine; Cis: Cisplatin.

10.3389/fphar.2024.1496917

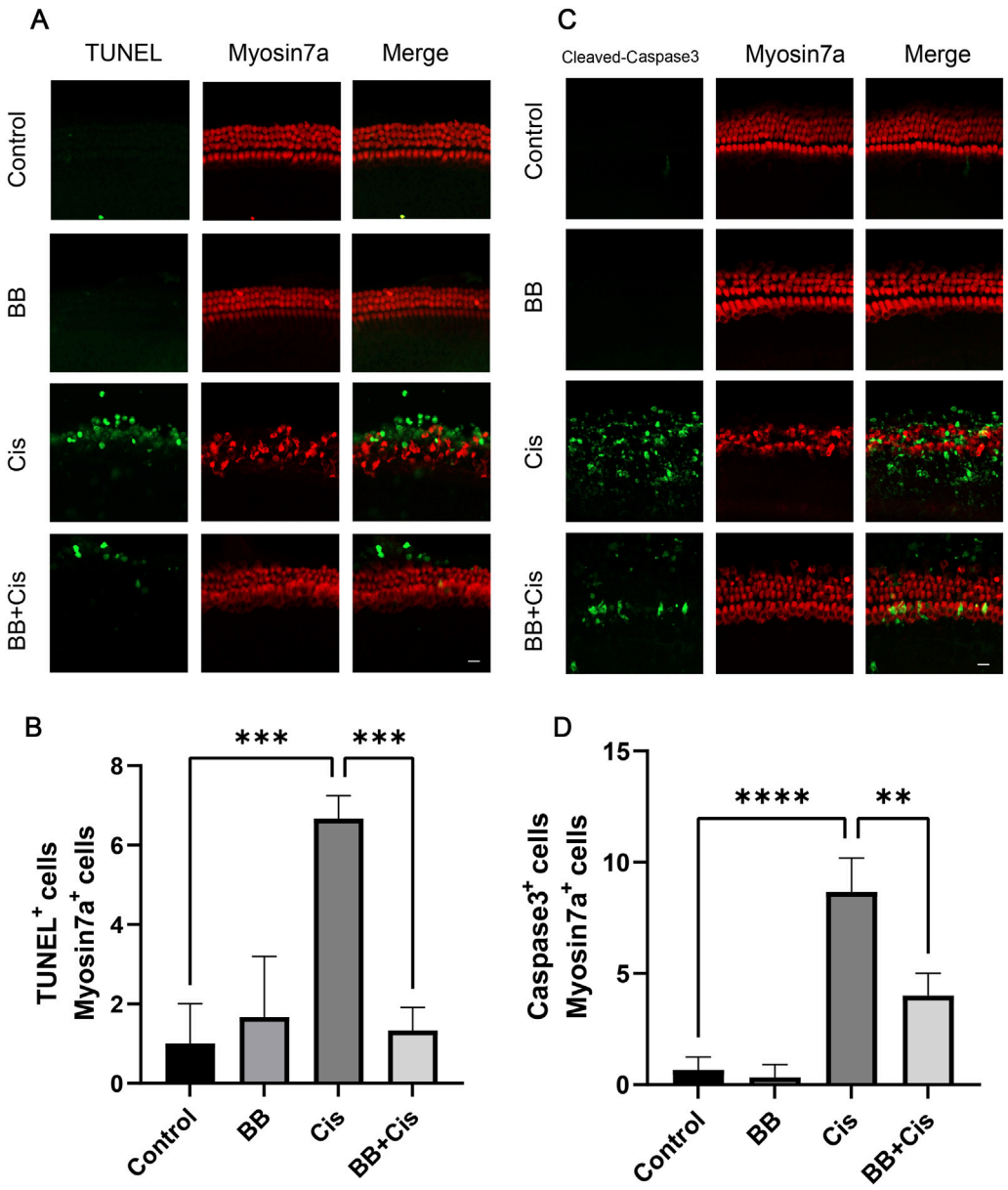


FIGURE 4
BB mitigates the apoptosis of hair cells in cochlear explants induced by cisplatin. **(A)** Midsection cochlear hair cells were pre-treated with BB and then exposed to cisplatin, followed by TUNEL staining. Scale bar: 20 μm. **(B)** Count of TUNEL and myosin 7a double-positive cells in **(A)** (n = 3). **(C)** Cochlear hair cells in the middle turn were stained for Cleaved Caspase-3 after BB pre-treatment and cisplatin exposure. Scale bar: 20 μm. **(D)** Numerical analysis of Cleaved Caspase-3 and myosin 7a double-positive cells in **(C)** (n = 3). $^{**}P < 0.01$, $^{***}P < 0.001$, $^{****}P < 0.0001$. BB: Berberrubine; Cis: Cisplatin.

(KEGG) database identified that one of the major pathways affected by BB treatment is the promotion of folate synthesis (Figure 6D). Following up with Gene Set Enrichment Analysis (GSEA), it was found that the pathway associated with folate biosynthesis was significantly enriched in the group treated with BB when compared to the untreated control group (Figure 6E). Notably, genes involved in folate biosynthesis and metabolism such as Ccnd2, Reln, Pgf, Mylk3, Ppplr12c, and Thbsl were significantly altered in the BB treatment group. Real-time fluorescence quantitative PCR further validated the changes in mRNA expression related to folate biosynthesis in the BB treatment group compared to the control group (Figure 6F). The expression of Ccnd2, Reln, Pgf, and Ppplr12 genes increased, while the expression of Mylk3 and Thbsl genes decreased. The overall effect of these changes is to promote folate synthesis. The collective results imply that Promoting folate synthesis may be one of the mechanisms by which berberine antagonizes cisplatin ototoxicity.

## 4 Discussion

Although cisplatin is a prevalent chemotherapy drug for malignancies, its associated ototoxicity poses a significant issue, affecting patients' quality of life and potentially necessitating the use

10.3389/fphar.2024.1496917

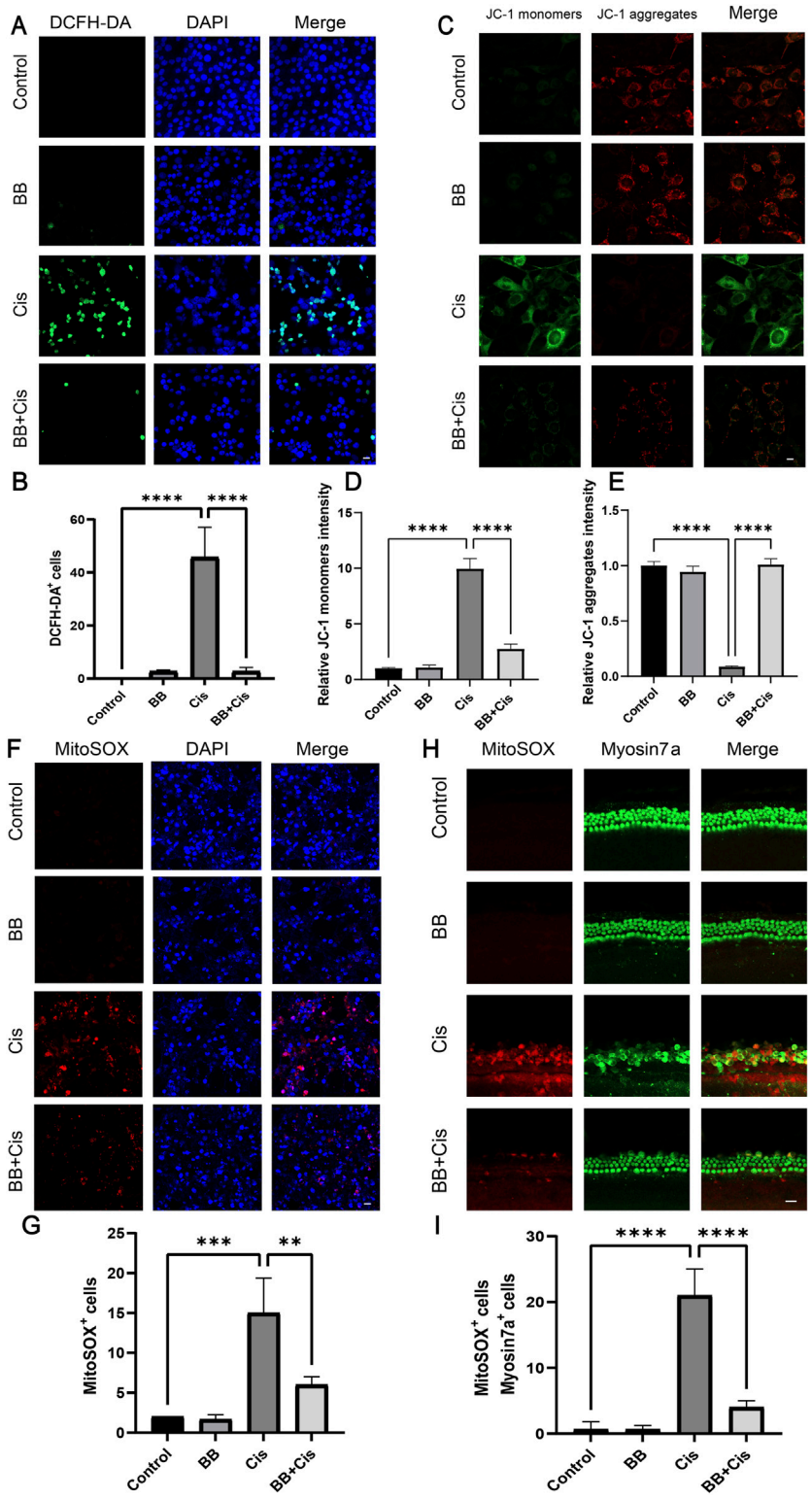


FIGURE 5
BB reduces cisplatin-induced oxidative stress response. **(A)** DCFH-DA fluorescence labeling of different experimental groups. Scale bar: 20 μm. **(B)** Numerical assessment of fluorescence intensity in **(A)**. **(C)** JC-1 staining of HEI-OC1 cells. Scale bar: 20 μm. **(D, E)** Numerical evaluation of JC-1 fluorescence in **(C)**. **(F)** MitoSOX staining for mitochondrial superoxide detection. Scale bar: 20 μm. **(G)** Numerical analysis of MitoSOX fluorescence in **(F)**. **(H)** MitoSOX staining in cochlea's middle turns from various groups. Scale bar: 20 μm. **(I)** Numerical evaluation of data in **(H)**. $^{**}P < 0.01$, $^{***}P < 0.001$, $^{****}P < 0.0001$. BB: Berberrubine; Cis: Cisplatin.

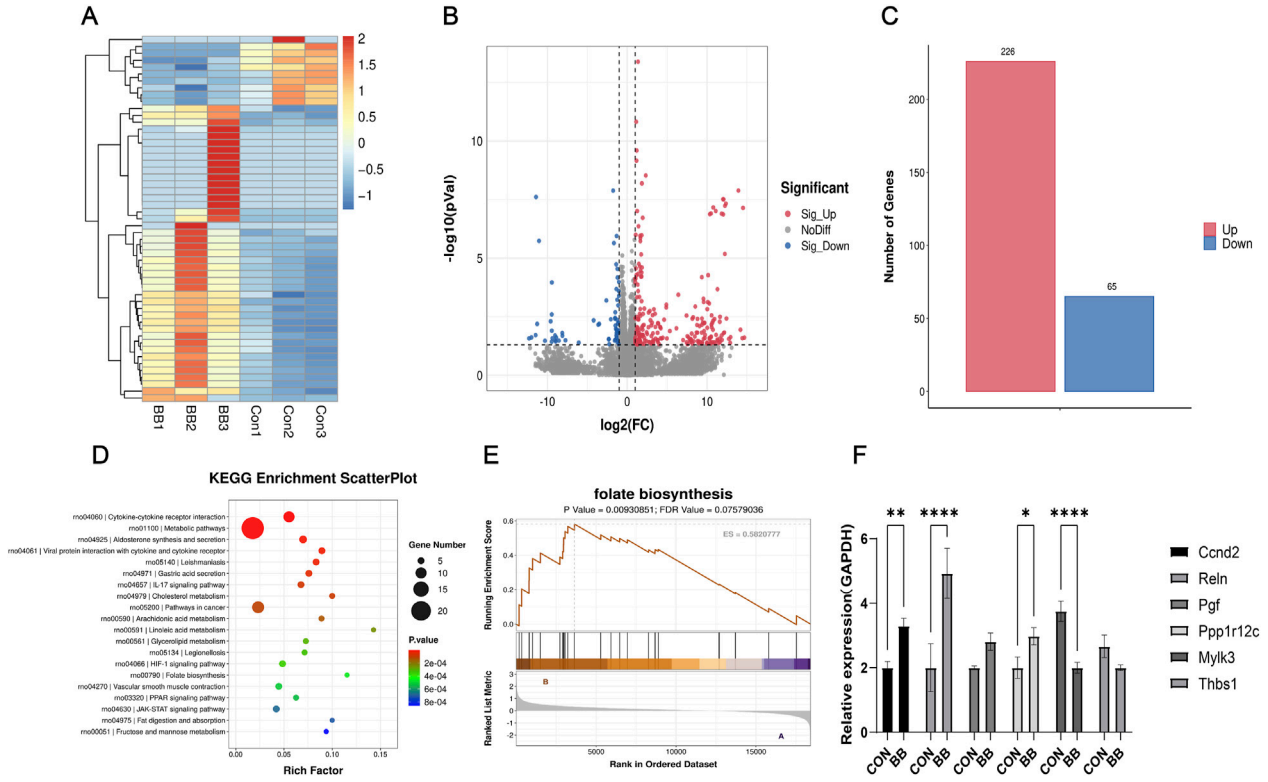


FIGURE 6
BB antagonizes cisplatin ototoxicity by promoting folate synthesis. **(A)** Heat map of genes with substantial expression changes post BB treatment. **(B)** Scatter plot of genes showing notable variance in expression post BB treatment. **(C)** Analysis of upregulated and downregulated gene quantities post BB treatment. **(D)** KEGG pathway enrichment of the most notably altered pathways post BB treatment. **(E)** Gene Set Enrichment Analysis (GSEA) contrasting gene expression in folate biosynthesis pathways between control and BB-treated groups. **(F)** qRT-PCR evaluation of gene expression levels in the folate biosynthesis pathway (n = 3). Statistical significance: $^{*}P < 0.05$, $^{**}P < 0.01$, $^{****}P < 0.0001$. BB: Berberrubine; Cis: Cisplatin.

of hearing aids or other supportive measures. Oxidative stress, primarily from overproduction of Reactive oxygen species (ROS) are central to cisplatin-induced ototoxicity, undermining the cochlea's natural defenses (Ramkumar et al., 2021; Tan et al., 2022; Li et al., 2023b). Cisplatin also provokes an inflammatory response characterized by the release of cytokines TNF-α, IL-1β, and IL-6 (Ramkumar et al., 2021; Zhang et al., 2020; Qiao et al., 2024). This response is amplified by heightened levels of COX-2, iNOS, and TNF-α, which are stimulated by ROS through STAT1 activation and NOX3 enzyme induction (Altun et al., 2014; Estfanous et al., 2020; Martins et al., 2017; Shalkami et al., 2018; Umugire et al., 2023; Yin et al., 2023). Furthermore, cisplatin's interaction with DNA leads to cytotoxic cross-linking, triggering apoptosis through increased Bax expression, mitochondrial permeability changes, and the activation of caspase-9 and caspase-3 (He et al., 2022; Umugire et al., 2023; Sheth et al., 2017; Wang et al., 2023). The complexity of these mechanisms underscores the need for continued research into effective strategies to combat cisplatin ototoxicity.

In our research, we exhibited the protective capabilities of BB against cisplatin-induced hearing damage and investigated the potential mechanisms behind it. Our findings indicated that BB reduces the detrimental effects on hair cells and the incidence of apoptosis induced by cisplatin, as observed in both the HEI-OC1 cell line cultures and the cochlear explants *in vitro*. Furthermore, BB was shown to attenuate the accumulation of reactive oxygen species (ROS) and the damage to mitochondria within these cells. To further authenticate BB's defense against cisplatin-induced hearing damage, we conducted mouse experiments using a cisplatin-induced injury model. In our study, oral administration of BB to mice effectively protected them from cisplatin-induced hearing loss, as evidenced by reduced hearing thresholds across a range of frequencies. However, this protective effect was not observed at the 32 kHz frequency. The lack of protection at this high frequency may be due to the greater severity of cisplatin's damage at higher frequencies, which could result in irreversible harm that BB is unable to counteract. Our immunofluorescence tests confirmed BB's protective role on hair cells in the cochlea's basal turn basement membrane. Nonetheless, the intricate physiological environment of animals could allow cisplatin to affect other unidentified critical structures. These unidentified effects might limit BB's ability to prevent high-frequency hearing loss, even when hair cell survival is improved. In summary, while BB demonstrates promise in mitigating cisplatin-induced ototoxicity, its protective effects are not absolute, particularly at the highest sound frequencies. Further research is needed to understand the full scope of cisplatin's impact on the auditory system and to explore additional strategies that may enhance BB's protective capabilities.

To further investigate the protective mechanisms of BB against cisplatin-induced hearing loss, we conducted RNA sequencing analysis. This analysis revealed that a total of 226 genes were upregulated and 65 genes were downregulated in HEI-OC1 cells

following BB treatment. KEGG and GSEA analysis showed significant enrichment of genes promoting folate synthesis pathway. Genes such as Ccnd2, Reln, Pgf, Mylk3, Ppplr12c, and Thbsl showed significant changes in expression. The overall effect of these gene expression changes is to upregulate the folate synthesis signaling pathway. Our experimental findings suggest that BB facilitates folate biosynthesis in organisms. Folate, a vital vitamin in the human body, possesses a wide array of physiological functions. Various studies have reported that folate contributes to the development of the nervous system, metabolism, epilepsy and depression management, cardiovascular health, pregnancy-related conditions, and cancer prevention (Balashova et al., 2018; Liwinski and Lang, 2023; Otsu et al., 2023; Ponziani et al., 2012; Shulpekova et al., 2021; Yang et al., 2012). A multitude of sources assert that folic acid plays a significant role in the prevention and management of hearing impairments. This includes sensorineural hearing loss that occurs with aging and cases of sudden sensorineural hearing loss with neurological origins (Kabagambe et al., 2018; Kose Celebi et al., 2023; Kundu et al., 2012). The protective mechanisms likely involve mitigating oxidative stress responses, inhibiting apoptosis, and promoting angiogenesis in the inner ear (Martínez-Vega et al., 2015; Martínez-Vega et al., 2016; Uchida et al., 2011). Additionally, there is clear evidence in the literatures stating that folate can prevent and treat cisplatin-induced ototoxicity (Tanyeli et al., 2019). Animal studies have corroborated this, aligning with our research findings. Therefore, it is probable that BB's antagonistic effect on cisplatin ototoxicity is mediated by enhancing the biosynthesis of folate substances.

Our study has several limitations. Firstly, we could have further optimized the selection of cisplatin and BB concentrations and doses. We selected these concentrations in cell experiments using different concentration gradients, which was a scientifically reliable approach. However, in the *in vitro* cochlear explant experiments, we relied on experience and logical deduction, increasing drug concentrations due to the greater tolerance of tissues compared to cells. Although the experiment achieved significant effects, there may still be an optimal drug concentration. For subsequent animal experiments, we referred to existing literatures on BB, but found no studies specifically on the ear. The optimal concentration of BB may vary across tissues, organs, and diseases. Our examination of BB's toxicity revealed it to be harmless at low and moderate levels but harmful at high levels, emphasizing the importance of careful BB concentration regulation in practical use. Therefore, further optimization of drug concentrations is necessary. Secondly, cisplatin ototoxicity damages a variety of tissues and structures, such as hair cells, vascular striae, spiral ganglia, and synapses (Wang et al., 2023; Gu et al., 2022; Waissbluth et al., 2022). Our research primarily focused on examining how BB can protect hair cells within the organ of Corti. We did not investigate and observe other structures, such as supportive cells, spiral ganglia, and vascular striae, while our findings provide valuable insights into the protective effects of BB on hair cells, they are limited in scope and do not encompass the full range of ototoxic effects of cisplatin on the auditory system. Further research is needed to explore the impact of BB on other affected structures and to gain a more comprehensive understanding of its protective mechanisms. Finally, we identified differentially expressed genes after BB treatment through RNA sequencing and performed qRT-PCR to assess mRNA expression at the cellular level. Our study's scope was limited, and further validation at different tissue and animal levels is necessary. We can also conduct Western blotting experiments to validate the results at the protein expression level, so that our conclusions will be more scientifically robust and persuasive.

## 5 Conclusion

It effectively showcases the protective benefits of BB against hearing damage induced by cisplatin by mechanisms involving the enhancement of folate biosynthesis, the reduction of ROS generation, and the mitigation of apoptosis. This concept may offer a novel approach to mitigating the ototoxic effects of cisplatin in a clinical setting.

## Data availability statement

The original contributions presented in the study are included in the article/supplementary material, further inquiries can be directed to the corresponding author.

## Ethics statement

The animal study was approved by the Animal Care and Use Committee of Southeast University. The study was conducted in accordance with the local legislation and institutional requirements.

## Author contributions

ZM: Conceptualization, Data curation, Methodology, Software, Writing–original draft, Writing–review and editing. DC: Conceptualization, Data curation, Methodology, Validation, Writing–review and editing. XD: Supervision, Writing–review and editing. CS: Conceptualization, Funding acquisition, Methodology, Project administration, Resources, Supervision, Validation, Visualization, Writing–review and editing.

## Funding

The author(s) declare that no financial support was received for the research, authorship, and/or publication of this article.

## Acknowledgments

Thank you to Professor Renjie Chai's laboratory teachers and classmates from the School of Life Sciences, Southeast University for their help.

## Conflict of interest

The authors declare that the research was conducted in the absence of any commercial or financial relationships that could be construed as a potential conflict of interest.

## Publisher's note



## References

Albera, R., Lacilla, M., Piumetto, E., and Canale, A. (2010). Noise-induced hearing loss evolution: influence of age and exposure to noise. *Eur. Arch. Otorhinolaryngol.* 267 (5), 665–671. doi:10.1007/s00405-009-1096-3

Altun, Z., Olgun, Y., Ercetin, P., Aktas, S., Kirkim, G., Serbetcioglu, B., et al. (2014). Protective effect of acetyl-l-carnitine against cisplatin ototoxicity: role of apoptosis-related genes and pro-inflammatory cytokines. *Cell Prolif.* 47 (1), 72–80. doi:10.1111/cpr.12080

Balashova, O. A., Visina, O., and Borodinsky, L. N. (2018). Folate action in nervous system development and disease. *Dev. Neurobiol.* 78 (4), 391–402. doi:10.1002/dneu.22579

Boulikas, T., and Vougiouka, M. (2003). Cisplatin and platinum drugs at the molecular level. (Review). *Oncol. Rep.* 10 (6), 1663–1682. doi:10.3892/or.10.6.1663

Callejo, A., Durochat, A., Bressieux, S., Saleur, A., Chabbert, C., Domènech Juan, I., et al. (2017). Dose-dependent cochlear and vestibular toxicity of trans-tympanic cisplatin in the rat. *Neurotoxicology* 60, 1–9. doi:10.1016/j.neuro.2017.02.007

Callejo, A., Sedó-Cabezón, L., Juan, I. D., and Llorens, J. (2015). Cisplatin-induced ototoxicity: effects, mechanisms and protection strategies. *Toxics* 3 (3), 268–293. doi:10.3390/toxics3030268

Crona, D. J., Faso, A., Nishijima, T. F., McGraw, K. A., Galsky, M. D., and Milowsky, M. I. (2017). A systematic review of strategies to prevent cisplatin-induced nephrotoxicity. *Oncologist* 22 (5), 609–619. doi:10.1634/theoncologist.2016-0319

Dasari, S., and Tchounwou, P. B. (2014). Cisplatin in cancer therapy: molecular mechanisms of action. *Eur. J. Pharmacol.* 740, 364–378. doi:10.1016/j.ejphar.2014.07.025

Estfanous, R. S., Elseady, W. S., Kabel, A. M., and Abd Ellatif, R. A. (2020). Amelioration of cisplatin-induced ototoxicity in rats by L-arginine: the role of nitric oxide, transforming growth factor beta 1 and Nrf2/HO-1 pathway. *Asian Pac J. Cancer Prev.* 21 (7), 2155–2162. doi:10.31557/APJCP.2020.21.7.2155

Fetoni, A. R., Paciello, F., and Troiani, D. (2022). Cisplatin chemotherapy and cochlear damage: otoprotective and chemosensitization properties of polyphenols. *Antioxid. Redox Signal* 36 (16-18), 1229–1245. doi:10.1089/ars.2021.0183

Gong, R., Hu, X., Gong, C., Long, M., Han, R., Zhou, L., et al. (2018). Hearing loss prevalence and risk factors among older adults in China. *Int. J. Audiol.* 57 (5), 354–359. doi:10.1080/14992027.2017.1423404

Gu, J., Tong, L., Lin, X., Chen, Y., Wu, H., Wang, X., et al. (2022). The disruption and hyperpermeability of blood-labyrinth barrier mediates cisplatin-induced ototoxicity. *Toxicol. Lett.* 354, 56–64. doi:10.1016/j.toxlet.2021.10.015

Guidotti, L., Tomassi, E., Marracci, S., Lai, M., Lapi, D., Pesi, R., et al. (2023). Effects of nutraceuticals on cisplatin-induced cytotoxicity in HEI-OC1 cells. *Int. J. Mol. Sci.* 24 (24), 17416. doi:10.3390/ijms242417416

Guo, X., Bai, X., Li, L., Li, J., and Wang, H. (2018). Forskolin protects against cisplatin-induced ototoxicity by inhibiting apoptosis and ROS production. *Biomed. Pharmacother.* 99, 530–536. doi:10.1016/j.biopha.2018.01.080

He, Y., Zheng, Z., Liu, C., Li, W., Zhao, L., Nie, G., et al. (2022). Inhibiting DNA methylation alleviates cisplatin-induced hearing loss by decreasing oxidative stress-induced mitochondria-dependent apoptosis via the LRP1-PI3K/AKT pathway. *Acta Pharm. Sin. B* 12 (3), 1305–1321. doi:10.1016/j.apsb.2021.11.002

Jin, Y., Khadka, D. B., and Cho, W. J. (2016). Pharmacological effects of berberine and its derivatives: a patent update. *Expert Opin. Ther. Pat.* 26 (2), 229–243. doi:10.1517/13543776.2016.1118060

Kabagambe, E. K., Lipworth, L., Labadie, R. F., Hood, L. J., and Francis, D. O. (2018). Erythrocyte folate, serum vitamin B12, and hearing loss in the 2003-2004 national health and nutrition examination survey (NHANES). *Eur. J. Clin. Nutr.* 72 (5), 720–727. doi:10.1038/s41430-018-0101-6

Kose Celebi, N., Deveci, H. S., Kulekci Ozturk, S., and Aslan Dundar, T. (2023). Clinical role of vitamin D, vitamin B12, folate levels and hematological parameters in patients with sudden sensorineural hearing loss. *Acta Otolaryngol.* 143 (7), 596–601. doi:10.1080/00016489.2023.2235398

Kros, C. J., and Steyger, P. S. (2019). Aminoglycoside- and cisplatin-induced ototoxicity: mechanisms and otoprotective strategies. *Cold Spring Harb. Perspect. Med.* 9 (11), A033548. doi:10.1101/cshperspect.a033548

Kundu, S., Munjal, C., Tyagi, N., Sen, U., Tyagi, A. C., and Tyagi, S. C. (2012). Folic acid improves inner ear vascularization in hyperhomocysteinemic mice. *Hear Res.* 284 (1-2), 42–51. doi:10.1016/j.heares.2011.12.006

Li, C., Wang, X., Qiao, X., Fan, L., Zhu, H., Chen, Y., et al. (2023b). 5,7-Dihydroxy-4-methylcoumarin modulates the JNK/FoxO1 signaling pathway to attenuate cisplatin-induced ototoxicity by suppressing oxidative stress and apoptosis *in vitro*. *Biochim. Biophys. Acta Mol. Cell Res.* 1870 (4), 119437. doi:10.1016/j.bbamcr.2023.119437

Li, Y., Zhang, T., Song, Q., Gao, D., Li, Y., Jie, H., et al. (2023a). Cisplatin ototoxicity mechanism and antagonistic intervention strategy: a scope review. *Front. Cell Neurosci.* 17, 1197051. doi:10.3389/fncel.2023.1197051

Li, Y. H., Li, Y., Yang, P., Kong, W. J., You, X. F., Ren, G., et al. (2010). Design, synthesis, and cholesterol-lowering efficacy for prodrugs of berberrubine. *Bioorg Med. Chem.* 18 (17), 6422–6428. doi:10.1016/j.bmc.2010.06.106

Liu, X. Z., and Yan, D. (2007). Ageing and hearing loss. *J. Pathol.* 211 (2), 188–197. doi:10.1002/path.2102

Liwinski, T., and Lang, U. E. (2023). Folate and its significance in depressive disorders and suicidality: a comprehensive narrative review. *Nutrients* 15 (17), 3859. doi:10.3390/nu15173859

Makovec, T. (2019). Cisplatin and beyond: molecular mechanisms of action and drug resistance development in cancer chemotherapy. *Radiol. Oncol.* 53 (2), 148–158. doi:10.2478/raon-2019-0018

Martínez-Vega, R., Garrido, F., Partearroyo, T., Cediel, R., Zeisel, S. H., Martínez-Álvarez, C., et al. (2015). Folic acid deficiency induces premature hearing loss through mechanisms involving cochlear oxidative stress and impairment of homocysteine metabolism. *Faseb J.* 29 (2), 418–432. doi:10.1096/fj.14-259283

Martínez-Vega, R., Murillo-Cuesta, S., Partearroyo, T., Varela-Moreiras, G., Varela-Nieto, I., and Pajares, M. A. (2016). Long-term dietary folate deficiency accelerates progressive hearing loss on CBA/Ca mice. *Front. Aging Neurosci.* 8, 209. doi:10.3389/fnagi.2016.00209

Martins, M. J. B., Batista, A. M. A., Brito, Y. N. F., Soares, P. M. G., Martins, C. D. S., Ribeiro, R. A., et al. (2017). Effect of remote ischemic preconditioning on systemic toxicity and ototoxicity induced by cisplatin in rats: role of TNF-α and nitric oxide. *ORL J. Otorhinolaryngol. Relat. Spec.* 79 (6), 336–346. doi:10.1159/000485514

Otsu, Y., Ae, R., and Kuwabara, M. (2023). Folate and cardiovascular disease. *Hypertens. Res.* 46 (7), 1816–1818. doi:10.1038/s41440-023-01307-w

Ponziani, F. R., Cazzato, I. A., Danese, S., Fagiuoli, S., Gionchetti, P., Annicchiarico, B. E., et al. (2012). Folate in gastrointestinal health and disease. *Eur. Rev. Med. Pharmacol. Sci.* 16 (3), 376–385. doi:10.1016/j.eurrev.2012.02.001

Qiao, X., Li, W., Zheng, Z., Liu, C., Zhao, L., He, Y., et al. (2024). Inhibition of the HMGB1/RAGE axis protects against cisplatin-induced ototoxicity via suppression of inflammation and oxidative stress. *Int. J. Biol. Sci.* 20 (2), 784–800. doi:10.7150/ijbs.82003

Ramkumar, V., Mukherjea, D., Dhukhwa, A., and Rybak, L. P. (2021). Oxidative stress and inflammation caused by cisplatin ototoxicity. *Antioxidants (Basel)* 10 (12), 1919. doi:10.3390/antiox10121919

Romani, A. M. P. (2022). Cisplatin in cancer treatment. *Biochem. Pharmacol.* 206, 115323. doi:10.1016/j.bcp.2022.115323

Shalkami, A. S., Hassan, M. I. A., and Abd El-Ghany, A. A. (2018). Perindopril regulates the inflammatory mediators, NF-κB/TNF-α/IL-6, and apoptosis in cisplatin-induced renal dysfunction. *Naunyn Schmiedeb. Arch. Pharmacol.* 391 (11), 1247–1255. doi:10.1007/s00210-018-1550-0

Sheth, S., Mukherjea, D., Rybak, L. P., and Ramkumar, V. (2017). Mechanisms of cisplatin-induced ototoxicity and otoprotection. *Front. Cell Neurosci.* 11, 338. doi:10.3389/fncel.2017.00338

Shulpekova, Y., Nechaev, V., Kardasheva, S., Sedova, A., Kurbatova, A., Bueverova, E., et al. (2021). The concept of folic acid in health and disease. *Molecules* 26 (12), 3731. doi:10.3390/molecules26123731

Song, D., Hao, J., and Fan, D. (2020). Biological properties and clinical applications of berberine. *Front. Med.* 14 (5), 564–582. doi:10.1007/s11684-019-0724-6

Steyger, P. S. (2021). Mechanisms of ototoxicity and otoprotection. *Otolaryngol. Clin. North Am.* 54 (6), 1101–1115. doi:10.1016/j.otc.2021.08.007

Sun, R., Kong, B., Yang, N., Cao, B., Feng, D., Yu, X., et al. (2021). The hypoglycemic effect of berberine and berberrubine involves modulation of intestinal farnesoid X receptor signaling pathway and inhibition of hepatic gluconeogenesis. *Drug Metab. Dispos.* 49 (3), 276–286. doi:10.1124/dmd.120.000215

Tan, M., Toplu, Y., Varan, E., Sapmaz, E., Özhan, O., Parlakpınar, H., et al. (2022). The effect of genistein on cisplatin induced ototoxicity and oxidative stress. *Braz J. Otorhinolaryngol.* 88 (1), 105–111. doi:10.1016/j.bjorl.2021.07.001

Tang, D., Wang, X., Wu, J., Li, Y., Li, C., Qiao, X., et al. (2024). Cinchonine and cinchonidine alleviate cisplatin-induced ototoxicity by regulating PI3K-AKT signaling. *CNS Neurosci. Ther.* 30 (2), e14403. doi:10.1111/cns.14403

Tanyeli, T. T., Karadaş, H., Akyıldız, İ., Gökdoğan, O., Sönmez, Ç., Çavuş, M. E., et al. (2019). Effect of folic acid on cisplatin-induced ototoxicity: a functional and morphological study. *J. Int. Adv. Otol.* 15 (2), 237–246. doi:10.5152/iao.2019.6208

Uchida, Y., Sugiura, S., Ando, F., Nakashima, T., and Shimokata, H. (2011). Hearing impairment risk and interaction of folate metabolism related gene polymorphisms in an aging study. *BMC Med. Genet.* 12, 35. doi:10.1186/1471-2350-12-35

Umugire, A., Nam, Y. S., Nam, Y. E., Choi, Y. M., Choi, S. M., Lee, S., et al. (2023). Protective effect of avenanthramide-C on auditory hair cells against oxidative stress, inflammatory cytokines, and DNA damage in cisplatin-induced ototoxicity. *Int. J. Mol. Sci.* 24 (3), 2947. doi:10.3390/ijms24032947

Waissbluth, S., Maass, J. C., Sanchez, H. A., and Martínez, A. D. (2022). Supporting cells and their potential roles in cisplatin-induced ototoxicity. *Front. Neurosci.* 16, 867034. doi:10.3389/fnins.2022.867034

Wang, K., Feng, X., Chai, L., Cao, S., and Qiu, F. (2017). The metabolism of berberine and its contribution to the pharmacological effects. *Drug Metab. Rev.* 49 (2), 139–157. doi:10.1080/03602532.2017.1306544

Wang, K., Rao, J., Zhang, T., Gao, Q., Zhang, J., Guang, C., et al. (2020). Metabolic activation and covalent protein binding of berberrubine: insight into the underlying mechanism related to its hepatotoxicity. *Drug Des. Devel Ther.* 14, 4423–4438. doi:10.2147/DDDT.S274627

Wang, X., Zhou, Y., Wang, D., Wang, Y., Zhou, Z., Ma, X., et al. (2023). Cisplatin-induced ototoxicity: from signaling network to therapeutic targets. *Biomed. Pharmacother.* 157, 114045. doi:10.1016/j.biopha.2022.114045

Yang, J., Vlashi, E., and Low, P. (2012). Folate-linked drugs for the treatment of cancer and inflammatory diseases. *Subcell. Biochem.* 56, 163–179. doi:10.1007/978-94-007-2199-9_9

Yin, H., Sun, Y., Ya, B., Guo, Y., Zhao, H., Zhang, L., et al. (2023). Apelin-13 protects against cisplatin-induced ototoxicity by inhibiting apoptosis and regulating STAT1 and STAT3. *Arch. Toxicol.* 97 (9), 2477–2493. doi:10.1007/s00204-023-03544-x

Zhang, N., Cai, J., Xu, L., Wang, H., and Liu, W. (2020). Cisplatin-induced stria vascularis damage is associated with inflammation and fibrosis. *Neural Plast.* 2020, 8851525. doi:10.1155/2020/8851525

frontiers | Frontiers in Pharmacology

TYPE Opinion
PUBLISHED 05 February 2025
DOI 10.3389/fphar.2025.1500955



OPEN ACCESS

EDITED BY
Qi Liang,
Air Force Medical University, China

REVIEWED BY
Yogan Khatri,
Cayman Chemical, United States

*CORRESPONDENCE
Mengquan Yang,
mqyang@sibs.ac.cn

RECEIVED 24 September 2024
ACCEPTED 20 January 2025
PUBLISHED 05 February 2025

CITATION
Yin Q, Zhu Z and Yang M (2025) Biosynthesis of plant neuroactive alkaloids treating Alzheimer's disease.
*Front. Pharmacol.* 16:1500955.
doi: 10.3389/fphar.2025.1500955



# Biosynthesis of plant neuroactive alkaloids treating Alzheimer's disease

Quanyu Yin, Zhengkang Zhu and Mengquan Yang*

National Tobacco Cultivation, Physiology and Biochemistry Research Center, Flavors and Fragrance Engineering and Technology Research Center of Henan Province, College of Tobacco Science, Henan Agricultural University, Zhengzhou, Henan, China

KEYWORDS

**Alzheimer's disease, biosynthesis, alkaloid, huperzine A, galantamine**

## Introduction

Alzheimer's disease (AD) is a debilitating neurodegenerative disorder characterized by cognitive decline and memory impairment. With increasing global prevalence, the need for effective therapeutic interventions is critical. Among the currently approved treatments, acetylcholinesterase inhibitors (AChEIs) like huperzine A and galantamine stand out due to their neuroprotective roles. These plant-derived alkaloids have demonstrated significant efficacy in alleviating symptoms by increasing acetylcholine levels in the brain.

While numerous other plant alkaloids exhibit varying degrees of neuroactive properties, huperzine A and galantamine remain the only plant-derived alkaloids currently approved and marketed as specific treatments for AD and other neurodegenerative diseases. For example, alkaloids such as berberine (from *Berberis* species) and rhynchophylline (from *Uncaria rhynchophylla*) have shown potential in targeting amyloid-beta (Aβ) aggregation, oxidative stress, and tau hyperphosphorylation. Similarly, harmine has demonstrated the ability to inhibit tau hyperphosphorylation through dual inhibition of glycogen synthase kinase-3 beta (GSK-3β) and dual specificity tyrosine phosphorylation regulated kinase 1A (DYRK1A). However, these metabolites have not yet advanced to clinical applications (Ng et al., 2015; Rezaul Islam et al., 2024).

The elucidation of the biosynthetic pathways of huperzine A and galantamine marks a significant advancement in understanding plant biochemistry and specialized metabolism. It not only advances our understanding of plant-derived neuroactive metabolites but also provides opportunities for sustainable and scalable production through synthetic biology approaches. By leveraging this approach, researchers can reconstruct the biosynthetic pathways of plant-derived natural products in microbial or plant systems, facilitating efficient production and reducing the reliance on native plant sources for these valuable compounds (Liu et al., 2023; Zhang et al., 2023; Bai et al., 2024; Teng et al., 2024). This opinion highlights the implications of these discoveries for future research and application in neurodegenerative disease treatment.

## Huperzine A: a lycopodium alkaloid

Huperzine A, derived from *Huperzia serrata* (Lycopodiaceae), is a well-known AChEI that has been widely used in traditional Chinese medicine (Ma and Gang, 2004; Yang et al., 2017; Wang et al., 2020; Zhang et al., 2024). The elucidation of the biosynthetic pathway of huperzine A has provided crucial insights into the formation of Lycopodium alkaloids and uncovered numerous enzymes with novel functions (Li et al., 2022; Ushimaru and Abe,

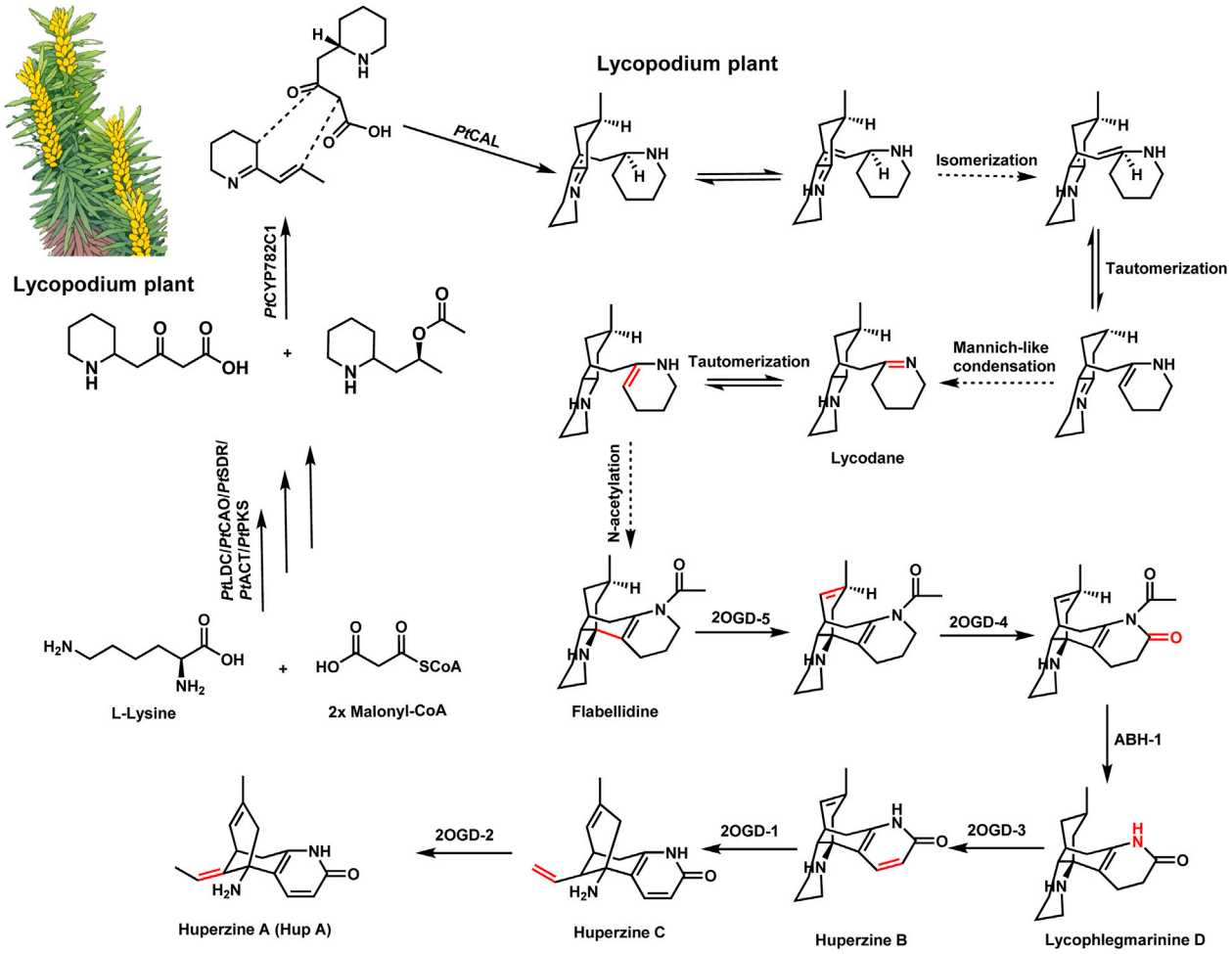


FIGURE 1
Schematic illustration of the biosynthesis of lycopodium alkaloids. Biosynthetic pathway of huperzine A (HupA). PtLDC, lycine decarboxylase; PtCAO, copper amine oxidase; PtPKS, piperidyl ketide synthase; PtSDR, short-chain dehydrogenase/reductase; PtCAT, acetyltransferase; PtCAL, alpha-carbonic anhydrases-like; 2OGD-1, 2-oxoglutarate-dependent dioxygenase 1; 2OGD-2, 2-oxoglutarate-dependent dioxygenase 2; 2OGD-3, 2-oxoglutarate-dependent dioxygenase 3; 2OGD-4, 2-oxoglutarate-dependent dioxygenase 4; 2OGD-5, 2-oxoglutarate-dependent dioxygenase 5.

2023; Cheng et al., 2024). Recent studies have identified three novel neofunctionalized α-carbonic anhydrase-like (CAL) enzymes responsible for the key Mannich-like condensations that form core carbon–carbon bonds in Lycopodium alkaloids, key steps in the construction of their polycyclic skeletons. Through transcriptome analysis and enzyme characterization, Nett et al. identified key enzymes such as CAL-1 and CAL-2, which promote crucial annulation reactions (Nett et al., 2023; Liu F. et al., 2024; Zamar et al., 2024). The pathway proceeds through stereospecific modifications and scaffold tailoring, involving additional enzymes like Fe(II)-dependent dioxygenases, which introduce oxidation steps crucial for the final bioactive form of huperzine A (Figure 1) (Nett et al., 2021; Nett et al., 2023; Ushimaru and Abe, 2023). These findings shed light on the complex evolution of neuroactive alkaloids in Lycopodium species, suggesting that such enzymes have evolved for specialized metabolite production as a defense mechanism.

Moreover, transient expression of huperzine A biosynthetic genes in *Nicotiana benthamiana* allowed for the successful production of Lycopodium alkaloid congeners, underscoring the potential for scalable biosynthesis through heterologous platforms. This breakthrough not only deepens our understanding of plant-derived alkaloids but also opens the door to bioengineering huperzine A production in microbial or plant chassis, reducing reliance on natural resources (Zhang et al., 2022; Gao et al., 2023; Liu et al., 2023; Bai et al., 2024; Golubova et al., 2024).

## Galantamine: an amaryllidaceae alkaloid

Galantamine, an alkaloid derived from plants in the *Amaryllidaceae* family, particularly daffodils (*Narcissus* spp.), is another crucial AChEI used in AD treatment (Prvulovic et al., 2010). Similar to huperzine A, the biosynthetic pathway of galantamine was recently elucidated, providing invaluable insights into its production (Kilgore et al., 2014; Li et al., 2018; Li et al., 2019; Hu et al., 2021; Mehta et al., 2024). The discovery began with identifying the key precursor, 4′-O-methylnorbelladine (4OMN), followed by oxidative coupling catalyzed by cytochrome P450 enzymes such as NtCYP96T6. This enzyme facilitates the

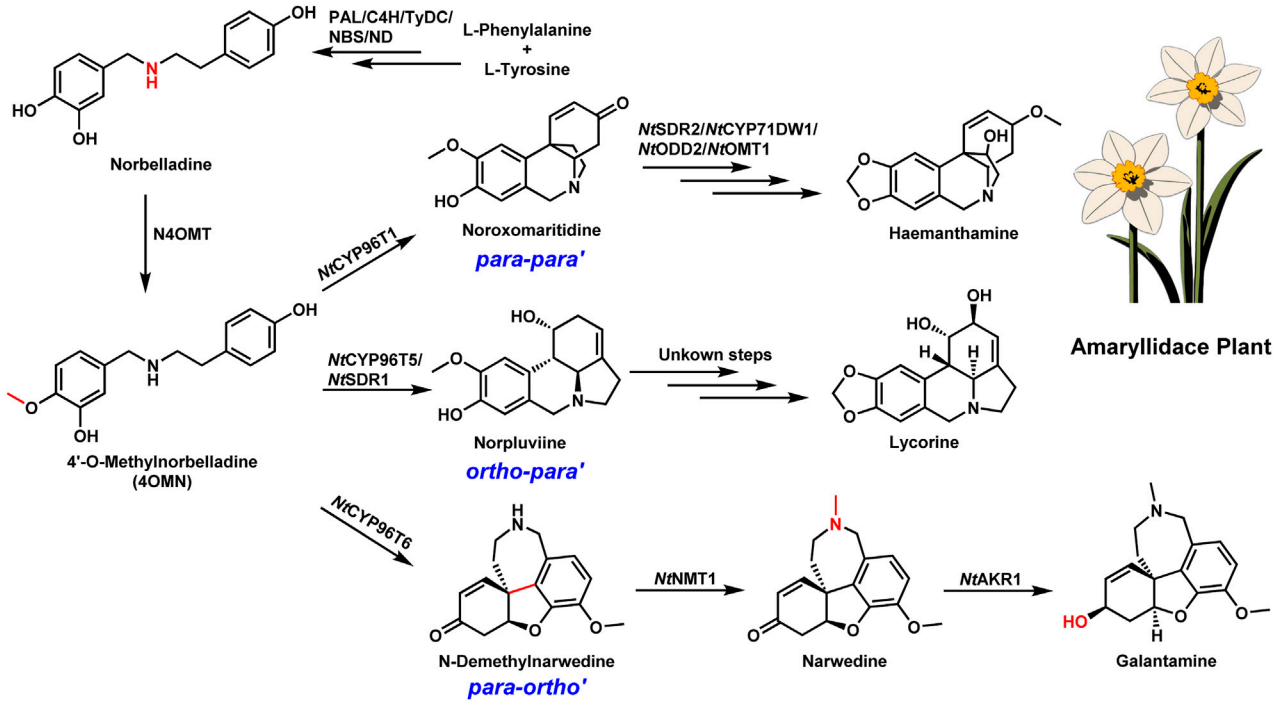


FIGURE 2
Schematic illustration of the biosynthesis of amaryllidaceae alkaloids. Biosynthetic pathway of galantamine. PAL, phenylalanine ammonia-lyase; C4H, cinnamate 4-hydroxylase; TyDC, tyrosine decarboxylase; NBS, norbelladine synthase; ND, norcraugsodine reductase; NtSDR2, short-chain dehydrogenase/reductase 2; NtCYP71DW1, cytochrome P450 71DW1; NtODD2, 2-oxoglutarate-dependent dioxygenase 2; NtOMT1, O-Methyltransferase 1; NtCYP 96T1, cytochrome P450 96T1; NtCYP 96T5, cytochrome P450 96T5; NtCYP 96T6, cytochrome P450 96T6; NtSDR1, short-chain dehydrogenase/reductase 1; NtNMT1, N-demethylnarwedine methyltransferase 1; NtAKR1, aldo-keto reductase 1. Dashed arrows represent steps that are hypothesized to occur spontaneously or without enzymatic catalysis.

para-ortho (p-o') oxidative coupling necessary to produce the galantamine skeleton. Subsequent methylation and reduction steps, catalyzed by NtNMT1 and NtAKR1 respectively, complete the biosynthesis of galantamine (Figure 2) (Mehta et al., 2024).

This discovery has profound implications for synthetic biology and metabolic engineering. With galantamine currently sourced primarily from natural populations of daffodils, the ability to biosynthesize it through engineered microbial systems holds significant promise for sustainable and scalable production (Zhang et al., 2022; Gao et al., 2023). Additionally, the elucidation of galantamine's pathway helps to understand how plants generate chemical diversity from simple precursors, providing a foundation for engineering other related alkaloids with potential therapeutic value.

## Challenges and future directions

The elucidation of huperzine A and galantamine biosynthetic pathways underscores the complexity and elegance of plant specialized metabolism. Both alkaloids share the common feature of acting as acetylcholinesterase inhibitors, though their evolutionary and biosynthetic origins differ significantly. The Lycopodium and Amaryllidaceae families, through distinct evolutionary pressures, have developed highly specialized enzymes that allow these plants to synthesize neuroactive metabolites with intricate polycyclic structures. While the elucidation of these biosynthetic pathways represents a significant advancement, several challenges remain.

First, the *in vivo* functional roles of these alkaloids in plants are not fully understood. It is speculated that they serve as defense metabolites against herbivores, but the regulatory mechanisms governing their production remain elusive (Chavez et al., 2024). Further research into the ecological roles of these alkaloids could provide important insights into the evolution of medicinal plants, the evolution of biosynthetic pathways, and their interactions with the environment (Szypuła and Pietrosiuk, 2023; Zhang et al., 2024).

Second, the scalability of producing huperzine A and galantamine through heterologous systems remains a key challenge. While transient expression in *N. benthamiana* has demonstrated proof-of-concept for biosynthesis, translating these findings into industrial-scale production will require optimization of gene expression, precursor supply, and enzymatic activity in microbial or plant-based platforms (Liu J. C. et al., 2024; Yang et al., 2024). Optimizing precursor supply, enhancing enzyme activity, and achieving high-yield production in heterologous systems are critical bottlenecks. Microbial synthetic biology platforms, such as *Saccharomyces cerevisiae* and *Pichia pastoris*, offer promising avenues for large-scale production due to their scalability and ease of genetic manipulation (Zhang et al., 2022; Gao et al., 2023; Yang et al., 2024). On the other hand, plant chassis like *N. benthamiana* provide unique advantages, including natural

metabolic environments and compartmentalized cells conducive to complex biosynthesis (Liu et al., 2023; Zhang et al., 2023; Golubova et al., 2024; Liu J. C. et al., 2024). Advances in CRISPR-based genome editing, multi-gene pathway assembly, and metabolic flux optimization are pivotal for overcoming current limitations (Liao et al., 2023; Xie et al., 2023; Teng et al., 2024). By leveraging these tools, researchers can create efficient production platforms not only for huperzine A and galantamine but also for other plant-derived neuroactive alkaloids, paving the way for accessible and sustainable therapeutics for Alzheimer's disease.

Finally, the potential for discovering new neuroactive alkaloids in related plant species should not be overlooked. The pathways for huperzine A and galantamine likely represent only a fraction of the neuroactive metabolites that plants produce. Systematic exploration of the metabolic pathways in related species could yield novel AChE inhibitors or other metabolites targeting neurodegenerative diseases.

## Conclusion

The elucidation of the biosynthetic pathways of huperzine A and galantamine marks a pivotal moment in plant biochemistry and neuropharmacology. These discoveries not only deepen our understanding of plant metabolism but also offer practical pathways for the sustainable production of crucial AD treatments. As the global population ages and the burden of neurodegenerative diseases grows, plant-derived neuroactive alkaloids like huperzine A and galantamine will continue to play an essential role in treatment. The future of this research lies in the intersection of synthetic biology, metabolic engineering, and traditional plant sciences, paving the way for innovative solutions to Alzheimer's disease and other neurological disorders.

## Author contributions

QY: Conceptualization, Writing–review and editing. ZZ: Conceptualization, Writing–review and editing. MY: Conceptualization, Writing–original draft, Writing–review and editing.

## Funding

The author(s) declare that financial support was received for the research, authorship, and/or publication of this article. This work was financially supported by the National Natural Science Foundation of China (32400218), the Key Technology R&D Program of Henan Province (242102110240, 232102110053), the Special Support Fund for High-level Talents and skills improvement of Henan Agricultural University (30501474).

## Conflict of interest

The authors declare that the research was conducted in the absence of any commercial or financial relationships that could be construed as a potential conflict of interest.

## Publisher's note



## References

Bai, Y., Liu, X., and Baldwin, I. T. (2024). Using synthetic biology to understand the function of plant specialized metabolites. *Annu. Rev. Plant Biol.* 75, 629–653. doi:10.1146/annurev-arplant-060223-013842

Chavez, B. G., Leite Dias, S., and D'auria, J. C. (2024). The evolution of tropane alkaloids: coca does it differently. *Curr. Opin. Plant Biol.* 81, 102606. doi:10.1016/j.pbi.2024.102606

Cheng, B., Song, L., and Chen, F. (2024). Huperzine alkaloids: forty years of total syntheses. *Nat. Prod. Rep.* 41, 59–84. doi:10.1039/d3np00029j

Gao, J., Zuo, Y., Xiao, F., Wang, Y., Li, D., Xu, J., et al. (2023). Biosynthesis of catharanthine in engineered Pichia pastoris. *Nat. Synth.* 2, 231–242. doi:10.1038/s44160-022-00205-2

Golubova, D., Tansley, C., Su, H., and Patron, N. J. (2024). Engineering Nicotiana benthamiana as a platform for natural product biosynthesis. *Curr. Opin. Plant Biol.* 81, 102611. doi:10.1016/j.pbi.2024.102611

Hu, J., Li, W., Liu, Z., Zhang, G., and Luo, Y. (2021). Molecular cloning and functional characterization of tyrosine decarboxylases from galanthamine-producing Lycoris radiata. *Acta Physiol. Plant.* 43, 84. doi:10.1007/s11738-021-03258-6

Kilgore, M. B., Augustin, M. M., Starks, C. M., O'neil-Johnson, M., May, G. D., Crow, J. A., et al. (2014). Cloning and characterization of a norbelladine 4'-O-methyltransferase involved in the biosynthesis of the Alzheimer's drug galanthamine in Narcissus sp. aff. pseudonarcissus. *PLoS One* 9, e103223. doi:10.1371/journal.pone.0103223

Li, W., Qiao, C., Pang, J., Zhang, G., and Luo, Y. (2019). The versatile O-methyltransferase LrOMT catalyzes multiple O-methylation reactions in amaryllidaceae alkaloids biosynthesis. *Int. J. Biol. Macromol.* 141, 680–692. doi:10.1016/j.ijbiomac.2019.09.011

Li, W., Yang, Y., Qiao, C., Zhang, G., and Luo, Y. (2018). Functional characterization of phenylalanine ammonia-lyase- and cinnamate 4-hydroxylase-encoding genes from Lycoris radiata, a galanthamine-producing plant. *Int. J. Biol. Macromol.* 117, 1264–1279. doi:10.1016/j.ijbiomac.2018.06.046

Li, X., Li, W., Tian, P., and Tan, T. (2022). Delineating biosynthesis of Huperzine A, A plant-derived medicine for the treatment of Alzheimer's disease. *Biotechnol. Adv.* 60, 108026. doi:10.1016/j.biotechadv.2022.108026

Liao, J., Liu, T., Xie, L., Mo, C., Qiao, J., Huang, X., et al. (2023). Heterologous mogrosides biosynthesis in cucumber and tomato by genetic manipulation. *Commun. Biol.* 6, 191. doi:10.1038/s42003-023-04553-3

Liu, F., Fernie, A. R., and Zhang, Y. (2024). Plant gene co-expression defines the biosynthetic pathway of neuroactive alkaloids. *Mol. Plant* 17, 372–374. doi:10.1016/j.molp.2024.02.002

Liu, J. C., De La Pena, R., Tocol, C., and Sattely, E. S. (2024). Reconstitution of early paclitaxel biosynthetic network. *Nat. Commun.* 15, 1419. doi:10.1038/s41467-024-45574-8

Liu, X., Zhang, P., Zhao, Q., and Huang, A. C. (2023). Making small molecules in plants: a chassis for synthetic biology-based production of plant natural products. *J. Integr. Plant Biol.* 65, 417–443. doi:10.1111/jipb.13330

Ma, X., and Gang, D. R. (2004). The Lycopodium alkaloids. *Nat. Product. Rep.* 21, 752–772. doi:10.1039/b409720n

Mehta, N., Meng, Y., Zare, R., Kamenetsky-Goldstein, R., and Sattely, E. (2024). A developmental gradient reveals biosynthetic pathways to eukaryotic toxins in monocot geophytes. *Cell* 187, 5620–5637.e10. doi:10.1016/j.cell.2024.08.027

Nett, R. S., Dho, Y., Low, Y. Y., and Sattely, E. S. (2021). A metabolic regulon reveals early and late acting enzymes in neuroactive Lycopodium alkaloid biosynthesis. *Proc. Natl. Acad. Sci. U. S. A.* 118, e2102949118. doi:10.1073/pnas.2102949118

Nett, R. S., Dho, Y., Tsai, C., Passow, D., Martinez Grundman, J., Low, Y. Y., et al. (2023). Plant carbonic anhydrase-like enzymes in neuroactive alkaloid biosynthesis. *Nature* 624, 182–191. doi:10.1038/s41586-023-06716-y

Ng, Y. P., Or, T. C. T., and Ip, N. Y. (2015). Plant alkaloids as drug leads for Alzheimer's disease. *Neurochem. Int.* 89, 260–270. doi:10.1016/j.neuint.2015.07.018

Prvulovic, D., Hampel, H., and Pantel, J. (2010). Galantamine for Alzheimer's disease. *Expert Opin. Drug Metabolism and Toxicol.* 6, 345–354. doi:10.1517/17425251003592137

Rezaul Islam, M., Akash, S., Murshedul Islam, M., Sarkar, N., Kumer, A., Chakraborty, S., et al. (2024). Alkaloids as drug leads in Alzheimer's treatment: mechanistic and therapeutic insights. *Brain Res.* 1834, 148886. doi:10.1016/j.brainres.2024.148886

Szypuła, W. J., and Pietrosiuk, A. (2023). "Biological and ecological roles of club mosses (lycopodiaceae) alkaloids," in *Plant specialized metabolites: phytochemistry, ecology and biotechnology*. Editors J.-M. Mérillon and K. G. Ramawat (Cham: Springer Nature Switzerland), 1–25.

Teng, Y., Jiang, T., and Yan, Y. (2024). The expanded CRISPR toolbox for constructing microbial cell factories. *Trends Biotechnol.* 42, 104–118. doi:10.1016/j.tibtech.2023.06.012

Ushimaru, R., and Abe, I. (2023). Assembling neuroactive alkaloids. *Nat. Plants* 9, 1946–1947. doi:10.1038/s41477-023-01586-8

Wang, J., Zhang, Z. K., Jiang, F. F., Qi, B. W., Ding, N., Hnin, S. Y. Y., et al. (2020). Deciphering the biosynthetic mechanism of pelletierine in lycopodium alkaloid biosynthesis. *Org. Lett.* 22, 8725–8729. doi:10.1021/acs.orglett.0c03339

Xie, L., Luo, Z., Jia, X., Mo, C., Huang, X., Suo, Y., et al. (2023). Synthesis of crocin I and crocin II by multigene stacking in Nicotiana benthamiana. *Int. J. Mol. Sci.* 24, 14139. doi:10.3390/ijms241814139

Yang, C., Wang, Y., Su, Z., Xiong, L., Wang, P., Lei, W., et al. (2024). Biosynthesis of the highly oxygenated tetracyclic core skeleton of Taxol. *Nat. Commun.* 15, 2339. doi:10.1038/s41467-024-46583-3

Yang, M., You, W., Wu, S., Fan, Z., Xu, B., Zhu, M., et al. (2017). Global transcriptome analysis of Huperzia serrata and identification of critical genes involved in the biosynthesis of huperzine A. *BMC Genomics* 18, 245. doi:10.1186/s12864-017-3615-8

Zamar, D. L., Papon, N., and Courdavault, V. (2024). SPOTLIGHT: alpha carbonic anhydrases join the club of alkaloid biosynthetic enzymes. *J. Plant Physiol.* 293, 154169. doi:10.1016/j.jplph.2023.154169

Zhang, J., Hansen, L. G., Gudich, O., Viehrig, K., Lassen, L. M. M., Schrubbers, L., et al. (2022). A microbial supply chain for production of the anti-cancer drug vinblastine. *Nature.* 609, 341–347. doi:10.1038/s41586-022-05157-3

Zhang, Y., Wiese, L., Fang, H., Alseekh, S., Perez De Souza, L., Scossa, F., et al. (2023). Synthetic biology identifies the minimal gene set required for paclitaxel biosynthesis in a plant chassis. *Mol. Plant* 16, 1951–1961. doi:10.1016/j.molp.2023.10.016

Zhang, Z. J., Jiang, S., and Zhao, Q. S. (2024). The chemistry and biology of lycopodium alkaloids. *Chem. Biodivers.* 21, e202400954. doi:10.1002/cbdv.202400954

frontiers | Frontiers in Pharmacology

TYPE Mini Review
PUBLISHED 07 February 2025
DOI 10.3389/fphar.2025.1497861



OPEN ACCESS

EDITED BY
Junfeng Wang,
Massachusetts General Hospital and Harvard Medical School, United States

REVIEWED BY
Luca Rastrelli,
University of Salerno, Italy

*CORRESPONDENCE
Yong Luo,
luoyong@zmu.edu.cn
Nanqu Huang,
hnq@zmu.edu.cn

RECEIVED 18 September 2024
ACCEPTED 20 January 2025
PUBLISHED 07 February 2025

CITATION
Wang M, Huang W, Huang J, Luo Y and Huang N (2025) Natural bioactive compounds form herbal medicine in Alzheimer's disease: from the perspective of GSK-3β.
*Front. Pharmacol.* 16:1497861.
doi: 10.3389/fphar.2025.1497861



# Natural bioactive compounds form herbal medicine in Alzheimer's disease: from the perspective of GSK-3β

Mei Wang[1], Wendi Huang[1], Juan Huang[2,3], Yong Luo[1,4]* and Nanqu Huang[4,5]*

[1]Department of Neurology, Third Affiliated Hospital of Zunyi Medical University (The First People's Hospital of Zunyi), Zunyi, Guizhou, China, [2]Key Laboratory of Basic Pharmacology and Joint International Research Laboratory of Ethnomedicine of Ministry of Education, Zunyi Medical University, Zunyi, Guizhou, China, [3]Chinese Pharmacological Society-Guizhou Province Joint Laboratory for Pharmacology, Zunyi, Guizhou, China, [4]Department of Geriatrics, Third Affiliated Hospital of Zunyi Medical University (The First People's Hospital of Zunyi), Zunyi, Guizhou, China, [5]National Drug Clinical Trial Institution, Third Affiliated Hospital of Zunyi Medical University (The First People's Hospital of Zunyi), Zunyi, Guizhou, China

Alzheimer's disease (AD) is a progressive neurodegenerative disorder characterized by cognitive decline and memory loss. Glycogen synthase kinase 3β (GSK-3β) plays a pivotal role in AD pathogenesis, particularly in tau protein hyperphosphorylation. Natural bioactive compounds have a wide range of sources, and medicinally valuable active compound can be extracted from plants, animals, and microorganisms. Currently, studies have found that various natural bioactive compounds from plants have the potential to improve AD symptoms, such as resveratrol and berberine. Therefore, this review examines the potential of natural bioactive compounds to modulate GSK-3β activity and inhibit the hyperphosphorylation of tau, offering a promising therapeutic strategy for AD. We summarize the current understanding of alkaloids, phenols, flavonoids, terpenoids and other natural compounds, highlighting their mechanisms of action and preclinical efficacy.

KEYWORDS

**Alzheimer's disease, GSK-3β, tau protein, tau hyperphosphorylation, natural bioactive compounds**

## Introduction

Alzheimer's disease (AD) is the most prevalent neurodegenerative disorder, with an increasing prevalence observed on an annual basis. The decline in memory and cognitive functions in patients places a significant burden on their families and society. A principal pathological characteristic of AD is the hyperphosphorylation of tau proteins, which results in the formation of neurofibrillary tangles (NFTs) (Rostagno, 2022). In a healthy state, tau proteins function as microtubule-associated proteins, contributing to the maintenance of cellular structural stability (Shahani and Brandt, 2002). However, hyperphosphorylated tau proteins are detached from microtubules and accumulate in the brain, forming NFTs, a process that is closely related to the activity of Glycogen synthase kinase 3β (GSK-3β) (Bielska and Zondlo, 2006; Liu et al., 2023). GSK-3β is a multifunctional serine/threonine protein kinase that plays a pivotal role in regulating cellular function by participating in a multitude of signaling pathways. The activity of GSK-3β is subject to dual regulation, it is

TABLE 1 Natural bioactive compounds regulate the phosphorylation of Tau by affecting the activity of GSK-3β.

| Metabolites | Source | Chemical structure | Mechanism | Test subject | Ref. |
|---|---|---|---|---|---|
| Berberine | *Coptis Salisb* | 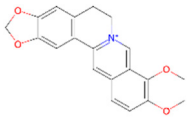 | GSK-3β and CDK-5↓ | Wistar rats with streptozotocin (STZ) | Saleh et al. (2024) |
| Gelsemine | *Gelsemium elegans Benth* | 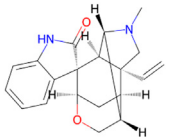 | pSer9-GSK-3β↑ | Aβ oligomer-treated mice | Chen et al. (2020) |
| Rutaecarpine | *Evodia rutaecarpa (Juss.) Benth* | 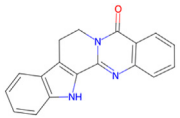 | GSK-3β↓ | C57BL/6 mice with high sucrose and pAAV-CMV-mGSK-3β | Zhao et al. (2021) |
| Dendrobium nobile Lindl. Alkaloid | *Dendrobium nobile Lindl* | 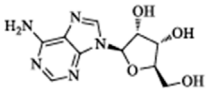 | PI3K/Akt/GSK-3β pathway↑ | Wortmannin (WM) and GF-109203X (GFX)-induced hyperphosphorylation of Tau in N2a cells and rats | Huang et al. (2024a) |
| Tetrahydroalstonine | *Cornus officinalis Sieb. et Zucc* | 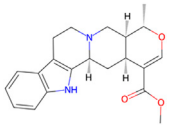 | PI3K/Akt pathway↑, BACE1, GSK-3β, insulin resistance↓ | Palmitate acid-induced SK-N-MC cells | Chen and Yu (2024) |
| Salidroside | *Rhodiola rosea L* | 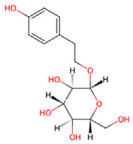 | GSK-3β phosphorylation↑ | Tau transgenic *Drosophila* line | Zhang et al. (2016) |
| Curcumin | *Curcuma longa L* | 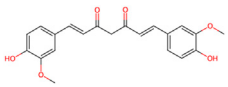 | CDK-5 and GSK-3β↓ | Scopolamine-induced AD rats | Das et al. (2019) |
| Resveratrol | Fruits | 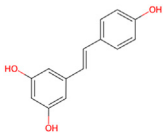 | GSK-3β and ERK1/2↓ | Hippocampal slice from 10-day-old Sprague–Dawley rat pup | Jhang et al. (2017) |

(Continued on following page)





10.3389/fphar.2025.1497861

TABLE 1 (*Continued*) Natural bioactive compounds regulate the phosphorylation of Tau by affecting the activity of GSK-3β.

| Metabolites | Source | Chemical structure | Mechanism | Test subject | Ref. |
|---|---|---|---|---|---|
| Gallic acid | Medicinal plants | 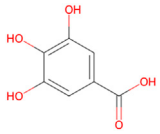 | GSK-3β↓ | APP/PS1 transgenic mouse | Ding et al. (2024) |
| Galangin | *Alpinia officinarum Hance* | 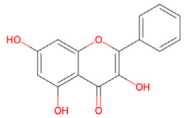 | Akt/GSK3β/mTOR pathway↑ | PC12 cells with Okadaic acid | Huang et al. (2019) |
| Scutellaria flavonoids | *Scutellaria Baicalensis Georgi* | 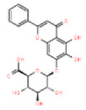 | PKA↑, CDK-5 and GSK-3β↓ | SD rats with Okadaic acid | Gao et al. (2021) |
| Icaritin | *Epimedium brevicornu Maxim* | 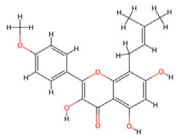 | GSK-3β↓ | SH-SY5Y cells with Okadaic acid | Li et al. (2022) |
| Icariin | *Epimedium brevicornu Maxim* | 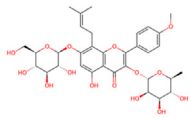 | GSK-3β↓ | SH-SY5Y cells with Okadaic acid | Li et al. (2022) |
| Genipin | *Gardenia jasminoides J. Ellis* | 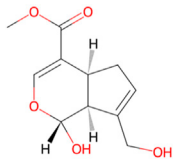 | CDK-5 and GSK-3β↓ | HEK293/Tau cells<br>N2a/SweAPP cells<br>SH-SY5Y/Tau cells | Li et al. (2021a) |
| Tanshinone IIA | *Salvia miltiorrhiza Bunge* | 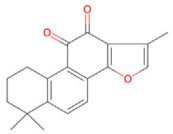 | PI3K/Akt/GSK-3β pathway↑ | APP/PS1 mice | Peng et al. (2022) |
| Ginsenoside Rd | *Panax ginseng C. A. Mey* | 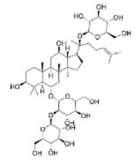 | GSK-3β and CDK-5↓ | APP transgenic mice | Li et al. (2021b) |

(Continued on following page)





10.3389/fphar.2025.1497861

TABLE 1 (*Continued*) Natural bioactive compounds regulate the phosphorylation of Tau by affecting the activity of GSK-3β.

| Metabolites | Source | Chemical structure | Mechanism | Test subject | Ref. |
|---|---|---|---|---|---|
| Ginsenoside Rh4 | *Panax ginseng C. A. Mey* | 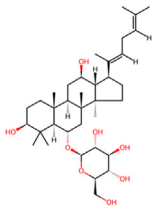 | Wnt2b/GSK-3β/SMAD4 pathway↑ | AD mouse induced by a combination of $AlCl_3{\cdot}6H_2O$ and d-galactose | Ren et al. (2023) |
| Atractylenolide III | *Atractylodes macrocephala Koidz* | 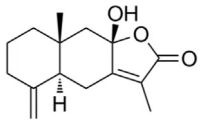 | PI3K/Akt/GSK-3β pathway↑ | SD rats through bilateral intracerebroventricular (ICV) administration of streptozotocin (STZ) | Liu et al. (2024) |
| Schisantherin B | *Schisandra chinensis (Turcz.) Baill* | 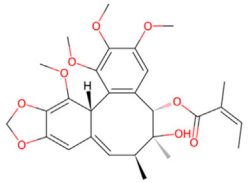 | PI3K/Akt/GSK-3β pathway↑ | Mice with $A\beta_{1\text{-}42}$ | Xu et al. (2016) |
| Sulforaphene | *Raphanus sativus L* | 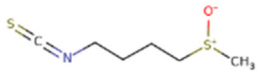 | PI3K/Akt/GSK-3β Pathway↑ | SD rats with Streptozotocin (STZ) and murine microglial BV-2 cell with lipopolysaccharide (LPS) | Yang et al. (2020) |

The arrow ↑ indicates upregulation, and the arrow ↓ indicates downregulation.





10.3389/fphar.2025.1497861

activated through auto-phosphorylation at tyrosine 216 and inactivated through phosphorylation at serine 9 (Krishnankutty et al., 2017). GSK-3β is capable of regulate the phosphorylation of multiple sites of the Tau proteins, including Thr181, Ser199, Ser202, and so forth (Liu et al., 2002). In the brains of AD patients, abnormal activation of GSK-3β is associated with the hyperphosphorylation of tau proteins and the formation of NFTs. Additionally, a decrease in the activity of Protein Phosphatase 2A (PP2A), the primary tau phosphatase, further exacerbates the imbalance of tau protein phosphorylation (Nicolia et al., 2010). Therefore, inhibiting the activity of GSK-3β is considered a potential therapeutic strategy for AD. Currently, a variety of GSK-3β inhibitors have been employed with some success in the evaluation of preclinical studies and experiments in AD (Arciniegas Ruiz and Eldar-Finkelman, 2021). However, the challenge of applying them to the clinic remains significant. This phenomenon can be attributed to the intricate nature of the pathogenesis of AD, and the likelihood of achieving therapeutic goals through a single mechanism is relatively low. Therefore, identifying drug with multi-target effects may prove to be a more efficacious approach for the treatment of AD.

Natural bioactive compounds widely distributed in plants, animals, marine organisms and microorganisms, and exhibit diverse chemical structures and a wide range of pharmacological activities. Researchers have used three-month-old male Albino Wistar rats to establish an AD model and have found that resveratrol, a naturally occurring compound derived from plants, has neuroprotective effects (Rao et al., 2024). Similarly, berberine, sourced from the plant *Coptis Salisb*, has demonstrated the ability to suppress the activation of GSK-3β and diminish the hyperphosphorylation of the tau protein in cellular models (Yu et al., 2011). Currently, the potential of natural bioactive compounds to treat AD by modulating GSK-3β activity is gradually being investigated (Huang et al., 2022; Santi et al., 2024; Xing et al., 2024). Thus, the aim of this work is to provide a comprehensive overview of *in vivo* and *in vitro* experiments investigating the regulation of Tau hyperphosphorylation by natural bioactive compounds through targeting GSK-3β (Table 1). This will facilitate the identification of novel therapeutic avenues for AD patients. Although GSK-3β inhibitors have shown some efficacy in preclinical studies, translating them into clinical applications remains challenging. Therefore, delving into the mechanisms of action and clinical application potential of these natural compounds is of great significance for the development of new AD therapeutic drugs.

## Alkaloids

Alkaloids are a class of nitrogen-containing organic bases primarily found in plants, known for their diverse physiological functions and biological activities. They typically have complex cyclic structures, with nitrogen atoms often included within the rings. Alkaloids have a broad range of pharmacological effects, including anti-cancer, anti-bacterial, anti-inflammatory, and antioxidant properties. Moreover, alkaloids also play a significant role in the treatment of neurological diseases.

Berberine, an isoquinoline alkaloid, is extracted from the *Coptis Salisb*, which is classified within the Ranunculaceae species. In the present study, researchers utilized berberine (BBR)-loaded poly (lactic-co-glycolic acid) (PLGA)/Tet-1 peptide nanoparticles (BBR/PLGA-Tet NPs) to evaluate the therapeutic potential of BBR in a rat AD model induced by streptozotocin (STZ). The findings revealed that both BBR and BBR/PLGA-Tet NPs significantly ameliorated cognitive impairments induced by STZ in AD rats, with BBR/PLGA-Tet NPs demonstrating a more pronounced effect. This improvement may be attributed to the reduction of GSK-3β and CDK-5 protein levels, thereby decreasing the hyperphosphorylation of Tau (Saleh et al., 2024). These nanoparticles can effectively penetrate the blood-brain barrier, enhancing the delivery efficiency of the drug within the brain, thereby providing a new strategy for the treatment of AD. This provides an experimental basis for the treatment of AD. Gelsemine, derived from *Gelsemium elegans Benth.*, which is classified within the Loganiaceae. It possesses not only anti-inflammatory and antioxidant effects but also inhibits the production of inflammatory factors. In a mouse model of β-amyloid (Aβ) oligomer-induced AD, Gelsemine demonstrated significant activity at a dose of 5 μg/kg. This activity was observed to reduce cognitive deficits and inflammatory responses induced by Aβ oligomers, as well as augment the phosphorylation level of GSK-3β at the Ser9 site. Consequently, this resulted in a reduction in the hyperphosphorylation of Tau, producing improved AD (Chen et al., 2020). However, this study injected the drug directly into the mouse brain via a stereotaxic device, a risky method of administration that is not directly applicable to human experimentation. Additionally, it is challenging to ascertain the accuracy of the drug injection into specific brain regions, owing to technological limitations. Another alkaloid, rutaecarpine, is extracted from the plant *Evodia rutaecarpa (Juss.) Benth.*, which is classified within the *Rutoideae*. Zhao et al. constructed an AD model using an adeno-associated virus carrying the GSK-3β gene (pAAV-CMV-mGSK-3β), which was injected by stereotaxic injection into the brains of mice. These mice had been fed a 20% sucrose solution and a 0.01% rutaecarpine chow for 24 weeks. They found that rutaecarpine at 0.01% was found to show significant pharmacological activity, ameliorating spatial memory deficits and enhancing synaptic plasticity in AD mice by modulating the GSK-3β signaling pathway (Zhao et al., 2021). However, this experimental method is not rigorous. Feeding through diet cannot guarantee that each mouse ingests the same amount of the drug. This may weaken the persuasiveness of the experimental results. Administering a fixed drug concentration via gavage to simulate oral drug intake in humans may better illustrate the pharmacological effects of the drug and reduce experimental errors. Dendrobium nobile Lindl. Alkaloid (DNLA), found in the valuable Orchidaceae species *Dendrobium nobile Lindl.* In experiments conducted *in vivo* and *in vitro*, Our previous research found that DNLA (20 mg/kg) could effectively reverse the hyperphosphorylation of the Tau protein in N2a cells and Wistar rats by regulating the PI3K/Akt/GSK-3β signaling pathway (Huang J. et al., 2024). Furthermore, tetrahydroalstonine (THA), another active compound extracted from Cornaceae species *Cornus officinalis Sieb. et Zucc*. In an *in vitro* experiment, THA (10 μM) activates the impaired PI3K/AKT signaling pathway, regulating insulin resistance and inhibiting the activity of BACE1 and GSK-3β, leading to a reduction in the production of Tau and Aβ (Chen and Yu, 2024). These findings indicate that some alkaloids, by modulating the activity of GSK-3β, have a significant inhibitory effect on the hyperphosphorylation of tau protein, offering new strategies for the treatment of AD.

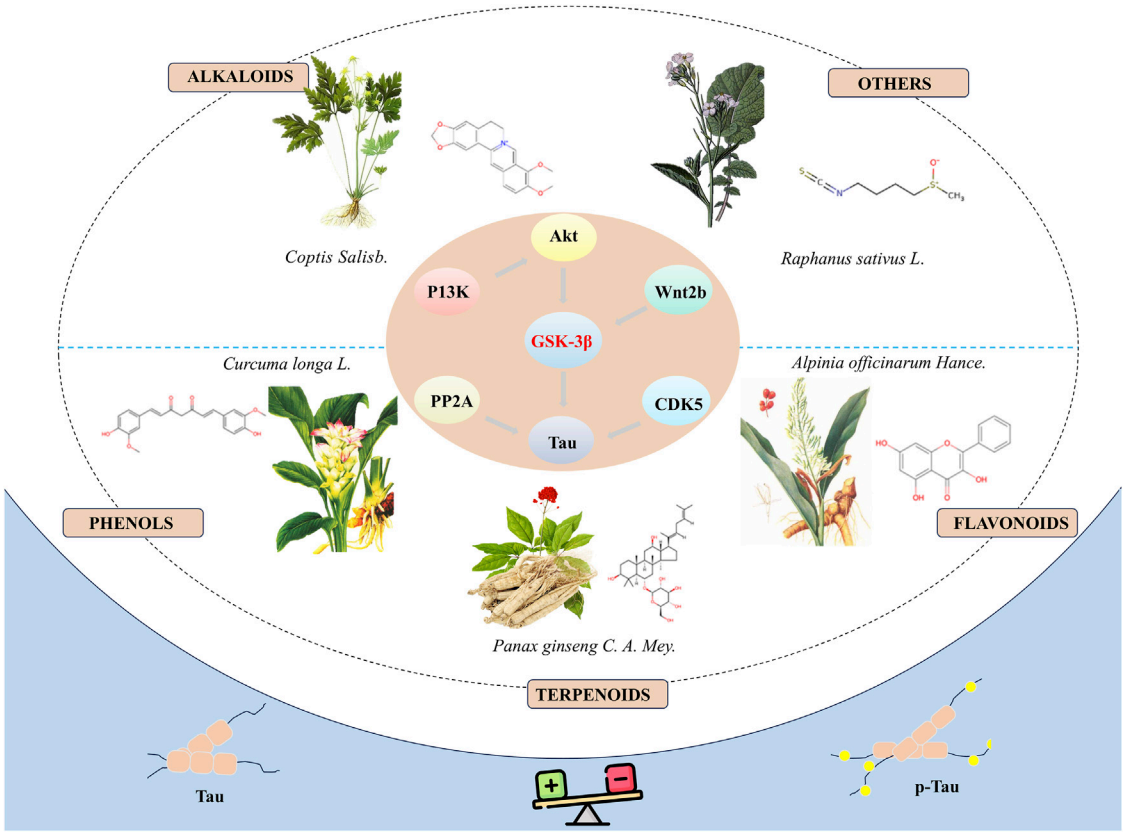


FIGURE 1
Natural bioactive compounds inhibit the hyperphosphorylation of tau protein by modulate the activity of GSK-3β and demonstrate the potential to treat AD.

## Phenols

Phenols are widely present in a variety of plants found in nature, such as fruits, tea leaves, grains, and vegetables. These compounds not only demonstrate potential health benefits in preventing cardiovascular diseases, inflammation, tumors, bacteria, and viruses, but some also exhibit neuroprotective effects, showing promise in improving symptoms of AD. Salidroside, extracted from *Rhodiola rosea L*, Crassulaceae family, has been demonstrated to alleviate the hyperphosphorylation of tau protein in a transgenic fruit fly model of AD. Using donepezil as a positive control group, the researchers ascertained that 2 μM of salidroside prolonged lifespan and enhanced locomotor activity in tau transgenic *Drosophila*, thereby demonstrating its potential for the treatment of AD. This effect was achieved by enhancing the phosphorylation of GSK-3β (Zhang et al., 2016). Curcumin, a naturally occurring yellow pigment derived from Zingiberaceae species *Curcuma longa L*, reverses spatial memory and motor deficits in scopolamine-induced AD rats by inhibiting the activity of GSK-3β and Cyclin dependent Kinase 5 (CDK-5), reducing the aggregation of Aβ and hyperphosphorylation of tau (Das et al., 2019). In this study, curcumin (80 mg/kg) demonstrated the same therapeutic effect as donepezil, with potential to treat AD. Resveratrol (RES), a polyphenolic compound with antioxidant, anti-inflammatory, and antimicrobial properties. Researchers utilized hippocampal slices from Sprague-Dawley rats to conduct their study. Initially, they increased the levels of p-S396-tau in the hippocampal slices through the application of Na3VO4. Subsequently, they intervened with resveratrol for a duration of 1 hour. It was discovered that RES (at a concentration of 20 μM) significantly enhanced the phosphorylation of GSK-3β at the Ser9 site, thereby inhibiting the activity of GSK-3β. This action led to a reduction in the Na3VO4-induced levels of p-S396-tau. Additionally, RES also suppressed the activation of ERK1/2 induced by Na3VO4, demonstrating its potential therapeutic role in AD (Jhang et al., 2017). The study was the first to reveal the connection between the generation of reactive oxygen species (ROS) caused by long-term exposure to Na3VO4 and the phosphorylation of tau protein, providing new insights into the pathological mechanisms of AD. Through the use of various drug pre-treatments and long-term exposure experiments, the protective effects of resveratrol were systematically evaluated. However, the sample size was relatively small (n = 3–5), which may increase the likelihood of randomness in the results, thereby affecting the reliability of the conclusions. Gallic acid (GA), isolated from medicinal plants, has been shown to significantly reduce abnormal phosphorylation levels of tau protein and the accumulation of Aβ in the APP/PS1 transgenic mouse model, thereby ameliorating spatial memory deficits in AD model mice. This effect is attributed to the interaction of GA with key phosphorylation sites of GSK-3β, thereby inhibiting its activity (Ding et al., 2024). These studies indicate that some phenols compounds show potential in the

treatment of AD by inhibiting the activity of GSK-3β and reducing the hyperphosphorylation of tau, offering new strategies for improving memory and cognitive functions in patients with AD. Future research should further explore the mechanisms of action and clinical application possibilities of these compounds.

## Flavonoids

Flavonoids are a class of secondary compounds found in plants. They are widely distributed in plant parts such as flowers, leaves, stems, and fruits. They are named for their yellow pigment properties. The pharmacological effects of these compounds have been confirmed by scientific research, which has demonstrated that they possess anti-inflammatory, antioxidant, antibacterial, and antiviral properties. In this article, we will present three natural compounds that have the potential to be used in the treatment of AD. Galangin is a bioactive compound that is extracted from Zingiberaceae family *Alpinia officinarum Hance*. In the PC12 cell model of AD, Galangin (1.0 μg/mL) has been observed to enhance cell viability and reduce tau protein phosphorylation by modulating the Akt/GSK-3β/mTOR signaling pathway, thereby inhibiting the activity of GSK-3β (Huang et al., 2019). Although the authors found that it has certain therapeutic effects on AD *in vitro* models, there is a lack of further verification *in vivo* models. There are certain differences between the *in vivo* environment and *in vitro* experiments. Conducting further animal experiments may better demonstrate the potential value of this compound. Moreover, stem and leaf flavonoids from *Scutellaria Baicalensis Georgi* (SSF), which is member of the Labiatae family, have been found to enhance learning and memory capabilities in AD rats by regulating the activity of CDK-5, PKA, and GSK-3β, which in turn inhibits the hyperphosphorylation of tau protein (Gao et al., 2021). Icaritin (ICT) and icariin (ICA), extracted from the Chinese botanical drug *Epimedium brevicornu Maxim*, Berberidaceae family. Our research found that 2.5 μmol/L of ICA and 1.0 μmol/L of ICT significantly reduced the levels of p-Tau and GSK-3β in the SH-SY5Y cell model induced by okadaic acid (OA), highlighting its neuroprotective potential, and that ICT was slightly more effective than ICA (Li et al., 2022). These evidences indicate that flavonoids have the potential to be a valuable therapeutic option for AD and further investigation into their neuroprotective capabilities is warranted. It will be instrumental in assessing the viability of flavonoids as therapeutic agents for the mitigation of AD pathology and related neurodegenerative processes.

## Terpenoids

Terpenoids constitute a class of natural hydrocarbon compounds that are widely distributed in plants and animals. They can be categorized based on the number of isoprene units they contain, resulting in the following classifications: monoterpenes ($C_{10}H_{16}$), sesquiterpenes ($C_{15}H_{24}$), diterpenoids ($C_{20}H_{32}$), triterpenoids ($C_{30}H_{48}$), and tetraterpenes ($C_{40}H_{64}$). A number of terpenoids have been found to possess biological activities, including antimalarial, anticancer, anti-inflammatory and antiviral properties. Additionally, the neuroprotective effects of terpenes are being increasingly investigated. Genipin is a bioactive compound that is extracted from *Gardenia jasminoides J. Ellis,* Rubiaceae family. The researchers observed the cell physiological changes after Genipin treatment at different concentrations in a variety of cell lines, and found that Genipin (20 μM) could inhibit Tau phosphorylation by down-regulating the expression of CDK-5 and GSK-3β. Genipin (20 μM) was found to inhibit Tau phosphorylation by down-regulating the expression of CDK-5 and GSK-3β, and to activate mTOR-dependent autophagy through the SIRT1/LKB1/AMPK signaling pathway, while inhibiting Aβ production, thus exerting neuroprotective effects (Li M. et al., 2021). Tanshinone IIA (TanIIA), extracted from the Chinese botanical drug Labiatae species *Salvia miltiorrhiza Bunge*. In the APP/PS1 mouse model of AD, following a 4-week period of TanIIA treatment, researchers observed the activation of the PI3K/Akt signaling pathway and inhibition of GSK-3β. This resulted in a significant attenuation of Tau hyperphosphorylation, as well as the reversal of cholinergic dysfunction and the reduction of oxidative stress. Notably, the low-dose group (15 mg/kg) and the high-dose group (30 mg/kg) exhibited comparable outcomes (Peng et al., 2022). However, it should be noted that the findings may be affected by the limited sample size, which could potentially compromise the representativeness and statistical validity of the results. Araliaceae species *Panax ginseng C. A. Mey* has been used for thousands of years in China. In one study, ginsenoside Rd effectively decreased the production and deposition of hyperphosphorylated tau protein by depressing the expression of GSK-3β and CDK-5 (Li L. et al., 2021). Further research has found that ginsenoside Rh4, which has higher pharmacological activity than ordinary ginsenosides, can not only inhibit the inflammatory response caused by over-activation of microglia and astrocytes, but also inhibit the excessive phosphorylation of tau protein in the hippocampus of AD mouse by regulating the Wnt2b/GSK-3β/SMAD4 signaling pathway (Ren et al., 2023). Atractylenolide III (Liu et al., 2024) extracted from *Atractylodes macrocephala Koidz*, Compositae family, has been demonstrated to enhance learning and memory capabilities in AD rats through modulate the PI3K/AKT/GSK-3β signaling pathway, and it has the same effect as donepezil. The results of these studies indicate that specific terpenoids have the potential to modulate the aberrant phosphorylation and aggregation of tau protein by regulating the phosphorylation of GSK-3β. In light of these findings, there is a scientific rationale for further investigation and development of terpenes as potential therapeutic strategies for AD.

## Others

In addition to the natural bioactive compounds mentioned above, there are other classes of compounds found in nature that can exert neuroprotective effects by modulating key cellular signaling pathways. Schisantherin B is a phenylpropanoid compound extracted from the plant *Schisandra chinensis (Turcz.) Baill.* of the Magnoliaceae family. In AD mouse model, Schisantherin B at a dose of 0.15 mg/kg has demonstrated the ability to reduce excessive phosphorylation of Tau, which may be achieved by modulating GSK-3β (Xu et al., 2016). Although this study used donepezil as a positive control group, which indicates the

therapeutic potential of Schisantherin B. However, the specific mechanism of action was not thoroughly investigated, and there is a lack of research on the biological toxicity of this compound. Future studies can include additional experimental content to further explore its molecular mechanisms. Sulforaphene (SF) represents a primary isothiocyanate compound that has been extracted from the Cruciferae species *Raphanus sativus L*. In the AD rat model, oral administration of SF (25 and 50 mg/kg) over a period of 6 weeks resulted in a significant improvement in cognitive function in rats. In addition, researchers conducted cell experiments and found that SF has potential anti-inflammatory effects in LPS-induced BV-2 cells. This may be achieved by regulating the PI3K/Akt/GSK-3β signaling pathway (Yang et al., 2020). Despite their disparate origins, these compounds share a common mechanism of action, namely, the inhibition of GSK-3β activity and the reduction of tau protein phosphorylation. These findings indicate the potential of natural products in the treatment of neurodegenerative diseases and provide a scientific basis for the development of new therapeutic drugs.

## Conclusion

In summary, natural bioactive compounds have demonstrated the potential to inhibit the hyperphosphorylation of tau protein by directly or indirectly modulating the activity of GSK-3β, thereby exhibiting potential therapeutic effects in neuroprotection (Figure 1). Although these bioactive molecules show promise in the prevention and treatment of neurodegenerative diseases, there are several limitations in current research: (1) Most studies are based on *in vitro* cell models and animal experiments, lacking relevant clinical trials to further verify the exact efficacy and side effects of these compounds. (2) The specific molecular mechanisms through which these bioactive molecules regulate the activity of GSK-3β remain to be fully elucidated and require further elucidation in future research. The broad role of GSK-3β suggests that its inhibition may have therapeutic benefits for a range of diseases, including diabetes (Lanzillotta et al., 2024) and cancer (Furuta et al., 2017). This extensive therapeutic potential provides opportunities for drug development but also increases the risks associated with drug use, as the role of GSK-3β can be completely different and even contradictory in different disease states. For instance, in certain tumour types, GSK-3β may act as a tumour suppressor, while in other tumour types, it may act as a tumour promoter (Luan et al., 2024). (3) Existing research has primarily focused on the short-term effects of these drugs, with a relative lack of systematic assessment of long-term efficacy and safety. (4) The reliability and generalizability of results may be affected by limitations in sample size or flaws in study design. The majority of experiments only utilize negative controls, which can exclude the influence of certain factors in the experiment, but cannot fully demonstrate that these compounds are more effective than currently used clinical drugs. (5) Although some compounds have shown promising results in cellular models, their toxicity and side effects *in vivo* are still unclear, necessitating further evaluation through more animal experiments and clinical trials. (6) Plant extracts are complex mixtures with compositions that vary depending on the preparation methods and the plant materials used. This complexity and variability impact the reproducibility and interpretation of research. To address these challenges, some guidelines for the classification of plant extract studies can be used to improve the reproducibility and interpretability of research (Heinrich et al., 2022). (7) Many of these compounds may suffer from poor absorption, rapid metabolism, or inadequate ability to cross the blood-brain barrier, which can significantly diminish their therapeutic effectiveness *in vivo*. Combining new materials to solve the problem of drug delivery is also a valuable research direction (Wu et al., 2023). Consequently, in subsequent research, it is essential to devise more comprehensive experimental plans and to explore related mechanisms in depth.

AD is a complex neurodegenerative disorder with limited treatment options. It is for this reason that researchers are committed to discovering more effective and safe treatment options. The unique chemical structures and multi-target mechanisms of action of natural bioactive compounds offer new avenues for the treatment of AD. Despite the current limitations in research, future clinical trials are expected to further verify the efficacy and safety of these compounds in AD patients, potentially leading to new breakthroughs in AD therapy. Future research could consider combining multiple models to more comprehensively assess the effects of compounds. For instance, integrating network pharmacology with *in vitro* and *in vivo* models can leverage the strengths of these models to provide more convincing scientific evidence. Utilizing novel technologies such as organoid construction (Qian et al., 2017) and human cell models can more accurately simulate the *in vivo* environment of the human body, allowing for a deeper exploration of the potential adverse effects of these compounds on humans, thereby laying the foundation for subsequent clinical trials. And the development of artificial intelligence and large language models may bring new ideas and perspectives to this type of research (Huang N. et al., 2024). We should embrace new technologies with a more inclusive attitude.

## Author contributions

MW: Writing–original draft. WH: Writing–review and editing. JH: Funding acquisition, Writing–review and editing. YL: Conceptualization, Funding acquisition, Writing–review and editing. NH: Conceptualization, Funding acquisition, Writing–review and editing.

## Funding

The author(s) declare that financial support was received for the research, authorship, and/or publication of this article. This work was supported by the Funds of National Natural Science Foundation of China (81860710, 82060728), Zunyi Science and Technology Bureau (HZ-2023-09, [2024] No. 6), Guizhou Provincial Science and Technology Department (Thousand Talents Program, ZK[2025-380]).

## Conflict of interest

The authors declare that the research was conducted in the absence of any commercial or financial relationships that could be construed as a potential conflict of interest.

## Publisher's note



## References

Arciniegas Ruiz, S. M., and Eldar-Finkelman, H. (2021). Glycogen synthase kinase-3 inhibitors: preclinical and clinical focus on CNS-A decade onward. *Front. Mol. Neurosci.* 14, 792364. doi:10.3389/fnmol.2021.792364

Bielska, A. A., and Zondlo, N. J. (2006). Hyperphosphorylation of tau induces local polyproline II helix. *Biochemistry* 45 (17), 5527–5537. doi:10.1021/bi052662c

Chen, K., and Yu, G. (2024). Tetrahydroalstonine possesses protective potentials on palmitic acid stimulated SK-N-MC cells by suppression of Aβ1-42 and tau through regulation of PI3K/Akt signaling pathway. *Eur. J. Pharmacol.* 962, 176251. doi:10.1016/j.ejphar.2023.176251

Chen, L., Pan, H., Bai, Y., Li, H., Yang, W., Lin, Z. X., et al. (2020). Gelsemine, a natural alkaloid extracted from Gelsemium elegans Benth. alleviates neuroinflammation and cognitive impairments in Aβ oligomer-treated mice. *Psychopharmacol. Berl.* 237 (7), 2111–2124. doi:10.1007/s00213-020-05522-y

Das, T. K., Jana, P., Chakrabarti, S. K., and Abdul Hamid, M. R. W. (2019). Curcumin downregulates GSK3 and Cdk5 in scopolamine-induced Alzheimer's disease rats abrogating aβ40/42 and tau hyperphosphorylation. *J. Alzheimers Dis. Rep.* 3 (1), 257–267. doi:10.3233/adr-190135

Ding, Y., He, J., Kong, F., Sun, D., Chen, W., Luo, B., et al. (2024). Gallic acid alleviates cognitive impairment by promoting neurogenesis via the gsk3β-nrf2 signaling pathway in an APP/PS1 mouse model. *J. Alzheimers Dis. Rep.* 8 (1), 461–477. doi:10.3233/adr-230171

Furuta, T., Sabit, H., Dong, Y., Miyashita, K., Kinoshita, M., Uchiyama, N., et al. (2017). Biological basis and clinical study of glycogen synthase kinase- 3β-targeted therapy by drug repositioning for glioblastoma. *Oncotarget* 8 (14), 22811–22824. doi:10.18632/oncotarget.15206

Gao, Y., Wang, X. Q., Ma, S., Dong, Y. C., and Shang, Y. Z. (2021). Flavonoids from stem and leaf of Scutellaria Baicalensis Georgi inhibit the phosphorylation on multi-sites of tau protein induced by okadaic acid and the regulative mechanism of protein kinases in rats. *Comb. Chem. High. Throughput Screen* 24 (7), 1126–1136. doi:10.2174/1386207323666200901101233

Heinrich, M., Jalil, B., Abdel-Tawab, M., Echeverria, J., Kulić, Ž., McGaw, L. J., et al. (2022). Best Practice in the chemical characterisation of extracts used in pharmacological and toxicological research-The ConPhyMP-Guidelines. *Front. Pharmacol.* 13, 953205. doi:10.3389/fphar.2022.953205

Huang, J., Huang, N., Qiu, Y., and Shi, J. (2024a). Dendrobium nobile Lindl. alkaloid decreases Tau hyperphosphorylation via regulating PI3K/Akt/GSK-3β pathway *in vitro* and *in vivo*. *J. Ethnopharmacol.* 322, 117592. doi:10.1016/j.jep.2023.117592

Huang, L., Lin, M., Zhong, X., Yang, H., and Deng, M. (2019). Galangin decreases p-tau, Aβ42 and β-secretase levels, and suppresses autophagy in okadaic acid-induced PC12 cells via an Akt/GSK3β/mTOR signaling-dependent mechanism. *Mol. Med. Rep.* 19 (3), 1767–1774. doi:10.3892/mmr.2019.9824

Huang, N., Huang, W., Wu, J., Long, S., Luo, Y., and Huang, J. (2024b). Possible opportunities and challenges for traditional Chinese medicine research in 2035. *Front. Pharmacol.* 15, 1426300. doi:10.3389/fphar.2024.1426300

Huang, Q., Zhang, C., Dong, S., Han, J., Qu, S., Xie, T., et al. (2022). Asafoetida exerts neuroprotective effect on oxidative stress induced apoptosis through PI3K/Akt/GSK3β/Nrf2/HO-1 pathway. *Chin. Med.* 17 (1), 83. doi:10.1186/s13020-022-00630-7

Jhang, K. A., Park, J. S., Kim, H. S., and Chong, Y. H. (2017). Resveratrol ameliorates tau hyperphosphorylation at Ser396 site and oxidative damage in rat hippocampal slices exposed to vanadate: implication of ERK1/2 and GSK-3β signaling cascades. *J. Agric. Food Chem.* 65 (44), 9626–9634. doi:10.1021/acs.jafc.7b03252

Krishnankutty, A., Kimura, T., Saito, T., Aoyagi, K., Asada, A., Takahashi, S. I., et al. (2017). *In vivo* regulation of glycogen synthase kinase 3β activity in neurons and brains. *Sci. Rep.* 7 (1), 8602. doi:10.1038/s41598-017-09239-5

Lanzillotta, C., Tramutola, A., Lanzillotta, S., Greco, V., Pagnotta, S., Sanchini, C., et al. (2024). Biliverdin Reductase-A integrates insulin signaling with mitochondrial metabolism through phosphorylation of GSK3β. *Redox Biol.* 73, 103221. doi:10.1016/j.redox.2024.103221

Li, L., Li, T., Tian, X., and Zhao, L. (2021a). Ginsenoside Rd attenuates tau phosphorylation in olfactory bulb, spinal cord, and telencephalon by regulating glycogen synthase kinase 3β and cyclin-dependent kinase 5. *Evid. Based Complement. Altern. Med.* 2021, 4485957. doi:10.1155/2021/4485957

Li, M., Cai, N., Gu, L., Yao, L., Bi, D., Fang, W., et al. (2021b). Genipin attenuates tau phosphorylation and Aβ levels in cellular models of Alzheimer's disease. *Mol. Neurobiol.* 58 (8), 4134–4144. doi:10.1007/s12035-021-02389-8

Li, Y., Dai, S., Huang, N., Wu, J., Yu, C., and Luo, Y. (2022). Icaritin and icariin reduce p-Tau levels in a cell model of Alzheimer's disease by downregulating glycogen synthase kinase 3β. *Biotechnol. Appl. Biochem.* 69 (1), 355–363. doi:10.1002/bab.2114

Liu, F., Iqbal, K., Grundke-Iqbal, I., and Gong, C. X. (2002). Involvement of aberrant glycosylation in phosphorylation of tau by cdk5 and GSK-3beta. *FEBS Lett.* 530 (1-3), 209–214. doi:10.1016/s0014-5793(02)03487-7

Liu, G., Xie, R., Tan, Q., Zheng, J., Li, W., Wang, Q., et al. (2024). Pharmacokinetic study and neuropharmacological effects of atractylenolide III to improve cognitive impairment via PI3K/AKT/GSK3β pathway in intracerebroventricular-streptozotocin rats. *J. Ethnopharmacol.* 333, 118420. doi:10.1016/j.jep.2024.118420

Liu, X., Lai, L. Y., Chen, J. X., Li, X., Wang, N., Zhou, L. J., et al. (2023). An inhibitor with GSK3β and DYRK1A dual inhibitory properties reduces Tau hyperphosphorylation and ameliorates disease in models of Alzheimer's disease. *Neuropharmacology* 232, 109525. doi:10.1016/j.neuropharm.2023.109525

Luan, H., Wang, T., Li, F., Sun, S., Wang, Z., Zhao, X., et al. (2024). IGSF9 promotes tumor invasion and metastasis through GSK-3β/β-catenin mediated EMT in lung cancer. *Neoplasia* 58, 101067. doi:10.1016/j.neo.2024.101067

Nicolia, V., Fuso, A., Cavallaro, R. A., Di Luzio, A., and Scarpa, S. (2010). B vitamin deficiency promotes tau phosphorylation through regulation of GSK3beta and PP2A. *J. Alzheimers Dis.* 19 (3), 895–907. doi:10.3233/jad-2010-1284

Peng, X., Chen, L., Wang, Z., He, Y., Ruganzu, J. B., Guo, H., et al. (2022). Tanshinone IIA regulates glycogen synthase kinase-3β-related signaling pathway and ameliorates memory impairment in APP/PS1 transgenic mice. *Eur. J. Pharmacol.* 918, 174772. doi:10.1016/j.ejphar.2022.174772

Qian, X., Nguyen, H. N., Jacob, F., Song, H., and Ming, G. L. (2017). Using brain organoids to understand Zika virus-induced microcephaly. *Development* 144 (6), 952–957. doi:10.1242/dev.140707

Rao, Y. L., Ganaraja, B., Suresh, P. K., Joy, T., Ullal, S. D., Manjrekar, P. A., et al. (2024). Outcome of resveratrol and resveratrol with donepezil combination on the β-amyloid plaques and neurofibrillary tangles in Alzheimer's disease. *3 Biotech.* 14 (8), 190. doi:10.1007/s13205-024-04034-2

Ren, Z., Yang, H., Zhu, C., Deng, J., and Fan, D. (2023). Ginsenoside Rh4 alleviates amyloid β plaque and tau hyperphosphorylation by regulating neuroinflammation and the glycogen synthase kinase 3β signaling pathway. *J. Agric. Food Chem.* 71 (37), 13783–13794. doi:10.1021/acs.jafc.3c02550

Rostagno, A. A. (2022). Pathogenesis of Alzheimer's disease. *Int. J. Mol. Sci.* 24 (1), 107. doi:10.3390/ijms24010107

Saleh, S. R., Abd-Elmegied, A., Aly Madhy, S., Khattab, S. N., Sheta, E., Elnozahy, F. Y., et al. (2024). Brain-targeted Tet-1 peptide-PLGA nanoparticles for berberine delivery against STZ-induced Alzheimer's disease in a rat model: alleviation of hippocampal synaptic dysfunction, Tau pathology, and amyloidogenesis. *Int. J. Pharm.* 658, 124218. doi:10.1016/j.ijpharm.2024.124218

Santi, M. D., Carvalho, D., Dapueto, R., Bentura, M., Zeni, M., Martínez-González, L., et al. (2024). Prenylated flavanone isolated from dalea species as a potential multitarget-neuroprotector in an *in vitro* Alzheimer's disease mice model. *Neurotox. Res.* 42 (2), 23. doi:10.1007/s12640-024-00703-5

Shahani, N., and Brandt, R. (2002). Functions and malfunctions of the tau proteins. *Cell Mol. Life Sci.* 59 (10), 1668–1680. doi:10.1007/pl00012495

Wu, D., Chen, Q., Chen, X., Han, F., Chen, Z., and Wang, Y. (2023). The blood-brain barrier: structure, regulation, and drug delivery. *Signal Transduct. Target Ther.* 8 (1), 217. doi:10.1038/s41392-023-01481-w

Xing, H., Chen, G., Raza, F., Zafar, H., Xing, L., Li, Q., et al. (2024). The protective effects of ecdysterone on cognitive impairment through regulating akt/GSK-3β/nrf2 signaling pathway and oxidative stress in cognitive mice model and aβ-

induced cell neurotoxicity. *Front. Biosci. Landmark Ed.* 29 (3), 109. doi:10.31083/j.fbl2903109

Xu, M., Dong, Y., Wan, S., Yan, T., Cao, J., Wu, L., et al. (2016). Schisantherin B ameliorates Aβ(1-42)-induced cognitive decline via restoration of GLT-1 in a mouse model of Alzheimer's disease. *Physiol. Behav.* 167, 265–273. doi:10.1016/j.physbeh.2016.09.018

Yang, W., Liu, Y., Xu, Q. Q., Xian, Y. F., and Lin, Z. X. (2020). Sulforaphene ameliorates neuroinflammation and hyperphosphorylated tau protein via regulating the PI3K/Akt/GSK-3β pathway in experimental models of Alzheimer's disease. *Oxid. Med. Cell Longev.* 2020, 4754195. doi:10.1155/2020/4754195

Yu, G., Li, Y., Tian, Q., Liu, R., Wang, Q., Wang, J. Z., et al. (2011). Berberine attenuates calyculin A-induced cytotoxicity and Tau hyperphosphorylation in HEK293 cells. *J. Alzheimers Dis.* 24 (3), 525–535. doi:10.3233/jad-2011-101779

Zhang, B., Li, Q., Chu, X., Sun, S., and Chen, S. (2016). Salidroside reduces tau hyperphosphorylation via up-regulating GSK-3β phosphorylation in a tau transgenic Drosophila model of Alzheimer's disease. *Transl. Neurodegener.* 5, 21. doi:10.1186/s40035-016-0068-y

Zhao, B., Wang, Y., Liu, R., Jia, X. L., Hu, N., An, X. W., et al. (2021). Rutaecarpine ameliorated high sucrose-induced Alzheimer's disease like pathological and cognitive impairments in mice. *Rejuvenation Res.* 24 (3), 181–190. doi:10.1089/rej.2020.2349

# Frontiers in Pharmacology

**Explores the interactions between chemicals and living beings**

The most cited journal in its field, which advances access to pharmacological discoveries to prevent and treat human disease.

---

## Discover the latest Research Topics

See more →


**Frontiers**

Avenue du Tribunal-Fédéral 34
1005 Lausanne, Switzerland
frontiersin.org

**Contact us**

+41 (0)21 510 17 00
frontiersin.org/about/contact